

Deciphering the molecular signaling cascade in neuronal death

Presented by

Minghui Jessica Chen
(B.Sc. (2nd Upper Hon), M.Sc.)

Submitted in total fulfillment of the requirements of the degree of

Doctor of Philosophy

Menzies Research Institute
University of Tasmania
(May 2011)

Abstract

Hydrogen sulphide (H₂S), an important physiological gaso-neurotransmitter involved in neuronal long-term potentiation, is a mediator of cerebral ischemic injury. Previous study has identified H₂S neuropathological implication in aggravation of ionotropic glutamate receptors (iGluRs) -induced excitotoxicity injury. Excitotoxicity is one of the earliest events in stroke, a leading cause of adult permanent disability globally. Despite extensive efforts to deduce effective therapeutic interventions, the only clinically approved stroke treatment yields limited efficacy and potential risk to intracranial hemorrhage. The purpose of my project is to formulate screening platforms and define potential manipulative targets for stroke intervention via comparative global transcriptional profiling of *in vitro* and *in vivo* models. This facilitates identification of common mechanistic pathways governing ischemic progression.

Cultured primary cortical neurons treated with selective iGluRs agonists were used as *in vitro* cerebral ischemia representations. Comparative microarray analysis revealed occurrence of inflammation, oxidative stress and particularly cell cycle re-activation during excitotoxicity. Since cerebral ischemia does not limit at excitotoxicity but also involves critical focal hypoperfusion to a localized brain region causing oxygen-glucose deprivation that leads to further complications (e.g. microvascular injury, blood-brain barrier impairment and post-ischemic inflammation), microarray analysis was performed on *in vivo* cerebral ischemia rodent models (hypoxic ischemia, transient and permanent focal ischemia). Again, oxidative stress and neuroinflammation were confirmed as primary events. Transient cerebral ischemia induces a secondary damage called

ischemia/reperfusion (I/R) injury, mediated by release of oxidative stressors into the bloodstream upon perfusion to the occluded artery. In order to accentuate the significance of oxidative stress during I/R injury, transgenic glutathione peroxidase-1 (a major antioxidant enzyme)-knockout mice were subjected to transient middle cerebral artery occlusion with observed downplay of Nrf2 (a cytoprotective transcription factor)-mediated anti-oxidative response, ubiquitin-proteasomal dysfunction and recruitment of additional cell death pathways mediated by p53 and Fas ligand.

As observed in the *in vitro* models, cell cycle re-activation is a major upstream signaling pathway in neuronal injury mediation, and in particular a group of cell cycle protein kinases known as aurora kinases (AURKs), has been identified to be up-regulated for the first time in stroke. A selective AURKs inhibitor was applied to permanent focal ischemia model to determine if cell cycle impediment could abrogate ischemic progression. Unprecedentedly, AURKs inhibition successfully attenuated infarct damage via down-regulation of the neuroinflammation particularly the chemokine signaling pathway. Overall, my research facilitates a tremendous step in understanding stroke pathogenesis and identified a novel target which manipulation has achieved promising therapeutic efficacy.

Declarations

Declaration of Originality

"This thesis contains no material which has been accepted for a degree or diploma by the University or any other institution, except by way of background information and duly acknowledged in the thesis, and to the best of the my knowledge and belief no material previously published or written by another person except where due acknowledgement is made in the text of the thesis, nor does the thesis contain any material that infringes copyright."

Authority of Access

This thesis may be made available for loan and limited copying in accordance with the Copyright Act 1968.

Statement of Ethical Conduct

—The research associated with this thesis abides by the international and Australian codes on human and animal experimentation, the guidelines by the Australian Government's Office of the Gene Technology Regulator and the rulings of the Safety, Ethics and Institutional Biosafety Committees of the University."

Minghui Jessica Chen

Statement of co-authorship

The following people and institutions contributed to the publication of the work undertaken as part of this thesis:

- Paper 1 Higgins, G.C., Beart, P.M., Shin, Y.S., **Chen, M.J.**[20%], Cheung, N.S., Nagley, P. (2010) Oxidative stress: emerging mitochondrial and cellular themes and variations in neuronal injury. *Journal of Alzheimer's Disease* **20**, S453–S473.
- Paper 2 †Choy, M.S. [35%], †**Chen, M.J.** [35%], Manikandan, J. [2.5%], Peng, Z.F.[2.5%], Jenner, A.M. [2.5%], Melendez, A.J.[2.5%], Cheung, N.S. [20%] (2010) Up-regulation of endoplasmic reticulum stress-related genes during the early phase of treatment of cultured cortical neurons by the proteasomal inhibitor lactacystin. *Journal of Cellular Physiology*, 2011 Feb;226(2):494-510. (†**Joint first author**)
- Paper 3 †**Chen, M.J.**[30%], †Peng, Z.F.[30%], Manikandan, J. [2%], Melendez, A.[2%], Tan, G.S.[2%] Chung, M.C.[2%], Li, Q.T.[2%], Tan, T.M. [2%], Deng, L.W.[2%], Whiteman, M.[2%], Beart, P.M.[2%], Moore, P.K. [2%], Cheung, N.S. [20%] (2010) Gene profiling reveals hydrogen sulphide recruits death signaling via the N-methyl-D-aspartate receptor identifying commonalities with excitotoxicity. *Journal of Cellular Physiology* 2011 May;226(5):1308-22. doi: 10.1002/jcp.22459. (†**Joint first author**)
- Paper 4 †Peng, Z.F.[32.5%], †**Chen, M.J.**[32.5%], Manikandan, J.[2.5%]., Melendez, A.J[2.5%]., Shui, G[2.5%]., Russo-Marie, F.[2.5%], Beart, P.M.[2.5%], Moore, P.K [2.5%]., Cheung, N.S.[20%] (2010) Multifaceted involvement of NO in neuronal injury: transcriptomic profiling defines the temporal recruitment of death signaling and reveals commonalities to excitotoxicity. *Journal of Cellular And Molecular Medicine* 2011 Feb 25. doi: 10.1111/j.1582-4934.2011.01288.x. (†**Joint first author**)
- Paper 5 †**Chen, M.J.**[37.5%], †Wong, C.H.[37.5%], Peng, Z.F.[2.5%], Manikandan, J.[2.5%], Melendez, A.J.[2.5%]., Tan, T.M.[2.5%], Crack, P.J.[5%]., Cheung, N.S.[10%] (2010) A global transcriptomic view of the multifaceted role of Glutathione Peroxidase-1 in cerebral ischemic-reperfusion injury. *Free Radical Biology and Medicine* 2011 Mar 15;50(6):736-48. (†**Joint first author**)
- Paper 6 **Chen, M.J.**[52.5%], Jones, N.M.[15%], Kesavapany, S.[2.5%], Peng, Z.F.[2.5%], Manikandan, J.[2.5%], Tan, T.M.[2.5%], Beart, P.M.[2.5%], Cheung, N.S.[20%] (2010) Oxidative stress and inflammation: Main pathophysiological mechanisms in neonatal hypoxic ischemia in an in vivo mouse model. (Manuscript preparation in progress)
- Paper 7 **Chen, M.J.**[52.5%], Peng, Z.F. [15%], Kesavapany, S. [2.5%], Manikandan, J.[2.5%], , Tan, T.M.[2.5%], Beart, P.M. [5%], Cheung, N.S. [20%] (2010) Comparative transcriptomic profiling of ionotropic glutamate receptors revealed

novel commonality and differences in induction of neuronal injury. (Manuscript preparation in progress)

Paper 8 **Chen, M.J.**[42.5%], Chan, S.J.[20%], Ng, J.M.[15%], Peng, Z.F.[2.5%], Manikandan, J.[2.5%], Tan, T.M. [2.5%], Beart, P.M [2.5%], Wong, P.T. [2.5%], Cheung, N.S. [10%] (2010) Aurora kinase inhibitor attenuates elevated infarct volume during permanent focal ischemia in rat brain. (Manuscript preparation in progress)

Paper 9 **Chen, M.J.**[50%], Peng, Z.F.[20%], Cheung, N.S.[30%] (2010) Cell cycle re-activation: a crucial mechanism to commit neurons to its demise? (Manuscript preparation in progress)

Details of the Authors roles:

Paper 1

- Candidate Chen M.J.: contributed to writing one of the four major sections entitled “NOVEL INSIGHTS INTO NEURONAL OXIDATIVE STRESS BASED ON MULTIPLE OXIDATIVE STRESSORS” with the respective microarray table.
- Cheung, N.S. (Candidate Supervisor): contributed to refinement and presentation and fostering of collaboration

Paper 2

- Choy, M.S.: contributed to writing of 50% of manuscript, experimental design and execution
- Candidate Chen M.J.: contributed to writing of 50% of manuscript, experimental design and execution
- Manikandan, J.: Contributed to bioinformatics microarray analysis
- Peng, Z.F.: Contributed to bioinformatics microarray analysis
- Jenner, A.M.: Offered general laboratory assistance
- Melendez, A.J.: Contributed personnel and software for bioinformatics analysis
- Cheung, N.S. (Senior corresponding author / Candidate Supervisor): Contributed the idea, its formalisation and development and provided research funding

Paper 3

- Candidate Chen M.J.: Contributed to writing of entire manuscript and performed experimental design and execution
- Peng, Z.F.: Contributed to microarray analysis, and performed experimental design and execution
- Manikandan, J.: Contributed to bioinformatics microarray analysis
- Melendez, A.J.: Contributed personnel and software for bioinformatics analysis
- Tan, G.S.: Offered general laboratory assistance
- Chung, M.C.: Offered general laboratory assistance
- Tan, T.M.: Offered general laboratory assistance
- Deng, L.W.: Offered general laboratory assistance

- Whiteman, M.: Offered general laboratory assistance
- Beart, P.M.: Assisted with refinement and presentation
- Moore, P.K.: Provide partial funding
- Cheung, N.S. (Senior corresponding author / Candidate Supervisor): Contributed the idea, its formalisation and development and provided research funding

Paper 4

- Peng, Z.F.: Contributed to microarray analysis writing of 50% manuscript and performed experimental design and execution
- Candidate Chen M.J.: Contributed to writing of 50% manuscript and performed experimental design and execution
- Manikandan, J.: Contributed to bioinformatics microarray analysis
- Melendez, A.J.: Contributed personnel and software for bioinformatics analysis
- Shui, G.: Offered general laboratory assistance
- Russo-Marie, F.: Offered general laboratory assistance
- Beart, P.M.: Assisted with refinement and presentation
- Moore, P.K.: Provide partial funding
- Cheung, N.S. (Senior corresponding author / Candidate Supervisor): Contributed the idea, its formalisation and development and provided research funding

Paper 5

- Candidate Chen M.J.: Contributed to writing of 90% manuscript and research data
- Wong, C.H.: Performed stroke surgeries on mice, wrote 10% of manuscript and assisted in refinement and presentation
- Peng, Z.F.: Contributed to microarray analysis
- Manikandan, J.: Contributed to bioinformatics microarray analysis
- Melendez, A.J.: Contributed personnel and software for bioinformatics analysis
- Tan, T.M.: Offered general laboratory assistance
- Crack, P.J.: Provide transgenic animals and assisted in refinement and presentation
- Cheung, N.S. (Senior corresponding author / Candidate Supervisor): Contributed the idea, its formalisation and development and provided research funding

Paper 6

- Candidate Chen M.J.: Contributed to writing of entire manuscript and research data
- Nicole, N.M.: Performed stroke surgeries on mice
- Kesavapany, S.: Offered general laboratory assistance
- Peng, Z.F.: Contributed to microarray analysis
- Manikandan, J.: Contributed to bioinformatics microarray analysis
- Tan, T.M.: Offered general laboratory assistance
- Beart, P.M.: Assisted in refinement and presentation
- Cheung, N.S. (Senior corresponding author / Candidate Supervisor): Contributed the idea, its formalisation and development and provided research funding

Paper 7

- Candidate Chen M.J.: Contributed to writing of entire manuscript and research experiment execution
- Peng, Z.F.: Contributed to microarray analysis, assisted in research planning and execution, data assembly and presentation
- Kesavapany, S.: Offered general laboratory assistance
- Manikandan, J.: Contributed to bioinformatics microarray analysis
- Tan, T.M.: Offered general laboratory assistance
- Beart, P.M.: Assisted in refinement and presentation
- Cheung, N.S. (Senior corresponding author / Candidate Supervisor): Contributed the idea, its formalisation and development and provided research funding

Paper 8

- Candidate Chen M.J.: Contributed to writing of manuscript and assembly research data
- Chan, S.J.: Performed stroke surgeries on rats
- Ng, J.M.: Contributed part of research work
- Peng, Z.F.: Contributed to microarray analysis
- Manikandan, J.: Contributed to bioinformatics microarray analysis
- Tan, T.M.: Offered general laboratory assistance
- Beart, P.M.: Assisted in refinement and presentation
- Wong, P.T.: Provided animals, manpower and stroke model technique
- Cheung, N.S. (Senior corresponding author / Candidate Supervisor): Contributed the idea, its formalisation and development and provided research funding

Paper 9

- Candidate Chen M.J.: Contributed to majority of manuscript writing
- Peng, Z.F.: Contributed to microarray analysis, assisted in data assembly and presentation
- Cheung, N.S. (Senior corresponding author / Candidate Supervisor): Contributed the idea, its formalisation and development and provided research funding

We the undersigned agree with the above stated “proportion of work undertaken” for each of the above published (or submitted) peer-reviewed manuscripts contributing to this thesis:

Signed: _____

A/P. Nam Sang Cheung
Supervisor
Menzies Research Institute
University of Tasmania

Date: _____

Preface

This thesis consists only of my original work towards the Ph.D. degree, and I received significant assistance for the following:

Chapter 4

Dr. Nicole Jones (Department of Pharmacology, University of New South Wales, Sydney, Australia) has rendered me tremendous assistance in imparting the surgical skills required to induce hypoxic ischemia in neonatal mice, and ensure my consistency in technique with regards to the induction of infarct injury in the animals.

Chapter 5

The Gpx-1^{-/-} transgenic mice were provided by Dr. Peter J. Crack's laboratory (Department of Pharmacology, The University of Melbourne, Melbourne, Australia). Suture-induced transient focal cerebral ischemia technique was taught by Dr. C.H. Wong.

Chapter 6

Surgical induction of permanent focal cerebral ischemia technique was imparted by Ms. Su Jing Chan who worked in Prof. Peter Wong's laboratory (Department of Pharmacology, National University of Singapore, Singapore).

Acknowledgements

I am more appreciative than I can express to my main supervisor, A/P Steve Nam Sang Cheung of Menzies Research Institute, University of Tasmania and my co-supervisor A/P Heung-Chin Cheng for their invaluable advices, motivations and endless encouragement that have been given to me. I am grateful to their patient and invaluable guidance and supervision towards the completion of my Ph.D. project. Special thanks goes out to A/P Cheung for sacrificing his precious time to meet me on a regular basis despite his busy schedule providing me with many research opportunities which eventually rewarded me with many research publications after my persistent hard work. A/P Cheung also demonstrates dedicated efforts to prepare me for my future post-doctoral career by providing room for independent thinking research and involvement in grant writing.

I would also like to show my gratitude to external collaborators for the tremendous help rendered which facilitate a much smoother route towards the completion of my Ph.D. project. They include Dr. Peter J. Crack and Dr. Connie H.Y. Wong (Department of Pharmacology, The University of Melbourne), Dr. Nicole Jones (Department of Pharmacology, University of New South Wales) and Prof. Peter T.H. Wong and Ms Su Jing Chan (Department of Pharmacology, National University of Singapore) for the technical assistance rendered and surgical skills rendered for the *in vivo* model studies. I would like to take this opportunity to show my appreciation to Prof. Philip M. Beart (Florey Institute of Neurosciences and Department of Pharmacology, The University of Melbourne), Dr. Jayapal Manikandan (Partek® Inc.) and Dr. Zhao Feng Peng (China University of Geosciences) whose help have truly accelerated my research.

I would also like to highlight and thank my peers, Mr. Jian Ming Jeremy Ng, Dr. Linda Lau and Mr. Soo Piang Chin for their great friendship and wonderful encouragements given to me in the course of this project. Last but not least, I want to thank my family (my parents and sister Rebecca) and husband Mark for the tremendous and relentless motivation and support they have provided me with to get me through all the ups and downs during my Ph.D. studies and at end of the day still stood by me and believed in me, despite the long distance apart from each other. To end this acknowledgement, I would like to say a very big thank you to all those whom I have unintentionally left out in this list and have in one way or another help in my Ph.D. project.

Table of contents

	Page
List of Tables	i
List of Figures	iv
Publications and Presentations	viii
List of Abbreviations	xi
Chapter 1: Introduction	1
1.1 L-glutamate (Glu): A crucial excitatory neurotransmitter in the mammalian brain	2
1.2 Mechanistic action of Glu via Glu receptors (GluRs)	2
1.2.1 Ionotropic GluRs (iGluRs)	2
1.2.1.1 N-methyl-D-aspartate receptors (NMDARs)	3
1.2.1.1.1 Structure and distribution of NMDARs	3
1.2.1.1.2 Physiological roles of NMDARs	6
1.2.1.1.3 NMDARs association with CNS diseases	8
1.2.1.2 Alpha-amino-3-hydroxy-5-methyl-4-isoxazolepropionic acid receptors (AMPARs)	9
1.2.1.2.1 Structure and distribution of AMPARs	9
1.2.1.2.2 Physiological roles of AMPARs	10
1.2.1.2.3 AMPARs association with CNS diseases	11

1.2.1.3 Kainate receptors (KARs)	12
1.2.1.3.1 Structure and distribution of KARs	12
1.2.1.3.2 Physiological roles of KARs	13
1.2.1.3.3 KARs association with CNS diseases	14
1.2.2 Metabotropic GluRs (mGluRs)	15
1.2.2.1 Structure and distribution of mGluRs	15
1.2.2.2 Physiological roles of mGluRs	16
1.2.2.3 mGluRs association with CNS diseases	17
1.3 Excitotoxicity in CNS due to GluRs over-stimulation	19
1.3.1 Calcium ion homeostasis	21
1.3.2 Nitric oxide (NO) generation	21
1.3.3 Free radical generation	23
1.3.4 Caspase activation	24
1.3.5 Calpains involvement	24
1.3.6 Organellar destabilization	25
1.3.6.1 Mitochondrial dysfunction	25
1.3.6.2 Lysosomal rupture	26
1.3.6.3 Endoplasmic reticulum (ER) stress	27
1.4 Ischemia	29
1.4.1 Types of cerebral ischemic stroke	30
1.4.1.1 Global ischemia	30
1.4.1.2 Focal ischemia	31
1.4.1.3 Hypoxic ischemia (HI)	32

1.5	Focal ischemia stroke	33
1.5.1	Epidemiology, symptoms and effects of focal cerebral ischemia	33
1.5.2	Current approved focal cerebral ischemia treatment	34
1.5.3	Post-ischemic physiological-response recovery	35
1.6	Patho-physiology of focal cerebral ischemia	36
1.6.1	Excitotoxicity, programmed cell death and ischemia	38
1.6.2	Programmed cell death (PCD) in focal ischemia	40
1.6.2.1	Apoptosis	42
1.6.2.2	Autophagy	44
1.6.2.3	Programmed necrosis	47
1.6.3	Oxidative stress	49
1.6.4	Neuroinflammation	52
1.6.5	Microvascular disruption	53
1.6.6	Blood-brain barrier (BBB) impairment	56
1.7	Inadequacy in knowledge of stroke pathogenesis: Missing pieces from the puzzle	58
1.8	Global transcriptomic profiling studies: An overview	58
1.8.1	Microarray technique: differential gene expression studies	60
1.8.2	Mechanistic concept behind microarray technology	61
1.8.3	Assignment of functional-biological pathway definition to significantly-modulated genes using online database tool	67
1.8.4	Relevance of global gene profiling to elucidation of	68

pathogenesis of neuropathological disorders

1.9	Aims of my Ph.D. project	69
2	Methodology	73
2.1	Buffers/Solutions and Consumables	74
2.2	Immunocytochemistry	74
2.3	Infarct volume assessment	75
2.4	Total RNA extraction and isolation from plated neuronal cultures	75
2.5	Total RNA extraction from animal brain cortice	76
2.6	Determination of RNA Concentration	77
2.7	Checking of RNA quality	77
2.8	cDNA Synthesis/ Reverse transcription	78
2.9	Real-time Polymerase Chain Reaction (PCR)	79
2.10	Microarray analysis	81
2.10.1	Microarray experiment using Illumina® Mouse Ref8 V1.1 / V2 and Rat Ref12 V1 hybridization beadchips	81
2.10.2	Microarray data collection and analysis	82
2.11	Statistical analysis	83
3	<i>In vitro</i> excitotoxicity models	84
3.1	Centralization of GluRs signaling cascades in H ₂ S-mediated neuronal injury	90
3.1.1	Background information	91
3.1.2	Introduction	99
3.1.3	Results	103

3.1.3.1	A high degree of global transcriptomic association between H ₂ S and NMDA/KA profiles: indication of high reliance of NMDARs and KARs –induced signaling transduction in H ₂ S-mediated neuronal injury	104
3.1.3.2	Functional-gene ontology classification revealed several key biological processes, crucial to neuronal survival/death	108
3.1.3.3	Validation of H ₂ S, NMDA and KA global transcriptomic profiles via real-time PCR	117
3.1.4	Discussion	119
3.1.4.1	Significance of iGluRs (NMDARs and KARs) activation in H ₂ S-mediated neuronal injury	119
3.1.4.2	Significance of enriched biological processes in H ₂ S-mediated neuronal injury	120
3.2	Comparative global gene profiling of iGluRs involvement in Glu – mediated excitotoxicity	130
3.2.1	Introduction	131
3.2.2	Results	134
3.2.2.1	Bi-model analyses of individual iGluRs profiles against that of Glu revealed the following decrease ordering of GluRs activation dependence NMDARs>KARs>AMPARs during excitotoxicity	135
3.2.2.2	Simultaneous comparison of all four excitotoxicity models identified several major common biological processes	140

3.2.2.3	Singular profile analysis highlight cell cycle re-activation as a prominent biological process during excitotoxicity	151
3.2.2.4	Validation of Glu global transcriptomic profiles via real-time PCR	165
3.2.3	Discussion	166
4	Hypoxic ischemia in <i>in vivo</i> neonatal mouse model	174
4.1	Introduction	177
4.2	Results	180
4.2.1	Hypoxic ischemia induced significant global transcriptional modulation	180
4.2.2	Validation of neonatal HI profiles via real-time PCR	187
4.3	Discussion	188
5	Transient focal cerebral ischemia	192
5.1	Transient focal cerebral ischemia in wild-type (WT) <i>in vivo</i> adult mouse model	196
5.1.1	Introduction	197
5.1.2	Results	199
5.1.2.1	tMCAO induced neural inflammation and oxidative stress, contributing to neuronal death in WT-mice	201
5.1.2.2	Validation of WT-tMCAO profiles via real-time PCR	214
5.1.3	Discussion	215
5.1.3.1	Neuroinflammation	216
5.1.3.2	Oxidative stress	219

5.2	Transient cerebral focal ischemia in glutathione peroxidase-1 knockout (Gpx-1 ^{-/-}) <i>in vivo</i> adult mouse model	221
5.2.1	Introduction	222
5.2.2	Results	225
5.2.2.1	Gpx-1 ^{-/-} mice displayed a distinct cortical global gene profile when compared to that of WT at physiological basal state	225
5.2.2.2	Gpx-1 ^{-/-} mice induced a substantially larger global gene profile as compared to WT mice upon tMCAO induction	235
5.2.2.3	Deletion of Gpx-1 induced transcriptional regulation of additional novel pathways, resulting in exacerbation of cerebral post-ischemic injury	244
5.2.2.4	Validation of Gpx-1 ^{-/-} profile via real-time PCR	252
5.2.3	Discussion	253
5.2.3.1	Gpx-1 ^{-/-} increases susceptibility to I/R injury via predisposition to oxidative stress	253
5.2.3.2	Absence of Gpx-1 modulates additional biological processes during I/R injury	254
6	Permanent focal cerebral ischemia	256
6.1	Permanent focal cerebral ischemia in adult rat model	260
6.1.1	Introduction	261
6.1.2	Results	265
6.1.2.1	pMCAO induces significant global transcriptional	267

regulation	
6.1.2.2 Validation of pMCAO global transcriptomic profile via real-time PCR	277
6.1.3 Discussion	278
6.2 Application of cell cycle inhibitor on permanent focal cerebral ischemia	281
6.2.1 Introduction	282
6.2.1.1 Aurora kinases (AURKs): A recently acknowledged family of crucial cell cycle protein kinases	284
6.2.2 Results	289
6.2.2.1 Cell cycle re-activation is an early upstream event during excitotoxicity <i>in vitro</i> : Significant role of AURKs	289
6.2.2.2 Inhibition of AURKs attenuates infarct damage upon pMCAO	291
6.2.2.3 AURKs inhibition significantly modulates pMCAO global transcriptomic profile	295
6.2.2.4 Comparative microarray analysis of differentially-expressed genes common to vehicle and treatment groups revealed AURKs inhibition induces a diminished transcriptional-amplitude response	298
6.2.2.5 AURKs inhibition suppresses the activation of several inflammation-related signaling cascades	306
6.2.2.6 Validation of AURKs inhibitor –treated pMCAO global	309

	transcriptomic profile via real-time PCR	
6.2.3	Discussion	310
7	Comparative in vitro global gene profiles: Focus on oxidative stress (Glu versus well known oxidative stressor neurodegenerative models)	313
7.1	Introduction	316
7.2	Results	320
7.2.1	Generation of NO global gene profile	320
7.2.2	Generation of hypochlorous acid (HOCl) global gene profile	321
7.2.3	Generation of rotenone global gene profile	322
7.2.4	Generation of lactacystin global gene profile	323
7.2.5	Comparative global transcriptomic analysis across all five distinct oxidative stressor models (Common genes perspective)	324
7.2.6	Comparative global transcriptomic analysis across all five distinct oxidative stressor models (Common pathway perspective)	327
7.3	Discussion	331
7.3.1	Response to oxidative stress	331
7.3.2	ER stress via unfolded protein response (UPR)	335
7.3.3	Ubiquitin-proteasome system (UPS)	338
7.3.4	Mitochondrial respiratory chain / Non-respiratory chain enzymes	340

7.3.5	Calcium ion binding and homeostasis	342
7.3.6	Cell death	343
7.3.7	Summary of the comparative microarray analysis across the five oxidative stressors models	347
8	Conclusion and future directions	349
8.1	Conclusion	350
8.1.1	Summary of major findings from <i>in vitro</i> models	350
8.1.2	Summary of major findings from <i>in vivo</i> models	352
8.2	Future directions	356
	References	360

List of tables

	Page
Table 3.1 Gene expression profiles of neuronal death-related families in cultured day 7 mouse primary cortical neurons treated with 200 μ M NaHS, 200 μ M NMDA and 100 μ M KA respectively.	111
Table 3.2 Validation of microarray data using real-time PCR technique on day 7 cultured murine primary cortical neurons treated with 200uM NaHS. Data are expressed as fold-change \pm sem.	117
Table 3.3 Validation of microarray data using real-time PCR technique on day 7 cultured murine primary cortical neurons treated with 200uM NMDA.	118
Table 3.4 Validation of microarray data using real-time PCR technique on day 7 cultured murine primary cortical neurons treated with 100uM KA.	118
Table 3.5 Gene expression profiles of neuronal death-related families in cultured day 7 mouse primary cortical neurons treated with E_{c50} of AMPA, KA, NMDA and Glu over a 24-hour period respectively.	145
Table 3.6 Genes encoding for proteins involved in mitotic cell division in individual excitotoxicity global transcriptomic profiles.	152
Table 3.7 Significantly expressed genes (with fold-change of at least ± 1.5 in a minimum one out of three time-points and passed One-way ANOVA, $p < 0.05$) encoding for proteins involved in mitotic cell cycle upon 300uM AMPA-mediated excitotoxicity in cultured primary cortical neurons.	156
Table 3.8 Significantly expressed genes (with fold-change of at least ± 1.5 in a minimum one out of three time-points and passed One-way ANOVA, $p < 0.05$) encoding for proteins involved in mitotic cell cycle upon 100uM KA-mediated excitotoxicity in cultured primary cortical neurons.	158

Table 3.9 Significantly expressed genes (with fold-change of at least ± 1.5 in a minimum one out of three time-points and passed One-way ANOVA, $p < 0.05$) encoding for proteins involved in mitotic cell cycle upon 200uM NMDA-mediated excitotoxicity in cultured primary cortical neurons	161
Table 3.10 Significantly expressed genes (with fold-change of at least ± 1.5 minimum one out of three time-points and passed One-way ANOVA, $p < 0$ encoding for proteins involved in mitotic cell cycle upon 250uM Glu-mediated excitotoxicity in cultured primary cortical neurons.	163
Table 3.11 Validation of microarray data using real-time PCR technique on D7 murine primary cortical neuronal cultures treated with 250uM Glu.	165
Table 4.1 Selected differentially-expressed gene profile of over-represented neuronal death-related biological processes in the infarct cortice of neonatal HI mice.	184
Table 4.2 Validation of microarray data using real-time PCR technique on the HI-induced neonatal murine cortice.	187
Table 5.1 Selected differentially-expressed gene profile of neuronal death-related families in the infarct cortice of WT-MCAO male adult mice.	210
Table 5.2 Validation of microarray data using real-time PCR technique on tMCAO-induced cortex RNA samples from WT mice respectively.	214
Table 5.3 Selected biological process-associated genes that were differentially expressed in Gpx-1 ^{-/-} mouse cortex when normalized against that of the WT strain at physiological basal condition.	231
Table 5.4 Gene expression profiles of neuronal death-related families in genes common to the infarct cortice of WT and Gpx-1 ^{-/-} -tMCAO models.	240
Table 5.5 Selected differentially-expressed gene profile of neuronal death-related families in Gpx-1 ^{-/-} -tMCAO infarct cortice.	248

Table 5.6 Validation of microarray data using real-time PCR technique on tMCAO-induced cortex RNA samples from Gpx-1 ^{-/-} mice respectively.	252
Table 6.1 Selected differentially-expressed temporal gene profile of neuronal death-related families in vehicle (<i>i.c.v.</i> injection of 80% DMSO 30min after surgery) pMCAO-induced adult male Wistar rat cortice.	273
Table 6.2 Validation of microarray data using real-time PCR technique on pMCAO-induced adult male Wistar rat infarcted cortice treated with 80% DMSO (vehicle).	277
Table 6.3 Transcriptional profiles of Aurks and associated cofactors in <i>in vitro</i> excitotoxicity models.	290
Table 6.4 Functional annotation of genes common to vehicle (80% DMSO) and 30mM ZM447439 treatment conditions induced via <i>i.c.v.</i> administration 30min post- pMCAO.	302
Table 6.5 Functional annotation of significantly-modulated genes demonstrating at least ± 1.5 fold-change in a minimum of one out of two time-points (8h and 24h) exclusive to vehicle (80% DMSO) condition induced via <i>i.c.v.</i> administration 30min post- pMCAO.	307
Table 6.6 Validation of microarray data using real-time PCR technique on pMCAO-induced adult male Wistar rat infarcted cortice treated with 30mM AURKs inhibitor (ZM447439; treatment).	309
Table 7.1 Selected enriched biological processes consisting of common differentially regulated genes common to five oxidative stressors-induced neuronal injury models.	326
Table 7.2 Selected enriched biological processes consisting of significantly up-regulated genes common to four oxidative stressors-induced neuronal injury models.	328

List of figures

	Pages
Figure 1.1 A simplified diagram summarizing the major biological processes implicated during neuronal excitotoxicity.	29
Figure 1.2 Diagram depicting the core and penumbra regions upon the infliction of focal cerebral ischemia in a localized brain region.	36
Figure 1.3 A summary of the major processes at work during the pathogenesis of focal cerebral ischemia.	37
Figure 1.4 A schematic diagram of the major steps in a microarray experiment.	64
Figure 1.5 A schematic diagram depicting a single-channel (one sample) microarray experiment layout.	65
Figure 1.6 A schematic diagram depicting a dual-channel (two samples: Target and Reference) microarray experiment layout.	66
Figure 3.1 Immunohistochemistry assay employing the neuronal microtubule-associated protein 2 (MAP2), demonstrated an increase in outgrowths with increasing days of culture.	86
Figure 3.2 Double immunohistochemistry labeling using MAP2 (neuronal marker) and glial fibrillary acidic protein (GFAP; astrocyte marker) demonstrated more than 95% of the cultures comprises of neurons.	87
Figure 3.3 Differential expressions of GluRs (GluR2/4-AMPA; NMDA R1-NMDARs) in cultured mouse primary cortical neurons from day 1-8 <i>in vitro</i> .	91
Figure 3.4 Concentration-dependent decrease in cell viability observed NaHS-treated day 7 neurons.	93

Figure 3.5 Potentiation of Glu-mediated neurotoxicity by NaHS application was seen only in day 7 neurons.	95
Figure 3.6 Successful attenuation of H ₂ S-induced neuronal death by NMDARs and KARs antagonists, which highlights the crucial role of NMDARs and KARs in the mediation of H ₂ S-induced neurotoxicity.	97
Figure 3.7 Bi-model global transcriptomic profile analysis of individual iGluRs agonists against H ₂ S-mediated neuronal injury model.	106
Figure 3.8 Venn diagram demonstrating the number of commonly occurring RefSeq transcripts overlapping across all three treatment profiles which have been subjected to the microarray analysis criteria of demonstrating at least ± 1.5 fold-change in one out of the three-points and passed statistical testing.	107
Figure 3.9 Summary of the prominent biological processes affected during H ₂ S-mediated neuronal injury.	128
Figure 3.10 Classification of individual global transcriptomic profiles of Glu, NMDA, AMPA and KA in cultured murine primary cortical neurons.	137
Figure 3.11 Bi-model global transcriptomic profile analysis of individual iGluRs agonists against Glu excitotoxicity model.	138
Figure 3.12 Consistency in the transcriptional regulatory trend of the commonly occurring gene probes in individual iGluRs against Glu excitotoxicity models.	139
Figure 3.13 Overall consistency in the transcriptional regulatory trend of the commonly occurring gene probes in all four excitotoxicity models.	140
Figure 3.14 A summarized diagram depicting the major role of cell cycle re-entry in the exacerbation of neuronal injury in concurrent with the simultaneous occurrence of oxidative stress and neuroinflammation during	172

excitotoxicity in cerebral ischemia.

Figure 5.1 Time-course profiling revealed a significant increase in number of up/down-regulated genes with transcriptional expression of a minimum of ± 1.5 -fold change from 8h to 24h timeframe. 209

Figure 5.2 Time-course profiling revealed a significant increase in number of up/down-regulated genes with transcriptional expression with a minimum of ± 1.5 -fold change from 8h to 24h timeframe. 237

Figure 5.3 (A) Venn diagram illustrated 422 DAVIDS-recognizable genes with significant regulation of at least ± 1.5 fold-change in a minimum of one out of three time-points were common to WT- and Gpx-1^{-/-}-tMCAO global gene profiles. (B) Stacked bar-chart depicted a high degree of consistency in regulatory trend of genes (at least ± 1.5 fold-change in at least one out of three time-points in individual treatment) common to both WT- and Gpx-1^{-/-}-tMCAO global gene profiles. 238

Figure 5.4 Sequential time-point comparisons (2-8h and 8-24h) of the 422 common up- and down-regulated genes did not reveal significant difference in gene expression increment/decrement (fold-change) between WT and Gpx-1^{-/-} mouse strains upon tMCAO induction. 239

Figure 6.1 TTC-stained 2mm- brain sections from anterior to posterior [1 – 6] of a male Wistar rat brain upon pMCAO induced on the left infarct hemisphere. 266

Figure 6.2 An overview of AURKA and AURKB involvements in the various phases of mitotic cell cycle process. 285

Figure 6.3 A simple signaling pathway demonstrating the most prominent transduction cascade of AURKA in the positive regulation of mitotic cell division. 287

- Figure 6.4** The main regulators of (A) Aurora A and (B) Aurora B kinases. Protein kinases are indicated in red and phosphorylation events by red arrows. Protein phosphatases are indicated in blue. (Image adapted from (Carmena et al., 2009)) 288
- Figure 6.5** TTC staining of 2mm sections of rat brain demonstrated a concentration-dependent reduction in infarct volume during pMCAO upon escalating dose application of selective pharmacological AURK inhibitor ZM447439 [1 – 6: anterior – posterior]. 293
- Figure 6.6** Quantitative analysis of the infarct volume corrected for brain edema and infarct tissue contraction demonstrated that 5ul *i.c.v.* injection of 30mM ZM447439 30min post-pMCAO successfully attenuated infarct damage. 294
- Figure 6.7** Venn diagram illustrating number of differentially-expressed annotated genes common and exclusive to both pMCAO + Vehicle and pMCAO + 30mM ZM447439 treatment global gene profiles at 8h and 24h. 297

Publications and presentations

Publications raised from this thesis

Higgins, G.C., Beart, P.M., Shin, Y.S., **Chen, M.J.**, Cheung, N.S., Nagley, P. (2010) Oxidative stress: emerging mitochondrial and cellular themes and variations in neuronal injury. *Journal of Alzheimer's Disease* 20: S453–S473.

†Choy, M.S., †**Chen, M.J.**, Manikandan, J., Peng, Z.F., Jenner, A.M., Melendez, A.J., Cheung, N.S. (2010) Up-regulation of endoplasmic reticulum stress-related genes during the early phase of treatment of cultured cortical neurons by the proteasomal inhibitor lactacystin. *Journal of Cellular Physiology*, 2011 Feb;226(2):494-510. (†**Joint first author**)

Chen, M.J., Peng, Z.F., Manikandan, J., Melendez, A., Li, Q.T., Tan, G.S., Chung, M.C., Li, Q.T., Tan, T.M., Deng, L.W., Whiteman, M., Beart, P.M., Moore, P.K., Cheung, N.S. (2010) Gene profiling reveals hydrogen sulphide recruits death signaling via the N-methyl-D-aspartate receptor identifying commonalities with excitotoxicity. *Journal of Cellular Physiology* 2011 May;226(5):1308-22. doi: 10.1002/jcp.22459.

†Peng, Z.F., †**Chen, M.J.**, Manikandan, J., Melendez, A.J., Shui, G., Russo-Marie, F., Beart, P.M., Moore, P.K., Cheung, N.S. (2010) Multifaceted involvement of NO in neuronal injury: transcriptomic profiling defines the temporal recruitment of death signaling and reveals commonalities to excitotoxicity. *Journal of Cellular And Molecular Medicine* 2011 Feb 25. doi: 10.1111/j.1582-4934.2011.01288.x. (†**Joint first author**)

Chen, M.J., Wong, C.H., Peng, Z.F., Manikandan, J., Melendez, A.J., Tan, T.M., Crack, P.J., Cheung, N.S. (2010) A global transcriptomic view of the multifaceted role of Glutathione Peroxidase-1 in cerebral ischemic-reperfusion injury. *Journal of Cellular And Molecular Medicine* 2011 Mar 15;50(6):736-48. (†**Joint first author**)

Other publications

†Chew, J., †**Chen, M.J.**, Lee, A., Peng, Z.F., Bay, B.H., Ng, J.M., Qi, R.Z., Cheung, N.S. (2010) Identification of p10 as a Neurotoxic Product Generated from the Proteolytic Cleavage of the Neuronal Cdk5 Activator, *Journal of Cellular Biochemistry*, in press (Accepted 9-Sep-2010) (†**Joint first author**)

†Yap, Y.W., †**Chen, M.J.**, Choy, M.S., Peng, Z.F., Whiteman, M., Manikandan, J., Melendez, A.J., Cheung, N.S. (2010) Temporal transcriptomic profiling revealed cellular targets that govern survival in HOCl-mediated neuronal apoptosis, *Life Sciences* in press (Accepted 17-Sep-2010) (†**Joint first author**)

†Chong, K.W., †**Chen, M.J.**, Koay, E.S., Wong, B.S., Lee, A.Y., Russo-Marie, F., Cheung, N.S. (2010) Annexin A3 is associated with cell death in lactacystin-mediated neuronal injury, *Neuroscience Letters* in press (Accepted 8-Sept-2010) (†**Joint first author**)

Chen, M.J., Soo, P.C., Choy, M.S., Peng, Z.F., Cheng, H.C., Cheung, N. S. (2010) Calpains-mediated PTEN cleavage in excitotoxic neuronal death, *Journal of Biochemistry- Molecular Biology at the Post-Genomic Era* in press (Accepted 31-Aug-2010).

Conference presentations

International Society of Neurochemistry (ISN) Summer School 2009 (Gyeongju South Korea) and The 22nd Biennial Meeting of the ISN/APSN Joint Meeting (Busan, South Korea): **Deciphering the mechanism of hydrogen sulphide-induced neuronal death in cultured murine cortical neurons, Chen, M.J.**, Peng, Z.F., Manikandan, J., Moore, P.K., Cheung, N.S.

40th Annual Meeting Society of Neuroscience (SfN) 2010 (San Diego, USA): **Multifaceted role of Gpx-1 in a cerebral ischemic-reperfusion transgenic mouse model: deletion of Gpx-1 enhanced the physiological basal oxidative state resulting in increased susceptibility to neuronal injury in a pro-oxidant environment, Chen, M.J.**, Wong, C.H., Peng, Z.F., Manikandan, J., Melendez, A.J., Crack, P.J., Cheung, N.S.

Abbreviations used in this thesis

3MST: 3-mercaptopyruvate sulfurtransferase
A β ₄₀: Abeta40
A β ₄₂: Abeta42
Acad: acetyl-coenzyme A dehydrogenase
AD: Alzheimer's disease
AIF: apoptosis-inducing factor
ALDH: mitochondrial aldehyde dehydrogenase
ALS: amyotrophic lateral sclerosis
AMPA: alpha-amino-3-hydroxy-5-methyl-4-isoxazolepropionic acid
AMPA_Rs: alpha-amino-3-hydroxy-5-methyl-4-isoxazolepropionic acid receptors
ANXs: annexins
ARE: antioxidant-response element
ATF4: activating transcription factor 4
ATP: adenosine triphosphate
AURKs: aurora kinases
BBB: blood-brain-barrier
BCL-2: B-cell lymphoma 2
BDNF: brain-derived neurotrophic factor
CAMK2: calcium/calmodulin kinase 2
cAMP: cyclic adenosine 3',5'-monophosphate
CAMs: cell adhesion molecules
CAPN-2: calpain-2
CASP: caspase
CBS: cystathionine- β -synthetase
CCND: cyclin D
CCND1/2: cyclin D 1/2
CCNG1: cyclin G1
CDK2: cyclin-dependent kinase 2
CEBPB2: CCAAT/enhancer binding protein (C/EBP) beta
cGMP: cyclic guanosine 3',5'-monophosphate
CGN: cerebellar granule neurons
CDKs: cyclin-dependent kinases
CNS: central nervous system
CNTF: ciliary neurotropic factor
CO₂: carbon dioxide
COX-2: cyclo-oxygenase 2
CPC: chromosomal passenger complex
CSE: cystathionine- γ -lyase
CTSB: cathepsin B
CYB5: cytochrome b5 reductase
CYP: cytochrome p450 family
DAB: 3,4-diaminobenzidine
DAMPs: damage-associated molecular pattern molecules

DAVID: Database for Annotation, Visualization, and Integrated Discovery
DDIT3: DNA-damage inducible transcript 3
DHRS8: Aldh dehydrogenase/reductase 8
DISC: death-inducing signaling complex
DLB: dementia with Lewy bodies tissue
DMEM: Dulbecco's modified Eagle medium
DMSO: dimethyl sulfoxide
DS: Down syndrome
EBSS: Earle's balanced salt solution
ECM: extracellular cell matrix
EDTA: ethylenediaminetetraacetate
Endo G: endonuclease G
ERK1: extracellular signal-regulated kinase 1
EPO: erythropoietin
EPSP: excitatory post-synaptic potential
ER: endoplasmic reticulum
ETC: electron transport chain
FAD⁺ / FADH₂: flavin adenine dinucleotide
FADD: Fas-associated death domain
FDR: Benjamini-Hochberg False Discovery Rate
FOS: FBJ osteosarcoma oncogene
GADD45G: Growth arrest and DNA-damage-inducible 45 gamma
GAPDH: glyceraldehydes 3-phosphate dehydrogenase
GC: guanylate cyclase
GEO: Gene Expression Omnibus
GFAP: glial fibrillary acidic protein
GluRs: glutamate receptors
GPD: glycerol-3-phosphate dehydrogenase
Gpx-1: glutathione peroxidase-1
Gpx-1^{-/-}: glutathione peroxidase-1 knockout
GSH: glutathione
GST: glutathione S-transferase
GTP: guanosine-5'-triphosphate
H₂O₂: hydrogen peroxide
HB-EGF: heparin-binding epidermal growth factor-like growth factor
HD: Huntington's disease
HI: hypoxic ischemia
HIF1: Hypoxia-inducible factor-1
HMOX1: heme oxygenase-1
HOCl: hypochlorous acid
H₂S: hydrogen sulphide
HSPs: heat shock proteins
HTRA2/OMI: HtrA serine peptidase 2
IAP: inhibitor of apoptosis
ICAD: inhibitor of caspase-3-activated DNase
i.c.v.: intra-cerebroventricular

IDH: isocitrate dehydrogenase
IGF-I: insulin-like growth factor I
IGF-2: insulin growth-like factor 2
iGluRs: ionotropic glutamate receptors
IL-1 β : interleukin-1-beta
IL-6: interleukin-6
IMS: mitochondrial intermembrane space
INK4C: cyclin-dependent kinase inhibitor 2c
I/R: ischemia/reperfusion
KA: kainate /kainic acid
KARs: kainate receptors
LAPTM5: lysosomal-associated protein transmembrane 5
KEAP1: (Nrf2)-Kelch-like ECH-associated protein 1
LC3: microtubule-associated protein 1-light chain 3
LDH: lactate dehydrogenase
LTP: long-term potentiation
MA: macroautophagy
MAF: v-maf musculoaponeurotic fibrosarcoma
MAP: microtubule-associated protein
MAP2: microtubule-associated protein 2
MAPK: mitogens-activated protein kinase
MCA: middle cerebral artery
MCAO: middle cerebral artery occlusion
MCP: monocyte chemoattractant protein
mGluRs: metabotropic glutamate receptors
MMPs: matrix metalloproteinases
MPO: myeloperoxidase
MPT: mitochondrial permeability transition
MT: metallothionein
NAD⁺ / NADH: nicotinamide adenine dinucleotide
NaHS: Sodium hydrosulphide
NB: Neurobasal[®] medium
NF- κ B: nuclear factor-kappaB
NK: natural killer
NMDA: N-methyl-D-aspartate
NMDARs: N-methyl-D-aspartate receptors
NO: nitric oxide
NO₂⁻: nitrite
NO₃⁻: nitrate
NOS: nitric oxide synthase
NOXA: phorbol-12-myristate-13-acetate-induced protein 1
Nrf2: nuclear factor, erythroid derived 2, like 2
NTC: no template control
OH \cdot : hydroxyl radical
O₂ \cdot^- : superoxide anion
OMMP: outer mitochondrial membrane permeability

ONOO⁻: peroxynitrite
PCD: programmed cell death
PCR: polymerase chain reaction
PD: Parkinson's disease
PERK: PKR-like ER kinase
PI: propidium iodide
PKC: protein kinase C
PKG: protein kinase G
PLAUR: plasminogen activator urokinase receptor
PLKs: polo-like kinases
pMCAO: permanent middle cerebral artery occlusion
PPI: protein phosphatase 1
PPP: pentose phosphate pathway
PUMA: p53-unregulated modulator of apoptosis
RNS: reactive nitrergic species
ROS: and reactive oxygen species
rt-PA: recombinant tissue plasminogen activator
RT-PCR: Reverse Transcriptional Polymerase Chain Reaction
SIAH1: seven in absentia homolog 1
Smac/DIABLO: second mitochondria-derived activator of caspases/direct inhibitor of apoptosis-binding protein with low pI
SOD: superoxide dismutase
SVZ: subventricular zone
TAE: Tris-acetate-EDTA excitatory post-synaptic potential
TBI: traumatic brain injury
TBS: Tris buffered saline
tBID: truncated BID
TLR: toll-like receptor
tMCAO: transient middle cerebral artery occlusion
TNF- α : tumour necrosis factor-alpha
TNFRs: tumour necrosis factor receptors
TRAIL: TNF-related apoptosis-inducing ligand
Trp53 / p53: transformation-related p53
TTC: 2,3,5-Triphenyl- 2H- tetrazolium chloride
TXNIP: thioredoxin interacting protein
TXNR: thioredoxin reductase
WT: wild-type
UPR: unfolded protein response
UPS: ubiquitin-proteasome system
VEGF: vascular endothelial cell growth factor

Chapter 1:

Introduction

1.1 L-glutamate (Glu): A crucial excitatory neurotransmitter in the mammalian brain

Glu is the major excitatory neurotransmitter in the mammalian central nervous system (CNS). It is involved in the stimulation of specific receptors resulting in regulation of basal excitatory synaptic transmission and numerous forms of synaptic plasticity such as long-term potentiation (LTP) and long-term depression, which are believed to underlie learning and memory. Glutamergic pathways are widespread throughout the brain accounting for synaptic transmission in approximately half of the synapses in the forebrain (McDonald and Johnston, 1990). Upon secretion from the presynaptic membranes, Glu attaches to both ionotropic and metabotropic receptors to mediate fast, slow, and persistent physiological effects on synaptic transmission and integrity. Under physio-pathological settings over-expression or hyper-activation of Glu receptors (GluRs) can result in neuronal injury and a variety of neurologic disorders (e.g. stroke, epilepsy, Alzheimer's disease (AD), amyotrophic lateral sclerosis (ALS)) (Simeone et al., 2004).

1.2 Mechanistic action of Glu via Glu receptors (GluRs)

GluRs are a superfamily of receptors that are activated upon Glu application and divided into two broad categories: ionotropic and metabotropic, with the former comprising N-methyl-D-aspartate (NMDA), alpha-amino-3-hydroxy-5-methyl-4-isoxazolepropionic acid (AMPA) and kainate (KA) subtypes based on their intrinsic ligand-gated ion channel activity that allows passage of Na^+ and Ca^{2+} ions through a pore, and the latter being G-protein coupled receptors and are further subdivided. The former are so named upon their high affinity to the respective synthetic agonists that specifically activate each subtype.

Metabotropic GluRs (mGluRs), on the other hand, are themselves not ionophores but are G protein-coupled receptors that trans-activate secondary messenger enzymes, conveying signals that can regulate a variety of cellular activities, including phosphorylation of voltage-gated and ligand-gated ion channels and gene transcription. Activities of these receptors are predominantly linked to CNS and each serves a distinct function.

1.2.1 Ionotropic GluRs (iGluRs)

1.2.1.1 N-methyl-D-aspartate receptors (NMDARs)

1.2.1.1.1 Structure and distribution of NMDARs

Functional NMDARs require the typical hetero-tetrameric assembly of both NR1, and NR2 subunits (occasionally NR3A-B subunits), which comprise any one of the four separate gene products (NR2A-D). The essentiality for the expression of both subunits arises from the formation of the Glu-binding domain at the junction of NR1 and NR2 subunits. Full activation of the NMDARs is achieved by the binding of Glu and glycine, a co-agonist binding on a site on the NR1 subunit. The glycine usually potentiates the Glu response by lowering the magnitude of desensitization of NMDARs (Aoshima et al., 1992; Chen et al., 1997; Mayer et al., 1989). In addition, the receptor complex also possesses binding sites for a variety of endogenous modulators, such as polyamines, zinc, and protons. The binding site for polyamines on the NR2 subunit is responsible for the regulation of the activity of NMDARs. NMDARs are permeable to influx of Na^+ and Ca^{2+} and efflux of K^+ ions (Simeone et al., 2004). NMDARs are intrinsically inhibited by Mg^{2+} binding-induced voltage-dependent block within the channel pore which can be alleviated by depolarization (MacDermott et al., 1986).

Chapter 1: Introduction

Each subunit comprises of a large extracellular NH₂-terminal; four transmembrane domains (M1-M4), of which the M2 segment forms a reentrant loop surrounding the pore; and an intracellular C-terminal (Kutsuwada et al., 1992). Although NR1 and NR2 share similar basic structure, they showed only ~ 20% homology to each other. A major distinguishing component of subunit identity is based on the observation that the NR2 subunits possess large intracellular C-terminal domains with various regions of conserved sequences. However as abovementioned, the four NR2 isoforms share considerable homology. NR2A, NR2B, and NR2C are 55% to 70% homologous (Monyer et al., 1992). Similarly, the NR3A and NR3B subunits shared ~ 50% sequence homology but have only ~27% and ~20% identity respectively with other NMDARs subunits (Chatterton et al., 2002; Ciabarra et al., 1995; Nishi et al., 2001; Sucher et al., 1995). The molecular biology of the NR1 subunit is significantly more complicated than that of the NR2 subunit. There are eight different NR1 subunit isoforms coming from the alternative splicing of three different exons: exon 5 in the N-terminus and the adjacent exons 21 and 22 in the C-terminus (Durand et al., 1993; Hollmann et al., 1993; Sugihara et al., 1992).

With the possible heteromeric combinations of NMDARs, it would not be difficult to deduce that the functional and pharmacological properties of NMDARs are governed by the NR1 and NR2 splice variants (Feldmeyer and Cull-Candy, 1996; Momiyama et al., 1996; Rumbaugh et al., 2000; Stern et al., 1992; Vicini et al., 1998), which determine Glu and glycine affinities (Buller and Monaghan, 1997; Ishii et al., 1993; Kutsuwada et al., 1992; Matsui et al., 1995; Woodward et al., 1995a; Woodward et al., 1995b) and NMDARs sensitivity for exogenous inhibitory compounds (Donevan and McCabe, 2000;

White et al., 2000; Williams, 1993). This in turn provides variation of age-dependent and regionally specific differences in NMDARs function and pharmacology.

NR1 subunit is expressed throughout all regions of the CNS (Danysz and Parsons, 1998). Accordingly, NR2A subunit is also ubiquitously distributed, with the highest expression level in the hippocampus, cerebral cortex, and cerebellar granule cells. NR2B subunit, on the other hand, is expressed selectively in the forebrain (cerebral cortex, hippocampus, thalamus, septum, caudate-putamen, and olfactory bulb) while the expression of the NR2C subunit is limited to cerebellar granule cells, with weak expression in the olfactory bulb and thalamus, and NR2D subunit is weakly expressed in the hippocampus, thalamus, brain stem, and olfactory bulb (Akazawa et al., 1994; Ishii et al., 1993; Kutsuwada et al., 1992; Meguro et al., 1992; Monyer et al., 1994; Moriyoshi et al., 1991; Watanabe et al., 1992; Watanabe et al., 1993a; Watanabe et al., 1993b; Watanabe et al., 1994a; Watanabe et al., 1994b). Last of all, NR3A subunit is highly localized in the brain stem, hypothalamus, thalamus, CA1, and amygdala (Ciabarra and Sevarino, 1997) whereas the NR3B subunit exists predominantly in motoneurons (Chatterton et al., 2002; Nishi et al., 2001).

Most NMDARs subtypes are distributed at glutaminergic synapses and concentrated at the center (Somogyi et al., 1998) or evenly distributed within the synaptic specialization (Clarke and Bolam, 1998). NMDA subtype of iGluRs is the principal mediator of Glu trophic activity (Balazs et al., 1988). NMDARs are permanently anchored on the plasma membrane. Activation of NMDARs has been demonstrated to exert survival-death

continuum effect with increasing concentrations of Glu (Cheung et al., 1998). It is suggested that this is a consequence of differential recruitment of diverse NMDARs subtypes stimulated by moderate and high doses of Glu respectively (Hardingham and Bading, 2002). This is observed in cortical neurons where NMDARs that contained the NR2A suppressed staurosporine-induced apoptosis, whereas those that comprised of the NR2B subunit led to excitotoxic cell death (Hardingham and Bading, 2002). However, a recent study by (Habas et al., 2006) demonstrated neuroprotection offered by NR2B against phosphatidylinositol-3 kinase (PI3K) inhibitor LY294002. As such, the significance of the relative ratio of NR2A to NR2B and their individual functions remain yet to be elucidated and may prove to be vital to the cell fate at any one time.

1.2.1.1.2 Physiological roles of NMDARs

In the past, it was perceived that NMDARs contributed less to basal synaptic transmission than AMPARs due to its voltage-dependent block by Mg^{2+} even though the NMDARs have an affinity for Glu that is - 500 times higher than that of AMPARs (Deisz et al., 1991; Patneau and Mayer, 1990). However, upon sufficient stimuli (e.g. intense activation of AMPARs and KARs) causing membrane depolarization, NMDARs can contribute significantly to synaptic transmission (Mayer and Westbrook, 1984; Mayer et al., 1984; Nowak et al., 1984). As such, NMDARs slower gating kinetics relative to AMPARs and KARs hold them accountable for the slow component of excitatory post-synaptic potentials (Lester et al., 1990).

NMDARs act as “plasticity gates” by enabling cells to possess an enhanced ability to

Chapter 1: Introduction

undergo plastic changes due to prolonged currents as a result of higher Ca^{2+} influx (Fox et al., 1999). The induction of LTP results in a delayed and transient increase in NR1 and NR2B subunit expression (Thomas et al., 1996; Thomas et al., 1994). Functional importance of NMDARs is highlighted by its involvement in cell migration, neuritic outgrowth, and neuronal survival [for a review, see (McDonald et al., 1990) and (Vallano, 1998)]. This is underscored by transgenic knockout and mutated mice studies where NR1^{-/-} mice completely devoid of functional NMDARs or carrying a single-point mutation at Asparagine 598 in the M2 segment of the NR1 subunit (an amino acid as a critical determinant of the ion selectivity of the channel) have reduced NMDARs-mediated Ca^{2+} permeability and Mg^{2+} block and showed embryonic lethality (Forrest et al., 1994; Single et al., 2000). Death of these transgenic mice at P0 emphasizes the criticality of Ca^{2+} permeability of NMDARs in mammalian development [for further review, see (Sprengel and Single, 1999)]. However, upon ectopic expression of a transgene encoding a NR1 splice variant, NR1^{-/-} mice survival is restored (Iwasato et al., 1997).

Initial reports demonstrated that basal or moderate activation of NMDARs offers neuroprotection in cultured cerebellar granule neurons (CGN). Exogenously administered NMDA inhibits death of CGN upon exposure to suboptimal KCl concentration media (Balazs et al., 1988), and pretreatment with NMDA further enhance protection against Glu-mediated excitotoxic neuronal death (Marini et al., 1998).

Modest NMDARs activation also promotes neuronal survival in the forebrain neurons. Application of exogenous NMDA attenuates neuronal death induced by staurosporine (Hardingham and Bading, 2002) or ethanol (Takadera and Ohyashiki, 2004) in cortical neurons. On the other hand, addition of antagonists of NMDARs trigger apoptosis in cultured rat primary cortical neurons (Takadera et al., 1999) and aggravates death induced by serum withdrawal (Hetman et al., 2000) or by a DNA-damaging agent, cisplatin (Gozdz et al., 2003). Induction of apoptosis in hippocampal, thalamic and cortical neurons *in vivo* is also seen in rats of post-natal day 7 and 8 upon blockade of NMDARs (Ikonomidou et al., 1999). These suggest that homeostatic activation of NMDARs is vital for neuronal survival and proliferation.

1.2.1.1.3 NMDARs association with CNS diseases

NMDARs playing a major role in the mediation of massive Ca^{2+} influx upon GluRs over-stimulation since it displays the highest Ca^{2+} permeability (Hara and Snyder, 2007). Excessive NMDARs activation induces Ca^{2+} influx and Ca^{2+} release from intracellular stores resulting in the activation of cytoplasmic proteases such as Ca^{2+} -dependent cysteine proteases [calpains; (Simpkins et al., 2003)] which hydrolyze cytoskeletal and other cellular proteins [e.g. alpha-fodrin; (Posner et al., 1995; Siman et al., 1989)]. NMDARs activation can also result in the destabilization of lysosomes and release of lysosomal proteases [cathepsins; (Graber et al., 2004; Tenneti et al., 1998)] resulting in cell death. Similarly, NMDARs activation also induces caspase-3 activation and apoptosis (Graber et al., 2004; Tenneti et al., 1998). Not surprisingly, over-stimulation of the NMDARs by Glu is implicated in neurodegenerative disorders including AD

(Doraiswamy, 2003a; Doraiswamy, 2003b; Hynd et al., 2004a; Hynd et al., 2004b), dementia associated with Down syndrome (Scheuer et al., 1996) and ischemic and traumatic brain injury (Arundine and Tymianski, 2004). Similarly, calpain activation (reviewed in (Carragher, 2006; Zatz and Starling, 2005)) and lysosomal dysfunction (Bahr and Bendiske, 2002; Nixon et al., 2000) are consistently observed in neurodegenerative diseases.

1.2.1.2 Alpha-amino-3-hydroxy-5-methyl-4-isoxazolepropionic acid receptors (AMPArs)

1.2.1.2.1 Structure and distribution of AMPARs

The AMPARs subfamily consists of four members: GluRs1-4 (Hollmann and Heinemann, 1994). These subunits demonstrated ~70% structural homology. AMPARs have a 5 to 10 -fold decreased elementary conductance (< 10 picoSiemen) relative to NMDARs and desensitize rapidly on application of Glu and AMPA but not to KA (Doble, 1999). Various homo- or hetero-tetrameric assemblies derived from these four different subunits give rise to functional AMPARs (Rosenmund et al., 1998). AMPARs travel in and out of the post-synaptic membrane, thus allowing regulation of synaptic strength through dynamic changes in synaptic AMPARs count (Malinow and Malenka, 2002). AMPARs are involved in the generation of fast excitatory post-synaptic potentials (EPSP) in the CNS of vertebrates. Homomeric and heteromeric AMPARs deprived of the GluRs2 subunit are porous to Ca^{2+} and zinc and exhibit voltage-dependent block by intracellular polyamines (Burnashev et al., 1992; Donevan and Rogawski, 1995; Hollmann et al., 1991; Verdoorn et al., 1991). In contrast, heteromeric receptors

harbouring both GluR2 and other AMPARs subunits are relatively impermeable to Ca^{2+} and are less responsive to voltage-dependent polyamine block (Bowie and Mayer, 1995; Geiger et al., 1995; Hollmann et al., 1991).

AMPARs subunits have extensive expression profiles scattered across brain regions and are mainly localized in principal neurons, interneurons, oligodendrocytes, and astrocytes (Bahr et al., 1996; Martin et al., 1993; Petralia and Wenthold, 1992). A prevalence of heteromeric AMPARs composed of GluR1 and GluR2, or GluR2 and GluR3 subunits, with a small population of homomeric GluR1 present in hippocampal CA1 and 2 neurons (Wenthold et al., 1996), whereas in CA3 principal neurons, AMPARs are mainly made up of GluR1 and GluR2 subunits (Geiger et al., 1995). Co-expression of the GluR1 and GluR2 or GluR3 subunits is observed in the dendritic spines of cultured hippocampal neurons (Craig et al., 1993) and the physio-functional properties of dendritic Glu receptors of CA1 and CA3 pyramidal neurons are comparable (Spruston et al., 1995). AMPARs subunit assembly in glia is distinct from that of neurons. The brain oligodendrocytes express GluR2, GluR3, and GluR4 subunits (Craig et al., 1993) while the hippocampal astrocytes express GluR1, GluR2, and GluR4 (Seifert et al., 1997; Seifert et al., 2003).

1.2.1.2.2 Physiological roles of AMPARs

AMPARs play a crucial role in maintenance of developmental and mature CNS plasticity. Ca^{2+} -permeable AMPARs are important in early development and especially critical to processes such as synaptogenesis (Durand and Zukin, 1993). Explicitly,

AMPA receptors (AMPAARs) are important in LTP (Bliss and Collingridge, 1993; Lledo et al., 1998; Madison and Schuman, 1991; Song and Huganir, 2002). Though exhibiting normal development, life expectancy, and neuronal cytoarchitecture, mice lacking the GluR1 subunit demonstrated an altered GluR2 immunoreactivity in the somata of hippocampal CA1 pyramidal cells with greatly reduced somatic AMPA currents. However, these mice continue to maintain normal miniature excitatory post-synaptic currents and fast excitatory post-synaptic potentials (Zamanillo et al., 1999). This indicates that GluR1 subunit might contribute to a large population of extrasynaptic AMPARs that could be delivered and inserted to specific synapses under certain conditions, thus increasing the potential of these synapses (Zamanillo et al., 1999).

1.2.1.2.3 AMPARs association with CNS diseases

AMPA receptors are involved not only in neuronal plasticity but also in excitotoxicity, mediated largely by the influx of Ca^{2+} (Choi et al., 1988). Their implication has been highlighted in animal models of ischemia and epilepsy. Studies of ischemic rodent models featured that prior to cell death, hippocampal CA1 pyramidal cells exhibit an increased AMPAR-mediated Ca^{2+} influx and decreased GluR2 and GluR3 mRNA and protein levels (Gorter et al., 1997; Heurteaux et al., 1995; Pellegrini-Giampietro et al., 1994; Pellegrini-Giampietro et al., 1992; Pollard et al., 1993; Tsubokawa et al., 1994). Interestingly, pharmacological prevention of GluR2 subunit down-regulation in the CA1 region offered neuroprotection (Heurteaux et al., 1995). Correspondingly in KA model of epileptogenesis, during the cellular injury prior to significant cell loss, lower GluR2 and GluR3 mRNA and protein expressions were detected in hippocampal CA1 and CA3

pyramidal neurons (Friedman et al., 1994; Friedman et al., 1997; Grooms et al., 2000; Pollard et al., 1993). GluR2 subunit level was also decreased in the hippocampal pyramidal cells of hypoxia-induced seizure rodent model (Sanchez et al., 2001) and in the piriform cortex and limbic forebrain of amygdala-kindled rats (Prince et al., 2000).

On the other hand, in a mouse model of fragile X syndrome (a hereditary form of mental retardation associated with hyperactivity, anxiety, seizures, and mild autism), decreased GluRs1 immunoreactivity with correlating reduced LTP occurred in cortical synapses but not in the hippocampus or cerebellum (Li et al., 2002). As such, it is hypothesized that the repression of cortical GluRs1 subunit level and LTP may have a patho-physiological association with fragile X mental retardation protein deficiency resulting in the cognitive and behavioral impairments observed in this syndrome (Li et al., 2002).

1.2.1.3 Kainate receptors (KARs)

1.2.1.3.1 Structure and distribution of KARs

KARs are tetrameric assemblies of GluRs5-7 and KA1-2 subunits. GluRs5-7 subunits have an approximately 10-fold lower affinity for KA than KA1-2 subunits. Each subunit contains four membrane segments (M1-M4), three of them transmembrane (M1, M3 and M4), and the remaining M2 segment comprising hydrophobic residues, which form a unique hairpin-like structure in the membrane. The M2 segment assists in the formation of pore of the receptor channel. Each monomer is approximately 900 amino acids long (MW = ~100 kDa) with the amino-terminal domain orientating towards the extracellular, and the carboxy-terminal end facing the intracellular side. Splice variants account for

GluR5 and GluR7 subunit formation, while post-transcriptional editing is present in GluR5 and GluR6 subunits. Physiological role in KARs in the CNS is still understated, but they are classically implicated in epileptogenesis where intraperitoneal injection of KA has long been used as a model for temporal lobe seizures. KARs activation, as opposed to that of AMPARs, results in inhibition of EPSP or the excitatory post synaptic current in the hippocampus (Vignes et al., 1998) via inhibitory post-synaptic current which can be abolished upon application of KARs antagonist (Clarke et al., 1997).

GluR5 mRNA expression is predominantly present in the subiculum, septal nuclei, piriform, and cingulate cortice and in cerebellar Purkinje cells while GluRs subunit is abundant in cerebellar granule cells and in the dentate gyrus and CA3 subfield of the hippocampus. On the contrary, GluR7 mRNA is generally expressed at low levels throughout the brain. KA1 is distinctively localized to the CA3 region of the hippocampus, whereas KA2 is distributed throughout the nervous system (Simeone et al., 2004).

1.2.1.3.2 Physiological roles of KARs

KARs activation triggers a fast-onset, rapidly desensitizing response. As rapid desensitization is one of the most notable attributes of non-NMDARs, it is of critical physiological regulation to ensure these receptors remain in inactive states. Relative to AMPA-evoked responses, KA-activated currents have slower onset and decay kinetics, as well as diminished peak amplitude (Simeone et al., 2004).

Post-synaptic KARs are responsible for the excitatory post-synaptic current in response to Glu release (Castillo et al., 1997; Vignes and Collingridge, 1997). This establishes an important role for KARs in activity-dependent synaptic plasticity (Lerma, 2003). KARs are evidently involved in frequency-dependent synaptic facilitation (a type of short-term plasticity in which the strength or integrity of synaptic transmission increases with repetitive stimulation) and LTP (Contractor et al., 2001; Schmidt and Hollmann, 2008). Apart from its actions on post-synaptic receptors, KA has long been postulated to modulate neurotransmitter release by a presynaptic mechanism (Represa et al., 1987). As such, KARs reside in a subset of both inhibitory and excitatory terminals.

1.2.1.3.3 KARs association with CNS diseases

It has long been established that in neurological disease models, KA is a potent excitotoxin, mediating acute limbic seizures and long-term morphologic changes in the hippocampus, which are hallmark characteristics seen in temporal lobe epilepsy (i.e. mossy-fiber sprouting, neuronal loss, and reactive gliosis) (Ben-Ari and Cossart, 2000). Persuasive clinical evidence employing KARs agonists further substantiate the detrimental effects of KA. For instance, domoic acid (a structural analogue of KA) has been found to inflict detrimental damage to the hippocampus through a real-life outbreak incident of toxic encephalopathy caused by ingestion of mussels contaminated with domoic acid (Perl et al., 1990). Common symptoms among those affected consisted of vomiting, cramps, diarrhea, and short-term memory loss; however, one-fifth of the patients developed intractable seizures or lapsed into coma, and 3% died.

1.2.2 Metabotropic GluRs (mGluRs)

1.2.2.1 Structure and distribution of mGluRs

mGluRs, unlike iGluRs, are G-protein-coupled receptors. They are subdivided into three categories which are further differentiated into 8 subtypes: Group I – mGluRs1 and 5, group II – mGluRs2 and 3, group III – mGluRs4, 6, 7, 8 (Simeone et al., 2004). Functional diversity is generated via the heterogeneity of the eight molecular mGluRs subtypes. They are made up of a heterogeneous family of receptors that are linked to numerous signal transduction pathways via guanine nucleotide or guanosine triphosphate-binding proteins (i.e. G-proteins). Unlike the molecular intrinsic function of iGluRs, Glu binding to mGluRs do not activate their intrinsic ionic channel, but rather indirectly modulates synaptic transmission and neuronal excitability through the activation or suppression of various G-protein-coupled effector systems (Conn and Pin, 1997). In the light of this signaling mechanism, mGluRs-mediated cellular outcomes are considerably slower in onset and longer lasting relative to that of the iGluRs activation (Simeone et al., 2004). Thus, mGluRs provide an alternative regulatory option for Glu to modulate neuronal activity over a longer time course in addition to its role as a fast-signaling neurotransmitter. They are involved in the regulation of neuronal excitation and synaptic transmission (Ossowska et al., 2007). Furthermore, the presence of mGluRs in the basal ganglia indicates their involvement in the nigrostriatal dopamine system (Feeley Kearney and Albin, 2003).

mGluRs are divided into group I, II and III based on the activation by their respective agonists. Group I mGluRs (mGluRs1/5) are selectively activated by 3,5-

dihydroxyphenylglycine (DHPG) (Schoepp et al., 1994); Group II mGluRs (mGluRs2/3) by (+)-1S,2S,5R,6S-2-aminobicyclo[3.1.0]hexane-2,6-dicarboxylic acid (LY354740) (Monn et al., 1997) and (2S,1 R,2 R,3 R)-2-(2,3-dicarboxycyclopropyl) glycine (DCG-IV) (Hayashi et al., 1993). The remaining mGluRs (mGluRs4/6/7/8) belongs to group III and are selectively activated by L-2-amino-4-phosphonobutyrate(L-AP4) (Conn and Pin, 1997).

Group I mGluRs are located primarily in somatodendritic domains. Group III mGluRs are predominantly localized in axon terminal domains, with group II mGluRs being found in both somatodendritic and axon terminal domains (Shigemoto and Mizuno, 2000). Prominently, among those mGluRs located presynaptically, group III mGluRs (except for mGluRs6) are found at axon terminal domains only in the presynaptic active zone, whereas group II mGluRs are found at extrasynaptic sites (Shigemoto et al., 1997; Wada et al., 1998).

1.2.2.2 Physiological roles of mGluRs

Group I mGluRs activation stimulates phosphoinositide hydrolysis via phospholipase C, which, in turn, leads to Ca^{2+} release from intracellular stores (Abe et al., 1992; Masu et al., 1991). On the contrary, activation of group II and group III mGluRs inhibits adenylate cyclase-mediated cyclic adenosine monophosphate production (cAMP) (Duvoisin et al., 1995; Nakajima et al., 1993; Okamoto et al., 1994; Saugstad et al., 1994; Tanabe et al., 1992; Tanabe et al., 1993). The downstream consequences of native mGluRs activation are dependent on the brain region and the specific cells studied. As a

general rule of thumb, group I mGluRs seem to be primarily involved in the increase of neuronal excitability through the inhibition of various voltage-gated and Ca^{2+} -activated K^+ channels. It is observed that in hippocampal pyramidal neurons, group I mGluRs activation decreases the resting leak K^+ conductance (Guerineau et al., 1994) and impedes Ca^{2+} -dependent after-hyperpolarization (Charpak et al., 1990; Desai and Conn, 1991) and a gradually inactivating voltage-dependent K^+ current (Luthi et al., 1996), all of which contribute to increased neuronal excitability. On the other hand, mGluRs negatively coupled to adenylate cyclase activity typically inhibit synaptic transmission by preventing neurotransmitter release at presynaptic terminals through indirect modulation of voltage-gated Ca^{2+} channels (Takahashi et al., 1996).

As group III mGluRs are typically located in the presynaptic active zone, they can serve as autoreceptors that specifically react to synaptic Glu release, whereas group II mGluRs at the extrasynaptic sites could counteract excessive Glu accumulation or spillover and play a more homeostatic protective role against excitotoxicity (Simeone et al., 2004). Presynaptic mGluRs not only modulate synaptic release of Glu but also can regulate that of GABA and decrease synaptic inhibition (Gereau and Conn, 1995; Hayashi et al., 1993; Salt and Eaton, 1995; Salt et al., 1996).

1.2.2.3 mGluRs association with CNS diseases

The ontogeny of mGluRs and their role in brain development are less well studied as compared to the iGluRs. Nevertheless, expression and function of mGluRs are crucial in developmental stages of the mammalian nervous system, with promotion of neuronal

Chapter 1: Introduction

excitability predominating in early life (Simeone et al., 2004). mGluRs have been involved in the pathogenesis of neurological and psychiatric disorders such as AD, Parkinson's disease (PD), anxiety, depression, and schizophrenia.

Group II mGluRs have recently been implicated in the pathogenesis of AD by inducing the synaptic activation of alpha-, beta- and gamma-secretases which are known to generate a family of released peptides, including Abeta40 ($A\beta_{40}$) and Abeta42 ($A\beta_{42}$) and stimulating the release of $A\beta_{42}$ from isolated intact nerve terminals (Kim et al., 2010). Post-synaptic group I mGluRs, on the other hand, induced a rapid accumulation of amyloid precursor protein C-terminal fragments in the synaptoneuroosomes, a family of membrane-bound intermediates generated from amyloid precursor protein metabolized by alpha- and beta-secretases (Kim et al., 2010).

Group I mGluRs have also been implicated in the pathogenesis of Huntington's disease (HD) through their interactions with the Huntingtin protein resulting in alteration of the mGluRs-mediated signaling pathways (Ribeiro et al., 2010). Dysfunctional glutaminergic signaling cascades have also been observed in the pathogenesis of L-DOPA-induced dyskinesia, a long-term motor complication of dopamine replacement in the treatment of PD. Selective mGlu5 inhibitors have been demonstrated to be successful in the amelioration of dyskinesia (Johnston et al., 2010).

1.3 Excitotoxicity in CNS due to GluRs over-stimulation

Induction of massive release of Glu from injured neurons is frequently observed during ischemic insults such as cardiac arrest, stroke, and head and spinal cord injury. Glutamnergic neurotransmission requires intricate regulatory management as otherwise improperly modulated will not only impair its physiological signaling properties, but also result in cell death via excitotoxicity. Excitotoxic death occurs as a result of excessive release of Glu from damaged neurons into the extracellular space, resulting in the over-stimulation of GluRs on the neighbouring cell surfaces and subsequently neuronal death. Over-stimulation of iGluRs triggers massive influx of extracellular Ca^{2+} , which together with release of Ca^{2+} intracellular stores from ruptured organelles e.g. lysosomes, into the cytosol results in activation of Ca^{2+} -dependent proteases calpains and protein phosphatase, calcineurin.

Excitotoxicity is one of the major mechanisms of cell death in numerous CNS diseases including stroke, brain trauma, epilepsy and chronic neurodegenerative disorders (Wang and Qin, 2010). The –excitotoxicity” theory was first formulated in 1969 by Dr Olney as an undesirable cytotoxic side-effect of excessive or prolonged activation of receptors by excitatory amino acids (EAAs) (Olney, 1969). Much research efforts have been attributed to the mechanistic elucidation of excitotoxicity with current understanding summarized as follow: iGluRs over-stimulation triggers multiple adverse effects comprising impaired intracellular calcium ion homeostasis, organellar dysfunctions, elevated nitric oxide (NO) and reactive oxygen species (ROS) production, unregulated persistent activation of proteases and kinases, and transcriptional activation of pro-death transcription factors and

Chapter 1: Introduction

immediate early genes (Wang and Qin, 2010). It has been demonstrated that in the event of excitotoxic neuronal death, all three subtypes of iGluRs (NMDARs, AMPARs and KARs) are actively involved, with the NMDARs playing a major role due to its abundant expression and highest Ca^{2+} permeability (Hara and Snyder, 2007).

Upon excess Glu application in experimental models, heterogeneity of neurodegenerative signaling cascades is observed. In neuronal cultures, an apoptotic-autophagic-necrotic continuum cell death is induced depending on the severity of NMDA insult (Berman and Murray, 1997). *In vivo*, cell death morphology is determined by GluRs subunit composition in neurons (Lev et al., 1995). This heterogenous population of cell death is evident in whole animal models of stroke (Panikashvili et al., 2005; Uberti et al., 2004) and traumatic brain injury (Panikashvili et al., 2005). At one extreme end of the spectrum, neurons display unregulated necrotic morphology upon intense glutaminergic insult (Berman and Murray, 1997). The mechanisms underlying neuronal necrosis are similar to those governing other cell types and include loss of cellular homeostasis with acute mitochondrial dysfunction leading to massive energy failure. Milder glutaminergic insults, however, have been shown to cause cell death ascribed to mechanistically regulated cell death pathways. These cell death pathways work coherently in excitotoxic neurodegeneration and include an array of molecular players such as cysteine proteases, mitochondrial endonucleases, poly(ADP-ribose) polymerase 1 (PARP-1) and glyceraldehyde 3-phosphate dehydrogenase (GAPDH; (Wang and Qin, 2010).

1.3.1 Calcium ion homeostasis

Ca^{2+} influx was demonstrated to be an early event essential for trigger of Glu excitotoxicity (Choi, 1985). It was shown that in Ca^{2+} -rich extracellular solution, Glu excitotoxicity in neuronal cultures was potentiated whereas a Ca^{2+} -free extracellular solution attenuated neurodegeneration. Further studies verified that the induction of Ca^{2+} influx by NMDARs, but not the Ca^{2+} load, was important in the GluRs-mediated neurodegenerative process (Choi, 1987; Tymianski et al., 1993), and that lower Ca^{2+} influxes via NMDARs evoked higher lethality as compared to higher Ca^{2+} influxes via other Ca^{2+} -permeable channels (Sattler et al., 1998). Majority of elevated cytosolic Ca^{2+} is sequestered into mitochondria, which can lead to mitochondrial toxicity resulting in metabolic acidosis and free radical generation (Thayer and Wang, 1995; Wang and Thayer, 1996).

1.3.2 Nitric oxide (NO) generation

Early study by Dawson et al. (1991) demonstrated the abrogation of Glu-induced neurodegeneration *in vitro* upon application of NO synthase (NOS) inhibitors, suggesting a prominent role of NO in Glu-induced excitotoxicity. NO once generated, can react with the heme group of guanylate cyclase (GC), triggering a conformational change in GC and the catalysis of guanosine-5'-triphosphate (GTP) to cyclic guanosine 3',5'-monophosphate [cGMP; (Ignarro, 1991)] and protein phosphorylation. GC activation is believed to be the main nitrenergic signal transduction pathway. cGMP acts as a second messenger that activates protein kinase G (PKG) 1 and 2, with the former involved in intracellular Ca^{2+} control and the latter regulating anionic influx e.g. Cl^- ion (French et al.,

1995; Lau et al., 2003). This transduction pathway can affect a broad range of proteins directly, e.g. phosphodiesterases of cyclic nucleotides and indirectly, e.g. protein kinase A, thus increasing the level of cAMP with activation of proteins involved in the cAMP downstream pathway (Ono and Trautwein, 1991; Whalin et al., 1991).

Furthermore, NO is also capable of affecting other cellular signaling pathways independent of GC activation. As NO is thermodynamically unstable, it is able to undergo various chemical reactions with gaseous molecules, anions and reactive oxygen species (ROS) to form nitrites, nitrates and peroxynitrites (ONOO⁻). NO reacts quickly with the superoxide anion (O₂^{•-}) to form ONOO⁻ to avoid its elimination by the antioxidant systems. ONOO⁻ has an action radius of 100µm and even shorter half-life of 1-2s, tending to generate multiple toxic products in its degradation (Beckman et al., 1990; Whiteman et al., 2002). During the process of these chemical reactions, intermediate-products such as ROS and other free radicals are produced. These nitregic intermediate- and end-products can induce modifications of cellular molecules (lipids, proteins and DNA) through oxidation (Poon et al., 2004), nitration (Souza et al., 1999) or nitrosylation (Stamler et al., 1997). For proteins, these modifications have special importance as they can modify protein conformation and affect their physiological functions. NO-mediated nitrosylation can alter the normal activity of a wide array of proteins by inducing conformational changes, which can hinder protein phosphorylation leading to a loss of function and/or gain-of-function, or affect signal transduction pathways of the growth factors (Amici et al., 2003; Cassina et al., 2000; Jonnala and Buccafusco, 2001; Newman et al., 2002). NO itself can also induce reversible inhibition of cytochrome c oxidase, thus

resulting in decreasing oxygen consumption and impeding energetic metabolism. Interestingly, NO also promote mitochondrial synthesis via enhancing the transcriptional activity of peroxisome proliferator-activated receptor gamma (PPAR γ) coactivator-1 (Nisoli et al., 2003; Scarpulla, 2002).

Recently, a novel cell death pathway implicating GAPDH and seven in absentia homolog 1 (SIAH1) has been linked to NO (Hara et al., 2005). GAPDH is an omnipresent housekeeping enzyme that, under physiological conditions, participates in glycolysis. However, with increasing intracellular levels, NO can nitrosylate GAPDH allowing it to bind SIAH1, an ubiquitin ligase. The newly formed duo can then translocate to the nucleus by virtue of the SIAH1 nuclear translocation domain and enhances p300/CBP-associated acetylation of nuclear proteins (Sen et al., 2008). The downstream activation of nuclear proteins including p53 causes pyknotic nuclei and morphological features suggestive of apoptosis.

1.3.3 Free radical generation

Free radical formation has been observed in CGN (Lafon-Cazal et al., 1993) and cortical cultures (Dugan et al., 1995; Reynolds and Hastings, 1995) upon excitotoxic stimulus. Pharmacological application of various antioxidant compounds including nitrone-based scavengers, free radical spin traps and 21-aminosteroids/lazaroids and/or over-expression of anti-oxidative enzyme overexpressing SOD showed successful attenuation of Glu and ischemia-induced neurotoxicity (Gonzalez-Zulueta et al., 1998). It is believed that rise in intracellular Ca²⁺ via Ca²⁺ influx is responsible for the trigger of free radical production

(Dykens, 1994) particularly by mitochondria. Mitochondria exposed to escalating Ca^{2+} and Na^+ concentrations activate a feed-forward system enhancing free radical production, which can be abolished by removal of extracellular Ca^{2+} but not NOS antagonists (Dugan et al., 1995). Similar dependence on NMDARs-mediated Ca^{2+} entry was substantiated by findings from Reynolds and Hastings (Reynolds and Hastings, 1995). In summary, it can be deduced that free radical generation in mitochondria is a secondary event to Ca^{2+} influx via NMDARs. Subsequently, these free radicals, particularly $\text{O}_2^{\bullet-}$, can interact with other radicals e.g. NO to form powerful oxidants (Huie and Padmaja, 1993).

1.3.4 Caspase activation

Caspases, a family of well-studied cysteine proteases notable for their role in classical apoptosis, was first demonstrated to be implicated in persistent excitotoxic injury in cerebrocortical (Tenneti et al., 1998) and cerebellar cultures (Du et al., 1997). Pre-treatment with caspase inhibitors showed neuroprotective efficacy in NMDA-mediated neurodegeneration. However, Ca^{2+} influx and mitochondrial dysfunction were not inhibited, indicating caspase activation occurs downstream of these events. Other than promoting cleavage of cytosolic proteins, nuclear caspase activation facilitates ICAD (a protein inhibiting the activity of caspase-3-activated DNase) truncation, resulting in DNA fragmentation and cell death (Enari et al., 1998).

1.3.5 Calpains involvement

Escalating intracellular Ca^{2+} level activates Ca^{2+} -dependent cytoplasmic proteases namely calpains. Proteolytic activation of one calpain isoform, μ -calpain, is necessary for the

cleavage and release of apoptosis-inducing factor (AIF) from mitochondria (Polster et al., 2005). Calpain/AIF pathway importance in excitotoxicity is further underscored by neuronal culture studies subjected to oxygen–glucose deprivation showing that calpain suppression attenuated AIF translocation and subsequent neuronal death (Cao et al., 2007). Mitochondrial AIF re-localization to the nucleus causes chromatin condensation, DNA fragmentation and cell death (Susin et al., 1999). An alternative route to excitotoxicity is via activation of PARP-1, a nuclear DNA repair enzyme, which incidentally also triggers the release of AIF and which involvement is highlighted by cortical cultures derived from PARP-1 knockout mice exhibiting reduced AIF translocation and neurodegeneration after NMDA treatment (Yu et al., 2002).

1.3.6 Organellar destabilization

1.3.6.1 Mitochondrial dysfunction

The mitochondrial network plays a vital role in the supply of cellular energy currency in the form of adenosine triphosphate (ATP) to ensure the proper functioning of a variety of metabolic processes within a cell. Simpler molecules resulting from the cellular cyclic processing of macromolecular nutrients transfer electrons to carrier proteins such as nicotinamide and flavin adenine dinucleotides (NAD^+ and FAD^+) producing NADH and FADH_2 , which transfer the electrons to the electron transport chain (ETC) localized at the inner mitochondrial membrane (Saraste, 1999). Due to the constitutive cyclic fluctuation of the redox status between ETC enzymatic protein complexes with consequent high consumption of cellular oxygen in the oxidative phosphorylation process, mitochondria are assumed to be the main cellular producers of ROS (Orrenius et al., 2007). Escaping

electrons from the ETC can potentially reduce oxygen to form the highly reactive $O_2^{\bullet-}$, which can undergo further Fenton reaction to generate hydroxyl radical (OH^{\bullet}) and hydrogen peroxide (H_2O_2) which similarly can cause detrimental cellular damages (Boveris et al., 1972).

As a result of this pivotal physiological function of mitochondria, which if not properly managed can have adverse effects on cell survival, mitochondrial functionality has been proposed to be a crucial regulator and indicator of cellular homeostasis. Indeed, decline in mitochondrial functionality has been closely linked to increasing age of mammals. This age-correlated respiratory chain deficiency is especially prevalent in only a subset of mammalian tissues, such as heart, skeletal muscle, colonic crypts and neurons (Dufour et al., 2008). A recent study by Dufour et al., 2008 demonstrated that the co-existence of functional respiratory chain-deprived and normal neurons accelerated the neurodegenerative process of the adjacent normal cells through a trans-neuronal signaling mechanism.

1.3.6.2 Lysosomal rupture

Calpain activation has been reported to associate with lysosomal rupture leading to the death of post-ischemic CA1 neurons (Yamashima et al., 2003). A “calpain-cathepsin hypothesis” was formulated by Yamashima et al. (1998) on the basis of the experimental paradigm of global brain ischemia in primates. The calpain-cathepsin cascade mechanism of cell death involves Ca^{2+} mobilization through the uptake of extracellular Ca^{2+} and/or the release from internal Ca^{2+} stores. Ca^{2+} mobilization can lead to the activation of

calpains which induces lysosomal rupture, possibly aided by ROS. The released lysosomal proteases, mainly the cathepsins, will then degrade the cell constituent proteins, ultimately leading to cell death. Cytoplasmic activation of cathepsin B (CTSB) upon lysosomal rupture mediates activation of pro-inflammatory caspase-1 and -11 upon focal cerebral ischemic induction and A β ₄₂-induced neurotoxicity (Benchoua et al., 2004; Gan et al., 2004). However, recent finding by (Mueller-Steiner et al., 2006) suggested CTSB by its endogenous proteolytic activity reduced amyloid plaque accumulation through increased protein turnover.

1.3.6.3 Endoplasmic reticulum (ER) stress

ER, with a pivotal pleiotropic physiological role in cellular biogenesis, metabolism, signaling and survival, is also a vital homeostatic organellar regulator of cellular stress (Travers et al., 2000). It is the site for the proper synthesis, folding and post-translational modification of cellular proteins (Ron and Walter, 2007) as well as production of steroids, cholesterol and other lipids (Chang et al., 2006). It also serves as a major intracellular Ca²⁺ ion store (Verkhratsky, 2005).

Presence of ER stress has been reported in AD (Hoozemans et al., 2005), PD (DeGracia and Montie, 2004) and ischemic stroke (Kitao et al., 2007). ER stress, characterized by the accumulation of unfolded proteins in the ER lumen, is frequently manifested upon presence of oxidative stress. This stress induction can occur upon perturbation of any of ER cellular functions, i.e. via protein oxidation, disturbance of Ca²⁺ signaling, and alteration of the homeostatic redox balance (Chakravarthi et al., 2006; Gorlach et al.,

2006). An intimate communicative, functional coupling relationship between ER and mitochondria has also been established on the basis of these cellular functions. One instance would be the maintenance of Ca^{2+} equilibrium, crucial for the proper functioning of both organelles (Csordas et al., 2006). Mitochondria act as an emergency Ca^{2+} store upon sudden transient surge in cytosolic Ca^{2+} level, to buffer the ER against any functional disruption. Furthermore, several members of the B-cell lymphoma 2 (BCL2) family prominent for their roles in regulation of mitochondrial-mediated apoptosis, also seem to participate in ER-induced cell death and Ca^{2+} signaling between the ER and mitochondria (Breckenridge et al., 2003; Gorchach et al., 2006; Rao et al., 2004; Szegezdi et al., 2006; Wu and Kaufman, 2006). Initiation of ER stress has been demonstrated to occur upon mitochondrial energy deficits (Flores-Diaz et al., 2004; Xu et al., 2004).

Extensive ER damage can trigger cell death via the production of unfolded proteins, the release of Ca^{2+} into the cytoplasm or altered redox homeostasis (Breckenridge et al., 2003) resulting in either classical programmed cell death (PCD) or other mitochondrial cell death pathways (Jimbo et al., 2003). As such, dysfunctional Ca^{2+} regulation arising from ER stress and increased molecular oxidative damage further potentiates activation of programmed necrotic pathway involving calpains, forming a positive feedback regulatory loop (Crocker et al., 2003; Nakagawa and Yuan, 2000).

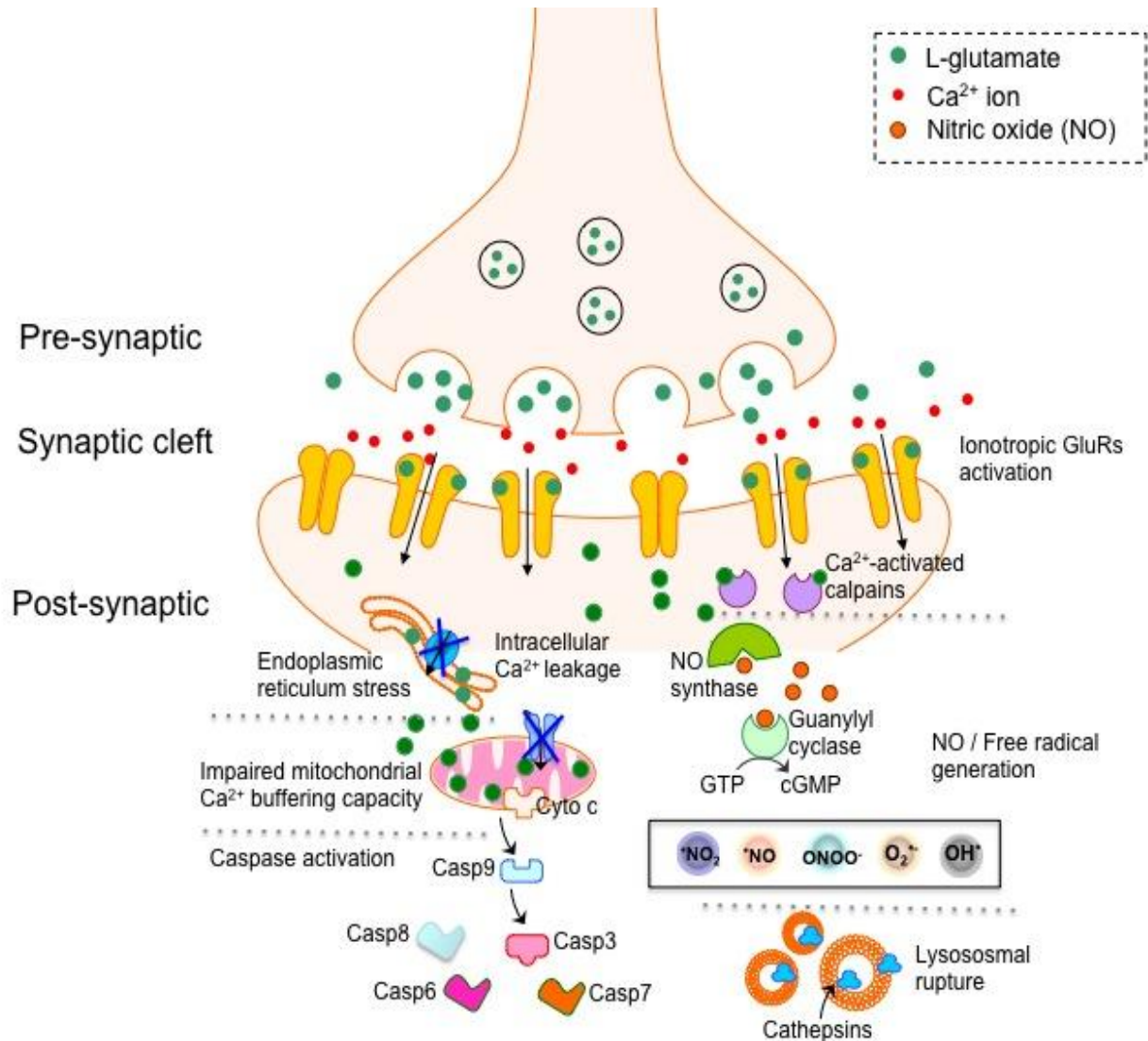


Figure 1.1 A simplified diagram summarizing the major biological processes implicated during neuronal excitotoxicity.

1.4 Ischemia

Stroke, a cerebro-vascular disease/accident, occurs when blood supply to the brain is disrupted in the event of occlusion or rupture of blood vessels, resulting in the loss of neurological function. As such, stroke can be subdivided into two types: ischemic stroke (lack of blood flow due to thrombosis or arterial embolism) and hemorrhagic stroke

(vascular leakage). It has been shown that majority of stroke cases (accounting for ~85%) is attributed to acute ischemic cause with the rest categorized as hemorrhage (Lakhan et al., 2009). Ischemic stroke is a general term with reference to a heterogeneous group of etiologies e.g. embolism, relative hypoperfusion and thrombosis. Nevertheless, ischemic stroke is ubiquitously caused by atherothrombosis of large cervical and intracranial arteries and embolism from the heart.

1.4.1 Types of cerebral ischemic stroke:

As a general rule of thumb, adult cerebral ischemia can be categorized into two mechanistically distinct modes namely, global and focal ischemia respectively. A third type of cerebral ischemia, known as hypoxic ischemia (HI), is commonly known to occur in neonates.

1.4.1.1 Global ischemia

Global ischemia, which occurs at a significantly lower incidence in human beings, takes place after transient circulatory arrest with resuscitation (e.g. hypoxic-ischemic encephalopathy secondary to a cardiac or pulmonary arrest), traumatic brain injury or after near-drowning incidents. In the event of circulatory arrest, absolute cerebral blood flow falls off from 0.8 ml/g/min to zero within seconds with the subsequent loss of consciousness that ensues after approximately 10s. Electroencephalography activity stops after 30 to 40s. The few minutes of global ischemia are sufficient to inflict irreversible, widespread brain damage that potentiates over days. Under normothermic conditions, 10min of global ischemia are lethal in man. The representative histological picture after

global ischemic insults is represented by delayed neuronal death sparing glial cells (sometimes even associated with astrogliosis). It is estimated that solely in the United States, approximately 500,000 people/year die because of circulatory arrest leading to global ischemia (NCBI » Bookshelf » Madame Curie Bioscience Database » Neurodegenerative Disease » Neuroprotective Strategies in Animal and *in Vitro* Models of Neuronal Damage: Ischemia and Stroke: <http://www.ncbi.nlm.nih.gov/bookshelf/br.fcgi?book=eurekah&part=A2331>).

1.4.1.2 Focal ischemia

Focal ischemia is triggered by the sudden significant reduction of blood supply to the brain, as a result of either the rupture or occlusion by thrombus/embolism of a blood vessel in the brain. The inhibition of normal cerebral blood flow can be transient or permanent. This impairs the supply of oxygen and nutrients, particularly glucose to a specific part of the brain, resulting in cerebral ischemia. As opposed to global ischemia, focal ischemia has an additional pathological feature called the ischemic penumbra. The penumbra defines the brain tissue representing the ischemia border-zone which is metabolically active but functionally silent, i.e. injured but alive. It is observed when absolute regional blood flow in the ischemic core is diminished to levels $<0.1\text{ml/g/min}$, blood flow in the penumbra typically remains at $0.2\text{-}0.4\text{ml/g/min}$. Histological image identifying focal ischemia is defined by pan-necrosis that includes all cell types in the brain (neurons, astrocytes, oligodendrocytes, endothelial cells). (NCBI » Bookshelf » Madame Curie Bioscience Database » Neurodegenerative Disease » Neuroprotective Strategies in Animal and *in Vitro* Models of Neuronal Damage: Ischemia and Stroke:

<http://www.ncbi.nlm.nih.gov/bookshelf/br.fcgi?book=eurekah&part=A2331>). Focal ischemia can be further subdivided into transient and permanent subtypes depending on the duration of occlusion. In transient focal ischemia, the temporary occlusion of cerebral blood flow to a particular part of the brain is restored via reperfusion. On the other hand, the occlusion in the cerebral artery is not relieved, impeding the blood supply to that specific part of the brain.

1.4.1.3 Hypoxic ischemia (HI)

HI brain damage is one of the most common causes of neonatal brain injuries, amidst other conditions such as intrauterine infection and perinatal cerebral hemorrhage (Bracci et al., 2006). HI, occurring during the perinatal period, severely affects brain integrity resulting in detrimental long-term neurological morbidity in terms of motor, intellectual, educational and neuropsychological performance deficits (e.g. cerebral palsy, mental retardation, learning disability and epilepsy), and even neonatal mortality (Cowan et al., 2003; Ferriero, 2004; Shalak and Perlman, 2004; van Handel et al., 2007). HI has been demonstrated to produce brain damages of differential severity comprising focal necrotic cell death, diffused white matter injury, and cystic/cavitary infarction resulting in intraventricular-periventricular hemorrhage and periventricular lesions (Leonardo and Pennypacker, 2009).

1.5 Focal ischemic stroke

1.5.1 Epidemiology, symptoms and effects of focal cerebral ischemia

Based on the World Health Organization 2007 health report, approximately 15 millions people globally suffer from stroke yearly. Of these, an estimation of 5.7 millions die (<http://www.who.int/chp/steps/stroke/en/index.html>), while another 5 millions suffer from permanent disability (<http://www.strokecenter.org/patients/stats.htm>). Stroke is the second global leading cause of death (<http://www.who.int/chp/steps/stroke/en/index.html>) and most common induction of adult permanent disability worldwide (Donnan et al., 2008). Solely in developed countries, stroke occupies the third position in the rank of human diseases which lead to mortality (Lo et al., 2003). The high incidence of stroke inflicts severe financial strain on the healthcare budgets for countries globally, as statistical analyses demonstrated three months after a stroke episode, 15-30% of the survivors are permanently disabled and 20% in need of institutional care (American Heart Association).

It is estimated that a typical large-vessel acute ischemic stroke results in the loss of 120 million neurons each hour. Relative to the rate of neuron loss during normal aging process, the ischemic brain suffers an ageing of 3.6 years for every hour the stroke is left untreated which explains why majority of stroke patients exhibit certain levels of motor weakness and sensory impairments [reviewed in Lakhan et al. (2009)].

The most commonly reported symptoms prior to stroke episode is sudden weakness or numbness of the face, arm or leg, most often on one side of the body. Other symptoms

comprise of: confusion, difficulty in speaking or understanding speech; difficulty seeing with one or both eyes; difficulty walking, dizziness, loss of balance or coordination; severe headache with no known cause; fainting or unconsciousness.

Occurrence of stroke, a cerebro-vascular disease, can significantly impair one's quality of life by causing physiological deficits such as motor impairments (hemiplegia, hemiparesis and dysphagia) and cognitive dysfunctions (apraxia and agnosia).

Definitions:

-Hemiplegia: One-sided paralysis.

-Hemiparesis: One-sided body weakness.

-Dysphagia: Problem with eating and swallowing as a result of damage to the part of the brain controlling the muscles to swallow.

-Apraxia: Inability to plan the steps involved in a complex task, carry the steps out in the proper sequence and/or follow a set of instructions.

1.5.2 Current approved focal cerebral ischemia treatment

Despite major steps achieved in the elucidation of the patho-physiology of cerebral ischemia, the available therapeutic avenues for acute ischemic stroke remain scarce (Donnan et al., 2008). The current approved clinical treatment of thrombolytic ischemic stroke is the intravenous injection of recombinant tissue plasminogen activator (rt-PA), which efficacy is reliant on the time of delivery (preferably 3 hours after symptoms onset) and comes with the risk of increased incidence of symptomatic intracranial hemorrhage (Furlan et al., 2003).

1.5.3 Post-ischemic physiological-response recovery

In most stroke cases regardless of fast or slow, patients will show signs of functional recovery as a result of brain reorganization and brain plasticity. Brain plasticity refers to the brain's dynamic modulation of its structure and function during development, learning, and pathology (Lakhan et al., 2009). For instance, within minutes following ischemia, the number and length of dendritic spines of the neurons in the penumbra region decreased rapidly. The initial deficit is then followed by the restoration of the dendritic spine synapses several months after the initial ischemic episode as part of the functional improvement processes (Brown et al., 2008).

Studies in experimental stroke models reveal that upon focal cerebral ischemia, neurogenesis is promoted in the subventricular zone (SVZ) and subgranular zone (SGZ) of the dentate gyrus and induces SVZ neuroblast migration towards the ischemic boundary. This phenomenon has further been verified to occur in the adult human brain, even in advanced age patients (Macas et al., 2006; Minger et al., 2007; Yamashita et al., 2006). Functional Magnetic Resonance Imaging studies have also reported that the injured adult brain has the ability to re-assemble to reduce motor impairment (Calautti and Baron, 2003; Eliassen et al., 2008). The major driving force behind this restoration of motor abilities seemingly is due to the energized activity in pre-existing networks. These reports shed a light of hope in the feasibility of usage of neuronal cell regenerative technique in stroke treatment which aims to influence endogenous neurogenesis and thereby promoting brain repair.

1.6 Patho-physiology of focal cerebral ischemia

The degree of brain ischemic damage is dependent on several factors, namely the severity and duration of ischemia and regenerative capability of the brain (Dirnagl et al., 1999). Cerebral ischemia activates the pathological ischemic cascades, resulting in almost instantaneous severe, irreversible neuronal damage to the primary site of blood supply blockage, known as the ischemic core (Dirnagl et al., 1999). A much larger viable but functionally impaired volume of the brain tissue encompassing the ischemic core, called the penumbra, though also sustaining certain degree of neuronal injury, can be rescued when the cerebral blood flow is promptly resumed (Lakhan et al., 2009).

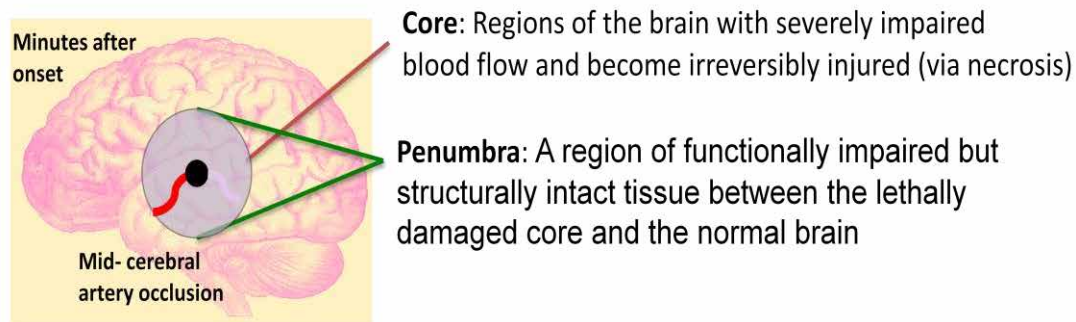


Figure 1.2 Diagram depicting the core and penumbra regions upon the infliction of focal cerebral ischemia in a localized brain region.

During focal cerebral ischemia, multiple undesirable cell signaling cascades are activated, aggravating the ischemic damage to the primary and surrounding sites of blood flow occlusion. Initial arterial occlusion results in oxygen/glucose deprivation causing a loss of function to the mitochondrial respiratory chain with a concomitant drop in ATP generation in neurons. This leads to neuronal depolarization and increase in extracellular

K^+ and Glu concentrations. Elevated Glu level in the extracellular matrix stimulates GluRs on neighbouring neurons, promoting excitotoxicity with increased oxidative load and inflammation, eventually causing cell demise. Elevated free radical production and pro-inflammatory molecules inflict microvascular injury and blood-brain barrier dysfunction, all in all contributing to irreversible cerebral damage. These processes occurring during focal cerebral ischemia are summarized in the Figure 1.3.

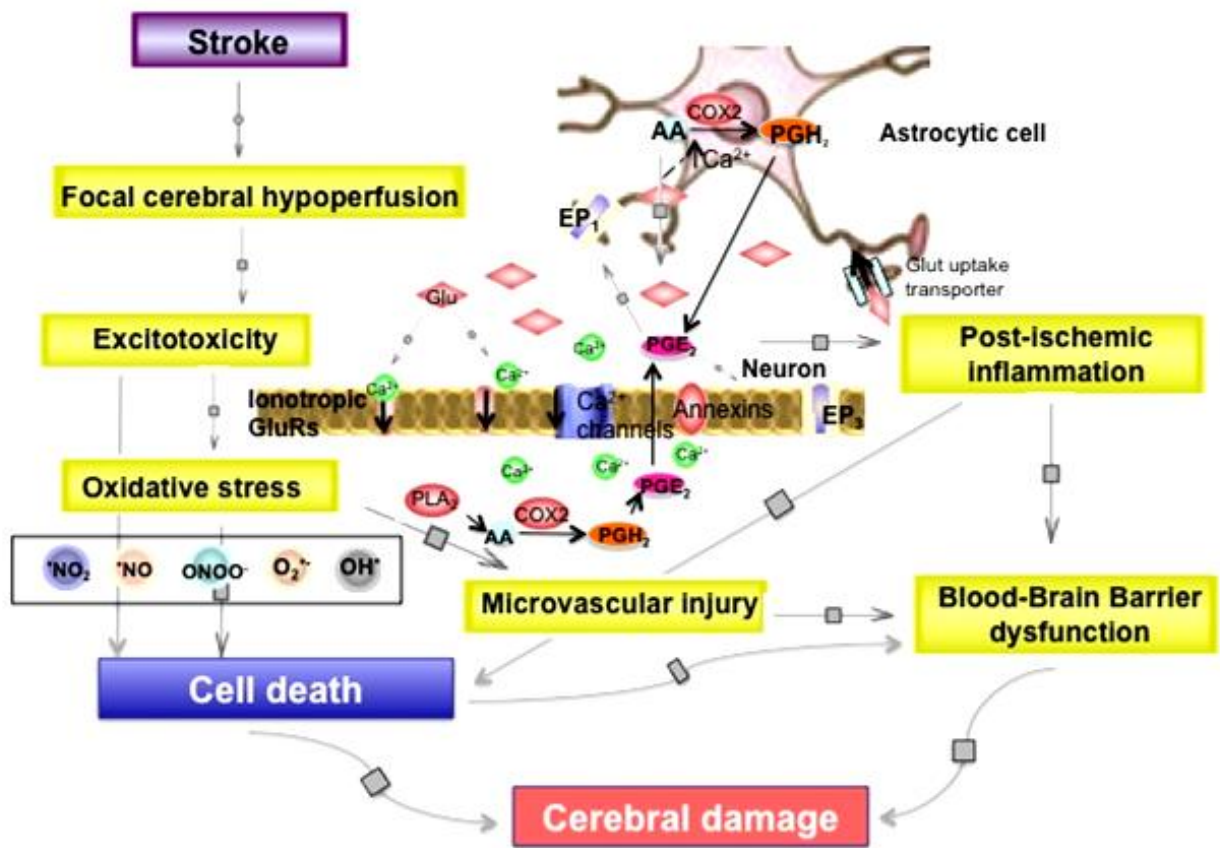


Figure 1.3 A summary of the major processes at work during the pathogenesis of focal cerebral ischemia.

Despite these mechanisms at work, residual perfusion from the collateral blood vessels slows down the progression of the ischemic cascade. As such, neuronal regeneration is still possible for several hours from the stroke onset even when blood supply drops to (30ml/100g/min; 20-40% of basal values) via prompt blood flow restoration (Hossmann, 1988b). This observation forms the foundation for the exploration of stroke therapeutic options directed at alleviating the cerebral blood flow blockage. The desired outcome is to achieve functional restoration of majority of the brain tissue subjected to ischemic condition and minimize post-stroke disability (Lakhan et al., 2009).

1.6.1 Excitotoxicity and ischemia

Initiation of ischemic stroke occurs via critical focal hypoperfusion in a localized brain region, which subsequently progresses to oxidative and excitotoxic damages that exacerbate to further complications such as microvascular injury, blood-brain barrier impairment and post-ischemic inflammation, aggravating the initial physical damage to the primary site of occlusion (Lakhan et al., 2009). Within the centre of the ischemic region, the cells are subjected to irreversible anoxic depolarization, whereas in the penumbra, the cells still retain ability to repolarize through increased energy consumption and depolarize in response to rising levels of extracellular Glu and K^+ ion. These persistent, rapid discharging of depolarization stimuli, also known as peri-infarct depolarizations, further promotes Glu release into the extracellular cell matrix (ECM), worsening excitotoxic damage (Hossmann, 1988a).

Chapter 1: Introduction

As previously mentioned, Glu is an excitatory neurotransmitter within the mammalian CNS. Over-activation of GluRs, especially the ionotropic receptor subtypes, has been demonstrated to result in excitotoxicity, characterized by increased influx of Ca^{2+} from extracellular matrix and release of intracellular Ca^{2+} store. This phenomenon is commonly noted in HI and focal cerebral ischemic stroke injury (Hara and Snyder, 2007; Simpkins et al., 2003). In HI injury, occlusion of cerebral blood flow lowers oxygen and glucose supplies to the brain. This slows down mitochondrial respiration considerably with concomitant drop in ATP production, eventually resulting in energy crisis (Nicholls et al., 1999). Membrane ionic pump dysfunction with concerted elevation cytosolic Ca^{2+} due to GluRs over-stimulation which overloads the mitochondrial Ca^{2+} buffering capacity resulting in mitochondrial permeability transition (Soane et al., 2007; Tsujimoto and Shimizu, 2007) which accelerates ROS production, NAD^+ exhaustion and PARP-1 (Moroni, 2008) and calpains (Siman et al., 1989) induction.

Even though this phenomenon has been ubiquitously detected in post-mortem brains of these neurological disorders, the significance of its implication during neuronal death progression remains unclear. As such, experimental models become an attractive avenue for deciphering the pathological mechanisms upstream and/or downstream of oxidative stress (Lakhan et al., 2009). As oxidative stress is a central dogma in numerous neuropathological conditions, novel insights into the signaling transduction pathways modulated upon its occurrence would form a foundation in the identification of potential biological targets useful in the area of therapeutic management.

1.6.2 Programmed cell death (PCD) in focal ischemia

Neurons are morphologically unique and functionally sophisticated mammalian cells. They possess the characteristic morphology of a cell body, with extensively elongated processes (axons and dendrites) that posed consequential problems for intracellular trafficking. In addition, the plethora of surface ion channels in neurons increases their vulnerability to injury and death through energy deprivation (ATP deficit) or via hyper-excitation by neurotransmitters leading to excitotoxicity by inducing elevation of intracellular and mitochondrial Ca^{2+} as previously mentioned, which forms one of the key determinants of PCD through various mechanisms (Chinopoulos and Adam-Vizi, 2006; Nicholls, 2008). Other crucial factors include ROS generation and presence of mitochondrial permeability transition (MPT) and/or outer mitochondrial membrane permeability (OMMP). Recent substantiation in non-neuronal cells indicates elevated Ca^{2+} in mitochondria to be a crucial signal in ROS-mediated apoptosis (Baumgartner et al., 2009). Finally, neurons function and are maintained in an adaptive cellular milieu made up of mainly glial cells such as astrocytes (Maragakis and Rothstein, 2006; Pekny and Nilsson, 2005). As such, neuronal exposure to glial cells-secreted cytokines during the inflammatory phase of injury in the CNS (Hanisch and Kettenmann, 2007; Pekny and Nilsson, 2005) can detrimentally activate extrinsic pathways to cell death.

Mitochondria in neurons have been recognized as a key crucial organelle under numerous pathological settings, playing the key regulatory roles in death processes in the affected cells [Reviewed extensively in Higgins et al. (2010)]. It is vital to cellular homeostatic and energy-yielding activities. The definition of PCD has broadened over the recent years

Chapter 1: Introduction

to incorporate more complex, distinctive cell death signaling cascades. Mitochondrial implication in PCD has been extensively studied (Reviewed by Nagley et al., 2010). Other than its prominent, well-explored effect on apoptosis (PCD-Type I), it also influences the progression of programmed necrosis (PCD-Type III), an alternative death pathway signified by the absence of caspase involvement (Clarke, 1990). Autophagy (PCD-Type II), perceived as a routine homeostatic mechanism for renewal and clearance of cellular constituents, has but recently been identified as a mode of PCD whose activation has been reported to lead to death under certain stress conditions (Boland and Nixon, 2006; Clarke, 1990; Mizushima et al., 2008). With the expansion in the subtypes of PCD, numerous cell death markers have been employed to distinguish the mechanistic mode of cellular injury or neurodegeneration under various pathological conditions in the nervous system.

To further add complexity to the picture, all these diverse signaling pathways are able to cross-regulate each other at both upstream and downstream of mitochondria. As a result, activation of one pathway may positively or negatively impact the development of other pathways instantaneously. The existence of these cross-talks can result in two cell death scenarios where firstly, in one initially homogeneous population of cultured neurons exposed to a given treatment, a heterogeneous set of responses between different cells of that population is likely to occur; Secondly, individual cells may display a subset of markers characteristic of explicitly defined cell death paradigms (e.g. PCD Types I, II or III) (Nagley et al., 2010). The former is reflective of the pathological features observed in ischemic stroke brains subjected to a single cellular insult. In stroke-affected and HI

brains, distinct necrotic features are concentrated in the core of the injury site. On the other hand, the penumbra surrounding this core is occupied by cells showing apoptotic features such as caspase activation and nuclear DNA fragmentation (Dirnagl et al., 1999).

1.6.2.1 Apoptosis

Apoptosis (PCD-Type I), dependent on caspase activation, is composed of two main pathways, the extrinsic (death receptor pathway) and intrinsic pathways (Reviewed extensively by Nagley et al., 2010). The stark difference lies in that the extrinsic pathway can occur independent of mitochondria while the intrinsic pathway is characterized by mitochondrial involvement. In the intrinsic pathway, apoptogenic proteins translocate from the mitochondrial intermembrane space (IMS) to the cytoplasm, leading to caspase activation that directly activates cell death. The occurrence of OMMP is regulated by the BCL2 protein family which is divided into pro-apoptotic and anti-apoptotic (pro-survival) subfamilies. The anti-apoptotic BCL2 proteins form the bridging intermediaries between the BH3-only proteins and the pro-apoptotic BCL2 family members, which include BAX and BAK. One postulation of this mechanistic association is that the anti-apoptotic BCL2 proteins inactivate BAX and BAK for as long as the pro-survival proteins remained uninhibited by the BH3-only proteins. The other view is that some BH3-only proteins may also act as facilitators, directly interacting with BAX and BAK to initiate their activation (reviewed by (Youle and Strasser, 2008)). BAX and BAK, upon activation, change conformation, oligomerise and form pores in the outer mitochondrial membrane (OMM). The “pore” is likely to be lipidic in nature, thus allowing transit of proteins from the IMS to the cytosol and vice versa (Smith et al., 2008).

The key executioners that re-localize from the IMS to the cytosol (reviewed in Hengartner, 2000; Kroemer et al., 2007) include cytochrome c (CYTC), antagonists of inhibitor of apoptosis (IAP), –second mitochondria-derived activator of caspases/direct inhibitor of apoptosis-binding protein with low pI” (Smac/DIABLO) and HTRA2/OMI that activate the caspase-signaling cascade, and the caspase-independent proteins, AIF and endonuclease G (Endo G) (Beart et al., 2007; Diwakarla et al., 2009b; Higgins et al., 2009; Kroemer et al., 2007). CYTC forms an apoptosome complex with APAF-1 and ATP in the cytosol to activate caspase-9. Caspase-9 then in turn activates its downstream effector caspase-3, caspase-6 and caspase-7, which consequently lead to chromatin condensation and DNA fragmentation (reviewed in Hengartner, 2000). The re-localization of AIF and Endo G during apoptosis frequently occurs much later than that of CYTC and Smac/DIABLO (Beart et al., 2007; Diwakarla et al., 2009b). Activation of both AIF and Endo G alone is able to result in nuclear degradation and DNA cleavage independent of caspases (Takano et al., 2005). As such, in an apoptotic process, AIF and Endo G are believed to be involved in a feed-forward mechanism whereby their redistribution from mitochondria is triggered by downstream caspase activation (reviewed in Hansen and Nagley, 2003).

BID, another BH3-only protein accountable for the Bax activation during OMMP in neurons, is also regulated by p53 (Desagher et al., 1999). For BID to become functional, it requires cleavage by active caspase-8 or caspase-2 to form truncated BID (tBID) (Konig et al., 2007; Niizuma et al., 2008). During focal cerebral ischemia and oxygen/glucose

deprivation in neurons, tBid presence is critical for apoptosis to proceed (Plesnila et al., 2001; Yin et al., 2002). Once migrated to the mitochondria, tBid participates in the direct redistribution of AIF to the nucleus in cultured neurons (Culmsee et al., 2005; Landshamer et al., 2008). However, it is recently reported that full length BID is involved in inducing caspase-independent cell death in neurons, implying the BID truncation is not crucial for the activation of the cell death signaling cascade and it may have an important role in AIF redistribution during cell death in the absence of caspase activity (Konig et al., 2007; Ward et al., 2006).

1.6.2.2 Autophagy

Autophagy is part of a cell's routine cellular homeostatic process to remove molecules and organelles via lysosomal clearance/degradation pathway (Nagley et al., 2010). Its importance in CNS is gaining increasing recognition (Jaeger and Wyss-Coray, 2009). Autophagy can be classified into several pathway subtypes (reviewed in (Todde et al., 2009)), namely macroautophagy (MA; most commonly associated with mitochondria and cell death), microautophagy (autophagy without vesicles) and chaperone-mediated autophagy. As such, we will focus on the discussion of MA involvement in neuronal death and the term "Autophagy" will be used to refer to MA. Autophagy requires the formation of a double membrane vesicle called an autophagosome which is involved in the sequestration and engulfment of organelles or molecules and target them for lysosomal clearance. Microtubule-associated protein 1-light chain 3 (LC3), an essential protein component of the autophagosome membrane, has been adopted as an autophagic biomarker for the localization studies of these vesicles (Kabeya et al., 2000). There is a

widely accepted belief that autophagy is essential for the homeostatic maintenance of functional organelles, such as mitochondria due to the post-mitotic nature of neurons (Terman et al., 2006). Due to the lack of cellular division in neurons, autophagy is essential for turnover of dysfunctional mitochondria and protein aggregates (i.e. β -amyloid or α -synuclein in AD and PD, respectively, believed to be detrimental to neuronal survival (reviewed in Klionsky, 2006; Terman et al., 2006). There are at least two situations in which autophagy come into play to induce neuronal death: in the first instance, when the autophagic process is insufficient to remove the toxic protein aggregates, as possibly occurs in AD and PD (reviewed in Kroemer and Levine, 2008); and secondly, autophagy is up-regulated as a direct contributor to cell death as in PCD Type II.

Existence of autophagic neuronal cell death was first proposed when an alternative death pathway independent of apoptosis was activated in sympathetic neurones (Xue et al., 1999). Subsequent similar studies reported multiple vesicles formation (Gomez-Santos et al., 2003), increase autophagic protein levels (Kanno et al., 2009) and cell death attenuation with autophagic inhibitors (Gomez-Santos et al., 2003; Xue et al., 1999). As the autophagic inhibitors such as 3 methyladenine or wortmannin used in these studies are non-specific and can also block apoptotic pathways (Canu et al., 2005), most did not classify the death explicitly as autophagic. Furthermore, cooperative signaling coupling between autophagy and apoptosis makes it even more difficult to distinctively classify cell death as belonging exclusively to a certain PCD type.

Another example of this signaling interplay implicating mitochondrial regulation, autophagic players and cell death is demonstrated by Beclin-1 function. This protein is not only a central component of the autophagic pathway, but also contains a BH3-only domain which can be negatively regulated by interacting with the anti-apoptotic BCL2 or BCL-xL proteins (Oberstein et al., 2007). Interference of these BCL2 family/Beclin-1 interactions by mutation of the BH3-only domain within Beclin-1 led to active autophagic death (Pattingre et al., 2005). Functional importance of Beclin-1 in PCD-Type II is further substantiated by over-expression studies that it induces massive autophagy which progresses to cell death (Pattingre et al., 2005). Suppression of the autophagic process by Beclin-1/BCL2(BCL-XL) interactions is alleviated through competitive disruption by BH3-only proteins such as BAD (Maiuri et al., 2007a). With the establishment of these molecular associations, Beclin-1 involvement in autophagy is much more prominent than in apoptosis. This is because current perspective is that the cross-talk is unidirectional (Ciechomska et al., 2009; Maiuri et al., 2007a), such that BCL2 family regulates autophagy but Beclin-1 does not affect apoptosis. However, these interactions do not necessary lead to cell death but can be beneficial to cellular homeostasis in other conditions such as starvation. For instance, during starvation in HeLa cells, ABT737 (a BH3- only peptide mimetic) triggered mitophagy rather than reticulophagy (also known as ERphagy), yet only ER-localized BCL2/BCL-xL (not mitochondrially-targeted BCL2/BCL-xL) was capable of inhibiting starvation-evoked autophagy, implying a significant importance of ER-stress/autophagic cross-talk (Maiuri et al., 2007b).

Further pathway interlocks between the apoptotic and autophagic signaling cascades can be illustrated via the roles of death signaling molecules such as the autophagy protein ATG5, as well as the BH3-only proteins BNIP3 and BIK. ATG5, an autophagy protein essential for autophagosome formation, can undergo truncation by calpains, transforming it to an effective apoptotic inducer (Mizushima et al., 2001). Once cleaved, ATG5 is able to freely translocate from the cytosol to mitochondria, where it binds to BCL-xL, triggering CYTC redistribution and downstream caspase activation (Yousefi et al., 2006). Hypoxia in HEK293 cells triggers BNIP3 up-regulation resulting in cell death (Azad et al., 2008). BNIP3 over-expression promotes autophagy, while knockdown diminishes hypoxia-induced autophagy and cell death. Similarly, silencing of Beclin-1 and ATG5 under the same cellular condition also inhibits hypoxia-induced cell death, indicating that all three proteins participate in the same autophagic cell death cascade. This postulation is further verified by BIK over-expression -induced cell death in $BCL2^{-/-}$ murine embryonic fibroblasts which could be abrogated by autophagic inhibitors and knockdown of Beclin-1 and ATG5 (Rashmi et al., 2008). Autophagy triggered by relevant BCL2 family members during cell death may be used as an alternative resort to provide additional supply of energy to fulfill the apoptotic process.

1.6.2.3 Programmed necrosis

Severe, massive cellular or tissue damages frequently lead to unregulated, accidental necrosis, when cells are subjected to drastic cellular ionic and osmotic perturbations leading to rapid swelling with consequential gross cellular debilitation (Blomgren et al., 2007; Boujrad et al., 2007; Gill and Perez-Polo, 2008; Kroemer et al., 2009; Nicotera and

Melino, 2004). This aberrant cytotoxic outcome differs from programmed necrosis (PCD-Type III) which is dependent on distinct regulated pathways (distinct from both apoptosis and autophagy). Cells undergoing PCD-Type III though possessing some morphological resemblance to truly necrotic cells, they on the other hand undergo a discrete loss of permeability of the plasma membrane (Boujrad et al., 2007). In both cases, mitochondrial energisation and ATP production were also inhibited.

Similar to PCD-Type I and PCD-Type II, mitochondria are also a central component to cell death regulation in programmed necrosis. However, as opposed to PCD-Type I, PCD-Type III does not rely on caspase activation (Kroemer et al., 2009). Instead, programmed necrosis triggers the MPT and is dependent on AIF and Endo G re-localization (Boujrad et al., 2007; Higgins et al., 2009). Calpains, a family of Ca^{2+} -dependent cysteine proteases, frequently form the hallmark of PCD-Type III (Golstein and Kroemer, 2007; Kroemer et al., 2009). While calpains have been implicated in all PCD subtypes in an apoptosis-necrosis continuum (e.g. calpains activation during apoptosis in motor neurons (Momeni and Kanje, 2006; Samantaray et al., 2006; Sribnick et al., 2007), their involvement in programmed necrosis has been especially highlighted due to elevation of intracellular Ca^{2+} in programmed necrosis (Diwakarla et al., 2009a; Pang et al., 2003; Yamashima et al., 2003). Calpains are categorized into tissue-specific isoforms (n-calpains), and two constitutively and ubiquitously expressed isozymes calpain I (μ -calpain) and calpain II (m-calpain), that are activated in vitro by micromolar and millimolar concentrations of Ca^{2+} , respectively (Polster et al., 2005). Unlike caspases, calpains do not recognize specific substrate cleavage sites and their activities

are tightly modulated by cofactors, such as the endogenous inhibitor, calpastatin, and phospholipids (Huang and Reichardt, 2001).

Cross-regulation between caspase-dependent and caspase-independent PCD pathways is evident from observations that calpastatin can be cleaved by caspase-3 to facilitate calpains activation in PCD-Type I (Porn-Ares et al., 1998; Wang et al., 1998) and that calpains too are able to activate endogenous caspases such as caspase-3, -7, -8 and -9 (Chua et al., 2000). It is demonstrated in a hypoglycemia model that neuronal death is dependent on both MPT and redistribution of CYTC and AIF triggered by both caspase-3 and calpain activation (Ferrand-Drake et al., 2003). Calpain I is directly accountable for the redistribution of AIF from intact mitochondria, and calpains inhibition is able to suppress AIF release, emphasizing calpains role in caspase-independent cell death (Polster et al., 2005). As such, AIF-dependent death (in the absence of caspase activation) associating with calpains activation has been classified as programmed necrosis (Boujrad et al., 2007). This emphasis is further highlighted by the significant reduction of damage induced by KA-mediated excitotoxicity *in vivo* upon calpastatin over-expression, demonstrated to be caused by a decrease in cleavage of BID to tBID and the redistribution of AIF and Endo G from mitochondria (Takano et al., 2005).

1.6.3 Oxidative stress

Neuronal oxidative stress is a prominent phenomenon frequently observed in chronic neurodegenerative disorders such as AD (Sultana and Butterfield, 2009) and PD (Jenner, 2007) and acute neurological disorders such as stroke (Niizuma et al., 2009). Oxidative

Chapter 1: Introduction

stress results from the aberrant disruption of the physiological balance between the pro-oxidants and anti-oxidants in favour of the former (Lakhan et al., 2009). It is characterized by a substantial rise in intracellular ROS level that is disruptive to cellular homeostatic balance through infliction of DNA, protein and lipid damages, release of Ca^{2+} from intracellular stores and chemotaxis which explains the accumulation of oxidized protein aggregates seen in numerous neuropathological conditions (Evans and Cooke, 2004; Halliwell, 2006; Lennon et al., 1991; Liu et al., 1996). Severe oxidative stress triggers cell death through necrosis while at moderate level can induce apoptosis (Evans and Cooke, 2004; Lennon et al., 1991; Liu et al., 1996).

Oxidative stress is one of the two main patho-physiological mechanisms frequently implicated in ischemic stroke as the formation of ROS/reactive nitrogen species (RNS) is significantly enhanced through numerous injury cascades e.g. mitochondrial inhibition, Ca^{2+} overload, reperfusion damage and inflammation (Coyle and Puttfarcken, 1993). Mitochondria, as the main cellular site for energy production, offer a rich primary source of ROS through its respiratory electron transport chain which constantly undergoes fluctuations in redox states (Halliwell, 2006). Other secondary cellular processes contributing to ROS production include lipid peroxidation, cation-associated Fenton reactions, NO-mediated protein nitrosylation and matrix enzymatic interactions (Chinopoulos and Adam-Vizi, 2006; Halliwell, 2006; Zundorf et al., 2009).

Brain ischemia generates $\text{O}_2^{\bullet-}$, a highly reactive primary radical, through xanthine oxidase and subsequently responsible for H_2O_2 formation and finally OH^{\bullet} generation (a

short-lived but most reactive type of oxygen species), thus activating a chain reaction cascade of ROS production after leakage from the mitochondrial electron transport chain (Lakhan et al., 2009). H_2O_2 is lipid-soluble and readily tranverses cell membranes. Concurrently, $O_2^{\bullet-}$ crosses cell membrane via anionic channels (Kontos, 2001). On the other hand, NO, a water- and lipid-soluble free radical that is produced from L-arginine by NOS, forms the basis for RNS formation. As NO itself is highly reactive due to its thermodynamic instability, it undergoes various chemical reactions with gaseous molecules, anions and ROS readily to form NO_2^- , NO_3^- and $ONOO^-$. Elevated NOS type -I and -III activities have been observed in neurons and vascular endothelium respectively upon cererbral ischemic onset. As time progresses, elevated NOS type II (iNOS) activity is also detected in other cell types within the brain including glia and infiltrating neutrophils (Lakhan et al., 2009).

Besides inflicting cerebral cellular damage, oxidative stress also elevates blood–brain barrier permeability through induction of matrix metalloproteinases (MMPs), especially MMP-9 (Montaner et al., 2003; Rosenberg et al., 1998), and endothelial cell injury (Chan, 2001; Kontos, 1985; Siesjo et al., 1989). Free radicals regulate cerebral blood flow by being strong cerebral vasodilators (Wei et al., 1985). However, further interaction between NO and $O_2^{\bullet-}$ alters vascular reactivity to CO_2 triggering an opposing effect of vasoconstriction (Kontos, 2001). Moreover, ROS promotes platelet aggregation (Love, 1999).

As a result, free radicals are considered as a potential therapeutic target for improving the

prognosis of an ischemic stroke. Compounds possessing strong intrinsic antioxidant properties such as ebselen (a mimic of glutathione peroxidase; (Yamagata et al., 2008)) and resveratrol (a natural phytoalexin found in some dietary sources such as grapes and red wine; (Ozkan et al., 2009)), have been demonstrated to reduce stroke-associated brain infarcts in animal models.

1.6.4 Neuroinflammation

The CNS has been misunderstood over the years to be an immune-privileged organ. However recent studies have uncovered the CNS to be engaging in substantial crucial, bi-directional crosstalk with the immune system. Emerging data from neuro-pathological studies further revealed that inflammatory cells participate in tissue remodeling after brain injury. Post-ischemic neuroinflammatory modulations cause dysfunction of the blood-brain barrier, cerebral edema, and neuronal cell death (Lakhan et al., 2009).

Microglial cells, as the resident macrophages of the brain, play a critical role as phagocytic scavengers to the immuno-competent CNS. Ekdahl and colleagues (2009) commented a two-hour middle cerebral artery occlusion (MCAO) in rats triggered an increase in the number of activated microglial cells that persists up to 16 weeks after (Ekdahl et al., 2009). Upon ischemia stimulation, microglia evolve into phagocytes secreting a variety of substances, many of which are cytotoxic and/or cytoprotective. These activated microglial cells are also capable of releasing several pro-inflammatory cytokines such as tumour necrosis factor-alpha (TNF- α), interleukin-1-beta (IL-1 β) and interleukin-6 (IL-6), as well as other potential cytotoxic molecules including NO, ROS,

and prostanoids (Lucas et al., 2006). Similarly to microglia, astrocytes can also secrete inflammatory factors such as cytokines, chemokines, and NO (Swanson et al., 2004). Interestingly, microglia may induce neuroprotection by secreting neurotrophic molecules such as brain-derived neurotrophic factor (BDNF), insulin-like growth factor I (IGF-I), and several other growth factors.

Cytokines promote the expression of cell adhesion molecules (CAMs), facilitating adherence of circulating leukocytes to vessel walls transmigrate into the brain with further release of additional pro-inflammatory mediators and secondary injury in the penumbra. This typically occurs within four to six hours after ischemia onset. Neutrophils are the earliest leukocyte subtype to infiltrate the ischemic brain and demonstrate substantial up-regulation in gene expression studies. Recently, Shichita et al. (2009) reported production of IL-23 from infiltrating macrophages attracts infiltrating γ dT cells three days after the onset of ischemia along side with IL-17 generation which amplify the inflammatory cascade (Shichita et al., 2009). Antibody-mediated inhibition of a γ dT cell receptor subtype effectively limited the infarct volume, even when delayed treatment was initiated at 24 hours after ischemic onset. As such, these γ dT cells may pose as potential clinical target providing a longer therapeutic window to inhibit secondary inflammatory expansion of cerebral damage after stroke (Lakhan et al., 2009).

1.6.5 Microvascular disruption

Maintenance of cerebrovascular autoregulation is important to retain the intrinsic ability of the cerebrovascular bed to buffer any changes in blood pressure by withstanding a

Chapter 1: Introduction

stable, constant perfusion (Paulson et al., 1990). When cerebral blood flow pressure drops, arteriolar vasodilation triggered by metabolic factors (hypoxia, adenosine, carbon dioxide (CO₂) and acidosis), myogenic processes (smooth muscle relaxation in response to drop in intravascular pressure) and endothelial mechanisms (NO, prostacyclin and endothelin-1) takes place to maintain cerebral perfusion pressure (Andresen et al., 2006). Focal and global dysfunction of cerebral autoregulation in reperfused ischemic brain have been observed, though its exact physio-pathological significance remains to be elucidated (Dawson et al., 2003; Eames et al., 2002; Reinhard et al., 2005).

Ischemia induces enhanced endothelial cell permeability, matrix degradation and loss of autoregulation. This in turns facilitates leukocyte-endothelial cell adhesion. Endothelial injury suppresses NO and prostacyclin release, and promotes endothelin-1 generation, resulting in elevated vascular tone limiting blood in the tissue and collateral vessels in the infarct area, inflicting a greater degree of ischemic injury. Endothelin-1 a highly potent vasoconstrictor when elevated in ischemic stroke has been found to be associated with cerebral edema (Estrada et al., 1994; Moldes et al., 2008). Further to the undesirable effects of vasoconstriction, systemic breakdown of autoregulation leaves the vulnerable ischemic penumbra exposed to potentially damaging blood pressure fluctuations induced during ischemia and post-ischemic thrombolytic treatment (Leonardi-Bee et al., 2002; Oliveira-Filho et al., 2003; Zazulia et al., 2007).

Apart from the structural microvascular damage, dynamic changes also occur at the molecular level that includes the presentation of leukocyte adhesion receptors on

Chapter 1: Introduction

endothelial cells (del Zoppo and Mabuchi, 2003; del Zoppo et al., 1991; Mori et al., 1992). This is an essential step towards a post-ischemic inflammatory response, further caused undesirably the obstruction of the downstream microvascular bed after reperfusion of the occluded supply arteries, an observation known as the “no-flow” phenomenon. All in all, this phenomenon is a result of extrinsic compression from edema, endothelial swelling and intravascular obstruction due to local activation of leukocytes, platelets and coagulation (Brouns and De Deyn, 2009).

Endothelial cell injury also causes the leakage of tissue factor to blood, where it interacts with coagulation factors to activate thrombin-mediated cleavage of fibrinopeptides from fibrinogen resulting in the fibrin molecules to aggregate, thus trapping platelets, clotting factors and erythrocytes to form the clot. Cleavage of procarboxypeptidase U, alternatively known as thrombin activatable fibrinolysis inhibitor, to its active form carboxypeptidase U by thrombin, plasmin or the thrombin/thrombomodulin complex abrogates fibrin resolution (Bjorkman et al., 2005; Bouma and Meijers, 2003; Leurs and Hendriks, 2005; Willemse and Hendriks, 2007). Substantial decrease in procarboxypeptidase U activity occurs in the first 72 h after ischemic stroke (Brouns et al., 2010) and in patients with poor response to thrombolytic therapy, is a probable indication of a stronger activation of the procarboxypeptidase U/carboxypeptidase U pathway and thrombus propagation (Brouns et al., 2009; Willemse et al., 2008).

Platelets activation has been observed in circumstances of ischemia and high shear stress (Gawaz, 2004; Zeller et al., 1999). Activated platelets accumulate within microvessels as

early as 2h of vascular occlusion (Fisher and Francis, 1990; Lip et al., 2002). They secrete a variety of biochemical mediators, thus permitting interactions between coagulation factors and contribute to the “no-reflow” phenomenon by adhering to both leukocytes and microvascular endothelial cells (Chong et al., 2001; Htun et al., 2006; Zeller et al., 2005). Furthermore, platelets also induce temporary vasospasm by releasing thromboxane A₂ and free radicals and propagate inflammatory cascade by releasing chemotactic mediators necessary for leukocyte transendothelial migration (Okada et al., 1994b; Zeller et al., 2005). In acute ischemic stroke, it is frequently observed that the endogenous fibrinolysis is usually outweighed by ongoing activation of the coagulation cascade and platelet activation (Eddleston et al., 1993). Coagulation is further enhanced by elevated levels of hemostatic indicators including D-dimer, fibrin monomer, thrombin–antithrombin III complex and fibrinopeptide 1.2 (Barber et al., 2006; Chong et al., 2001; Haapaniemi et al., 2004; Tanne et al., 2006).

1.6.6 Blood-brain-barrier (BBB) impairment

Uphold of blood–brain-barrier (BBB) integrity is important in the protection of the neuronal microenvironment. Upon cerebral ischemia onset, endothelial basal lamina dissolution occurs as rapid as 2h after the onset of ischemia, resulting in an increase in BBB permeability (Hamann et al., 1995). Ischemic damages inflicted to the BBB occurred in a biphasic manner, especially after blood reperfusion to the ischemic region (Belayev et al., 1996; Huang et al., 1999; Kuroiwa et al., 1985). Although early reperfusion may temporarily limit BBB modifications, use of thrombolytic rt-PA treatment and delayed reperfusion may on the contrary aggravate the endothelial injury

(Bang et al., 2007; Hjort et al., 2008; Kastrup et al., 1999; Kidwell et al., 2008). Oxidative stress initiates BBB injury and aggravates the extent of damage through promotion of digestion of the endothelial basal lamina by inducing MMP-9 release by neurons, glia and endothelial cells (Gasche et al., 2001; Gidday et al., 2005; Heo et al., 2005). Other players involved in mediation of BBB injury include accumulation of bradykinin (Aschner et al., 1997; Kamiya et al., 1993), vascular endothelial growth factor (Abumiya et al., 1999), thrombin (Okada et al., 1994a), active matrix metalloproteinases and other protease activities (Gasche et al., 2001; Gidday et al., 2005; Heo et al., 2005; Hosomi et al., 2001; Opdenakker et al., 2001; Rosell et al., 2008). With the infliction of the first wave of BBB damage, a second stage of severe BBB injury occurred within 24–72 h after infarction (Kastrup et al., 1999; Lorberboym et al., 2003). Its etiology is more complex and results in greater tissue damage via leukocyte infiltration and marked MMP-9 release from neutrophils that transmigrated to the ischemic region (Gidday et al., 2005; Rosell et al., 2008).

BBB impairment allows non-selective leakage of blood components into the brain parenchyma (Brouns and De Deyn, 2009). Inflammatory cells transmigrate into the ischemic region, potentiating post-ischemic inflammation (del Zoppo and Hallenbeck, 2000). By means of osmosis, high molecular weight molecules followed by water is extravasated into the brain leading to vasogenic edema, which subsequently progresses to intracranial hypertension. Furthermore, red blood cell entry into the brain leads to hemorrhagic transformation of the infarcted area.

1.7. Inadequacy in knowledge of stroke pathogenesis: Missing pieces from the puzzle

A quick search from PubMed easily revealed an enormous number of publications providing molecular mechanistic insights into the pathogenesis of stroke. These invaluable research works are like pieces of clue to a puzzle, providing multiple angle glimpses to the molecular signaling cascades at work in cerebral ischemia. Even then the etiology still calls for more research effort to be elucidated, as demonstrated by the current presence of only yet a single clinically approved therapeutic treatment (i.e. rt-PA) with inconsistent efficacy, short therapeutic window and high risk to detrimental side effects. This is further complicated by the multifunctionality of most cellular proteins, making the timing of manipulation of their expression levels a critical task under neuropathological conditions. As such, it is crucial and beneficial to develop screening platforms for identification of more novel primary cellular players governing the progression of the ischemic cascade, whose manipulations can achieve therapeutic interventions.

1.8 Global transcriptomic profiling studies: An overview

Traditional molecular research tools for gene expression studies e.g. Reverse Transcriptional Polymerase Chain Reaction (RT-PCR), *in situ* hybridization, Northern blotting and RNase protection assays, only permit a low-throughput analysis of one or a small group of genes at any one time. As such, it becomes critical with respect to the availability and selection of the probes of interest by the commercial companies and researchers respectively to dictate the genes to be studied in a research project, a huge

limitation to the elucidation of functional and biological significance of a gene with respect to its interactions with other partners.

However, with the complete sequence of the human genome in 2001 by the Human Genome Project Consortium (Lander et al., 2001) in concurrence with Celera Genetics (Venter et al., 2001), it also marks the revolution in biomedical technological development. Microarray technology allows a simultaneous high-throughput identification of many novel genes, and bettering the understanding of their biological and functional significance, sparking off the ‘post-genomic era’ (Lockhart and Winzeler, 2000). These high-throughput and efficiently -generated vast sequencing data contributed to ‘functional genomics’ screening which aims to determine the function of genes and their interactions/modulations eventually contributing to the large paradigms of biological functions.

Microarray technology started its humble beginning in 1995 where it is used to determine the gene expression of 45 genes in *Arabidopsis* (Schena et al., 1995) and gained vast popularity in 2001 with its successful implementation in the sequencing of the human genome. Since then, it has been also been employed for various research purposes including differential gene expression, single nucleotide polymorphism genotyping, splice-variant analysis, novel gene identification, protein-RNA interaction, DNA mapping and epigenetics (reviewed in Hheisel, 2006). These all in all contribute to development of diagnostic tools for diseases (Gershon, 2005), and drug discovery (Marton *et al.*, 1998; Geschwind, 2003). In accordance with my current Ph.D. project, we will focus on the molecular biology behind its use in gene expression profiling,

facilitating a short period efficient elucidation of the temporal patterns of expression and generation of large transcriptional profiles of different disease models.

Due to the thousands of distinct gene reporters on a single array, each microarray experiment is therefore equivalent to the same number of genetic tests carried out in parallel. Since microarrays have the possibility to incorporate tens of thousands of gene probes, it becomes feasible to screen the entire genome of a particular organism, thus enabling a complete comparison of the expression levels of almost all transcribed genes on a genomic scale (Brown and Botstein, 1999). The influence of microarray analysis has been powerful in both basic and applied biology. This technology has substantially accelerated many scientific investigations by clearing the path biologists approach complex problems. Processing of incredibly large amount of microarray data also quickens the development of bioinformatics as a new science area (Schulze and Downward, 2001; Gershon, 2002).

1.8.1 Microarray technique: differential gene expression studies

Global gene expression profiles in cells or tissues assist in the elucidation of the molecular basis of disease pathology, drug treatment or phenotype. Microarray analysis facilitates the detection of global changes of gene expression in samples derived from normal and diseased tissues, treated and non-treated time courses, or different stages of differentiation and development (Schulze and Downward, 2001). Significant data on gene expression profiles under different conditions can be obtained with the addition of appropriate controls and repeated experiments. Computational analysis of all microarray

data further permits reliable interpretation after the classification of known and unknown genes based on their expression patterns (Armstrong and van de Wiel, 2004).

1.8.2 Mechanistic concept behind microarray technology

Microarray technology is formulated on the basis of three major design criteria: firstly the probe type employed on the array, secondly the assembly of the arrays and thirdly the number of samples (single or double-channel) which can be concurrently determined on the same array (Tarca et al., 2006). Conventional microarray offered by Affymetrix® is made up of probe attachment via surface engineering to a solid surface (e.g. glass or silicon chip) by a covalent bond to a chemical matrix such as epoxy-silane, amino-silane, lysine, polyacrylamide. Later developed microarray platforms by Illumina® employed microscopic beads, as opposed to the large solid support. Nevertheless, microarrays from different companies are typically made up of an arrayed series of thousands of microscopic spots of DNA oligonucleotides, called features, each containing picomoles (10^{-12} moles) of a specific DNA sequence, known as probes (or reporters). Each of these probes was repeated tens of times on the same array. These can be a short section of a gene or other DNA element that are used to hybridize a cDNA or cRNA sample (called target) under high-stringency conditions. Probe-target hybridization is usually detected and quantified by detection of fluorophore- (Cy3 or Cy5) labeled targets to determine relative abundance of nucleic acid sequences in the target.

The basic principle behind microarray technology is the high specificity hybridization between first DNA strand (target sequence) and the second DNA strand (probe on

microarray) (Southern et al., 1999). This is dependent on the property of complementary nucleic acid sequences to exclusively pair with each other via hydrogen bonds between corresponding nucleotide base pairs. The higher the degree of base pair complementation in a nucleotide sequence, the stronger and tighter the non-covalent bonding between the two strands. After removal of non-specific bonding sequences by repeated washings, only DNA strands specific to the probes will remain hybridized. As such, fluorescently labeled (Cy3 or Cy5) target sequences that bind to a probe sequence emit a signal that is subjected to the strength of the hybridization (determined by the number of paired bases), the hybridization conditions (temperature and duration), and washing after hybridization. Total strength of the signal, from a spot (feature), is quantitated by the amount of target sample binding to the probes present on that spot. Microarrays use relative quantitation in which the intensity of a feature is compared to the intensity of the same feature under a different condition (e.g. treatment and diseased state), and the identity of the feature is known by its position. A simplified workflow of a microarray experiment is shown in Figure 1.4.

Fluorescently labeled target sequences could be DNAs, RNAs or cDNAs. Microarray analysis of mRNA samples required the mRNAs to be reversed transcribed using an oligo-d(T) primers to form cDNAs. The cDNA templates are then amplified using RNA polymerase to form cRNAs using fluorescently labeled nucleotides. These target sequences can be hybridized onto the arrays in a single (one sample) or dual (two samples) -channel array formats. Single-channel arrays, employing only one fluorophore for detection, commonly used oligonucleotides as probes, although in some cases cDNA

or PCR fragments are adopted. Employing this array layout implies that only one sample can be hybridized per array, and differential gene expression data is obtainable through comparative normalization with other arrays upon completion of whole microarray experiment. The single-channel array format is depicted in Figure 1.5.

Similarly, dual-channel arrays also adopt oligonucleotides, cDNA or PCR fragments as probes. The distinct difference is that this array format highly relies upon the competitive hybridization between two samples (target and control reference), each differentiated by different fluorophore labeling, on a single array. Advantage of this technique is that relative gene expression differences between the two samples are observedly simultaneously. Its difference in layout from single-channel format is shown in Figure 1.6.

Three key points need to be taken into consideration when designing a microarray experiment: Firstly, the number of biological samples to ensure the reliability of the conclusions drawn from the experiment; secondly, technical replicates (two RNA samples obtained from each experimental unit) to ensure precision by the handler and allow for testing differences within treatment groups. The technical replicates may be two independent RNA extractions or two aliquots of the same extraction; and lastly, the number of replicates of each cDNA clone or oligonucleotide presented as replicates (at least duplicates) on the microarray slide, to provide a measure of technical precision in each hybridisation. It is important to formulate a good and meticulous microarray experimental design so that high quality results can be yielded in conjunction with valid

and sound conclusions. As such, guidelines on microarray designs have been published in MIAME (minimum information about a microarray experiment) standards (<http://www.mged.org/Workgroups/MIAME/miame.html>).

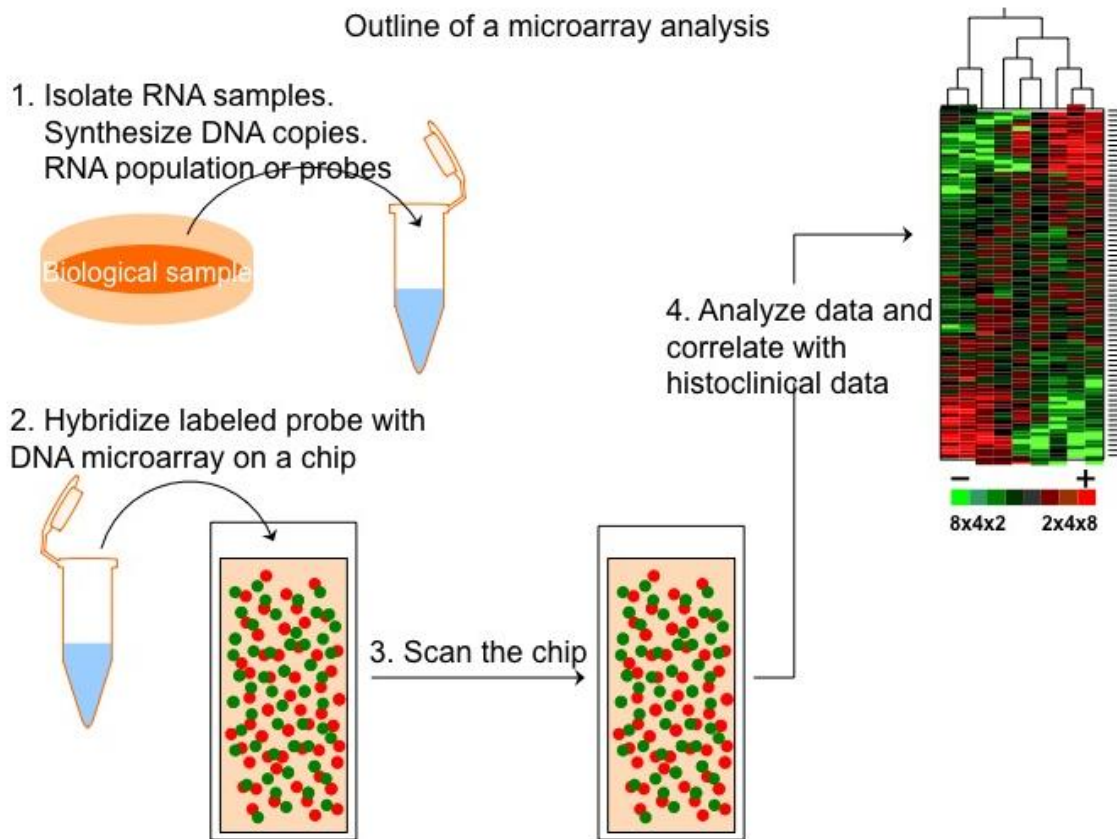


Figure 1.4 A schematic diagram of the major steps in a microarray experiment.

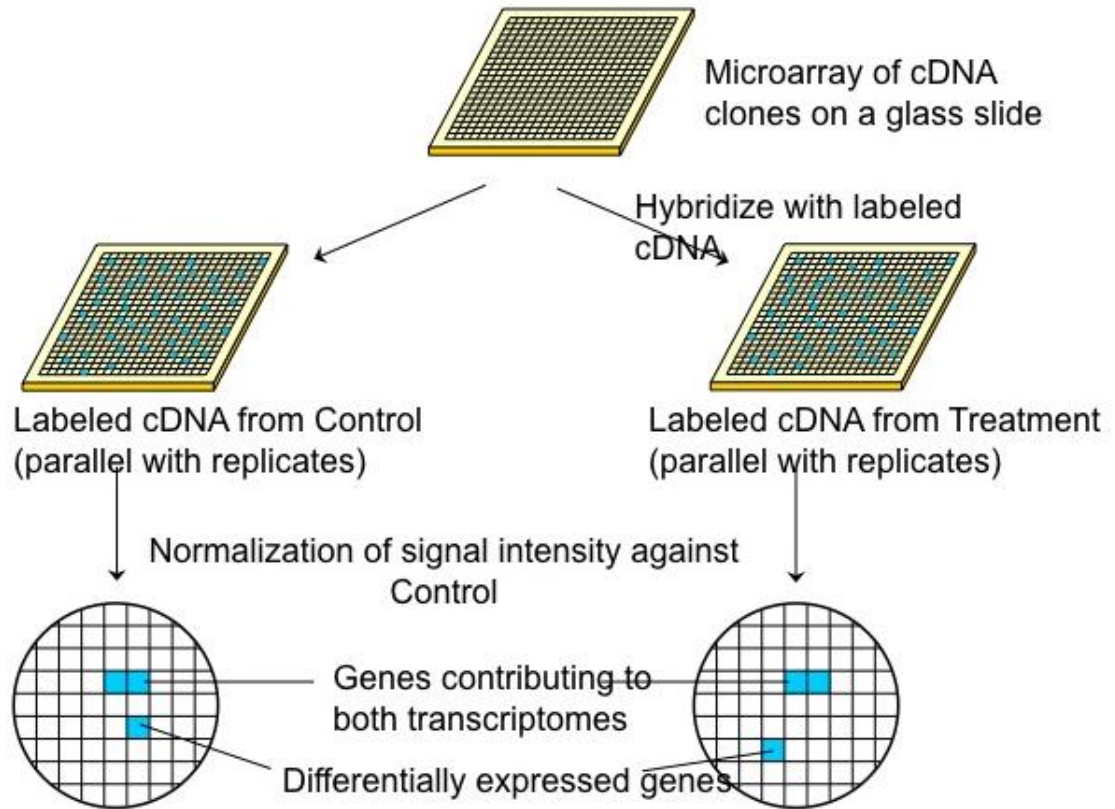


Figure 1.5 A schematic diagram depicting a single-channel (one sample) microarray experiment layout.

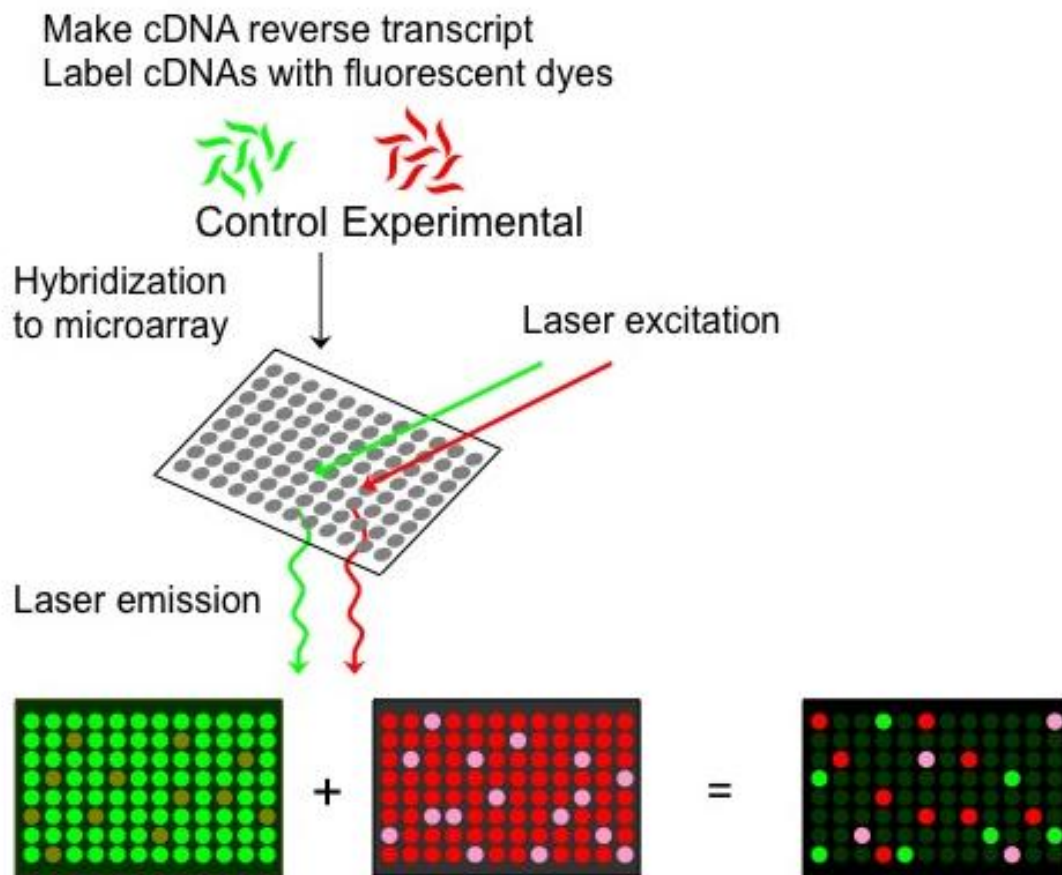


Figure 1.6 A schematic diagram depicting a dual-channel (two samples: Target and Reference) microarray experiment layout.

1.8.3 Assignment of functional-biological pathway definition to significantly-modulated genes using online database tool

Database for Annotation, Visualization, and Integrated Discovery (DAVID) 6.7 is a high-throughput and integrative data-mining bioinformatics environment, which is able to identify and assign biological pathway significance associated with large gene lists through classification of co-functioning genes to biological annotations and statistically highlight those enriched (over-represented) annotations (Dennis et al., 2003; Huang et al., 2009). This exploratory, computational-cum-statistical instrument of clustering and enrichment is crucial in the identification of biological processes most pertinent to the biological phenomena of interest.

Differentially modulated, statistically significant gene probes identified from biostatistical software (e.g. GeneSpring® and Partek®) were input onto the functional classification interface on DAVID for functional genomic analysis. The results emergent from this stepwise DAVID analysis suggested gene functional classification based on their biological-function annotations (setting the background to the respective microarray platform and array type use i.e. companies and species) and clustering annotation was carried out to rank the importance of the overall annotation term groups through enrichment and statistically validation by gene-term enrichment score through modified Fisher's exact test and Benjamini correction.

1.8.4 Relevance of global gene profiling to elucidation of pathogenesis of neuropathological disorders

The study of gene expression on a global scale using microarrays has significantly accelerated the analysis of diseases and the unraveling of cellular signaling pathways. One area in which microarray analysis has received significant attention is in neurobiology (Geschwind, 2000; Lockhart and Barlow, 2001). Differential gene expression mapping in multiple brain regions has been used to determine the genetic etiologies and molecular mechanisms accountable for the neurobehavioral differences in mice (Sandberg et al., 2000). Studies using microarrays to determine gene expression changes occurring in the neocortex and cerebellum of aging mice have shown that brain aging in the mice might be comparable to changes in human neurodegenerative disorders at the transcriptional level (Lee et al., 2000). Similarly, microarrays have been extensively used to measure transcript expression profiles or search for molecular markers and pathways involved in the pathogenesis of AD, multiple sclerosis and stroke (Colangelo et al., 2002; Emilsson et al., 2006; Ginsberg et al., 2000; Rink et al., 2010; Tseveleki et al., 2010). Studies for the development of new therapies for diseases without suitable animal models, such as schizophrenia, also involved microarray analysis of gross brain samples to reveal alterations in specific metabolic pathways (Hakak et al., 2001; Middleton et al., 2002; Mirnics et al., 2000).

1.9 Aims of my Ph.D. project

The objective of my Ph.D. project is to lay the foundation for development of screening platforms for stroke using comparative global transcriptional profiling analyses of *in vitro* and *in vivo* models to define novel biological target, and via pharmacological manipulation to determine its effectiveness in neuronal injury abrogation. My aims are as follow:

1. To identify common signaling pathways *in vitro* stroke models of excitotoxicity
2. To verify and correlate the occurrence of common signaling pathways also in different *in vivo* stroke subtypes animal models
3. Using transgenic knockout animals to further illustrate the importance of primary mechanistic events during stroke
4. To ascertain if manipulation of the expression level of an identified novel biological target would attenuate ischemic-induced infarct damage
5. To determine if the identified signaling pathways in stroke are universal to other neurodegenerative disorders

Chapter 1: Introduction

Global gene profiling of stroke has been reported in several recent literatures (Rink et al., 2010; Tseveleki et al., 2010) to identify genes which influence the pathological and clinical changes during focal cerebral ischemia. In my current project, a more in-depth and extensive microarray approach was adopted to facilitate a comprehensive elucidation of the pathogenesis of cerebral ischemia, which subsequently facilitated the identification of a novel family of biological targets (Auora kinase A (AURKA) and B (AURKB)). Functional genomics study of cerebral ischemia is made more detailed in two ways: firstly, temporal global transcriptomic profiling over a 24h-period is conducted and secondly, both *in vitro* and *in vivo* cerebral ischemia models are adopted for microarray analyses. Furthermore, a concurrent comparative microarray analysis of various *in vitro* neurodegenerative models offers unprecedented novel mechanistic insights common to numerous neurodegenerative disorders. In this Ph.D. study, great emphasis is placed on over-represented biological processes related to neuronal injury. For the purpose of clear distinction during reference to proteins and genes, gene symbols in the text are denoted in sentence case, while that with reference to proteins are in uppercase.

Temporal microarray analysis of *in vitro* ischemia models using specific iGluRs agonists on cultured murine primary cortical neurons elucidates the significance of excitotoxicity, an upstream process during cerebral ischemia. This provides invaluable insights into significantly modulated biological processes triggered by excitotoxicity (discussed in Chapter 3), and thereby facilitates the identification of novel biological targets which would theoretically show promising efficacy in the abrogation of infarct damage due to their implications in the pathogenesis of cerebral ischemia (Discussed in Chapter 6).

Chapter 1: Introduction

As focal cerebral ischemia can be subdivided into more specific disorder categories depending on the etiology, the age of the affected and the duration of ischemia, my present study has for the first time looked into the temporal global transcriptomic profiling of three subtypes: neonatal hypoxic ischemia, transient and permanent cerebral ischemia (Discussed in Chapter 4 -6). Oxidative stress is one of the two main pathio-pathological mechanisms in cerebral ischemia in addition to inflammation. The importance of intact functional anti-oxidant mechanisms to combat oxidative stress during cerebral ischemia is accentuated by the employment of glutathione peroxidase 1 – knockout (Gpx-1^{-/-}) transgenic mice, and its temporal microarray analysis is conducted in parallel with and compared against that of the wild-type mice (Discussed in Chapter 5).

A novel biological target, AURKs family, has been identified to be involved in cell cycle re-activation during excitotoxicity in *in vitro* cerebral ischemia models. Functional translational study involving administration of AURKs inhibitor in *in vivo* permanent cerebral ischemia model demonstrated substantial attenuation of infarct volume and this neuroprotective effect has been attributed to the suppression of the neuro-inflammatory cascades as shown by comparative temporal microarray analysis (Discussed in Chapter 6).

To ascertain the common pathways of neurodegeneration in the pathogeneses of different neurodegenerative diseases, unprecedented comparative microarray analysis of *in vitro* models of cerebral ischemia against that of other neuropathological conditions mainly AD, PD and ALS induced by pharmacological agents rotenone, lactacystin, hypochlorous acid

Chapter 1: Introduction

(HOCl) and NO is conducted (Discussed in Chapter 7). Invaluable mechanistic modulatory insights from as general as biological processes down to specific gene regulation aids the identification of more novel biological targets whose manipulations would provide even more effective therapeutic intervention across the neurodegenerative disease spectrum.

Chapter 2: Methodology

2.1 Buffers/Solutions and Consumables

Distilled water passed through a purification system (Milli-Q water; Millipore Corporation, Bedford, MA, USA) was used for all purposes. Most stock solutions were purchased from Sigma-Aldrich-Aldrich: phosphate-buffered saline (PBS) was supplied as 10× stock solution, Tris-HCl stock solutions were supplied as 1M, sodium chloride (NaCl) stock solution was supplied as 5M, ethylenediaminetetraacetate (EDTA) stock solution was supplied as 0.5M, and sodium dodecyl sulfate (SDS) stock solution was supplied as 10% (w/v), Stock 5× electrophoresis buffer and 10× Tris-acetate-EDTA (TAE) buffer. Multiwell plates for cell culture were from Nunc (Roskilde, Denmark). Disposable 15ml and 50ml centrifuge tubes (FALCON), and disposable 3ml syringes with 22½-gauge needles were from Becton Dickinson (Franklin Lakes, NJ, USA). Disposable 1.5ml and 2ml microfuge tubes were from Eppendorf (Hamburg, Germany). Nalgene[®] disposable filter units for sterile filtration were from Nalgene Nunc International (Rochester, NY, USA). Cell scrapers were from Techno Plastic Products (TPP; Zollstrasse, Schweiz).

2.2 Immunocytochemistry

- H₂O₂ solution
- Normal goat serum
- 0.1% Triton X-100
- Tris buffered saline (TBS)
- 3,4-diaminobenzidine (DAB) substrate solution

Fixed cells were quenched in 1% H₂O₂ and non-specific binding was subsequently blocked with 10% normal goat serum and 0.1% Triton X-100 in TBS for 1h at 4°C. Cells were incubated with polyclonal antibody to microtubule associated protein 2 (MAP2) (1:10000) overnight at 4°C and then secondary antibody for 3 h in solution with 2% normal goat serum and 0.1% Triton X-100 in TBS. Detection of immunoreactive cells was carried out using DAB substrate solution (0.5mg/ml DAB and 0.01% H₂O₂ in TBS). Immunoreactive cells were visualized under bright-field microscopy.

2.3 Infarct volume assessment

- 2,3,5-Triphenyl- 2H- tetrazolium chloride (TTC) stain

The whole brains were cut into 2-mm coronal sections and immediately stained by 2% TTC (Sigma Aldrich) at 37°C for 30min. The infarct volume was calculated by Image J 1.42q and corrected for brain edema and contraction of infarct tissues.

2.4 Total RNA extraction and isolation from plated neuronal cultures

- RNeasy Mini Kit (50) (Qiagen Cat. No. 74104)
- Filtered pipette tips
- Pipetman
- Eppendorf tubes

RNA from samples was extracted using RNeasy Mini Kit according to the manufacturer's instructions. All pipette tips used for RNase-free and filtered. The following procedures were suited for 1 million cultured cells per sample.

2.5 Total RNA extraction from animal brain cortice

- Trizol reagent (Sigma-Aldrich-Aldrich Cat. No. 15596-018)
- RNeasy Mini Kit (50) (Qiagen Cat. No. 74104)
- Filtered pipette tips
- Pipetman
- Eppendorf tubes

At selected time-points post-reperfusion, animals were deeply anesthetized and then decapitated. Brains were reperused with ice-cold PBS, removed quickly and the infarct cortex was dissected. Cortex from the same hemisphere was removed from the sham control animals. The whole cortex was frozen immediately in liquid nitrogen, and stored at -80°C . Brain samples were ground and homogenized as described in (Bozinovski et al., 2002). Total RNA from homogenized cortex samples was extracted using the conventional phenol-chloroform extraction method with Trizol reagent. The obtained RNA samples were further purified using RNeasy Mini Kit according to the manufacturer's instructions. All pipette tips used were RNase-free and filtered.

2.6 Determination of RNA Concentration

- Distilled-treated water
- Total RNA samples
- Nanodrop ND-1000 Version 3.2.1

RNA concentration was determined by adding 1.5 μ l of the RNA sample on the pedestal of the equipment. The pedestal was thoroughly cleaned with distilled water using laboratory wipe before usage and measurement was blanked with water. It was necessary to ensure that the RNA solution was mixed well. Absorbance reading was taking at 260nm and 280nm. One unit of OD_{260nm} was equivalent to 40 μ g/ml RNA content. In this case, concentration of RNA was obtained by multiplying 40 to the absorbance reading at 260nm and then to 50 (dilution factor). Ratio of OD_{260nm}:OD_{280nm} would give the purity of the RNA sample.

2.7 Checking of RNA Quality

- RNA loading buffer (Sigma-Aldrich Cat. No. 1486)
- RNA dilution buffer
- Heat block
- E-gene HDA-GT12 genetic analyzer

1 μ l of total RNA sample was mixed with 1 μ l RNA loading buffer in 0.2ml tube. The mixture is heated at 70°C for 4min on a heat block and then spun down to collect any condensation. The total volume of the mixture was topped up to 10 μ l with the RNA

Dilution buffer and mix by gently pipetting up and down a few times. Sample mixtures were analyzed immediately on the E-gene HDA-GT12 System. Two bands, both 18S and 26S ribosomal RNA, should be observed at a ratio of 1:2 respectively.

2.8 cDNA Synthesis/ Reverse transcription

- Taqman reverse transcription reagents (Applied Biosystems)
- DEPC-treated water
- MicroAmp Optical Reaction tubes
- Filtered pipette tips
- Pipetman
- Thermal cycler

Reverse transcription was carried out according to steps specified by the manufacturer. In a 0.2ml microcentrifuge tube, a reaction mix was prepared for total RNA to be reversed transcribed. The following volumes were recommended for each sample.

Component	Per Sample (ul)
10X RT-buffer	1
25 mM MgCl ₂	2.2
deoxyNTPs Mixture	2
Random Hexamers	0.5
Rnase Inhibitor	0.2
Reverse Transcriptase (50 U/μl)	0.625
Total	6.525

In labelled microcentrifuge tube (MicroAmp Reaction Tube), volume corresponding to 200μg of each RNA sample was added to the reaction mix corresponding to one sample (6.525μl), and the volume of RNase-free water used was 3.475 – RNA sample volume in

a 10- μ l reaction (μ l). The tube was capped and centrifuged to eliminate any bubbles and force the solution to the bottom. All the reaction tubes were loaded into a thermal cycler.

The thermal cycler was set to the following conditions:

Step	Hexamer Incubation	Reverse Transcription	Reverse Transcription Inactivation
	HOLD	HOLD	HOLD
Temperature	25°C	37°C	95°C
Time	10min	60min	5min
Volume	10 μ l		

A primer incubation step of 25°C for 10min is necessary to maximise primer-RNA template binding when using random hexamers for first strand cDNA synthesis. 37°C for 60min in the reverse transcription step is necessary for reverse transcribing 18S only. After thermal cycling, all cDNA samples were stored at -15 to -25°C.

2.9 Real-time Polymerase Chain Reaction (Real-time PCR)

- Taqman Probes (Applied Biosystems)
- 18S Taqman Probe
- Taqman Master Mix
- DEPC-treated water
- cDNA
- 96-well optical reaction plates and adhesive cover
- Eppendorf tubes
- Pipetmans
- Filtered Pipette tips

- Benchtop microcentrifuge

Each sample was triplicated with three No Template Control (NTC) for each probe used. The PCR reaction master mix was prepared for No. of reactions \times 20 μ l (excluding the cDNA).

Reaction component	Per reaction (ul)
Taqman Universal Master Mix (2X)	12.5
20X Assay Mix of Gene of Interest	1.25
20X 18S RNA Assay Mix	1.25
cDNA (total 100 ng)	5
DEPC-treated Water	5
Total	25

20 μ l of the master mix was pipetted to the bottom of each well of the optical 96-well fast reaction plate. 5 μ l of cDNA or water (NTC) was added to the designated reaction well. The reaction plate was sealed with an Optical Adhesive Cover. The plate was then centrifuged at 4000rpm for 5min using the eppendorf centrifuge to eliminate air bubbles and force all solution to the bottom of well.

The plate was then read by the 7000 Fast Real-Time PCR System with the following conditions:

PCR Setup	Carryover decontamination via UNG	AmpliTag Gold Pre-activation	Melting Point	Anneal/Extend Step (Combined)
Temperature	50°C	95°C	95°C	60°C
Time	2min	10min	15s	1min
No. of cycles	1	1	40	

2.10 Microarray analysis

2.10.1 Microarray experiment using Illumina® Mouse Ref8 V1.1 / V2 and Rat Ref12

V1 hybridization beadchips

- Illumina® TotalPrep RNA Amplification Kit (Ambion)
- Total RNA
- RNase-free water
- Streptavidin-Cy3
- Hybridization and blocking buffers
- Streptavidin-Cy3

500ng total RNA sample was brought up to an initial start volume of 11µl. RNA was reverse transcribed to form first strand cDNA with the T7 Oligo(dT) Primer to synthesize cDNA containing a T7 promoter sequence., which was subsequently used for the second strand cDNA synthesis (employs DNA polymerase and Rnase H to simultaneously degrade the RNA and synthesize second strand cDNA). The cDNA were purified to remove RNA, primers, enzymes, and salts that would inhibit *in vitro* transcription. Finally *in vitro* transcription is employed to generate multiple copies of biotinylated cRNA from the double-stranded cDNA templates. All the previously mentioned procedures were performed using Illumina® TotalPrep RNA Amplification Kit. The yield of cRNA was quantitated using the NanoDrop ND-1000.

750ng cRNA in a total volume of 5µl RNase-free water was mixed with 10µl hybridization buffer and preheated to 65°C for 5min. The assay sample was then fully

loaded onto the large sample port of each array on the beadchip. After loading of all assay samples had been completed, the beadchip contained in the humidified hybridization chamber was placed in the 58°C oven for 17h. The following day, the IntelliHyb seal on the beadchip was removed to expose all the arrays. The arrays underwent different buffer wash, blocked, labeled with streptavidin-Cy3 and dried. The beadchip was then ready for scanning on the Illumina scanner using Bead Studio software at Scan Factor = 0.8 for mouse arrays and 0.65 for rat arrays.

The Illumina beadchips adopted in this Ph.D. study employ the single-channel (one-sample) format. For *Mus musculus* beadchip arrays, each array contains multiple replicates of gene-specific probes which enable the detection of transcriptional regulatory change for a total of 24,613 and 25,697 well-annotated RefSeq transcripts pooled from the NCBI, Meebo and RIKEN databases for V1.1 and V2 respectively. On the other hand, a pool of 22,523 RefSeq transcripts was observed for *Rattus norvegicus* beadchip arrays.

2.10.2 Microarray data collection and analysis

Initial analysis of the scanned images was performed using BeadScan (Illumina®). For absolute analysis, each chip was scaled to a target intensity of 1000-2000, and probe. The absolute data (signal intensity, detection call and detection P-value) were exported into GeneSpringGX 7.3 (Agilent Technologies, CA, USA) software for analysis by parametric test based on crossgene error model (PCGEM). One-way ANOVA approach is been used to identify differentially expressed genes.

Array data were globally normalized using GeneSpring® V7.3 software. Firstly, all of the measurements on each chip were divided by the 50th percentile value (per chip normalization). Secondly, each gene was normalized to the baseline value of the control samples (per gene normalization) using median. Then genes were filtered on fold change 1.5 fold against controls in at least one of total number of time-points or conditions to facilitate observation of gene regulatory trend, one-way ANOVA ($p < 0.05$) and Benjamini-Hochberg false discovery rate (FDR) Correction were used to seek differentially expressed genes. Genes which were differentially expressed are annotated according to Gene Ontology-Biological process provided by the online bioinformatics resources Database for Annotation, Visualization and Integrated Discovery (DAVID) 6.7 (<http://david.abcc.ncifcrf.gov/>) (Dennis et al., 2003; Huang et al., 2009). All microarray data reported here are described in accordance with MIAME guidelines, and has been deposited in the NCBI's Gene Expression Omnibus (GEO; <http://www.ncbi.nlm.nih.gov/geo/>).

2.11 Statistical analysis

All experiments were repeated at least three times. Data were analyzed using Tukey test with one-way analysis of variance (ANOVA) to assess significant differences in multiple comparisons. Values of $*p < 0.05$, $** p < 0.01$, $***p < 0.001$ were considered as statistically significant. Microarray data was expressed as mean \pm sem.

Chapter 3:
In vitro
Excitotoxicity
Models

3 Description of *in vitro* excitotoxicity models using cultured murine primary cortical neurons

Mouse Neocortical Neuronal Cell Culture Preparation

Neocortical neurons (gestational days 15 or 16) obtained from foetal cortices of Swiss albino mice were used to prepare the primary cultures employing previous described procedures with modifications (Cheung et al., 1998). Microdissected cortices were subjected to trypsin digestion and mechanical trituration. Cells were collected by centrifugation and resuspended in NB medium containing 2.5% B-27 supplement, 1% penicillin, 1% streptomycin, 0.25% GlutaMAX-1 supplement and 10% dialyzed FCS. 24-well plates previously coated with poly-D-lysine (100µg/ml) were seeded with cells to a density of 2×10^5 cells/cm² and used for subsequent experiments. The cultures were maintained in a humidified 5% CO₂ and 95% air incubator at 37°C. Immunocytochemical staining of the cultures at day 5 *in vitro* for microtubule-associated protein 2 and glia fibrillary acidic protein revealed > 95% of the cells were neurons with minimal contamination by glia (Cheung et al., 1998). All experiments involving animals were approved by the National University of Singapore, and were in accordance with the US Public Health Service guide for the care and use of laboratory animals.

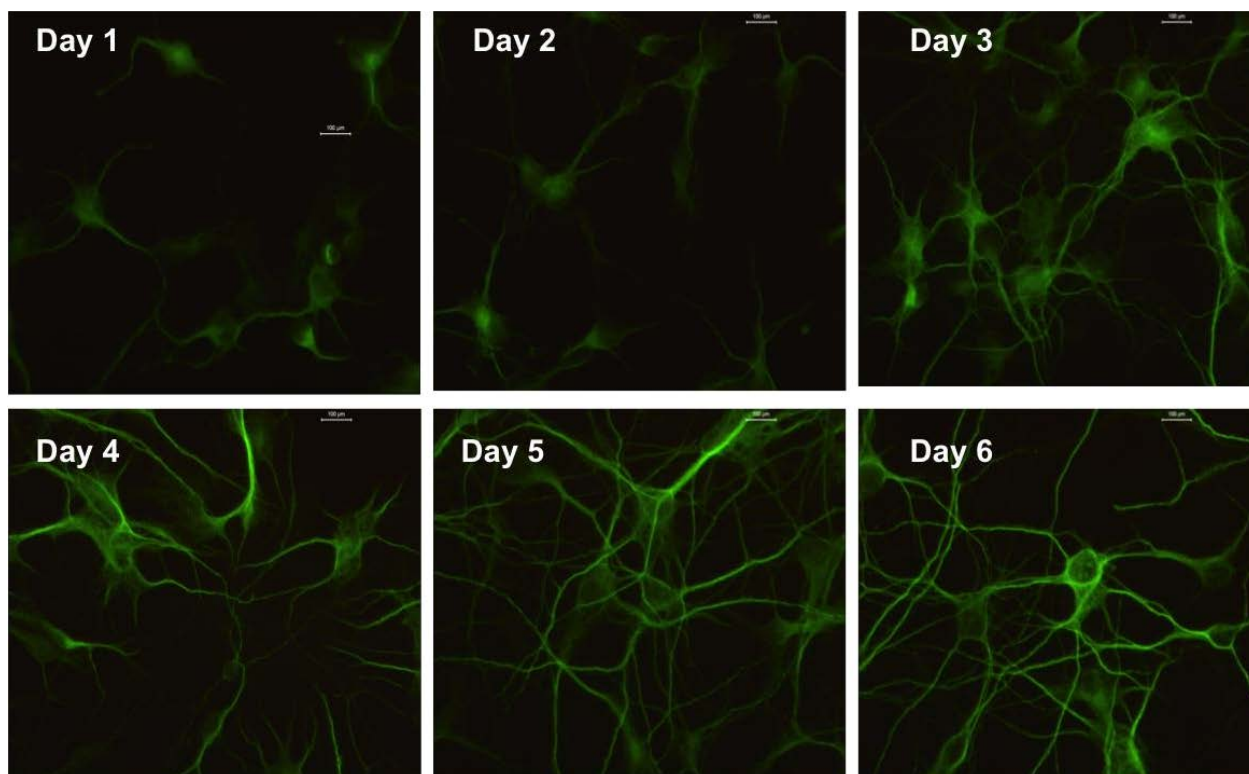


Figure 3.1 Immunohistochemistry assay employing the neuronal marker, microtubule-associated protein 2 (MAP2), demonstrated an increase in neurite outgrowths with increasing days of culture.

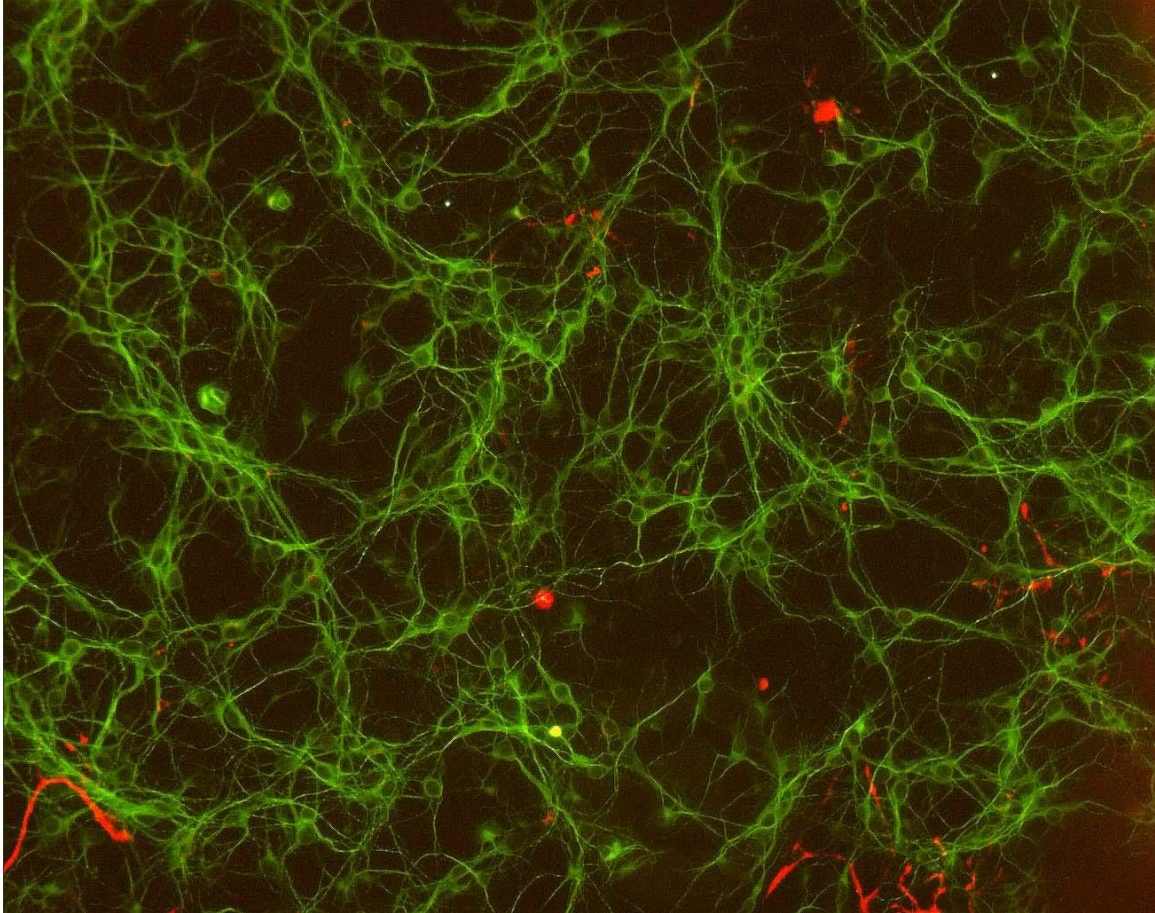


Figure 3.2 Double immunohistochemistry labeling using MAP2 (neuronal marker; Green) and glial fibrillary acidic protein (GFAP; astrocyte marker; Red) demonstrated more than 95% of the cultures comprises of neurons. (Published in Yew et al., 2005)

Drug preparation for application on neuronal cultures over a 24h period

All pharmacological drugs listed in the table below were freshly prepared individually in their respective solvent before each neuronal culture treatment. Desired concentrations were achieved via dilution with NB medium. EC₅₀ for each drug has been previously ascertained in our laboratory via 3-(4,5-Dimethylthiazol-2-yl)-2,5-diphenyltetrazolium bromide (MTT) colorimetric reduction cell viability assay, and this concentration is employed to induce neuronal injury over a 24-hour incubation period in day 7 cultured neurons. Total RNA was harvested at 5h, 15h and 24h post-treatment, and subjected to microarray analysis using Illumina® Mouse Ref8 V1 gene chips. For each treatment analysis via microarray, the arrays were assigned as follow: Control (n=6) and Treatment: 5h (n=3), 15h (n=3) and 24h (n=3). n represents the number of biological replicates. All microarray data reported here are described in accordance with MIAME guidelines, and has been deposited in the NCBI's Gene Expression Omnibus (GEO; <http://www.ncbi.nlm.nih.gov/geo/>) and are accessible through the following GEO Series accession number.

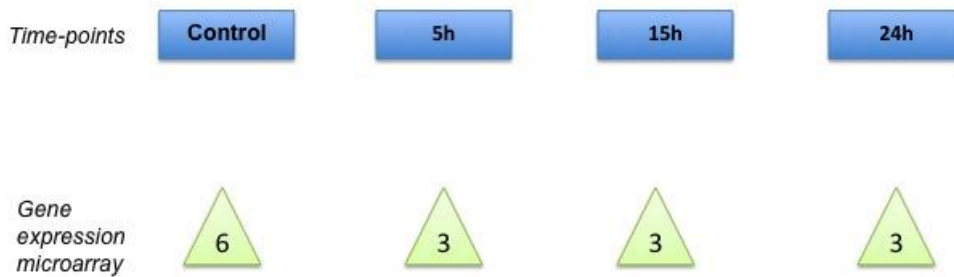
Drug Treatment	Solvent	Stock Concentration	Treatment concentration	GEO Accession
Sodium hydrosulphide (NaHS)	Water	100mM	200uM	GSE16035
Glu	100mM sodium hydroxide (NaOH)	100mM	250uM	GSE19936
NMDA	100mM NaOH	100mM	200uM	GSE16035
KA	100mM NaOH	100mM	100uM	GSE22994
AMPA	100mM NaOH	55mM	300uM	GSE22993

All drugs were purchased from Sigma-Aldrich.

Chapter 3:
***In vitro* excitotoxicity models**

NaHS have been widely adopted in many research studies as a convenient, water-soluble H₂S donor. NaHS dissociates to Na⁺ and HS⁻ in solution, then HS⁻ associates with H⁺ to produce H₂S. In physiological saline (pH 7.4) at 37°C, approximately 18.5 - 33% of the H₂S exists as the undissociated form (H₂S), and the remaining exists as HS⁻ at equilibrium with H₂S of a molar concentration of NaHS (Dombkowski et al., 2004; Zhao and Wang, 2002).

***In vitro* Excitotoxicity Model Experimental Plan**



- GluRs agonists of choice:***
- 300uM AMPA
 - 100uM KA
 - 200uM NMDA
 - 250uM L-glutamate

**Chapter 3.1:
Centralization of
GluRs signaling cascade in
Hydrogen Sulphide (H₂S) –
mediated neuronal injury**

3.1.1 Background information

A previous study in our laboratory had ascertained that the expression of iGluRs plays a pivotal role in the determination of H₂S-mediated neuronal effects (Cheung et al., 2007). Immunoblotting analysis was carried out to assess the expression of iGluRs in our *in vitro* primary neuronal cultures. From day 5 cultures, neurons showed initial expression of AMPARs and NMDARs with maximum expression optimized at day 7 and 8. In order to attribute the bi-functional effect of H₂S is a result of GluRs expression, day 3 (with no GluRs expression) and day 7 (stable GluRs level) were used for treatment-effect comparison.

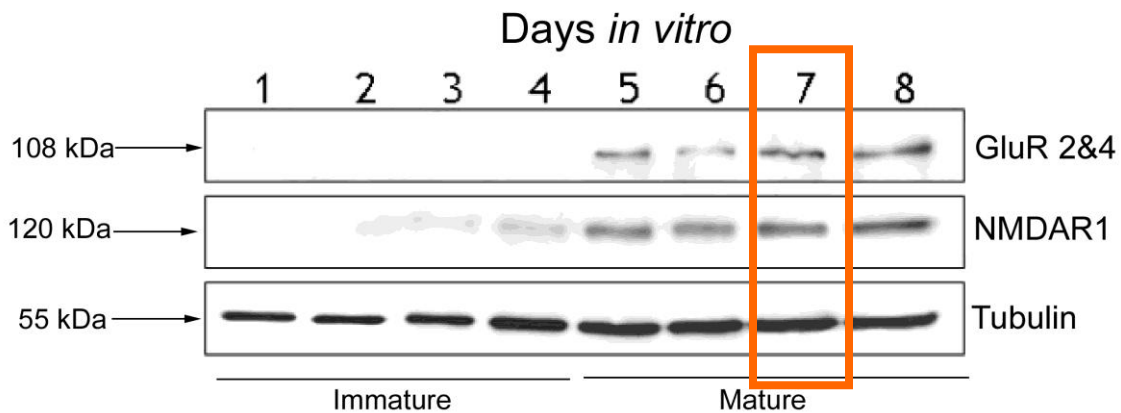


Figure 3.3 Differential expressions of GluRs (GluR2/4 - AMPARs; NMDAR1 - NMDARs) in cultured mouse primary cortical neurons from day 1-8 *in vitro*. Cultures of mouse embryonic day 15-16 cortical neurons were cultured in NB medium with B-27 and GlutaMAX supplements for up to 8 days *in vitro*. During this time cells were lysed and analyzed by western blotting for GluR 2/4 and NMDAR1 receptor expression. 10 μ g of proteins was loaded per lane. Data are representative of 3 or more immunoblots. Data published in Cheung et al., (2007).

Chapter 3.1: GluRs in H₂S neuronal injury

As shown in Figure 3.4, NaHS, a H₂S donor, induced a contrasting cell survival effect between day 3 and day 7 cultured neurons after 24h. Day 3 neurons treated with escalating doses of NaHS demonstrated consistent cell viability comparable to control, a phenomenon which occurred irrespective of NaHS treatment. Instead, in sharp contrast, NaHS induced a dose-dependent reduction in cell viability as revealed by the MTT reduction assay with an EC₅₀ of 200μM (Figure 3.4A). Concurrently, day 7 neurons when treated with NaHS concentrations less than or equal 200μM showed no significant occurrence of accidental necrosis as determined by lactate dehydrogenase (LDH) release. Upon treatment with NaHS doses above 200μM, LDH release was significantly elevated, an indication of neurons undergoing necrotic cell death (Cheung et al., 2007).

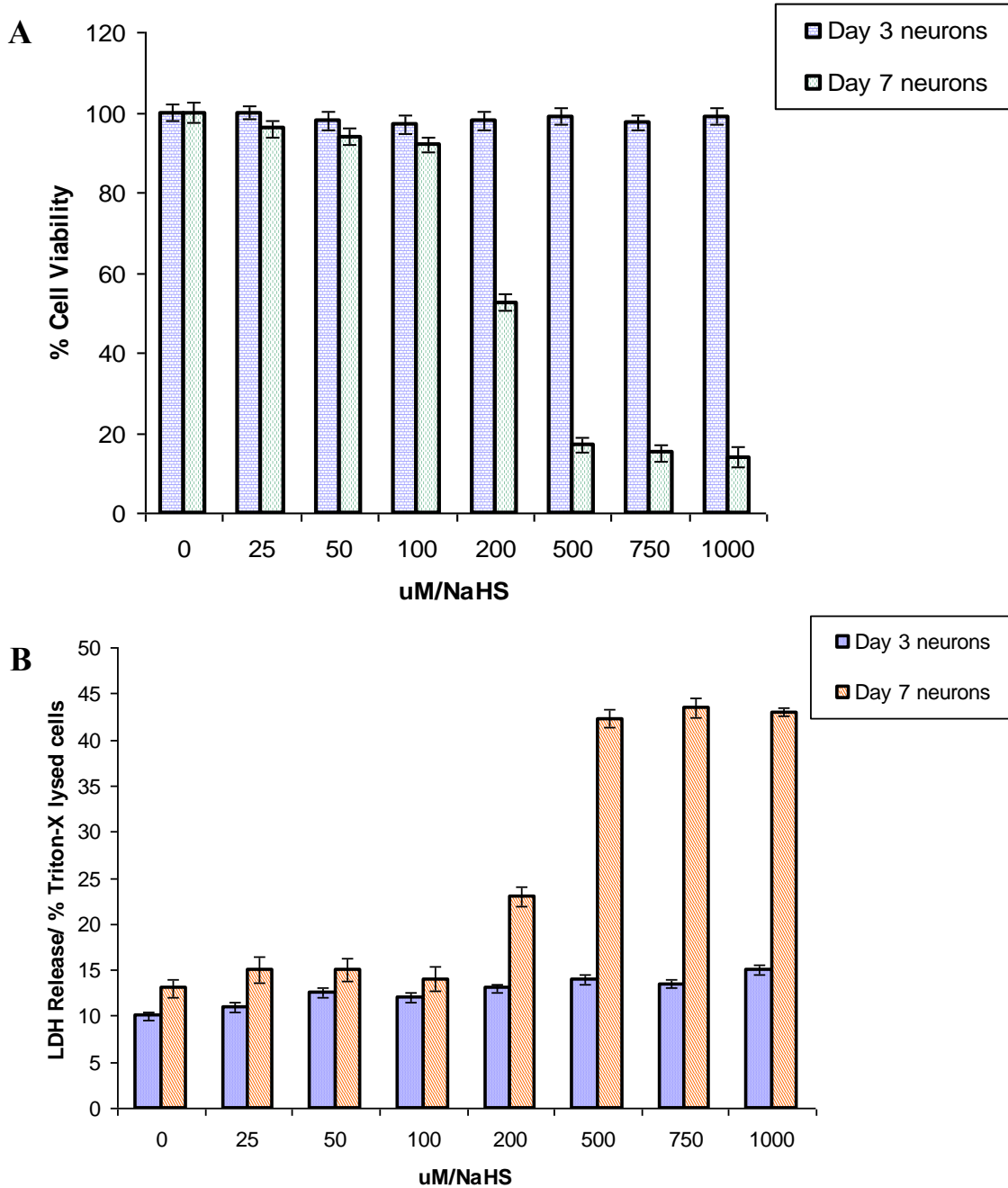


Figure 3.4 Concentration-dependent decrease in cell viability observed NaHS-treated day 7 neurons. Cells were exposed for 24h to NaHS at the stated concentrations and cell viability analyzed by **(A)** MTT and **(B)** LDH assays. Data are expressed as Mean \pm S. D. of 6 or more separate determinations. *** $p < 0.001$ compared to control neurons. Data published in Cheung et al., (2007).

Chapter 3.1: GluRs in H₂S neuronal injury

After having ascertained that sole application of NaHS induced neuronal death in day 7 neurons but not that of day 3 neurons, the present author then moved on to determine if co-application of NaHS would confer any effects on Glu-induced neuronal excitotoxicity. As demonstrated in Figure in day 3 neurons, 100 μ M Glu treatment was unable to cause any significant cell death due to lack of functional GluRs in trigger excitotoxicity. Instead, 25 μ M NaHS offers neuroprotection to day 3 neurons against oxidative stress-induced neuronal injury triggered by 100 μ M Glu.

On the contrary, in day 7 neurons, sole and co- administration of 100 μ M Glu with 25 μ M NaHS demonstrated a significant reduction of cell viability (Figure 3.5). This suggested that H₂S was capable of potentiating neuronal death when administered with Glu, by working synergistically with GluRs to induce neuronal death (Cheung et al., 2007).

Chapter 3.1:
GluRs in H₂S neuronal injury

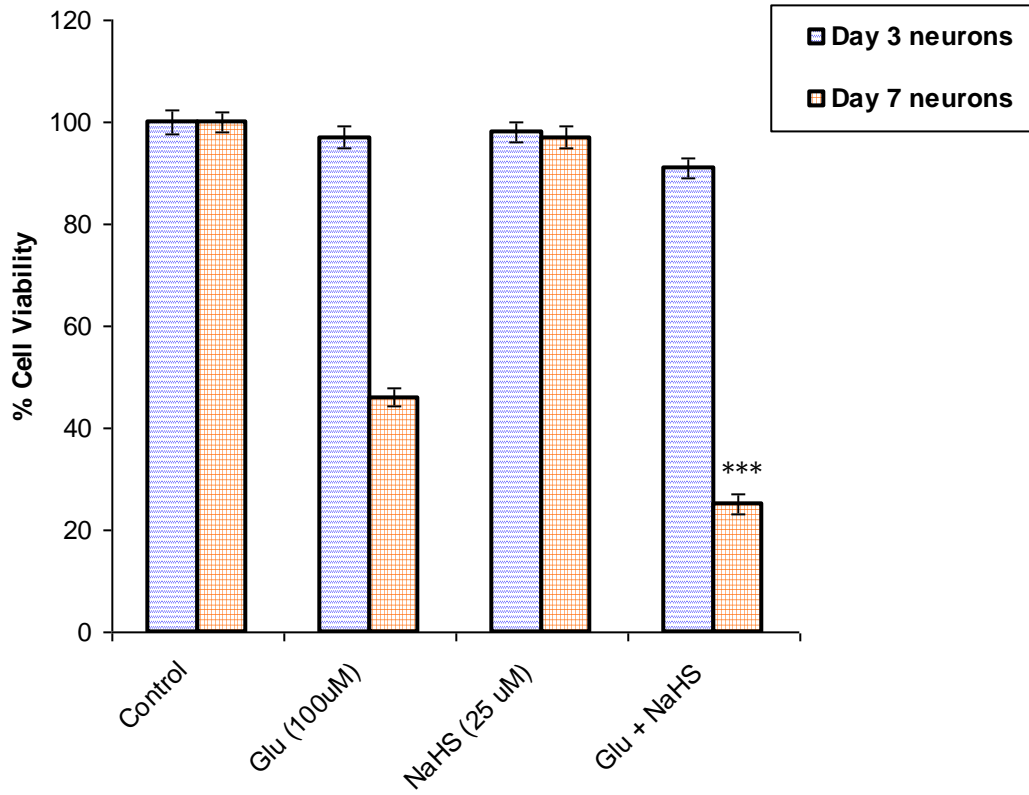


Figure 3.5 Potentiation of Glu-mediated neurotoxicity by NaHS application was seen only in day 7 neurons. Neurons were exposed to the stated conditions for 24h and cell viability assessed by MTT reduction assay. Data are expressed as Mean \pm S. D. of 6 or more separate determinations. *** $p < 0.001$ compared to Glu-treated neurons. Data published in Cheung et al., (2007).

Chapter 3.1: GluRs in H₂S neuronal injury

To determine which GluR subtypes were involved in the mediated of H₂S-induced neurotoxicity, various GluR subtype antagonists were employed to assess their effectiveness in attenuating H₂S-mediated neuronal death (Figure 3.6). Selective AMPAR antagonists, kynureate, GYKI52466 and CYZ20, were ineffective in the abrogation of H₂S-mediated neuronal death. Only application of pharmacological NMDAR antagonists, MK801 and APV, and KAR antagonist, CNQX was the neurotoxic effect of 200 μ M NaHS treatment able to be substantially attenuated, suggesting the importance of NMDARs and KARs activation in the triggering of H₂S-mediated receptor-dependent signaling pathway.

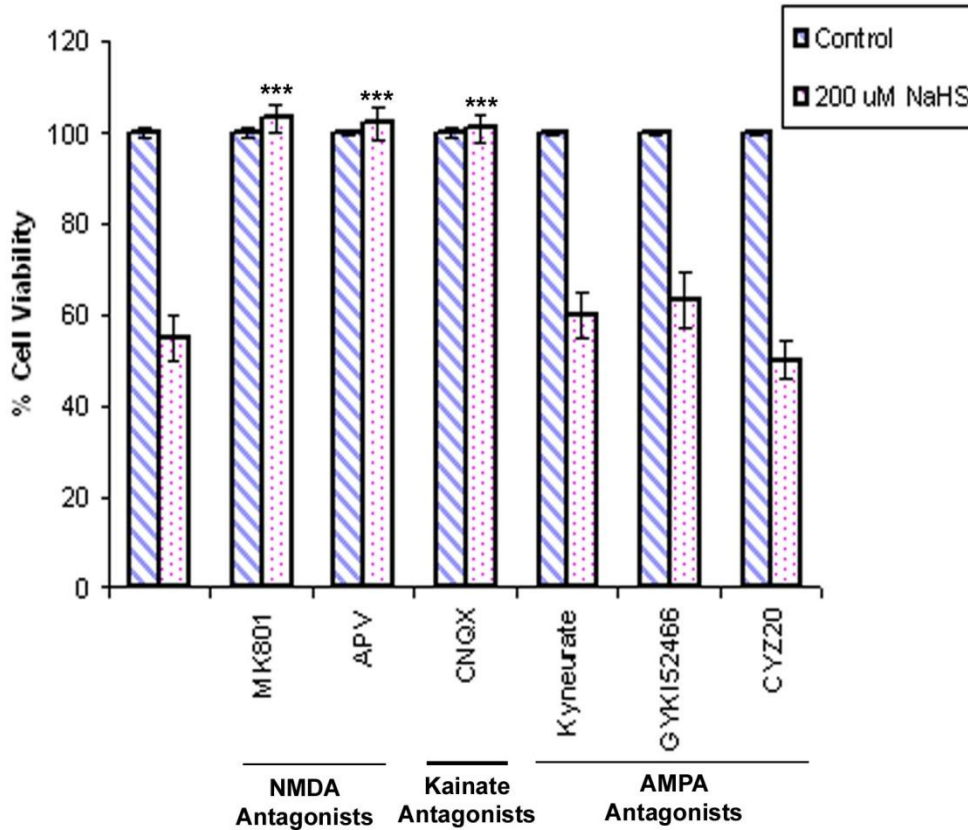


Figure 3.6 Successful attenuation of H₂S-induced neuronal death by NMDARs and KARs antagonists, which highlights the crucial role of NMDARs and KARs in the mediation of H₂S-induced receptor-dependent neurotoxicity. Day 7 neurons were treated with respective antagonists (10 μ M) for 1h prior to the addition of 200 μ M NaHS and incubated 24h. Data are expressed as Mean \pm S. D. of 6 or more separate determinations. *** p < 0.001 compared to NaHS (200 μ M) treated neurons. Data published in Cheung et al., (2007).

Chapter 3.1: GluRs in H₂S neuronal injury

From these published observations in Cheung et al., (2007), two conclusions can be drawn.

Conclusion 1: H₂S-mediated receptor-dependent signaling cascade is dependent on GluRs-activated signaling cascade.

Conclusion 2: H₂S-mediated neuronal injury revolves around iGluRs, particularly NMDARs and KARs, -induced excitotoxicity.

3.1.2 Introduction

Endogenous hydrogen sulphide (H₂S) expression has been detected in the brains of humans, rats and cattle (Goodwin et al., 1989; Savage and Gould, 1990; Warena et al., 1989) via the quantification of its release from acid-labile sulfur (Ishigami et al., 2009), indicating its physiological functions in the mammalian nervous system. *In vitro* quantification employing tissue homogenates indicated that H₂S is present in highest concentrations (three-folds of normal tissue level; 50-160μM) in the mammalian brain, liver and kidneys (Richardson et al., 2000). H₂S is produced intrinsically from the activity of key transsulfuration enzymes, cystathionine-γ-lyase (CSE), cystathionine-β-synthetase (CBS) and the recently discovered 3-mercaptopyruvate sulfurtransferase (3MST; reviewed in (Kimura, 2010)), all of which are expressed in the brain. CBS, whose activity is enhanced by a CBS activator, S-adenosyl methionine in the brain, plays a major role in the generation of H₂S.

It has been established under physiological condition, H₂S mediates NMDAR-triggered hippocampal LTP, an important cellular mechanism in regulation of synaptic plasticity and memory-building (Abe and Kimura, 1996). The underlying signaling process of H₂S-mediated NMDARs-dependent potentiation is unclear, but it has been suggested that redox modulation of thiol groups scattered along the extracellular domains of neuronal NMDARs, which are sensitive to oxidizing/reducing agents may be responsible. An identified likely redox modulatory site is the Cysteine pair (Cys744 and Cys798) located on the extracellular domains of the NR1 subunit (Sullivan et al., 1994).

Abnormal biosynthesis of H₂S has been implicated in the pathogenesis of several

Chapter 3.1: GluRs in H₂S neuronal injury

neurodegenerative diseases such as stroke (Qu et al., 2006), PD (Hu et al., 2010; Hu et al., 2009; Yin et al., 2009) and AD (Beyer et al., 2004; Clarke et al., 1998). Brains of AD patients possess substantially lower H₂S level, and higher levels of brain protein nitration by ONOO⁻ than normal subjects, without any change in L-cysteine level or CBS disease (Beyer et al., 2004; Clarke et al., 1998). In PD models, H₂S is reported to confer neuroprotection through attenuation of elevated ROS level, prevention of mitochondrial membrane potential loss, inhibition of microglial activation and accumulation of pro-inflammatory factors (e.g. TNF- α and NO) via the nuclear factor-kappaB (NF- κ B) pathway (Hu et al., 2010; Hu et al., 2009; Yin et al., 2009). On the contrary, H₂S is involved in the aggravation of cerebral ischemic damage (Qu et al., 2006). As such, the role of H₂S under different neuropathological conditions still remains elusive.

The role of H₂S under patho-physiological conditions in the brain remains equivocal. H₂S has previously been shown to confer neuroprotection mouse primary cortical neurons by acting as a free radical scavenger in the event of oxidative stress mediated by radical species such as H₂O₂, NO, ONOO⁻ and HOCl (Kimura et al., 2010; Whiteman et al., 2004; Whiteman et al., 2005a; Whiteman et al., 2006) and toxins such as rotenone (a commonly used toxin to establish PD models; (Hu et al., 2009)), and against oxidative Glu-mediated receptor-independent toxicity through elevation of intracellular glutathione levels and opening of K⁺_{ATP} and Cl⁻ channels (Kimura and Kimura, 2004). However, evidence from our previous study strongly favoured H₂S increasing Glu-induced cell death through a NMDAR-dependent pathway involving calpains rather than caspase-3 activation, with concomitant lysosomal rupture in GluRs-expressing cultured cortical

Chapter 3.1: GluRs in H₂S neuronal injury

neurons (Cheung et al., 2007). These apparently divergent results could well be explained through the existence of two forms of Glu toxicity; ionotropic receptor-initiated excitotoxicity and receptor-independent oxidative Glu toxicity (Murphy et al., 1989), which upon H₂S stimulates distinctive downstream signaling cascades. H₂S role as a neuroprotectant in Glu oxidative stress-mediated programmed cell death pathway occurring independent of iGluRs and thus, its cell death induction is not attenuated by antagonists of iGluRs (Murphy et al., 1989). It is triggered by high extracellular Glu concentrations in cultures of neurons lacking functional iGluRs where Glu competes with cystine (a major source of intracellular cysteine essential for glutathione biosynthesis) for cellular entry via the same amino acid transporter, resulting in decreased production of glutathione (a major antioxidant tripeptide made up of cysteine, Glu and glycine) and increased vulnerability to oxidative stress (Bannai and Kitamura, 1980). This observation has been consistently reported in primary cultures of neuronal cells (Kimura and Kimura, 2004), neuronal cell lines (Kimura et al., 2006; Murphy et al., 1989), and brain slices. H₂S-mediated neuroprotective effect is also extended to other oxidative stress agents, such as H₂O₂ (Kimura et al., 2010), NO (Whiteman et al., 2006), ONOO⁻ (Whiteman et al., 2004), myeloperoxidase-derived oxidant hypochlorous acid (HOCl) (Whiteman et al., 2005a) and rotenone (a commonly used toxin to establish Parkinson's disease models; Hu et al., 2009 (Hu et al., 2009)).

On the other hand, research work from our group provided evidence of H₂S involvement in the positive regulation of neuronal death in an iGluRs-expressing neuronal model which more closely resembles the adult mammalian brain (Cheung et al., 2007). This is

Chapter 3.1: GluRs in H₂S neuronal injury

in consistent with the report by Qu et al., (2006) that demonstrated in an *in vivo* adult rodent stroke model (i.e. functional GluRs), H₂S is a mediator of cerebral ischemic injury. Thus in presence of high levels of extracellular Glu during neuropathological conditions such as ischemia leads to constitutive activation of the iGluRs leading to excitotoxicity. This underscores the bi-directional neuromodulator role of H₂S determined by the presence/absence of iGluRs.

As a continuation of previous research findings, a comparative microarray strategy was employed to define the mechanistic significance of NMDARs and KARs involvement in H₂S-mediated neuronal death and hence to elucidate the consequent patterns of recruitment of cellular signaling.

3.1.3 Results

Previous data from our laboratory (Cheung et al., 2007) demonstrated that H₂S-mediated neuronal injury is highly dependent on the GluRs, particularly NMDARs and KARs, -induced excitotoxic pathways. In this current chapter, with particular emphasis placed on the importance of excitotoxicity in H₂S-mediated signaling pathway through employment of comparative analysis of H₂S, NMDA and KA global transcriptomic profiles using day 7 cultured murine primary cortical neurons as the basis of an *in vitro* model. Microarray analyses using Illumina® Mouse Ref8 V1.1 beadchips revealed differential, time-dependent global gene regulation in NaHS (a H₂S donor), NMDA and KA -treated cortical neurons. All differentially expressed genes in this study were selected based on the criteria of a minimum of ± 1.5 fold change in at least one out of three time-points and has passed statistical testing of one-way ANOVA, $p < 0.05$ and Benjamini-Hochberg FDR.

Cell viability assay conducted previously in our laboratory ascertained the EC₅₀ concentrations in cultured murine primary cortical neurons to be 100uM for KA and 200uM for NaHS and NMDA. These selected pharmacological dosages were employed respectively for neuronal culture treatment over a 24-hour period (5h, 15h and 24h) in preparation of total RNA samples for microarray study.

3.1.3.1 A high degree of global transcriptomic association between H₂S and NMDA/KA profiles: indication of high reliance of NMDARs and KARs –induced signaling transduction in H₂S-mediated neuronal injury

Out of a total of 24,613 well-annotated RefSeq transcripts, NaHS treatment generated a differentially regulated gene profile of 3,395 RefSeq transcripts, while NMDA and KA induced a significant transcriptional regulation in 2,309 and 3,800 transcripts. A Venn diagram comparison of the commonality of the gene probes regulated in all three profiles provided a total 1,510 transcript candidates. This figure amounted to a reasonably high, 44.4% overlapping transcriptional regulatory occurrence of H₂S profile attributed to that of NMDA and KA. Bi-model commonality comparison demonstrated a stunningly overlap of 82.7% (1,911 out of 2,309 RefSeq transcripts; Figure 3.7A) of NMDA profile, and a slightly lower, of 57.2% (2176 out of 3,800 RefSeq transcripts; Figure 3.7B) of KA profile being present in that of H₂S respectively.

As previous pharmacological inhibitor study has demonstrated AMPARs antagonists inability to inhibit H₂S-mediated neuronal injury, it would be important to verify if this observation was a result of receptor abundance or the diversity/minimal participation of the downstream signaling cascade contributing to excitotoxicity. As such, global gene profiling of specific AMPARs agonist, AMPA, was performed, generating a gene profile of 1,563 significantly differentially regulated RefSeq transcripts. This was followed by a bi-model comparison to that of H₂S. As shown in Figure 3.7C, 55.9% (842 out of 1,563 RefSeq transcripts) of AMPARs-mediated signaling cascade at the transcriptional level was present in H₂S-mediated neuronal injury. This implies that AMPARs also play a major role in H₂S-

Chapter 3.1: GluRs in H₂S neuronal injury

mediated neuronal damage, and as such the inability of AMPARs antagonists to attenuate neuronal death is most likely a result of physiological distribution of AMPARs, i.e. low receptor abundance coupled with the decreased in number of AMPARs with free permeability to Ca²⁺ on the post-synaptic membrane. Under physiological condition, NMDARs and KARs are present in greater abundance than AMPARs, explaining the effectiveness of selective NMDARs and KARs antagonists from previous pharmacological findings, thus concluding that NMDARs and KARs –triggered signaling cascades play a major role in H₂S-mediated neuronal damage.

To determine the downstream mechanistic implications that NMDARs and KARs activation played in H₂S induction of neuronal injury, the 1,510 RefSeq transcripts common to all three profiles were subjected to functional-gene ontology classification using DAVID 6.7 analysis (Figure 3.8). DAVID 6.7 provides a high-throughput and integrative data-mining bioinformatics environment, which is able to identify and assign biological definition through classification of co-functioning genes to biological annotations and statistically highlight those enriched (over-represented) annotations (Dennis et al., 2003; Huang et al., 2009). This exploratory, computational-cum-statistical instrument of clustering and enrichment is crucial in the identification of biological processes most pertinent to the biological phenomena of interest. DAVID interpretation recognized 1,215 biologically- and functionally-reported genes from various biological databases respectively for differentially regulated RefSeq transcripts common to all three treatments.

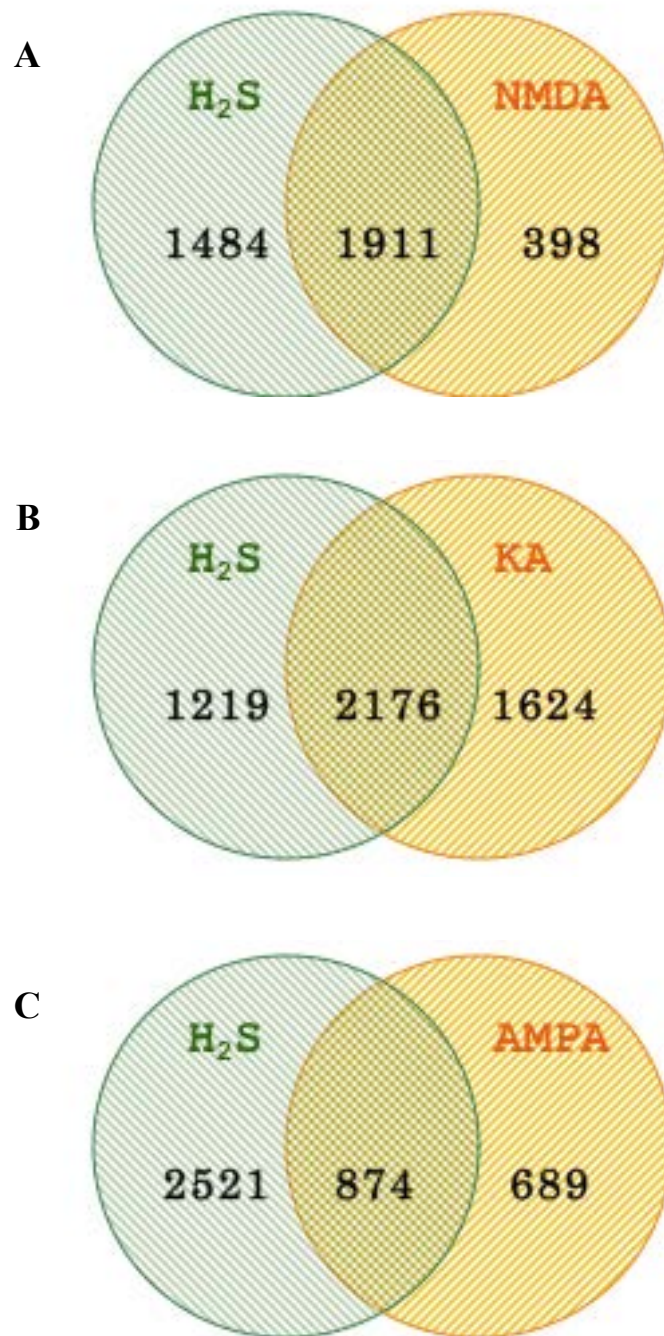


Figure 3.7 Bi-model global transcriptomic profile analysis of individual iGluRs agonists against H₂S-mediated neuronal injury model. Venn diagrams demonstrating the number of gene probes common and mutually exclusive to both models [A] H₂S against NMDA [B] H₂S against AMPA and [C] H₂S against KA.

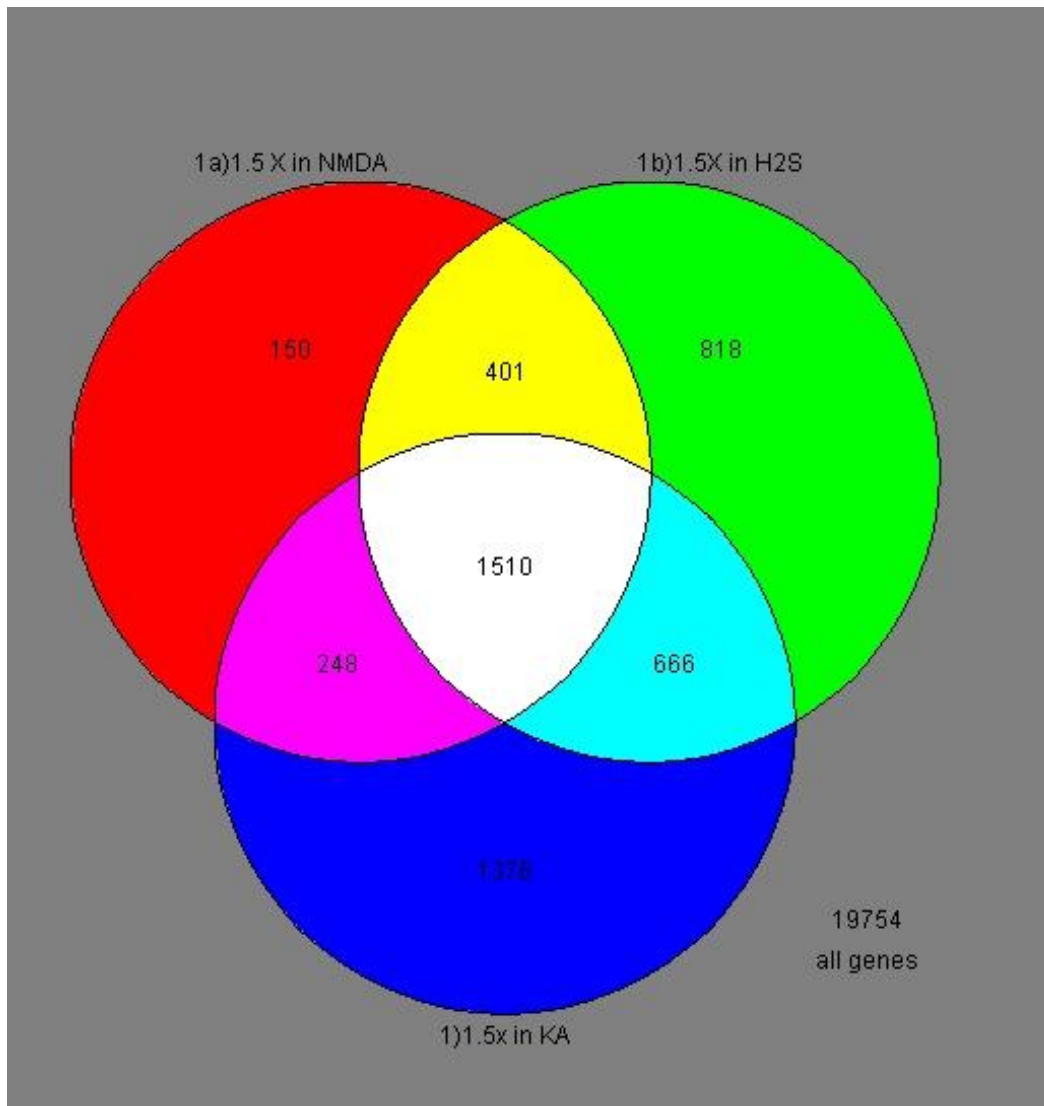


Figure 3.8 Venn diagram demonstrating the number of commonly occurring RefSeq transcripts overlapping across all three treatment profiles which have been subjected to the microarray analysis criteria of demonstrating at least ± 1.5 fold-change in one out of the three-points and passed statistical testing.

3.1.3.2 Functional-gene ontology classification revealed several key biological processes, crucial to neuronal survival/death

Since H₂S-mediated neuronal injury depends largely on NMDARs and KARs, which both simultaneously participate in the damage-inflicting excitotoxicity process, it could be deduced that excitotoxicity might be a primary, major upstream event assisting in H₂S induction of neuronal death. Indeed, functional clustering of the differentially expressed gene probes common to all three profiles demonstrated several significantly enriched biological pathways relevant to the progression of excitotoxicity. They are discussed in greater details below.

- CALCIUM ION BINDING AND INTERACTION

Cellular Ca²⁺ level is a key index for the progression of neuronal injury (Nagley et al., 2010) and majority of the genes encoding proteins involved in and/or required Ca²⁺ binding and interaction were significantly up-regulated between 5h and 15h post-treatment in all three neuronal injury models (Table 3.1).

- ENDOPLASMIC RETICULUM (ER) / LYSOSOMAL STRESS

Organellar stress, particularly that of the ER and lysosomes, was particularly prominent in H₂S, NMDA and KA profiles with significant transcriptional up-regulation of ER and lysosomal housing enzymatic (e.g. Retsat, Cln5 and Ctsz) and membrane (e.g. Lamp2, Laptm4b and Laptm5) proteins, and ER stress inducible genes (Cebpb and Notch1) (Table 3.1) taking place throughout the whole 24h profiling period. A recent article by Inoue et al., (2009) reported lysosomal-associated protein transmembrane 5 (LAPTM5)

Chapter 3.1: GluRs in H₂S neuronal injury

accumulation induces a non-apoptotic cell death with autophagic vacuoles and lysosomal destabilization with lysosomal-membrane permeabilization in a caspase-independent fashion (Inoue et al., 2009). On the other hand, lysosomal Atp6v0a1 and Ap1 which are respectively involved in the acidification of organellar compartment for generation of proton gradient and endocytotic synaptic vesicle recycling demonstrated significant down-regulation, a further indication of functional impairment of lysosomes.

- ANTI-OXIDANT RESPONSE

The elevation of cytosolic Ca²⁺ during excitotoxicity mediated by over-activation of iGluRs can inflict oxidative and electrophilic stresses (Higgins et al., 2010; McCullough et al., 2001). In response to the heightened cellular stress, substantial increase in the number of anti-oxidant enzymes with significant transcriptional up-regulation was induced, as a counteractive measure to suppress any oxidative and free radical stress-mediated damages (Table 3.1). These genes which encode for molecular chaperones and heat shock proteins (HSPs) were up-regulated from the 15h phase, and comprised of Bag3, ApoE, Hspb8, Hmox1, Serpinh1 (Hsp47) and metal ion chaperones, metallothioneins (Mt1 and Mt3). Up-regulation of the oxidative stress-inducible cytoprotective transcription factor, Nuclear factor, erythroid derived 2, like 2 (Nrf2), of which one of its downstream targets is Hmox1, was also observed. Prominently, numerous genes encoding for members of the major anti-oxidant glutathione (GSH) pathway, namely Gst (b1 and m6), mGst (1 and a4), Gsr and Idh2, demonstrated significant up-regulation from 15h.

- CELL DEATH

Majority of cell death cascade-involving genes such as *Angpt4*, *Casp6*, *Dap*, *Tnfrsf5* and *Adamt14* showed initial up-regulation at 15h post-treatment in all three neuronal injury models (Table 3.1). Interestingly, members of the intrinsic mitochondrial-dependent apoptotic pathway (*Casp3*, *Bok* and *Cidea*) and its endogenous inhibitor *Bcl-XL* all demonstrated a down-regulatory trend.

- CELL HOMEOSTASIS, SURVIVAL AND PROLIFERATION

Most of the pro-survival players including mitogenic factors (*Spp1*, *Nr2e1*, *Igf2*, *Cntf* and *Birc7*) demonstrated significant gene up-regulation across all three pharmacological types of neuronal death (Table 3.1).

- MITOTIC CELL CYCLE REGULATION

As shown in Table 3.1, microarray analysis revealed most genes that protect genome integrity, promote DNA repair and impede cell cycle re-activation, such as *Gadd45g*, *Ccng1*, *Cdk2* and *Ink4c* gene expression showed an up-regulatory role in NaHS, NMDA and KA treatment models.

Chapter 3.1:
GluRs in H₂S neuronal injury

Table 3.1 Gene expression profiles of neuronal death-related families in cultured day 7 mouse primary cortical neurons treated with 200µM NaHS, 200µM NMDA and 100µM KA respectively. All expression values (given as fold-changes) were selected based on having at least minimum of ±1.5 fold change in at least one out of three time-points subjected to one-way ANOVA analysis and Benjamini Hochberg FDR correction, and were significant at $p < 0.05$. Values are given as mean ± sem.

Genbank	Gene Title	Symbol	Time-points								
			200 µM NaHS			200 µM NMDA			100 µM KA		
			5 h	15 h	24 h	5 h	15 h	24 h	5 h	15 h	24 h
Calcium ion binding and interaction											
NM_011309	S100 calcium binding protein A1	S100a1	1.35 ± 0.23	1.57 ± 0.31	2.01 ± 0.36	1.24 ± 0.31	1.92 ± 0.40	1.63 ± 0.37	1.33 ± 0.26	1.77 ± 0.36	1.53 ± 0.34
NM_011313	S100 calcium binding protein A6 (calcyclin)	S100a6	1.74 ± 0.33	2.12 ± 0.43	3.48 ± 0.62	-1.02 ± 0.18	1.93 ± 0.38	1.91 ± 0.37	1.35 ± 0.24	2.12 ± 0.39	1.66 ± 0.30
NM_009113	S100 calcium binding protein A13	S100a13	1.04 ± 0.26	1.28 ± 0.39	1.81 ± 0.53	1.09 ± 0.36	1.50 ± 0.43	1.16 ± 0.32	1.23 ± 0.47	1.51 ± 0.44	1.57 ± 0.47
NM_007585	Annexin A2	Anxa2	1.22 ± 0.26	1.57 ± 0.43	2.50 ± 0.37	1.52 ± 0.25	1.93 ± 0.31	2.05 ± 0.43	2.31 ± 0.45	1.98 ± 0.34	1.48 ± 0.35
NM_013470	Annexin A3	Anxa3	1.59 ± 0.40	2.00 ± 0.70	4.98 ± 1.00	1.18 ± 0.31	3.64 ± 0.81	3.23 ± 0.63	1.01 ± 0.23	1.95 ± 0.43	1.61 ± 0.42
NM_009673	Annexin A5	Anxa5	1.23 ± 0.26	1.43 ± 0.34	2.42 ± 0.48	1.15 ± 0.20	1.69 ± 0.29	1.61 ± 0.38	-1.02 ± 0.19	1.50 ± 0.33	1.10 ± 0.21
NM_008861	Polycystic kidney disease 2	Pkd2	1.04 ± 0.25	1.28 ± 0.35	1.57 ± 0.30	1.14 ± 0.27	1.54 ± 0.28	1.48 ± 0.31	1.39 ± 0.24	1.65 ± 0.30	1.23 ± 0.25
NM_007616	Caveolin, caveolae protein 1	Cav1	1.07 ± 0.26	1.12 ± 0.28	1.55 ± 0.37	1.48 ± 0.37	1.04 ± 0.19	-1.31 ± 0.19	1.69 ± 0.46	-1.21 ± 0.18	-1.96 ± 0.15
NM_012056	FK506 binding protein 9	Fkbp9	1.23 ± 0.30	1.54 ± 0.47	2.40 ± 0.42	1.43 ± 0.30	2.24 ± 0.43	1.44 ± 0.30	1.20 ± 0.23	1.98 ± 0.39	1.40 ± 0.31
NM_016863	FK506 binding protein 1b	Fkbp1b	-1.11 ± 0.25	-1.20 ± 0.26	-2.77 ± 0.11	-1.25 ± 0.23	-1.80 ± 0.15	-1.27 ± 0.22	-1.02 ± 0.33	-1.81 ± 0.15	-1.68 ± 0.16
NM_008855	Protein kinase C, beta 1	Pkcb1	-1.26 ± 0.19	-1.38 ± 0.29	-3.45 ± 0.05	-1.03 ± 0.28	-2.76 ± 0.16	-2.61 ± 0.12	-1.04 ± 0.20	-1.82 ± 0.10	-2.38 ± 0.08
Endoplasmic reticulum/lysosomal stress											
NM_009883	CCAAT/enhancer binding protein (C/EBP) beta (Cebpb)	Cebpb	-1.24 ± 0.17	-1.06 ± 0.18	1.88 ± 0.34	1.79 ± 0.39	1.41 ± 0.23	1.84 ± 0.48	4.79 ± 0.95	2.26 ± 0.40	2.14 ± 0.40
NM_026159	Retinol saturase	Retsat	1.28 ± 0.25	1.66 ± 0.65	2.05 ± 0.39	1.31 ± 0.29	2.55 ± 0.50	1.30 ± 0.21	-1.25 ± 0.21	2.26 ± 0.38	1.46 ± 0.80
NM_008714	Notch gene homolog 1 (drosophilia)	Notch1	1.13 ± 0.25	1.55 ± 0.52	2.51 ± 0.50	1.32 ± 0.26	2.25 ± 0.43	1.66 ± 0.38	-1.09 ± 0.19	2.39 ± 0.44	1.68 ± 0.37

Chapter 3.1:
GluRs in H₂S neuronal injury

Table 3.1 (continued)

Genbank	Gene Title	Symbol	Time-points								
			200 μ M NaHS			200 μ M NMDA			100 μ M KA		
			5 h	15 h	24 h	5 h	15 h	24 h	5 h	15 h	24 h
Endoplasmic reticulum/lysosomal stress (continue)											
NM_009906	Tripeptidyl peptidase i	Cln2	1.15 ± 0.28	1.45 ± 0.47	1.67 ± 0.40	1.24 ± 0.36	1.70 ± 0.40	1.31 ± 0.31	1.52 ± 0.40	1.95 ± 0.53	1.65 ± 0.54
XM_127882	Ceroid lipofuscinosis, neuronal 5	Cln5	1.09 ± 0.26	1.44 ± 0.55	2.82 ± 0.53	1.83 ± 0.43	2.25 ± 0.45	1.61 ± 0.30	1.29 ± 0.32	1.90 ± 0.41	1.37 ± 0.35
NM_019972	Sortilin 1	Nltr3	1.11 ± 0.33	1.29 ± 0.38	2.03 ± 0.55	1.52 ± 0.45	3.71 ± 0.81	2.47 ± 0.64	1.21 ± 0.38	1.71 ± 0.50	1.56 ± 0.53
NM_022325	Cathepsin Z	Ctsz	1.13 ± 0.30	1.35 ± 0.45	1.98 ± 0.62	1.35 ± 0.43	1.79 ± 0.44	1.44 ± 0.40	1.34 ± 0.50	1.65 ± 0.48	1.57 ± 0.52
NM_001017 959	Lysosomal-associated membrane protein 2	Lamp2	1.63 ± 0.30	2.23 ± 0.41	1.54 ± 0.34	1.44 ± 0.31	2.31 ± 0.41	1.77 ± 0.43	1.63 ± 0.30	2.23 ± 0.41	1.54 ± 0.34
NM_033521	Lysosomal-associated protein transmembrane 4B	Laptm4b	1.08 ± 0.38	1.61 ± 0.50	1.70 ± 0.47	1.37 ± 0.50	1.84 ± 0.47	1.45 ± 0.48	1.38 ± 0.54	1.86 ± 0.68	1.56 ± 0.68
NM_010686	Lysosomal-associated protein transmembrane 5	Laptm5	1.46 ± 0.26	1.47 ± 0.27	3.95 ± 0.71	1.71 ± 0.46	2.31 ± 0.98	2.13 ± 0.34	-1.52 ± 0.18	1.81 ± 0.34	1.36 ± 0.50
NM_016920	ATPase, H ⁺ transporting, lysosomal V0 subunit A1	Atp6Voa1	-1.24 ± 0.20	-1.24 ± 0.29	-2.29 ± 0.08	-1.28 ± 0.17	-1.99 ± 0.10	-1.21 ± 0.26	1.54 ± 0.36	-1.36 ± 0.16	-1.50 ± 0.24
NM_007457	Adaptor protein complex AP-1, sigma 1	Ap1	-1.16 ± 0.22	-1.12 ± 0.23	-2.18 ± 0.13	-1.25 ± 0.23	-1.58 ± 0.16	-1.47 ± 0.21	1.01 ± 0.31	-1.67 ± 0.15	-1.69 ± 0.19
Anti-oxidant response											
NM_013863	Bcl2-associated athanogene 3	Bag3	1.18 ± 0.19	1.59 ± 0.48	2.62 ± 0.41	2.28 ± 0.47	2.65 ± 0.36	2.44 ± 0.48	2.52 ± 0.37	2.49 ± 0.37	2.09 ± 0.31
NM_009696	Apolipoprotein E	ApoE	1.25 ± 0.20	1.58 ± 0.54	2.19 ± 0.40	1.15 ± 0.27	2.28 ± 0.52	1.75 ± 0.27	1.31 ± 0.28	2.36 ± 0.43	1.98 ± 0.36
NM_029688	Sulfiredoxin 1 homolog (S. cerevisiae)	Npn3	1.14 ± 0.36	1.59 ± 0.78	3.73 ± 0.63	1.91 ± 0.39	1.62 ± 0.28	1.02 ± 0.19	2.68 ± 0.80	1.73 ± 0.43	1.21 ± 0.38
NM_030704	Heat shock 27kDa protein 8	Hspb8	1.35 ± 0.35	1.97 ± 1.33	4.00 ± 0.75	1.98 ± 0.46	3.85 ± 0.80	1.83 ± 0.46	1.42 ± 0.37	2.61 ± 0.59	1.60 ± 0.38
NM_013602	Metallothionein 1	Mt1	1.15 ± 0.19	1.56 ± 0.72	2.19 ± 0.35	1.58 ± 0.25	1.97 ± 0.34	1.47 ± 0.24	1.97 ± 0.40	2.29 ± 0.38	1.92 ± 0.38
NM_013603	Metallothionein 3	Mt3	1.16 ± 0.20	1.58 ± 0.52	1.94 ± 0.32	1.35 ± 0.27	1.90 ± 0.27	1.77 ± 0.55	2.34 ± 0.48	1.90 ± 0.34	2.01 ± 0.49

Table 3.1 (continued)

Genbank	Gene Title	Symbol	Time-points								
			200 μ M NaHS			200 μ M NMDA			100 μ M KA		
			5 h	15 h	24 h	5 h	15 h	24 h	5 h	15 h	24 h
Anti-oxidant response (continue)											
NM_016892	Copper chaperone for superoxide dismutase	Ccs	1.17 ± 0.22	1.45 ± 0.31	1.63 ± 0.27	1.47 ± 0.32	1.90 ± 0.33	1.46 ± 0.26	1.27 ± 0.27	1.69 ± 0.30	1.43 ± 0.34
NM_009825	Serine (or cysteine) proteinase inhibitor clade H member 1	Serpinh1	1.04 ± 0.19	1.44 ± 0.55	2.23 ± 0.46	1.69 ± 0.31	2.02 ± 0.39	1.12 ± 0.24	1.27 ± 0.23	1.58 ± 0.27	1.08 ± 0.23
NM_016764	Peroxiredoxin 4	Prdx4	1.11 ± 0.25	1.33 ± 0.25	1.79 ± 0.28	1.31 ± 0.31	1.65 ± 0.31	1.40 ± 0.27	1.66 ± 0.31	1.53 ± 0.26	1.24 ± 0.24
NM_010902	Nuclear factor, erythroid derived 2, like 2	Nrf2	1.22 ± 0.33	1.37 ± 0.39	2.66 ± 0.77	1.65 ± 0.49	2.00 ± 0.45	1.26 ± 0.33	1.59 ± 0.53	1.70 ± 0.66	1.25 ± 0.40
NM_010442	Heme oxygenase (decycling) 1	Hmox1	-1.05 ± 0.19	1.45 ± 0.77	4.40 ± 0.67	2.70 ± 0.58	3.11 ± 0.48	1.59 ± 0.29	2.34 ± 0.39	2.17 ± 0.39	2.04 ± 0.37
NM_145079	Udp glucuronosyltransferase 1 family, polypeptide a6a	Ugta6a	1.39 ± 0.37	1.52 ± 0.39	2.53 ± 0.57	1.07 ± 0.35	1.93 ± 0.45	2.03 ± 0.46	1.38 ± 0.42	2.19 ± 0.56	1.92 ± 0.54
NM_010358	Glutathione S-transferase, mu 1	Gstb1	1.37 ± 0.25	1.88 ± 0.60	2.57 ± 0.51	1.45 ± 0.32	2.23 ± 0.46	1.43 ± 0.30	1.57 ± 0.33	2.12 ± 0.40	1.42 ± 0.40
NM_008184	Glutathione S-transferase, mu 6	Gstm6	1.25 ± 0.42	1.86 ± 0.55	2.11 ± 0.54	1.45 ± 0.45	2.09 ± 0.63	1.34 ± 0.35	1.52 ± 0.50	1.89 ± 0.52	1.18 ± 0.36
NM_013541	Glutathione S-transferase, pi 1	Gstp1	-1.23 ± 0.15	-1.04 ± 0.19	-1.66 ± 0.12	-1.13 ± 0.20	-1.41 ± 0.14	-1.71 ± 0.11	1.19 ± 0.23	-1.51 ± 0.15	-1.79 ± 0.14
NM_019946	Microsomal glutathione s-transferase 1	mGst	1.52 ± 0.39	2.14 ± 1.12	3.68 ± 0.72	1.71 ± 0.42	2.96 ± 0.60	1.67 ± 0.37	1.41 ± 0.44	2.55 ± 0.53	1.91 ± 0.51
NM_025569	Microsomal glutathione S-transferase 3	mGst3	-1.28 ± 0.13	-1.33 ± 0.21	-3.87 ± 0.06	-1.39 ± 0.17	-2.15 ± 0.11	-1.99 ± 0.11	-1.03 ± 0.23	-2.27 ± 0.08	-2.31 ± 0.09
NM_010357	Glutathione s-transferase, alpha 4	mGsta4	1.74 ± 0.34	2.35 ± 1.05	3.83 ± 0.93	1.29 ± 0.39	3.05 ± 0.70	2.14 ± 0.52	1.14 ± 0.31	2.30 ± 0.60	2.03 ± 0.48
NM_010344	Glutathione reductase 1	Gsr	1.24 ± 0.33	1.57 ± 0.40	1.90 ± 0.42	1.42 ± 0.38	1.62 ± 0.42	1.18 ± 0.30	1.69 ± 0.49	1.31 ± 0.36	1.12 ± 0.36
NM_010497	Isocitrate dehydrogenase 1 (NADP+), soluble	Idh1	-1.10 ± 0.17	1.00 ± 0.18	-1.76 ± 0.09	1.12 ± 0.27	-1.46 ± 0.13	-1.75 ± 0.10	1.11 ± 0.23	-2.08 ± 0.09	-2.69 ± 0.10
NM_173011	Isocitrate dehydrogenase 2 (NADP+), mitochondrial	Idh2	1.03 ± 0.25	1.51 ± 0.77	1.79 ± 0.50	1.59 ± 0.48	2.23 ± 0.62	1.43 ± 0.34	1.60 ± 0.46	2.22 ± 0.62	1.86 ± 0.66

Chapter 3.1:
GluRs in H₂S neuronal injury

Table 3.1 (continued)

Genbank	Gene Title	Symbol	Time-points								
			200 μ M NaHS			200 μ M NMDA			100 μ M KA		
			5 h	15 h	24 h	5 h	15 h	24 h	5 h	15 h	24 h
Cell death											
NM_020581	Angiopoietin-like 4	Angptl4	2.20 ± 0.84	3.44 ± 3.73	9.33 ± 1.72	1.52 ± 0.44	2.50 ± 0.66	1.49 ± 0.38	4.74 ± 0.84	11.98 ± 2.14	10.21 ± 2.28
NM_009811	Caspase 6	Casp6	1.28 ± 0.29	1.58 ± 0.56	2.44 ± 0.49	1.52 ± 0.39	2.42 ± 0.48	1.74 ± 0.27	1.29 ± 0.30	2.08 ± 0.35	1.59 ± 0.36
NM_009810	Caspase 3 apoptosis related cysteine protease	Casp3	-1.13 ± 0.21	-1.19 ± 0.28	-2.33 ± 0.09	1.17 ± 0.31	-2.03 ± 0.18	-2.01 ± 0.09	1.13 ± 0.26	-1.62 ± 0.14	-2.33 ± 0.13
NM_146057	Death-associated protein	Dap	1.30 ± 0.28	1.63 ± 0.43	1.97 ± 0.44	1.34 ± 0.27	1.93 ± 0.38	1.39 ± 0.27	1.23 ± 0.34	1.81 ± 0.39	1.41 ± 0.38
NM_009818	Catenin (cadherin associated protein), alpha 1	Ctnna1	1.28 ± 0.24	1.63 ± 0.41	2.68 ± 0.40	1.55 ± 0.28	2.39 ± 0.33	1.78 ± 0.32	1.29 ± 0.23	2.09 ± 0.29	1.43 ± 0.27
NM_013749	Tumor necrosis factor receptor superfamily, member 12a	Tnfrsf12a	-1.02 ± 0.22	1.12 ± 0.26	3.20 ± 0.59	1.72 ± 0.46	1.53 ± 0.31	1.21 ± 0.27	3.05 ± 0.63	2.05 ± 0.48	1.31 ± 0.28
NM_011609	Tumor necrosis factor receptor superfamily, member 1a	Tnfrsf1a	1.16 ± 0.30	1.51 ± 0.52	2.59 ± 0.57	1.70 ± 0.55	2.09 ± 0.58	1.30 ± 0.29	1.13 ± 0.27	1.53 ± 0.33	1.03 ± 0.30
NM_144899	Adamts-like 4	Adamt14	1.30 ± 0.32	1.35 ± 0.29	1.63 ± 0.34	1.02 ± 0.28	1.77 ± 0.35	1.65 ± 0.37	-1.07 ± 0.25	1.77 ± 0.41	1.39 ± 0.35
NM_009743	Bcl2-like 1	Bcl2l1/ Bcl-XL	-1.06 ± 0.20	-1.20 ± 0.35	-1.89 ± 0.12	-1.38 ± 0.18	-1.62 ± 0.15	-1.21 ± 0.22	1.26 ± 0.22	-1.77 ± 0.16	-1.83 ± 0.15
NM_016778	BCL2-related ovarian killer protein	Bok	-1.09 ± 0.16	-1.05 ± 0.24	-2.10 ± 0.08	1.02 ± 0.19	-1.57 ± 0.12	-1.74 ± 0.12	-1.08 ± 0.14	-1.47 ± 0.12	-1.65 ± 0.12
NM_001025 296	Cell death-inducing DNA fragmentation factor, alpha subunit	Cidea	-1.14 ± 0.21	-1.18 ± 0.24	-1.81 ± 0.14	-1.12 ± 0.25	-1.63 ± 0.19	-1.53 ± 0.17	1.45 ± 0.21	-1.52 ± 0.19	-1.58 ± 0.21
Cell homeostasis, survival and proliferation											
NM_009263	Secreted phosphoprotein 1	Spp1	2.07 ± 0.42	1.80 ± 0.96	5.52 ± 1.40	1.85 ± 0.83	3.35 ± 3.20	4.30 ± 1.17	-1.01 ± 0.32	2.43 ± 0.68	2.23 ± 0.67
NM_010234	Fbj osteosarcoma oncogene	c-Fos	-1.69 ± 0.16	-1.58 ± 0.14	1.56 ± 0.41	2.81 ± 0.72	7.73 ± 2.49	13.41 ± 9.70	53.97 ± 10.04	27.35 ± 4.76	19.53 ± 3.89
NM_152229	Nuclear receptor subfamily 2, group e, member 1	Nr2e1	1.12 ± 0.21	1.57 ± 0.58	1.67 ± 0.32	1.37 ± 0.35	1.94 ± 0.32	1.56 ± 0.50	1.86 ± 0.40	2.25 ± 0.42	1.68 ± 0.35

Chapter 3.1:
GluRs in H₂S neuronal injury

Table 3.1 (continued)

Genbank	Gene Title	Symbol	Time-points								
			200 μ M NaHS			200 μ M NMDA			100 μ M KA		
			5 h	15 h	24 h	5 h	15 h	24 h	5 h	15 h	24 h
Cell homeostasis, survival and proliferation (continued)											
NM_010514	Insulin-like growth factor 2	Igf2	1.15 ± 0.25	1.66 ± 1.04	1.74 ± 0.38	1.56 ± 0.36	1.72 ± 0.41	1.24 ± 0.28	1.78 ± 0.35	2.06 ± 0.43	1.56 ± 0.39
NM_010053	Distal-less homeobox	Dlx1	1.20 ± 0.27	1.31 ± 0.28	1.52 ± 0.31	1.40 ± 0.37	1.92 ± 0.57	1.98 ± 0.71	1.50 ± 0.32	1.47 ± 0.26	1.33 ± 0.34
NM_053007	Ciliary neurotropic factor	Cntf	1.11 ± 0.24	1.18 ± 0.32	1.43 ± 0.30	1.18 ± 0.27	1.50 ± 0.41	1.24 ± 0.29	1.57 ± 0.52	1.51 ± 0.39	1.37 ± 0.52
NM_001025 250	Vascular endothelial growth factor A	Vegfa	-1.80 ± 0.16	-1.40 ± 0.21	-1.01 ± 0.25	1.15 ± 0.46	-1.47 ± 0.16	-1.69 ± 0.13	-1.23 ± 0.17	-1.74 ± 0.16	-2.41 ± 0.13
XM_283820	Baculoviral IAP repeat-containing 7 (livin)	Birc7	1.14 ± 0.31	1.45 ± 0.48	1.76 ± 0.46	1.08 ± 0.44	1.59 ± 0.43	1.39 ± 0.40	1.15 ± 0.45	1.90 ± 0.59	1.56 ± 0.49
Mitotic cell cycle regulation											
NM_007891	E2F transcription factor 1	E2f1	-1.09 ± 0.19	-1.01 ± 0.25	-1.52 ± 0.13	1.15 ± 0.27	-1.53 ± 0.14	-1.50 ± 0.14	1.35 ± 0.24	-1.60 ± 0.14	-1.77 ± 0.14
NM_007631	Cyclin D1	Ccnd1	-1.31 ± 0.21	-1.20 ± 0.24	-1.80 ± 0.14	-1.04 ± 0.33	-1.96 ± 0.12	-1.98 ± 0.12	1.55 ± 0.46	-1.04 ± 0.27	-1.67 ± 0.16
NM_009831	Cyclin G1	Ccng1	1.26 ± 0.23	1.43 ± 0.31	2.75 ± 0.58	1.30 ± 0.34	1.55 ± 0.33	1.25 ± 0.34	1.53 ± 0.33	1.35 ± 0.25	-1.01 ± 0.22
NM_016756	Cyclin-dependent kinase 2	Cdk2	1.08 ± 0.19	1.24 ± 0.31	1.62 ± 0.32	1.60 ± 0.28	1.48 ± 0.26	1.33 ± 0.29	1.55 ± 0.39	1.31 ± 0.29	1.16 ± 0.30
NM_007668	Cyclin-dependent kinase 5	Cdk5	-1.24 ± 0.15	-1.26 ± 0.20	-2.92 ± 0.08	-1.29 ± 0.46	-2.25 ± 0.10	-1.86 ± 0.15	-1.11 ± 0.15	-2.58 ± 0.08	-2.57 ± 0.10
NM_009668	Bridging integrator 1	Bin1	1.04 ± 0.30	-1.08 ± 0.30	-1.76 ± 0.14	-1.48 ± 0.21	-1.66 ± 0.17	-1.35 ± 0.19	1.14 ± 0.27	-1.50 ± 0.18	-1.59 ± 0.19
NM_008179	G1 to phase transition 2 (Gsp2)	Gsp2	-1.02 ± 0.18	-1.07 ± 0.26	-1.92 ± 0.08	-1.25 ± 0.15	-1.60 ± 0.11	-1.37 ± 0.12	-2.44 ± 0.07	-1.87 ± 0.10	-1.98 ± 0.10
NM_011817	Growth arrest and DNA-damage-inducible 45 gamma	Gadd45g	-1.04 ± 0.25	1.30 ± 0.48	2.50 ± 0.64	1.64 ± 0.48	3.16 ± 0.75	4.04 ± 0.96	13.29 ± 3.83	16.58 ± 3.90	16.21 ± 3.59
NM_007569	B-cell translocation gene 1 anti-proliferative	Btg1	1.62 ± 0.38	1.64 ± 0.34	2.00 ± 0.44	1.05 ± 0.33	1.83 ± 0.49	1.53 ± 0.37	1.89 ± 0.61	1.38 ± 0.44	1.12 ± 0.31
NM_007671	Cyclin-dependent kinase inhibitor 2c (p18, inhibits cdk4)	Ink4c	1.16 ± 0.28	1.38 ± 0.33	1.74 ± 0.46	1.61 ± 0.46	1.80 ± 0.42	1.33 ± 0.30	1.54 ± 0.48	1.85 ± 0.44	1.61 ± 0.49

Chapter 3.1:
GluRs in H₂S neuronal injury

Table 3.1 (continued)

Genbank	Gene Title	Symbol	Time-points								
			200 μ M NaHS			200 μ M NMDA			100 μ M KA		
			5 h	15 h	24 h	5 h	15 h	24 h	5 h	15 h	24 h
Mitotic cell cycle regulation (continued)											
NM_008316	Hus1 homolog	mHus	-1.11 ± 0.19	1.04 ± 0.26	1.38 ± 0.36	1.49 ± 0.34	1.95 ± 0.42	1.46 ± 0.33	1.22 ± 0.20	1.59 ± 0.28	1.05 ± 0.24
NM_21356	Growth factor receptor bound 2-associated protein 1	Gab1	1.35 ± 0.25	1.67 ± 0.40	3.06 ± 0.43	1.50 ± 0.25	2.58 ± 0.46	1.81 ± 0.30	1.06 ± 0.17	2.03 ± 0.23	1.42 ± 0.24
NM_010754	MAD homolog 2 (Drosophila)	Mad2	-1.36 ± 0.16	-1.22 ± 0.17	-1.59 ± 0.13	-1.25 ± 0.17	-1.55 ± 0.13	-1.31 ± 0.16	-1.36 ± 0.18	-1.86 ± 0.12	-2.12 ± 0.10

3.1.3.3 Validation of H₂S, NMDA and KA global transcriptomic profiles via real-time PCR

Microarray data was validated via real-time PCR using on the same total RNA samples previously employed in microarray analyses. These selected gene probes demonstrated identical transcriptional regulatory trend at 15h and 24h (Table 3.2).

Table 3.2 Validation of microarray data using real-time PCR technique on day 7 cultured murine primary cortical neurons treated with 200uM NaHS. Data are expressed as fold-change \pm sem. All fold-change expressions are statistically significant at $p < 0.05$. Each expression data is representative of 3 independent replicates. Data are expressed as fold-change \pm sem.

GenBank	Gene Title	Symbol	200 μ M NaHS			
			15h		24h	
			Microarray	Real-time PCR	Microarray	Real-time PCR
NM_007837	DNA damage-inducible transcript 3	Ddit3	-1.26 \pm 0.19	-1.89 \pm 0.65	1.59 \pm 0.41	3.24 \pm 0.83
NM_011817	Growth arrest and DNA-damage-inducible 45 gamma	Gadd45g	1.30 \pm 0.48	1.70 \pm 0.88	2.50 \pm 0.64	1.64 \pm 0.66
NM_030704	Heat shock protein 8	Hspb8	1.97 \pm 1.33	2.77 \pm 0.82	4.00 \pm 0.75	3.10 \pm 0.76
NM_010442	Heme oxygenase 1	Hmox1	1.45 \pm 0.77	2.00 \pm 0.72	4.40 \pm 0.67	
NM_029688	Sulfiredoxin 1 homolog (S. cerevisiae)	Npn3	1.59 \pm 0.78	3.91 \pm 0.86	3.73 \pm 0.63	
NM_013743	Pyruvate dehydrogenase kinase, isoenzyme 4	Pdk4	2.44 \pm 1.51	2.55 \pm 0.90	2.09 \pm 0.53	7.28 \pm 0.82

Chapter 3.1:
GluRs in H₂S neuronal injury

Table 3.3 Validation of microarray data using real-time PCR technique on day 7 cultured murine primary cortical neurons treated with 200uM NMDA. Data are expressed as fold-change \pm sem. All fold-change expressions are statistically significant at $p < 0.05$. Each expression data is representative of 3 independent replicates. Data are expressed as fold-change \pm sem.

			200 μ M NMDA			
GenBank	Gene Title	Symbol	15h		24h	
			Microarray	Real-time PCR	Microarray	Real-time PCR
NM_153553	Neuronal PAS domain protein 4	Npas4	4.77 \pm 1.80	2.89 \pm 0.68	6.72 \pm 3.23	
NM_011817	Growth arrest and DNA-damage-inducible 45 gamma	Gadd45g	3.16 \pm 0.75		4.04 \pm 0.96	6.65 \pm 0.75
NM_030704	Heat shock protein 8	Hspb8	3.85 \pm 0.80		1.83 \pm 0.46	4.52 \pm 0.82
NM_010442	Heme oxygenase 1	Hmox1	3.11 \pm 0.48	4.39 \pm 0.63	1.59 \pm 0.29	4.00 \pm 0.71
NM_029688	Sulfiredoxin 1 homolog (S. cerevisiae)	Npn3	1.95 \pm 0.53	3.69 \pm 0.88	1.11 \pm 0.21	-1.28 \pm 0.68
NM_013743	Pyruvate dehydrogenase kinase, isoenzyme 4	Pdk4	5.15 \pm 1.34	3.94 \pm 0.65	3.34 \pm 0.61	
NM_023556	Mevelonate kinase	Mvk	-2.35 \pm 0.13	-6.88 \pm 0.68	-2.37 \pm 0.14	-11.16 \pm 0.78

Table 3.4 Validation of microarray data using real-time PCR technique on day 7 cultured murine primary cortical neurons treated with 100uM KA. Data are expressed as fold-change \pm sem. All fold-change expressions are statistically significant at $p < 0.05$. Each expression data is representative of 3 independent replicates. Data are expressed as fold-change \pm sem.

			100 μ M KA			
GenBank	Gene Title	Symbol	15h		24h	
			Microarray	Real-time PCR	Microarray	Real-time PCR
NM_013743	Pyruvate dehydrogenase kinase, isoenzyme 4	Pdk4	4.53 \pm 1.22	3.93 \pm 0.54	2.97 \pm 1.02	5.65 \pm 0.86
NM_023556	Mevalonate kinase	Mvk	-3.42 \pm 0.08	-4.51 \pm 0.80	-3.73 \pm 0.09	-12.73 \pm 0.54
NM_029688	Sulfiredoxin 1 homolog (S. cerevisiae)	Npn3	1.93 \pm 0.36		1.38 \pm 0.30	
NM_010442	Heme oxygenase 1	Hmox1	2.17 \pm 0.39		2.04 \pm 0.37	1.74 \pm 0.67
NM_011817	Growth arrest and DNA damage-inducible 45 gamma	Gadd45g	16.58 \pm 3.90	8.69 \pm 0.59	16.21 \pm 3.59	
NM_153553	Neuronal PAS domain protein 4	Npas4	14.85 \pm 3.18	19.63 \pm 0.64	12.38 \pm 3.11	
NM_030704	Heat shock protein 8	Hspb8	2.61 \pm 0.59	1.53 \pm 0.82	1.60 \pm 0.38	

3.1.4 Discussion

3.1.4.1 Significance of iGluRs (NMDARs and KARs) activation in H₂S-mediated neuronal injury

From the simultaneous comparative analysis of the transcriptomic profiles of H₂S, NMDA and KA –mediated neuronal injuries which demonstrates a 44.4% commonly occurring, differentially regulated genes of the former attributed to both latter, it can be inferred that there is a relatively high dependency of the iGluRs, namely NMDARs and KARs - transduced signaling cascade in H₂S-mediated neuronal injury. This is further supported by bi-model comparisons which indicate an overwhelming 82.7% of NMDA profile, and concurrently a still considerably high 57.2% transcriptomic incidence of KA profile in that of H₂S (Figure 3.7A and B). This is unsurprising as NMDARs are the major iGluRs subtype in terms of abundance in the mammalian brain, and demonstrate the highest intrinsic Ca²⁺ permeability which explains the numerous research findings that report the physiological association between NMDARs and H₂S role as a neuromodulator.

H₂S is able to induce NMDAR activation via two possible pathways. H₂S has the ability to reduce disulfide bonds or make bound sulfane sulfur (one of the endogenous H₂S storage form) with free thiols in NMDARs. In the case of the former scenario, it is worthy to appreciate that disulfide bonds play a role in the functional regulation of many proteins, including NMDARs (Aizenman et al., 1989). Recent studies have demonstrated H₂S-mediated S-sulphydration of key sulphydryl groups regulating NMDAR activity alter Ca²⁺ influx through the receptor and/or indirectly activate cAMP-dependent protein kinase

known to regulate NMDAR-mediated signaling (Gadalla and Snyder, 2010; Tang et al., 2010).

Up-to-date, no literature has clearly addressed the neuromodulator role of H₂S under patho-physiological conditions in association with KARs. As such, our previous and existing findings have unprecedentedly established the relationship of H₂S-mediated neuronal injury with KARs via pharmacological inhibition study (Cheung et al., 2007) and comparative global transcriptomic profiling. It is possible that H₂S triggers the activation of KARs via the same mechanism as that of NMDARs, i.e. S-sulphydration of key sulphhydryl groups. Even though the overall average sequence identity in the entire iGluRs family is only about 20-30%, with NMDARs subunits demonstrating the highest degree of distinction from the closely-related AMPARs and KARs, all the three subtypes generally exhibit the same topology, thus making them concurrently unique and similar.

3.1.4.2 Significance of enriched biological processes in H₂S- mediated neuronal injury

Based on time-course of global transcriptomic profiling, we are able to devise an overview of H₂S-mediated neuronal injury formulated from the pattern of gene expression changes.

- **Early- and medium-term events (5h -15h processes)**
 1. Application of exogenous H₂S induces iGluRs activation, and while taking into account NMDAR high Ca²⁺-permeability, a massive Ca²⁺ influx from the ECM would be effected, which would in turn stimulate release from intracellular ER store. Together these sources contribute to drastic rise in Ca²⁺ concentration, which

- is evident from the transcriptional up-regulation of Ca²⁺-binding proteins (e.g. Anxs and S100bp; Table 3.1: Calcium ion binding and homeostasis).
2. Perturbed Ca²⁺ regulation elicited early activation of Ca²⁺-dependent proteases calpains, demonstrated previously to occur 5h after NaHS treatment with subsequent destabilization of the lysosomal membrane (Cheung et al., 2007).

 3. In addition, triggering of extrinsic apoptotic mechanism was also evident from the H₂S global transcriptomic profile. Members involved in the Fas/FasL-mediated cell death cascade (e.g. Tnfrsf5 and Casp6) demonstrated significant up-regulation at 15h (Table 3.1: Cell death). Tumor necrosis factor receptor superfamily, subtype 1 (Tnfrsf1) has been implicated in the early establishment of inflammatory response and elevated neuronal damage upon neurotrauma induction. Tnfrsf1, capable of induction of both apoptosis and necrosis via intracellular signaling has been reported to enhance expression of cell death-related genes, MMPs and their inhibitors (Quintana et al., 2005). On the contrary, the classical intrinsic mitochondrial-dependent cytochrome c-induced cell death mechanism was not triggered in H₂S-mediated neuronal injury. This observation is in agreement with our previous immunoblot analysis which revealed a lack of caspase-3 activation but extensive activations of calpains (Cheung et al., 2007).

 4. Activation of the cell death signaling cascade concurrently triggered the cellular pro-survival response. Only a handful of the pro-survival candidates including Igf2

Chapter 3.1: GluRs in H₂S neuronal injury

and Nre1 demonstrated significant transcriptional up-regulation at 15h. Insulin growth-like factor 2 (IGF2) is a potent mitogen which possess growth-promoting ability mediated via the Igf type 1 and type 2 receptors as well as through the insulin receptors, all of which are widely expressed throughout the brain (Silva et al., 2009). In this case, its gene expression showed significant elevation at 15h in NaHS-treated neurons. Ciliary neurotropic factor (CNTF) functions as a survival factor for numerous neuronal cell types through transcriptional modulation. In the event of oxidative stress commonly observed in neurodegenerative diseases, ROS has been reported to inhibit CNTF activation of Jak/STAT pathway in neurons resulting in increased neuronal damage (Kaur et al., 2005). Together this evidence suggested that the cell survival cascades were suppressed at the intermediate stage of H₂S-mediated neuronal injury.

- ***Late processes (15h-24h)***

5. Disruption of homeostatic balance imposed by elevated level of H₂S results in organellar (e.g. ER and lysosomes) oxidative stress and disruption:

a) A “calpain-cathepsin hypothesis” was formulated by (Yamashima et al., 1998) on the basis of the experimental paradigm of global brain ischemia in primates. The calpain-cathepsin cascade mechanism of cell death involves Ca²⁺ mobilization through the uptake of extracellular Ca²⁺ and/or the release from internal Ca²⁺ stores. Ca²⁺ mobilization can lead to the activation of calpains which induces lysosomal rupture, possibly aided by ROS. The released lysosomal proteases, cathepsins, will then degrade the cell constituent proteins, ultimately leading to cell

Chapter 3.1: GluRs in H₂S neuronal injury

death. Indeed, a significant increase in gene expression of lysosomal cathepsin Z (CtSZ; Table 3.1) was observed at 24h of H₂S-mediated neuronal injury.

b) The ER is an important organelle with the capability to regulate cellular stress through modulation of protein synthesis and metabolism (Travers et al., 2000). Extensive ER damage can trigger cell death via the production of unfolded proteins, the release of Ca²⁺ into the cytoplasm or altered redox homeostasis (Breckenridge et al., 2003) resulting in either classical programmed cell death or other mitochondrial cell death pathways (Jimbo et al., 2003). As such, dysfunctional Ca²⁺ regulation arising from ER stress and increased molecular oxidative damage further potentiates activation of programmed necrotic pathway involving calpains, forming a positive feedback regulatory loop (Crocker et al., 2003; Nakagawa and Yuan, 2000).

Significant transcriptional elevation of severe ER stress-induced pro-apoptotic gene, CCAAT/enhancer binding protein (C/EBP) beta (Cebpb) was observed at 24 h in H₂S-mediated neuronal death (Table 3.1: ER/Lysosomal stress). CEBPB together with its binding partner DNA-damage-inducible transcript 3 (DDIT3; also known as CHOP) forms a dimerized repressor complex which inhibits transcription of survival-promoting genes, facilitating the development of PCD (Hayashi et al., 2005; Zinszner et al., 1998). The increase in Ddit3 protein expression (demonstrated in Figure 3.2) is believed to lead to the suppression of the BCL2 family expression in the cells, which make them more susceptible to apoptosis

(McCullough et al., 2001). This is consistent with the observed down-regulation of Bcl-xl.

6. Presence of ER stress, lysosomal rupture, activated pro-apoptotic protein members and elevated Ca²⁺ level contributes to elevated production of ROS in H₂S-mediated neuronal death (Eghbal et al., 2004). Cells under oxidative stress would be more predisposed to their death fate as ROS have the ability to react with and modify any cellular molecules (e.g. DNA, proteins and lipids), and thus in the process affect their physiological functions and disrupt the cellular homeostatic balance (Higgins et al., 2010). Hsps and molecular chaperones are crucial in the alleviation of oxidative stress through facilitation of the refolding of misfolded proteins to avoid their aggregation and accumulation in the cell (Meriin and Sherman, 2005). In addition, HSP27 (HSPB8) can also suppress the activity of the pro-apoptotic member of the BCL2 family, BID, thus preventing cytochrome c release (Franklin et al., 2005). In H₂S-induced neuronal injury, substantial mRNA expression up-regulation of HSPs and chaperones generally demonstrated at 15h (Table 3.1).

Similarly, genes encoding for proteins involved in the anti-oxidant GSH pathway were also significantly up-regulated from 15h. H₂S has been demonstrated to confer neuroprotective effect through elevation of GSH level, a major and effective cellular antioxidant in the concentration range of 1–8mM (Kimura and Kimura, 2004). This is induced through H₂S-mediated potentiation of cystine/Glu antiporter

Chapter 3.1: GluRs in H₂S neuronal injury

activity to promote production of cysteine, a substrate for GSH synthesis, whose effect is especially important in offering neuroprotection upon injury induced by Glu-mediated non-receptor oxidative stress where transport of cystine is impeded by high extracellular level of Glu. This is because Glu competes with cystine for the same amino acid transporter to enter the cells (Bannai and Kitamura, 1980). Furthermore, H₂S also facilitates effective translocation of cysteine (reduced form of cystine) into cells for glutathione production (Kimura et al., 2010). In addition, the reducing property of H₂S facilitates sequestration of reactive oxygen species and hydrogen peroxide which is frequently up-regulated in the mitochondria under oxidative stress, since the mitochondria play a pivotal role in cell death induction via multiple converging signaling cascades (Higgins et al., 2010). The transcriptional up-regulation of these genes is clearly an indication of an attempt to buffer neurons against any oxidative and ER stress, consequentially averting cellular death.

7. Raised oxidative stress increases the vulnerability of cellular DNA to damage.

A study by Baskar et al., (2007) reported the ability of H₂S to induce DNA damage in cultured human lung fibroblasts, thus triggering a p53 response to guard the genome integrity of the cell. Downstream targets of p53 which demonstrated increased transcriptional expression during H₂S-mediated neuronal injury include, growth arrest and DNA-damage-inducible 45 gamma (Gadd45g), cyclin G1 (Ccng1) and cyclin-dependent kinase 2 (Cdk2). GADD45G impedes CDC2/cyclin B1 kinase complex formation and thus cell cycle progression in the S and G2/M

Chapter 3.1: GluRs in H₂S neuronal injury

cell cycle phases upon genotoxic stress (Vairapandi et al., 2002), and its activation of downstream signaling cascade strongly potentiates cell death (Mak and Kültz, 2004). Simultaneously, GADD45G also mediates activation of stress-responsive gene MEKK (expression fold-change data under cell survival), thus explaining parallel up-regulation in both at 24h after NaHS treatment. CCNG1, a transcriptional p53 target whose expression is induced upon DNA damage, regulates p53 function through modulation of p53 stability (Kimura and Nojima, 2002; Okamoto et al., 2002). Cell cycle arrest can also occur via a p53-independent pathway through cyclin-dependent kinase inhibitor 2c (INK4C), which in H₂S-mediated neuronal injury demonstrated significant transcriptional up-regulation at 24h, and whose activity has a strong correlation with activities of the retinoblastoma protein and other retinoblastoma family members (p107 and p130) at the G1 phase. INK4C is able to inhibit the enzymatic activities of cyclin D-dependent kinases through interaction with CDK4 and CDK6, thus negatively regulating cell growth and proliferation and at the same time control the production of diffusible mitogens and chemokines which affects post-natal development of neurons (Zindy et al., 2003).

This is the first time that the H₂S neuropathological implication with NMDARs and particularly, KARs has been established in the context of iGluRs-mediated excitotoxicity, a major neuropathological mechanism (summarized in Figure 3.9). As H₂S and NMDARs cooperate to mediate physiological function under regulated homeostasis, it cannot be ruled out that upon hyper-stimulation of this pathway

Chapter 3.1: GluRs in H₂S neuronal injury

could be detrimental to cell survival. Indeed in an *in vivo* adult rodent stroke model expressing functional GluRs, Qu et al., (2006) reported that H₂S is a mediator of cerebral ischemic injury. Concurrently, we cannot eliminate the possibility of H₂S-induced iGluRs-independent neuroprotective effect, especially pertaining to stimulation of glutathione production. It can be postulate that H₂S-induced neuronal injury takes place when the balance between H₂S-triggered GluRs-dependent pro-death and receptor-independent anti-death stimuli is disrupted in favour of the former.

In conclusion, it can be deduced that excitotoxicity plays a major role in H₂S-mediated neuronal death, and based on the physiological neuronal expression of different iGluRs subtypes, both NMDARs and KARs played a much substantial role as compared to AMPARs due to the higher in abundance of the former two. Since H₂S and Glu have been concurrently implicated in many neuropathies, this suggests a possibility of a synergistic relationship between these two signaling pathways, evoking an addictive detrimental effect which sends the neurons to demise. Findings of this subchapter in relation to H₂S-mediated neuronal injury have been summarized in the following illustration.

Chapter 3.1: GluRs in H₂S neuronal injury

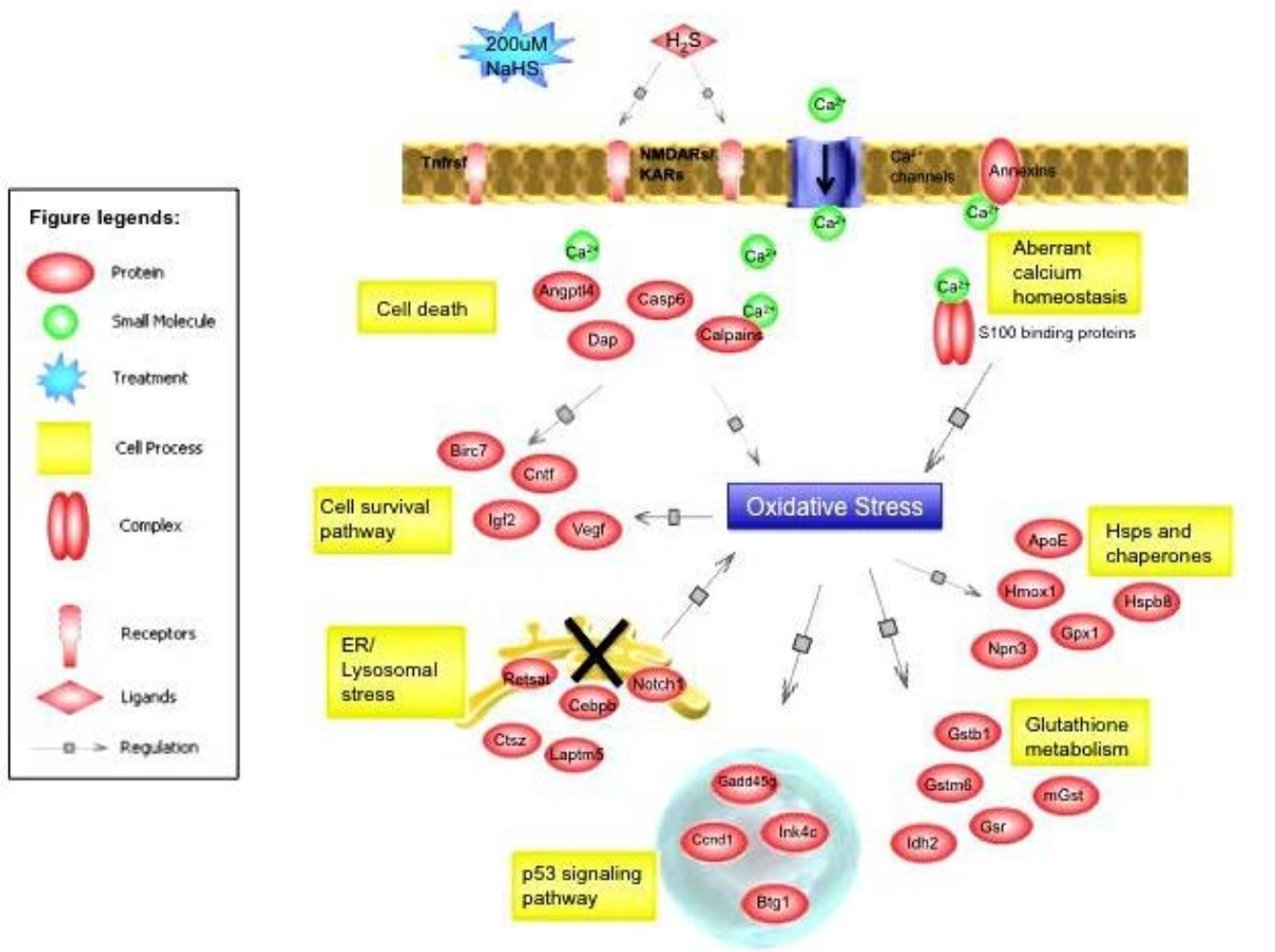


Figure 3.9 Summary of the prominent biological processes affected during H₂S-mediated neuronal injury.

Chapter 3.1: GluRs in H₂S neuronal injury

Excitotoxicity involving all three iGluRs subtypes has been reported to be a central dogma event in many neurodegenerative conditions. However, it remains to be elucidated what is their mechanistic contribution as an iGluRs subfamily during Glu-mediated neuronal injury, which would theoretically also simultaneously trigger mGluRs activation. Due to the differential cellular expression of iGluRs subtypes on the post-synaptic membrane as well the selectivity of Ca²⁺ permeability in AMPARs governed by subunit assembly, it would be unjustifiable to eliminate AMPARs contribution in excitotoxicity during Glu-mediated neuronal injury due to its probable low receptor expression. Furthermore, under physiological condition, AMPARs activation is crucial to facilitate activation of Ca²⁺ channel activity in NMDARs by indirectly inducing repulsion of Mg²⁺ out of the latter's gate during LTP. As such, it would be worthwhile to assess in details the overall mechanistic involvement of the iGluRs subfamily in mediation of excitotoxicity during Glu-mediated neuronal injury.

Chapter 3.2:
Comparative global gene profiling
of
iGluRs Involvement
in
Glu –mediated
Excitotoxicity

3.2.1 Introduction

Excitotoxicity is one of the earliest cellular processes commonly detected in the pathogenesis of neurodegenerative diseases such as AD (Hynd et al., 2004a), dementia associated with Down syndrome (DS; (Scheuer et al., 1996)) and acute neurological deficits like traumatic brain injury (TBI) and stroke (Arundine and Tymianski, 2004). It is believed to be one of the upstream primary events at work to induce neuronal injury at cellular level. It is believed to be triggered by the rise of Glu concentration in the micro-environment of the brain, as a result of conditions such as hypoglycemia or status epilepticus. Hypoglycemia is commonly observed during stroke or TBI episode where ischemic reduction in blood flow limits supply of oxygen and glucose to a localized region of the brain. This leads to an inadequacy of ATP production which abolishes the electrochemical gradients of ions required to be maintained to ensure functionality of the Glu transporters on the astrocytes to uptake Glu from the extracellular matrix, leading to a buildup of extracellular Glu. To further complicate matter, the loss of electrochemical gradients reverses the transporters, causing them to release Glu and aspartate into the extracellular space. This promotes an accelerated accumulation of Glu, leading to enhanced activation of GluRs.

In excitotoxic neuronal death, it has been suggested that iGluRs particularly NMDARs play a major role in the mediation of a large Ca^{2+} influx upon over-stimulation as a consequence of its high Ca^{2+} -permeability and abundance (Hara and Snyder, 2007; Takahashi et al., 2010). This consequential influx of extracellular Ca^{2+} , together with release of Ca^{2+} intracellular stores from ruptured organelles (e.g. lysosomes) into the

Chapter 3.2: iGluRs in excitotoxicity

cytosol, results in activation of Ca^{2+} -dependent proteases, calpains, and the protein phosphatase, calcineurin resulting in hydrolysis of cytoskeletal and other cellular proteins [e.g. α -fodrin; (Siman et al., 1989; Simpkins et al., 2003)]. Glu-induced excitotoxicity has been associated with simultaneous calpain activation (Zatz and Starling, 2005) and lysosomal dysfunction (Bahr and Bendiske, 2002) consistently observed in these neurodegenerative diseases.

It is important to keep in mind that in the mammalian brain, Glu is the only physiological excitatory neurotransmitter agonist for GluRs activation, be it metabotropic or ionotropic, even though the GluRs superfamily has been extensively categorized based on their subunit composition and sequence homology, which are determinants of their downstream signaling mechanisms as well as intrinsic activities. As such, Glu-mediated neuronal death comprises of two concurrent branching signaling components mediated by ionotropic and metabotropic GluRs respectively. Unlike iGluRs which possess intrinsic ionic channel activity, metabotropic GluRs are G-protein coupled receptors. It is believed that Glu is able to mediate the differential multi-GluRs activation by adoption of different conformations when interact with different types of GluRs. Since individual GluRs also demonstrate differential expression pattern in different parts of the brain as well as selective orientation in local region (i.e. pre- or post-synaptic membranes), this further provides the opportunity for differential temporal activation of receptors, permitting regulation of basal excitatory synaptic transmission and numerous forms of synaptic plasticity such as LTP and long-term depression, which are believed to underlie learning and memory. Concurrently, under patho-physiological conditions where excitotoxicity is

Chapter 3.2: iGluRs in excitotoxicity

triggered, this structured hierarchy may promote a synchronized temporal activation of different GluRs, leading to a simultaneously converged, as well as diverse downstream cellular events, eliciting differential cellular outcome.

Excitotoxicity is a general term that defines a damage-inflicting cellular process that is signified by the rise in cytosolic Ca^{2+} level as a result of a constitutive and hyper-activation of ion channel-gated iGluRs subfamily. It is commonly demonstrated that all three iGluRs subtypes are involved, and that NMDARs play the pivotal role due to its highest intrinsic permeability to Ca^{2+} and its abundance. However, it is important to remember that during neuropathological state when marked elevation of extracellular Glu was released by damaged neurons and astrocytes, Glu not only activates iGluRs resulting in excitotoxicity, but also mGluRs. In addition, much remains to be elucidated with regards to the amplification and divergence of downstream signaling pathways with respect to the concerted iGluRs activation triggered during excitotoxicity. In this subchapter, microarray technique is applied on four excitotoxicity representations induced by a) the general GluRs agonist Glu, b) AMPAR agonist, AMPA, c) NMDAR agonist, NMDA and, d) KARs agonist, KA. Comparative global gene profile analysis is performed to elucidate the major primary biological processes regulated by iGluRs in the trigger of excitotoxicity during Glu-mediated neuronal injury. This is the first time that global gene profiling of this type and scale to elucidate pathogenesis of excitotoxicity has been performed.

3.2.2 Results

Employing D7 murine primary cortical neurons, cultures were treated with the following previously reported EC₅₀ concentrations of iGluRs agonists for 24 h: 200uM NMDA (Chen et al., 2010b), 100uM KA (Moldrich et al., 2000; Moldrich et al., 1999) and 300uM AMPA (Larm et al., 1997), and the intrinsic general GluRs activator 250uM Glu (Cheung et al., 1998).

Overall cellular transcriptional regulation was assessed in Glu, NMDA, AMPA and KA excitotoxicity models respectively over a 24-hour period using Illumina® Mouse Ref8 V1.1 genechips. The raw transcriptional signal data from individual arrays was then subjected to statistical filtering using one-way ANOVA, $p < 0.05$ and Benjamini-Hochberg FDR (FDR), and gene probes were considered to be significantly regulated when they demonstrated gene expression of at least ± 1.5 in a minimum of one out of the three time-points (5h, 15h and 24h). All gene probes that passed these selection criteria were put together to form the global transcriptomic data for each excitotoxicity model. Glu (1,842 gene probes), NMDA (2,309 gene probes), AMPA (1,863 gene probes) and KA (3,800 gene probes) neuronal treatments induced transcriptomic profiles that were lined up side-by-side in Figure 3.10 and partitioned to different fold-change categories. Clearly demonstrated in Figure 3.10, substantial number of gene probes demonstrated greater than ± 1.5 fold-change in gene expression over the 24-hour assessment period, with KA treatment generating the largest transcriptomic profile.

3.2.2.1 Bi-model analyses of individual iGluRs profiles against that of Glu revealed the following decrease ordering of GluRs activation dependence NMDARs>KARs>AMPARs during excitotoxicity

Since Glu is involved in the activation of all GluRs, including both ionotropic and metabotropic subtypes, it would be interesting to determine the relative contribution of each iGluR-triggered signaling cascade attributing to Glu-induced neurotoxicity. Bi-model global transcriptomic profile comparisons using Glu model as the basis of analysis demonstrated that in order of highest to lowest degree of overlap, i.e. commonly occurring, differentially regulated gene probes, NMDA > KA > AMPA were observed (Figure 3.11). NMDA (Figure 3.11A) and KA (Figure 3.11C) profiles respectively demonstrated comparable and nearly double the number of with-Glu commonly occurring genes relative to AMPA profile (Figure 3.11B). This signifies a greater reliance of NMDARs and KARs -mediated signaling pathways to induce excitotoxicity during Glu-mediate neurotoxicity. A more in-depth analysis into the consistency in the transcriptional regulatory trend demonstrated that majority of the gene probes were similarly regulated at 15h and 24h respectively in all three iGluRs models (Figure 3.12).

However, AMPARs involvement cannot be neglected as it may play a crucial role in the upstream initiation of excitotoxicity, as seen in during LTP under physiological state, promoting activation of NMDARs and KARs. This is because during LTP, AMPARs open their intrinsic ionic pores directly upon Glu ligand binding, facilitating Na⁺ influx into the post-synaptic neurons resulting in depolarization. This promotes the opening of ionic channel activity within NMDARs as depolarization from the AMPAR activation leads to

Chapter 3.2: iGluRs in excitotoxicity

repulsion of the Mg^{2+} out into the extracellular space, allowing the pore to pass current. The pores of NMDARs are occluded at resting membrane potential by Mg^{2+} . As opposed to AMPARs which demonstrated selective permeability to Ca^{2+} depending on its subunit composition, NMDARs are freely permeable to Ca^{2+} and Na^+ . The Ca^{2+} that enters the cell promotes AMPARs on the plasma membrane, resulting in a long-lasting increase in (EPSP) size underlying LTP. The Ca^{2+} entry also phosphorylates calcium/calmodulin kinase 2 (CAMK2), which phosphorylates AMPARs, increasing their single-channel conductance. As such, AMPARs activation is crucial for activation of NMDARs intrinsic channel activity in addition to Glu ligand binding, and NMDARs in turn amplify AMPARs signaling cascade by promoting its plasma membrane localization, further facilitating Ca^{2+} influx mediated by selected AMPARs with permeability to Ca^{2+} channels.

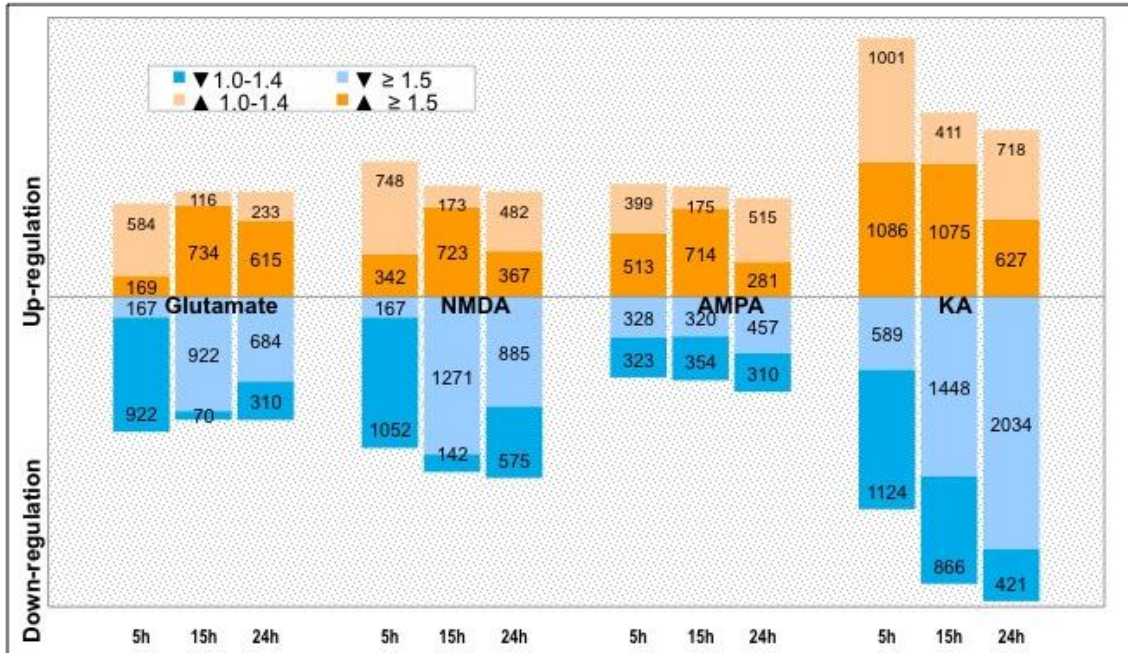


Figure 3.10 Classification of individual global transcriptomic profiles of Glu, NMDA, AMPA and KA in cultured murine primary cortical neurons. The genes in these categories passed microarray selection criteria: gene expression of at least ± 1.5 in a minimum of one out of the three time-points (5h, 15h and 24h) and statistical examination using one-way ANOVA, $p < 0.05$ and FDR) according to specific time-points and fold-change expression up/down-regulated.

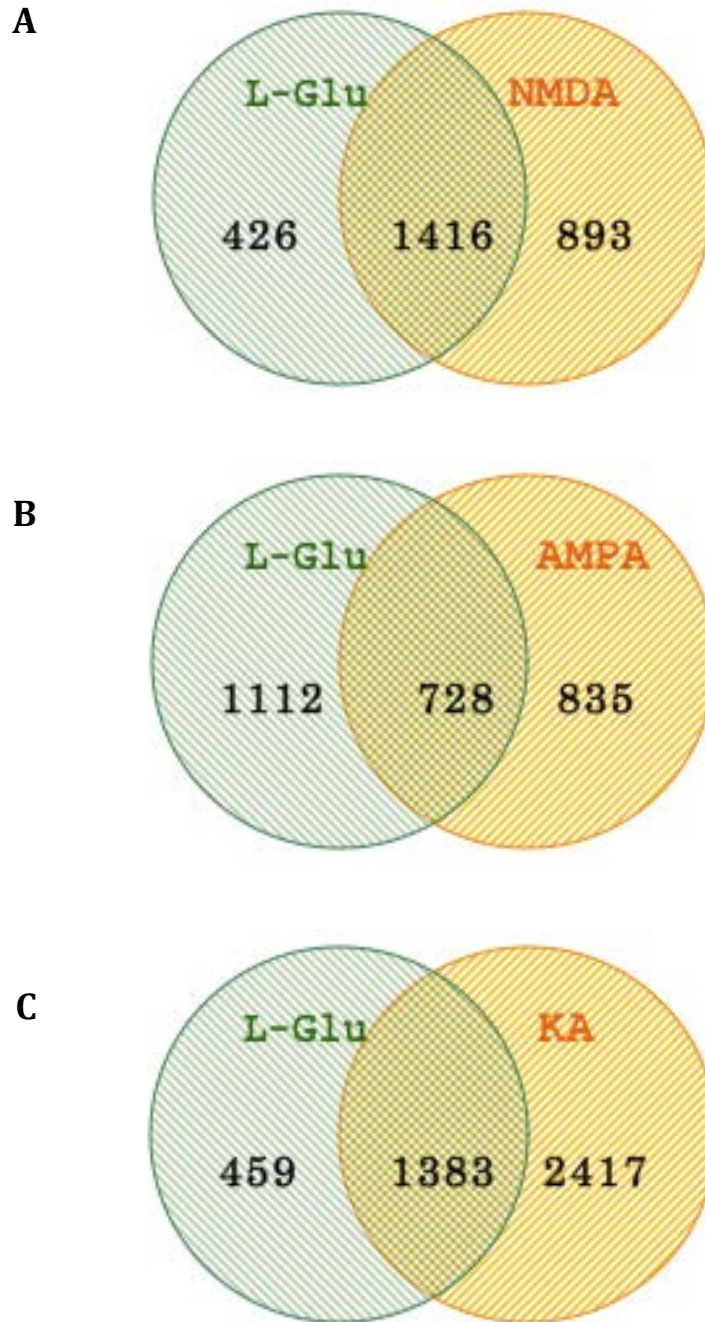


Figure 3.11 Bi-model global transcriptomic profile analysis of individual iGluRs agonists against Glu excitotoxicity model. Venn diagrams demonstrating the number of gene probes common and mutually exclusive to both models [A] Glu against NMDA [B] Glu against AMPA and [C] Glu against KA.

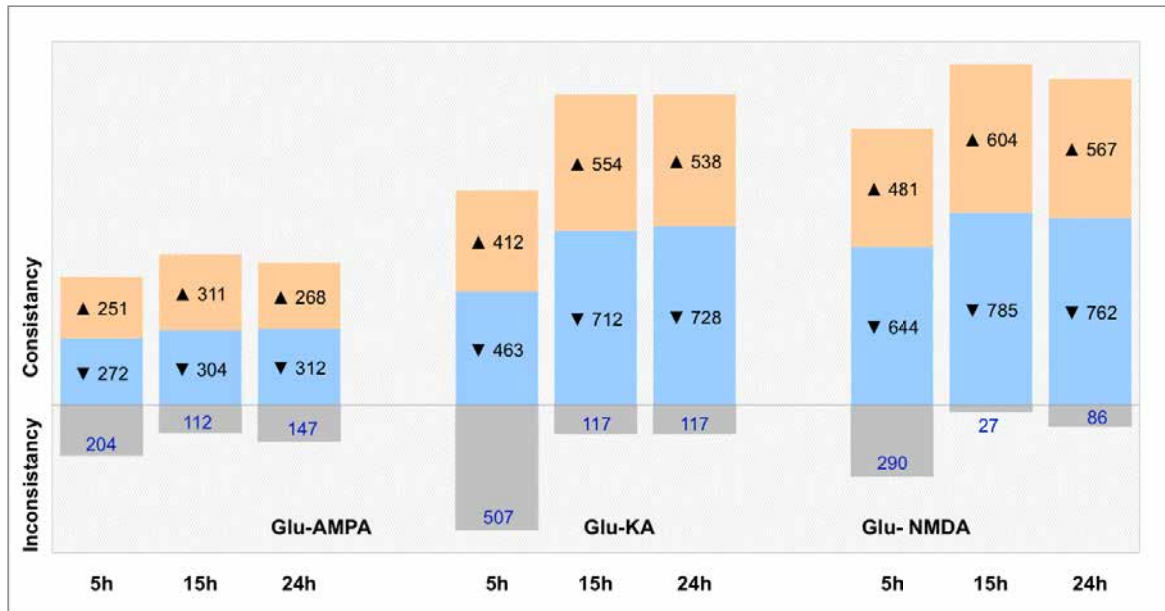


Figure 3.12 Consistency in the transcriptional regulatory trend of the commonly occurring gene probes in individual iGluRs against Glu excitotoxicity models.

3.2.2.2 Simultaneous comparison of all four excitotoxicity models identified several major common biological processes

In order not to miss the overall contributory effect of iGluRs in Glu-mediated excitotoxicity, a comparative microarray analysis of all four excitotoxicity models was performed. A total of 583 gene probes have been identified. The consistency of the transcriptional regulatory trend from the individual time-point –specific and inter-time-point perspective across all four models was studied. As shown in Figure 3.13 , high level of consistency was demonstrated for within time-point –limiting analyses particularly at 15h and 24h. However, inter-time-point comparison (5h -24h) of the commonly occurring gene probes in all four models demonstrated a decreased degree of consistency.

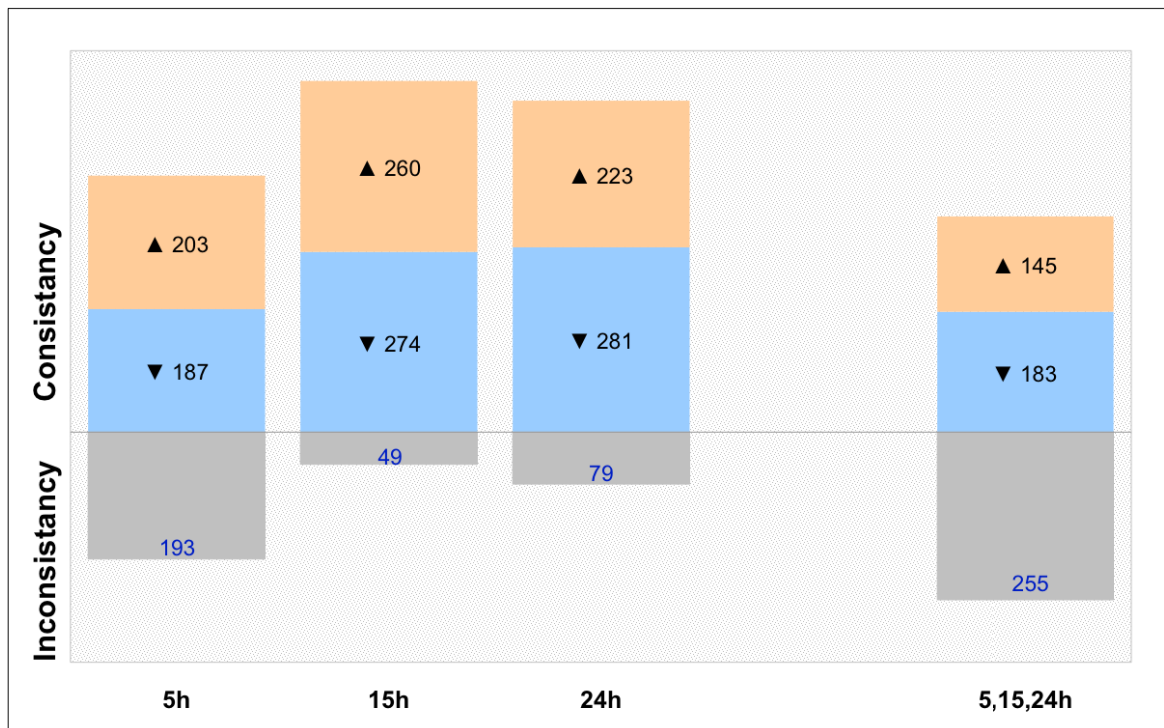


Figure 3.13 Overall consistency in the transcriptional regulatory trend of the commonly occurring gene probes in all four excitotoxicity models.

Chapter 3.2: iGluRs in excitotoxicity

Gene ontology-functional classification of these 583 RefSeq transcripts, which corresponded to 485 biologically-annotated genes, facilitated identification of several important and over-represented biological pathways imminent to the progression of excitotoxicity (Table 3.5). These include calcium ion homeostasis and binding, anti-oxidant response, cell death and cell survival processes. Prominently, an overwhelming number of candidates involved in the promotion of mitotic cell cycle progression were transcriptionally elevated in all four models of excitotoxicity. Consistently, all members of these over-represented biological processes were significantly modulated at the expression level between the 5h and 15h time-points, implying the reported pathways constitute the early upstream cellular events in excitotoxicity.

-CALCIUM ION HOMEOSTASIS AND BINDING

In all four excitotoxicity models, genes encoding for Ca^{2+} -dependent proteins and receptors (Gpcr12, Pkcb and Rln3r1) were significantly down-regulated, indicating the occurrence of aberrant calcium ion homeostasis (Table 3.5). On the contrary, genes encoding for Ca^{2+} -binding proteins (Cacy and Anx(A2, A3 and A5)) showed increase in gene expression, a further evidence of elevation of cytosolic Ca^{2+} level during excitotoxicity due to activation of iGluRs which open up the intrinsic Ca^{2+} channels.

-LYSOSOMAL STRESS

Aberrant elevation of cytosolic Ca^{2+} level and overproduction of ROS imposes organellar stresses through disruption of the delicate balance of cellular ionic gradients and unregulated modifications of cellular proteins resulting in detrimental loss/gain-of

function, all contributing to disturbance of normal cellular signaling. Analysis of the profiles of genes common to all four excitotoxicity models revealed significant transcriptional activation of lysosomal resident proteins, indication of some form of disorientation and/or stress imposed on the normal functioning of the lysosomes (Table 3.5).

- ANTI-OXIDANT RESPONSE

- Heat shock proteins (Hsps) and molecular chaperones

Organellar (endoplasmic reticulum and lysosomal) stress is especially prominent in excitotoxicity and evokes the cellular counteractive response to minimize electrophilic and oxidative burdens. Interestingly, comparative microarray analysis demonstrated that in the specific iGluRs excitotoxic models up-regulation of majority of genes encoding for HSPs and molecular chaperones (Hmox1, Npn3, Hspa2, and Hspb8) and metal chaperones (Mt3) occurred at the 5h time-point, much earlier than that of Glu at 15h (Table 3.5).

- Glutathione metabolism

Genes transcribing for members of the GSH anti-oxidative pathway were significantly up-regulated in all four models (Table 3.5). However, AMPA and Glu models demonstrated significant elevation of GSH pathway genes at 15h, while NMDA and KARs demonstrated earlier transcriptional response at 5h.

-CELL DEATH

Majority of the genes encoding for proteins directly/indirectly involved in promotion of cell death (Notch1, Angptl4, Casp6 and Catna1) were transcriptionally up-regulated as demonstrated in Table 3.5. Cell death was further accelerated by the down-regulation of anti-cell death protein (Bcl11b).

-CELL HOMEOSTASIS, SURVIVAL AND PROLIFERATION

In all four excitotoxicity models, genes encoding for pro-survival/mitogenic proteins (Spp1 and Birc5 (also known as Survivin)) and growth factors (Igf2, Ilgfbp7 and Igfbp5) were up-regulated between the 5h and 15h time-points, a cellular response to suppress the cell death mechanisms (Table 3.5).

-MITOTIC CELL CYCLE

Numerous genes encoding for cell cycle proteins that promote cell cycle re-entry were up-regulation in all four excitotoxicity models between 5h and 15h. This was an unprecedented observation made during excitotoxicity. Under physiological condition, neurons were in the post-mitotic and differentiated state. Aberrant cell cycle re-entry has been implicated in the pathogenesis of several neurological conditions such as AD, DS, HD, Niemann-Pick's disease and stroke (Camins et al., 2008; Pelegri et al., 2008). Recent studies on AD suggested that this cellular event is a part of the neuronal death process (Lopes et al., 2009a; Lopes et al., 2009b). p53, the main keeper of genome integrity, demonstrated a significant pursuing down-regulation (denoted as Trp53 in the table),

**Chapter 3.2:
iGluRs in excitotoxicity**

indicating a failure in the cell cycle checkpoint system, further making the re-activation of
cell cycle process easier.

Chapter 3.2:
iGluRs in excitotoxicity

Table 3.5 Gene expression profiles of neuronal death-related families in cultured day 7 mouse primary cortical neurons treated with Ec_{50} of AMPA, KA, NMDA and Glu over a 24-hour period respectively. All expression values (given as fold-changes) were selected based on having at least minimum of ± 1.5 fold change in at least one out of three time-points, subjected to one-way ANOVA analysis and Benjamini Hochberg FDR correction, and were significant at $p < 0.05$. Values are given as mean \pm sem.

Genbank	Gene Title	Symbol	Time-points											
			300uM AMPA			100uM KA			200uM NMDA			250uM Glu		
			5h	15h	24h									
<u>Calcium ion homeostasis and binding</u>														
NM_008151	G-protein coupled receptor 12	Gpcr12	-2.40 \pm 0.09	-1.70 \pm 0.15	-1.70 \pm 0.14	-2.10 \pm 0.13	-2.66 \pm 0.12	-2.89 \pm 0.11	-1.50 \pm 0.19	-2.20 \pm 0.11	-2.00 \pm 0.13	-1.50 \pm 0.19	-1.80 \pm 0.17	-1.40 \pm 0.18
NM_007587	Calcitonin/calcitonin-related polypeptide, alpha	Calc1	1.10 \pm 0.36	1.50 \pm 0.47	1.20 \pm 0.34	1.20 \pm 0.40	2.30 \pm 0.47	2.20 \pm 0.67	1.10 \pm 0.35	1.90 \pm 0.54	1.70 \pm 0.43	-1.10 \pm 0.31	2.30 \pm 0.66	2.80 \pm 0.71
NM_008855	Protein kinase C, beta 1	Pkcb	-1.10 \pm 0.21	-1.60 \pm 0.16	-2.00 \pm 0.12	1.20 \pm 0.27	-2.00 \pm 0.12	-2.40 \pm 0.12	-1.20 \pm 0.26	-2.80 \pm 0.09	-2.50 \pm 0.09	-1.10 \pm 0.23	-1.90 \pm 0.12	-1.60 \pm 0.18
NM_178717	Relaxin family peptide receptor 3	Rln3r1	-2.30 \pm 0.13	-2.10 \pm 0.13	-1.90 \pm 0.14	-2.80 \pm 0.10	-2.95 \pm 0.11	-3.52 \pm 0.10	-1.50 \pm 0.16	-2.40 \pm 0.10	-2.20 \pm 0.10	-1.20 \pm 0.21	-1.50 \pm 0.22	-1.30 \pm 0.22
NM_011313	S100 calcium binding protein A6 (calyculin)	Cacy	1.10 \pm 0.23	1.60 \pm 0.36	1.10 \pm 0.19	1.30 \pm 0.24	2.12 \pm 0.39	1.66 \pm 0.30	1.50 \pm 0.29	2.80 \pm 0.51	2.30 \pm 0.35	1.00 \pm 0.18	2.00 \pm 0.38	1.90 \pm 0.37
NM_007585	Annexin A2	Anxa2	1.90 \pm 0.38	1.80 \pm 0.42	1.30 \pm 0.31	2.30 \pm 0.45	1.98 \pm 0.34	1.48 \pm 0.35	1.90 \pm 0.38	2.30 \pm 0.43	1.60 \pm 0.31	1.60 \pm 0.25	2.00 \pm 0.31	2.10 \pm 0.43
NM_013470	Annexin A3	Anxa3	1.30 \pm 0.30	1.80 \pm 0.48	1.60 \pm 0.58	1.00 \pm 0.23	1.95 \pm 0.43	1.61 \pm 0.42	1.50 \pm 0.45	3.20 \pm 0.77	2.60 \pm 0.58	1.20 \pm 0.31	3.60 \pm 0.81	3.20 \pm 0.63
NM_009673	Annexin A5	Anxa5	-1.00 \pm 0.23	1.50 \pm 0.31	1.10 \pm 0.24	-1.00 \pm 0.19	1.50 \pm 0.33	1.10 \pm 0.21	1.40 \pm 0.27	2.00 \pm 0.40	1.80 \pm 0.35	1.20 \pm 0.20	1.70 \pm 0.29	1.60 \pm 0.38
<u>Lysosomal stress</u>														
NM_017372	Lysozyme	Lys	1.70 \pm 0.40	1.50 \pm 0.36	-1.20 \pm 0.24	-1.10 \pm 0.29	1.50 \pm 0.36	1.40 \pm 0.43	1.60 \pm 0.61	2.10 \pm 0.69	2.10 \pm 0.48	1.20 \pm 0.30	1.60 \pm 0.40	1.50 \pm 0.44
NM_010686	Lysosomal-associated protein transmembrane 5	Laptm5	1.70 \pm 0.31	1.40 \pm 0.34	-1.10 \pm 0.19	-1.50 \pm 0.18	1.80 \pm 0.34	1.40 \pm 0.50	1.80 \pm 0.46	2.40 \pm 0.98	2.20 \pm 0.34	1.20 \pm 0.25	1.80 \pm 0.37	1.70 \pm 0.40

Table 3.5 (continue)

Genbank	Gene Title	Symbol	Time-points											
			300uM AMPA			100uM KA			200uM NMDA			250uM Glu		
			5h	15h	24h	5h	15h	24h	5h	15h	24h	5h	15h	24h
<u>Lysosomal stress (continue)</u>														
NM_010685	Lysosomal-associated membrane protein 2	Lamp2	1.60 ± 0.39	1.70 ± 0.41	1.30 ± 0.32	1.90 ± 0.39	2.10 ± 0.50	1.40 ± 0.37	1.50 ± 0.36	2.00 ± 0.41	1.50 ± 0.30	1.10 ± 0.30	2.10 ± 0.51	1.70 ± 0.38
NM_019972	Sortilin 1	Nltr3	1.20 ± 0.35	1.70 ± 0.50	1.50 ± 0.54	1.50 ± 0.51	2.40 ± 0.56	1.80 ± 0.46	1.50 ± 0.45	3.70 ± 0.81	2.50 ± 0.64	1.50 ± 0.45	2.00 ± 0.63	1.40 ± 0.44
NM_009906	Tripeptidyl peptidase i	Cln2	1.20 ± 0.29	1.70 ± 0.53	1.10 ± 0.30	1.50 ± 0.40	2.00 ± 0.53	1.70 ± 0.54	1.20 ± 0.36	1.70 ± 0.40	1.30 ± 0.31	-1.10 ± 0.32	1.60 ± 0.41	1.60 ± 0.40
<u>Anti-oxidant response</u>														
-Heat shock proteins and molecular chaperones														
NM_010442	Heme oxygenase (decycling) 1	Hmox1	1.90 ± 0.45	1.40 ± 0.29	1.10 ± 0.51	1.90 ± 0.39	2.17 ± 0.39	2.04 ± 0.37	2.90 ± 0.58	3.30 ± 0.48	1.70 ± 0.29	1.40 ± 0.34	2.10 ± 0.41	1.30 ± 0.38
NM_029688	Sulfiredoxin 1 homolog (S. cerevisiae)	Npn3	2.60 ± 0.56	1.70 ± 0.34	1.30 ± 0.41	3.10 ± 0.54	1.93 ± 0.36	1.38 ± 0.30	2.00 ± 0.39	1.70 ± 0.28	1.10 ± 0.19	-1.30 ± 0.21	2.30 ± 0.46	1.10 ± 0.30
NM_007453	Peroxiredoxin 6	Prdx6	1.20 ± 0.41	1.60 ± 0.55	1.10 ± 0.37	1.80 ± 0.54	2.34 ± 0.76	1.95 ± 0.61	1.20 ± 0.36	1.70 ± 0.47	1.20 ± 0.28	-1.10 ± 0.27	2.10 ± 0.60	1.80 ± 0.56
NM_008301	Heat shock protein 2	Hspa2	1.50 ± 0.44	3.00 ± 0.76	2.30 ± 0.64	1.60 ± 0.44	2.77 ± 0.65	2.26 ± 0.64	1.00 ± 0.26	2.10 ± 0.52	2.10 ± 0.47	-1.30 ± 0.19	1.70 ± 0.36	1.60 ± 0.39
NM_030704	Heat shock protein 8	Hspb8	1.80 ± 0.45	2.20 ± 0.63	1.40 ± 0.59	1.50 ± 0.37	2.70 ± 0.59	1.60 ± 0.38	2.00 ± 0.46	3.90 ± 0.80	1.90 ± 0.46	1.30 ± 0.31	4.40 ± 1.06	2.60 ± 0.70
NM_013602	Metallothionein 1	Mt1	1.40 ± 0.28	1.60 ± 0.28	1.10 ± 0.17	1.80 ± 0.40	2.29 ± 0.38	1.92 ± 0.38	1.60 ± 0.25	2.00 ± 0.34	1.50 ± 0.24	1.10 ± 0.16	1.80 ± 0.26	1.80 ± 0.39
NM_013603	Metallothionein 3	Mt3	1.60 ± 0.26	1.80 ± 0.69	1.10 ± 0.20	2.40 ± 0.48	2.00 ± 0.34	2.10 ± 0.49	1.40 ± 0.27	2.00 ± 0.27	1.80 ± 0.55	-1.10 ± 0.17	1.60 ± 0.28	1.60 ± 0.30

Table 3.5 (continue)

Genbank	Gene Title	Symbol	Time-points											
			300uM AMPA			100uM KA			200uM NMDA			250uM Glu		
			5h	15h	24h									
-Glutathione metabolism														
NM_010357	Glutathione S-transferase, alpha 4	mGsta4	1.10 ± 0.29	1.90 ± 0.44	1.40 ± 0.33	1.20 ± 0.31	2.30 ± 0.60	2.10 ± 0.48	1.30 ± 0.39	3.20 ± 0.70	2.20 ± 0.52	-1.20 ± 0.18	2.60 ± 0.63	2.10 ± 0.59
NM_008184	Glutathione S-transferase, mu 6	Gstm6	1.20 ± 0.40	1.50 ± 0.53	-1.00 ± 0.35	1.50 ± 0.50	1.90 ± 0.52	1.20 ± 0.36	1.50 ± 0.45	2.10 ± 0.63	1.40 ± 0.35	-1.20 ± 0.22	2.10 ± 0.58	1.70 ± 0.52
NM_173011	Isocitrate dehydrogenase 2 (NADP+), mitochondrial	Idh2	1.30 ± 0.38	1.70 ± 0.47	1.20 ± 0.38	1.60 ± 0.46	2.22 ± 0.62	1.86 ± 0.66	1.60 ± 0.48	2.30 ± 0.62	1.50 ± 0.34	1.00 ± 0.26	1.80 ± 0.51	1.90 ± 0.62
NM_019946	Microsomal glutathione S-transferase 1	mGst	1.10 ± 0.30	1.80 ± 0.46	1.30 ± 0.42	1.40 ± 0.44	2.55 ± 0.53	1.91 ± 0.51	1.80 ± 0.42	3.20 ± 0.60	1.80 ± 0.37	1.00 ± 0.27	3.20 ± 0.87	2.90 ± 0.90
NM_025569	Microsomal glutathione S-transferase 3	mGst3	-1.20 ± 0.19	-1.50 ± 0.15	-1.40 ± 0.16	-1.20 ± 0.20	-2.26 ± 0.09	-2.14 ± 0.12	-1.30 ± 0.18	-2.00 ± 0.10	-1.70 ± 0.12	-1.20 ± 0.14	-1.70 ± 0.11	-1.60 ± 0.12
NM_010358	Glutathione S-transferase, mu 1	Gstb1	1.30 ± 0.26	1.60 ± 0.27	1.10 ± 0.18	1.50 ± 0.33	2.12 ± 0.40	1.42 ± 0.40	1.50 ± 0.32	2.30 ± 0.46	1.50 ± 0.30	-1.10 ± 0.14	1.90 ± 0.37	1.70 ± 0.35
Cell death														
NM_008714	Notch gene homolog 1 (Drosophila)	Notch1	1.00 ± 0.20	1.50 ± 0.29	1.30 ± 0.29	-1.10 ± 0.19	2.40 ± 0.44	1.70 ± 0.37	1.30 ± 0.26	2.30 ± 0.43	1.70 ± 0.38	-1.30 ± 0.18	1.80 ± 0.44	2.10 ± 0.48
NM_020581	Angiopoietin-like 4	Angptl4	2.70 ± 0.59	5.20 ± 1.14	2.30 ± 0.63	4.60 ± 0.84	11.98 ± 2.14	10.21 ± 2.28	4.20 ± 0.65	9.80 ± 1.61	6.60 ± 1.00	1.90 ± 0.46	7.90 ± 1.62	7.90 ± 1.58
NM_009811	Caspase 6	Casp6	1.10 ± 0.28	1.60 ± 0.33	1.20 ± 0.32	1.30 ± 0.30	2.10 ± 0.35	1.60 ± 0.36	1.50 ± 0.39	2.50 ± 0.48	1.80 ± 0.27	1.20 ± 0.31	2.00 ± 0.37	1.70 ± 0.46
NM_009818	Catenin (cadherin associated protein), alpha 1	Catna1	1.30 ± 0.21	1.60 ± 0.24	1.20 ± 0.18	1.30 ± 0.23	2.20 ± 0.29	1.50 ± 0.27	1.60 ± 0.28	2.40 ± 0.33	1.80 ± 0.32	1.20 ± 0.20	1.90 ± 0.34	1.80 ± 0.36
NM_021399	B-cell leukemia/lymphoma 11B	Bcl11b	-1.00 ± 0.17	-1.80 ± 0.11	-1.60 ± 0.12	-1.30 ± 0.16	-1.53 ± 0.12	-1.82 ± 0.11	-1.00 ± 0.21	-2.20 ± 0.09	-1.90 ± 0.11	1.00 ± 0.17	-1.70 ± 0.10	-1.50 ± 0.12

Table 3.5 (continue)

Genbank	Gene Title	Symbol	Time-points											
			300uM AMPA			100uM KA			200uM NMDA			250uM Glu		
			5h	15h	24h	5h	15h	24h	5h	15h	24h	5h	15h	24h
Cell homeostasis, survival and proliferation														
NM_010835	Homeo box, msh-like 1	Msh	1.10 ± 0.35	1.60 ± 0.48	1.00 ± 0.29	1.90 ± 0.63	2.02 ± 0.54	1.82 ± 0.46	1.30 ± 0.33	1.60 ± 0.34	1.50 ± 0.36	-1.30 ± 0.25	1.90 ± 0.57	1.80 ± 0.47
NM_152229	Nuclear receptor subfamily 2, group E, member 1	Nr2e1	1.40 ± 0.28	1.80 ± 0.38	1.30 ± 0.29	1.90 ± 0.40	2.30 ± 0.42	1.70 ± 0.35	1.40 ± 0.35	2.00 ± 0.32	1.60 ± 0.50	1.00 ± 0.21	2.00 ± 0.48	2.10 ± 0.47
NM_009263	Secreted phosphoprotein 1	Spp1	1.60 ± 0.40	1.40 ± 0.38	1.00 ± 0.28	1.00 ± 0.32	2.43 ± 0.68	2.23 ± 0.67	1.90 ± 0.83	3.50 ± 3.20	4.50 ± 1.17	1.30 ± 0.30	2.00 ± 0.44	2.00 ± 0.45
NM_009129	Secretogranin II	SgII	6.80 ± 2.32	7.90 ± 2.39	6.20 ± 1.77	7.40 ± 2.47	14.06 ± 2.73	12.03 ± 1.93	2.50 ± 0.44	3.20 ± 0.82	5.30 ± 0.85	1.00 ± 0.22	-3.80 ± 0.07	-3.50 ± 0.08
NM_009696	Apolipoprotein E	Apoe	1.00 ± 0.23	1.70 ± 0.29	1.30 ± 0.24	1.30 ± 0.28	2.36 ± 0.43	1.98 ± 0.36	1.20 ± 0.27	2.40 ± 0.52	1.80 ± 0.27	-1.20 ± 0.14	1.70 ± 0.32	1.70 ± 0.37
NM_009689	Baculoviral IAP repeat-containing 5	Birc5	1.70 ± 0.50	1.10 ± 0.37	1.00 ± 0.26	1.80 ± 0.59	1.39 ± 0.35	1.21 ± 0.31	2.00 ± 0.56	1.40 ± 0.33	-1.00 ± 0.22	1.40 ± 0.36	1.70 ± 0.50	1.20 ± 0.30
NM_013863	Bcl2-associated athanogene 3	Bag3	1.80 ± 0.24	2.40 ± 0.39	2.40 ± 0.48	2.50 ± 0.37	2.49 ± 0.37	2.09 ± 0.31	2.30 ± 0.47	2.70 ± 0.36	2.50 ± 0.48	1.60 ± 0.34	2.00 ± 0.38	1.80 ± 0.45
NM_010514	Insulin-like growth factor 2	Igf2	1.40 ± 0.28	1.50 ± 0.30	1.00 ± 0.21	1.80 ± 0.35	2.10 ± 0.43	1.60 ± 0.39	1.60 ± 0.36	1.70 ± 0.41	1.30 ± 0.28	1.40 ± 0.32	2.20 ± 0.52	1.90 ± 0.52
NM_133662	Immediate early response 3	Ier3	1.40 ± 0.32	1.40 ± 0.37	1.80 ± 0.45	-1.00 ± 0.26	1.60 ± 0.31	1.60 ± 0.35	1.20 ± 0.32	1.70 ± 0.31	1.60 ± 0.27	1.90 ± 0.48	1.10 ± 0.34	1.00 ± 0.21
NM_008048	Insulin-like growth factor binding protein 7	Ilgfbp7	1.20 ± 0.27	1.50 ± 0.32	1.30 ± 0.27	1.40 ± 0.30	2.20 ± 0.41	1.70 ± 0.45	1.30 ± 0.27	2.20 ± 0.44	1.70 ± 0.35	1.10 ± 0.27	2.20 ± 0.43	2.20 ± 0.58
NM_008520	Latent transforming growth factor beta binding protein 3	Ltbp2	1.10 ± 0.25	1.80 ± 0.43	1.60 ± 0.32	1.30 ± 0.33	1.98 ± 0.41	1.94 ± 0.41	1.20 ± 0.26	1.60 ± 0.34	1.80 ± 0.35	1.00 ± 0.22	1.50 ± 0.25	1.90 ± 0.41

Table 3.5 (continue)

Genbank	Gene Title	Symbol	Time-points											
			300uM AMPA			100uM KA			200uM NMDA			250uM Glu		
			5h	15h	24h									
Cell homeostasis, survival and proliferation (continue)														
NM_010518	Insulin-like growth factor binding protein 5	Igfbp5	-1.10 ± 0.25	1.60 ± 0.32	1.10 ± 0.26	1.30 ± 0.26	2.20 ± 0.38	1.70 ± 0.40	1.10 ± 0.25	2.00 ± 0.40	1.80 ± 0.39	-1.20 ± 0.12	1.70 ± 0.28	1.90 ± 0.40
NM_021099	Kit oncogene	Kit	-2.30 ± 0.10	-1.30 ± 0.20	-1.30 ± 0.18	-2.00 ± 0.11	-3.20 ± 0.07	-2.60 ± 0.10	-1.50 ± 0.13	-2.10 ± 0.10	-1.20 ± 0.18	-1.70 ± 0.12	-1.90 ± 0.12	-1.70 ± 0.17
Mitotic cell cycle														
NM_025565	SPC25, NDC80 kinetochore complex component, homolog (<i>S. cerevisiae</i>)	Spbc25	1.60 ± 0.52	1.36 ± 0.52	-1.00 ± 0.32	2.10 ± 0.81	1.83 ± 0.57	1.34 ± 0.45	2.10 ± 0.48	1.80 ± 0.49	1.20 ± 0.32	1.50 ± 0.41	1.60 ± 0.65	1.30 ± 0.63
NM_028390	Anillin, actin binding protein (scraps homolog, <i>Drosophila</i>)	Anilin	1.80 ± 0.51	1.20 ± 0.28	-1.00 ± 0.19	1.80 ± 0.48	1.60 ± 0.35	1.19 ± 0.32	1.80 ± 0.41	1.50 ± 0.33	1.20 ± 0.26	1.50 ± 0.40	1.60 ± 0.51	1.40 ± 0.41
NM_011497	Aurora kinase A	Aurka	1.90 ± 0.56	1.20 ± 0.36	1.00 ± 0.25	1.90 ± 0.55	1.46 ± 0.37	1.07 ± 0.29	1.70 ± 0.40	1.30 ± 0.32	1.10 ± 0.26	1.50 ± 0.42	1.60 ± 0.50	1.30 ± 0.44
NM_028109	TPX2, microtubule-associated protein homolog (<i>Xenopus laevis</i>)	Tpx2	1.60 ± 0.46	1.20 ± 0.41	-1.00 ± 0.26	1.70 ± 0.49	1.49 ± 0.45	1.06 ± 0.35	1.80 ± 0.49	1.50 ± 0.33	1.10 ± 0.25	1.40 ± 0.42	1.70 ± 0.55	1.30 ± 0.46
NM_007659	Cell division cycle 2 homolog A (<i>S. pombe</i>)	Cdc2	2.20 ± 0.62	1.30 ± 0.45	-1.00 ± 0.26	2.60 ± 0.71	1.74 ± 0.38	1.18 ± 0.32	2.10 ± 0.51	1.70 ± 0.39	1.20 ± 0.26	1.80 ± 0.42	1.70 ± 0.47	1.30 ± 0.39
NM_023223	Cell division cycle 20 homolog (<i>S. cerevisiae</i>)	Cdc20	2.00 ± 0.50	1.30 ± 0.38	1.00 ± 0.24	1.90 ± 0.55	1.88 ± 0.50	1.46 ± 0.46	2.00 ± 0.39	1.50 ± 0.31	-1.10 ± 0.24	1.40 ± 0.41	1.80 ± 0.50	1.20 ± 0.36
NM_013538	Cell division cycle associated 3	Cdca3	1.80 ± 0.65	1.20 ± 0.45	1.00 ± 0.28	1.60 ± 0.55	1.96 ± 0.56	1.34 ± 0.41	2.30 ± 0.62	1.80 ± 0.42	1.10 ± 0.26	1.40 ± 0.39	1.80 ± 0.48	1.30 ± 0.39
NM_026410	Cell division cycle associated 5	Cdca5	1.70 ± 0.38	1.00 ± 0.32	-1.10 ± 0.22	1.60 ± 0.34	1.20 ± 0.30	-1.03 ± 0.23	1.90 ± 0.44	1.30 ± 0.22	-1.10 ± 0.20	1.60 ± 0.45	1.30 ± 0.35	1.10 ± 0.33
NM_172301	Cyclin B1	Ccnb1	2.20 ± 0.63	1.30 ± 0.40	1.00 ± 0.30	3.00 ± 0.82	1.85 ± 0.60	1.32 ± 0.43	2.10 ± 0.50	1.60 ± 0.41	1.20 ± 0.29	1.50 ± 0.42	1.80 ± 0.54	1.30 ± 0.51

Table 3.5 (continue)

Genbank	Gene Title	Symbol	Time-points											
			300uM AMPA			100uM KA			200uM NMDA			250uM Glu		
			5h	15h	24h									
<u>Mitotic cell cycle (continue)</u>														
NM_009831	Cyclin G1	Ccng1	1.30 ± 0.32	1.60 ± 0.49	1.10 ± 0.23	1.80 ± 0.47	1.40 ± 0.36	-1.20 ± 0.27	1.30 ± 0.34	1.60 ± 0.33	1.30 ± 0.34	1.40 ± 0.34	1.60 ± 0.43	1.30 ± 0.35
NM_031166	Inhibitor of DNA binding 4	Idb4	1.30 ± 0.38	1.60 ± 0.48	1.10 ± 0.28	1.60 ± 0.47	2.20 ± 0.65	1.70 ± 0.59	1.50 ± 0.41	2.00 ± 0.53	1.20 ± 0.34	-1.40 ± 0.21	2.00 ± 0.56	2.10 ± 0.76
NM_010578	Integrin beta 1 (fibronectin receptor beta)	Fnrp	1.50 ± 0.33	1.20 ± 0.23	1.10 ± 0.22	1.50 ± 0.30	1.64 ± 0.31	1.13 ± 0.23	1.60 ± 0.31	1.50 ± 0.29	1.10 ± 0.20	1.30 ± 0.22	1.60 ± 0.28	1.40 ± 0.32
NM_023317	Nuclear distribution gene E homolog 1 (A nidulans)	Nude	1.30 ± 0.39	1.60 ± 0.45	1.00 ± 0.27	1.50 ± 0.42	1.89 ± 0.47	1.57 ± 0.45	1.30 ± 0.32	1.60 ± 0.35	1.30 ± 0.30	1.10 ± 0.30	1.80 ± 0.43	1.30 ± 0.35
NM_133851	Nucleolar and spindle associated protein 1	Nusp1	1.90 ± 0.58	1.10 ± 0.30	1.00 ± 0.24	2.00 ± 0.52	1.93 ± 0.47	1.24 ± 0.37	2.20 ± 0.51	1.90 ± 0.37	1.10 ± 0.21	1.50 ± 0.30	1.80 ± 0.44	1.50 ± 0.42
NM_007595	Calcium/calmodulin-dependent protein kinase II, beta	Camk2d	-1.10 ± 0.16	-1.60 ± 0.13	-1.50 ± 0.11	1.00 ± 0.16	-2.10 ± 0.08	-2.30 ± 0.10	-1.30 ± 0.13	-2.50 ± 0.06	-1.70 ± 0.11	-1.20 ± 0.13	-2.40 ± 0.09	-1.80 ± 0.11
NM_008913	Protein phosphatase 3, catalytic subunit, alpha isoform	Pp3ca	1.00 ± 0.23	-1.40 ± 0.25	-1.90 ± 0.09	1.40 ± 0.25	-1.74 ± 0.10	-2.12 ± 0.10	-1.00 ± 0.23	-2.20 ± 0.09	-1.80 ± 0.21	1.00 ± 0.20	-1.70 ± 0.11	-1.40 ± 0.12
NM_023396	Reprimo, TP53 dependent G2 arrest mediator candidate	Trp53	-1.30 ± 0.15	-1.50 ± 0.16	-1.50 ± 0.13	-1.40 ± 0.17	-1.80 ± 0.12	-1.80 ± 0.11	-1.20 ± 0.18	-1.80 ± 0.10	-1.60 ± 0.10	1.00 ± 0.18	-2.00 ± 0.09	-1.90 ± 0.11

3.2.2.3 Singular profile analysis highlight cell cycle re-activation as a prominent biological process during excitotoxicity

Demonstrated in Table 3.6, majority of the proteins involved in mitotic cell cycle process demonstrated significant transcriptional modulation across all four profiles. Gene expression of proteins promoting positive regulation of mitosis occurred at the 5-15h post-treatment interval but predominantly at the earlier 5h time-point, a strong advocate of an early occurrence of cell cycle re-entry upon iGluRs induction. Fold-change expression of individual cell cycle genes for respective treatments (AMPA, KA, NMDA and Glu) was demonstrated in Table 3.7, 3.8, 3.9 and 3.10 accordingly due to page size constraint.

Table 3.6 Genes encoding for proteins involved in mitotic cell division in individual excitotoxicity global transcriptomic profiles. Genes were selected on the basis of demonstrating at least ± 1.5 fold-change expression in at least one out of three time-points (5h, 15h and 24h) and passed statistical testing of one-way ANOVA, $p < 0.05$ and FDR correction. The genes were classified in the table according to the first time-point where significant regulation above or below 1.5 is detected.

	300uM AMPA	200uM NMDA	100uM KA	250uM Glu
Up-regulation (5h)	<ul style="list-style-type: none"> • Anillin, actin binding protein • Aurora kinase A • baculoviral IAP repeat-containing 5 • Buninhibited by benzimidazoles 1 homolog, beta (S. cerevisiae) • Cell division cycle 2 homolog A (S. pombe) • cell division cycle 20 homolog (S. cerevisiae) • cell division cycle associated 2 • cell division cycle associated 3 • cell division cycle associated 5 • cyclin D1 • cyclin D2 • DBF4 homolog (S. cerevisiae) • E4F transcription factor 1 • integrin beta 1 (fibronectin receptor beta) • neural precursor cell expressed, developmentally down-regulated gene 9 • non-SMC condensin I complex, subunit H 	<ul style="list-style-type: none"> • Anillin, actin binding protein • Aurora kinase A • Baculoviral IAP repeat-containing 5 • Budding uninhibited by benzimidazoles 1 homolog, beta (S. cerevisiae) • Cell division cycle 2 homolog A (S. pombe) • Cell division cycle 20 homolog (S. cerevisiae) • Cell division cycle associated 2 • Cell division cycle associated 3 • Cell division cycle associated 5 • Cell division cycle associated 8 • Cyclin B1 • Cyclin-dependent kinase 2 • DBF4 homolog (S. cerevisiae) • Integrin beta 1 (fibronectin receptor beta) • Kinesin family member C1 • MAD2 mitotic arrest deficient-like 1 (yeast) • Microtubule-associated protein, RP/EB family, 2 	<ul style="list-style-type: none"> • Anillin, actin binding protein • Asp (abnormal spindle)-like, microcephaly associated (Drosophila) • AT hook containing transcription factor 1 • Aurora kinase A • Baculoviral IAP repeat-containing 5 • Budding uninhibited by benzimidazoles 1 homolog, beta (S. cerevisiae) • Cell division cycle 2 homolog A (S. pombe) • Cell division cycle 20 homolog (S. cerevisiae) • Cell division cycle 6 homolog (S. cerevisiae); • Cell division cycle associated 3 • Cell division cycle associated 5 • Coiled-coil domain containing 99 • Cyclin D1 • Cyclin D2 • Cyclin G1 • Cyclin B1 • Cyclin-dependent kinase 2 	<ul style="list-style-type: none"> • Anillin, actin binding protein • Aurora kinase A • Baculoviral IAP repeat-containing 5 • Cyclin B1 • Cell division cycle 2 homolog A (S. pombe) • Cell division cycle associated 2 • Cell division cycle associated 3 • Cell division cycle associated 5 • Cell division cycle associated 8 • E4F transcription factor 1 • Nucleolar and spindle associated protein 1 • Polo-like kinase 1 (Drosophila) • Pescadillo homolog 1, containing BRCT domain (zebrafish) • SPC24, NDC80 kinetochore complex component, homolog (S. cerevisiae) • SPC25, NDC80 kinetochore complex component, homolog (S. cerevisiae) • Sperm associated antigen 5

Table 3.6 (continue)

	300uM AMPA	200uM NMDA	100uM KA	250uM Glu
<p>Up-regulation (5h) <i>(continue)</i></p>	<ul style="list-style-type: none"> • polo-like kinase 1 (Drosophila) • predicted gene 8416; predicted gene 5593; cyclin B1; similar to cyclin B1; predicted gene 4870 • regulator of chromosome condensation 2; hypothetical protein LOC100047340 • SPC25, NDC80 kinetochore complex component, homolog (S. cerevisiae) 	<ul style="list-style-type: none"> • Neural precursor cell expressed, developmentally down-regulated gene 1 • Non-SMC condensin I complex, subunit H • Nucleolar and spindle associated protein 1 • Pituitary tumor-transforming gene 1 • Polo-like kinase 1 (Drosophila) • SPC24, NDC80 kinetochore complex component, homolog (S. cerevisiae) • SPC25, NDC80 kinetochore complex component, homolog (S. cerevisiae) • Sperm associated antigen 5 	<ul style="list-style-type: none"> • DBF4 homolog (S. cerevisiae) • E4F transcription factor 1 • Inhibitor of DNA binding 4 • Integrin beta 1 (fibronectin receptor beta) • Microtubule-associated protein, RP/EB family, member 2 • Neural precursor cell expressed, developmentally down-regulated gene 9 • Non-SMC condensin II complex, subunit G2 • Nuclear distribution gene E homolog 1 (A nidulans) • Nucleolar and spindle associated protein 1 • ribosomal protein S6 • SET domain containing (lysine methyltransferase) 8 • Kinesin family member C1 • MAD2 mitotic arrest deficient-like 1 (yeast) • SPC25, NDC80 kinetochore complex component, homolog (S. cerevisiae) • sperm associated antigen 5 	

Table 3.6 (continue)

	300uM AMPA	200uM NMDA	100uM KA	250uM Glu
Up-regulation at 15h (continue)	<ul style="list-style-type: none"> • Nuclear distribution gene E homolog 1 (A nidulans) • Nucleolar and spindle associated protein 1 	<ul style="list-style-type: none"> • Nuclear distribution gene E homolog 1 (A nidulans) 		<ul style="list-style-type: none"> • Integrin beta 1 (fibronectin receptor beta) • Neural precursor cell expressed, developmentally down-regulated gene 1 • Non-SMC condensin I complex, subunit H • Nuclear distribution gene E homolog 1 (A nidulans) • Nuclear factor of activated T-cells, cytoplasmic, calcineurin-dependent 1 • Pituitary tumor-transforming gene 1
Down-regulation at 5h	<ul style="list-style-type: none"> • NIMA (never in mitosis gene a)-related expressed kinase 3 	<ul style="list-style-type: none"> • Calcium/calmodulin-dependent protein kinase II alpha 	<ul style="list-style-type: none"> • CDK5 and Abl enzyme substrate 1 • NIMA (never in mitosis gene a)-related expressed kinase 3 • SAC3 domain containing 1 • tubulin, gamma 1 	
Down-regulation at 15h	<ul style="list-style-type: none"> • Calcium/calmodulin-dependent protein kinase II, beta • Tubulin, beta 3 	<ul style="list-style-type: none"> • Calcium/calmodulin-dependent protein kinase II, beta • Cyclin D1 • Fibronectin type 3 and SPRY domain-containing protein • Protein phosphatase 3, catalytic subunit, alpha isoform • Ras homolog gene family, member U 	<ul style="list-style-type: none"> • Budding uninhibited by benzimidazoles 3 homolog (S. cerevisiae) • Calcium/calmodulin-dependent protein kinase II alpha • Calcium/calmodulin-dependent protein kinase II, beta • Centromere protein V 	<ul style="list-style-type: none"> • Amyloid beta (A4) precursor protein • Calcium/calmodulin-dependent protein kinase II alpha • Calcium/calmodulin-dependent protein kinase II, beta • Microtubule-associated protein, RP/EB family, member 2

Table 3.6 (continue)

	300uM AMPA	200uM NMDA	100uM KA	250uM Glu
Down-regulation at 15h (continue)		<ul style="list-style-type: none"> • Stathmin 1 • Tubulin, beta 3 	<ul style="list-style-type: none"> • Protein phosphatase 3, catalytic subunit, alpha isoform • Ras homolog gene family, member U • Regulator of chromosome condensation 2; hypothetical protein LOC100047340 • Calcium/calmodulin-dependent protein kinase II gamma gamma • Stathmin 1 	<ul style="list-style-type: none"> • Polo-like kinase 2 (Drosophila) • Protein phosphatase 3, catalytic subunit, alpha isoform • Ras homolog gene family, member U
Down-regulation at 24h	<ul style="list-style-type: none"> • Centrin 2 • Protein phosphatase 3, catalytic subunit, alpha isoform 	<ul style="list-style-type: none"> • Tubulin, gamma 1 	<ul style="list-style-type: none"> • ADP-ribosylation factor-like 8A • Activating transcription factor 6 beta • Centrin 2 • Centrin 3 • Checkpoint with forkhead and ring finger domains • Chromatin modifying protein 1A; predicted gene 8515 • Thioredoxin-like 4B • Tubulin, beta 3 	

Chapter 3.2:
iGluRs in excitotoxicity

Table 3.7 Significantly expressed genes (with fold-change of at least ± 1.5 in a minimum one out of three time-points and passed One-way ANOVA, $p < 0.05$ and Benjamini Hochberg FDR correction) encoding for proteins involved in mitotic cell cycle upon 300uM AMPA-mediated excitotoxicity in cultured primary cortical neurons.

Genbank	Title	Symbol	300uM AMPA		
			5h	15h	24h
Mitotic cell cycle					
NM_172301	Cyclin B1	Ccnb1	2.75 \pm 0.63	1.66 \pm 0.40	1.03 \pm 0.30
NM_007659	Cell division cycle 2 homolog A (<i>S. pombe</i>)	Cdc2	2.58 \pm 0.62	1.54 \pm 0.45	-1.10 \pm 0.26
NM_011121	Polo-like kinase 1 (<i>Drosophila</i>)	Plk	2.40 \pm 0.52	1.19 \pm 0.42	-1.08 \pm 0.20
NM_013726	DBF4 homolog (<i>S. cerevisiae</i>)	Dbf4	2.32 \pm 0.55	1.76 \pm 0.45	1.25 \pm 0.35
NM_011497	Aurora kinase A	AurkA	2.31 \pm 0.56	1.48 \pm 0.36	1.04 \pm 0.25
NM_009829	Cyclin D2	Ccnd2	2.22 \pm 0.61	1.50 \pm 0.33	1.01 \pm 0.18
NM_133851	Nucleolar and spindle associated protein 1	NuSap1	2.18 \pm 0.58	1.35 \pm 0.30	-1.04 \pm 0.24
NM_013538	Cell division cycle associated 3	Cdca3	2.17 \pm 0.65	1.45 \pm 0.45	1.01 \pm 0.28
NM_009773	Budding uninhibited by benzimidazoles 1 homolog, beta (<i>S. cerevisiae</i>)	Bubr1	2.15 \pm 0.62	1.34 \pm 0.54	-1.09 \pm 0.26
NM_028390	Anillin, actin binding protein	Anl	1.97 \pm 0.51	1.28 \pm 0.28	-1.10 \pm 0.19
NM_009689	Baculoviral IAP repeat-containing 5	Birc5	1.94 \pm 0.50	1.25 \pm 0.37	-1.03 \pm 0.26
NM_175384	Cell division cycle associated 2	Cdca2	1.92 \pm 0.42	1.12 \pm 0.29	-1.12 \pm 0.19
NM_173867	Regulator of chromosome condensation 2	Td60	1.90 \pm 0.59	1.92 \pm 0.55	1.64 \pm 0.47
NM_026410	Cell division cycle associated 5	Cdca5	1.86 \pm 0.38	1.10 \pm 0.32	-1.21 \pm 0.22
NM_144818	Non-SMC condensin I complex, subunit H	Nsc1h	1.83 \pm 0.69	1.32 \pm 0.63	1.02 \pm 0.46
NM_025565	SPC25, NDC80 kinetochore complex component, homolog (<i>S. cerevisiae</i>)	Spc25	1.79 \pm 0.52	1.50 \pm 0.52	-1.08 \pm 0.32
NM_017464	Neural precursor cell expressed, developmentally down-regulated gene 9	Npcdr9	1.72 \pm 0.47	1.97 \pm 0.56	1.31 \pm 0.36
NM_023223	Cell division cycle 20 homolog (<i>S. cerevisiae</i>)	Cdc20	1.65 \pm 0.52	1.14 \pm 0.34	1.03 \pm 0.33
NM_010578	Integrin beta 1 (fibronectin receptor beta)	Fnrp	1.58 \pm 0.33	1.29 \pm 0.23	1.13 \pm 0.22
NM_007893	E4F transcription factor 1	E4f1	1.53 \pm 0.45	1.42 \pm 0.41	1.28 \pm 0.38
NM_007631	Cyclin D1	Ccnd1	1.46 \pm 0.45	-1.00 \pm 0.25	-1.63 \pm 0.18

Table 3.7 (continue)

Genbank	Title	Genbank	300uM AMPA		
			5h	15h	24h
Mitotic cell cycle					
NM_023317	Nuclear distribution gene E homolog 1 (A nidulans)	Nude	1.40 ± 0.39	1.74 ± 0.45	1.11 ± 0.27
NM_009831	Cyclin G1	Ccng1	1.28 ± 0.32	1.58 ± 0.49	1.05 ± 0.23
NM_023813	Calcium/calmodulin-dependent protein kinase II, delta	Camk2	1.28 ± 0.38	1.57 ± 0.41	1.24 ± 0.29
NM_031166	Inhibitor of DNA binding 4	Idb4	1.27 ± 0.38	1.65 ± 0.48	1.07 ± 0.28
NM_008913	Protein phosphatase 3, catalytic subunit, alpha isoform	Ppca3	1.01 ± 0.23	-1.45 ± 0.25	-1.93 ± 0.09
NM_007595	Calcium/calmodulin-dependent protein kinase II, beta	Camk2d	-1.04 ± 0.16	-1.56 ± 0.13	-1.52 ± 0.11
NM_019405	Centrin 2	Calt	-1.07 ± 0.24	-1.33 ± 0.24	-1.83 ± 0.21
NM_023279	Tubulin, beta 3	Tubb3	-1.39 ± 0.23	-1.82 ± 0.18	-1.75 ± 0.19
NM_011848	NIMA (never in mitosis gene a)-related expressed kinase 3	Nek3	-1.78 ± 0.13	-1.12 ± 0.16	-1.30 ± 0.13

Table 3.8 Significantly expressed genes (with fold-change of at least ± 1.5 in a minimum one out of three time-points and passed One-way ANOVA, $p < 0.05$ and Benjamini Hochberg FDR correction) encoding for proteins involved in mitotic cell cycle upon 100uM KA-mediated excitotoxicity in cultured primary cortical neurons.

Genbank	Gene title	Symbol	100uM KA		
			5h	15h	24h
Mitotic cell cycle					
NM_172301	Cyclin B1	Ccnb1	3.13 \pm 0.75	1.85 \pm 0.39	1.42 \pm 0.37
NM_007659	Cell division cycle 2 homolog A (<i>S. pombe</i>)	Cdc2	3.02 \pm 0.71	1.74 \pm 0.38	1.18 \pm 0.32
NM_013726	DBF4 homolog (<i>S. cerevisiae</i>)	Dbf4	2.63 \pm 0.59	1.76 \pm 0.41	1.36 \pm 0.32
NM_025565	SPC25, NDC80 kinetochore complex component, homolog (<i>S. cerevisiae</i>)	Spc25	2.38 \pm 0.81	1.83 \pm 0.57	1.34 \pm 0.45
NM_009773	Budding uninhibited by benzimidazoles 1 homolog, beta (<i>S. cerevisiae</i>)	Bubr1	2.33 \pm 0.58	1.67 \pm 0.50	1.27 \pm 0.51
NM_017464	Neural precursor cell expressed, developmentally down-regulated gene 9	Npcdr9	2.31 \pm 0.74	1.58 \pm 0.48	1.38 \pm 0.36
NM_011497	Aurora kinase A	AurkA	2.30 \pm 0.55	1.46 \pm 0.37	1.07 \pm 0.29
NM_133851	Nucleolar and spindle associated protein 1	NuSap1	2.30 \pm 0.52	1.93 \pm 0.47	1.24 \pm 0.37
NM_023223	Cell division cycle 20 homolog (<i>S. cerevisiae</i>)	Cdc20	2.22 \pm 0.55	1.88 \pm 0.50	1.46 \pm 0.46
NM_009829	Cyclin D2	Ccnd2	2.18 \pm 0.33	1.26 \pm 0.25	1.01 \pm 0.34
NM_009689	Baculoviral IAP repeat-containing 5	Birc5	2.09 \pm 0.59	1.39 \pm 0.35	1.21 \pm 0.31
NM_028390	Anillin, actin binding protein	Anl	1.96 \pm 0.48	1.60 \pm 0.35	1.19 \pm 0.32
NM_009791	Asp (abnormal spindle)-like, microcephaly associated (<i>Drosophila</i>)	Asp	1.95 \pm 0.61	1.39 \pm 0.45	1.22 \pm 0.49
NM_013538	Cell division cycle associated 3	Cdc3	1.94 \pm 0.55	1.96 \pm 0.56	1.34 \pm 0.41
NM_173867	Regulator of chromosome condensation 2	Td60	1.88 \pm 0.64	2.00 \pm 0.56	1.97 \pm 0.51
NM_053173	Kinesin family member C1	Kifc5a	1.88 \pm 0.50	1.41 \pm 0.38	1.17 \pm 0.34
NM_007893	E4F transcription factor 1	E4f1	1.84 \pm 0.46	1.83 \pm 0.47	1.91 \pm 0.51
NM_026410	Cell division cycle associated 5	Cdea5	1.82 \pm 0.34	1.20 \pm 0.30	-1.03 \pm 0.23
NM_009096	Ribosomal protein S6	S6	1.75 \pm 0.45	1.29 \pm 0.41	1.23 \pm 0.47
NM_133762	Non-SMC condensin II complex, subunit G2	Nsc2g2	1.66 \pm 0.45	1.17 \pm 0.41	-1.03 \pm 0.34
NM_010578	Integrin beta 1 (fibronectin receptor beta)	Fnr1	1.59 \pm 0.30	1.64 \pm 0.31	1.13 \pm 0.23
NM_023317	Nuclear distribution gene E homolog 1 (<i>A. nidulans</i>)	Nude	1.58 \pm 0.42	1.89 \pm 0.47	1.57 \pm 0.45
NM_019499	MAD2 mitotic arrest deficient-like 1 (yeast)	Mad2	1.58 \pm 0.58	1.15 \pm 0.41	-1.13 \pm 0.40
NM_017407	Sperm associated antigen 5	Mastrin	1.57 \pm 0.49	1.63 \pm 0.39	1.10 \pm 0.28

Table 3.8 (continue)

Genbank	Gene title	Symbol	100uM KA		
			5h	15h	24h
Mitotic cell cycle (continue)					
NM_031166	Inhibitor of DNA binding 4	Idb4	1.57 ± 0.47	2.19 ± 0.65	1.72 ± 0.59
NM_016756	Cyclin-dependent kinase 2	Cdk2	1.55 ± 0.39	1.31 ± 0.29	1.16 ± 0.30
NM_026375	AT hook containing transcription factor 1	At1	1.55 ± 0.38	1.27 ± 0.29	1.07 ± 0.29
NM_027411	Coiled-coil domain containing 99	Ccd99	1.54 ± 0.52	1.10 ± 0.29	1.07 ± 0.38
NM_011799	Cell division cycle 6 homolog (S. cerevisiae)	Cdc6	1.53 ± 0.42	1.06 ± 0.27	1.10 ± 0.34
NM_009831	Cyclin G1	Ccng1	1.53 ± 0.33	1.35 ± 0.25	-1.01 ± 0.22
NM_007631	Cyclin D1	Ccnd1	1.51 ± 0.42	1.06 ± 0.31	-1.28 ± 0.24
NM_030241	SET domain containing (lysine methyltransferase) 8	Sdc8	1.51 ± 0.43	-1.07 ± 0.25	-1.14 ± 0.24
NM_153058	Microtubule-associated protein, RP/EB family, member 2	Eb2	1.50 ± 0.49	1.44 ± 0.42	1.08 ± 0.39
NM_008682	Neural precursor cell expressed, developmentally down-regulated gene 1	Nedd1	1.43 ± 0.33	1.67 ± 0.33	1.23 ± 0.34
NM_008913	Protein phosphatase 3, catalytic subunit, alpha isoform	Ppca3	1.41 ± 0.25	-1.74 ± 0.10	-2.12 ± 0.10
NM_019641	Stathmin 1	Stamn1	1.40 ± 0.39	-2.29 ± 0.13	-1.60 ± 0.27
NM_019405	Centrin 2	Calt	1.36 ± 0.39	-1.41 ± 0.23	-1.91 ± 0.17
NM_009774	Budding uninhibited by benzimidazoles 3 homolog (S. cerevisiae)	Bub3	1.17 ± 0.31	-1.59 ± 0.14	-1.66 ± 0.16
NM_007684	Centrin 3	Cen3	1.16 ± 0.32	-1.25 ± 0.19	-1.61 ± 0.19
NM_008569	Anaphase promoting complex subunit 1	Apc1	1.16 ± 0.25	1.61 ± 0.39	1.31 ± 0.35
NM_026823	ADP-ribosylation factor-like 8A	Arfl8a	1.15 ± 0.23	-1.37 ± 0.18	-1.78 ± 0.14
NM_145606	Chromatin modifying protein 1A	Cmp1a	1.11 ± 0.26	-1.43 ± 0.13	-1.59 ± 0.12
NM_178597	Calcium/calmodulin-dependent protein kinase type II gamma chain	Camkg	1.10 ± 0.24	-1.69 ± 0.12	-1.71 ± 0.17
XM_203393	Centromere protein V	Cenv	1.03 ± 0.28	-1.52 ± 0.15	-1.36 ± 0.18
NM_007595	Calcium/calmodulin-dependent protein kinase II, beta	Camk2d	1.01 ± 0.16	-2.09 ± 0.08	-2.25 ± 0.10
NM_017406	Activating transcription factor 6 beta	Atf6b	-1.01 ± 0.21	-1.38 ± 0.14	-1.76 ± 0.14
NM_023279	Tubulin, beta 3	Tubb3	-1.13 ± 0.33	-2.22 ± 0.15	-2.58 ± 0.13
NM_177407	Calcium/calmodulin-dependent protein kinase II alpha	CaMKII	-1.15 ± 0.31	-1.62 ± 0.20	-1.54 ± 0.20

Table 3.8 (continue)

Genbank	Gene title	Symbol	100uM KA		
			5h	15h	24h
Mitotic cell cycle (continue)					
NM_172717	Checkpoint with forkhead and ring finger domains	Frfd	-1.16 ± 0.30	-1.42 ± 0.25	-1.67 ± 0.22
NM_133955	Ras homolog gene family, member U	Rasu	-1.32 ± 0.16	-1.98 ± 0.10	-2.18 ± 0.09
NM_175646	Thioredoxin-like 4B	Trxl4b	-1.41 ± 0.21	-1.29 ± 0.20	-1.68 ± 0.16
NM_022021	CDK5 and Abl enzyme substrate 1	Cables	-1.56 ± 0.14	-1.87 ± 0.12	-2.11 ± 0.12
NM_133678	SAC3 domain containing 1	Shd1	-1.58 ± 0.26	-1.55 ± 0.23	-1.80 ± 0.17
NM_134024	Tubulin, gamma 1	Tubg	-1.66 ± 0.13	-1.52 ± 0.13	-1.70 ± 0.15
NM_011848	NIMA (never in mitosis gene a)-related expressed kinase 3	Nek3	-1.79 ± 0.14	-1.20 ± 0.17	-1.68 ± 0.13

Table 3.9 Significantly expressed genes (with fold-change of at least ± 1.5 in a minimum one out of three time-points and passed One-way ANOVA, $p < 0.05$ and Benjamini Hochberg FDR correction) encoding for proteins involved in mitotic cell cycle upon 200uM NMDA-mediated excitotoxicity in cultured primary cortical neurons.

Genbank	Genbank	Symbol	200uM NMDA		
			5h	15h	24h
Mitotic cell cycle					
NM_013538	Cell division cycle associated 3	Cdca3	2.18 \pm 0.62	1.78 \pm 0.42	1.04 \pm 0.26
NM_133851	Nucleolar and spindle associated protein 1	NuSap1	2.18 \pm 0.51	1.83 \pm 0.37	1.11 \pm 0.21
NM_025565	SPC25, NDC80 kinetochore complex component, homolog (<i>S. cerevisiae</i>)	Spc25	2.11 \pm 0.48	1.82 \pm 0.49	1.21 \pm 0.32
NM_007659	Cell division cycle 2 homolog A (<i>S. pombe</i>)	Cdc2	2.10 \pm 0.51	1.66 \pm 0.39	1.20 \pm 0.26
NM_172301	Cyclin B1	Ccnb1	2.07 \pm 0.50	1.62 \pm 0.41	1.19 \pm 0.29
NM_009689	Baculoviral IAP repeat-containing 5	Birc5	1.96 \pm 0.56	1.41 \pm 0.33	-1.02 \pm 0.22
NM_011121	Polo-like kinase 1 (<i>Drosophila</i>)	Plk	1.90 \pm 0.38	1.44 \pm 0.21	-1.10 \pm 0.20
NM_019499	MAD2 mitotic arrest deficient-like 1 (yeast)	Mad2	1.87 \pm 0.62	1.09 \pm 0.34	-1.12 \pm 0.25
NM_023223	Cell division cycle 20 homolog (<i>S. cerevisiae</i>)	Cdc20	1.87 \pm 0.39	1.43 \pm 0.31	-1.02 \pm 0.24
NM_026410	Cell division cycle associated 5	Csca5	1.85 \pm 0.44	1.26 \pm 0.22	-1.11 \pm 0.20
NM_144818	Non-SMC condensin I complex, subunit H	Nsc1h	1.85 \pm 0.64	1.28 \pm 0.45	1.10 \pm 0.34
NM_028390	Anillin, actin binding protein	Anl	1.84 \pm 0.41	1.50 \pm 0.33	1.18 \pm 0.26
NM_008682	Neural precursor cell expressed, developmentally down-regulated gene 1	Nedd1	1.71 \pm 0.42	1.85 \pm 0.40	1.36 \pm 0.27
NM_011497	Aurora kinase A	AurkA	1.65 \pm 0.40	1.31 \pm 0.32	1.11 \pm 0.26
NM_016756	Cyclin-dependent kinase 2	Cdk2	1.60 \pm 0.28	1.48 \pm 0.26	1.33 \pm 0.29
NM_009773	Budding uninhibited by benzimidazoles 1 homolog, beta (<i>S. cerevisiae</i>)	Bubr1	1.60 \pm 0.41	1.28 \pm 0.39	-1.06 \pm 0.26
NM_053173	Kinesin family member C1	Kifc5a	1.59 \pm 0.44	1.19 \pm 0.26	1.01 \pm 0.21
NM_026560	Cell division cycle associated 8	Cdc8	1.58 \pm 0.48	1.22 \pm 0.32	1.01 \pm 0.27
NM_175384	Cell division cycle associated 2	Cdca2	1.57 \pm 0.30	1.32 \pm 0.25	-1.01 \pm 0.20
NM_013917	Pituitary tumor-transforming gene 1	Pttg1	1.57 \pm 0.62	1.09 \pm 0.29	-1.23 \pm 0.21
NM_026282	SPC24, NDC80 kinetochore complex component, homolog (<i>S. cerevisiae</i>)	Spc24	1.55 \pm 0.50	1.29 \pm 0.37	-1.06 \pm 0.25
NM_017407	Sperm associated antigen 5	Mastrin	1.54 \pm 0.37	1.43 \pm 0.32	1.02 \pm 0.22
NM_010578	Integrin beta 1 (fibronectin receptor beta)	Fnr1	1.54 \pm 0.31	1.45 \pm 0.29	1.10 \pm 0.20

Table 3.9 (continue)

Genbank	Genbank	Symbol	200uM NMDA		
			5h	15h	24h
Mitotic cell cycle (continue)					
NM_013726	DBF4 homolog (S. cerevisiae)	Dbf4	1.51 ± 0.40	1.11 ± 0.23	1.28 ± 0.35
NM_033270	E2F transcription factor 6	E2F6	1.41 ± 0.32	1.50 ± 0.24	1.15 ± 0.23
NM_031166	Inhibitor of DNA binding 4	Idb4	1.36 ± 0.41	1.89 ± 0.53	1.15 ± 0.34
NM_027985	MAD2 mitotic arrest deficient-like 2 (yeast)	Mad2b	1.33 ± 0.29	1.50 ± 0.37	1.05 ± 0.27
NM_009831	Cyclin G1	Ccng1	1.30 ± 0.34	1.55 ± 0.33	1.25 ± 0.34
NM_023317	Nuclear distribution gene E homolog 1 (A nidulans)	Nude	1.28 ± 0.32	1.56 ± 0.35	1.24 ± 0.30
NM_019641	Stathmin 1	Stamn1	1.19 ± 0.39	-1.80 ± 0.16	-1.34 ± 0.22
NM_023279	Tubulin, beta 3	Tubb3	1.02 ± 0.31	-1.77 ± 0.17	-1.66 ± 0.17
NM_007631	Cyclin D1	Ccnd1	1.02 ± 0.31	-1.61 ± 0.15	-1.65 ± 0.15
NM_008913	Protein phosphatase 3, catalytic subunit, alpha isoform	Ppca3	-1.00 ± 0.23	-2.14 ± 0.09	-1.82 ± 0.21
NM_134024	Tubulin, gamma 1	Tubg1	-1.04 ± 0.18	-1.34 ± 0.15	-1.76 ± 0.13
NM_153058	Microtubule-associated protein, RP/EB family, member 2	Eb2	-1.29 ± 0.16	-1.63 ± 0.11	-1.27 ± 0.25
NM_183178	Fibronectin type 3 and SPRY domain-containing protein	Fsd1	-1.30 ± 0.15	-1.72 ± 0.12	-1.69 ± 0.11
NM_007595	Calcium/calmodulin-dependent protein kinase II, beta	Camk2d	-1.31 ± 0.13	-2.47 ± 0.06	-1.71 ± 0.11
NM_133955	Ras homolog gene family, member U	Rasu	-1.53 ± 0.14	-1.50 ± 0.12	-1.22 ± 0.20
NM_177407	Calcium/calmodulin-dependent protein kinase II alpha	Camk2	-1.62 ± 0.18	-1.68 ± 0.16	-1.43 ± 0.17

Chapter 3.2:
iGluRs in excitotoxicity

Table 3.10 Significantly expressed genes (with fold-change of at least ± 1.5 in a minimum one out of three time-points and passed One-way ANOVA, $p < 0.05$) encoding for proteins involved in mitotic cell cycle upon 250uM Glu-mediated excitotoxicity in cultured primary cortical neurons.

Genbank	Gene	Symbol	250uM Glu		
			5h	15h	24h
Mitotic cell cycle					
NM_011121	Polo-like kinase 1 (Drosophila)	Plk	2.08 \pm 0.32	2.06 \pm 0.37	1.62 \pm 0.30
NM_007659	Cell division cycle 2 homolog A (S. pombe)	Cdc2	2.06 \pm 0.42	1.91 \pm 0.47	1.50 \pm 0.39
NM_011497	Aurora kinase A	AurkA	1.91 \pm 0.42	1.98 \pm 0.50	1.59 \pm 0.44
NM_026410	Cell division cycle associated 5	Cdca5	1.88 \pm 0.45	1.60 \pm 0.35	1.35 \pm 0.33
NM_175384	Cell division cycle associated 2	Cdca2	1.82 \pm 0.37	1.70 \pm 0.35	1.52 \pm 0.34
NM_028390	Anillin, actin binding protein	Anl	1.80 \pm 0.40	1.86 \pm 0.51	1.67 \pm 0.41
NM_026282	SPC24, NDC80 kinetochore complex component, homolog (S. cerevisiae)	Spc24	1.71 \pm 0.32	1.67 \pm 0.55	1.18 \pm 0.33
NM_172301	Cyclin B1	Ccnb1	1.68 \pm 0.42	2.09 \pm 0.54	1.48 \pm 0.51
NM_025565	SPC25, NDC80 kinetochore complex component, homolog (S. cerevisiae)	Spc25	1.66 \pm 0.41	1.85 \pm 0.65	1.47 \pm 0.63
NM_133851	Nucleolar and spindle associated protein 1	NuSap1	1.66 \pm 0.30	2.09 \pm 0.44	1.67 \pm 0.42
NM_023223	Cell division cycle 20 homolog (S. cerevisiae)	Cdc20	1.61 \pm 0.41	2.03 \pm 0.50	1.32 \pm 0.36
NM_026560	Cell division cycle associated 8	Cdca8	1.61 \pm 0.57	1.43 \pm 0.48	1.06 \pm 0.36
NM_013538	Cell division cycle associated 3	Cdca3	1.57 \pm 0.39	2.03 \pm 0.48	1.43 \pm 0.39
NM_009689	Baculoviral IAP repeat-containing 5	Birc5	1.54 \pm 0.36	1.88 \pm 0.50	1.34 \pm 0.30
NM_017407	Sperm associated antigen 5	Mastrin	1.52 \pm 0.38	1.85 \pm 0.46	1.55 \pm 0.48
NM_007893	E4F transcription factor 1	E4f1	1.52 \pm 0.40	1.09 \pm 0.33	1.03 \pm 0.35
NM_008682	Neural precursor cell expressed, developmentally down-regulated gene 1	Nedd4	1.40 \pm 0.29	1.84 \pm 0.42	1.65 \pm 0.42
NM_009831	Cyclin G1	Ccng	1.36 \pm 0.31	1.52 \pm 0.39	1.31 \pm 0.29
NM_010578	Integrin beta 1 (fibronectin receptor beta)	Fnrb	1.34 \pm 0.22	1.64 \pm 0.28	1.46 \pm 0.32
NM_013917	Pituitary tumor-transforming gene 1	Securin	1.29 \pm 0.44	1.71 \pm 0.72	1.27 \pm 0.45
NM_144818	Non-SMC condensin I complex, subunit H	Nsc1h	1.24 \pm 0.49	1.71 \pm 0.55	1.53 \pm 0.49
NM_033270	E2F transcription factor 6	E2f6	1.22 \pm 0.24	1.68 \pm 0.42	1.53 \pm 0.39
NM_023317	Nuclear distribution gene E homolog 1 (A nidulans)	Nude	1.13 \pm 0.30	1.77 \pm 0.43	1.35 \pm 0.35
NM_022889	Pescadillo homolog 1, containing BRCT domain (zebrafish)	Pes1	1.12 \pm 0.22	1.49 \pm 0.33	1.31 \pm 0.28
NM_007471	Amyloid beta (A4) precursor protein	Abeta	1.06 \pm 0.20	-1.64 \pm 0.12	-1.56 \pm 0.14
NM_008913	Protein phosphatase 3, catalytic subunit, alpha isoform	Pp3ca	1.03 \pm 0.20	-1.71 \pm 0.11	-1.48 \pm 0.12

Table 3.10 (continue)

Genbank	Gene	Symbol	250uM Glu		
			5h	15h	24h
<u>Mitotic cell cycle (continue)</u>					
NM_007595	Calcium/calmodulin-dependent protein kinase II, beta	Camk2b	-1.18 ± 0.13	-2.33 ± 0.09	-1.74 ± 0.11
NM_198429	Nuclear factor of activated T-cells, cytoplasmic, calcineurin-dependent 1	Nfat2	-1.29 ± 0.23	1.50 ± 0.41	1.61 ± 0.45
NM_153058	Microtubule-associated protein, RP/EB family, member 2	Eb2	-1.29 ± 0.15	-1.51 ± 0.14	-1.27 ± 0.17
NM_133955	Ras homolog gene family, member U	Ras	-1.30 ± 0.16	-1.62 ± 0.15	-1.31 ± 0.14
NM_152804	Polo-like kinase 2 (Drosophila)	Snk	-1.37 ± 0.18	-1.82 ± 0.12	-1.46 ± 0.20
NM_031166	Inhibitor of DNA binding 4	Id4	-1.41 ± 0.21	1.93 ± 0.56	2.11 ± 0.76
NM_177407	Calcium/calmodulin-dependent protein kinase II alpha	Camk2a	-1.42 ± 0.19	-1.67 ± 0.21	-1.44 ± 0.24

3.2.2.4 Validation of Glu global transcriptomic profiles via real-time PCR

Microarray data was validated via real-time PCR using on the same total RNA samples previously employed in microarray analysis. Similar temporal transcriptional regulatory trend was observed for the following genes (Table 3.11).

Table 3.11 Validation of microarray data using real-time PCR technique on D7 murine primary cortical neuronal cultures treated with 250uM Glu. All fold-change expressions are statistically significant at $p < 0.05$. Each expression data is representative of 3 independent replicates. Data are expressed as fold-change \pm sem.

GenBank	Gene Title	Symbol	5h		15h		24h	
			Microarray	Real-time PCR	Microarray	Real-time PCR	Microarray	Real-time PCR
NM_030704	Heat shock protein 8	Hspb8	1.29 \pm 0.31	1.42 \pm 0.69	4.40 \pm 1.06	9.29 \pm 0.55	2.63 \pm 0.70	2.24 \pm 0.72
NM_010442	Heme oxygenase 1	Hmox1	1.59 \pm 0.34		2.37 \pm 0.41	1.78 \pm 0.62	1.51 \pm 0.38	
NM_029688	Sulfiredoxin 1 homolog	Npn3	-1.20 \pm 0.29		2.16 \pm 0.73	2.99 \pm 0.55	1.17 \pm 0.43	
NM_011121	Polo-like kinase 1	Plk	2.08 \pm 0.32		2.06 \pm 0.37	1.64 \pm 0.59	1.62 \pm 0.30	
NM_007585	Annexin A2	AnxA2	1.52 \pm 0.25		1.93 \pm 0.31		2.05 \pm 0.43	8.25 \pm 0.61
NM_020581	Angiopoietin-like 4	Angptl4	2.00 \pm 0.46	3.28 \pm 0.66	8.27 \pm 1.62		8.24 \pm 1.58	5.63 \pm 0.58
NM_011497	Aurora kinase A	Aurka	1.91 \pm 0.42	3.31 \pm 0.69	1.98 \pm 0.50	1.95 \pm 0.72	1.59 \pm 0.44	2.97 \pm 1.11
NM_028109	TPX2, microtubule-associated protein homolog	Tpx2	1.70 \pm 0.42	5.78 \pm 0.47	2.09 \pm 0.55	4.79 \pm 0.78	1.57 \pm 0.46	4.21 \pm 0.60

3.2.3 Discussion

Comparative global transcriptomic profile analysis of iGluRs-specific agonists (AMPA, KA and NMDA) and the general GluRs agonist, Glu revealed several enriched biological processes pivotal to the progression of excitotoxicity. Temporal global gene profiling study revealed that AMPA and Glu –mediated neuronal injury evoke a delayed activation of downstream signaling cascade as compared to that of NMDA and KA. This temporal discrepancy arises probably as a result of surface receptor abundance and voltage conductance ability of individual iGluRs in the situation of the later transcriptional modulation of signaling cascades in AMPA model, and an additional factor of metabotropic GluRs activation in Glu model.

Lending further support from H₂S-mediated neuronal death where only selective NMDARs and KARs antagonists have the ability to evoke attenuation, it implies that NMDARs and KARs have a greater surface expression on the post-synaptic membrane for activation as compared to AMPARs. Furthermore, AMPARs limitation in the conductance of Ca²⁺ influx is imposed by its selective permeability to Ca²⁺ governed by the GluR2 subunit, even though they are still freely permeable to other cations such as Na⁺ and K⁺. NMDARs and KARs do not demonstrate selective permeability to Ca²⁺. The presence of a GluR2 subunit has the ability to occlude the channel conductance of Ca²⁺ influx as a result of its post-translational modification that alters the uncharged amino acid glutamine to the positively-charged arginine in the receptor's ion channel. The positively-charged amino acid at the critical point makes it energetically adverse for Ca²⁺ to enter the cell through the pore. Majority of the GluR2 subunits in CNS undergoes this single amino acid

Chapter 3.2: iGluRs in excitotoxicity

alteration, implying the main ions gated by AMPARs are Na⁺ and K⁺. As such, it has been postulated that activation of GluR2-containing AMPARs guards against excitotoxicity through inhibition of Ca²⁺ entry into the neuron (Kim et al., 2001). However, it is important to keep in mind, that given sufficient time for influx of Ca²⁺ into the cytosol via non- GluR2-containing receptors, AMPARs still have the ability to initiate excitotoxicity as reported in literature.

Oxidative stress is a prominent patho-physiological mechanism during excitotoxicity as demonstrated by the significant transcriptional activation of anti-oxidative enzymes such as HSPs and molecular chaperones, and GSH metabolic pathway. Mitochondria has been shown to be the primary source of ROS in excitotoxicity-mediated neuronal injury, where an overproduction of ROS leads to an inactivation of anti-oxidant enzymes thus fast consuming the cellular antioxidant ability, eventually causing a dysfunction of the natural defense mechanisms to protect the neurons. ROS, being thermodynamically active, modify cellular proteins, lipids and DNA in a detrimental way, thereby disrupting normal cellular signaling and gene regulation. Frequently, oxidative stress, a crucial component of neurodegeneration seen in AD, ALS and PD, with increasing participation in their pathogenesis has been identified as concordant with markers of unregulated cell cycle re-entry and its aberrations (Wang et al., 2009; Zhu et al., 2007).

Temporal global transcriptomic profiles of models of excitotoxicity demonstrated significant modulation of mitotic cell cycle process, with an up-regulation observed for majority of the cell cycle-promoting proteins. Over the years, the precise origins of mitotic

Chapter 3.2: iGluRs in excitotoxicity

dysfunction have not been fully understood. Cell cycle re-activation association to excitotoxicity has previously been reported on numerous occasions in models of excitotoxicity and stroke, amidst models of other neurodegenerative diseases such as the MPTP model of PD and superoxide dismutase (SOD)-1 mouse model of ALS (Hoglinger et al., 2007; Nguyen et al., 2003; Verdaguer et al., 2004a; Verdaguer et al., 2003), indicating a similar neuropathological incidence between two cellular events which may not be a coincidence. For the first time, employing comparative temporal microarray technique, the present project has demonstrated that iGluRs activation plays an important role in the trigger of cell cycle re-activation during Glu-mediated excitotoxicity, and that iGluRs may promisingly be the origin of mitotic dysfunction.

Aberrant expression of neuronal cell cycle proteins with resultant neuronal loss has been observed in the central nervous system of patients with neurodegenerative diseases such as AD, PD, ALS, Niemann-Pick's disease, DS and progressive supranuclear palsy (Nunomura et al., 2007; Woods et al., 2007) and acute neurological disorder such as stroke and traumatic brain injury ((Byrnes and Faden, 2007; Timsit and Menn, 2007)). Accumulating evidence from postmortem studies has demonstrated aberrant expression of cell-cycle-related molecules in the neurons of the hippocampus, subiculum, locus coeruleus and dorsal raphe nuclei. This is further substantiated by proof of DNA replication in brains of patients with AD (Busser et al., 1998; McShea et al., 1997; Vincent et al., 1997; Yang et al., 2001), epilepsy (Nagy and Esiri, 1998), PD (Jordan-Sciutto et al., 2003) and ALS (Ranganathan and Bowser, 2003).

Chapter 3.2: iGluRs in excitotoxicity

Neurons in the adult central nervous system exist in the quiescent state, i.e. a non-dividing, silent phase, called G_0 . Cells in this state are designated as terminally differentiated as they do not have the ability to re-enter cell cycle (McShea et al., 1999). Increasing evidence from neurodegenerative diseases studies demonstrate frequently these mitotically inactive neurons formed the vulnerable targets of aberrant cell cycle re-entry (Lee et al., 2009; McShea et al., 2007; Zhu et al., 2007; Zhu et al., 1999). Re-entrant cells that proceed beyond the late G_1 , or even enter and complete S-phase, cannot return to G_0 . As a result of some undefined cellular constraints of terminally differentiated neurons, the cell cycle re-entrant cells being neither able to return to quiescent state or complete mitosis, induced their own deaths via the PCD pathways (Meikrantz and Schlegel, 1995; Wang et al., 2009).

During cell transitions from S-phase to M-phase in mitosis, cyclins and their associated CDKs fluctuate in their expression and activity as the (Grana and Reddy, 1995). In particular, the expression and activation of cyclin D (CCND)/CDK4,6 complex, triggered by the presence of mitotic growth factors, facilitates the passing from resting (G_0) cells into the G_1 phase of cell cycle (Sherr, 1994; Sherr, 1995). Similarly, the G_1 /S transition is governed by the activation of the cyclin E/CDK2 complex (Sherr, 1994), such that the absence of cyclin E and/or the inhibition of the cyclin E/CDK2 complex by p21, p27 and p53 would impose cell cycle arrest at the G_1 checkpoint.

From Table 3.6 of the genes involved in mitotic cell division for individual excitotoxicity profiles, it is apparent that numerous cell cycle-promoting proteins were transcriptionally

Chapter 3.2: iGluRs in excitotoxicity

up-regulated from 5h and 15h, in concurrent with an increase in gene expression of pro-mitogenic signals from growth factors. Interestingly, transcriptional up-regulation of Ccnd1 and Ccnd2 was observed in AMPA and KA models, but not that of NMDA and Glu models. This discrepancy in temporal modulation of CCND could be explained by the earlier occurrence of cell cycle re-activation before the selected 5h time-points in NMDA and Glu profiles as a result of the highest physiological abundance and Ca²⁺ permeability of NMDARs out of the three iGluRs subtypes, which leads to the failure of capturing the timeframe of Ccnd transcriptional modulation. As such, NMDA profile demonstrated basal fold-change (~1.0) at 5h, followed by significant pursuing down-regulation at 15h and 24h. On the other hand, Ccnd transcriptional regulation was not present in Glu profile, indicating an overall close to basal (between -1.50 to 1.50 fold) expression due to a neutralizing effect from the up- and down -regulation of Ccnd in AMPA/KA and NMDA profiles respectively upon all iGluRs activation.

While activation of iGluRs during excitotoxicity may be the answer to the initiation of cell cycle reactivation, oxidative stress may further facilitate and promote the latter's progression (Bonda et al., 2010). Indeed, significant oxidative load, represented by the substantial transcriptional activation of Hsps, molecular chaperones and GSH pathway, was observed across all four excitotoxicity models. A "two-hit" hypothesis, originally put forward for neurodegeneration in AD and implicating both oxidative stress and cell cycle malfunctioning, seemingly also apply to neuronal excitotoxicity (Zhu et al., 2001;2007) . In the current study, the two conditions that must be met in order for aberrant cell cycle re-entry to occur in neurons namely, (a) an elevation in cell cycle proteins and (b) an increase

Chapter 3.2: iGluRs in excitotoxicity

in pro-mitogenic signals, have been fulfilled. This is because even though mature neurons may express some cell cycle proteins, the amount produced is not sufficient to produce a substantial pro-mitogenic signal to drive the mature neurons to re-enter the cell cycle. Furthermore, some cell cycle proteins demonstrates diverse post-mitotic multi-functions that span various developmental stages of a neuron, including neuronal migration, axonal elongation, axonal pruning, dendrite morphogenesis and synaptic maturation and plasticity (Frank and Tsai, 2009; Kim et al., 2009). As such, final ingredient to put neurons to their demise most likely requires the stimulus of additional pro-mitogenic molecules, such as thrombin, A β ₄₂, ROS, NO and others, which elevation will trigger the mitogenic signal cascades in the injured neurons. Once mitogenic signaling is stimulated beyond a certain threshold, neurons appear to exit their quiescent state and re-enter the cell cycle (Bonda et al., 2010).

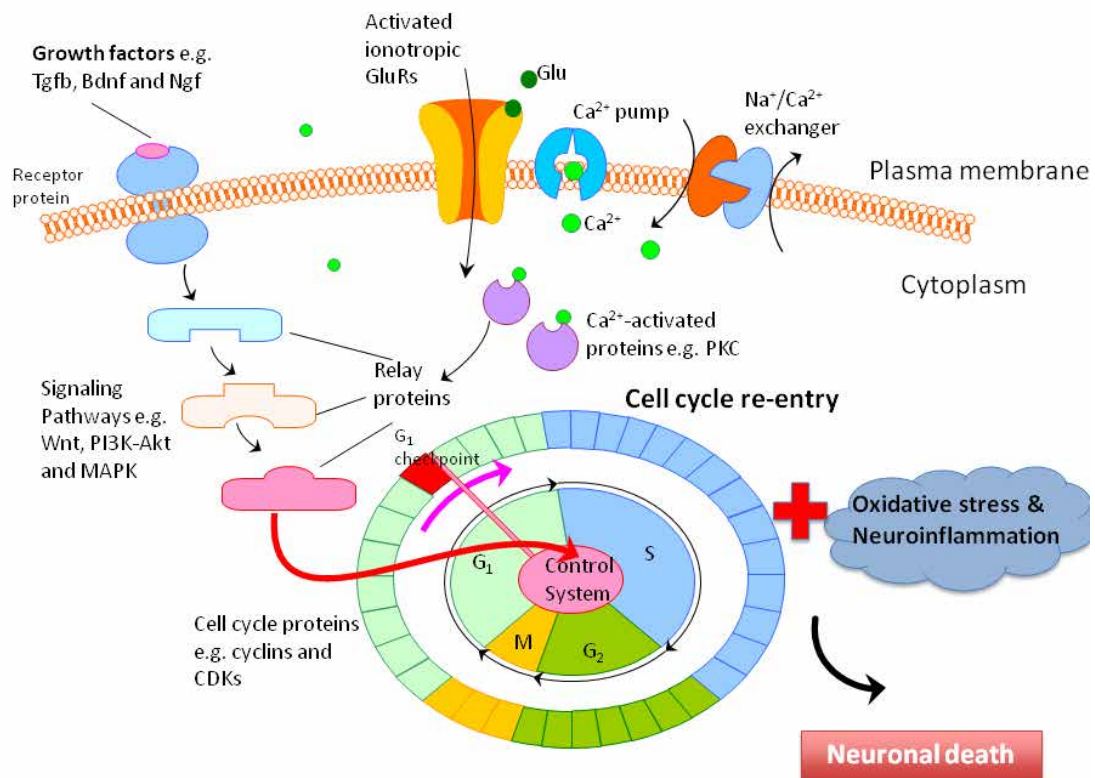


Figure 3.14 A summarized diagram depicting the major role of cell cycle re-entry in the exacerbation of neuronal injury in concurrence with the simultaneous occurrence of oxidative stress and neuroinflammation during excitotoxicity in cerebral ischemia. Cell cycle re-activation is highly dependent on the presence of pro-mitogenic stimuli (growth factors) and cell cycle proteins (CDKs and cyclins)

In conclusion, this subchapter reported that activation of iGluRs induces cell cycle re-activation during excitotoxicity, in addition to tremendously heightened oxidative stress. The two aforementioned processes with concomitant transcriptional activation cooperate as per the “two-hit” hypothesis to inflict cellular damages and eventually death

Chapter 3.2: iGluRs in excitotoxicity

As such, cell cycle abnormalities potentially define a target for finding new therapeutic possibilities treatment of neurodegenerative disorders where excitotoxicity is causative, which would be addressed in Chapter 6.2. Current *in vitro* models of excitotoxicity were inadequate in providing insights into the role of excitotoxicity under patho-physiological conditions within the mammalian brain which comprises of a heterogeneity of cell type populations (cell-cell interactions that play an important role in neuropathological cell communication) and a complex structural-biological architecture (e.g. vasculature structure and blood-brain barrier). Furthermore, pharmacological activation of iGluRs would be insufficient to mimic the upstream patho-physiological events triggering the accumulation of extracellular Glu. As Glu –mediated excitotoxicity is commonly defined in cerebral ischemia commonly known as stroke, and the pathogenesis of the latter has not been fully elucidated, employment of *in vivo* models of cerebral ischemia for microarray analyses (Chapter 4, 5 and 6) would provide the opportunity to understand the significance of excitotoxicity, and simultaneously provide insights into the mechanistic regulation in this acute neurological disorder.

Chapter 4:

Hypoxic Ischemia (HI)

in

***in vivo* Neonatal Mouse model**

4 Description of neonatal hypoxic ischemia (HI) model

All animal work conducted in this study was approved by the University of New South Wales (UNSW) Animal Ethics and Experimentation Committee and performed in accordance with the guidelines of the National Health and Medical Research Council (Australia). C57 Black 6(C57/Bl6) mouse pups were obtained from Animal Resources Centre (Perth, WA) and were housed under standard housing conditions in the UNSW Biological Resources Centre animal facility throughout experiments.

HI was carried out as previously described in (Jones et al., 2008). Pups were anesthetized with 1.5% isoflurane in 30% O₂/70% N₂ mixture and underwent unilateral HI. The right common carotid artery was exposed through a ventral midline neck incision and permanently occluded by electrocoagulation (Aaron Medical Industries Inc, Florida, USA), where the occlusion was verified. The wound was sutured and mouse pups were returned to their mother for 1.5–2h. Sham control mice underwent the identical procedure, without carotid artery occlusion. Pups were then placed in an 8% O₂/92% N₂ humidified chamber at 37°C for 1h. This combined procedure results in select neuronal damage or infarction in the hemisphere ipsilateral to the carotid occlusion, whereas hypoxia alone (contralateral hemisphere) does not produce any significant brain injury (originally described by (Levine, 1960; Levine and Klein, 1960) and later refined by (Rice et al., 1981)). Following the HI or sham surgery procedure, all pups were returned to their dam and kept under standard housing conditions for the remainder of the study.

Chapter 4:
***In vivo* neonatal hypoxic ischemia**

Neonatal mice were randomly decapitated at 3h and 24h post 1-hour exposure to HI, along with their respective time-point specific sham controls. Assessment of the volume of the infarct lesion (n=6) was performed with Nissl stain (cresyl violet). Global gene profiling was performed on the right infarct cortice. Four biological replicates from each time-point/condition (sham control or HI) were used for microarray analysis. The schematic microarray experimental design is demonstrated as follow:

**Mouse Neonatal Hypoxic Ischemia (HI) Microarray
Experimental Plan**



4.1 Introduction

Unregulated hyper-activation of GluRs has been demonstrated to play a detrimental role in the initial phase of injury infliction during HI especially in term neonates where extracellular Glu accumulates to cytotoxic level, leading to a condition known as hypoxic encephalopathy commonly characterized by cortical infarction. On the other hand, HI insults in preterm neonates frequently results in selective white matter injury called periventricular leukomalacia with insignificant or absence of cortical pathology. This is because the perinatal age window represents a dynamic development period of alterations of neuronal and glial structure and function, which in turn translates into differential vulnerability to age-specific patterns of injury. This means that even though HI can occur in both term and pre-term neonates, the pattern of response is highly dependent on the age of the infant, which in turn is correlated to the expression profile and functionality of the GluRs, in this case the iGluRs (Reviewed in Jensen, 2002a; b). Since excitotoxicity played a substantial role in term neonates, current study in the chapter would focus on the temporal global transcriptomic profiling of HI in term mouse neonates.

HI brain damage is one of the most common causes of neonatal brain injuries, amidst other conditions such as intrauterine infection and perinatal cerebral hemorrhage (Bracci et al., 2006). HI, occurring during the perinatal period, severely affects brain integrity resulting in detrimental long-term neurological morbidity in terms of motor, intellectual, educational and neuropsychological performance deficits (e.g. cerebral palsy, mental retardation, learning disability and epilepsy), and even neonatal mortality (Cowan et al., 2003; Ferriero, 2004; Shalak and Perlman, 2004; van Handel et al., 2007). HI has been

Chapter 4:
***In vivo* neonatal hypoxic ischemia**

demonstrated to produce brain damages of differential severity comprising of focal necrotic cell death, diffused white matter injury, and cystic/cavitary infarction resulting in intraventricular-periventricular hemorrhages and periventricular lesions (Leonardo and Pennypacker, 2009).

Oxidative stress is the main injurious trigger component of different cell death phenotypes in HI (Gill and Perez-Polo, 2008). Oxidative stress-induced cell deaths can be divulged into apoptotic (i.e. caspase-dependent and programmed tightly) under chronic conditions and necrotic (i.e. caspase-independent and unregulated) under more acute oxidative insults. However, with the revelation of existence of alternate cell death routes, PCD, originally an alternative name for apoptosis (PCD-I), has revolutionized its definition to include further two cell death subtypes namely the caspase-independent autophagy (PCD-II) and programmed necrosis (PCD-III) (Nagley et al., 2010).

Heterogeneous modes of cell death (apoptosis and necrosis) were consistently observed in the neuronal population in the cortex, hippocampus, thalamus and striatum after HI (Malinak and Silverstein, 1996). Recently, autophagy was also demonstrated to play a pivotal role in the infliction of neonatal HI injury (Carlioni et al., 2008; Higgins et al., 2010). Autophagy has been actively involved in numerous neuronal processes such as development, starvation, neurodegeneration and excitotoxic stimulation (Boland and Nixon, 2006; Matyja et al., 2005; Shacka et al., 2007; Wang et al., 2008). More specifically in neurological disorders context, an increase in autophagosome formation suggestive of an enhancement of the autophagic flux during cerebral HI in rodent

Chapter 4:
***In vivo* neonatal hypoxic ischemia**

neonates and adults has been identified (Adhami et al., 2006; Koike et al., 2008; Wen et al., 2008; Zhu et al., 2005).

Current therapeutic interventions fail to provide substantial reversal of HI brain injuries and improvement in overall cognitive function. Recent clinical studies demonstrated that post-HI hypothermia provide moderate neuroprotection but fail to show any significant reduction in neonatal morbidity and mortality (Shankaran et al., 2005). Concurrently, erythropoietin therapy is only found to be effective against neurological deficits when use in high dose upon induction of a moderate degree of HI (Juul et al., 2008; Zhu et al., 2009). This is due to the multiplicity of cell death mechanisms induced by neonatal HI, occurring in different cells or even as a continuum in the same cell, which makes neuroprotective treatment against neonatal HI more difficult to achieve. As such, temporal global gene profiling of neonatal hypoxic ischemia would provide worthy mechanistic insights into the disease pathogenesis.

4.2 Results

HI was induced in post-natal day 7 C57/Bl6 pups via unilateral carotid artery ligation with a subsequent 1-hour exposure to a hypoxic environment (8% oxygen). This model inflicts a unilateral infarct in the hemisphere ipsilateral to the ligation as hypoxia induction alone at this age is sub-threshold for injury. The area of damage is typically restricted to the periventricular regions of the brain, particularly the cortical and hippocampal areas. This is reminiscent of hypoxic encephalopathy in term babies where cortical infarction is commonly observed (Jensen, 2002). Previous study had demonstrated substantial infarct damage occurred in the cortical and hippocampal regions in the neonates upon HI (Jones et al., 2008). As such, the infarct cortice along with its sham controls were chosen for temporal microarray analysis to understand the pathophysiological mechanisms at work during neonatal HI.

4.2.1 Hypoxic ischemia induced significant global transcriptional modulation

Right infarct cortice were harvested at 3h and 24h post-hypoxic ischemia, concurrently with their respective time-point sham controls. Four biological replicates were collected at each time-points. Their RNAs were extracted and subjected to microarray analysis using Illumina® Mouse Ref8 V2 beadchip arrays (the latest version at the time of experiment as V1.1 has been discontinued. It comprises of the initial RefSeq transcripts in Ver 1.1 and additional added sequences from newly identified genes). Raw signal data from the arrays were analyzed using GeneSpring V7.3 and normalized against their respective sham control. Only gene probes with a) fold-change of at least ± 1.5 in a minimum of one out of the two time-points and b) passed statistical testing of one-way

ANOVA, $p < 0.05$ and Benjamini-Hochberg FDR correction. 342 differentially expressed RefSeq transcripts passed these parameters and they were subjected to functional-gene ontology classification using DAVID 6.7. They corresponded to 314 DAVID-identifiable genes.

Functional clustering revealed several over-represented biological processes broadly categorized as follow: a) inflammatory response, b) cell homeostasis, survival and proliferation, c) cell cycle regulation and d) response to oxidative stress and e) cell death.

-INFLAMMATORY RESPONSE

-Chemokine signaling pathway

Chemokines are involved in the guidance of leukocytes to the ischemic site of inflammation by creating a concentration gradient in the extracellular matrix. Majority of genes encoding for chemokines of the C-C and the C-X-C motifs (Ccl3, Ccl9, Ccl12 and Cxcl1) demonstrated significant transcriptional up-regulation particularly at the early 3h post-HI time-point (Table 4.1).

-Toll-like receptor (TLR) signaling pathway

TLR signaling cascade is part of the innate immunity response to initiate inflammation via promotion of cytokine production and immune cell activation. As shown in Table 4.1, members implicated in the TLR transduction pathway (Cd68, Cd86, c-Fos, c-Jun and Spp1) showed early substantial early increase in gene expression at 3h. Interestingly, Tlr2 demonstrated a late (24h) elevation in transcriptional expression.

-Leukocyte mediated cytotoxicity

Genes encoding for Fc receptors (Cd16, Cd23, Cd68 and Fcrl3) expressed on the surface of leukocytes demonstrated significant transcriptional up-regulation between 3h and 24h post-HI (Table 4.1).

-VASCULATURE DEVELOPMENT

Early vasculature disruption was evident from the transcriptional up-regulation of proteins involved in the maintenance of vasculature homeostasis and integrity (Agpt2, Serpina8, Cys61, Cx30, Lcn2 and Socs3) at 3h post-HI.

-CELL HOMEOSTASIS, SURVIVAL AND PROLIFERATION

Genes encoding for proteins involved in the pro-survival pathway (MAPK signaling cascade), pro-mitogenic factors (Igfbp3) and transcription factors (Egr2 and Egr4) demonstrated early transcriptional elevation at 3h post-HI. However, Bdnf, a physiological important neurotropic factor that promotes cell survival showed a pursuing down-regulatory trend prominent at 24h post-HI.

-CELL CYCLE REGULATION

Only a handful of genes involved in the positive regulation of cell cycle process (Hls7 and Myd116) showed transcriptional up-regulation at 3h post-HI. On the contrary, numerous genes involved in the cell cycle checkpoints triggered by p53 (Gadd45(a,b and g), p21 and Ink4b) demonstrated increased expression concurrently at the same time-point (Table 4.1).

-RESPONSE TO OXIDATIVE STRESS

Oxidative and electrophilic stresses characterized by aberrant ionic homeostasis and elevated ROS, reactive nitrengic species and free radical production triggered the cell's innate anti-oxidant response via transcriptional induction of Hsps (Hspb1, Hsp90 and Dnajb), endoplasmic reticulum stress-inducible cytoprotective transcription factor (Aft4) and metal ion chaperones (Mt1 and Mt2) between 3h and 24h post-HI (Table 4.1).

-CELL DEATH

Cell death induced via extrinsic stimulus was apparent with the transcriptional up-regulation of the Fas ligand-mediated pathway (Litaf, Traf7, Tnfrsf12a). Fas ligand-mediated extrinsic apoptotic pathway is triggered in the hippocampus and thalamus after HI in neonatal rat brain, and its incidence associated with extent of HI damage (Northington et al., 2001). Simultaneously, endogenous cytoprotective antagonist of Fas ligand-induced cell death, Ier3, also demonstrated similar temporal up-regulation at 3h post-HI. Further, lysosomal stress was evident with the increase in mRNA expression of lysosomal enzymes Lys and Ctsz at 24h post-HI. Genes encoding for proteins involved in intracellular signaling pathways which suppress cell survival and promote cell death (Met, Axud1, Nfkbia, Lys and Lapf) showed transcriptional activation also at the later time-point (Tsble 4.1).

Chapter 4:
***In vivo* neonatal hypoxic ischemia**

Table 4.1 Selected differentially-expressed gene profile of over-represented neuronal death-related biological processes in the infarct cortice of neonatal HI mice. All fold-change expressions were subjected to one-way ANOVA analysis and Benjamini Hochberg FDR correction , and significant at $p < 0.05$. Data are expressed as fold-change \pm sem.

Genbank	Gene Title	Symbol	<u>Hypoxic ischemia</u>	
			3h	24h
<u>Inflammatory response</u>				
<u>-Chemokine signaling pathway</u>				
NM_011337	Chemokine (C-C motif) ligand 3	Ccl3	3.89 \pm 2.39	1.97 \pm 0.66
NM_011338	Chemokine (C-C motif) ligand 9	Ccl9	2.03 \pm 0.48	1.98 \pm 1.03
NM_011331	Chemokine (C-C motif) ligand 12	Ccl12	1.44 \pm 0.22	2.40 \pm 0.99
NM_008176	Chemokine (C-X-C motif) ligand 1	Cxcl1	1.65 \pm 0.44	2.18 \pm 1.70
NM_013655	Chemokine (C-X-C motif) ligand 12	Cxcl12	-1.38 \pm 0.12	-1.51 \pm 0.13
NM_009142	Chemokine (C-X3-C motif) ligand 1	Cxc3	1.22 \pm 0.18	-1.54 \pm 0.13
<u>-TLR signaling pathway</u>				
NM_009853	CD68 antigen	Cd68	1.22 \pm 0.18	1.57 \pm 0.49
NM_019388	CD86 antigen	Cd86	1.51 \pm 0.38	-1.05 \pm 0.09
NM_010234	FBJ osteosarcoma oncogene	c-Fos	17.63 \pm 2.98	1.15 \pm 0.63
NM_010591	Jun oncogene	c-Jun	1.83 \pm 0.23	1.21 \pm 0.18
NM_009263	Secreted phosphoprotein 1	Spp1	1.87 \pm 0.16	4.13 \pm 3.36
NM_011905	TLR 2	Tlr2	1.20 \pm 0.23	1.59 \pm 0.31
<u>-Leukocyte mediated cytotoxicity</u>				
NM_010188	Fc receptor, IgG, low affinity III	Cd16	1.57 \pm 0.24	1.85 \pm 0.81
NM_010185	Fc receptor, IgE, high affinity I, gamma polypeptide	Cd23	1.55 \pm 0.34	1.64 \pm 0.59
NM_144559	Fc receptor, IgG, low affinity IV	Fcrl3	1.25 \pm 0.10	1.92 \pm 0.76
<u>Vasculature development</u>				
NM_008416	Jun-B oncogene	Junb	1.86 \pm 0.37	-1.10 \pm 0.09
NM_007426	Angiopoietin 2	Agpt2	2.25 \pm 0.25	1.18 \pm 0.19
NM_007428	Angiotensinogen (serpin peptidase inhibitor, clade A, member 8)	Serpina8	1.64 \pm 0.43	1.50 \pm 0.67
NM_010516	Cysteine rich protein 61	Cyr61	1.67 \pm 0.52	-1.00 \pm 0.15
NM_008128	Gap junction membrane channel protein beta 6	Cx30	1.75 \pm 0.58	1.62 \pm 0.53
NM_008491	Lipocalin 2	Lcn2	5.05 \pm 2.65	7.33 \pm 19.87
NM_194054	Reticulon 4	Rtn4	1.06 \pm 0.09	1.66 \pm 0.25
NM_007585	Annexin A2	Anxa2	1.72 \pm 0.14	1.47 \pm 0.23
NM_007707	Suppressor of cytokine signaling 3	Socs3	2.74 \pm 1.18	1.85 \pm 0.77
NM_009373	Transglutaminase 2, C polypeptide	Tg2	1.53 \pm 0.36	1.48 \pm 0.46
NM_183261	Nuclear receptor subfamily 2, group F, member 2	Nr2f2	-1.60 \pm 0.09	1.02 \pm 0.29

Table 4.1 (continue)

Genbank	Gene Title	Symbol	<u>Hypoxic ischemia</u>	
			3h	24h
<u>Cell homeostasis, survival and proliferation (continue)</u>				
NM_001048141	Brain derived neurotrophic factor	Bdnf	1.32 ± 0.17	-1.52 ± 0.09
NM_008343	Insulin-like growth factor binding protein 3	Igfbp3	1.23 ± 0.29	1.80 ± 0.42
NM_010118	Early growth response 2	Egr2	1.78 ± 0.27	-1.13 ± 0.14
NM_020596	Early growth response 4	Egr4	1.54 ± 0.36	-1.71 ± 0.22
NM_007498	Activating transcription factor 3	Atf3	2.30 ± 0.97	-1.09 ± 0.07
NM_010495	Inhibitor of DNA binding 1	Idb1	1.29 ± 0.13	1.58 ± 0.24
NM_013642	Dual specificity phosphatase 1	Dusp1	1.52 ± 0.64	1.17 ± 0.26
NM_019819	Dual specificity phosphatase 14	Dusp14	1.72 ± 0.13	1.12 ± 0.25
NM_008927	Mitogen activated protein kinase kinase 1	Mek1	1.51 ± 0.33	1.36 ± 0.70
<u>Cell cycle regulation</u>				
NM_001039543	Myeloid leukemia factor 1	Hls7	1.82 ± 0.27	-1.22 ± 0.14
NM_008654	Myeloid differentiation primary response gene 116	Myd116	1.75 ± 0.22	-1.04 ± 0.06
NM_011750	Splicing factor 1	Spf1	1.12 ± 0.31	-1.72 ± 0.03
NM_007836	Growth arrest and DNA-damage-inducible 45 alpha	Gadd45a	1.71 ± 0.34	1.14 ± 0.16
NM_008655	Growth arrest and DNA-damage-inducible 45 beta	Gadd45b	2.47 ± 0.62	1.02 ± 0.13
NM_011817	Growth arrest and DNA-damage-inducible 45 gamma	Gadd45g	2.18 ± 0.95	1.25 ± 0.26
NM_007669	Cyclin-dependent kinase inhibitor 1A (P21)	p21	1.62 ± 0.08	1.01 ± 0.18
NM_007670	Cyclin-dependent kinase inhibitor 2B (p15, inhibits CDK4)	Ink4b	1.78 ± 0.25	-1.07 ± 0.14
<u>Response to oxidative stress</u>				
XM_139474	Activating transcription factor 4	Atf4	1.51 ± 0.15	1.04 ± 0.21
NM_013560	Heat shock protein 1	Hspb1	1.78 ± 1.28	1.13 ± 0.38
NM_010480	Heat shock protein 90kDa alpha (cytosolic), class A member 1	Hsp90	1.65 ± 0.17	1.19 ± 0.44
NM_001037941	DnaJ (Hsp40) homolog, subfamily B, member 6	Dnajb	-1.06 ± 0.18	1.52 ± 0.16
NM_013602	Metallothionein 1	Mt1	2.10 ± 0.29	2.17 ± 0.97
<u>Cell death</u>				
NM_013863	Bcl2-associated athanogene 3	Bag3	2.13 ± 0.17	-1.06 ± 0.23
NM_019980	LPS-induced TN factor	Litaf	1.52 ± 0.28	1.29 ± 0.32
NM_153792	Tnf receptor-associated factor 7	Traf7	1.09 ± 0.10	1.81 ± 0.43
NM_013749	Tumor necrosis factor receptor superfamily, member 12a	Tnfrsf12a	3.47 ± 0.26	1.28 ± 0.42
NM_133662	Immediate early response 3	Ier3	2.28 ± 0.61	2.26 ± 1.11
NM_025690	SAFB-like, transcription modulator	Met	1.02 ± 0.07	1.64 ± 0.29
NM_153287	AXIN1 up-regulated 1	Axud1	2.28 ± 0.82	1.22 ± 0.17

Table 4.1 (continue)

Genbank	Gene Title	Symbol	<u>Hypoxic ischemia</u>	
			3h	24h
<u>Cell homeostasis, survival and proliferation (continue)</u>				
NM_010907	Nuclear factor of kappa light chain gene enhancer in B-cells inhibitor, alpha	Nfkbia	1.51 ± 0.27	1.19 ± 0.24
NM_017372	Lysozyme	Lys	1.16 ± 0.08	1.61 ± 0.39
NM_022325	Cathepsin Z	Ctsz	1.06 ± 0.14	1.68 ± 0.37
NM_024413	Pleckstrin homology domain containing, family F (with FYVE domain) member 1	Lapf	1.52 ± 0.22	1.07 ± 0.12

4.2.2 Validation of neonatal HI profile via real-time PCR

Microarray data was validated via real-time PCR on the same HI-induced cortical RNA samples used in microarray analysis. Two time-points namely 3h and 24h were selected for validation. The selected gene probes demonstrated identical transcriptional regulatory trend (Table 4.2).

Table 4.2 Validation of microarray data using real-time PCR technique on the HI-induced neonatal murine cortice. Data are expressed as fold-change \pm sem.

GenBank	Gene Title	Symbol	3h		24h	
			Microarray	Real-time PCR	Microarray	Real-time PCR
NM_007498	Activating transcription factor 3	Atf3	2.38 \pm 1.00	4.16 \pm 0.70		
NM_008491	Lipocalin 2	Lcn2	5.27 \pm 2.76	18.25 \pm 0.48		
NM_011817	Growth arrest and DNA damage-inducible 45gamma	Gadd45g	1.95 \pm 0.99	2.06 \pm 0.71		
NM_007585	Annexin A2	AnxA2	1.53 \pm 0.12	5.62 \pm 0.72		
NM_009263	Secreted phosphoprotein 1	Spp1	1.83 \pm 0.16	4.39 \pm 0.60	4.13 \pm 3.36	6.61 \pm 0.84
NM_133662	Immediate early response 3	Ier3	2.12 \pm 0.57	5.15 \pm 0.92	2.26 \pm 1.11	3.08 \pm 1.20

4.3 Discussion

The immature developing brain is just as susceptible to hypoxic-ischemic encephalopathy and focal arterial stroke as an adult brain. This is evidenced by the comparable incidence of arterial stroke between the newborns and elderly, about 1/4,000 term babies (deVeber et al., 2000).

Temporal global transcriptomic profiling revealed that inflammation and oxidative stress were two main patho-physiological mechanisms at work in neonatal HI. These two processes are closely correlated in babies manifesting asphyxic insult and hypoxic-ischemic encephalopathy (Perrone et al., 2010). During neuro-inflammation, intrinsic vulnerability of developing oligodendroglia to excitotoxic, oxidative and inflammatory forms of injuries coupled with activated microglia and astrogliosis are major determinants to the pathogenesis of HI-induced white matter (cortical) injury (Deng, 2010). Microglia, the only resident macrophages in the brain, are main cell type providing immunosurveillance by stimulus-dependent activation when triggered upon brain insults (Kreutzberg, 1996; Raivich et al., 1999). Activated microglial cells and macrophages can potentially inflict damages on various cell types comprising of endothelial cells, oligodendrocytes, astrocytes and neurons (Flavin et al., 1997; Li et al., 2005; Yenari et al., 2006), thereby aggravating injury. However, it is still uncertain whether microglial activation is beneficial or harmful after stroke (Imai et al., 2007; Lalancette-Hebert et al., 2007). During birth, microglia would have established a stronghold population in the brain which is eventually ramified after the first 2 post-natal weeks, in accordance with a diminishing of PCD at this developmental stage (Carson and

Chapter 4: ***In vivo* neonatal hypoxic ischemia**

Sutcliffe, 1999). However, during neonatal HI, substantial macrophage activation and accumulation at the site of injury is evident and faster along with the elevated production of inflammatory cytokines and NO as compared to adult models (Bona et al., 1999; Cowell et al., 2002; Ivacko et al., 1996; McRae et al., 1995; Tsuji et al., 2000). This phenomenon can continue to persist even after several weeks (Benjelloun et al., 1999; Fox et al., 1999). Activation of macrophages, derived from resident microglia, is evident from the significant transcription up-regulation of Cd68 macrophage surface antigen at 24h post-HI in the injured cortex (Table 4.1: TLR signaling cascade).

Chemoattractant cytokines, or chemokines, regulate an array of physiological functions including cell migration, proliferation, differentiation and angiogenesis (Gerard and Rollins, 2001). They bind and activate G-protein-coupled receptors and are classified as C, CC, CXC, and CX3C based on the positions of key cysteine residues (Gerard and Rollins, 2001). CXCL12 is suggested to play a crucial role in homing stem cells to regions of ischemic injury (Hill et al., 2004). CXCL12 expression is especially enhanced in reactive astrocytes in the ischemic penumbra (a region of functionally impaired but viable cells) promoting stem cell migration (Wang et al., 2002b). In stark contrast, in our current temporal microarray study of neonatal HI employing infarct cortex, which corresponded to the penumbra, a decrease in transcriptional expression of Cxcl12 is observed. This could be accounted for by findings from a previous study which demonstrated a brief upregulation of CXCL12 by reactive astrocytes following neonatal HI injury, suggesting that the timeframe of endogenous CXCL12-mediated chemotaxis and recruitment of reparative cells may be narrow (Miller et al., 2005). As such, the

Chapter 4:
***In vivo* neonatal hypoxic ischemia**

chosen 3h time-point for our current neonatal HI microarray study is not early enough to detect the transcriptional peak of Cxcl12.

Acceleration of the inflammatory response was accelerated by vascular injury as demonstrated by the transcriptional up-regulation of vasculature-related proteins, leading to increased blood vessel permeability that permits leukocyte transendothelial migration from the blood-brain-barrier. The significance of inflammation in HI was accentuated by the transcriptional activation of chemokine-mediated chemotaxis, TLR signaling pathway and leukocyte-mediated cytotoxicity.

Oxidative stress and inflammation are tightly associated during cerebral ischemia. Once induced, the inflammatory cells generate ROS which in turns positively potentiate the inflammatory response through a positive feedback loop while concurrently induces cellular oxidative stress. Oxidative stress experience was denoted mainly by the upheaval in gene expression of ER-stress inducible transcription factor Atf4, Hsps (Hspb1, Hsp90 and Dnajb) and metal ion chaperones (Mt1) as shown in Table 4.1: Response to oxidative stress. The neonatal brain, particularly, is especially susceptible to HI as compared to a mature adult brain. This is because it contains high concentrations of unsaturated fatty acids coupled with accelerated rate of oxygen consumption, and unfavorably paralleled with low levels of anti-oxidants and redox-active iron, thus putting the neonatal brain at a “pro-oxidant” state when subjected to HI (Halliwell, 1992). As such, a recent study using sulforaphane, an isothiocyanate involved in the induction of cytoprotective transcription factor Nrf2-mediated anti-oxidant response, demonstrated efficacy in the protection

Chapter 4:
***In vivo* neonatal hypoxic ischemia**

against HI (Ping et al., 2010). Furthermore, genes encoding for pro-mitogenic proteins (Egr2, Egr4, Atf3 and Mek1; in Table 4.1 under Cell homeostasis, survival and proliferation) demonstrated significant transcriptional elevation at early 3h time-point, indication of an increased pro-survival response. MEK1, commonly known as extracellular signal-regulated kinase 1 (ERK1), has been reported to demonstrate neuroprotection in both adult and neonatal brain injury (Kyriakis and Avruch, 2001). However, genes involved in mitotic cell cycle checkpoints (Gadd45(a, b and g), p21 and Ink4b) showed substantial increase in gene expression at the early 3h time-point, indicating a counteractive impediment to cell cycle re-activation, which might occur at earlier hours preceding the 3h selected time-point, explaining why not many mitosis-related proteins were detected at significant mRNA level by microarray. Instead only a handful of mitosis-associated candidates (Hls7, Myd116 and Spf1) demonstrated enhanced mRNA expression.

In conclusion, neuro-inflammation and oxidative stress are two potential neuropathological mechanisms responsible for the high incidence of morbidity and mortality in infants and children sustaining HI injury during prenatal and perinatal stages and often resulting in mental retardation, seizures and motor dysfunction (cerebral palsy) (Vannucci, 1990).

Chapter 5:
Transient
Focal Cerebral Ischemia

5 Description of transient focal cerebral ischemia model in adult mice

All animal procedures used in this project were approved by The University of Melbourne Animal Ethics Committee. The mice used in the present studies were of C57BL/6 background at eight to ten weeks of age (body weight 25 ± 32 g) with their specific genotype being either wild-type (WT) or Gpx-1^{-/-}. The Gpx-1 null mutant mice were previously generated in Dr. Peter J. Crack's laboratory (Centre of Functional Genomics and Human Disease, Monash Institute of Medical Research) and the method was outlined in de Haan et al. (1998).

Anaesthesia

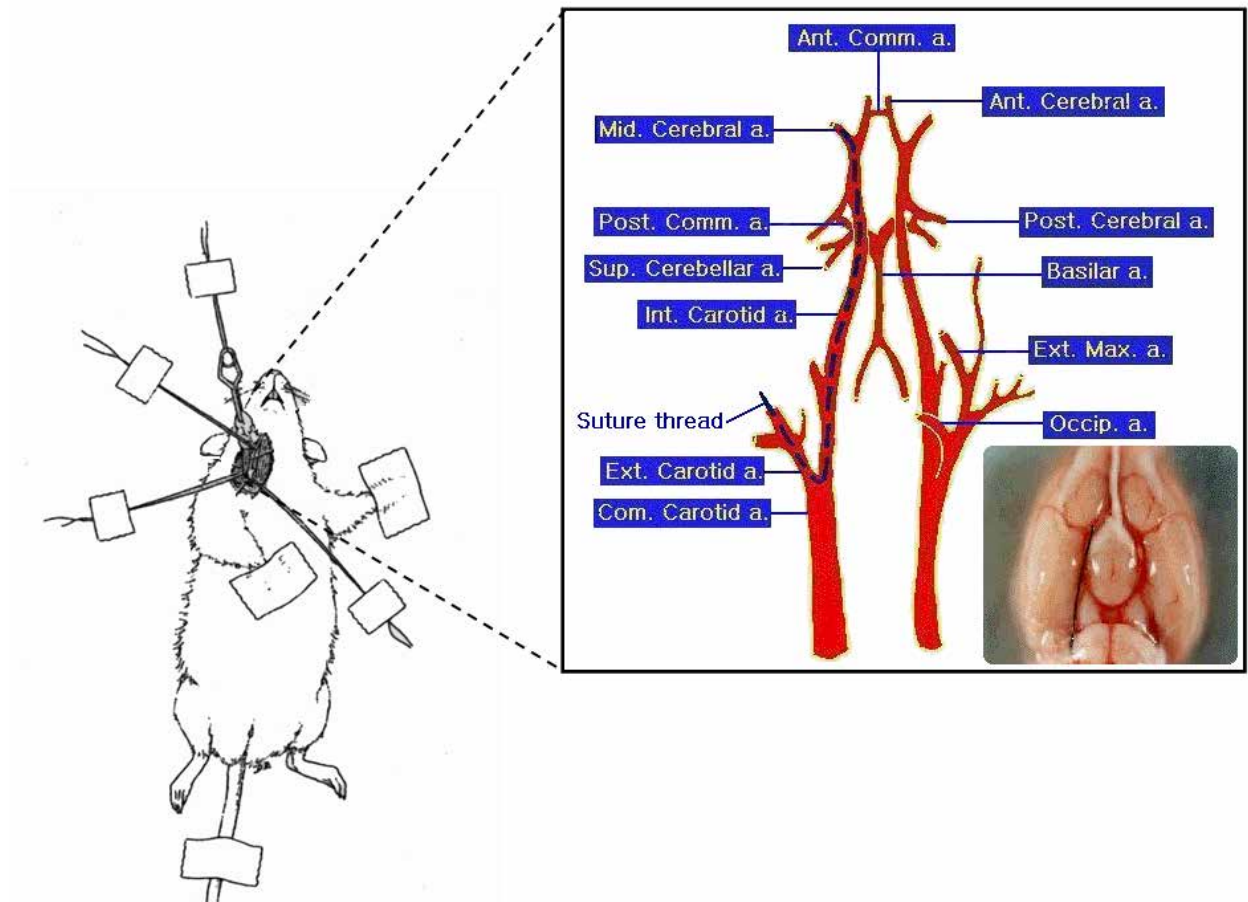
In preparation for surgery, eight to ten week old male WT and Gpx-1^{-/-} mice were anaesthetised by intraperitoneal injection of a cocktail consisting of ketamine hydrochloride (200mg/kg, Pfizer, West Ryde, NSW, Australia) and xylazine (10mg/kg, Troy Laboratories, Smithfield, NSW, Australia).

Mouse Transient Focal Cerebral Ischemia (tMCAO) Model

Mice underwent tMCAO model of cerebral ischemia-reperfusion injury as previously described (Connolly et al., 1996). Briefly, mice were anaesthetised intraperitoneally as described in previously. Experiments examining biochemical end-points and infarct size, a 2-hour ischemic period was used. After ligation of the right proximal common carotid artery, a 6-0 nylon monofilament with a silicone rubber coating tip diameter of 0.21 - 0.23mm (Doccol Co., NM, USA) was introduced into the distal internal carotid artery and was advanced 12mm distally to the carotid bifurcation where it occluded the mid-

Chapter 5: *In vivo* transient focal cerebral ischemia

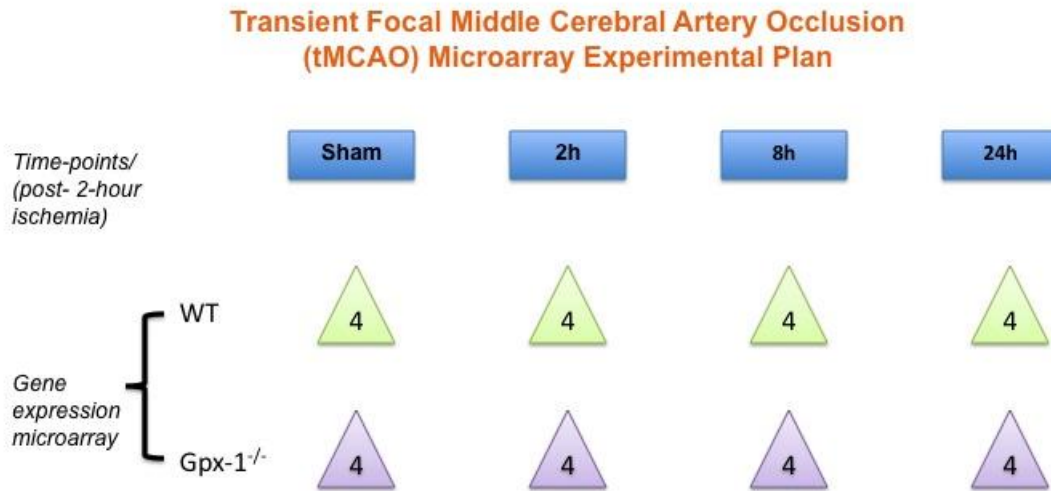
cerebral artery (see illustration below). The wound was closed and the animal returned to its cage. Uninjured control (sham) animals were subjected to the initial anesthetic and neck incision only. The animals were then allowed to recover from anesthetic. Body temperature was monitored and maintained at 37 ± 0.5 °C via a heating pad.



To ensure effective occlusion of the middle cerebral artery, cerebral blood flow was monitored throughout the surgical procedure via a laser Doppler (Perimed PX5010, Stockholm, Sweden). After a skin incision, CBF measurements were conducted with the probe holder placed at the level of the skull, directly above the infarct region after

Chapter 5:
***In vivo* transient focal cerebral ischemia**

MCAO. The arbitrary Doppler flow units were recorded every second before, during and 2h after MCAO. The baseline Doppler arbitrary values for each mouse varies thus to examine relative changes in blood flow throughout an experiment, CBF of each mouse was normalised to its own baseline value and expressed as a percentage. At the end of the 2-hour ischemic period, the mouse was re-anaesthetised and the neck incision reopened allowing the suture to be withdrawn from the carotid artery. The animals were then returned to the heating pad until euthanized at designated time-points of 2h, 8h and 24h for right infarct cortex total RNA collection for microarray analysis (microarray setup demonstrated on below).



Chapter 5.1:
Transient focal cerebral ischemia
in
Wild-Type (WT)
***in vivo* adult mouse model**

5.1.1 Introduction

Minutes after the onset of focal cerebral ischemia, severe hypoperfusion to the primary site of blockage leads to the formation of an ischemic core, a region of severe, irreversible neuronal damage. Encompassing this core is a border of brain tissue which is barely viable and functionally and metabolically impaired due to the infliction of certain degree of neuronal injury. This region is known as the penumbra, and its formation occurs as a result of the residual perfusion from the collateral blood vessels deterring the progression of the ischemic cascade. Unlike the core, the damage it sustained is still reversible to a certain extent if the blood flow is promptly restored (Hossmann, 1988b).

Paradoxically, even though restoration of blood flow to the ischemic tissue is critical for recovery of normal neurological function, it can result in secondary damage, known as ischemia/reperfusion (I/R) injury. This can be explained as a deterioration of ischemic but salvageable brain tissue after blood flow restoration and has a multifactorial etiology (Aronowski et al., 1997; Dietrich, 1994). Early recanalisation in patients with severe ischemia faces an increased susceptibility of reperfusion-related brain hemorrhage, believed to be the result of microvascular injury (Albers et al., 2006). The ischemic cascade does not cease progression even after blood reperfusion. A number of biochemical cascades including the production and release of ROS (Love, 1999), inflammatory changes (Wong and Crack, 2008), and necrotic and apoptotic cell death pathways (Ferrer and Planas, 2003) have been documented in this penumbra area of infarction (Dirnagl et al., 1999).

The pathophysiology of I/R injury still awaits further elucidation. However, leukocyte-

Chapter 5.1: Wild-type transient-MCAO

mediated signaling cascades appear to be centered in reperfusion injury through its infiltration into the brain tissue via disruption of the endothelium, obstruction of the microcirculation and destruction of the blood–brain barrier where they release cytokines and promote inflammation (Pan et al., 2007). Oxidative stress mediators such as ROS released by inflammatory cells e.g. leukocytes around the I/R injured areas evokes the expression of several pro-inflammatory genes by inducing the synthesis of transcription factors, including NF- κ B, hypoxia inducible factor 1, interferon regulator factor 1 and Stat3 (Wong and Crack, 2008). This in turn leads to cytokine up-regulation in the cerebral tissue with consequential expression of adhesion molecules on the endothelial cell surface e.g. intercellular adhesion molecule 1 (Icam1), P-selectin and E-selectin, which promotes leukocyte adhesion to the endothelia in the periphery of the infarct (Yilmaz and Granger, 2008). Leukocyte migration to the ischemic site promotes the activation of the complement cascade with generation of active fragments such as C3a and C5a anaphylatoxins (D'Ambrosio et al., 2001). Induction of MCAO in mouse is demonstrated to elevate C3a and complement 5a receptors expressions significantly and inhibition of the complement cascade offers neuroprotection, highlighting an active role of the complement system in cerebral ischemic injury (Arumugam et al., 2009).

Platelets work synergistically with leukocytes in reperfusion injury via the release of a variety of biochemical mediators that can progress to vasospasm and exacerbation of oxidative stress and the inflammatory cascade (Chong et al., 2001; Wong and Crack, 2008; Zeller et al., 2005). Finally, the disintegration of the blood–brain barrier integrity and post-ischemic hyperperfusion can further induce vasogenic brain edema and hemorrhage (Rosenberg et al., 2001).

5.1.2 Results

From the comparative global transcriptomic analysis of *in vitro* excitotoxic models, oxidative stress and neuroinflammation have been demonstrated to be the primary pathophysiological upstream events facilitating the propagation of the ischemic cascades that further aggravate cellular damages and thus promote cell demise. As previously mentioned, though restoration of blood flow at the primary site of occlusion is critical for recovery of neurological function, continued propagation of the ischemic cascade causes reperfusion to the focal ischemic site (in the case of cerebral transient ischemic stroke) to induce secondary I/R injury. It has been demonstrated that free radical (ROS/RNS) production and NO generation are especially pronounced upon reperfusion of ischemic tissue (Hallenbeck and Dutka, 1990). As such, employment of *in vivo* mouse transient focal ischemic model would be ideal and extremely useful in the elucidation of pathophysiological significance of oxidative stress and the inflammatory cascades during excitotoxic stimulation. The approach adopted to achieve this objective is to perform a global transcriptomic profiling of the temporal recruitment of cell death signaling cascades in the brain cortex upon tMCAO induction. During I/R injury, an apoptotic-necrotic continuum sparked off by the significant escalated free radical production and release promotes apoptosis, and ended with pan-necrosis in the territory supplied by the occluded artery with glial and endothelial cell death is observed (Hara et al., 1996; Leist et al., 1997; Murakami et al., 1997).

Two-hour ischemic period was induced via the intraluminal suture method on the WT C57/Bl6 male adult mice, followed by simultaneous cortical tissue collection after 2h, 8h and 24h of reperfusion respectively. Previous reported infarct measurement based on

Chapter 5.1: Wild-type transient-MCAO

brain slices (area in mm²) collected at 24h after reperfusion confirmed successful induction of focal ischemia in the brains (Crack et al., 2001). Only the cortex tissues were collected for microarray analysis because the global transcriptomic data collected would complement that of the *in vitro* which utilized primary mouse cortical neurons, and furthermore, it has been reported that in the intraluminal suture-induced tMCAO model, the occlusion typically spares striatum and primarily involves the neocortex (Hara et al., 1996; Leist et al., 1997; Murakami et al., 1997).

The technique of intraluminal suture (also known as endovascular filament) as a representative animal model of ischemic stroke was first introduced by Koizumi et al. (1986) and subsequently modified by Longa et al. (1989). It is applied to rats and mice. In my current study, the modified intraluminal suture method is employed to induce tMCAO. A strand of surgical filament is inserted via the external carotid artery, channel to the internal carotid artery and advanced until the tip occludes the origin of the middle cerebral artery, causing a cessation of blood flow and subsequent brain infarction in its area of supply. Insertion via the external carotid artery facilitates closure of the access point with preserved blood supply via the common and internal carotid artery to the brain after the removal of the filament. Withdrawal of the suture results in reperfusion, thus achieving a tMCAO model.

Global gene profiling of cortical tissues from tMCAO-induced WT mouse brain was performed using arrays on Illumina[®] Mouse Ref8 V2 beadchips. All differentially expressed genes in this chapter were selected based on the following parameters: 1) a minimum of ± 1.5 fold change in at least one out of three time-points and 2) passed the statistical screening test

Chapter 5.1: Wild-type transient-MCAO

of one-way ANOVA, $p < 0.05$ and Benjamini-Hochberg FDR Correction. The GeneSpring v7.3 software-generated genelists were then classified according to their involvement in reported biological processes employing DAVID 6.7.

5.1.2.1 tMCAO induced neural inflammation and oxidative stress, contributing to neuronal death in WT-mice

Only 572 gene probes were significantly regulated in the cortex for WT mice undergoing tMCAO, with most of them undergoing up-regulation (Figure 5.1). Among these gene probes, majority of them were involved in the mediation of inflammatory and immune defense responses. These include the complement and coagulation cascades, cytokine-cytokine receptor interaction, natural killer cell-mediated cytotoxicity, TLR signaling pathway and leukocyte transendothelial migration. Significant signs of the activation of the inflammatory signaling cascades occurred at 8h after tMCAO reperfusion, with subsequent remarkable elevated gene expression of nearly all inflammatory-participating players at 24h. Apart from the activation of the immune system, other prominent pathways significantly over-represented in the WT-tMCAO global gene profile comprise of those involved in the anti-oxidative stress response, pro-survival pathway, cell death cascade and calcium ion binding and homeostasis etc.

- INFLAMMATORY RESPONSE

-Cytokine-cytokine receptor interaction

Numerous chemokine ligands (Ccl and Cxcl families) and receptors (Ccr5) , as well as interleukins (Il11) and their receptors (Il1r2, Il8rb, Il13ra1 and Il17rb), and cytokine tumour

Chapter 5.1: **Wild-type transient-MCAO**

necrosis factor (TNF)-receptors (Tnfrsh1a and Tnfrsf12a) demonstrated increase in gene expression between 8h and 24h post-reperfusion after tMCAO induction (Table 5.1). It is worthy to take note of the transcriptional up-regulation of interferon gamma receptor 2 (Ifngr2) and LPS-induced TN factor (Litaf) at 8h and 24h post-reperfusion respectively. Mitogen-induced interferon-gamma (IFN- γ), and intracellular tumour necrosis factor-alpha (TNF- α), which are major T-helper 1 cell pro-inflammatory cytokines, has been reported to demonstrate decrease production in model of focal ischemia and in whole blood cell preparation a day after stroke onset, contributing to acute immunodeficiency in ischemic stroke (Klehmet et al., 2009; Young and Bream, 2007). In our study, the increase in gene expression of Ifngr2 may present a cellular effort to increase the brain immuno-resistance to infections after ischemic stroke.

-Facilitation of leukocyte transendothelial migration

It has been reported that within hours after the onset of ischemia, circulating leukocytes migrate from the blood into the brain, inducing further pro-inflammatory factors release and secondary damages. During this diapedesis, the leukocytes bind to endothelial CAMs and then migrate across the vascular endothelium. Transcriptomic analysis revealed majority of the mediators involved in the facilitation of leukocyte adherence and diapedesis demonstrated up-regulation at 24h post-reperfusion (Table 5.1).

-Immune cell mediated-cytotoxicity

As it is known that the brain is poorly infiltrated by the mammalian immune system, the resident glial cells, namely microglial cells and astrocytes, play an especially important role

Chapter 5.1: Wild-type transient-MCAO

as the immuno-competent and phagocytic macrophages and secretion of inflammatory factors (e.g. cytokines, chemokines and NO), even neurotropic molecules such as brain-derived neurotropic factor (Bdnf) and insulin-like growth factor 1 (Igf1) in the CNS (See Table 5.1: Cell homeostasis, survival and proliferation) (Ekdahl et al., 2009; Lucas et al., 2006; Swanson et al., 2004). As shown in WT-tMCAO model, elevated transcriptomic response of majority of the genes involved in glial cell-mediated cytotoxicity (Prf1, Fc receptors (Fcgr4 and Fcrlg) and Ifngr2) took place at 8h post-reperfusion. Ca²⁺-dependent granule exocytosis and intracytoplasmic granular release of cytotoxic proteins, namely perforin (Prf1) and granzymes, together with Tnfrsfs which possess an intrinsic conserved intracytoplasmic "death domain" lead to the activation of the caspase enzymatic cascade and ultimately apoptotic mechanisms in numerous cell types through interaction with distinct intermediary adaptor molecules (Zamai et al., 1998). Other than mediating the release of pro-inflammatory cytokines, activated microglial cells have also been shown to be able to induce generation of other cytotoxic products such as prostanoid, ROS and nitric oxide (NO), of which the enzyme responsible for the latter production, Nos3, demonstrated transcriptional up-regulation at 24h.

-TLR signaling pathway

Transcriptional up-regulation of the TLRs (Tlr2 and Tlr13), which play an important role in the elimination of foreign and microbial pathogens through activation of the innate immunity, occurred just 2h after tMCAO, with consistent increment in gene expression over the whole time-course study (Table 5.1). Stimulation of Tlr7 gene expression occurred slightly later at 8h, with subsequent down-regulation at 24h. On the other hand, lipopolysaccharide binding protein (Lbp) and myeloid differentiation primary response 88

Chapter 5.1: Wild-type transient-MCAO

(Myd88) with a specific role in TLR signaling pathway demonstrated a late increase in gene expression at 24h.

-Complement and coagulation signaling cascade

Complements, which form the non-adaptive component of the innate immunity system, are involved in the osmotic lysis of cells through formation of transmembrane channels (membrane-attack complexes) upon activation. Activation of the complement cascade has been demonstrated to be crucial in inducing an inflammatory response in I/R injury through production of the active components such as C3a and C5a anaphylatoxins after tMCAO in mouse model (D'Ambrosio et al., 2001). Concurrently, its inhibition exhibits a neuroprotective effect in in vivo models (Arumugam et al., 2009). As demonstrated from the WT-tMCAO global gene profile in Table 5.1, various complement components such as C1qa, C1qb, C1qc, C3 and C4b were transcriptionally up-regulated at 24h post-reperfusion.

The coagulation signaling cascade plays a pivotal role in the haemostasis process to impede blood loss from a ruptured blood vessel through formation of a fibrin- and platelet-derived blood clot. As it has been previously established that tMCAO-induced vascular leakages in the brain (Crack et al., 2001), it is reasonable to propose the existence of damages to the blood vasculature network. Analysis of the WT-tMCAO transcriptional profile identified several pro-coagulant players (Vwf, Plaur, F10 and F13a1) being significantly up-regulated at the 24h time-point (Table 5.1). Infliction of damages to blood vessel walls revealed subendothelium proteins, especially von Willebrand factor (vWF), a protein secreted by healthy endothelium localized between the endothelium and underlying basement membrane. When the endothelium is ruptured, the normally unexposed vWF is exposed to the flowing

Chapter 5.1: Wild-type transient-MCAO

blood which further recruits additional clotting factors such as collagen and factor VIII. Particular attention is paid to the transcriptional up-regulation of the plasminogen activator, urokinase receptor (Plaur), as the current thrombolytic therapeutic treatment to acute cerebral ischemic stroke is only limited to the intravenous injection of recombinant tissue plasminogen activator (Donnan et al., 2008; Furlan et al., 2003). On the other hand, thrombomodulin (Thbd), an anti-coagulant protein involved in activation of protein S (Pros1) to prevent excessive thrombin formation (thrombosis), showed a substantial up-regulation at the 2h time-point which is followed by a corresponding transcriptional up-regulation of its downstream target Pros1. This is an additional piece of evidence of infliction of damage to the brain vasculature in the event of tMCAO.

- VASCULATURE DEVELOPMENT

During I/R injury, the vasculature integrity is compromised with increase in vascular permeability to facilitate leukocytes migration from the bloodstream to the ischemic region. As demonstrated in Table 5.1, genes encoding for proteins primarily involved in the maintenance of vasculature homeostasis (Angpt2, Angptl4, Lox, Pdpn and Emcn) showed increase in mRNA expression from 8h post- reperfusion.

- RESPONSE TO OXIDATIVE STRESS

During I/R injury, elevation of oxidative mediators particularly ROS surrounding the damaged core induce aberrant modifications to biological components including proteins, DNA and lipids resulting in further cellular stress. The experienced stress in turns triggers anti-oxidant response to buffer against the rising oxidative pressure through up-regulation of anti-oxidant proteins such as Hsps and chaperones which promote correct folding and

Chapter 5.1: **Wild-type transient-MCAO**

clearance of misfolded proteins and for certain members (Hsp27 and70) inhibit the pro-apoptotic signaling cascade. Hspb1 (also known as Hsp27), Hspb6, Dnajb1 and Srxn1 were significantly transcriptionally up-regulated individually throughout the whole temporal course of reperfusion study (Table 5.1). Further, dual role transcription factors such as Stat3 could be activated to induce the transcriptional elevation of numerous pro-survival and – apoptotic biological targets. Indeed, as demonstrated from the microarray data (Table 5.1), Stat3 showed increased gene expression at 24h post-reperfusion respectively.

- CALCIUM ION BINDING AND HOMEOSTASIS

Oxidative stress arising from I/R injury can inflict multiple mechanistic cell death-contributing signaling cascades. One of them would be intracellular Ca^{2+} overload which occurs as a result of excess Ca^{2+} influx from the extracellular matrix through iGluRs in the event of excitotoxicity with subsequent Ca^{2+} -induced Ca^{2+} release from endoplasmic reticulum as a result of organellar stress. Temporal transcriptomic profiling suggested the presence of elevated intracellular Ca^{2+} level through the increase in gene expression of Ca^{2+} -dependent proteins such as the S100 calcium binding protein family and annexins family throughout the whole time-course study (Table 5.1).

- CELL DEATH

The oxidative stress-activated transcription factor NF- κ B has been reported to be induced, both expression and binding activity, in the glial cells of the penumbra after cerebral ischemia and *in vivo* MCAO models, and whose main role is in the transcription of downstream death-promoting and pro-inflammatory protein targets (Clemens et al., 1997; Terai et al., 1996). Zhang and Peng (2005) on the other hand reported NF- κ B localisation and

Chapter 5.1: **Wild-type transient-MCAO**

activation occurred in neurons instead during cerebral ischemia. Our transcriptomic profiling tMCAO data on WT mice demonstrated prominent Nfkbiz gene up-regulation, an inhibitor of NF- κ B, from the early onset (2h) of I/R injury which might be a cellular mechanism to counteract the cell machinery under oxidative stress. Increased in gene expression of the endoplasmic reticulum stress-responsive pro-apoptotic proteins, Cebpb and Ddit3 at 2h and 8h respectively were also observed, where both of which form a repressor complex to inhibit the transcription of pro-survival genes. Lysosomal enzymes, cathepsin c and z (Ctsc and Ctsz), also showed increase in mRNA levels at 24h post-reperfusion, indicative of lysosomal rupture (Table 5.1).

Cell proliferative response, i.e. in the case of aberrant cell cycle re-entry (which is unfeasible under physiological condition due to the post-mitotic differentiated state of the adult brain neurons), is impeded by the transcriptional up-regulation of Mif1 and Atf3, and members of the growth arrest and DNA-damage-inducible 45 (Gadd45) family. Myeloid leukemia factor 1 (Mif1) and activating transcription factor 3 (Atf3) have recently been identified as stress-induced upstream positive regulators of p53 activity and stability thereby maintaining genome integrity (Yan et al., 2005; Yoneda-Kato et al., 2005). Gadd45 members, on the other hand, are p53-transcribed downstream transcriptional targets which play an important role in preventing unregulated cell cycle re-entry and promoting of DNA repairs upon genotoxic insults, highly probable under heightened oxidative stress condition. Other death-promoting players (Btg1, Uvrug and Uaca) also showed increase in gene expression during the temporal course of tMCAO study (Table 5.1). Uveal autoantigen with coiled-coil domains and ankyrin repeats (Uaca) is involved in the regulation of stress-induced apoptosis through modulation of Apaf-1 nuclear localisation, resulting in apoptosome up-regulation,

Chapter 5.1: Wild-type transient-MCAO

LGALS3/galectin-3 down-regulation and NF- κ B inactivation. On the other hand, UV radiation resistance associated gene (Uvrags) participates in the activation of the Beclin1-PI₃KC3 complex, promoting autophagy and suppressing cell proliferation.

- CELL HOMEOSTASIS, SURVIVAL AND PROLIFERATION

Cellular survival-promoting protein-encoding genes, particularly growth factors e.g. Bdnf, Hbegf and Fgf12, and their related binding partners and receptors e.g. Tgfr2 and Igfbp3 showed elevated gene expression throughout the whole-course of I/R injury (Table 5.1). Transcription factors such as Jun oncogenes (Jun and Junb) which target pro-survival genes demonstrated substantial transcriptional up-regulation at 2h post-reperfusion.

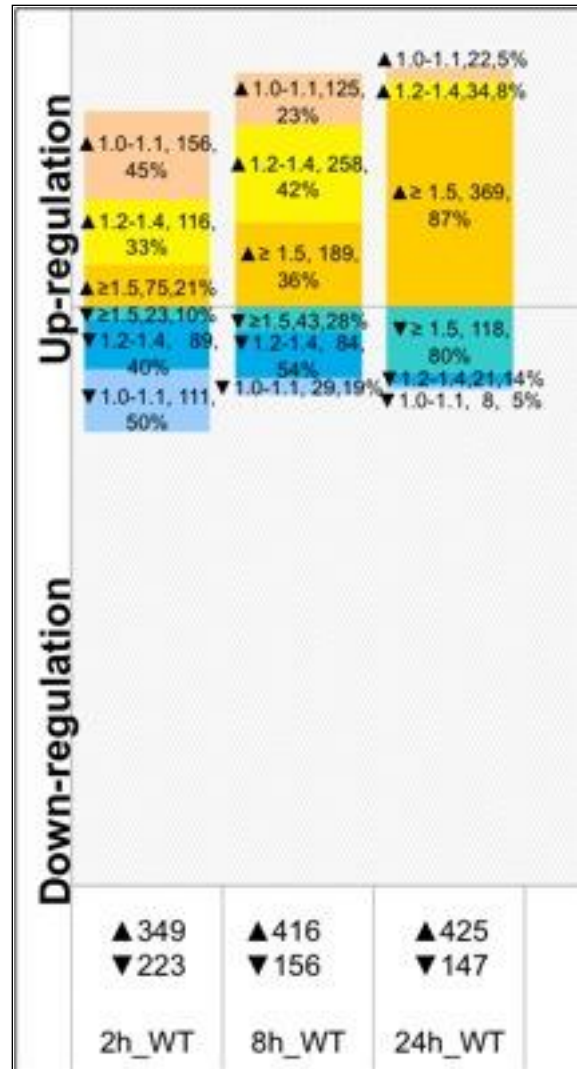


Figure 5.1 Time-course profiling revealed a significant increase in number of up/down-regulated genes with transcriptional expression of a minimum of ± 1.5 -fold change from 8h to 24h timeframe. Only genes with transcriptional fold-change of at least ± 1.5 in at least one out of three time-points and had passed stringent statistical analyses were included into WT (572 gene probes) –MCAO global gene profiles. Genes were then segregated into fold-change categories at respective time-points.

Chapter 5.1:
Wild-type transient-MCAO

Table 5.1 Selected differentially-expressed gene profile of neuronal death-related families in the infarct cortice of WT-MCAO male adult mice. All fold-change expressions are subjected to one-way ANOVA analysis and significant at $p < 0.05$. Data are expressed as fold-change \pm sem.

Genbank	Gene Title	Symbol	Time-points		
			2h	8h	24h
Cytokine-Cytokine receptor interaction					
NM_011609	Tumor necrosis factor receptor superfamily, member 1a	Tnfrsf1a	1.10 \pm 0.10	1.34 \pm 0.20	1.71 \pm 0.54
NM_013749	Tumor necrosis factor receptor superfamily, member 12a	Tnfrsf12a	1.57 \pm 0.32	1.53 \pm 0.80	2.84 \pm 3.22
NM_023785	Pro-platelet basic protein	Ppbp	1.01 \pm 0.10	1.06 \pm 0.11	1.50 \pm 1.26
NM_001013365	Oncostatin M	Osm	1.66 \pm 0.47	1.45 \pm 0.34	1.87 \pm 1.12
NM_011333	Chemokine (C-C motif) ligand 2	Ccl2	1.29 \pm 0.13	2.28 \pm 0.83	2.48 \pm 2.03
NM_013653	Chemokine (C-C motif) ligand 5	Ccl5	1.17 \pm 0.06	1.33 \pm 0.26	1.94 \pm 1.19
NM_013654	Chemokine (C-C motif) ligand 7	Ccl7	2.32 \pm 1.23	2.68 \pm 1.46	3.25 \pm 3.80
NM_011330	Small chemokine (C-C motif) ligand 11	Ccl11	1.08 \pm 0.13	1.86 \pm 0.92	1.77 \pm 1.26
NM_009140	Chemokine (C-X-C motif) ligand 2	Cxcl2	1.26 \pm 0.08	1.34 \pm 0.35	1.81 \pm 1.14
NM_019932	Chemokine (C-X-C motif) ligand 4	Cxcl4	1.43 \pm 0.38	1.50 \pm 0.31	2.46 \pm 1.59
NM_021274	Chemokine (C-X-C motif) ligand 10	Cxcl10	1.28 \pm 0.13	1.88 \pm 0.77	2.63 \pm 2.26
NM_023158	Chemokine (C-X-C motif) ligand 16	Cxcl16	1.19 \pm 0.15	1.62 \pm 0.58	2.15 \pm 1.04
NM_009917	Chemokine (C-C motif) receptor 5	Ccr5	1.37 \pm 0.15	1.69 \pm 0.37	2.11 \pm 0.85
NM_008361	Interleukin 1 beta	Il1b	1.50 \pm 0.33	1.91 \pm 0.73	2.17 \pm 1.87
NM_010555	Interleukin 1 receptor, type II	Il1r2	1.03 \pm 0.04	1.29 \pm 0.07	1.64 \pm 1.00
NM_009909	Interleukin 8 receptor, beta	Il8rb	1.01 \pm 0.07	1.13 \pm 0.06	1.64 \pm 1.02
NM_008350	Interleukin 11	Il11	1.12 \pm 0.09	1.73 \pm 0.30	5.85 \pm 12.87
NM_133990	Interleukin 13 receptor, alpha 1	Il13ra1	1.14 \pm 0.17	1.41 \pm 0.23	1.70 \pm 0.63
NM_019583	Interleukin 17 receptor B	Il17rb	1.21 \pm 0.10	1.58 \pm 0.62	1.31 \pm 0.37
Facilitation of Leukocyte Transendothelial Migration					
NM_008677	Neutrophil cytosolic factor 4	Ncf4	1.05 \pm 0.06	1.34 \pm 0.20	2.18 \pm 0.91
NM_027102	Endothelial cell-specific adhesion molecule	Esam1	-1.26 \pm 0.06	1.11 \pm 0.10	1.61 \pm 0.65
NM_010493	Intercellular adhesion molecule	Icam1	1.47 \pm 0.52	1.83 \pm 0.58	1.68 \pm 0.58
NM_010494	Intercellular adhesion molecule 2	Icam2	-1.19 \pm 0.11	1.39 \pm 0.11	1.50 \pm 0.40
NM_008816	Platelet/endothelial cell adhesion molecule 1	Pecam1	-1.13 \pm 0.09	1.03 \pm 0.15	1.73 \pm 0.74
NM_007806	Cytochrome b-245, alpha polypeptide	Cyba	1.15 \pm 0.19	1.44 \pm 0.07	2.71 \pm 1.33
NM_009510	Villin 2	Vil2	1.27 \pm 0.11	1.68 \pm 0.05	1.39 \pm 0.40
NM_010833	Moesin	Msn	1.07 \pm 0.10	1.45 \pm 0.08	2.23 \pm 1.15
NM_033268	Actinin alpha 2	Actn2	-1.19 \pm 0.08	1.33 \pm 0.21	-1.72 \pm 0.15
Immune Cell-Mediated Cytotoxicity					
NM_013545	Protein tyrosine phosphatase, non-receptor type 6	Ptpn6	1.11 \pm 0.11	1.10 \pm 0.06	1.86 \pm 0.70
NM_011073	Perforin 1 (pore forming protein)	Prfl	-1.77 \pm 0.09	1.86 \pm 0.12	-1.27 \pm 0.27
NM_144559	Fc receptor, IgG, low affinity IV	Fcgr4	-1.09 \pm 0.06	1.80 \pm 0.56	3.47 \pm 2.85
NM_010185	Fc receptor, IgE, high affinity I, gamma polypeptide	Fcer1g	1.15 \pm 0.14	1.48 \pm 0.16	2.20 \pm 1.30
NM_008338	Interferon gamma receptor 2	Ifngr2	-1.55 \pm 0.04	1.60 \pm 0.10	-1.18 \pm 0.19
NM_011662	TYRO protein tyrosine kinase binding protein	Tyrobp	1.04 \pm 0.14	1.05 \pm 0.12	1.64 \pm 0.49
NM_008713	Nitric oxide synthase 3	Nos3	1.08 \pm 0.17	1.02 \pm 0.06	1.75 \pm 0.51

Chapter 5.1:
Wild-type transient-MCAO

Table 5.1 (continue)

Genbank	Gene Title	Symbol	Time-points		
			2h	8h	24h
<u>Immune Cell-Mediated Cytotoxicity (continue)</u>					
NM_011368	Src homology 2 domain-containing transforming protein C1	Shc1	1.01 ± 0.11	1.52 ± 0.14	1.54 ± 0.55
<u>TLR signaling pathway</u>					
NM_008489	Lipopolysaccharide binding protein	Lbp	1.17 ± 0.40	1.32 ± 0.18	1.61 ± 0.26
NM_019388	CD86 antigen	Cd86	1.37 ± 0.16	1.86 ± 0.63	1.73 ± 0.77
NM_011905	TLR 2	Tlr2	1.89 ± 0.72	2.33 ± 0.98	2.93 ± 1.76
NM_133211	TLR 7	Tlr7	1.40 ± 0.03	1.50 ± 0.05	1.21 ± 0.32
NM_205820	TLR 13	Tlr13	1.54 ± 0.21	1.89 ± 0.48	2.02 ± 0.98
NM_010851	Myeloid differentiation primary response gene 88	Myd88	-1.02 ± 0.06	1.31 ± 0.26	1.83 ± 0.99
<u>Complement and coagulation cascades</u>					
NM_008878	Serine (or cysteine) peptidase inhibitor, clade F, member 2	Serpinf2	1.20 ± 0.04	1.58 ± 0.31	1.37 ± 0.10
NM_009776	Serine (or cysteine) peptidase inhibitor, clade G, member 1	Serping1	1.14 ± 0.16	1.29 ± 0.18	2.02 ± 0.68
NM_007572	Complement component 1, q subcomponent, alpha polypeptide	C1qa	1.07 ± 0.08	1.13 ± 0.11	1.51 ± 0.41
NM_009777	Complement component 1, q subcomponent, beta polypeptide	C1qb	1.14 ± 0.08	1.49 ± 0.09	1.79 ± 0.56
NM_007574	Complement component 1, q subcomponent, C chain	C1qc	1.14 ± 0.13	1.21 ± 0.17	1.70 ± 0.36
NM_009778	Complement component 3	C3	-1.05 ± 0.05	1.05 ± 0.14	1.60 ± 0.65
NM_009780	Complement component 4B (Childo blood group)	C4b	-1.13 ± 0.18	1.07 ± 0.09	1.54 ± 0.47
NM_011708	Von Willebrand factor homolog	Vwf	-1.44 ± 0.02	1.37 ± 0.10	2.20 ± 0.22
NM_009929	procollagen, type XVIII, alpha 1	Col18a1	-1.01 ± 0.11	1.06 ± 0.13	1.56 ± 0.53
NM_007972	Coagulation factor X	F10	1.04 ± 0.10	1.01 ± 0.05	1.51 ± 0.48
NM_028784	Coagulation factor XIII, A1 subunit	F13a1	1.04 ± 0.12	1.18 ± 0.04	1.87 ± 0.35
NM_011113	Plasminogen activator, urokinase receptor	Plaur	1.28 ± 0.20	1.30 ± 0.17	1.68 ± 0.59
NM_011173	Protein S (alpha)	Pros1	1.16 ± 0.15	1.57 ± 0.15	2.04 ± 0.72
NM_009378	Thrombomodulin	Thbd	1.75 ± 0.66	1.68 ± 0.44	2.26 ± 1.13
<u>Vasculature development</u>					
NM_007426	Angiopoietin 2	Angpt2	1.14 ± 0.05	1.90 ± 0.33	2.38 ± 1.75
NM_020581	Angiopoietin-like 4	Angptl4	1.18 ± 0.11	1.76 ± 0.20	1.50 ± 0.47
NM_009263	Secreted phosphoprotein	Spp1	1.15 ± 0.23	2.07 ± 0.51	6.98 ± 12.94
NM_198724	EGF-like domain 7	Egfl7	1.04 ± 0.01	1.00 ± 0.07	1.62 ± 0.37
NM_205536	ELK3, member of ETS oncogene family	Elk3	1.05 ± 0.06	1.05 ± 0.10	1.90 ± 0.57
NM_009022	Aldehyde dehydrogenase family 1, subfamily A2	Aldh1a2	1.17 ± 0.17	1.58 ± 0.23	1.94 ± 0.87
NM_010516	Cysteine rich protein 61	Cyr61	2.64 ± 2.26	1.46 ± 0.42	1.82 ± 1.20
NM_010728	Lysyl oxidase	Lox	1.20 ± 0.05	1.54 ± 0.06	2.01 ± 1.47
NM_008608	Matrix metalloproteinase 14 (membrane-inserted)	Mmp14	1.01 ± 0.17	1.16 ± 0.08	1.62 ± 0.22
NM_010329	Podoplanin	Pdpn	1.39 ± 0.29	1.70 ± 0.25	2.38 ± 1.69
NM_011451	Sphingosine kinase 1	Sphk1	1.16 ± 0.13	2.03 ± 0.67	1.89 ± 1.19
NM_009373	Transglutaminase 2, C polypeptide	Tgm2	1.17 ± 0.23	1.75 ± 0.30	2.94 ± 2.34

Chapter 5.1:
Wild-type transient-MCAO

Table 5.1 (continue)

Genbank	Gene Title	Symbol	Time-points		
			2h	8h	24h
Vasculature development (continue)					
NM_007564	Zinc finger protein 36, C3H type-like 1	Zfp3611	1.33 ± 0.59	1.53 ± 0.32	1.96 ± 0.41
NM_009929	Procollagen, type XVIII, alpha 1	Col18a1	1.01 ± 0.11	1.10 ± 0.13	1.56 ± 0.53
NM_016885	Endomucin	Emcn	1.13 ± 0.10	1.10 ± 0.16	1.63 ± 0.69
NM_015768	Prokineticin 2	Prok2	1.03 ± 0.25	1.50 ± 0.26	1.39 ± 0.66
Response to oxidative stress					
NM_011486	Signal transducer and activator of transcription 3	Stat3	1.09 ± 0.17	1.26 ± 0.21	1.74 ± 1.00
NM_173011	Isocitrate dehydrogenase 2 (NADP+), mitochondrial	Idh2	1.00 ± 0.23	1.22 ± 0.17	1.60 ± 0.18
NM_021491	Sphingomyelin phosphodiesterase 3, neutral	Smpd3	-1.31 ± 0.11	1.27 ± 0.12	-1.87 ± 0.18
NM_013560	Heat shock protein 1 (Hsp27)	Hspb1	1.70 ± 1.27	2.14 ± 1.40	3.07 ± 3.82
NM_001012401	Heat shock protein, alpha-crystallin-related, B6	Hspb6	1.30 ± 0.15	1.74 ± 0.17	2.85 ± 0.94
NM_013863	Bcl2-associated athanogene 3	Bag3	1.63 ± 0.56	1.67 ± 0.73	1.57 ± 0.57
NM_018808	DnaJ (Hsp40) homolog, subfamily B, member 1	Dnajb1	1.53 ± 0.89	1.21 ± 0.26	-1.19 ± 0.07
NM_011451	Sphingosine kinase 1	Sphk1	1.16 ± 0.13	2.03 ± 0.67	1.89 ± 1.19
NM_010931	Ubiquitin-like, containing PHD and RING finger domains, 1	Uhrf1	1.11 ± 0.12	1.12 ± 0.09	1.87 ± 0.38
NM_029688	Sulfiredoxin 1 homolog (S. cerevisiae)	Srxn1	1.25 ± 0.17	1.72 ± 0.27	1.58 ± 0.45
Calcium ion binding and homeostasis					
NM_010809	Matrix metalloproteinase 3	Mmp3	1.05 ± 0.07	1.70 ± 0.43	4.03 ± 4.27
NM_008605	Matrix metalloproteinase 12	Mmp12	-1.04 ± 0.06	1.46 ± 0.69	1.68 ± 0.68
NM_011313	S100 calcium binding protein A6 (calcyclin)	S100a6	1.13 ± 0.14	1.37 ± 0.16	2.27 ± 0.96
NM_016740	S100 calcium binding protein A11 (calgizzarin)	S100a11	1.07 ± 0.18	1.76 ± 0.18	3.82 ± 3.06
NM_009113	S100 calcium binding protein A13	S100a13	1.18 ± 0.16	1.27 ± 0.10	1.50 ± 0.31
NM_007585	Annexin A2	Anxa2	1.25 ± 0.22	1.94 ± 0.25	3.22 ± 2.57
NM_013470	Annexin A3	Anxa3	-1.18 ± 0.13	1.15 ± 0.16	2.05 ± 0.83
NM_016789	Neuronal pentraxin 2	Nptx2	2.44 ± 0.41	1.64 ± 1.17	1.07 ± 0.22
NM_146118	Solute carrier family 25 (mitochondrial carrier, phosphate carrier), member 25	Slc25a25	1.63 ± 0.33	1.37 ± 0.16	-1.05 ± 0.08
NM_016745	ATPase, Ca ⁺⁺ transporting, ubiquitous	Atp2a3	-1.19 ± 0.07	1.81 ± 0.08	-1.34 ± 0.16
Cell death					
NM_030612	Nuclear factor of kappa light polypeptide gene enhancer in B-cells inhibitor, zeta	Nfkbiz	2.22 ± 1.08	1.84 ± 0.51	1.57 ± 0.54
NM_009883	CCAAT/enhancer binding protein (C/EBP), beta	Cebpb	1.60 ± 0.39	1.95 ± 0.31	1.87 ± 1.10
NM_007837	DNA-damage inducible transcript 3	Ddit3	1.36 ± 0.17	1.52 ± 0.31	1.43 ± 0.55
NM_001039543	Myeloid leukemia factor 1	Mlf1	1.86 ± 0.52	1.49 ± 0.54	1.07 ± 0.16
NM_007498	Activating transcription 3	Atf3	4.06 ± 3.68	3.22 ± 2.64	3.00 ± 3.68
NM_007836	Growth arrest and DNA-damage-inducible 45 alpha	Gadd45a	1.39 ± 0.25	1.34 ± 0.18	1.54 ± 0.76
NM_008655	Growth arrest and DNA-damage-inducible 45 beta	Gadd45b	2.72 ± 0.97	2.09 ± 1.19	2.20 ± 1.96
NM_011817	Growth arrest and DNA-damage-inducible 45 gamma	Gadd45g	2.36 ± 1.79	1.55 ± 0.79	1.55 ± 1.41

Chapter 5.1:
Wild-type transient-MCAO

Table 5.1 (continue)

Genbank	Gene Title	Symbol	Time-points		
			2h	8h	24h
<u>Cell death (continue)</u>					
NM_178635	UV radiation resistance associated gene	Uvrag	1.54 ± 0.11	1.62 ± 0.11	1.37 ± 0.28
NM_009982	Cathepsin C (Ctsc)	Ctsc	-1.17 ± 0.10	1.14 ± 0.15	2.27 ± 0.83
NM_022325	Cathepsin Z (Ctsz)	Ctsz	1.27 ± 0.14	1.32 ± 0.18	1.91 ± 0.66
NM_007569	B-cell translocation gene 1, anti-proliferative	Btg1	1.32 ± 0.47	1.26 ± 0.18	1.71 ± 0.50
NM_028283	Uveal autoantigen with coiled-coil domains and ankyrin repeats	Uaca	1.21 ± 0.20	1.08 ± 0.09	1.90 ± 0.57
<u>Cell homeostasis, survival and proliferation</u>					
NM_153553	Neuronal PAS domain protein 4	Npas4	6.39 ± 12.48	1.74 ± 0.92	1.38 ± 0.26
NM_019713	Ras association (RalGDS/AF-6) domain family 1	Rassf1	1.66 ± 0.37	1.56 ± 0.24	1.64 ± 0.59
NM_207246	RAS, guanyl releasing protein 3	Rasgrp3	-1.23 ± 0.08	1.65 ± 0.09	-1.15 ± 0.10
NM_011368	Src homology 2 domain-containing transforming protein C1	Shc1	1.01 ± 0.11	1.52 ± 0.14	1.54 ± 0.55
NM_011691	Vav 1 oncogene	Vav1	-1.04 ± 0.07	1.25 ± 0.05	1.65 ± 0.68
NM_026014	Chromatin licensing and DNA replication factor 1	Cdt1	1.38 ± 0.08	1.51 ± 0.54	1.38 ± 0.39
NM_008885	Peripheral myelin protein	Pmp22	1.86 ± 0.17	1.67 ± 0.19	1.69 ± 0.75
NM_008416	Jun-B oncogene	Junb	2.42 ± 1.20	1.12 ± 0.24	1.17 ± 0.46
NM_007557	Bone morphogenetic protein 7	Bmp7	1.22 ± 0.05	1.42 ± 0.19	1.91 ± 0.81
NM_009371	Transforming growth factor, beta receptor II	Tgfbr2	-1.03 ± 0.06	1.04 ± 0.06	1.53 ± 0.29
NM_007540	Brain derived neurotrophic factor	Bdnf	1.65 ± 0.29	1.17 ± 0.24	-1.30 ± 0.10
NM_008343	Insulin-like growth factor binding protein 3	Igfbp3	1.01 ± 0.06	1.54 ± 0.28	2.77 ± 2.62
NM_010415	Heparin-binding EGF-like growth factor	Hbegf	1.27 ± 0.19	1.30 ± 0.22	1.70 ± 0.71
NM_010199	Fibroblast growth factor 12	Fgf12	-1.33 ± 0.08	1.58 ± 0.09	-1.54 ± 0.17
NM_054051	Phosphatidylinositol-4-phosphate 5-kinase, type II, beta	Pip5k2b	-1.33 ± 0.07	-1.77±0.06	-2.19 ± 0.09
NM_173370	CDP-diacylglycerol synthase 1	Cds1	-1.05 ± 0.05	-1.24±0.09	-1.69 ± 0.10
NM_138306	Diacylglycerol kinase zeta	Dgkz	-1.05 ± 0.09	-1.36±0.05	-1.84 ± 0.13

5.1.2.2 Validation of WT-tMCAO profiles via real-time PCR

Microarray data was validated on the same tMCAO-induced WT cortical RNA samples used in microarray analysis via real-time PCR. These selected gene probes demonstrated identical transcriptional regulatory trend at 2h, 8h and 24h post-reperfusion (Table 5.2).

Table 5.2 Validation of microarray data using real-time PCR technique on tMCAO-induced cortex RNA samples from WT mice respectively. All fold-change expressions are statistically significant at $p < 0.05$. Each expression data is representative of 3 independent replicates. Data are expressed as fold-change \pm sem.

Genbank	Gene Title	Symbol	WT-tMCAO					
			2h		8h		24h	
			Microarray	Real-time PCR	Microarray	Real-time PCR	Microarray	Real-time PCR
NM_153553	Neuronal PAS domain protein 4	Npas4	6.39 \pm 12.48	4.17 \pm 0.43	1.74 \pm 0.92		1.38 \pm 0.26	
NM_007498	Activating transcription 3	Atf3	4.06 \pm 3.68	8.80 \pm 0.38	3.22 \pm 2.64	5.39 \pm 0.44	3.00 \pm 3.68	
NM_011905	Toll-like receptor 2	Tlr2	1.89 \pm 0.72	7.85 \pm 0.95	2.33 \pm 0.98	9.09 \pm 0.97	2.93 \pm 1.76	
NM_009263	Secreted phosphoprotein	Spp1	1.15 \pm 0.23		2.07 \pm 0.51	2.68 \pm 0.97	6.98 \pm 12.94	
NM_007585	Annexin A2	AnxA2	1.25 \pm 0.22		1.94 \pm 0.25		3.22 \pm 2.57	7.57 \pm 0.95
NM_020581	Angiopoietin-like 4	Angptl4	1.18 \pm 0.11		1.76 \pm 0.20		1.50 \pm 0.47	1.96 \pm 1.05
NM_011817	Growth arrest and DNA-damage-inducible 45 gamma	Gadd45g	2.36 \pm 1.79	3.84 \pm 0.84	1.55 \pm 0.79	1.61 \pm 0.87	1.55 \pm 1.41	2.36 \pm 0.91

5.1.3 Discussion

Ischemic stroke is triggered off with severe focal hypoperfusion i.e. a reduction in blood flow with concomitant oxygen-glucose deprivation, resulting in excitotoxicity and oxidative injury which manifested as microvascular damage, blood-brain barrier dysfunction and post-ischemic inflammation (Lakhan et al., 2009). Unlike focal ischemia, transient focal cerebral ischemia which is followed by restoration of blood flow to the affected infarct region usually results in secondary I/R injury frequently incurred through two main patho-physiological mechanisms namely, oxidative stress and neuroinflammation. The cerebral ischemic core usually underwent the most severe irreversible neuronal injury through simultaneous activation of pathological cascades (Dirnagl et al., 1999). Injured brain tissue surrounding this ischemic core, known as penumbra, would be subjected to lesser neuronal damages if cerebral blood flow is restored promptly, a process known as reperfusion. However, despite the immediate re-delivery of blood to the affected brain region, the ischemic cascade usually remains active for hours to days post-reperfusion.

The brain being poorly equipped with anti-oxidative cytoprotective mechanisms is especially susceptible to oxidative stress as it is unable to buffer detrimental elevation of ROS level and other forms of free radicals and/or oxidants produced by inflammatory cells. Within a short period of time after the trigger of ischemia, resident macrophages (microglial cells) transformed into phagocytes releasing pro- (e.g. prostanoids, NO, TNF- α , interleukins; latter two-associated receptors demonstrated increased mRNA expression) and anti- (e.g. neurotropic factors: Bdnf and insulin-like growth factor; transcriptional up-regulation evident from Table 1: Cell survival and proliferation)

Chapter 5.1: Wild-type transient-MCAO

inflammatory molecules, thus playing a pivotal role in neuronal survival and post-injury tissue remodeling (Lucas et al., 2006; Madinier et al., 2009). Furthermore, microglia have also been reported to neuroprotect against excitotoxicity through the uptake of extracellular Glu (Nakajima et al., 2008), the removal of dying neurons and cell debris (Stoll and Jander, 1999) and direct sequestration of infiltrating neutrophil granulocytes (Neumann et al., 2008). Astrocytes residing in the brain also contribute to the inflammation process via secretion of inflammatory molecules including NO, cytokines and chemokines (Swanson et al., 2004).

Occurrence of neuroinflammation is particularly prominent in experimental stroke models and acute ischemic stroke patients, where a decrease in cell count and an impaired functioning of innate T lymphocytes and natural killer (NK) cells in peripheral blood were been observed, implying an immunity alteration which manifested into an increased susceptibility to brain infections after stroke (Haeusler et al., 2008; Klehmet et al., 2009; Peterfalvi et al., 2009; Urra et al., 2009; Vogelgesang et al., 2008). This opens up a new perspective of the immune system playing a vital role in tissue remodelling after neuronal injury, even though it has been initially perceived that the CNS to be an immuno-privileged region (Lakhan et al., 2009).

5.1.3.1 Neuroinflammation

- Complement and coagulation cascade

The present temporal transcriptomic profiling of transient cerebral ischemia in the cortex of WT mouse revealed substantial and credential evidence of activation of neuroinflammatory cascades. Temporal recruitment of the immune system via infiltrating

Chapter 5.1: Wild-type transient-MCAO

leukocytes through the blood-brain-barrier and resident glial cells (microglia and astrocytes) was observed to occur from as early as 2h and majority at 8h post-reperfusion (Table 5.1: Complement and coagulation cascades). The complement and coagulation pathways play important role in the induction of immunity-mediated neuronal death and occlusion of the cerebral artery, aggravating the degree of severity of I/R injury. Expression of active complement fragments such as C3a and C5a receptors have been reported to increase significantly after MCAO induction in mouse (Arumugam et al., 2009). Interestingly, a transcriptional up-regulation of the anti-thrombolytic factor-associated receptor, plasminogen activator urokinase receptor (Plaur), is observed. This verifies the only current intravenous usage of recombinant tissue plasminogen activator for the thrombolytic therapeutic treatment of acute ischemic stroke, which demonstrated a short efficacy window timeframe of three hours after the trigger of ischemic stroke (Furlan et al., 2003).

-Cytokine-cytokine receptor interaction

Cytokine-cytokine receptor interactions are crucial in the regulation of innate and adaptive immune systems in a variety of inflammatory-related diseases including stroke. In the mammalian brain, expression and secretion of cytokines are not limited to blood-circulating peripherally-derived leukocytes (T lymphocytes, NK cells, phagocytes), but also to the neurons and glia (Barone and Feuerstein, 1999; Ferrarese et al., 1999). Reperfusion-mediated accentuation of chemokine expression has been suggested to evoke an intense inflammatory reaction. ELR motif-containing CXC chemokines are implicated in neutrophil infiltration in the ischemic area, while CXCR3 ligands serve as

Chapter 5.1: Wild-type transient-MCAO

chemoattractants to recruit T-helper 1 cells. Similarly, CC chemokines, promotes mononuclear cell infiltration and macrophage activation (Frangogiannis, 2007).

Transcriptional up-regulation of interleukins (Ils) and tumour necrosis factor receptors (Tnfrsfs) indicates an activation of pro-inflammatory cytokines-mediated signaling cascade, playing a role in the increase in brain infarct and edema volumes (Table 5.1: Cytokine-cytokine receptor interaction) (Acalovschi et al., 2003; Boutin et al., 2001). Concurrently, chemokines, a group of leukocyte chemoattractant proteins which are involved in inflammatory cell recruitment, demonstrated significant transcriptional activation, exacerbating I/R injury by increasing leukocyte infiltration (Kim et al., 1995). On the other hand, neuroprotection is exerted via the increase in gene expression of transforming growth factor beta receptor (Tgfb2) (Zhu et al., 2002). Upon immune cell chemokines-guided migration to site of ischemia, CAMs promote leukocyte rolling and adherence to the endothelial surface of the vascular endothelium (Yilmaz and Granger, 2008). In particular, Icam1 had been reported to demonstrated high protein expression in patients with acute ischemic stroke and correlated with poor prognosis (Rallidis et al., 2009). In the present transient *in vivo* cerebral ischemic stroke model, significant gene expression was observed at 8h post-reperfusion (Table 1: Facilitation of leukocyte transendothelial migration). Upon arrival at target cell, immune cell activation triggered cytotoxicity via transcriptional elevation of perforin (Prf1; Table 5.1: Immune cells-mediated cytotoxicity). Perforin, enveloped in cytotoxic granules with serine esterase molecules and exocytosed by immune cells, induced target cell lysis via pore formation in the cell membrane (Griffiths and Mueller, 1991; Podack et al., 1991). Innate immune system activation is further evident from the transcriptional activation of the TLR

Chapter 5.1: **Wild-type transient-MCAO**

pathway at 2h post-reperfusion (Table 5.1: TLR pathway). On the contrary, IFN- γ whose associated interferon gamma receptor 2 (Ifngr2; Table 5.1: Immune cells-mediated cytotoxicity) demonstrated as primarily secreted by T helper and NK cells, is suggested that it plays an important role in the protection against complications caused by post-ischemic infections with observations of its significant decrease in stroke patients (Klehmet et al., 2009; Urta et al., 2009). The decrease in IFN- γ secretion occurred in conjunction with an early decrease in T cell frequencies in peripheral blood of patients with acute ischemia stroke (Urta et al., 2009; Vogelgesang et al., 2008).

5.1.3.2 Oxidative Stress

Oxidative stress is a potential mediator of ischemic injury through the generation of plenty of reactive free radicals including ROS, reactive nitrogen species and electrophiles during acute ischemic stroke, leading to mitochondrial dysfunction, Ca²⁺ overload, aggravation of I/R injury and inflammation (Coyle and Puttfarcken, 1993; Cuzzocrea et al., 2001). As demonstrated in Table 5.1: Immune cell-mediated cytotoxicity, nitric oxide synthase 3 (Nos3), with a reported increase in activity in vascular endothelium upon ischemia, demonstrated transcriptional up-regulation at 24h post-reperfusion. Aberrant calcium ion homeostasis is reflected from the transcriptional elevation of Ca²⁺-binding proteins and Ca²⁺-associated transporters throughout the temporal course of I/R injury (Table 5.1: Calcium ion binding and homeostasis). Oxidative stress induced lysosomal disruption and endoplasmic reticulum stress, further exacerbating Ca²⁺ overload through release of its intracellular store, and simultaneously induced the expression of pro-apoptotic genes and transcription factors such as Cebpb, Ddit3 and Atf3 (Table 5.1: Cell death). Brain infarct regional susceptibility to oxidative stress damage is increased via the

Chapter 5.1:
Wild-type transient-MCAO

transcriptional down-regulation of members of the PI3K-Akt pathway (Pip5k2b, Cds and Dgkz; Table 5.1: Cell survival and proliferation). Increased Akt phosphorylation has been detected and critical for survival in transient cerebral ischemia (Noshita et al., 2001). Elevated cellular oxidative load evoked a counteractive anti-oxidative response through immediate early activation of Hsps and chaperones (Hspb1, Hspb6, Bag3 and Dnajb1), and transcriptional factor (Stat3) induction of neuroprotective downstream targets to diminish oxidative damages such as aberrant protein accumulation and neutralization of reactive free radicals (Table 5.1: Response to oxidative stress). The cellular pro-survival and proliferative mitogens-induced signaling pathways were also triggered with the increase in mRNA expression of growth factors (Bdnf, Hbegf and Fgf12) and mitogenic proteins (Rassf1, Rasgrp3, Shc1 and Vav1; Table 5.1: Cell survival and proliferation).

Chapter 5.2:
Transient focal cerebral ischemia
in
Glutathione peroxidase-1
– knockout (Gpx-1^{-/-})
***in vivo* adult mouse model**

5.2.1 Introduction

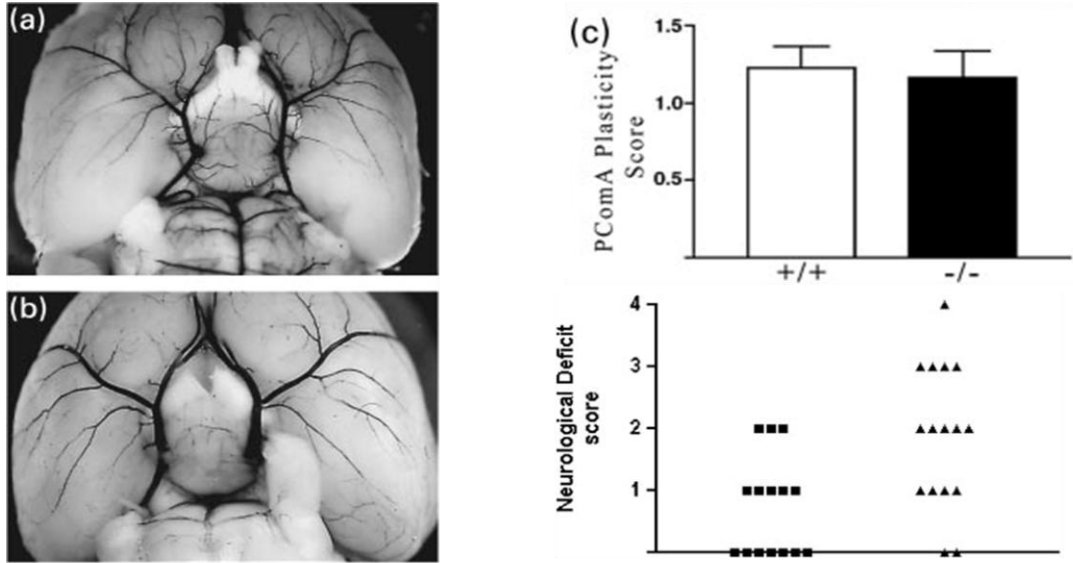
Oxidative brain damage is considered to be the most significant contributor to ischemic brain injury (Love, 1999). Deregulated excess production of ROS, derived from cellular oxygen metabolism and exogenous sources, can result in oxidative stress and even cell death. ROS levels within cells are modulated by synergistic action of enzymatic and non-enzymatic antioxidants. Gpx is a selenium-containing enzyme that catalyses the reduction of a variety of ROS e.g. H₂O₂ at the expense of reduced GSH. There are at least five isoforms of Gpx found in mammalian cells. Of these, the cytosolic and mitochondrial Gpx-1 is most abundant and localises in most tissues (de Haan et al., 1998). Role of Gpx-1 has been implicated in neurodegenerative disorders such as PD and dementia with Lewy bodies tissue (DLB) (Power and Blumbergs, 2009) and traumatic brain injury (Tsuru-Aoyagi et al., 2009). It has been shown in PD and DLB models, Gpx-1 surrounds Lewy bodies rich in alpha-synuclein in an effort to promote their degradation as alpha-synuclein proved to be capable of H₂O₂ generation (Power and Blumbergs, 2009). Furthermore, Gpx-1 role in aided recovery of spatial memory after traumatic brain injury possibly through its early response to oxidative stress and selective, long-term sparing of neurons in the dentate nucleus has been reported (Tsuru-Aoyagi et al., 2009).

Due to its high abundance, mutation of the Gpx-1 allele would lower overall Gpx activity in the brain significantly. Gpx-1 knockout (Gpx-1^{-/-}) mice do not show overt phenotypic differences, all indications suggest that these mice are in a chronic “pro-oxidant” state (Cheng et al., 1999; de Haan et al., 2004). Indeed, a recent study illustrated that the absence of Gpx-1 exacerbated stroke injury via increased ROS production and vascular

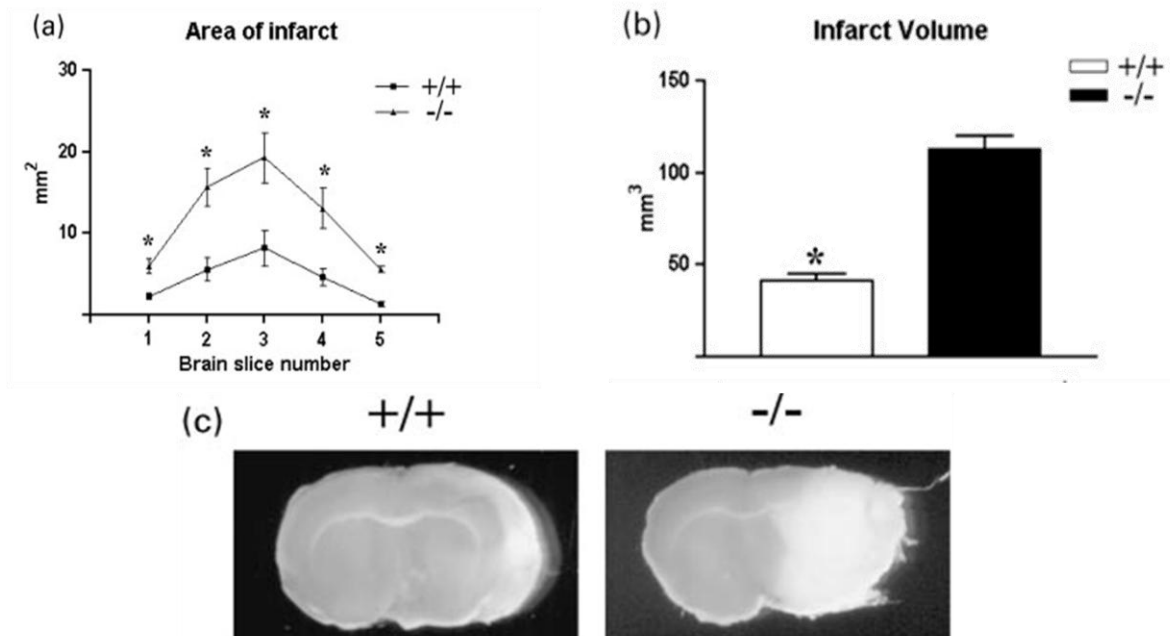
Chapter 5.2: Gpx-1^{-/-}-transient MCAO

permeability (Wong et al., 2008). Furthermore, Gpx-1^{-/-} mice demonstrated an increase in caspase-3 activation and greater infarct volume (Crack et al., 2001). As such, it has been proposed that selenium dietary supplementation may provide cytoprotection against neurodegenerative and cardiovascular disorders through the maintenance of Gpx-1 activity and other detoxifying seleno-enzymes such as thioredoxin reductase and selenoprotein (Steinbrenner and Sies, 2009).

Background information of Gpx-1^{-/-} mouse



Adapted from Crack et al., (2001) Increased infarct size and exacerbated apoptosis in the glutathione peroxidase-1 (Gpx-1) knockout mouse brain in response to ischemia/reperfusion injury. *J Neurochem.* 78:1389-1399.



Adapted from Crack et al., (2001) Increased infarct size and exacerbated apoptosis in the glutathione peroxidase-1 (Gpx-1) knockout mouse brain in response to ischemia/reperfusion injury. *J Neurochem.* 78:1389-1399.

5.2.2 Results

In order to further in-depth highlight the role of augmented free radical species generation in infliction of oxidative cellular damage during cerebral ischemia and assign importance of functional anti-oxidant enzymes and proteins, a global gene profiling analysis was performed on Gpx-1^{-/-} transgenic male C57/Bl6 mice with identical ischemic/reperfusion surgical procedures.

5.2.2.1 Gpx-1^{-/-} mice displayed a distinct cortical global gene profile when compared to that of WT at physiological basal state

Previous study by Crack et al. (2001) has reported a deletion of Gpx-1 expression increased the vulnerability to cerebral ischemia-reperfusion injury as a result of significant reduction in post-ischemic microvascular perfusion. A significantly greater infarct was observed in the Gpx-1^{-/-} (area in mm²) when compared with the WT mice (Crack et al., 2001). This highlights the essentiality of Gpx-1, as an anti-oxidant enzyme, in the alleviation of the increased oxidative stress resulting from accelerated reactive oxygen species (ROS) production which imposed detrimental cellular effects such as microvascular and tissue damages in the post-ischemic brains (Crack et al., 2001; Gursoy-Ozdemir et al., 2004; Weisbrot-Lefkowitz et al., 1998). As such, it can be inferred that Gpx-1 plays a major role in the protection of the mammalian brain against cerebral I/R injury.

It has been shown previously that there exist no cerebral vasculature abnormalities in Gpx-1^{-/-} transgenic mouse brain which might predispose these mice to increased

Chapter 5.2: Gpx-1^{-/-}-transient MCAO

susceptibility to focal cerebral ischemia (Crack et al., 2001). Also, it has been verified there is no obvious difference in ROS generation between uninjured WT and Gpx-1^{-/-} mice (Crack et al., 2001). As such, the other objective of the present study is to decipher the impact on tMCAO induction on the temporal activation/inhibition of the cellular signaling pathways upon deletion of Gpx-1 functional expression. Identical TMCAO surgical experimental technique, cortical tissue collection and microarray analysis were imposed on the Gpx-1^{-/-} transgenic mice.

In order to ensure valid, unbiased transcriptomic profiling comparison between WT and Gpx-1^{-/-} upon I/R injury, it is crucial to ascertain the global gene expression at the basal physiological state between both mouse types. Upon bioinformatics and statistical analyses, the present author discovered a total of 662 gene probes which demonstrated significant gene expression of at least ± 1.5 fold change in at least one out of three time-points in Gpx-1^{-/-} condition when normalized against that of the WT.

-RESPONSE TO OXIDATIVE STRESS

Genes encoding for proteins involved in the alleviation of cellular oxidative and/or electrophilic stresses (Prdx5, Txnrd2, Mt3, Hsp90b1 and Dnajc2) demonstrated heightened transcriptional elevation in Gpx-1^{-/-} mice cortex (Table 5.3). Hsps and chaperones play a pivotal role in conferring cytoprotection through the delicate control of aberrant and misfolded protein accumulation through promotion of correct formation and maintenance of native conformation of cytosolic proteins and stabilization of actin filaments and in some cases, in the negative regulation of programmed cell death progression (Meriin and Sherman, 2005). Peroxiredoxins (Prdxs), though indirectly

involved in the anti-oxidative response through sequestration of peroxides, play an important part in cellular redox state regulation (Egler et al., 2005; Wang et al., 2003). Oxidized peroxiredoxins are then subsequently reduced via the action of the thioredoxin reductase family (Txnr). Electrophilic stress which usually concurrently with oxidative stress is counteracted by metallothioneins (Mt) which bind to heavy metal ions. Mt3 with a unique localisation pattern in the brain has been involved in tissue repair and protection under neuronal injuries (Ono et al., 2007).

- CELL HOMEOSTASIS, SURVIVAL AND PROLIFERATION

Mitogenic cellular signal transduction pathways such as MAPK/ERK and Wnt signaling cascades, which promote cellular growth and survival demonstrated transcriptional activation through the observed elevation in gene expression of majority of its pathway members (Table 5.3). The Wnt pathway plays an important role in the developmental growth of organisms through association of the Wnt protein with β -catenin (Ctnnb1) and upon Wnt ligand stimulation (Wnt5a) leading to subsequent transcriptional activation of pro-proliferative Wnt-regulated genes (Axin2, Celsr2, Tle1 and Wnt5a) (Table 5.3). Wnt-associated pathway players demonstrated significant up-regulation in gene expression in Gpx-1^{-/-} mouse cortice. Similarly, majority of genes encoding for proteins involved in MAPK/ERK pathway showed transcriptional activation.

- CELL DEATH

Multiple cell death signaling transduction cascades are present within the mammalian cells which can be triggered via intrinsic and/or extrinsic stimuli. As demonstrated from

the global transcriptomic profile of Gpx-1^{-/-} mouse cortex, genes involved in promotion of cell death demonstrated down-regulation, while those involved in its suppression showed opposing elevated expression (Table 5.3).

- CELLULAR PROTEIN CATABOLISM VIA UBIQUITIN-PROTEASOME SYSTEM

The mammalian ubiquitin-proteasome system (UPS) is a coordinated multiple-step degradation pathway of misfolded and unfolded proteins, primarily involves mainly the molecularly marking with proteins and/or polypeptides with poly-ubiquitins for targeted degradation in the proteasome (Schroder and Kaufman, 2005; Sherman and Goldberg, 2001). The genes encoding ubiquitins and proteasome subunits were highly up-regulated in Gpx-1^{-/-} mouse cortex under basal condition (Table 5.3). These genes include those encoding for the proteasome subunits (Psm4, Psm1, Psm6, Psm3), ubiquitin carboxyl-terminal esterases (Uch13 and Ubch15), ubiquitin-conjugating enzyme E2 (Ube2a and Ube2g1) and ubiquitin-specific proteases (Usp14).

- CELL CYCLE CHECKPOINT RESPONSE

Cellular DNA is susceptible to damages upon induction of various stress stimuli such as UV irradiation, heat shock insult and oxidative and/or electrophilic stress. In the event of genotoxic injury, initial phase of p53 response is triggered to guard the genome integrity by initiation of the DNA repair machinery. p53 activation is evident from the transcriptional up-regulation of to the p53-inducible cell survival factor Traip1 (Table 5.3: Cell death). Various cell cycle checkpoints are in place to detect and repair DNA

damages such as single/double strand breaks. In the Gpx-1^{-/-} mouse cortex, the genes encoding for these proteins (Rad17, Rad23b, Obfc2b and Smc1a) demonstrated increase in gene expression (Table 5.3).

- MITOTIC CELL CYCLE

Cell cycle re-activation has been identified as a central component of genotoxic injury response of post-mitotic neurons which eventually lead to neuronal death instead of survival (Kruman et al., 2004). With the increase in vulnerability of the cellular DNA to genotoxic damages upon oxidative and/or electrophilic stresses in Gpx-1^{-/-} mouse, global transcriptomic profiling revealed a significant increase in mRNA expression of cell cycle progression promoting proteins which comprise of Nek9, Mapk6, Ccnd2, Mapre2, Mcm6 and Sep(3,5,9) (Table 5.3). However, this aberrant cell cycle re-entry is kept in check and impeded by the transcriptional activation of cell cycle point proteins mentioned previously.

- MITOCHONDRIAL RESPIRATORY CHAIN

Imbalance of mitochondrial dynamics has been suggested to play a major role in the physio-pathogenesis of neurological disorders where oxidative stress is consistently noted. Oxidative phosphorylation is primarily dependent on the proper coordinated functioning of a series of electron carriers (ubiquinone, flavoproteins, iron-sulfur proteins and cytochromes) that are spatially organized on the basis of their redox potentials into four complexes, creating a rich potential energy pool through a proton electrochemical gradient which is harnessed by the fifth complex (ATP synthase) (Darley-Usmar et al.,

1994). As demonstrated in Gpx-1^{-/-} profile, several main players of the mitochondrial electron transport chain, namely complexes I (Ndufb9 and Ndufs4), and IV (Cox6c), demonstrated significant up-regulation (Table 5.3).

- DEFENSE AND INFLAMMATORY RESPONSE

Transcriptomic profiling revealed a transcriptional activation of majority of the proteins [Chst2, Ccl(17, 21a, 21b and 21c), Mlf2 and H47] involved in immune response through cytokine and/or chemokine production, participation in lymphocyte homing, transendothelial migration and adhesion and subsequently activation of the inflammatory cascade (Table 5.3).

Chapter 5.2:
Gpx-1^{-/-}-transient MCAO

Table 5.3 Selected biological process-associated genes that were differentially expressed in Gpx-1^{-/-} mouse cortex when normalized against that of the WT strain at physiological basal condition. All fold-change expressions were subjected to one-way ANOVA analysis and Benjamini-Hochberg FDR correction, and were significant at $p < 0.05$. Data are expressed as fold-change \pm sem.

Genbank	Gene Title	Symbol	Gpx-1 ^{-/-}
<u>Response to oxidative stress</u>			
NM_012021	Peroxiredoxin 5	Prdx5	1.61 \pm 0.08
NM_013711	Thioredoxin reductase 2	Txnrd2	-1.54 \pm 0.07
NM_013603	Metallothionein 3	Mt3	2.03 \pm 0.20
NM_011631	Heat shock protein 90kDa beta (Grp94), member 1	Hsp90b1	1.56 \pm 0.14
NM_009584	DnaJ (Hsp40) homolog, subfamily C, member 2	Dnajc2	1.50 \pm 0.14
NM_030206	Cytoglobin	Cygb	-1.52 \pm 0.07
<u>Cell homeostasis, survival and proliferation</u>			
<u>-MAPK/ERK signaling cascade</u>			
NM_008306	N-deacetylase/N-sulfotransferase (heparan glucosaminy) 1	Ndst1	1.50 \pm 0.19
NM_001008533	Adenosine A1 receptor	Adora1	1.64 \pm 0.15
NM_011162	Mitogen-activated protein kinase 8 interacting protein 1	Mapk8ip1	-1.85 \pm 0.09
NM_021921	Mitogen-activated protein kinase 8 interacting protein 2	Mapk8ip2	-1.51 \pm 0.07
NM_010897	Neurofibromatosis 1	Nf1	1.70 \pm 0.16
NM_013612	Solute carrier family 11 (proton-coupled divalent metal ion transporters), member 1	Slc11a1	-1.69 \pm 0.19
NM_013881	Unc-51 like kinase 2 (C. elegans)	Ulk2	1.53 \pm 0.07
NM_010216	c-fos induced growth factor	Figf	1.61 \pm 0.10
NM_009506	Vascular endothelial growth factor C	Vegfc	1.74 \pm 0.07
<u>-Wnt receptor signaling pathway</u>			
NM_172815	R-spondin 2 homolog (Xenopus laevis)	Rspo2	1.60 \pm 0.23
NM_015732	Axin2	Axin2	1.65 \pm 0.11
NM_017392	Cadherin, EGF LAG seven-pass G-type receptor 2 (flamingo homolog, Drosophila)	Celsr2	1.85 \pm 0.18
NM_026192	Calcium binding and coiled coil domain 1	Calcoc1	1.49 \pm 0.22
NM_009974	Casein kinase 2, alpha prime polypeptide;	Csnk2a2	-1.75 \pm 0.07
NM_007614	Catenin (cadherin associated protein), beta 1	Ctnnb1	1.74 \pm 0.14
NM_011599	Transducin-like enhancer of split 1, homolog of Drosophila E(spl)	Tle1	1.60 \pm 0.14
NM_009524	Wingless-related MMTV integration site 5A	Wnt5a	1.95 \pm 0.25
NM_009528	Wingless-related MMTV integration site 7B	Wnt7b	-1.59 \pm 0.12
<u>Cell death</u>			
NM_026933	TP53 regulated inhibitor of apoptosis 1	Triap1	1.61 \pm 0.09
NM_007537	BCL2-like 2	Bcl2l2	1.78 \pm 0.14
NM_134131	Tumor necrosis factor, alpha-induced protein 8	Tnfaip8	1.50 \pm 0.24
NM_011632	TNF receptor-associated factor 3	Traf3	1.69 \pm 0.16
NM_025816	Tax1 (human T-cell leukemia virus type I) binding protein 1	Tax1bp1	1.82 \pm 0.12
NM_013556	Hypoxanthine guanine phosphoribosyl transferase 1	Hprt1	1.58 \pm 0.20
NM_008410	Integral membrane protein 2B	Itm2b	1.59 \pm 0.13

Table 5.3 (continue)

Genbank	Gene Title	Symbol	Gpx-1 ^{-/-}
<u>Cell death (continue)</u>			
NM_009402	Peptidoglycan recognition protein 1	Pglyrp1	2.32 ± 0.60
NM_009344	Pleckstrin homology-like domain, family A, member 1	Phlda1	2.06 ± 0.53
NM_011221	Purine rich element binding protein B	Purb	2.33 ± 0.52
NM_007483	Ras homolog gene family, member B	Rhob	1.71 ± 0.09
NM_019812	Sirtuin 1 (silent mating type information regulation 2, homolog) 1 (<i>S. cerevisiae</i>)	Sirt1	1.54 ± 0.23
NM_009472	Unc-5 homolog C (<i>C. elegans</i>)	Unc5c	1.52 ± 0.18
NM_009517	Zinc finger matrin type 3	Zmat3	2.00 ± 0.18
NM_029083	DNA-damage-inducible transcript 4	Ddit4	-1.60 ± 0.13
NM_001013829	Src homology 2 domain containing F	Shf	-1.75 ± 0.08
NM_019567	Apoptotic chromatin condensation inducer 1	Acin1	-2.19 ± 0.10
NM_133882	Complement component 8, beta polypeptide	C8b	-1.66 ± 0.10
NM_011817	Growth arrest and DNA-damage-inducible 45 gamma	Gadd45g	-1.64 ± 0.10
NM_011073	Perforin 1 (pore forming protein)	Prf1	-2.18 ± 0.15
NM_176833	Protein phosphatase 1F (PP2C domain containing)	Ppm1f	-1.60 ± 0.07
NM_011361	Serum/glucocorticoid regulated kinase 1	Sgk	-1.55 ± 0.13
<u>Cellular protein catabolism via ubiquitin-proteasome system</u>			
NM_016877	CCR4-NOT transcription complex, subunit 4	Cnot4	1.72 ± 0.28
NM_172637	HECT domain containing 2	Hectd2	1.59 ± 0.11
NM_025745	Mus musculus endoplasmic reticulum lectin 1 (Erlec1)	Erlec1	1.81 ± 0.17
NM_026402	Autophagy-related 3 (yeast)	Atg3	1.59 ± 0.18
NM_144859	Praja 2, RING-H2 motif containing	Pja2	1.53 ± 0.23
NM_011931	Predicted gene 6206; ring finger and WD repeat domain 2	Rfwd2	1.76 ± 0.30
NM_027314	Predicted gene 7684; membrane-associated ring finger (C3HC4) 5	Rnf153	1.69 ± 0.08
NM_011966	Proteasome (prosome, macropain) subunit, alpha type 4; predicted gene 6542	Psma4	1.50 ± 0.11
NM_027357	Proteasome (prosome, macropain) 26S subunit, non-ATPase, 1	Psmc1	1.53 ± 0.29
NM_025550	Proteasome (prosome, macropain) 26S subunit, non-ATPase, 6	Psmc6	1.63 ± 0.17
NM_011192	Proteasome (prosome, macropain) 28 subunit, 3	Psme3	1.93 ± 0.28
NM_016723	Ubiquitin carboxyl-terminal esterase L3 (ubiquitin thiolesterase)	Uchl3	1.87 ± 0.18
NM_019562	Ubiquitin carboxyl-terminal esterase L5	Uchl5	2.27 ± 0.18
NM_021522	Ubiquitin specific peptidase 14	Usp14	1.59 ± 0.10
NM_021323	Ubiquitin specific peptidase 29	Usp29	-1.63 ± 0.07
NM_019668	Ubiquitin-conjugating enzyme E2A, RAD6 homolog (<i>S. cerevisiae</i>)	Ube2a	1.86 ± 0.07
NM_025985	Ubiquitin-conjugating enzyme E2G 1 (UBC7 homolog, <i>C. elegans</i>)	Ube2g1	1.50 ± 0.10
<u>Cell cycle checkpoint response to DNA damage stimuli</u>			
NM_001044371	RAD17 homolog (<i>S. pombe</i>)	Rad17	1.52 ± 0.20
NM_009009	RAD21 homolog (<i>S. pombe</i>)	Rad21	-1.54 ± 0.04

Table 5.3 (continue)

Genbank	Gene Title	Symbol	Gpx-1 ^{-/-}
<u>Cell cycle checkpoint response to DNA damage stimuli (continue)</u>			
NM_009011	RAD23b homolog (<i>S. cerevisiae</i>)	Rad23b	1.63 ± 0.29
NM_026933	TP53 regulated inhibitor of apoptosis 1	Triap1	1.61 ± 0.09
NM_027355	Ring finger protein 168	Rnf168	1.53 ± 0.06
NM_027257	Oligonucleotide/oligosaccharide-binding fold containing 2B	Obfc2b	1.66 ± 0.13
NM_019710	Structural maintenance of chromosomes 1A	Smc1a	1.80 ± 0.06
NM_025372	Timeless interacting protein	Tipin	1.51 ± 0.09
NM_025613	EP300 interacting inhibitor of differentiation 1	Eid1	2.00 ± 0.18
NM_009517	Zinc finger matrin type 3	Zmat3	2.00 ± 0.18
<u>Cell cycle</u>			
NM_145138	NIMA (never in mitosis gene a)-related expressed kinase 9	Nek9	1.56 ± 0.15
NM_027418	Mitogen-activated protein kinase 6	Mapk6	1.71 ± 0.23
NM_009829	Cyclin D2	Ccnd2	1.61 ± 0.25
NM_009831	Cyclin G1	Ccng1	1.52 ± 0.22
NM_009833	Cyclin T1	Ccnt1	1.55 ± 0.12
NM_153058	Microtubule-associated protein, RP/EB family, member 2	Mapre2	1.58 ± 0.09
NM_008567	Minichromosome maintenance deficient 6 (MIS5 homolog, <i>S. pombe</i>) (<i>S. cerevisiae</i>)	Mcm6	1.60 ± 0.19
NM_011889	Septin 3	Sep3	1.50 ± 0.18
NM_213614	Septin 5	Sep5	1.74 ± 0.18
NM_017380	Septin 9	Sep9	1.52 ± 0.15
NM_021884	Tumor susceptibility gene 101	Tsg101	1.58 ± 0.06
<u>Mitochondrial respiratory chain</u>			
NM_016920	ATPase, H ⁺ transporting, lysosomal V0 subunit A1	Atp6v0a1	1.52 ± 0.27
NM_009729	ATPase, H ⁺ transporting, lysosomal V0 subunit C, pseudogene 2; ATPase, H ⁺ transporting, lysosomal V0 subunit C	Atp6v0c	-1.73 ± 0.10
NM_023172	NADH dehydrogenase (ubiquinone) 1 beta subcomplex, 9	Ndufb9	1.77 ± 0.41
NM_010887	NADH dehydrogenase (ubiquinone) Fe-S protein 4	Ndufs4	1.53 ± 0.10
NM_053071	Cytochrome c oxidase, subunit VIc	Cox6c	1.81 ± 0.12
NM_146141	Pyrophosphatase (inorganic) 2	Ppa2	1.75 ± 0.15
<u>Defense and inflammatory response</u>			
NM_008306	N-deacetylase/N-sulfotransferase (heparan glucosaminyl) 1	Ndst1	1.50 ± 0.19
NM_018763	Carbohydrate sulfotransferase 2	Chst2	1.76 ± 0.43
NM_011332	Chemokine (C-C motif) ligand 17	Ccl17	1.60 ± 0.27
NM_011335	Chemokine (C-C motif) ligand 21a	Ccl21a	4.43 ± 0.31
NM_011124	Chemokine (C-C motif) ligand 21b	Ccl21b	6.70 ± 0.28
NM_023052	Chemokine (C-C motif) ligand 21c (leucine)	Ccl21c	5.52 ± 0.51
NM_145385	Myeloid leukemia factor 2	Mlf2	1.60 ± 0.08
NM_024439	Histocompatibility 47	H47	1.64 ± 0.06
NM_010895	Neurogenic differentiation 2	Neurod2	1.55 ± 0.12
NM_009402	Peptidoglycan recognition protein 1	Pglyrp1	2.32 ± 0.60

Table 5.3 (continue)

Genbank	Gene Title	Symbol	Gpx-1^{-/-}
<u>Defense and inflammatory response (continue)</u>			
NM_009780	Complement component 4B (Chido blood group)	C4b	-1.55 ± 0.08
NM_133882	Complement component 8, beta polypeptide	C8b	-1.66 ± 0.10
NM_011486	Signal transducer and activator of transcription 3	Stat3	-1.57 ± 0.06

5.2.2.2 Gpx-1^{-/-} mice induced a substantially larger global gene profile as compared to WT mice upon tMCAO induction

Interestingly, Gpx-1^{-/-} mice demonstrated a promisingly larger group of gene probes (1,456) significantly modulated, but majority being down-regulated. Shown in Figure 5.2, a comparative graphical representation of the number of genes partitioned and clustered accordingly to their time-specific transcriptional expression. It could be generally inferred that deletion of Gpx-1 induced substantially more transcriptional down-regulation of genes upon tMCAO induction. The larger global transcriptomic profile from the Gpx-1^{-/-} mice upon tMCAO induction could be accounted by the heightened cellular response to elevated predisposition to cerebral injury following a localized ischemic event, attributed by atypical responses within the microvasculature, including inflammation, diminished endothelial barrier function (increased vascular permeability), endothelial activation, and reduced microvascular perfusion (Wong et al., 2008).

A comparative examination of the gene probes common to both mouse types demonstrated a reasonably high level of overlap (422 probe sets), which accounted for over 70% and 28% of the WT and Gpx-1^{-/-} global gene profiles respectively (Figure 5.3A). Within this subset of 422 common probe sets, more than 75% demonstrated identical regulatory trend over the time-course of 2h, 8h and 24h with majority showing further up/down-regulatory fold-changes in gene expression in Gpx-1^{-/-} condition (Figure 5.3B). Sequential time-point comparisons of the common up- and down-regulated genes respectively did not reveal significant difference in level of gene expression (fold-change) between mouse types upon tMCAO induction, as shown in Figure 5.4. This is

Chapter 5.2: Gpx-1^{-/-}-transient MCAO

further confirmed by the in-depth analysis of the regulatory trend of genes common to both tMCAO-induced mouse models as demonstrated in Table 5.4. Genes classified under the respective biological processes did not show marked difference in transcriptional fold-changes between WT and Gpx-1^{-/-} mice upon tMCAO treatment, implying that the deletion of Gpx-1^{-/-} did not affect the regulation of the originally activated/inhibited cellular signaling cascades seen in the WT mice. Interestingly, deletion of Gpx-1^{-/-} induced differential gene expression regulation of substantially additional more genes, implying the modulation of supplementary pathways affected by the absence of Gpx-1 expression and activity. As such, the author proceeded to focus on the remaining 1,034 genes exclusive to Gpx-1^{-/-}-tMCAO global transcriptome (Table 5.5).

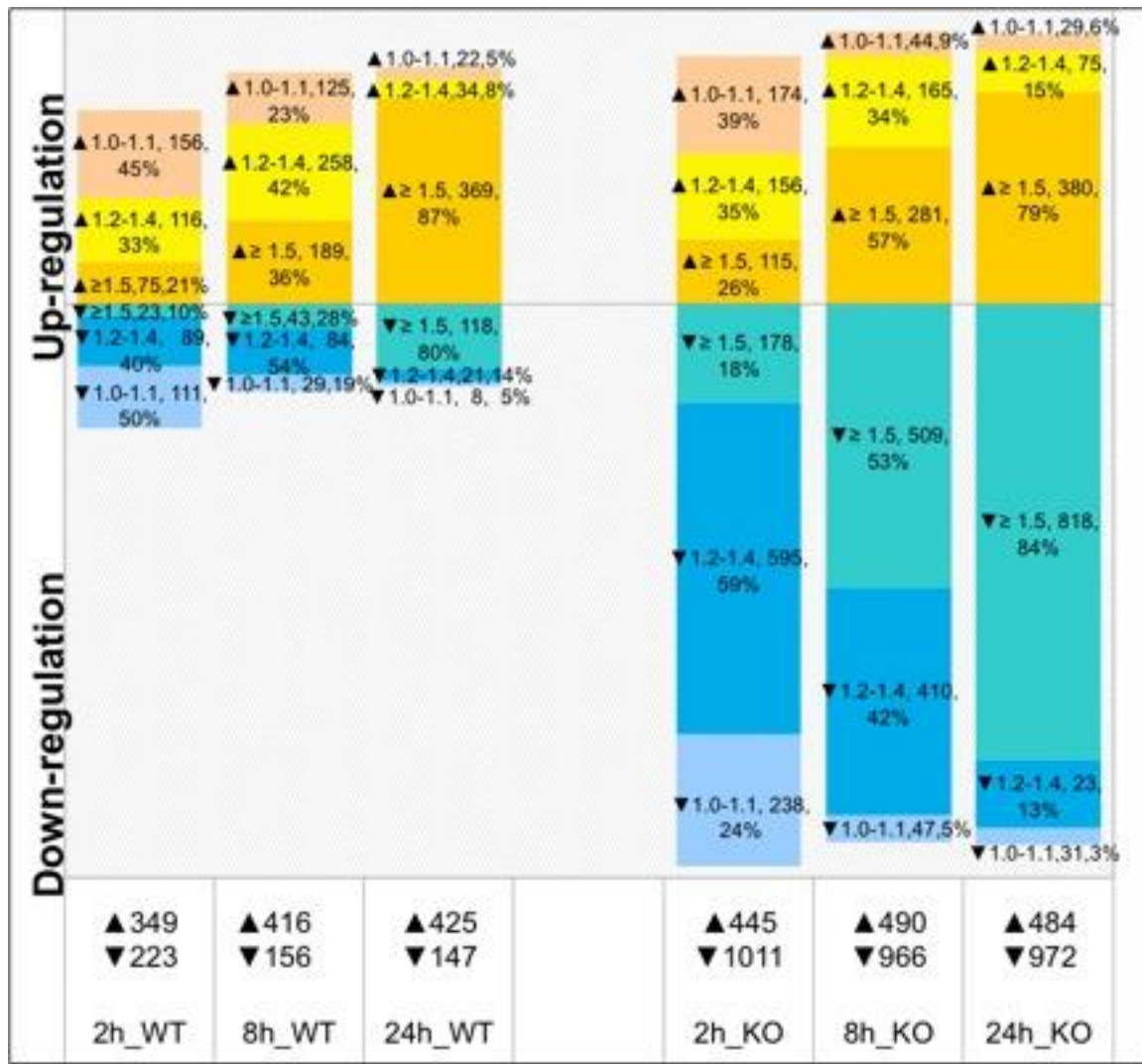
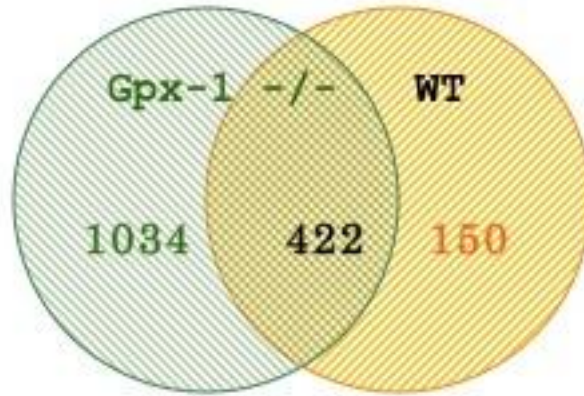


Figure 5.2 Time-course profiling revealed a significant increase in number of up/down-regulated genes with transcriptional expression with a minimum of ± 1.5 -fold change from 8h to 24h timeframe. Only genes with transcriptional fold-change of at least ± 1.5 in at least one out of three time-points and had passed stringent statistical analyses were included into WT (572 gene probes) and Gpx-1^{-/-} (1,456 gene probes) -tMCAO global gene profiles. Genes were then segregated into fold-change categories at respective time-points. The excess differentially expressed genes in Gpx-1^{-/-} -tMCAO profile were accounted in the transcriptionally down-regulated category.

A



B

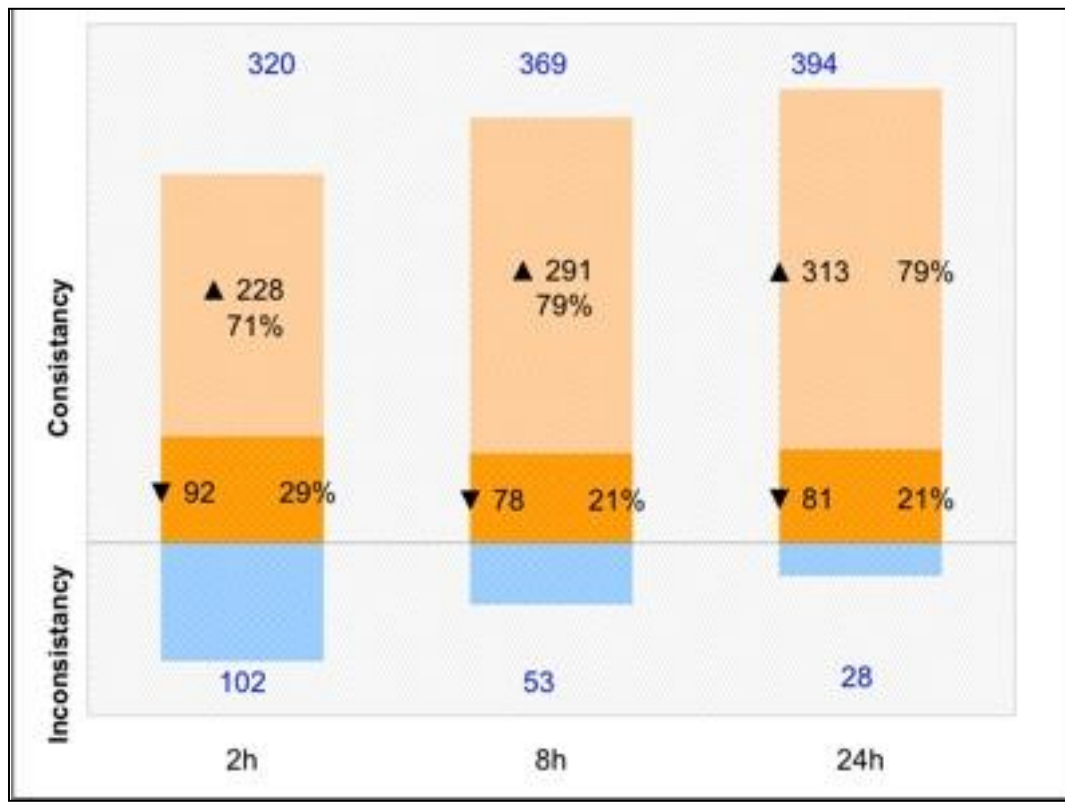


Figure 5.3 (A) Venn diagram illustrated 422 DAVIDS-recognizable genes with significant regulation of at least ± 1.5 fold-change in a minimum of one out of three time-points were common to WT- and Gpx-1^{-/-}-tMCAO global gene profiles. (B) Stacked bar-chart depicted a high degree of consistency in regulatory trend of genes (at least ± 1.5 fold-change in at least one out of three time-points in individual treatment) common to both WT- and Gpx-1^{-/-}-tMCAO global gene profiles.

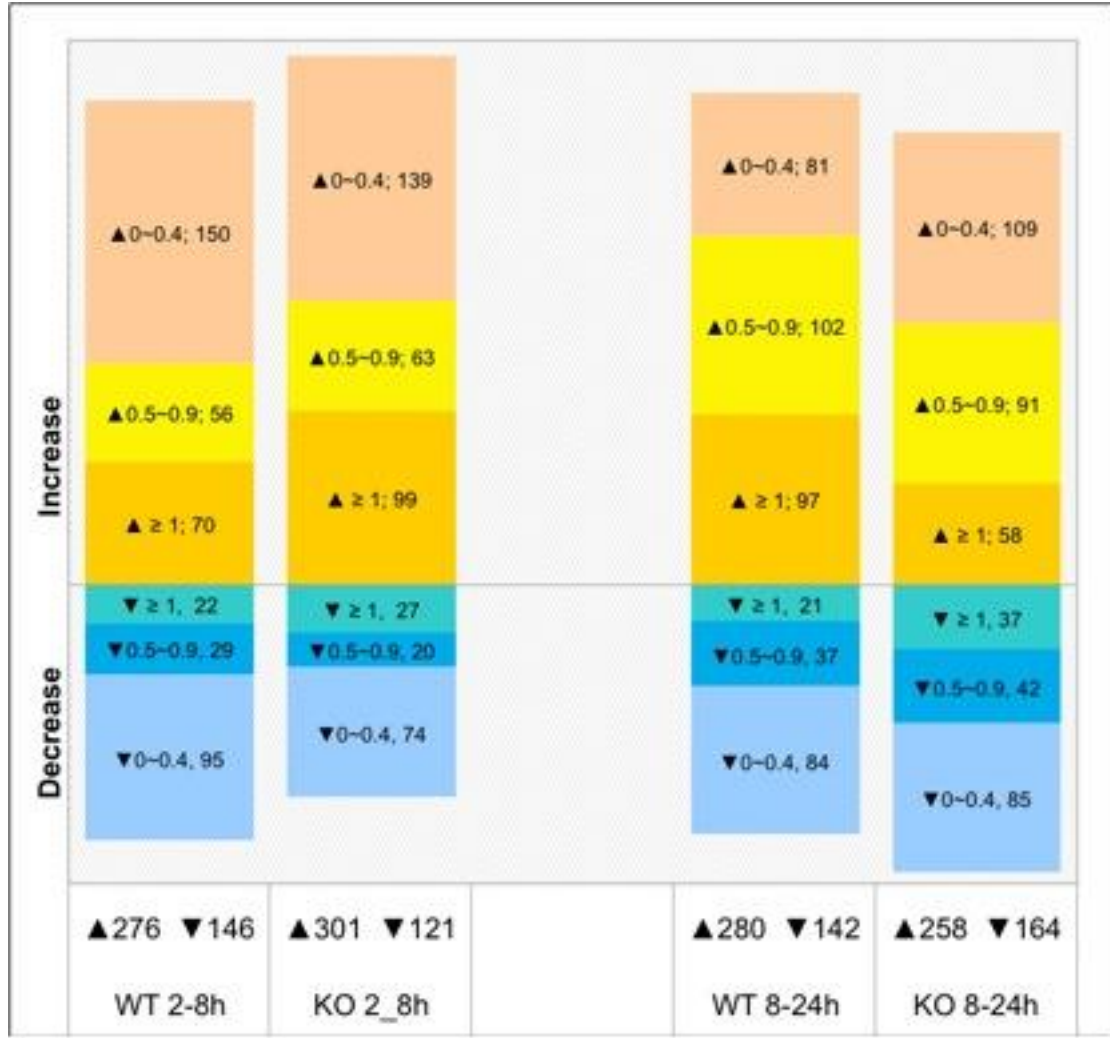


Figure 5.4 Sequential time-point comparisons (2-8h and 8-24h) of the 422 common up- and down-regulated genes did not reveal significant difference in gene expression increment/decrement (fold-change) between WT and Gpx-1^{-/-} mouse strains upon tMCAO induction. Sequential time-point fold-change variation was assigned to various fold-change categories and summarized on a plotted chart. Genes with fold-difference <0.1 between time-points were omitted from the count.

Chapter 5.2:
Gpx-1^{-/-}-transient MCAO

Table 5.4 Gene expression profiles of neuronal death-related families in genes common to the infarct cortice of WT and Gpx-1^{-/-}-tMCAO models. All fold-change expressions are subjected to one-way ANOVA analysis and Benjamini-Hochberg FDR correction, and significant at $p < 0.05$. Data are expressed as fold-change \pm sem.

Genbank	Gene Title	Symbol	Time-points					
			WT-tMCAO			Gpx-1 ^{-/-} -tMCAO		
			2h	8h	24h	2h	8h	24h
<u>Calcium ion binding and homeostasis</u>								
NM_008597	Matrix glia protein	Mgp	-1.10 \pm 0.06	1.20 \pm 0.23	1.77 \pm 0.31	-1.55 \pm 0.14	-1.04 \pm 0.10	1.04 \pm 0.16
NM_011313	S100 calcium binding protein A6 (calyculin)	S100a6	1.13 \pm 0.14	1.37 \pm 0.16	2.27 \pm 0.96	-1.02 \pm 0.17	1.41 \pm 0.17	3.35 \pm 2.37
NM_009114	S100 calcium binding protein a9 (calgranulin b)	S100a9	1.73 \pm 0.41	1.86 \pm 0.59	8.05 \pm 36.86	2.56 \pm 1.36	1.82 \pm 1.02	4.42 \pm 16.41
NM_007585	Annexin A2	Anxa2	1.25 \pm 0.22	1.94 \pm 0.25	3.22 \pm 2.57	1.33 \pm 0.29	2.29 \pm 1.41	3.35 \pm 2.37
NM_011607	Tenascin C	Tnc	1.17 \pm 0.12	1.16 \pm 0.08	2.12 \pm 1.58	1.17 \pm 0.10	1.20 \pm 0.35	1.87 \pm 0.91
<u>Cell death</u>								
NM_030612	Nuclear factor of kappa light polypeptide gene enhancer in B-cells inhibitor, zeta	Nfkbiz	2.22 \pm 1.08	1.84 \pm 0.51	1.57 \pm 0.54	1.73 \pm 0.05	1.93 \pm 0.16	1.40 \pm 0.62
NM_007837	DNA-damage inducible transcript 3 (Ddit3)	Ddit3	1.36 \pm 0.17	1.52 \pm 0.31	1.43 \pm 0.55	1.53 \pm 0.17	2.00 \pm 0.77	1.53 \pm 0.34
NM_009883	CCAAT/enhancer binding protein (C/EBP) beta (Cebpb)	Cebpb	1.60 \pm 0.39	1.95 \pm 0.31	1.87 \pm 1.10	1.72 \pm 0.24	1.88 \pm 0.77	1.41 \pm 0.95
NM_028283	Uveal autoantigen with coiled-coil domains and ankyrin repeats	Uaca	1.21 \pm 0.20	1.08 \pm 0.09	1.90 \pm 0.57	1.07 \pm 0.07	1.27 \pm 0.17	1.65 \pm 0.55
NM_007498	Activating transcription 3	Atf3	4.06 \pm 3.68	3.22 \pm 2.64	3.00 \pm 3.68	3.09 \pm 1.03	4.04 \pm 5.10	2.29 \pm 1.57
NM_007836	Growth arrest and dna-damage-inducible 45 alpha	Gadd45a	1.39 \pm 0.25	1.34 \pm 0.18	1.54 \pm 0.76	1.28 \pm 0.07	1.64 \pm 0.73	1.54 \pm 0.48
NM_008655	Growth arrest and dna-damage-inducible 45 beta	Gadd45b	2.72 \pm 0.97	2.09 \pm 1.19	2.20 \pm 1.96	2.50 \pm 0.28	2.67 \pm 1.82	1.71 \pm 1.02
NM_011817	Growth arrest and dna-damage-inducible 45 gamma	Gadd45g	2.36 \pm 1.79	1.55 \pm 0.79	1.55 \pm 1.41	3.02 \pm 1.83	2.95 \pm 2.10	1.90 \pm 1.32
NM_007669	Cyclin-dependent kinase inhibitor 1a (p21)	Cdkn1a	1.84 \pm 0.14	2.68 \pm 0.82	1.66 \pm 1.18	1.80 \pm 0.05	2.92 \pm 0.66	1.62 \pm 0.92

Chapter 5.2:
Gpx-1^{-/-}-transient MCAO

Table 5.4 (continue)

Genbank	Gene Title	Symbol	Time-points					
			WT-tMCAO			Gpx-1 ^{-/-} -tMCAO		
			2h	8h	24h	2h	8h	24h
<u>Cell death (continue)</u>								
NM_009982	Cathepsin C (Ctsc)	Ctsc	-1.17 ± 0.10	1.14 ± 0.15	2.27 ± 0.83	-1.25 ± 0.07	-1.05 ± 0.29	1.91 ± 0.61
NM_022325	Cathepsin Z (Ctsz)	Ctsz	1.27 ± 0.14	1.32 ± 0.18	1.91 ± 0.66	1.21 ± 0.14	1.29 ± 0.22	1.59 ± 0.42
<u>Cell homeostasis, survival and proliferation</u>								
NM_153553	Neuronal PAS domain protein 4	Npas4	6.39 ± 12.48	1.74 ± 0.92	1.38 ± 0.26	3.31 ± 8.58	1.26 ± 1.06	-1.24 ± 0.46
NM_020581	Angiopoietin-like 4	Angptl4	1.18 ± 0.11	1.76 ± 0.20	1.50 ± 0.47	2.03 ± 0.30	3.95 ± 0.76	2.72 ± 1.23
NM_008343	Insulin-like growth factor binding protein 3	Igfbp3	1.01 ± 0.06	1.54 ± 0.28	2.77 ± 2.62	-1.17 ± 0.09	1.27 ± 0.19	2.14 ± 1.60
NM_016693	Mitogen-activated protein kinase kinase kinase 6	Map3k6	1.39 ± 0.15	1.99 ± 0.20	1.48 ± 0.40	1.30 ± 0.10	1.66 ± 0.34	1.47 ± 0.61
NM_011368	Src homology 2 domain-containing transforming protein c1	Shc1	1.01 ± 0.11	1.52 ± 0.14	1.54 ± 0.55	-1.05 ± 0.11	1.51 ± 0.21	1.59 ± 0.44
NM_010851	Myeloid differentiation primary response gene 88	Myd88	-1.02 ± 0.06	1.31 ± 0.26	1.83 ± 0.99	1.29 ± 0.19	1.84 ± 0.41	2.42 ± 1.19
NM_010234	Fbj osteosarcoma oncogene	Fos	4.37 ± 4.85	1.64 ± 1.19	1.36 ± 1.29	3.24 ± 2.03	1.41 ± 1.38	1.07 ± 0.48
NM_010591	Jun oncogene	Jun	1.54 ± 0.80	1.22 ± 0.20	1.04 ± 0.24	1.73 ± 0.16	1.94 ± 0.61	1.48 ± 0.42
NM_009263	Secreted phosphoprotein 1	Spp1	1.15 ± 0.23	2.07 ± 0.51	6.98 ± 12.94	-1.26 ± 0.17	1.80 ± 1.22	4.73 ± 6.48
NM_013614	Ornithine decarboxylase, structural 1	Odc1	1.34 ± 0.26	1.43 ± 0.22	1.70 ± 0.86	1.12 ± 0.09	1.43 ± 0.45	1.66 ± 0.83
NM_009929	Procollagen, type xviii, alpha 1	Col18a1	-1.01 ± 0.11	-1.06 ± 0.13	1.56 ± 0.53	1.02 ± 0.08	1.22 ± 0.17	1.53 ± 0.55
NM_011451	Sphingosine kinase 1	Sphk1	1.16 ± 0.13	2.03 ± 0.67	1.89 ± 1.19	-1.05 ± 0.12	2.12 ± 1.21	1.75 ± 1.54
NM_027253	Ras interacting protein 1	Rasip1	1.02 ± 0.09	1.21 ± 0.23	1.57 ± 0.61	1.33 ± 0.04	1.76 ± 0.53	1.34 ± 0.59

Chapter 5.2:
Gpx-1^{-/-}-transient MCAO

Table 5.4 (continue)

Genbank	Gene Title	Symbol	Time-points					
			WT-tMCAO			Gpx-1 ^{-/-} -tMCAO		
			2h	8h	24h	2h	8h	24h
<u>Cell homeostasis, survival and proliferation (continue)</u>								
NM_010415	Heparin-binding egf-like growth factor	Hbegf	1.27 ± 0.19	1.30 ± 0.22	1.70 ± 0.71	1.17 ± 0.04	1.53 ± 0.63	1.61 ± 0.80
<u>Response to oxidative stress</u>								
NM_013863	Bcl2-associated athanogene 3 (Bag3)	Bag3	1.63 ± 0.56	1.67 ± 0.73	1.57 ± 0.57	1.55 ± 0.08	2.11 ± 1.43	1.47 ± 0.69
NM_013560	Heat shock protein 1	Hspb1	1.70 ± 1.27	2.14 ± 1.40	3.07 ± 3.82	2.10 ± 0.50	3.75 ± 3.11	3.61 ± 4.78
NM_001012401	Heat shock protein, alpha-crystallin-related, b6	Hspb6	1.30 ± 0.15	1.74 ± 0.17	2.85 ± 0.94	1.01 ± 0.12	1.57 ± 0.36	2.49 ± 0.91
NM_009825	Serine (or cysteine) proteinase inhibitor clade H member 1 (Serpinh1)	Serpinh1	-1.01 ± 0.10	3.82 ± 0.61	6.93 ± 7.71	1.04 ± 0.25	2.79 ± 1.44	7.36 ± 6.77
NM_018808	DnaJ (Hsp40) homolog, subfamily B, member 1	Dnajb1	1.53 ± 0.89	1.21 ± 0.26	-1.19 ± 0.07	1.37 ± 0.19	1.70 ± 0/90	-2.09 ± 0.29
<u>Inflammatory response</u>								
NM_023065	Interferon gamma inducible protein 30	Ifi30	-1.04 ± 0.06	1.03 ± 0.07	1.64 ± 0.49	1.12 ± 0.05	1.22 ± 0.10	1.55 ± 0.33
NM_001013365	Oncostatin m	Osm	1.66 ± 0.47	1.45 ± 0.34	1.87 ± 1.12	1.77 ± 0.32	1.59 ± 0.41	1.72 ± 0.77
NM_009841	Cd14 antigen	Cd14	3.37 ± 1.79	5.96 ± 5.65	5.10 ± 9.25	3.72 ± 0.80	6.54 ± 10.56	4.58 ± 7.73
NM_019980	Lps-induced tn factor	Litaf	1.49 ± 0.39	1.27 ± 0.38	1.83 ± 1.03	1.76 ± 0.02	1.96 ± 0.69	2.35 ± 1.43
NM_011157	Proteoglycan 1, secretory granule	Srgn	1.13 ± 0.13	1.78 ± 0.38	2.27 ± 1.53	1.28 ± 0.22	1.66 ± 0.49	1.91 ± 0.72
NM_009780	Complement component 4b (childo blood group)	C4b	-1.13 ± 0.18	1.07 ± 0.09	1.54 ± 0.47	1.01 ± 0.15	1.15 ± 0.11	1.95 ± 0.44
NM_013749	Tumor necrosis factor receptor superfamily, member 12a	Tnfrsf12a	1.57 ± 0.32	1.53 ± 0.80	2.84 ± 3.22	2.31 ± 0.35	3.03 ± 2.20	3.06 ± 1.06
NM_011905	Toll-like receptor 2	Tlr2	1.89 ± 0.72	2.33 ± 0.98	2.93 ± 1.76	1.30 ± 0.17	1.87 ± 1.17	1.93 ± 1.05
NM_205820	Toll-like receptor 13	Tlr13	1.54 ± 0.21	1.89 ± 0.48	2.02 ± 0.98	1.13 ± 0.09	1.54 ± 0.48	1.85 ± 0.63

Chapter 5.2:
Gpx-1^{-/-}-transient MCAO

Table 5.4 (continue)

Genbank	Gene Title	Symbol	Time-points					
			WT-tMCAO			Gpx-1 ^{-/-} -tMCAO		
			2h	8h	24h	2h	8h	24h
<u>Inflammatory response (continue)</u>								
NM_010185	Fc receptor, ige, high affinity i, gamma polypeptide	Fcgr1g	1.15 ± 0.14	1.48 ± 0.16	2.20 ± 1.30	1.18 ± 0.17	1.51 ± 0.44	2.14 ± 1.13
NM_011333	Chemokine (c-c motif) ligand 2	Ccl2	1.29 ± 0.13	2.28 ± 0.83	2.48 ± 2.03	1.77 ± 0.48	2.24 ± 1.31	2.55 ± 2.13
NM_011330	Small chemokine (c-c motif) ligand 11	Ccl11	1.08 ± 0.13	1.86 ± 0.92	1.77 ± 1.26	1.09 ± 0.11	1.94 ± 0.90	2.24 ± 1.53
NM_011331	Chemokine (c-c motif) ligand 12	Ccl12	1.29 ± 0.24	2.15 ± 0.85	7.03 ± 8.91	1.47 ± 0.51	2.19 ± 1.39	7.00 ± 10.57
NM_008176	Chemokine (c-x-c motif) ligand 1	Cxcl1	3.50 ± 2.61	7.35 ± 6.41	6.05 ± 11.39	5.07 ± 1.71	7.07 ± 8.91	5.41 ± 12.72
NM_021274	Chemokine (c-x-c motif) ligand 10	Cxcl10	1.28 ± 0.13	1.88 ± 0.77	2.63 ± 2.26	1.08 ± 0.06	1.48 ± 0.58	2.62 ± 2.06

5.2.2.3 Deletion of Gpx-1 induced transcriptional regulation of additional novel pathways, resulting in exacerbation of cerebral post-ischemic injury

It has been previously reported that Gpx-1 deficiency resulted in an elevated oxidant production, causing an aggravation of post-ischemic cerebral injury (Crack et al., 2001), which can be abrogated through transgenic overexpression of functional Gpx-1 (Weisbrodt-Lefkowitz et al., 1998). Previous studies from our laboratory also revealed that tMCAO induced a significant increase in infarct size and vascular permeability in Gpx-1^{-/-} brains as compared to that of WT (Crack et al., 2001; Wong et al., 2008). Neuronal deficit scores showed close association to histological data, and caspase-3 activation occurred much early in Gpx-1^{-/-} mice upon tMCAO induction (Crack et al., 2001). Current global gene profiling study further substantiated Gpx-1^{-/-} mice increased susceptibility to neuronal damage and subsequently death during I/R process. Biological pathway assignment of the 1,034 genes having exclusive significant transcriptional regulation to Gpx-1^{-/-} -tMCAO condition identified several cellular signaling pathways which play a prominent role in the regulation of cell death and survival (Table 5.5).

-INDUCTION OF CELL DEATH: FAS/FASL AND p53 -MEDIATED PRO-APOPTOTIC PATHWAYS

It is evident from the microarray analysis of tMCAO-induced Gpx-1^{-/-} mouse cortex that genes encoding for proteins involved extrinsic (Fas/FasL) and intrinsic p53 -triggered pro-apoptotic pathways were transcriptionally up-regulated (Table 5.5). The Fas/FasL-mediated extrinsic apoptotic pathway is evident at the early 2h time-point upon tMCAO induction in Gpx-1^{-/-} mice (Table 5.5: Induction of cell death). RCHY1 is an ubiquitin-protein E3 ligase

that promotes p53 degradation demonstrated down-regulation allowing up-regulation of p53 expression, and contributing to its activity. The increase in Ddit3/CHOP protein expression facilitates the suppression of the BCL2 expression making them more susceptible to apoptosis (McCullough et al., 2001). Previously we have reported an increase in protein expression of the transcription factor NF-κB in Gpx-1^{-/-} after transient ischemic stroke whose up-regulation exacerbated neuronal death (Crack et al., 2006). This is further verified in the present study which demonstrated an elevated transcriptional up-regulation of the p65 subunit of NF-κB (Rela) in Gpx-1^{-/-} mouse cortex. Interestingly, endogenous inhibitor of NF-κB transcription activity (IκBα), Nfkbia, also demonstrated an increasing regulatory trend (Table 5.5).

- CELLULAR CALCIUM ION BINDING AND HOMEOSTASIS

Genes encoding for both intrinsic and extrinsic Ca²⁺ ionotropic receptors (Gpr12, Grin1, Ryr3) and ion channels (Atp2a2, Cacnb4, Slc24a3) demonstrated substantial down-regulation in Gpx-1^{-/-} mouse cortex (Table 5.5).

- MITOGEN-ACTIVATED PROTEIN KINASE (MAPK) SIGNALING PATHWAYS

MAPK pathways, which can be further divided into three types (p38 MAPK, SAPK/JNK, MAPK/ERK and BMK-1/ERK5, are involved in the transduction of a large variety of external signals, (e.g. growth factors, cytokine, Fas) leading to a variety of cellular responses, including growth, differentiation, inflammation and apoptosis. The former two are important in pathways controlling T cell differentiation, production of inflammatory cytokines and eicosanoids (Ichijo et al., 1997), and apoptotic cell death, whereas the latter two are

Chapter 5.2: Gpx-1^{-/-}-transient MCAO

implicated in pro-proliferative, mitogenic and cell cycle progression cascades (Kato et al., 1998; Xia et al., 1995). As shown in Table 5.5: MAPK signaling pathway, majority of the players involved in MAPK signaling pathways showed substantial transcriptional down-regulation. On the other hand, dual specificity phosphatase (Dusp) 1(Dusp1) and 3(Dusp3) demonstrated significant up-regulation at the early time-point of 2h. Dusps, an emerging subclass of the protein tyrosine phosphatase (PTP) gene superfamily which are selective for dephosphorylating the critical phosphothreonine and phosphotyrosine residues within MAPKs, are strongly transcriptionally induced by various growth factors and/or cellular stresses, resulting in a sophisticated transcriptional regulatory mechanism for targeted inactivation of MAPK activities (Camps et al., 2000).

- CYTOPROTECTIVE RESPONSE TO OXIDATIVE STRESS: SUPPRESSION OF NRF2-INDUCED PATHWAY

Deletion of functional Gpx-1 induced a mixed transcriptional anti-oxidative response, with Hsps and chaperones such Mt3 and Hsp90b1 being down-regulated while Hmox1, Hspa1a and Naprt1 up-regulated. Nrf2, a recently acknowledged protective-survival transcription factor induced upon oxidative and electrophilic stresses, plays a pivotal role in the transcriptional activation of antioxidant-response element (ARE) -harbouring genes encoding detoxifying enzymes and cytoprotective antioxidant proteins including superoxide dehydrogenase, NAD(P)H dehydrogenase quinone-1 (Nqo1) and heme oxygenase-1 (Hmox1) (reviewed in Higgins et al. 2010). In the event of cellular stress, Nrf2 normally kept inactive through interaction with its inhibitory partner (Nrf2)-Kelch-like ECH-associated protein 1 (Keap1) dissociates and migrates to the nucleus upon its phosphorylation

Chapter 5.2: Gpx-1^{-/-}-transient MCAO

by protein kinases such as protein kinase C (PKC), ERK, and MAPK (Buckley et al., 2003; De Long et al., 1987). Nrf2 DNA-binding activity is conferred by a heterodimer consisting of an ubiquitous small v-maf musculoaponeurotic fibrosarcoma (Maf) protein (Maff and Mafg) the tissue-restricted protein p45 Nrf2. Transcriptomic profiling revealed up-regulation of Hmox1 and Maff and down-regulation of Mafg, Prkcb1 and Mapk4 (Table 5.5: MAPK signaling pathway and oxidative stress induced gene expression via NRF2). Thioredoxin interacting protein (Txnip), an Nrf2 negatively regulated target, also showed transcriptional elevation at 2h. Further, FBJ osteosarcoma oncogene (Fos) reported to exert antagonistic effect on the ARE element Nqo1 (Venugopal and Jaiswal, 1996) demonstrated significant up-regulation at 2h (Table 5.5).

- UBIQUITIN-PROTEASOME SYSTEM (UPS) -DEPENDENT PROTEIN CATABOLISM

The UPS function is impaired in Gpx-1^{-/-} mouse cortex with the decrease in mRNA level of its associated pathway players (Psm1, Uchl(3,5) and Usp(2,11), eventually resulting in accumulation of cellular proteins (Table 5.5).

- MITOTIC CELL CYCLE

Majority of genes encoding for mitogenic proteins involved in the mediation of cell proliferation (Cyclin(d2, t1), Rhob, Src, and Foxg1) demonstrated pursuing down-regulation with a concurrent correlated increase in mRNA level for inhibitor of cell cycle (Cdkn1a) (Table 5.5).

Chapter 5.2:
Gpx-1^{-/-}-transient MCAO

Table 5.5 Selected differentially-expressed gene profile of neuronal death-related families in Gpx-1^{-/-}-tMCAO infarct cortex. All fold-change expressions were subjected to one-way ANOVA analysis and Benjamini Hochberg FDR correction, and were significant at $p < 0.05$. Data are expressed as fold-change \pm sem.

Genbank	Gene Title	Symbol	Time-points		
			2h	8h	24h
Cell death					
NM_007987	Fas (TNF receptor superfamily member)	Fas	1.56 \pm 0.18	1.81 \pm 0.35	1.61 \pm 0.20
NM_021897	Transformation related protein 53 inducible nuclear protein 1	Trp53inp1	1.25 \pm 0.15	1.56 \pm 0.32	1.20 \pm 0.13
NM_021451	Phorbol-12-myristate-13-acetate-induced protein 1	Pmaip1	1.24 \pm 0.10	1.78 \pm 0.42	1.19 \pm 0.15
NM_007837	DNA-damage inducible transcript 3	Ddit3	1.57 \pm 0.18	1.89 \pm 0.67	1.51 \pm 0.24
NM_009045	v-rel reticuloendotheliosis viral oncogene homolog A (avian)	Rela	1.18 \pm 0.07	1.46 \pm 0.27	1.51 \pm 0.43
NM_007915	Etoposide induced 2.4 mRNA	Ei24	-1.52 \pm 0.03	-1.54 \pm 0.04	-1.37 \pm 0.04
NM_011931	Ring finger and WD repeat domain 2	Rfwd2	-1.24 \pm 0.08	-1.39 \pm 0.08	-1.77 \pm 0.05
NM_026557	Ring finger and CHY zinc finger domain containing 1	Rchyl	-1.29 \pm 0.14	-1.53 \pm 0.10	-1.15 \pm 0.11
NM_174991	Brain-specific angiogenesis inhibitor 1	Bai1	-1.16 \pm 0.20	-1.30 \pm 0.06	-1.99 \pm 0.07
NM_009517	Zinc finger matrin type 3	Zmat3	-1.42 \pm 0.06	-1.76 \pm 0.03	-2.23 \pm 0.10
NM_009370	Transforming growth factor, beta receptor I	Tgfr1	-1.06 \pm 0.09	-1.08 \pm 0.18	-1.59 \pm 0.12
Calcium ion binding and homeostasis					
NM_009722	ATPase, Ca ⁺⁺ transporting, cardiac muscle, slow twitch 2	Atp2a2	-1.23 \pm 0.04	-1.40 \pm 0.04	-1.57 \pm 0.07
NM_008151	G-protein coupled receptor 12	Gpr12	-1.18 \pm 0.06	-1.54 \pm 0.13	-1.21 \pm 0.15
NM_146123	Calcium channel, voltage-dependent, beta 4 subunit	Cacnb4	-1.23 \pm 0.07	-1.44 \pm 0.10	-1.68 \pm 0.18
NM_010104	Endothelin 1	Edn1	1.81 \pm 0.22	2.11 \pm 1.04	1.72 \pm 0.67
NM_008169	Glu receptor, ionotropic, NMDA1 (zeta 1)	Grin1	-1.11 \pm 0.09	-1.42 \pm 0.08	-1.65 \pm 0.08
NM_177652	Ryanodine receptor 3	Ryr3	-1.45 \pm 0.04	-1.42 \pm 0.12	-1.52 \pm 0.22
NM_053195	Solute carrier family 24 (sodium/potassium/calcium exchanger), member 3	Slc24a3	-1.29 \pm 0.04	-1.39 \pm 0.09	-1.70 \pm 0.11
MAPK Signaling Pathway					
NM_013642	Dual specificity phosphatase 1	Dusp1	1.69 \pm 0.60	1.29 \pm 0.24	1.17 \pm 0.48
NM_028207	Dual specificity phosphatase 3 (vaccinia virus phosphatase VH1-related)	Dusp3	1.80 \pm 0.68	1.32 \pm 0.23	1.32 \pm 0.18
NM_026268	Dual specificity phosphatase 6	Dusp6	1.26 \pm 0.23	-1.32 \pm 0.25	-1.59 \pm 0.21
NM_008748	Dual specificity phosphatase 8	Dusp8	-1.00 \pm 0.05	-1.31 \pm 0.14	-1.96 \pm 0.16
NM_172632	Mitogen-activated protein kinase 4	Mapk4	1.04 \pm 0.04	-1.12 \pm 0.11	-1.67 \pm 0.09
NM_008854	Protein kinase, cAMP dependent, catalytic, alpha	Prkaca	-1.35 \pm 0.10	-1.77 \pm 0.06	-2.11 \pm 0.05
NM_021420	Serine/threonine kinase 4	Stk4	-1.38 \pm 0.02	-1.62 \pm 0.16	-1.67 \pm 0.11
NM_011697	Vascular endothelial growth factor B	Vegfb	-1.13 \pm 0.09	-1.33 \pm 0.08	-1.53 \pm 0.10
NM_009506	Vascular endothelial growth factor C	Vegfc	-1.35 \pm 0.06	-1.63 \pm 0.06	-1.42 \pm 0.14

Table 5.5 (continue)

Genbank	Gene Title	Symbol	Time-points		
			2h	8h	24h
MAPK Signaling Pathway (continue)					
NM_010216	c-Fos induced growth factor	Figf	-1.55 ± 0.08	-1.46 ± 0.04	-1.32 ± 0.05
NM_145452	RAS p21 protein activator 1	Rasa1	-1.24 ± 0.09	-1.54 ± 0.12	-1.36 ± 0.10
NM_010592	Jun proto-oncogene related gene d1	Jund1	-1.04 ± 0.11	-1.05 ± 0.27	-1.51 ± 0.13
NM_007581	Calcium channel, voltage-dependent, beta 3 subunit	Cacnb3	-1.19 ± 0.05	-1.34 ± 0.10	-1.51 ± 0.04
NM_008855	Protein kinase C, beta 1	Prkeb1	-1.11 ± 0.05	-1.38 ± 0.11	-1.61 ± 0.17
NM_133189	Calcium channel, voltage-dependent, gamma subunit 7	Cacng7	-1.45 ± 0.07	-1.60 ± 0.03	-1.65 ± 0.13
NM_009785	Calcium channel, voltage-dependent, alpha2/delta subunit 3	Cacna2d3	-1.09 ± 0.03	-1.42 ± 0.13	-1.53 ± 0.24
NM_010897	Neurofibromatosis 1	Nf1	-1.10 ± 0.06	-1.61 ± 0.06	-2.42 ± 0.11
NM_019430	Calcium channel, voltage-dependent, gamma subunit 3	Cacng3	-1.09 ± 0.08	-1.48 ± 0.15	-1.61 ± 0.19
NM_013643	Protein tyrosine phosphatase, non-receptor type 5	Ptpn5	-1.19 ± 0.07	-1.34 ± 0.07	-1.68 ± 0.08
NM_011102	Protein kinase C, gamma	Prkcc	-1.33 ± 0.04	-1.52 ± 0.13	-1.79 ± 0.12
NM_010838	Microtubule-associated protein tau	Mapt	1.04 ± 0.09	-1.18 ± 0.13	-1.61 ± 0.08
Response to oxidative stress					
NM_010442	Heme oxygenase (decycling) 1	Hmox1	1.67 ± 0.61	2.76 ± 1.86	4.01 ± 3.64
NM_010479	Heat shock protein 1A	Hspa1a	11.50 ± 1.85	8.74 ± 26.80	2.47 ± 2.64
NM_172607	Nicotinate phosphoribosyltransferase domain containing 1	Naprt1	1.07 ± 0.10	1.12 ± 0.10	1.62 ± 0.14
NM_010755	v-Maf musculoaponeurotic fibrosarcoma oncogene family, protein F (avian)	Maff	1.63 ± 0.07	1.53 ± 0.25	1.32 ± 0.36
NM_001009935	Thioredoxin interacting protein	Txnip	2.02 ± 0.45	2.45 ± 0.28	1.90 ± 0.73
NM_133662	Immediate early response 3	Ier3	2.51 ± 0.44	2.12 ± 0.53	2.24 ± 1.29
NM_007742	Collagen, type I, alpha 1	Col1a1	-1.19 ± 0.14	-1.36 ± 0.04	-1.55 ± 0.05
NM_010137	Endothelial PAS domain protein 1	Epas1	-1.14 ± 0.16	-1.41 ± 0.12	-1.56 ± 0.04
NM_013603	Metallothionein 3	Mt3	-1.12 ± 0.10	-1.47 ± 0.23	-2.21 ± 0.15
NM_011631	Heat shock protein 90, beta (Grp94), member 1	Hsp90b1	-1.06 ± 0.07	-1.26 ± 0.09	-1.73 ± 0.05
NM_009221	Synuclein, alpha	Snca	-1.42 ± 0.13	-1.52 ± 0.11	-1.13 ± 0.17
NM_010756	v-Maf musculoaponeurotic fibrosarcoma oncogene family, protein G (avian)	Mafg	-1.31 ± 0.04	-1.33 ± 0.08	-1.50 ± 0.07
Ubiquitin-proteasome system-dependent protein catabolism					
NM_027357	Proteasome (prosome, macropain) 26S subunit, non-ATPase, 1	Psm1	-1.35 ± 0.05	-1.36 ± 0.09	-1.58 ± 0.11
NM_028774	Ring finger protein (C3H2C3 type) 6	Rnf6	-1.42 ± 0.06	-1.24 ± 0.07	-1.52 ± 0.09
NM_016723	Ubiquitin carboxyl-terminal esterase L3 (ubiquitin thiolesterase)	Uchl3	-1.44 ± 0.06	-1.60 ± 0.20	-1.67 ± 0.07
NM_019562	Ubiquitin carboxyl-terminal esterase L5	Uchl5	-1.52 ± 0.09	-1.67 ± 0.04	-1.70 ± 0.08
NM_198091	Ubiquitin specific peptidase 2	Usp2	-1.12 ± 0.04	-1.31 ± 0.08	-1.58 ± 0.05
NM_145628	Ubiquitin specific peptidase 11	Usp11	-1.30 ± 0.02	-1.45 ± 0.10	-1.66 ± 0.16
NM_025745	Endoplasmic reticulum lectin 1	Erlec1	-1.49 ± 0.06	-1.68 ± 0.01	-1.75 ± 0.13

Chapter 5.2:
Gpx-1^{-/-}-transient MCAO

Table 5.5 (continue)

Genbank	Gene Title	Symbol	Time-points		
			2h	8h	24h
Mitotic Cell cycle					
NM_007631	Cyclin D1	Ccnd1	1.25 ± 0.21	1.16 ± 0.14	1.54 ± 0.29
NM_009829	Cyclin D2	Ccnd2	-1.23 ± 0.12	-1.36 ± 0.25	-1.63 ± 0.08
NM_009833	Cyclin T1	Ccnt1	-1.13 ± 0.03	-1.21 ± 0.16	-1.71 ± 0.08
NM_153058	Microtubule-associated protein, RP/EB family, member 2	Mapre2	-1.26 ± 0.06	-1.44 ± 0.05	-1.59 ± 0.09
NM_010021	Deleted in azoospermia-like	Dazl	-1.37 ± 0.04	-1.51 ± 0.03	-1.56 ± 0.06
NM_010329	Podoplanin	Pdpn	1.11 ± 0.16	1.47 ± 0.44	2.05 ± 1.33
NM_007483	Ras homolog gene family, member B	Rhob	-1.14 ± 0.08	-1.17 ± 0.14	-1.75 ± 0.05
NM_008552	MAS1 oncogene	Mas1	-1.27 ± 0.04	-1.78 ± 0.05	-1.76 ± 0.07
NM_001003920	ER serine/threonine kinase 1	Brsk1	-1.24 ± 0.11	-1.58 ± 0.10	-1.80 ± 0.11
NM_021491	Sphingomyelin phosphodiesterase 3, neutral	Smpd3	-1.25 ± 0.09	-1.29 ± 0.18	-1.71 ± 0.18
NM_015732	Axin2	Axin2	-1.40 ± 0.06	-1.55 ± 0.07	-2.00 ± 0.12
NM_009703	v-Raf murine sarcoma 3611 viral oncogene homolog	Araf	-1.01 ± 0.07	1.03 ± 0.09	1.51 ± 0.23
NM_010436	H2A histone family, member X	H2afx	-1.13 ± 0.07	-1.20 ± 0.03	-1.58 ± 0.07
NM_008241	Forkhead box G1	Foxg1	-1.38 ± 0.12	-1.56 ± 0.14	-1.59 ± 0.09
NM_007591	Calreticulin	Calr	-1.19 ± 0.17	-1.44 ± 0.10	-1.87 ± 0.03
NM_148930	RNA binding motif protein 5	Rbm5	-1.54 ± 0.08	-1.56 ± 0.14	-1.32 ± 0.16
NM_133833	Dystonin	Dst	-1.06 ± 0.20	-1.31 ± 0.04	-1.51 ± 0.06
NM_007668	Cyclin-dependent kinase 5	Cdk5	-1.19 ± 0.02	-1.34 ± 0.04	-1.56 ± 0.13
NM_147151	Euchromatic histone lysine N-methyltransferase 2	Ehmt2	-1.11 ± 0.05	-1.41 ± 0.08	-1.50 ± 0.11
NM_008583	Multiple endocrine neoplasia 1	Men1	-1.25 ± 0.02	-1.36 ± 0.05	-1.55 ± 0.13
NM_001025395	Rous sarcoma oncogene	Src	-1.50 ± 0.01	-1.51 ± 0.08	-1.90 ± 0.07
NM_008036	FBJ osteosarcoma oncogene B	Fosb	4.07 ± 1.18	1.21 ± 0.89	-2.05 ± 0.06
NM_025613	EP300 interacting inhibitor of differentiation 1	Eid1	-1.45 ± 0.15	-1.64 ± 0.10	-1.74 ± 0.09
NM_007669	Cyclin-dependent kinase inhibitor 1A (p21)	Cdkn1a	2.02 ± 0.16	3.40 ± 0.85	2.01 ± 1.15
NM_019710	Structural maintenance of chromosomes 1A	Smc1a	-1.38 ± 0.03	-1.61 ± 0.02	-1.65 ± 0.07
NM_148952	E2F transcription factor 4	E2f4	-1.15 ± 0.08	-1.12 ± 0.15	-1.55 ± 0.07
Immune response					
NM_018770	Cell adhesion molecule 1	Cadm1	-1.41 ± 0.09	-1.62 ± 0.04	-1.83 ± 0.06
NM_053202	Forkhead box P1	Foxp1	-1.10 ± 0.09	-1.39 ± 0.04	-1.69 ± 0.12
NM_019654	Suppressor of cytokine signaling 5	Socs5	-1.22 ± 0.06	-1.46 ± 0.05	-1.63 ± 0.11
NM_010789	Meis homeobox 1	Meis1	-1.63 ± 0.08	-1.64 ± 0.08	-1.74 ± 0.08
NM_001024458	Adducin 1 (alpha)	Add1	-1.08 ± 0.11	-1.38 ± 0.08	-1.73 ± 0.09
NM_007614	Catenin (cadherin associated protein), beta 1	Ctnnb1	-1.40 ± 0.12	-1.33 ± 0.04	-1.62 ± 0.06
NM_010137	Endothelial PAS domain protein 1	Epas1	-1.14 ± 0.16	-1.41 ± 0.12	-1.46 ± 0.04
NM_001077696	Histone deacetylase 5	Hdac5	-1.28 ± 0.11	-1.83 ± 0.06	-1.77 ± 0.10
NM_016713	Misshapen-like kinase 1 (zebrafish)	Mink1	-1.43 ± 0.05	-1.55 ± 0.12	-1.61 ± 0.07
NM_008583	Multiple endocrine neoplasia 1	Men1	-1.24 ± 0.05	-1.36 ± 0.08	-1.62 ± 0.12

Chapter 5.2:
Gpx-1^{-/-}-transient MCAO

Table 5.5 (continue)

Genbank	Gene Title	Symbol	Time-points		
			2h	8h	24h
Immune response (continue)					
NM_008783	Rre B-cell leukemia transcription factor 1	Pbx1	-1.34 ± 0.04	-1.60 ± 0.11	-1.77 ± 0.07
NM_021344	Tescalcin	Tesc	-1.14 ± 0.05	-1.26 ± 0.14	-2.03 ± 0.02

5.2.2.4 Validation of Gpx-1^{-/-} profile via real-time PCR

Microarray data was validated on the same tMCAO-induced Gpx-1^{-/-} cortical RNA samples used in microarray analysis via real-time PCR. These selected gene probes demonstrated identical transcriptional regulatory trend at 2h, 8h and 24h post-reperfusion (Table 5.6).

Table 5.6 Validation of microarray data using real-time PCR technique on tMCAO-induced cortex RNA samples from Gpx-1^{-/-} mice respectively. All fold-change expressions are statistically significant at $p < 0.05$. Each expression data is representative of 3 independent replicates. Data are expressed as fold-change \pm sem.

Genbank	Gene Title	Symbol	Gpx-1 ^{-/-} -MCAO					
			2h		8h		24h	
			Microarray	Real-time PCR	Microarray	Real-time PCR	Microarray	Real-time PCR
NM_153553	Neuronal PAS domain protein 4	Npas4	3.31 \pm 8.58	6.71 \pm 0.32	1.26 \pm 1.06		-1.24 \pm 0.46	
NM_008491	Lipocalin 2	Lcn2	1.46 \pm 0.45		6.20 \pm 4.42	3.26 \pm 1.05	5.67 \pm 6.74	
NM_009263	Secreted phosphoprotein	Spp1	-1.26 \pm 0.17		1.80 \pm 1.22	1.54 \pm 1.09	4.73 \pm 6.48	16.19 \pm 0.12
NM_020581	Angiopoietin-like 4	Angptl4	2.03 \pm 0.30		3.95 \pm 0.76	2.33 \pm 1.14	2.72 \pm 1.23	1.96 \pm 1.05
NM_007585	Annexin A2	AnxA2	1.33 \pm 0.29	1.72 \pm 0.56	2.29 \pm 1.41		3.35 \pm 2.37	5.08 \pm 0.89
NM_007498	Activating transcription 3	Atf3	3.09 \pm 1.03	10.11 \pm 0.61	4.04 \pm 5.10		2.29 \pm 1.57	
NM_010479	Heat shock protein 1A	Hspa1a	11.50 \pm 1.85	5.74 \pm 0.68	8.74 \pm 26.80	12.33 \pm 1.12	2.47 \pm 2.64	
NM_010442	Heme oxygenase 1	Hmox1	1.67 \pm 0.61	2.18 \pm 0.66	2.76 \pm 1.86	1.71 \pm 0.75	4.01 \pm 3.64	
NM_011905	Toll-like receptor 2	Tlr2	1.30 \pm 0.17	1.67 \pm 0.63	1.87 \pm 1.17	2.47 \pm 1.15	1.93 \pm 1.05	7.91 \pm 0.99
NM_011817	Growth arrest and DNA-damage-inducible 45 gamma	Gadd45g	3.09 \pm 1.95	6.07 \pm 0.42	1.26 \pm 1.06		-1.24 \pm 0.46	2.36 \pm 0.91
NM_133662	Immediate early response 3	Ier3	2.51 \pm 0.44	3.93 \pm 0.60	6.20 \pm 4.42	3.26 \pm 1.05	5.67 \pm 6.74	3.10 \pm 0.96

5.2.3 Discussion

Spontaneous surge in ROS and free reactive radicals in the brain during ischemic stroke trigger a chain reaction of signaling cascades that converge to apoptosis, necrosis and inflammation, manifesting into neuronal loss, memory and motor deficits (Dirnagl et al., 1999). As neurons do not have sufficient intrinsic anti-oxidative enzymes e.g. catalase installed to combat with dramatic oxidative stress, they rely primarily on Gpx-1 to control the levels of H₂O₂ and OH•, and SOD to lower O₂• (Chan, 1996; de Haan et al., 1998). Gpx-1, predominantly localized in the mitochondria and cytoplasm, catalyzed the reduction of H₂O₂ to alcohols and water. Overexpression of Gpx-1 in transgenic mice have demonstrated a greater neuronal resistance to I/R injury in transient cerebral ischemic model induced by MCAO which occurred as a result of its regulatory function in oxidative stress progression such as delayed caspase-3 activation (Crack et al., 2001; Weisbrot-Lefkowitz et al., 1998).

5.2.3.1 Gpx-1^{-/-} increases susceptibility to I/R injury via predisposition to oxidative stress

The present study attempts to address the effects of Gpx-1 knockdown expression on the global transcriptional profile of tMCAO I/R injury in transgenic mice. Prior to this, a microarray analysis of Gpx-1^{-/-} sham control cortex at physiological basal state before tMCAO treatment was performed and normalized against that of WT. Intriguingly, the present data revealed that a significant transcriptional up-regulation of anti-oxidative proteins (Hsps and chaperones), and members of several distinct mechanisms associating with cell survival, death, UPS, cell cycle, DNA damage response, mitochondrial

respiratory chain (oxidative phosphorylation) and defense and inflammatory response (Table 5.3). Previously, we have demonstrated no cerebral vasculature abnormalities and significant difference in ROS generation between WT and Gpx-1^{-/-} mouse brains which would increase the latter's susceptibility to I/R injury (Crack et al., 2001). This is highly suggestive of a compensatory cellular response induced by Gpx-1^{-/-} absence to maintain physiological balance by combating against rise in ROS level. As such, it can be inferred from our current microarray comparison that Gpx-1 not only plays an important role in homeostatic regulation not only under heightened oxidative stress condition during I/R injury as previously demonstrated (Crack et al., 2001), but also under physiological basal condition.

5.2.3.2 Absence of Gpx-1 modulates additional biological processes during I/R injury

A step further into the temporal transcriptomic profile comparison of WT and Gpx-1^{-/-} cortice during I/R injury unraveled an overwhelming 70% of gene probes with significant transcriptional regulation from MCAO-induced WT condition also being present in that of Gpx-1^{-/-} transgenic mice (accounting for only 28%), within which three-quarter of these common gene probes demonstrated similar regulatory trend and expression (Table 5.4). However, this implied that absence of Gpx-1 does not affect the existing activated and inhibited signaling pathways already triggered upon I/R cortex injury. However, what is noteworthy to mention is the identification of several cellular pathways from the remaining 72% of MCAO-induced Gpx-1^{-/-} transgenic mice, which can be classified into two groups: a) exclusive to Gpx-1^{-/-} model, b) transcriptional regulation of additional

Chapter 5.2: Gpx-1^{-/-}-transient MCAO

genes already revealed in MCAO-induced WT cortex and having opposing regulatory trend to that of WT. Distinct cellular pathways exclusive to I/R injury in MCAO-induced Gpx-1^{-/-} cortex which were transcriptional regulated include the activation of pro-apoptotic p53 and Fas ligand (CD95/Apo1)-mediated pathways, downplay of Nrf2 anti-oxidative cascade, UPS dysfunction, inhibition of MAPK and cell cycle pathways, and finally repression of the immunity response (Table 5.5). All these pathways, all in all, revealed the patho-physiological mechanisms behind the increased neuronal damages, i.e. increased infarct size and exacerbated cell death, of Gpx-1^{-/-} transgenic mice to transient cerebral ischemic stroke.

In conclusion, the present temporal transcriptomic profiling provides a comprehensive in-depth summary of the cellular pathways being regulated in the cortex upon I/R injury in an *in vivo* transient cerebral ischemic stroke mediated in the presence and absence of Gpx-1. The present data further signifies a crucial regulatory role of Gpx-1 in the protection of brain against oxidative stress and inflammation unleashed during I/R injury. Furthermore, the present report for the first time that absence of Gpx-1 elevates the heightened redox status of cortex by pre-conditioning the brain cells in a pro-oxidant state at physiological condition through activation of an anti-oxidant response to uphold cellular homeostasis, thus increasing the vulnerability of the brain cells to subsequent neuronal traumas (such as ischemic stroke).

Chapter 6:
Permanent
Focal cerebral ischemia

6 Description of permanent focal cerebral ischemia model in adult rats

All experiments involving animals were approved by the National University of Singapore, and were in accordance with the US Public Health Service guide for the care and use of laboratory animals. Selective Aurora kinase inhibitor, ZM447439 (Cat. No. 2458) was purchased from Tocris, Bristol, UK), and prepared in 100% di-methyl sulfoxide (DMSO) as 100mM stock. Desired concentration of 30mM was achieved via dilution with 80% DMSO in normal saline.

Anaesthesia

In preparation for surgery, male Wistar rats of 260 – 300g were anaesthetised by intraperitoneal injection of a cocktail consisting of ketamine hydrochloride (37.5mg/ml) and xylazine (5mg/ml) purchased from the Animal Holding Unit of National University of Singapore.

Rat Permanent Focal Cerebral Ischemia Model

Modified transcranial permanent middle cerebral artery occlusion (pMCAO) is carried out as previously described (Qu et al., 2006). Young adult male Wistar rats were allowed free access to food and water before and after all procedures. Rats were weighed and anesthetized intraperitoneally with rat anaesthesia cocktail as previously mentioned at 1ml/kg body weight, and supplemented as necessary during the procedures. Body temperature was monitored and maintained within normal limits with a $37 \pm 0.5^{\circ}\text{C}$ heating pad. Under the operating microscope the left middle cerebral artery (MCA) was exposed transcranially without damage to the zygomatic bone. Transection of the facial

Chapter 6:
***In vivo* permanent focal cerebral ischemia**

nerve was avoided during exposure of the temporalis muscle, which was divided caudally and retracted inferiorly to avoid compression of the orbital contents. The circle of Willis and the origin of the MCA was exposed in all rats by gently retracting the brain with a spatula on a flexible arm. The MCA was occluded with micro-bipolar coagulation using a low power setting and continuous saline irrigation, and then transected to avoid recanalization. Temporalis muscle and skin were closed in layers, and rats were allowed to recover from anesthesia on a heating pad. 30min post-pMCAO surgery, rats were subjected to a 5ul *i.c.v.* injection of either vehicle (80% DMSO) or 30mM ZM447439 (in 80% DMSO) at the following coordinates from the Bregma: AP = - 0.9mm, ML = + 1.4mm, VD = - 3.8mm. They were returned to their cages for the remainder of the period.

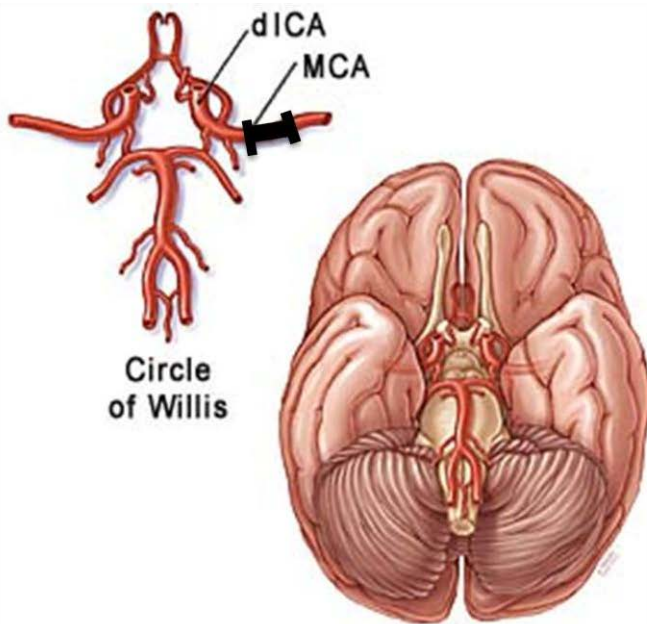
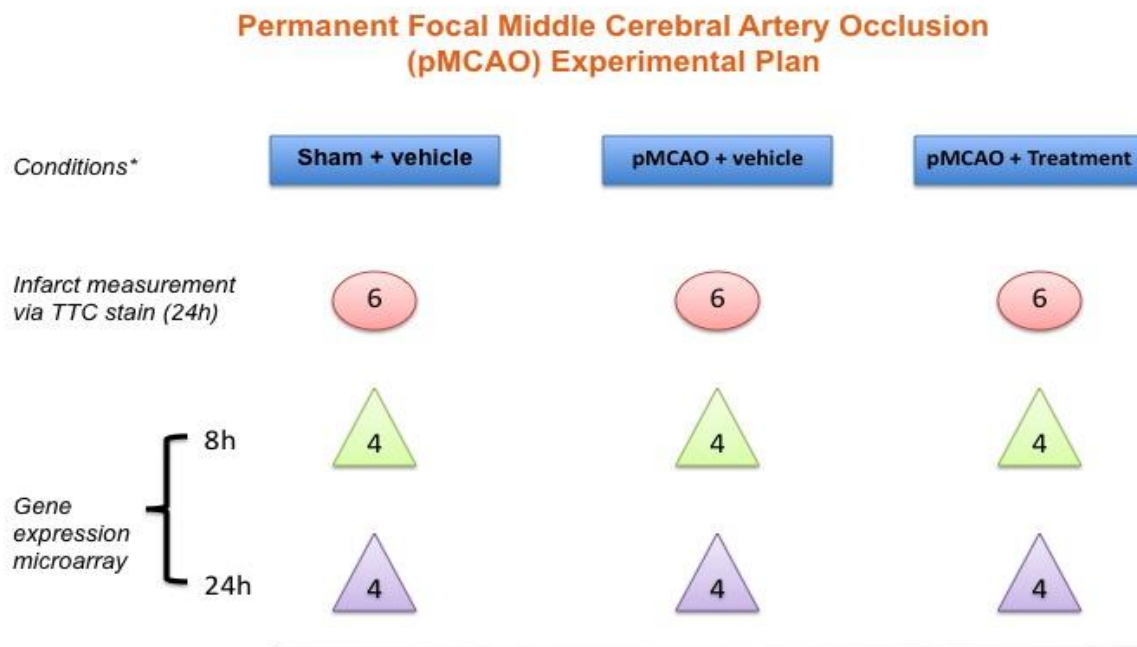


Image adapted from
<http://www.mcg.edu/neurology/research/strokesicklecell/sicklepatients.html>

Chapter 6:
***In vivo* permanent focal cerebral ischemia**

Rats were randomized into six groups namely: Sham, pMCAO + Vehicle (80% DMSO), pMCAO + 30mM ZM447439 (in 80% DMSO) for 8h and 24h post-injection, with consequent euthanization, removal and perfusion of brain with saline for TTC staining (n = 6) and removal of brain for microarray analysis (n= 4) for each condition/time-point. TTC staining was used to ascertain the infarct volume induced upon pMCAO (detailed methodology can be found in Chapter 2). Individual rat cortex sample was loaded for each gene array using Illumina Rat Ref12 V1 genechips in microarray analysis. A schematic diagram for the experimental layout is shown below.



* Vehicle = 80% DMSO; Treatment = 30mM selective Aurk inhibitor ZM447439 in 80% DMSO. 5ul of either conditions was injected intra-cerebroventricularly (i.c.v.) 30min post-pMCAO surgery. Rats were then sacrificed at 8h or 24h after i.c.v. injection.

**Chapter 6.1:
Permanent
Focal Cerebral Ischemia
In
Adult Rat Model**

6.1.1 Introduction

Permanent focal cerebral ischemia results when blood flow to the hypoperfused ischemic region is not promptly restored upon onset or period of ischemia is too long resulting in incomplete reperfusion due to microvascular occlusion, an observation coined as “no-re flow phenomenon” back in the sixties (Ames et al., 1968). The eventual outcome is the consumption of the penumbra region, an initially functionally impaired but viable region surrounding the ischemic centre, by the ischemic cascade, resulting in the expansion of the infarct core.

At the site of ischemic injury, heterogeneity in mode of cell death is present. Occurrence of necrosis, an unregulated form of cell death commonly associated with rupture of the plasma membrane and cytotoxic uncontrollable swelling of both the cell and internal organelles, is especially prominent due to the physical mechanical damage to the cells e.g. neurons, endothelial cells and glia at the immediate site of hypoperfusion (Johnson and Deckwerth, 1993; Martin et al., 1998). Necrotic neuronal death results in the release of high level of Glu and toxins into the extracellular matrix, causing de-regulated mechanistic stimulation of surrounding uninjured neurons via GluRs activation. Concurrently, many brain cells undergo apoptosis, a genetically regulated mechanism that commit cell to its demise with minimal disruption to surrounding micro-environment via diminished level of inflammation or release of genetic materials (Choi, 1996; Hara et al., 1997; Lee et al., 1999; Namura et al., 1998). Several determinants govern the predominating form of neuronal death at the ischemic site. These include the local degree of ischemia, cell maturity, the concentration of free intracellular Ca^{2+} and the cellular

Chapter 6.1: Permanent-MCAO

microenvironment (Choi, 1995; Lee et al., 1999; Leist and Nicotera, 1998b). Activation of GluRs induces excitotoxicity, leading to the manifestation of apoptosis and/or programmed necrosis, both of which activate downstream signaling cascades that cross-regulate each other (Choi, 1995; Choi, 1996; Leist and Nicotera, 1998a; Leist and Nicotera, 1998b; Leist et al., 1997; Namura et al., 1998; Thornberry and Lazebnik, 1998). For instance, calpains, Ca^{2+} -dependent proteases involved in programmed necrosis, have been implicated in the mediation of the apoptosis in neurons (Crocker et al., 2003) and cleavage endogenous caspases such as caspase-3, -7, -8 and -9 (Chua et al., 2000; McGinnis et al., 1999). In addition or alternatively, early mitochondrial ROS generation (Yu et al., 1997), depletion of intracellular K^+ (Yu et al., 1997), and potentiation of toxic Zn^{2+} influx (Koh, 2001) may trigger apoptosis.

Activated caspases are cysteine-dependent aspartate-directed proteases that modify crucial homeostasis and repair proteins. Caspase -1 and -3 has been suggested to play a pivotal role in ischemia-mediated apoptosis amidst the participation of the other members of the caspase family in the late stages of cell death (Leist et al., 1997; Namura et al., 1998; Thornberry and Lazebnik, 1998). Caspase-mediated apoptosis is triggered by release of cytochrome *c* from mitochondria, through assembly of the apoptosome complex, which in turn activates caspase 3 (Green and Reed, 1998). Programmed necrosis, on the other hand, plays a significant role in delayed neuronal death following ischemic stroke through mitochondrial proteins such as apoptosis-inducing factor and BCL2/adenovirus E1B—interacting protein (Cho and Toledo-Pereyra, 2008). Typically, necrosis is the overwhelmed mechanism that follows acute, permanent vascular

occlusion, whereas milder injury, often results in apoptosis especially within the ischemic penumbra.

Permanent focal cerebral ischemia is commonly observed in patients who seek medical attention after a prolonged period of time upon onset, allowing the prognosis of stroke to progress from mild to severe. Current available therapeutic treatment for focal cerebral ischemic stroke is through intravenous delivery of rt-PA exerting a thrombolytic effect on the site of occlusion. Two rationales exist behind this treatment: firstly, to target the insult itself by lysing the arterial thrombus in order to restore focal cerebral blood flow; secondly, to decrease the intrinsic vulnerability of the penumbra thus enhancing neuroprotection of the penumbra (Brouns and De Deyn, 2009). The shortfall of the rt-PA treatment is that it is only effective within a short therapeutic window of 3 hours after stroke symptom onset, to facilitate significant improvement in neurological deficits and functional outcome of stroke patients (Lakhan et al., 2009). However, when focal cerebral ischemia is left medically unattended for long duration, even upon blood reperfusion to the ischemic region is attempted, microvascular occlusion would already have formed, resulting in partial reperfusion and unwanted increased risk of symptomatic intracranial hemorrhage (which occurs in ~6 % of patients) from the use of rt-PA. Furthermore, since a large percentage of patients with acute ischemic stroke do not have gain access to appropriate medical help within three hours of stroke onset, most do not receive rt-PA treatment (Furlan et al., 2003). This presents a challenge in the successful treatment rate of acute ischemic stroke and a deficiency of therapeutic option with a longer therapeutic window. In order to make up for the latter shortfall, it is important to

Chapter 6.1: Permanent-MCAO

elucidate the pathogenesis of permanent focal cerebral ischemia, a comparative equivalent to acute and/or chronic ischemic stroke left untreated for long duration, so that foundation can be laid for the search of suitable novel biological targets in such cases.

6.1.2 Results

In the etiology of permanent focal cerebral ischemia, the blood flow in the occluded artery is not relieved, resulting in prolonged and constitutive propagation of the ischemic cascades particularly at the penumbra. This leads to the functionally impaired but viable cells in the penumbra to subside with a consequential expansion of the ischemic core. In the present pMCAO adult rat model, the middle cerebral artery is coagulated and transected, resulting in irrevocable blood flow occlusion. To reflect the extensiveness of the infarct damage inflicted upon pMCAO, TTC staining was carried out. TTC is a tetrazolium compound commonly employed as a germinator indicator that in the presence of viable cells, is reduced by metabolic processes e.g. mitochondrial respiratory chain, to form a water-insoluble deep red pigment by oxidizing aldoses and ketoses. Figure 6.1 shows TTC-stained 2-mm transverse sections (From anterior to posterior [1 - 6]) of a rat brain upon pMCAO. The white area indicates the infarct region of dead brain tissue, which covered both the striatum and the cortex.

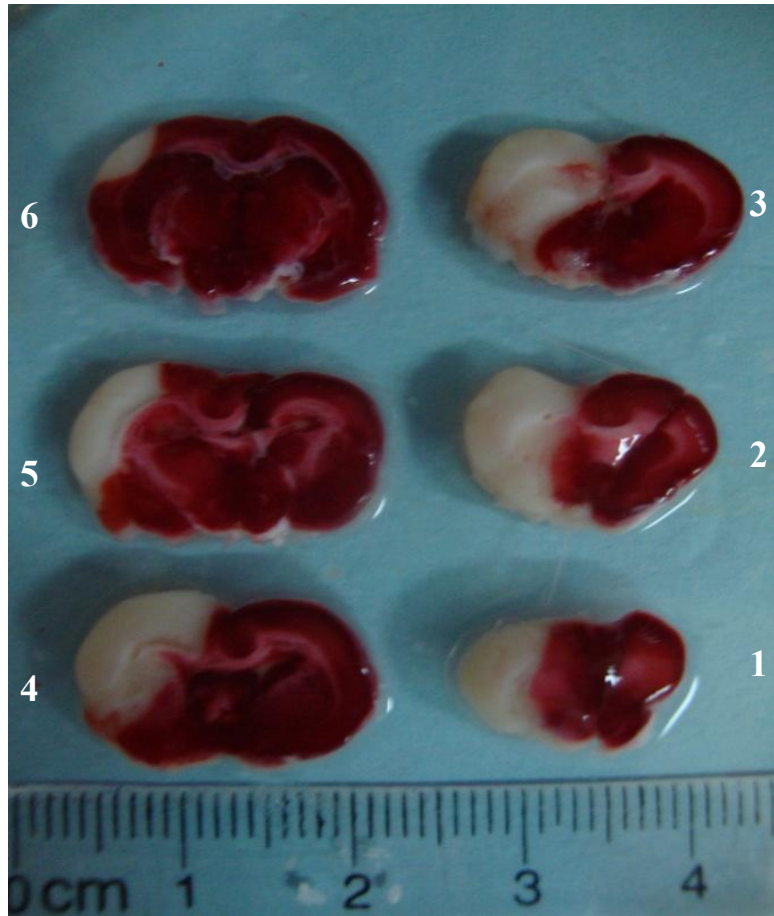


Figure 6.1 TTC-stained 2mm- brain sections from anterior to posterior [1 – 6] of a male Wistar rat brain upon pMCAO induced on the left infarct hemisphere. The white area indicates the dead cells (Infarct region) while the red area refers to viable tissues.

6.1.2.1 pMCAO induces significant global transcriptional regulation

To facilitate an extensive understanding of the pathogenesis of permanent focal cerebral ischemia, temporal global transcriptomic profiling (8h and 24h) was performed on pMCAO adult rat model. For genes to be considered significant in their differential expressions, they need to firstly pass stringent statistical analyses: One-way ANOVA, $p < 0.05$ and Benjamini Hochberg FDR, and secondly demonstrating a fold-change of at least ± 1.5 in at least one out of the two time-points (8h and 24h). These criteria generated a genelist of 1,201 differentially-expressed RefSeq transcripts which was then subjected to functional gene-ontology classification using the online bioinformatics database DAVID 6.7 and corresponded to 1,140 biologically-annotated genes. Particularly in pMCAO, reminiscent of the global gene profile of tMCAO model, occurrence of inflammation and oxidative stress, and disruption of vasculature development were observed, with a yet even more pronounced i.e. evoke a higher transcriptional response, than the latter. Activation of the inflammatory response is prominent from the significant transcriptional regulation of the cytokines, chemokines, CAMs and interleukins which all promote leukocyte (neutrophils) infiltration. In addition, vasculature disruption, DNA damage infliction and cell death pathway induction were also demonstrated from the microarray analysis. Detailed transcriptional regulation of these biological processes during pMCAO will be discussed in this chapter.

-VASCULATURE DEVELOPMENT

Microvascular injury is evident from the transcriptional up-regulation of genes encoding for proteins involved in promoting angiogenesis (Angptl2, Ctgf, Cysr61, Hif1a, Sphk1

and Vegfa) at 24h after pMCAO initiation, indicative of disruption to the vasculature structure (shown in Table 6.1). Hypoxia-inducible factor-1 (HIF1), a heterodimer made up of HIF1A and HIF1B is involved in the regulation of several key genes under hypoxic condition during cerebral ischemia (Chen et al., 2009). HIF1A elicits neuro-protective as well as –toxic functions (reviewed in (Fan et al., 2009)). It is known to regulate the transcription of erythropoietin (EPO), which induces several pathways related to neuroprotection and vascular endothelial cell growth factor (VEGF), which facilitates neovascularization in hypoxic-ischemic brain areas. On the contrary, HIF1A induces activation of the apoptotic and programmed necrosis by increasing the stability of the tumor suppressor protein p53 and encouraging interaction between calcium ion and calpains respectively. HIF1A can also exacerbate brain edema via increasing the permeability of the BBB. Indeed, neurotoxic role of HIF1A has been reported in focal ischemia where its elevated protein expression in ischemic brain tissues, correlated to an increase hemorrhage conversion of cerebral infarction, which could be abrogated by its inhibitor (Chen et al., 2010a). Increase in blood vessel permeability was further implied by the transcriptional up-regulation of anti-thrombolytic proteins, Plat and Plau, with the former taking place earlier at 8h post-pMCAO (Table 6.1).

-INFLAMMATORY RESPONSE

-Chemokine signaling pathway

Proteins closely associated and participated in chemokine signaling pathway, which eventually contribute to leukocyte chemotaxis (members of CCL and CXCL families and, Jak2 and Rock2) demonstrated substantial increase in gene expression from 8h after

pMCAO initiation. With the transcriptional elevation of these inflammatory markers, this implied the presence of an intense inflammatory response to cerebral ischemic injury. Ccl2 and Ccl12, also known as monocyte chemoattractant protein 1 (Mcp1) and 5 (Mcp5) respectively, have been reported to be downstream transcriptional targets of HIF1, with HIF1A playing a significant role in the induction of the other heterodimeric partner HIF1B to form HIF1 functional transcription complex (Mojsilovic-Petrovic et al., 2007). This would explain the heightened transcriptional up-regulation of Ccl2 and Ccl12 which correlated to that of Hif1a as shown in Table 6.1.

-Leukocyte transendothelial migration

Majority of the proteins involved in the promotion of leukocyte transendothelial migration (adhesion, rolling and infiltration) showed significant transcriptional up-regulation at 24h post-pMCAO (evident from Table 6.1), in accordance with that observed in vasculature development and chemokine signaling pathway. These three biological processes worked in coordinated and concerted effort to facilitate leukocyte infiltration to the site of ischemia to mediate deleterious effects on the progression of tissue damage or beneficial roles during post-ischemia recovery and repair. Particularly Icam1 and Mmp9 were substantially up-regulated as compared to other genes. ICAM1 protein expression on the vascular endothelium is enhanced upon TNF α and IL-1 stimulations, and serves as a bridge for stabilizing endothelial cell and leukocyte adhesion through binding to its receptor integrin(transcriptional up-regulation of Itgb1 shown in Table 6.1) on the leukocytes (Rothlein et al., 1986). On the other hand, MMP9, a member of the MMPs family facilitates propagation and regulation of

neuroinflammatory responses to ischemic brain injury via enzymatic digestion of protein components of the extracellular matrix such as collagen, proteoglycan and laminin, as well as cell-surface and soluble proteins, including receptors and cytokines (Amantea et al., 2009).

-TLRs signaling pathway

TLRs signaling pathway has consistently been implicated in the pathogenesis of cerebral ischemia to remove cell debris and start regenerative process (Brea et al., 2009; Kriz and Lalancette-Hebert, 2009; Marsh et al., 2009), and indeed, genes encoding for players in this pathway (Il1b, Il6, Tlr2) demonstrated significant transcriptional up-regulation between 8-24h post-pMCAO (Table 6.1). A recent article by Tu et al., 2010 reported a prominent role of TLR2/4 signaling pathway in aggravation of ischemic brain injury through mediating the inflammatory reaction (Tu et al., 2010). As shown in Table 6.1, Tlr2 is significantly up-regulated at 24h time-point. Origin of TLRs activation has recently been attributed to damage-associated molecular pattern molecules (DAMPs) that are released during conditions of oxidative stress (Gill et al., 2010).

-CELL HOMEOSTASIS, SURVIVAL AND PROLIFERATION

Recent studies have demonstrated that neurotrophic factors are critical in neurogenesis promotion after cerebral ischemia (Kernie and Parent, 2010; Leker et al., 2009). As shown in Table 6.1, numerous genes encoding for neurotrophic and pro-mitogenic factors were significantly up-regulation over the 24-hour profiling period: c-Fos, Jun, Dtr, Bdgf, Fgf2 and Myc showed early up-regulation at 8h, and Birc2/3, Igfbp3, Fgf2, Ngfb and

Tgfb2 transcriptional activation occurred at 24h post-pMCAO (Table 6.1). Among all, Dtr, also known as heparin-binding epidermal growth factor-like growth factor (Hb-egf), demonstrated the highest transcriptional elevation. HB-EGF is a potent neurotropic factor whose post-administration has been reported to reduce infarct size, thus playing an important role in the stimulation of neurogenesis and angiogenesis after cerebral ischemia (Jin et al., 2004; Kawahara et al., 1999; Sugiura et al., 2005).

-MITOTIC CELL CYCLE REGULATION

Genes encoding for proteins which impede mitotic cell cycle re-activation (Cank1d, Gadd45 (a,b and g) and Inbba) showed transcriptional elevation prominently from 8h post-pMCAO. Accordingly, transcriptional down-regulation was seen in cell cycle-promoting proteins (Camk2(a, b, and g) and Clasp2) (Table 6.1). Paradoxically, Mdm2, endogenous p53-inhibitory binding partner also demonstrated increase in gene expression. Taken together with the transcriptional modulation of p53 downstream target Gadd45, this indicates that the p53 signaling pathway plays an important role during focal cerebral ischemia, indirectly implying an attempt at cell cycle re-activation.

-RESPONSE TO OXIDATIVE STRESS

Anti-oxidant response was strongly evoked during pMCAO as represented by the transcriptional activation of genes encoding for molecular chaperones (Hmox1, Ptgs2, Serpine1, Sod2 and Txndr1) and heat shock proteins (Hsp1b and Hsp2a), especially taking place at 8h (Table 6.1).

-CELL DEATH

Proteins involved directly (Cflar, Casp3 and Casp7) and indirectly (Cebpb, Ddit3 and Nfkbia) in promotion of cell death were transcriptionally up-regulated at 24h and 8h post-pMCAO respectively (Table 6.1). DDIT3 is an endoplasmic reticulum stress-inducible protein which dimerizes with its partner CCAAT/enhancer-binding protein beta (CEBPB) to form a transcription factor to induce expression of downstream pro-death proteins expression, whereas NFKBIA, an inhibitor to the transcription factor NF- κ B, is implicated in the suppression of the pro-survival and proliferative pathways. Since Ddit3 and Nfkbia transcriptional activation preceded that of the caspases (Cflar, Casp3 and Casp7), and taken together with the presence of oxidative stress and cell survival pathway activation at 8h post-pMCAO (as implicated by the early initiation of anti-oxidant response and neurotrophic response), this implied that organellar stress due to overwhelming oxidative burden might be responsible for the activation of caspases-mediated cell death.

Chapter 6.1:
Permanent-MCAO

Table 6.1 Selected differentially-expressed temporal gene profile of neuronal death-related families in vehicle (*i.c.v.* injection of 80% DMSO 30min after surgery) pMCAO-induced adult male Wistar rat cortice. All fold-change expressions are subjected to one-way ANOVA analysis and significant at $p < 0.05$ with Benjamini Hochberg FDR correction. Data are expressed as fold-change \pm sem.

Genbank	Gene Title	Symbol	Vehicle (80% DMSO)	
			8h	24h
<u>Vasculature development</u>				
XM_001065522	Angiopoietin 2	Agpt2	1.43 \pm 0.26	2.82 \pm 1.44
NM_022266	Connective tissue growth factor	Ctgf	-1.19 \pm 0.11	1.76 \pm 0.38
NM_031327	Cysteine rich protein 61	Cyr61	1.97 \pm 0.41	6.33 \pm 0.49
NM_012548	Endothelin 1	Edn1	1.23 \pm 0.32	1.59 \pm 0.35
NM_021654	Gap junction membrane channel protein alpha 4	Gja4	1.29 \pm 0.28	2.68 \pm 0.23
NM_024359	Hypoxia inducible factor 1, alpha subunit	Hif1a	1.09 \pm 0.29	2.20 \pm 0.22
NM_013151	Plasminogen activator, tissue	Plat	2.06 \pm 0.81	2.56 \pm 0.58
NM_013085	Plasminogen activator, urokinase	Plau	1.00 \pm 0.12	1.75 \pm 0.17
NM_013114	Selectin, platelet	Selp	1.03 \pm 0.08	2.20 \pm 0.31
NM_133386	Sphingosine kinase 1	Sphk1	2.23 \pm 0.69	5.55 \pm 1.79
NM_173116	Sphingosine phosphate lyase 1	Sgpl1	1.09 \pm 0.24	1.60 \pm 0.06
NM_053565	Suppressor of cytokine signaling 3	Socs3	1.37 \pm 0.23	1.99 \pm 0.19
NM_031836	Vascular endothelial growth factor A	Vegfa	1.44 \pm 0.31	1.88 \pm 0.52
<u>Inflammatory response</u>				
<u>-Chemokine signaling pathway</u>				
NM_024145	Gardner-Rasheed feline sarcoma viral (Fgr) oncogene homolog	Fgr	-1.00 \pm 0.03	1.84 \pm 0.28
NM_031514	Janus kinase 2	Jak2	1.50 \pm 0.38	2.21 \pm 0.39
NM_013022	Rho-associated coiled-coil forming kinase 2	Rock2	1.07 \pm 0.25	1.83 \pm 0.10
NM_019285	Adenylate cyclase 4	Ancy4	-1.00 \pm 0.18	1.80 \pm 0.29
NM_031530	Chemokine (C-C motif) ligand 2	Ccl2	2.94 \pm 1.40	12.52 \pm 3.18
XM_213425	Chemokine (C-C motif) ligand 12	Ccl12	-1.12 \pm 0.07	2.00 \pm 0.61
NM_019233	Chemokine (C-C motif) ligand 20	Ccl20	1.48 \pm 1.22	6.50 \pm 2.63
NM_053858	Small inducible cytokine A4	Ccl4	3.74 \pm 1.69	2.52 \pm 0.84
NM_001007612	Chemokine (C-C motif) ligand 7	Ccl7	2.81 \pm 1.18	8.86 \pm 2.61
NM_030845	Chemokine (C-X-C motif) ligand 1	Cxcl1	2.14 \pm 0.34	6.62 \pm 2.42
NM_053647	Chemokine (C-X-C motif) ligand 2	Cxcl2	2.39 \pm 0.81	4.96 \pm 9.38
NM_001017478	Chemokine (C-X-C motif) ligand 16	Cxcl16	1.52 \pm 0.66	3.51 \pm 1.59
NM_013106	Guanine nucleotide binding protein, alpha inhibiting 3	Gnai3	1.21 \pm 0.30	1.63 \pm 0.23
NM_133307	Protein kinase C, delta	Prkcd	1.29 \pm 0.31	2.37 \pm 0.77
NM_022380	Signal transducer and activator of transcription 5B	Stat5b	1.22 \pm 0.17	1.52 \pm 0.16
XM_001071741	RAS guanyl releasing protein 2 (calcium and DAG-regulated)	Rasgrp2	-1.08 \pm 0.15	-2.25 \pm 0.05

Chapter 6.1:
Permanent-MCAO

Table 6.1 (continue)

Genbank	Gene Title	Symbol	Vehicle (80% DMSO)	
			8h	24h
<u>-Chemokine signaling pathway (continue)</u>				
NM_012776	Adrenergic receptor kinase, beta 1	Adrbk1	-1.18 ± 0.34	-1.69 ± 0.05
NM_024138	Guanine nucleotide binding protein, gamma 7	Gng7	-1.21 ± 0.20	-2.83 ± 0.03
XM_342524	Phospholipase C, beta 1	Plcb1	-1.21 ± 0.45	-1.96 ± 0.11
<u>-Leukocyte transendothelial migration</u>				
NM_022205	Chemokine (C-X-C motif) receptor 4	Cxcr4	1.12 ± 0.12	2.15 ± 0.60
NM_013106	Guanine nucleotide binding protein, alpha inhibiting 3	Gnai3	1.21 ± 0.30	1.63 ± 0.23
NM_012711	Integrin alpha M	Itgam	1.12 ± 0.18	1.68 ± 0.35
NM_017022	Integrin beta 1 (fibronectin receptor beta)	Itgb1	1.18 ± 0.23	1.65 ± 0.31
NM_012967	Intercellular adhesion molecule 1	Icam1	1.89 ± 0.31	4.47 ± 0.51
NM_031055	Matrix metalloproteinase 9	Mmp9	1.13 ± 0.20	2.95 ± 0.49
NM_030863	Moesin	Msn	1.24 ± 0.16	3.30 ± 0.50
NM_017318	Protein tyrosine kinase 2 beta	Ptk2b	-1.12 ± 0.27	-1.77 ± 0.10
XM_214499	Actinin alpha 2	Actn2	1.02 ± 0.21	-1.96 ± 0.05
XM_215659	Ras homolog gene family, member C	Rhoc	1.30 ± 0.30	1.94 ± 0.09
NM_012628	Protein kinase C, gamma	Prkcc	-1.14 ± 0.28	-1.60 ± 0.07
XM_001074876	Claudin 10	Cldn10	-1.31 ± 0.23	-4.68 ± 0.07
<u>-TLR signaling pathway</u>				
NM_021744	CD14 antigen	Cd14	1.94 ± 0.52	7.30 ± 1.42
NM_031512	Interleukin 1 beta	Il1b	1.55 ± 0.13	3.86 ± 4.08
NM_012589	Interleukin 6	Il6	1.60 ± 0.56	2.08 ± 0.58
XM_239239	Mitogen activated protein kinase kinase 3	Map2k3	1.32 ± 0.31	2.25 ± 0.59
NM_012881	Secreted phosphoprotein 1	Spp1	5.14 ± 3.62	5.02 ± 1.97
XM_001063419	Toll interacting protein	Tollip	1.01 ± 0.09	1.64 ± 0.27
NM_198769	Toll-like receptors 2	Tlr2	1.35 ± 0.16	2.34 ± 0.55
NM_053703	Mitogen-activated protein kinase kinase 6	Map2k6	-1.14 ± 0.06	-3.90 ± 0.04
<u>Cell homeostasis, survival and proliferation</u>				
NM_022197	c-Fos oncogene	c-fos	3.92 ± 2.29	4.34 ± 1.16
NM_021835	v-Jun sarcoma virus 17 oncogene homolog (avian)	Jun	1.73 ± 0.29	1.93 ± 0.19
NM_012945	Diphtheria toxin receptor	Dtr	1.89 ± 0.69	4.96 ± 0.44
NM_021752	Baculoviral IAP repeat-containing 2	Birc2	1.15 ± 0.19	1.84 ± 0.13
NM_023987	Baculoviral IAP repeat-containing 3	Birc3	1.42 ± 0.30	1.98 ± 0.61
NM_012588	Insulin-like growth factor binding protein 3	Igfbp3	1.28 ± 0.40	3.33 ± 0.63
NM_012513	Brain derived neurotrophic factor	Bdnf	1.56 ± 1.11	2.30 ± 0.93
NM_019305	Fibroblast growth factor 2	Fgf2	1.62 ± 0.18	1.60 ± 0.28

Table 6.1 (continue)

Genbank	Gene Title	Symbol	Vehicle (80% DMSO)	
			8h	24h
<u>Cell homeostasis, survival and proliferation (continue)</u>				
NM_012603	Myelocytomatosis viral oncogene homolog (avian)	Myc	1.61 ± 0.27	3.61 ± 0.49
XM_227525	Nerve growth factor, beta	Ngfb	-1.08 ± 0.48	1.75 ± 0.29
XM_001061815	Nuclear factor of activated T-cells, cytoplasmic, calcineurin-dependent 4	Nfatc4	1.58 ± 0.62	3.05 ± 0.86
NM_031131	Transforming growth factor, beta 2	Tgfb2	1.00 ± 0.34	2.19 ± 0.30
NM_053429	Fibroblast growth factor receptor 3	Fgfr3	-1.56 ± 0.10	-1.44 ± 0.05
XM_235565	Mitogen-activated protein kinase 8 interacting protein 2	Mapk8ip2	-1.14 ± 0.20	-1.58 ± 0.09
NM_012513	RAS guanyl releasing protein 2 (calcium and DAG-regulated)	Rasgrp2	-1.08 ± 0.15	-2.25 ± 0.05
NM_022185	Phosphatidylinositol 3-kinase, regulatory subunit, polypeptide 2	Pik3r2	-1.19 ± 0.17	-1.77 ± 0.09
<u>Mitotic cell cycle regulation</u>				
NM_139060	Casein kinase 1, delta	Csnk1d	1.22 ± 0.28	1.52 ± 0.27
XM_001080981	Transformed mouse 3T3 cell double minute 2	Mdm2	1.21 ± 0.33	2.00 ± 0.60
NM_017128	Inhibin beta-A	Inhba	1.54 ± 0.49	2.91 ± 1.32
NM_024127	Growth arrest and DNA-damage-inducible 45 alpha	Gadd45a	1.84 ± 0.66	3.72 ± 1.20
NM_001008321	Growth arrest and DNA-damage-inducible 45 beta	Gadd45b	2.33 ± 0.52	3.28 ± 1.02
XM_001053888	Growth arrest and DNA-damage-inducible 45 gamma	Gadd45g	2.89 ± 0.97	5.94 ± 2.31
NM_012920	Calcium/calmodulin-dependent protein kinase II alpha subunit	Camk2a	-1.21 ± 0.30	-1.81 ± 0.02
NM_021739	Calcium/calmodulin-dependent protein kinase II beta subunit	Camk2b	-1.20 ± 0.20	-2.05 ± 0.13
NM_133605	Calcium/calmodulin-dependent protein kinase II gamma	Camk2g	-1.31 ± 0.15	-2.40 ± 0.10
NM_053722	CLIP associating protein 2	Clasp2	-1.13 ± 0.31	-1.97 ± 0.09
<u>Response to oxidative stress</u>				
NM_012580	Heme oxygenase (decycling) 1	Hmox1	2.31 ± 0.49	4.47 ± 1.54
NM_017232	Prostaglandin-endoperoxide synthase 2	Ptgs2	2.77 ± 1.04	4.44 ± 1.61
NM_012620	Serine (or cysteine) proteinase inhibitor, clade E, member 1	Serpine1	1.73 ± 0.63	6.85 ± 1.04
NM_017051	Superoxide dismutase 2, mitochondrial	Sod2	1.44 ± 0.28	2.04 ± 0.52
NM_031614	Thioredoxin reductase 1	Txnrd1	1.15 ± 0.12	1.95 ± 0.05
NM_031970	Heat shock 27kDa protein 1	Hspb1	2.54 ± 1.15	3.38 ± 0.95
NM_021863	Heat shock protein 2	Hspa2	1.37 ± 0.38	1.78 ± 0.44
<u>Cell death</u>				
NM_024125	CCAAT/enhancer binding protein (C/EBP), beta	Cebpb	1.69 ± 0.68	2.23 ± 0.85

Table 6.1 (continue)

Genbank	Gene Title	Symbol	Vehicle (80% DMSO)	
			8h	24h
Cell death (continue)				
NM_024134	DNA-damage inducible transcript 3	Ddit3	1.62 ± 0.22	1.93 ± 0.38
XM_343065	Nuclear factor of kappa light chain gene enhancer in B-cells inhibitor, alpha	Nfkbia	1.61 ± 0.42	2.37 ± 0.88
NM_057138	CASP8 and FADD-like apoptosis regulator	Cflar	1.12 ± 0.31	4.33 ± 1.09
NM_012922	Caspase 3, apoptosis related cysteine protease	Casp3	1.23 ± 0.28	2.80 ± 0.46
NM_022260	Caspase 7	Casp7	1.07 ± 0.22	1.90 ± 0.36

6.1.2.2 Validation of pMCAO global transcriptomic profile via real-time PCR

Global gene profile of pMCAO model was verified using quantitative real-time PCR which demonstrated similar transcriptional regulation, indicating the high reliability in data interpretation from the microarray analysis.

Table 6.2 Validation of microarray data using real-time PCR technique on pMCAO-induced adult male Wistar rat infarcted cortice treated with 80% DMSO (vehicle). Data are expressed as fold-change \pm sem.

GenBank	Gene Title	Symbol	Vehicle (80% DMSO)			
			8h		24h	
			Microarray	Real-time PCR	Microarray	Real-time PCR
NM_031970	Heat shock 27kDa protein 1	Hspb1	2.54 \pm 1.15	5.10 \pm 0.55	3.38 \pm 0.95	6.43 \pm 0.71
NM_053612	Heat shock 22kDa protein 8	Hspb8	1.88 \pm 0.65	1.95 \pm 0.74	2.69 \pm 0.87	4.84 \pm 0.73
NM_017232	Prostaglandin-endoperoxide synthase 2	Ptgs2	2.77 \pm 1.04	6.19 \pm 0.83	4.44 \pm 1.61	6.59 \pm 0.72
NM_031530	Chemokine (C-C motif) ligand 2	Ccl2	2.94 \pm 1.40	5.45 \pm 0.48	12.52 \pm 3.18	
NM_030845	Chemokine (C-X-C motif) ligand 1	Cxcl1	2.14 \pm 0.34	4.26 \pm 0.71	6.62 \pm 2.42	
NM_021744	CD14 antigen	Cd14	1.94 \pm 0.52	2.93 \pm 0.89	7.30 \pm 1.42	16.06 \pm 0.76
NM_012924	CD44 antigen	Cd44	1.25 \pm 0.30		3.60 \pm 0.29	6.34 \pm 0.94
NM_053819	Tissue inhibitor of metalloproteinase 1	Timp1	2.84 \pm 1.42	10.13 \pm 0.95	6.30 \pm 1.22	10.02 \pm 0.73

6.1.3 Discussion

Permanent focal cerebral ischemia occurs when timely reperfusion to the occluded region is not provided, resulting in the penumbra region succumbing to irreversible cellular injury and subsequent demise, with consequential expansion of the ischemic core. As such, it represents the highest degree of severity in terms of infarct damage. During permanent focal ischemia, prolonged period of oxygen/glucose deprivation as a result of no blood flow enhances Glu accumulation in the extracellular space and inflict microvascular injury, aggravating excitotoxicity and BBB impairment respectively. These two aforementioned neuropathological processes eventually contribute to oxidative stress and neuroinflammation.

As permanent focal cerebral ischemia presents a rapid and severe disease progression, global gene profiling of its pathogenesis would provide useful temporal transcriptional information pertaining to its downstream biological outcomes. Furthermore, the pMCAO model adopted in the present study involved the removal of a section of the middle cerebral artery, which implies that the blood flow to the affected brain region was instantaneously dropped to zero, and the detrimental impact of ischemia was experienced at most intense, with immediate cutoff of oxygen and glucose supply. This rapidly accelerated the ischemic cascade progression. This is unlike that of the suture-induced transient cerebral ischemia model where there is still a 20-30% residual blood supply to the occluded region to slow down the transduction of ischemic cascade signaling. This would explain why neuroinflammation and oxidative stress are the two major pathophysiological mechanisms demonstrated in these models, as both constitute the

downstream cellular outcomes of cerebral ischemia.

Occurrence of neuroinflammation as a result of leukocyte infiltration into the brain during BBB dysfunction is especially prominent from the transcriptional activation of proteins involved in the inflammatory and defense cascades: chemokine signaling, leukocyte transendothelial migration and TLR cascade. Within hours after the ischemic insult, enhanced circulating level of cytokines and chemokines promotes elevation of CAMs on cerebral endothelial cells to enable attachment and transendothelial migration of activated neutrophils and monocytes. Undesirable buildup and aggregation of these immune cells may further diminish cerebral blood flow, or extravasate into the brain parenchyma. Extensive release of the pro-inflammatory mediators such as cytokines, chemokines and ROS/RNS from infiltrating leukocytes and resident brain cells, including neurons and glia, accelerates the progression of tissue damage (Reviewed in (Amantea et al., 2009)).

TLRs, critical components of the innate immune system, play an important role in cerebral ischemia through mediation of inflammatory response that could inflict secondary ischemic damage, and simultaneously remove cell debris to pave the route for post-ischemia regeneration. A recent study by marsh et al. (2009) suggested that systemic administration of TLR ligands induces a state of tolerance to subsequent ischemic injury via suppression of pro-inflammatory molecules expression and induction of numerous anti-inflammatory mediators that concertedly confer robust neuroprotection (Marsh et al., 2009).

Chapter 6.1: Permanent-MCAO

Similarly, oxidative stress is apparent from the strong transcriptional up-regulation of anti-oxidative pathways made up of Hsps and molecular chaperones, Nrf2-mediated transcriptional anti-oxidant response and GSH metabolic pathway. A recent article by Gill et al. (2010) associated oxidative stress with neuroinflammation through the activation of TLRs by DAMPs. In conclusion, current global gene profiling of permanent focal cerebral ischemia further highlights the significant implications of oxidative stress and neuroinflammation and their coordinated cooperation in inducing neuronal demise during the disease pathogenesis, which are consistent with the observations made in transient model (Gill et al., 2010).

**Chapter 6.2:
Application of
Cell Cycle Inhibitor
on
Permanent
Focal Cerebral Ischemia**

6.2 .1 Introduction

Global transcriptomic profiles of *in vivo* models of cerebral ischemia (hypoxic, transient and permanent focal ischemia) demonstrated elevation in gene expression of pro-mitogenic proteins such as growth factors and cell cycle proteins. Specifically, no significant or down-regulation of Ccnd (Ccnd1 and Ccnd2) or cyclin-dependent kinase 4 or 6 (Cdk4 and Cdk6) was observed. The proteins of these encoding genes form a complex [CCND/CDK(4 or 6)] crucial to initiate mitotic cell cycle entry from quiescent G0 state to G1 state. This discrepancy could be a result of the rapid occurrence of cell cycle re-entry much earlier before the 5h studied time-point, causing a miss in the timeframe for detection of their transcriptional peak. As such, in order to verify that cell cycle re-activation was indeed triggered during cerebral ischemia as a result of iGluRs-induced excitotoxicity, a specific cell cycle protein kinase family, aurora kinases (AURKs) was chosen as the biological target for pharmacological inhibition study to determine its efficacy in abrogation of cerebral infarct damage.

De-regulated, aberrant expression of neuronal cell cycle proteins have been consistently reported in the CNS of patients with neurodegenerative pathologies such as AD, PD and ALS, neurological disorders including stroke, Niemann Pick's disease, DS and progressive supranuclear palsy as well as schizophrenia (Camins et al., 2008; Camins et al., 2007; Nunomura et al., 2007; Woods et al., 2007). Its extensive prevalence in the pathogenesis of numerous CNS-associated pathological conditions suggested that its involvement in the mediation of neuronal death could not be undermined. Existing evidence supporting the occurrence of cell cycle re-entry in post-mitotic, differentiated

Chapter 6.2: AURKs inhibitor on permanent-MCAO

neurons upon neuronal insults includes the activation of cyclin-dependent kinases (CDKs) and cyclins, inhibition of cell cycle checkpoint proteins e.g. p27 and retinoblastoma protein and the expression of the transcription factor E2F-1 (Akashiba et al., 2008; Camins et al., 2007; Krantic et al., 2005; Lopes and Casares, 2010).

In *in vivo* models, cell cycle re-activation has been suggested to play a pivotal role in the mediation of neuronal loss in excitotoxicity induced by kainic acid, models of stroke, MPTP-induced PD model, 3-nitropropionic acid-induced HD model, and the SOD-1 mouse model of ALS (Hoglinger et al., 2007; Nguyen et al., 2003; Pelegri et al., 2008; Verdaguer et al., 2003). Similar observation has been reported in *in vitro* neuronal culture models challenged with apoptotic stimuli such as K^+ deprivation in cerebellar granule cells (Yeste-Velasco et al., 2007), treatment with excitatory amino acid Glu and KA (Gendron et al., 2001; Smith et al., 2003; Verdaguer et al., 2004a; Verdaguer et al., 2003), $A\beta$ treatment (Iqbal and Grundke-Iqbal, 2008; Majd et al., 2008) and camptothecin treatment (Park et al., 2000). These studies consistently report that neuronal insults elevate cell cycle-involved proteins and the pro-apoptotic transcription factor E2F-1, and that cell cycle re-activation may be a central event to the initiation of neuronal death in numerous neurodegenerative diseases and disorders. This theory is supported by evidence that inhibition of CDKs by drugs such as flavopiridol and roscovitine offer neuroprotection in neuronal cell cultures (Verdaguer et al., 2004a). This is because CDK5 and E2F-1 can be regulated by calpain activation during neuronal loss in the pathogenesis of neurodegenerative diseases (Crespo-Biel et al., 2007).

6.2.1.1 Aurora kinases (AURKs): A recently acknowledged family of crucial cell cycle protein kinases

Successful facilitation of normal cell division is governed by the physiological role of key regulatory protein kinases which comprise of CDKs, polo-like kinases (PLKs) and aurora kinases (AURKs). These protein kinases regulate mitotic entry and coordinates chromosomal and cytoskeletal events, ensuring correct separation of identical genetic material into the two daughter cells. Compromised function and deregulated expression of these players frequently result in aneuploidy and have been closely associated with tumourigenesis, highlighting them as potential targets for anti-cancer therapeutic treatments.

In particular, AURKs, a conserved family of Serine/Threonine kinases consisting of three family members (AURKA, AURKB and AURKC), has been gaining increasing recognition for their critical roles in mitosis and cytokinesis. The occurrence of AURK members differs from species to species: Only a single aurora gene is found in fungi, while in majority of higher eukaryotes, the incidence of AURK members increases with AURKA and AURKB adopting distinct localizations and functions. The third member, AURKC primarily expressed in the testis only occurs in mammals. In our current study we will focus on AURKA and AURKB implication in the excitotoxicity, a major event in the pathogenesis of cerebral ischemia, as evident from their transcriptional up-regulation from in vitro models (discussed later in Results section 6.2.2.1)

Chapter 6.2:
AURKs inhibitor on permanent-MCAO

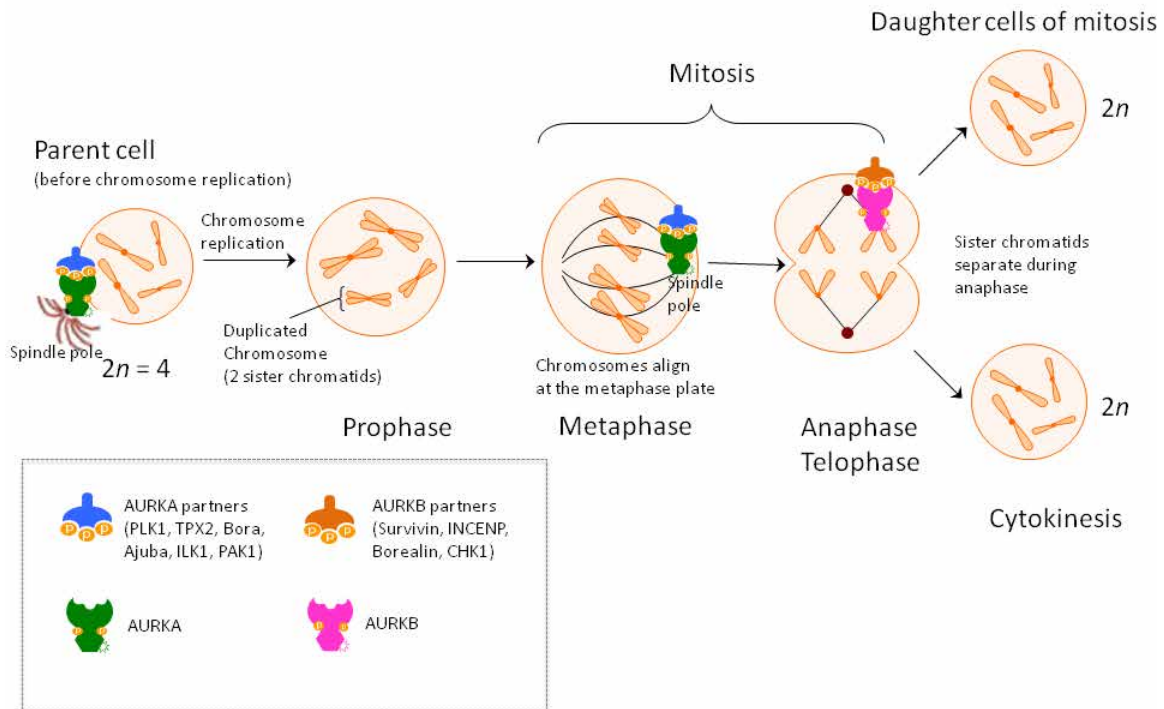


Figure 6.2 An overview of AURKA and AURKB involvements in the various phases of mitotic cell cycle process.

Even though AURKA and AURKB share high degree of sequence and structural homology with 70% identity in the catalytic domain, they adopt unique subcellular localization and diverse functions during mitosis due to their specific association with distinct cofactors, and temporal expression and pathway-specific degradation. AURKA is essential for mitotic entry via spindle pole association, centrosome maturation and separation, G2 to M transition and spindle bipolarity (Barr and Gergely, 2007; Fu et al., 2007; Hirota et al., 2003; Vader and Lens, 2008). AURKA functions are attributed to its ability to bind to microtubules coupled with its location at the spindle poles. Aberrant

Chapter 6.2: AURKs inhibitor on permanent-MCAO

AURKA over-expression has been identified in the pathogenesis of a variety of human cancer types such as breast, colorectal, bladder, pancreatic, esophageal, lung and ovarian as well as leukemia (Comperat et al., 2007; Lassmann et al., 2007; Li et al., 2003; Nishida et al., 2007; Tanaka et al., 1999; Tong et al., 2004).

The most well known AURKA cofactor is TPX2, a microtubule-associated protein (MAP) that directs the kinase to the mitotic spindle, but not the centrosome, and activates it (Kufer et al., 2002). TPX2 has a dual role in AURKA activation. Its N-terminus binds the kinase, inducing a conformational change that facilitates auto-phosphorylation of Thr288 in AURKA T-loop (Bayliss et al., 2003; Eysers et al., 2003). Bound TPX2 then shields this residue from dephosphorylation by protein phosphatase 1 (PP1) on entry into mitosis (Bayliss et al., 2003; Eysers et al., 2003).

Other activating cofactors comprising of Ajuba, Bora, inhibitor-2, integrin-like kinase and PAK1 co-localise with, and seemingly positively regulate, AURKA at the centrosome and/or microtubule asters. On the contrary, protein phosphatase 1 (PP1) and 2A (PP2A) attach and inhibit AURKA via dephosphorylation of Thr288, keeping AURKA inactive at interphase by stabilizing PTTG1 (pituitary tumor transforming gene 1; a mammalian securing protein that inactivates AURKA) (Tong et al., 2008). Particularly, the most prominent *in vivo* protein that may inhibit AURKA activity directly and/or indirectly is p53, where itself and its downstream target GADD45a co-localize at the centrosome to inhibit AURKA (Shao et al., 2006). TPX2 binding harbours AURKA T-loop from p53 inactivation (Eysers and Maller, 2004).

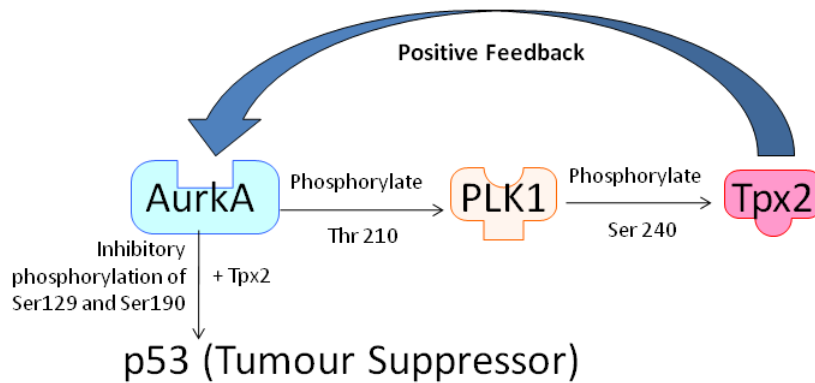


Figure 6.3 A simple signaling pathway demonstrating the most prominent transduction cascade of AURKA in the positive regulation of mitotic cell division.

On the other hand, AURKB being the enzymatically active member of the chromosomal passenger complex (CPC) amidst other protein components which include the scaffolding protein INCENP and the target subunits Survivin and Borealin/Dasra B. Up to the metaphase stage, CPC interacts with the inner centromere and subsequently progresses to the spindle midzone, equatorial cell cortex and midbody in the late mitosis and cytokinesis (Ruchaud et al., 2007; Vader and Lens, 2008). AURKB plays a pivotal role in the regulation of chromosomal interactions with microtubules, chromatid cohesion, spindle stability and cytokinesis (Ruchaud et al., 2007).

Chapter 6.2:
AURKs inhibitor on permanent-MCAO

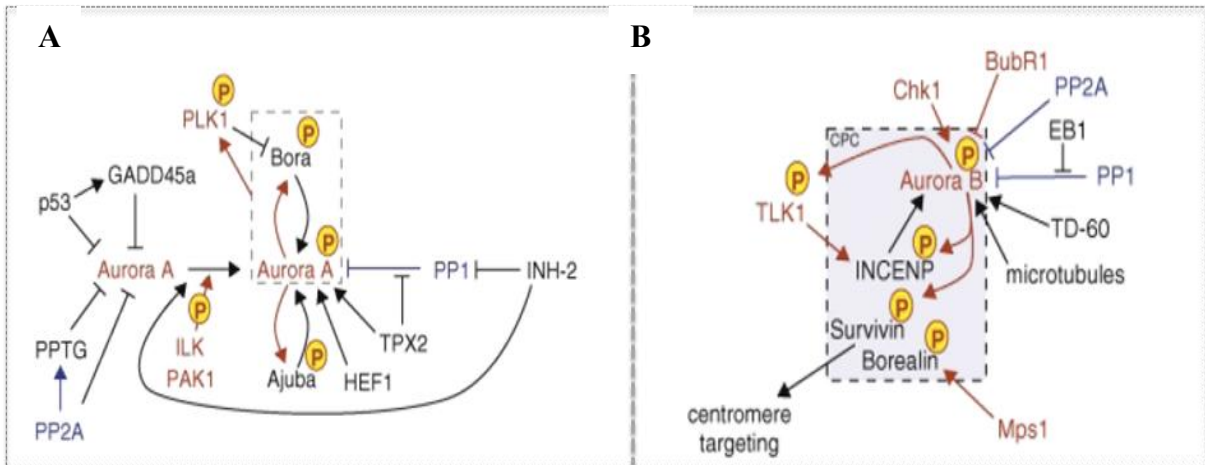


Figure 6.4 The main regulators of **(A)** Aurora A and **(B)** Aurora B kinases. Protein kinases are indicated in **red** and phosphorylation events by red arrows. Protein phosphatases are indicated in **blue**. (Image adapted from Carmena et al. 2009)

6.2.2 Results

6.2.2.1 Cell cycle re-activation is an early upstream event during excitotoxicity *in vitro*: Significant role of AURKs

Comparative microarray analysis of Glu and specific iGluR agonists (NMDA, AMPA and KA) demonstrated the occurrence of cell cycle re-activation in excitotoxicity during the early 5h time-point post-treatments. This is in consistent with existing literature reports and that pharmacological application of CDKs inhibitors is able to successfully attenuate excitotoxicity-induced neuronal death (Smith et al., 2003; Verdaguer et al., 2004a; Verdaguer et al., 2003). Taken together, all observations are directed to cell cycle re-activation being an early upstream process during excitotoxicity, and highlighting that its occurrence is crucial to the mediation of downstream neuronal injury and death. Furthermore, what is interesting is that the present *in vitro* excitotoxicity models for the first time identified AURKs involvement in excitotoxicity.

Specifically, AurkA, and its activating cofactor Tpx2 and downstream effector Plk demonstrated significant early transcriptional up-regulation as shown in Table 6.3. Concurrently and interestingly, AurkB and its activating cofactor Survivin also showed elevated gene expression at 5h post-treatment in all excitotoxicity-induced treatments except Glu (demonstrated in Table 6.3). Other than activating iGluRs, Glu can also trigger G-protein coupled mGluRs. This slight discrepancy is probably attributed to AURKB distinct functions from AURKA, resulting in its transcriptional downplay by the metabotropic subtype of GluRs, an effect as opposed to that of ionotropic subtype. This is

Chapter 6.2:
AURKs inhibitor on permanent-MCAO

then reflected by the absence of significant differential expression in the Glu global transcriptomic profile.

Table 6.3 Transcriptional profiles of Aurks and associated cofactors in *in vitro* excitotoxicity models. All fold-change expressions are subjected to one-way ANOVA analysis and significant at $p < 0.05$. Data are expressed as fold-change \pm sem.

Genbank	Gene Title	Symbol	Time-points		
			5h	15h	24h
<u>Glu</u>					
NM_011497	Aurora kinase A	AurkA	1.91 \pm 0.42	1.98 \pm 0.50	1.59 \pm 0.44
NM_011121	Polo-like kinase 1 (Drosophila)	Plk	2.08 \pm 0.32	2.06 \pm 0.37	1.62 \pm 0.30
NM_028109	TPX2, microtubule-associated protein homolog (Xenopus laevis)	Tpx2	1.70 \pm 0.42	2.09 \pm 0.55	1.57 \pm 0.46
<u>NMDA</u>					
NM_011497	Aurora kinase A	AurkA	1.65 \pm 0.40	1.31 \pm 0.32	1.11 \pm 0.26
NM_011121	Polo-like kinase 1 (Drosophila)	Plk	1.90 \pm 0.38	1.44 \pm 0.21	-1.10 \pm 0.20
NM_028109	TPX2, microtubule-associated protein homolog (Xenopus laevis)	Tpx2	1.79 \pm 0.49	1.48 \pm 0.33	1.11 \pm 0.25
XM_181344	Aurora kinase B	AurkB	1.61 \pm 0.45	1.33 \pm 0.43	1.02 \pm 0.36
NM_009689	Baculoviral IAP repeat-containing 5	Survivin	1.99 \pm 0.47	1.34 \pm 0.31	-1.07 \pm 0.22
<u>AMPA</u>					
NM_011497	Aurora kinase A	AurkA	2.31 \pm 0.56	1.48 \pm 0.36	1.04 \pm 0.25
NM_011121	Polo-like kinase 1 (Drosophila)	Plk	1.80 \pm 0.46	1.27 \pm 0.41	-1.08 \pm 0.26
NM_028109	TPX2, microtubule-associated protein homolog (Xenopus laevis)	Tpx2	2.40 \pm 0.52	1.19 \pm 0.42	-1.08 \pm 0.20
XM_181344	Aurora kinase B	AurkB	1.74 \pm 0.62	1.05 \pm 0.40	-1.24 \pm 0.24
NM_009689	Baculoviral IAP repeat-containing 5	Survivin	1.94 \pm 0.50	1.25 \pm 0.37	-1.03 \pm 0.26
<u>KA</u>					
NM_011497	Aurora kinase A	AurkA	2.30 \pm 0.55	1.46 \pm 0.37	1.07 \pm 0.29
NM_011121	Polo-like kinase 1 (Drosophila)	Plk	1.75 \pm 0.41	1.55 \pm 0.26	1.15 \pm 0.37
NM_028109	TPX2, microtubule-associated protein homolog (Xenopus laevis)	Tpx2	1.90 \pm 0.49	1.49 \pm 0.45	1.06 \pm 0.35
XM_181344	Aurora kinase B	AurkB	2.01 \pm 0.73	1.09 \pm 0.43	1.10 \pm 0.46
NM_009689	Baculoviral IAP repeat-containing 5	Survivin	2.09 \pm 0.59	1.39 \pm 0.35	1.21 \pm 0.31

6.2.2.2 Inhibition of AURKs attenuates infarct damage upon pMCAO

Supposedly if AURKs play a pivotal role in cell cycle re-entry as that of CDKs during excitotoxicity, it would be worthwhile to ascertain in parallel the patho-physiological importance of AURKs in *in vivo* ischemic stroke model where excitotoxicity is causative. As such, a selective AURKs (particularly AURKA and AURKB) pharmacological inhibitor, ZM447439 has been employed to determine its efficacy in reduction of infarct damage during pMCAO. As ZM447439 is only soluble in organic solvent e.g. DMSO and not polar solvents e.g. water, much attention has been focused on reducing DMSO solvent concentration during drug preparation to prevent physiological disturbance by DMSO presence yet achieve complete solubilization of the compound. As it turns out, 80% DMSO in normal saline is the most optimal solvent composition attained. 5ul volume of the desired concentration of ZM447439 was designed to be injected intracerebroventricularly (*i.c.v*) into the left hemisphere of the rat brain 30min post-pMCAO surgery so as to mimic real-life re-enactment of stroke episode. A randomized pilot study to ascertain the concentration-dependent effect of ZM447439 upon pMCAO was conducted using n = 4 for each condition. As shown in Figure 6.5, the area of infarct diminishes with escalating doses of ZM447439 from 10mM up to 30mM. Furthermore, 80% DMSO did not induce any change to the infarct volume induced by pMCAO. Much higher concentrations of ZM447439 were not performed, as the pharmacological specificity of the drug would be altered, resulting in inhibition of other protein kinases such as protein kinase C and phosphatidylinositol-3-kinase.

Chapter 6.2: AURKs inhibitor on permanent-MCAO

Based on the concentration-effect observations from Figure 6.5, 30mM ZM447439 seemingly appeared to be effective in abrogation of infarct injury induced by 30min. As such, a repeated experiment employing 30mM ZM447439 together with its corresponding vehicle control was conducted (n = 8 each) to validate its effect 30min post-pMCAO. Quantitative analysis using Image J software on the infarct volume which has been corrected for brain edema and brain tissue contraction demonstrated a significant decrease in the infarct damage upon 5ul *i.c.v.* injection of 30mM ZM447439 as shown in Figure 6.6.

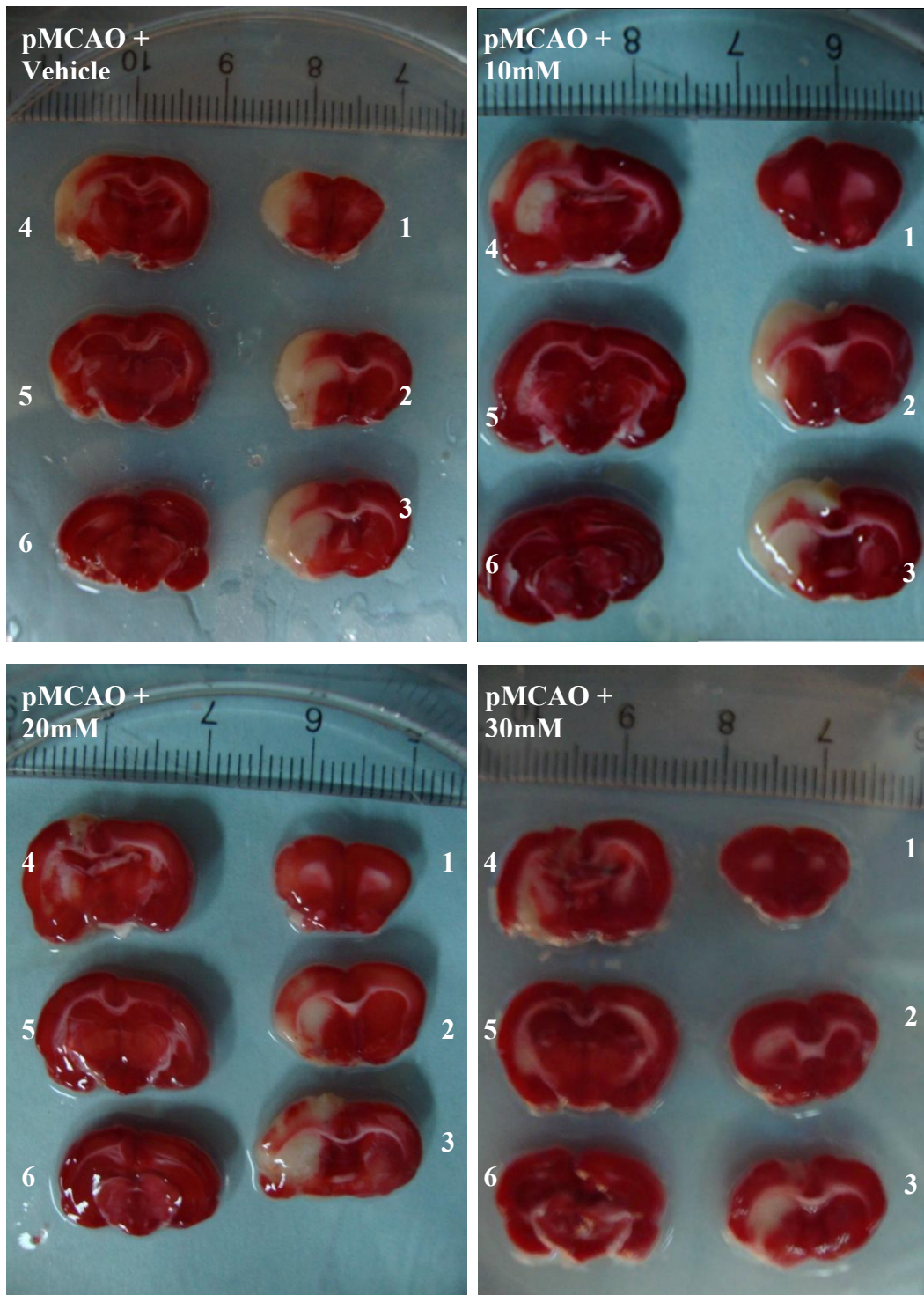


Figure 6.5. TTC staining of 2mm sections of rat brain demonstrated a concentration-dependent reduction in infarct volume during pMCAO upon escalating dose application of selective pharmacological AURK inhibitor ZM447439 [1 – 6: anterior – posterior].

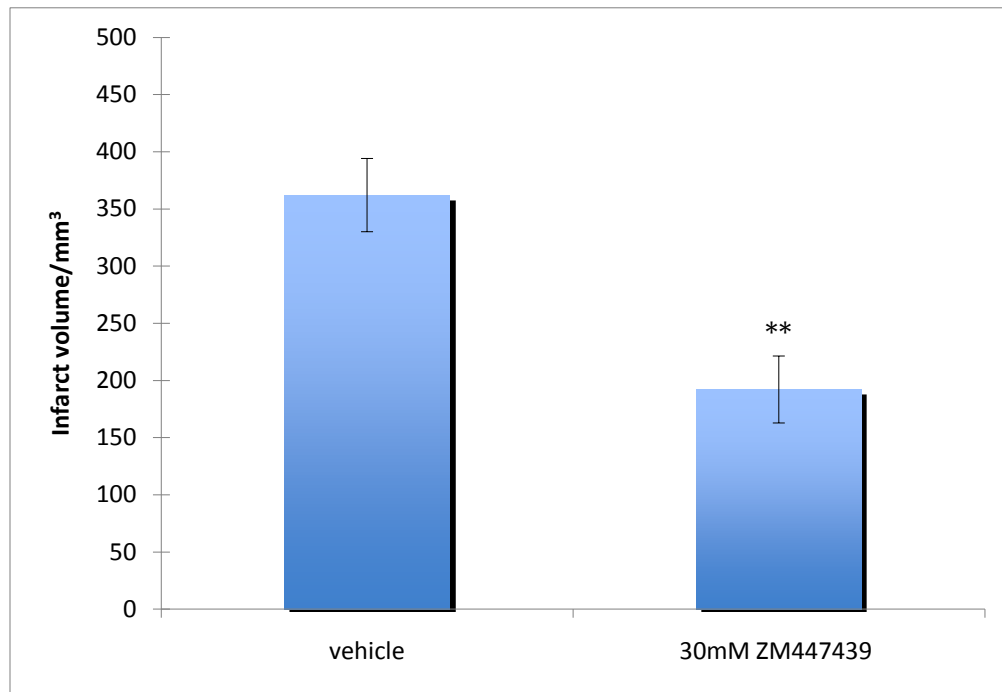


Figure 6.6 Quantitative analysis of the infarct volume corrected for brain edema and infarct tissue contraction demonstrated that 5ul *i.c.v.* injection of 30mM ZM447439 30min post-pMCAO successfully attenuated infarct damage. Data generated here is representative of 6 replicates. Data is statistically significant at ** $p < 0.01$.

6.2.2.3 AURKs inhibition significantly modulates pMCAO global transcriptomic profile

In order to understand the mechanistic influence behind AURKs inhibition on the attenuation of infarct damage, a temporal global transcriptomic profiling of 30mM ZM447439 treatment after pMCAO was conducted in complement to that of the microarray data analysis of pMCAO alone using Illumina® Rat Ref12V1 genechips. The schematic experimental layout is identical to that of vehicle-pMCAO and demonstrated previously on Page 259. Four biological replicates were used for each time-point (8h and 24h post-*i.c.v.* injection). As a refresher, significantly/differentially-expressed genes refer to those demonstrating at least ± 1.5 fold-expression in at least one out of the two time-points and have passed statistical testing of one-way ANOVA with $p < 0.05$ and Benjamini-Hochberg FDR correction. As before, the significantly-modulated list of genes was subjected to DAVID analysis which through gene enrichment classified genes according to their respective biological processes.

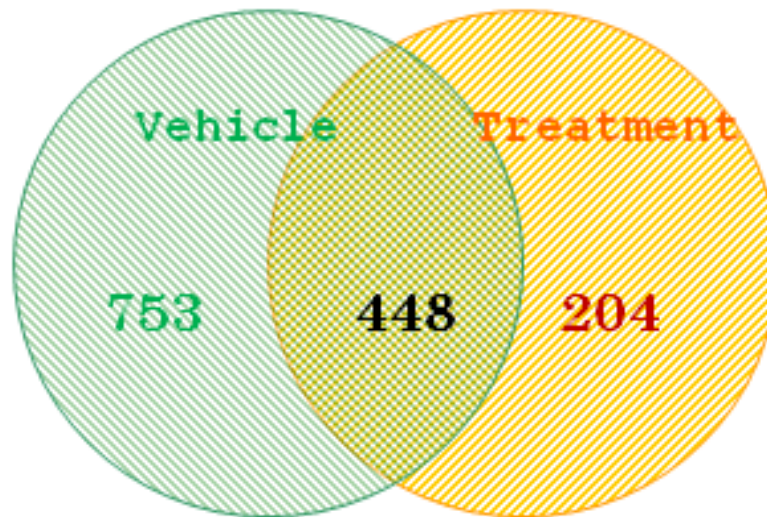
30mM AURK inhibitor treatment after pMCAO generated a genelist of 652 statistically significant differentially expressed candidates. DAVID-processed functional gene ontology clustering of these genes (corresponding to 612 biologically-annotated genes) demonstrated that majority of them were related to the inflammation cascades from chemotaxis and facilitation of leukocyte infiltration to activation of an immune response.

In order to determine the signaling pathways affected when 30mM ZM447439 was post-administered to pMCAO and that consequentially lead to infarct reduction, a comparative

Chapter 6.2: AURKs inhibitor on permanent-MCAO

microarray analysis of significantly-expressed genes between vehicle-pMCAO and AURKs inhibitor treatment-pMCAO was performed. The result of this bi-model comparison was demonstrated in a Venn diagram shown in Figure 6.7. It yielded gene counts of 448 differentially expressed RefSeq transcripts common to both models and, 753 and 204 gene probes exclusive to the vehicle and treatment conditions respectively. Functional annotation and clustering using DAVID 6.7 was performed on all three distinct genelists to determine the effects of AURKs inhibition on the inhibition/activation of signaling cascades and if additional pathways were recruited. Several enriched biological processes were recognized from the lists of differentially-expressed gene probes common to vehicle and treatment conditions and exclusive to the former. On the other hand, functional-gene ontology classification of the 204 differentially-expressed gene probes significantly modulated only in AURKs inhibitor treatment-pMCAO condition (correspond to 192 DAVID-recognizable genes) did not yield any over-represented biological signaling pathways, demonstrating that AURKs inhibition did not recruit additional downstream biological processes to aid in its abrogation of infarct damage.

pMCAO



8 - 24h

Figure 6.7 Venn diagram illustrating number of differentially-expressed annotated genes common and exclusive to both pMCAO + Vehicle and pMCAO + 30mM ZM447439 treatment global gene profiles at 8h and 24h. Gene count is made up of genes with significant regulation of at least ± 1.5 fold-change in one out of two time-points in each condition and have passed one-way ANOVA, $p < 0.05$.

6.2.2.4 Comparative microarray analysis of differentially-expressed genes common to vehicle and treatment groups revealed AURKs inhibition induces a diminished transcriptional-amplitude response

Functional clustering of commonly-occurring genes in both vehicle and treatment conditions revealed vasculature disruption, and inflammation (chemokine signaling pathway, transendothelial migration, complement and coagulation cascade and TLR signaling pathway) and cell death and survival as the main over-represented biological processes being modulated upon pMCAO (Table 6.4).

-VASCULATURE DEVELOPMENT

Majority of the genes involved in regulation of the blood vessel structural integrity and permeability demonstrated up-regulation, indication of microvascular injury leading to increase vascular leakage to permit infiltration of leukocytes and other molecules. However, a smaller-amplitude but similar transcriptional response was demonstrated upon AURKs inhibition (Table 6.4). Interestingly, Mmp14 and Nos3 demonstrated an opposing trend i.e. AURKs suppression promotes their expression at 24h time-point.

-INFLAMMATORY RESPONSE

Majority of the genes encoding for proteins involved in initiation and propagation of an inflammatory response demonstrated significant transcriptional regulation at 8h for the chemokine signaling pathway, and at 24h for those involved in facilitation of leukocyte transendothelial migration, complement and coagulation cascade and TLR signaling pathway (Table 6.4). However, upon fold-expression between vehicle and AURKs

Chapter 6.2: **AURKs inhibitor on permanent-MCAO**

inhibitor treatment, it becomes apparent that a lower transcriptional response was observed in the latter, a probable indication of less degree of neuroinflammation when AURKs were functionally inhibited.

-Chemokine signaling pathway

Vehicle and treatment conditions demonstrated difference in transcriptional modulation of the chemokine signaling pathway prominently at 24h post-i.c.v. injection, where the latter demonstrated a reduced increase in gene expression of implicated members upon AURKs inhibition (Table 6.4). This is especially true for members of the C-C (Ccls) and C-X-C (Cxcls) motifs chemokine families, particularly Ccl2, Ccl7, Cxcl1 and Cxcl2.

-Leukocyte transendothelial migration

Similar lower expression-amplitude observation in AURKs inhibitor treatment condition than that of vehicle was observed for the cell adhesion molecules (F11r, Ecam, Igam and Icam1), all of which promote leukocyte migration into ischemic region (Table 6.4). Similar trend is observed for matrix metalloproteinase-9 (Mmp9) and its endogenous inhibitor, Timp.

-Complement and coagulation cascade

While majority of the genes encoding for proteins in the complement and coagulation cascade demonstrated significant up-regulation in the vehicle condition, the contrary is observed in the treatment condition with most of the genes showing close to basal and

Chapter 6.2:
AURKs inhibitor on permanent-MCAO

insignificant regulation, indicative of an absence of this biological process occurring during AURKs inhibition (Table 6.4).

-TLRs signaling pathway

Transcriptional up-regulation of members involved in the TLRs signaling pathway was observed throughout the 8 - 24h profiling period, with the direct players (Tlr2 and Tollip) showing increase in expression at the later time-point (Table 6.4). In accordance with the observations made in other inflammation-related processes, a smaller transcriptional response was evoked upon AURKs inhibition.

-CELL HOMEOSTASIS, SURVIVAL AND PROLIFERATION

Genes encoding for growth factors (Bdnf, Ngfb and Igfbp3) and pro-mitogenic proteins (Birc3 and Birc5) demonstrated lower heightened transcriptional regulation upon AURKs inhibition, a probable indication of reduced cellular death stimuli from decreased degree of inflammation and oxidative stress (Table 6.4).

-MITOTIC CELL CYCLE

Cell cycle proteins involved in the impediment of cell cycle re-activation (Gadd45a, Gadd45g and Inhba) were significantly up-regulated while those promoting mitosis (Camk2(a and g), Csnk1d and Mdm2) were up-regulated especially in the vehicle condition. On the contrary, an insignificant or lower transcriptional response was demonstrated for these genes in the AURKs inhibitor treatment condition after pMCAO (Table 6.4). This is expected as AURKs are involved in mitosis, and their inhibition

Chapter 6.2:
AURKs inhibitor on permanent-MCAO

would be translated to a decreased stimulation in cell cycle re-entry, indicative of successful inhibition of this family of cell cycle protein kinases.

-RESPONSE TO OXIDATIVE STRESS

Genes encoding for heat shock proteins (Hsps) and molecular chaperones (Ptgs2, Sod2, Txnrd1, Hsp(a2, b1 and b8) and Hmox1) demonstrated comparable up-regulation in vehicle and treatment conditions, an indication that AURKs inhibition did not suppress oxidative stress (Table 6.4).

-CELL DEATH

As shown in Table 6.4, Cebpb and Ddit3, endoplasmic reticulum stress-inducible pro-apoptotic genes, demonstrated comparable transcriptional up-regulation with or without AURKs inhibition, further suggesting that oxidative stress was not affected by the pharmacological suppression of AURKs. On the other hand, a lower transcriptional activation of the caspase family has been observed, especially with Cflar and Casp3 after AURKs inactivation.

Chapter 6.2:
AURKs inhibitor on permanent-MCAO

Table 6.4 Functional annotation of genes common to vehicle (80% DMSO) and 30mM ZM447439 treatment conditions induced via *i.c.v.* administration 30min post- pMCAO. All fold-change expressions were subjected to one-way ANOVA analysis and Benjamini-Hochberg correction, and significant at $p < 0.05$. Data are expressed as fold-change \pm sem.

Genbank	Title	Symbol	Vehicle-pMCAO		Treatment-pMCAO	
			8h	24h	8h	24h
<u>Vasculature development</u>						
NM_012924	CD44 antigen	Cd44	1.25 \pm 0.30	3.60 \pm 0.29	-1.06 \pm 0.12	2.21 \pm 0.53
NM_139104	EGF-like domain 7	Egfl7	-1.05 \pm 0.20	1.79 \pm 0.25	1.02 \pm 0.15	1.68 \pm 0.76
XM_001065522	Angiopoietin 2	Agpt2	1.43 \pm 0.26	2.82 \pm 1.44	1.24 \pm 0.07	2.13 \pm 0.46
NM_022266	Connective tissue growth factor	Ctgf	-1.19 \pm 0.11	1.76 \pm 0.38	-1.49 \pm 0.17	1.59 \pm 0.38
NM_031327	Cysteine rich protein 61	Cyr61	1.97 \pm 0.41	6.33 \pm 0.49	1.50 \pm 0.38	4.35 \pm 1.59
NM_001004228	Endomucin	Emcn	-1.79 \pm 0.07	-1.04 \pm 0.41	-1.73 \pm 0.20	-1.17 \pm 0.26
NM_021654	Gap junction membrane channel protein alpha 4	Gja4	1.29 \pm 0.28	2.68 \pm 0.23	1.15 \pm 0.13	2.04 \pm 0.58
NM_024359	Hypoxia inducible factor 1, alpha subunit	Hif1a	1.09 \pm 0.29	2.20 \pm 0.22	-1.18 \pm 0.08	1.63 \pm 0.12
NM_031056	Matrix metalloproteinase 14 (membrane-inserted)	Mmp14	-1.03 \pm 0.34	1.48 \pm 0.26	-1.01 \pm 0.09	1.92 \pm 0.61
NM_021838	Nitric oxide synthase 3, endothelial cell	Nos3	1.07 \pm 0.24	1.77 \pm 0.60	1.18 \pm 0.29	2.03 \pm 0.56
NM_013114	Selectin, platelet	Selp	1.03 \pm 0.08	2.20 \pm 0.31	1.06 \pm 0.24	1.61 \pm 0.49
NM_133386	Sphingosine kinase 1	Sphk1	2.23 \pm 0.69	5.55 \pm 1.79	1.75 \pm 0.52	4.54 \pm 1.35
NM_053565	Suppressor of cytokine signaling 3	Socs3	1.37 \pm 0.23	1.99 \pm 0.19	1.26 \pm 0.05	1.71 \pm 0.10
<u>Inflammatory response</u>						
-Chemokine signaling pathway						
NM_031514	Janus kinase 2	Jak2	1.50 \pm 0.38	2.21 \pm 0.39	-1.03 \pm 0.15	1.75 \pm 0.32
NM_019285	Adenylate cyclase 4	Adcy4	-1.00 \pm 0.18	1.80 \pm 0.29	1.04 \pm 0.17	1.69 \pm 0.39
NM_031530	Chemokine (C-C motif) ligand 2	Ccl2	2.94 \pm 1.40	12.52 \pm 3.18	2.09 \pm 0.60	7.02 \pm 3.08
NM_013025	chemokine (C-C motif) ligand 3 (Ccl3),	Ccl3	3.36 \pm 1.69	4.51 \pm 4.33	3.53 \pm 2.66	2.14 \pm 1.11
NM_053858	Small inducible cytokine A4	Ccl4	3.74 \pm 1.69	2.52 \pm 0.84	3.96 \pm 2.03	2.27 \pm 0.74
NM_001007612	Chemokine (C-C motif) ligand 7	Ccl7	2.81 \pm 1.18	8.86 \pm 2.61	1.86 \pm 0.97	5.95 \pm 2.08
XM_213425	Chemokine (C-C motif) ligand 12	Ccl12	-1.12 \pm 0.07	2.00 \pm 0.61	-1.11 \pm 0.06	2.21 \pm 0.35
NM_020542	Macrophage inflammatory protein-1 alpha receptor gene	Ccr1	1.02 \pm 0.20	3.55 \pm 2.39	-1.02 \pm 0.36	1.99 \pm 0.62
NM_030845	Chemokine (C-X-C motif) ligand 1	Cxcl1	2.14 \pm 0.34	6.62 \pm 2.42	3.19 \pm 0.80	3.80 \pm 1.55
NM_053647	Chemokine (C-X-C motif) ligand 2	Cxcl2	2.39 \pm 0.81	4.96 \pm 9.38	2.62 \pm 0.67	1.96 \pm 1.15
NM_001017478	Chemokine (C-X-C motif) ligand 16	Cxcl16	1.52 \pm 0.66	3.51 \pm 1.59	1.63 \pm 0.40	2.86 \pm 0.55

Chapter 6.2:
AURKs inhibitor on permanent-MCAO

Table 6.4 (continue)

Genbank	Title	Symbol	Vehicle-pMCAO		Treatment-pMCAO	
			8h	24h	8h	24h
-Chemokine signaling pathway (continue)						
NM_022205	Chemokine (C-X-C motif) receptor 4	Cxcr4	1.12 ± 0.12	2.15 ± 0.60	1.10 ± 0.14	1.62 ± 0.06
NM_133307	Protein kinase C, delta	Prkcd	1.29 ± 0.31	2.37 ± 0.77	-1.30 ± 0.11	2.23 ± 1.26
XM_215659	Ras homolog gene family, member C	Rhoc	1.30 ± 0.30	1.94 ± 0.09	1.07 ± 0.15	1.82 ± 0.32
XM_001071741	RAS guanyl releasing protein 2 (calcium and DAG-regulated)	Rasgrp2	-1.08 ± 0.15	-2.25 ± 0.05	-1.06 ± 0.16	-1.56 ± 0.17
-Leukocyte transendothelial migration						
NM_053796	Junctional adhesion molecule 1	F11r	-1.05 ± 0.21	1.81 ± 0.76	-1.14 ± 0.07	1.58 ± 0.32
NM_001004245	Endothelial cell adhesion molecule	Ecam	1.11 ± 0.38	1.51 ± 0.51	1.19 ± 0.27	1.59 ± 0.27
NM_012967	Intercellular adhesion molecule 1	Icam1	1.89 ± 0.31	4.47 ± 0.51	1.65 ± 0.22	2.72 ± 0.65
NM_031055	Matrix metalloproteinase 9	Mmp9	1.13 ± 0.20	2.95 ± 0.49	-1.10 ± 0.15	2.06 ± 0.79
NM_053819	Tissue inhibitor of metalloproteinase 1	Timp1	2.84 ± 1.42	6.30 ± 1.22	1.58 ± 0.80	4.75 ± 1.19
NM_030863	Moesin	Msn	1.24 ± 0.16	3.30 ± 0.50	1.14 ± 0.08	1.85 ± 0.70
-Complement and coagulation cascade						
NM_001008515	Complement component 1, q subcomponent, alpha polypeptide	C1qa	-1.19 ± 0.17	-1.13 ± 0.16	-1.52 ± 0.09	1.15 ± 0.45
NM_013151	Plasminogen activator, tissue	Plat	2.06 ± 0.81	2.56 ± 0.58	1.73 ± 0.27	2.40 ± 0.51
NM_012620	Serine (or cysteine) proteinase inhibitor, clade E, member 1	Serpine1	1.49 ± 0.29	7.02 ± 1.48	1.37 ± 0.14	4.60 ± 2.04
NM_031771	Thrombomodulin	Thbd	1.63 ± 0.97	2.32 ± 0.68	1.42 ± 0.28	1.89 ± 0.24
TLR signaling pathway						
NM_021744	CD14 antigen	Cd14	1.94 ± 0.52	7.30 ± 1.42	1.47 ± 0.49	4.95 ± 1.70
NM_022197	c-Fos oncogene	c-Fos	3.92 ± 2.29	4.34 ± 1.16	2.32 ± 0.91	4.75 ± 3.45
NM_021835	v-Jun sarcoma virus 17 oncogene homolog (avian)	Jun	1.73 ± 0.29	1.93 ± 0.19	1.41 ± 0.26	1.94 ± 0.09
NM_012589	Interleukin 6	Il6	1.60 ± 0.56	2.08 ± 0.58	1.56 ± 0.48	1.86 ± 0.35
XM_239239	Mitogen activated protein kinase kinase 3	Map2k3	1.32 ± 0.31	2.25 ± 0.59	1.20 ± 0.12	2.15 ± 0.13
NM_053703	Mitogen-activated protein kinase kinase 6	Map2k6	-1.14 ± 0.06	-3.90 ± 0.04	-1.29 ± 0.16	-2.34 ± 0.13
NM_198130	Myeloid differentiation primary response gene 88	Myd88	1.44 ± 0.58	1.72 ± 0.52	1.24 ± 0.15	1.94 ± 0.44
NM_012881	Secreted phosphoprotein 1	Spp1	5.14 ± 3.62	5.02 ± 1.97	3.28 ± 1.68	4.52 ± 1.78
NM_198769	Toll-like receptor 2	Tlr2	1.35 ± 0.16	2.34 ± 0.55	1.30 ± 0.32	1.83 ± 0.30

Chapter 6.2:
AURKs inhibitor on permanent-MCAO

Table 6.4 (continue)

Genbank	Title	Symbol	Vehicle-pMCAO		Treatment-pMCAO	
			8h	24h	8h	24h
Cell homeostasis, survival and proliferation						
NM_012513	Brain derived neurotrophic factor	Bdnf	1.56 ± 1.11	2.30 ± 0.93	1.03 ± 0.70	1.68 ± 1.02
NM_019216	Growth differentiation factor 15	Gdf15	1.81 ± 0.62	1.62 ± 0.90	2.17 ± 0.78	1.97 ± 0.67
NM_021752	Baculoviral IAP repeat-containing 2	Birc2	1.15 ± 0.19	1.84 ± 0.13	-1.13 ± 0.11	1.72 ± 0.16
NM_198130	Myeloid differentiation primary response gene 88	Myd88	1.44 ± 0.58	1.72 ± 0.52	1.24 ± 0.15	1.94 ± 0.44
XM_227525	Nerve growth factor, beta	Ngfb	-1.08 ± 0.48	1.75 ± 0.29	-1.10 ± 0.16	1.74 ± 0.51
NM_012588	Insulin-like growth factor binding protein 3	Igfbp3	1.28 ± 0.40	3.33 ± 0.63	-1.16 ± 0.09	2.43 ± 0.42
Mitotic cell cycle						
NM_012920	Calcium/calmodulin-dependent protein kinase II alpha subunit	Camk2a	-1.21 ± 0.30	-1.81 ± 0.02	-1.33 ± 0.05	-1.61 ± 0.06
NM_133605	Calcium/calmodulin-dependent protein kinase II gamma	Camk2g	-1.31 ± 0.15	-2.40 ± 0.10	-1.26 ± 0.12	-1.51 ± 0.17
NM_024127	Growth arrest and DNA-damage-inducible 45 alpha	Gadd45a	1.84 ± 0.66	3.72 ± 1.20	1.40 ± 0.09	3.06 ± 0.82
XM_001053888	Growth arrest and DNA-damage-inducible 45 gamma	Gadd45g	2.89 ± 0.97	5.94 ± 2.31	1.99 ± 0.29	5.92 ± 0.71
XM_001080981	Transformed mouse 3T3 cell double minute 2	Mdm2	1.21 ± 0.33	2.00 ± 0.60	1.01 ± 0.07	1.65 ± 0.27
Response to oxidative stress						
NM_017232	Prostaglandin-endoperoxide synthase 2	Ptgs2	2.77 ± 1.04	4.44 ± 1.61	1.71 ± 0.58	3.09 ± 1.56
NM_017051	Superoxide dismutase 2, mitochondrial	Sod2	1.44 ± 0.28	2.04 ± 0.52	1.07 ± 0.15	1.56 ± 0.28
NM_031614	Thioredoxin reductase 1	Txnrd1	1.15 ± 0.12	1.95 ± 0.05	1.00 ± 0.27	2.42 ± 0.23
NM_031970	Heat shock 27kDa protein 1	Hspb1	2.54 ± 1.15	3.38 ± 0.95	2.04 ± 0.74	3.73 ± 1.24
NM_021863	Heat shock protein 2	Hspa2	1.37 ± 0.38	1.78 ± 0.44	1.06 ± 0.14	1.86 ± 0.35
NM_053612	Heat shock 22kDa protein 8	Hspb8	1.88 ± 0.65	2.69 ± 0.87	1.17 ± 0.28	1.86 ± 0.29
NM_012580	Heme oxygenase (decycling) 1	Hmox1	2.31 ± 0.49	4.47 ± 1.54	2.10 ± 0.59	4.01 ± 1.23
Cell death						
NM_024125	CCAAT/enhancer binding protein (C/EBP), beta	Cebpb	1.69 ± 0.68	2.23 ± 0.85	1.41 ± 0.16	2.63 ± 0.55
NM_024134	DNA-damage inducible transcript 3	Ddit3	1.62 ± 0.22	1.93 ± 0.38	1.22 ± 0.20	1.95 ± 0.35
NM_057138	CASP8 and FADD-like apoptosis regulator (Cflar),	Cflar	1.12 ± 0.31	4.33 ± 1.09	-1.15 ± 0.11	2.55 ± 0.62
NM_012922	Caspase 3, apoptosis related cysteine protease	Casp3	1.23 ± 0.28	2.80 ± 0.46	-1.04 ± 0.11	2.04 ± 0.09
NM_022260	Caspase 7	Casp7	1.07 ± 0.22	1.90 ± 0.36	-1.14 ± 0.10	1.68 ± 0.16
XM_343065	Nuclear factor of kappa light chain gene enhancer in B-cells inhibitor, alpha	Nfkbia	1.61 ± 0.42	2.37 ± 0.88	1.52 ± 0.24	2.08 ± 0.27

Chapter 6.2:
AURKs inhibitor on permanent-MCAO

Table 6.4 (continue)

Genbank	Title	Symbol	Vehicle-pMCAO		Treatment-pMCAO	
			8h	24h	8h	24h
Cell death (continue)						
NM_012904	Annexin A1	Anxa1	1.40 ± 0.54	2.79 ± 0.99	1.16 ± 0.21	2.20 ± 0.60

6.2.2.5 AURKs inhibition suppresses the activation of several inflammation-related signaling cascades

Comparative microarray analysis on the consequential transcriptional effect of AURKs inhibition of pMCAO revealed an overwhelming 753 gene transcripts being significantly modulated in vehicle condition. Functional clustering of these differentially-expressed gene probes which corresponded to 722 annotated genes on DAVID 6.7 presented additional candidates involved in enriched biological processes already identified in the commonly-occurring genes. The transcriptionally activated processes included inflammatory responses (leukocyte chemotaxis, coagulation and complement signaling pathway, and TLR-mediated cascade), vasculature development, and promotion of cell homeostasis, survival and proliferation (Table 6.5). Taking note that the differentially-expressed genes in this vehicle-MCAO exclusive category were simultaneously absent from the treatment-pMCAO condition (due to their insignificant modulation), this implies that AURKs inhibition evokes a less intense neuro-inflammation and vasculature disturbance which consequentially translated to a weaker pro-injury/death stimuli, thus counteracted with a diminished pro-survival transcriptional response.

Chapter 6.2:
AURKs inhibitor on permanent-MCAO

Table 6.5 Functional annotation of significantly-modulated genes demonstrating at least ± 1.5 fold-change in a minimum of one out of two time-points (8h and 24h) exclusive to vehicle (80% DMSO) condition induced via *i.c.v.* administration 30min post- pMCAO. All fold-change expressions were subjected to one-way ANOVA analysis and Benjamini-Hochberg correction, and significant at $p < 0.05$. Data are expressed as fold-change \pm sem.

Genbank	Gene title	Symbol	Vehicle-pMCAO	
			8h	24h
<u>Inflammatory response</u>				
NM_024131.	D-dopachrome tautomerase	Ddt	-1.20 \pm 0.08	-1.72 \pm 0.04
NM_012896	Adenosine A3 receptor	Adora3	-1.38 \pm 0.05	-1.55 \pm 0.08
NM_019233	Chemokine (C-C motif) ligand 20	Ccl20	1.48 \pm 1.22	6.50 \pm 2.63
NM_022924	Coagulation factor 2	F2	1.01 \pm 0.05	1.57 \pm 0.25
NM_013057	Coagulation factor III	F3	1.68 \pm 0.10	1.30 \pm 0.13
NM_031019	Corticotropin releasing hormone	Crh	-1.21 \pm 0.18	1.50 \pm 0.29
NM_019143	Fibronectin 1	Fn1	1.19 \pm 0.13	2.10 \pm 0.48
NM_031512	Interleukin 1 beta	Il1b	1.55 \pm 0.13	3.86 \pm 4.08
XM_001071294	Interleukin 1 receptor antagonist	Il1rn	1.10 \pm 0.09	3.10 \pm 1.64
XM_001059899	ADP-ribosyltransferase (NAD ⁺ ; poly (ADP-ribose) polymerase)-like 1	Adprt1l	1.01 \pm 0.25	1.46 \pm 0.16
NM_012704	Prostaglandin E receptor 3 (subtype EP3)	Ptger3	1.01 \pm 0.06	1.59 \pm 0.33
NM_022380	Signal transducer and activator of transcription 5B	Stat5b	1.22 \pm 0.17	1.52 \pm 0.16
NM_053757	Small inducible cytokine subfamily E, member 1	Scye1	-1.07 \pm 0.21	1.52 \pm 0.16
XM_001063419	Toll interacting protein	Tollip	1.01 \pm 0.09	1.64 \pm 0.27
<u>Vasculature development</u>				
NM_139104	EGF-like domain 7	Egfl7	-1.05 \pm 0.20	1.79 \pm 0.25
NM_001004228	Endomucin	Emcn	-1.79 \pm 0.07	-1.04 \pm 0.41
NM_012548	Endothelin 1	Edn1	1.23 \pm 0.32	1.59 \pm 0.35
NM_019305	Fibroblast growth factor 2	Fgf2	1.62 \pm 0.18	1.60 \pm 0.28
NM_021836	Jun-B oncogene	Junb	2.27 \pm 1.02	2.14 \pm 0.72
NM_017061	Lysyl oxidase	Lox	1.58 \pm 0.58	3.72 \pm 1.01
NM_013085	Plasminogen activator, urokinase	Plau	1.00 \pm 0.12	1.75 \pm 0.17
NM_022669	Secretogranin 2	Scg2	1.04 \pm 0.48	2.35 \pm 0.58
NM_013114	Selectin, platelet	Selp	1.03 \pm 0.08	2.20 \pm 0.31
NM_173116	Sphingosine phosphate lyase 1	Sgpl1	1.09 \pm 0.24	1.60 \pm 0.06
XM_575397	Wingless-related MMTV integration site 2	Wnt2	-1.11 \pm 0.08	1.60 \pm 0.32
<u>Cell homeostasis, survival and proliferation</u>				
<u>-MAPK signaing pathway</u>				
XM_001071741	RAS guanyl releasing protein 2 (calcium and DAG-regulated)	Rasgrp2	-1.08 \pm 0.15	-2.25 \pm 0.05
NM_012513	Brain derived neurotrophic factor	Bdnf	1.56 \pm 1.11	2.30 \pm 0.93
NM_053851	Calcium channel, voltage-dependent, beta 2 subunit	Cacnb2	1.06 \pm 0.20	-1.55 \pm 0.09

Chapter 6.2:
AURKs inhibitor on permanent-MCAO

Table 6.5 (continue)

Genbank	Gene title	Symbol	Vehicle-pMCAO	
			8h	24h
<u>-MAPK signaing pathway (continue)</u>				
NM_012828	Calcium channel, voltage-dependent, beta 3 subunit	Cacnb3	-1.09 ± 0.23	-2.26 ± 0.12
NM_053769	Dual specificity phosphatase 1	Dusp1	1.98 ± 0.69	1.96 ± 0.49
NM_133578	Dual specificity phosphatase 5	Dusp5	1.45 ± 0.29	2.03 ± 0.92
NM_053883	Dual specificity phosphatase 6	Dusp6	1.38 ± 0.51	1.54 ± 0.25
XM_001063880	Dual specificity phosphatase 8	Dusp8	-1.21 ± 0.24	-1.56 ± 0.05
XM_340861	Dual specificity phosphatase 14	Dusp14	1.18 ± 0.09	1.62 ± 0.31
XM_235565	Mitogen-activated protein kinase 8 interacting protein 2	Mapk8ip2	-1.14 ± 0.20	-1.58 ± 0.09
XM_227525.3	Nerve growth factor, beta	Ngfb	-1.08 ± 0.48	1.75 ± 0.29
XM_001061815	Nuclear factor of activated T-cells, cytoplasmic, calcineurin-dependent 4	Nfatc4	1.58 ± 0.62	3.05 ± 0.86
NM_053306	P21 (CDKN1A)-activated kinase 2	Pak2	1.14 ± 0.11	1.48 ± 0.26
NM_012628	Protein kinase C, gamma	Prkcc	-1.14 ± 0.28	-1.60 ± 0.07
<u>TGF-beta signaling pathway</u>				
NM_013022	Rho-associated coiled-coil forming kinase 2	Rock2	1.07 ± 0.25	1.83 ± 0.10
XM_001053727	Bone morphogenetic protein 7	Bmp7	1.25 ± 0.30	2.54 ± 0.96
NM_017128	Inhibin beta-A	Inhba	1.54 ± 0.49	2.91 ± 1.32
NM_021587	Latent transforming growth factor beta binding protein 1	Ltbp1	-1.01 ± 0.19	2.12 ± 0.56
XM_001081231	Noggin	Nog	-1.24 ± 0.18	-1.69 ± 0.05
NM_031131	Transforming growth factor, beta 2	Tgfb2	1.00 ± 0.34	2.19 ± 0.30
<u>Pro-mitogenic/Anti-apoptotic signaling pathways</u>				
NM_133416	B-cell leukemia/lymphoma 2 related protein A1 (Bcl2a1)	Bcl2a1	1.54 ± 0.25	2.92 ± 1.27
NM_031345	Delta sleep inducing peptide, immunoreactor	Dsipi	-1.14 ± 0.22	-1.76 ± 0.10
NM_023987	Baculoviral IAP repeat-containing 3	Birc3	1.42 ± 0.30	1.98 ± 0.61
XM_001060919	Death associated protein kinase 1	Dapk1	-1.04 ± 0.37	-1.62 ± 0.08
NM_001004279	Peptidylprolyl isomerase D (Ppid)	Ppid	1.17 ± 0.08	1.52 ± 0.25
NM_033539	Eukaryotic translation elongation factor 1 alpha 1	Eef1a1	1.27 ± 0.38	1.97 ± 0.37
NM_001024800	Thioredoxin domain containing 1	Txndc1	1.30 ± 0.27	2.00 ± 0.31

Chapter 6.2:
AURKs inhibitor on permanent-MCAO

6.2.2.6 Validation of AURKs inhibitor –treated pMCAO global transcriptomic profile via real-time PCR

Global gene profiles of AURKs inhibitor-treated pMCAO model was verified using quantitative real-time PCR which demonstrated similar transcriptional regulation, indicating the high reliability in data interpretation from the microarray analysis (Table 6.6).

Table 6.6 Validation of microarray data using real-time PCR technique on pMCAO-induced adult male Wistar rat infarcted cortice treated with 30mM AURKs inhibitor (ZM447439; treatment). Data are expressed as fold-change \pm sem.

GenBank	Gene Title	Symbol	Treatment (30mM AURKs inhibitor in 80% DMSO)			
			8h		24h	
			Microarray	Real-time PCR	Microarray	Real-time PCR
NM_031970	Heat shock 27kDa protein 1	Hspb1	2.04 \pm 0.74	3.05 \pm 1.52	3.73 \pm 1.24	3.84 \pm 1.02
NM_053612	Heat shock 22kDa protein 8	Hspb8	1.17 \pm 0.28		1.86 \pm 0.29	4.76 \pm 0.83
NM_017232	Prostaglandin-endoperoxide synthase 2	Ptgs2	1.71 \pm 0.58	2.63 \pm 0.52	3.09 \pm 1.56	2.41 \pm 0.89
NM_031530	Chemokine (C-C motif) ligand 2	Ccl2	2.09 \pm 0.60	4.50 \pm 0.61	7.02 \pm 3.08	9.88 \pm 0.95
NM_030845	Chemokine (C-X-C motif) ligand 1	Cxcl1	3.19 \pm 0.80	7.04 \pm 0.68	3.80 \pm 1.55	4.04 \pm 1.14
NM_021744	CD14 antigen	Cd14	1.47 \pm 0.49		4.95 \pm 1.70	4.14 \pm 0.67
NM_012924	CD44 antigen	Cd44	-1.06 \pm 0.12		2.21 \pm 0.53	6.23 \pm 0.94
NM_031055	Matrix metalloproteinase 9	Mmp9	-1.10 \pm 0.15		2.06 \pm 0.79	8.88 \pm 0.80
NM_053819	Tissue inhibitor of metalloproteinase 1	Timp1	1.58 \pm 0.80	2.41 \pm 0.89	4.75 \pm 1.19	7.44 \pm 0.95

6.2.3 Discussion

In vivo animal works on cerebral ischemia demonstrated employment of antioxidants, NMDAR modulators, cytokine inhibitors, i/eNOS inhibitors, cyclo-oxygenase 2 (COX-2) inhibitors very often showed fairly well efficacy in the abrogation of disease progression, but with majority subsequently failed to pass clinical trials (Abe, 2008; Richardson et al., 2000; Robinson and Keating, 2006). Many of these clinical evaluations took place before cell cycle re-entry was implicated as a mechanism for neuronal death.

Current available therapeutic treatment using rt-PA, developed on the basis of its thrombolytic effect to remove the occlusion, is only effective within a short 3 hours window after ischemic onset, and the potential risk of continuous thrombolysis resulting in intracranial hemorrhage is high even after treatment. This reveals a substantial shortfall in the availability of therapeutic options for cerebral ischemia, and call for more promising treatment methods.

Treatment with an inhibitor of cell cycle protein kinase family, AURKs, i.e. ZM447439 which is selective for AURKA and AURKB, showed significant therapeutic efficacy towards the reduction of infarct damage during acute, permanent cerebral ischemia (the most severe form of focal ischemia). Generally, genes involved in cell death-associated processes showed a reduced transcriptional amplitude response after AURKs inhibition. Particularly, significant differential temporal modulation was observed in the inflammatory cascades involved in chemokine signaling, leukocyte transendothelial migration, complement and coagulation cascade, and TLRs signaling. Comparable anti-

Chapter 6.2: AURKs inhibitor on permanent-MCAO

oxidant response was observed with and without AURKs suppression. All in all, these differential transcriptional responses contributed to a lower cell death stimulus, as verified by the decreased transcriptional activation of cell death molecules e.g. caspases. Even though cell cycle re-entry has not been identified as an enriched biological process in pMCAO model, but based on ability of AURKs inhibitor to attenuate ischemic infarct damage, it could be interpreted that cell cycle re-activation is a primary event in the acute disorder pathogenesis and plays a prominent upstream role in the induction of neuronal death; and furthermore, AURKs functionality is important in the initiation of cell cycle re-entry. The inability to detect cell cycle re-activation via microarray in the vehicle process could be attributed to this process occurring earlier than the first profiling time-point (8h).

This is the first time that AURKs inhibition has been demonstrated to be effective against infliction of ischemic damage, and this neuroprotective effect might be closely associated with the modulation of inflammatory response. AURKs have been identified to be a promising biological target in the intervention of acute cerebral ischemia. This is because, the expression of cell cycle proteins is not at all time associated with cell cycle re-entry by neurons. Some core cell cycle proteins possess postmitotic functions that span across various developmental phases of a neuron, including neuronal migration, axonal elongation, axonal pruning, dendrite morphogenesis and synaptic maturation and plasticity (Frank and Tsai, 2009; Kim et al., 2009). Numerous studies have reported that sporadic expression of CCND in unperturbed normal primary neurons without the presence of active CDK4, indicative of other physiological role of CCND (Liu et al.,

Chapter 6.2:
AURKs inhibitor on permanent-MCAO

2008; Rao et al., 2007). Furthermore, in addition to cell cycle protein expression, pro mitogenic stimuli are also required to initiate cell cycle re-entry. When normal neurons with elevated CCND expression are subjected to a mitogenic stimulus like thrombin, the neurons re-activate cell cycles resulting in their demise (Liu et al., 2008; Rao et al., 2007). Up-to-date, AURKA and AURKB roles have only been pertained to mitotic cell cycle. As such, much work still needs to be performed to establish the relationship between AURKs function in cell cycle re-entry and its relation to neuro-inflammation.

Chapter 7:

Comparative *in vitro* global gene profiles

Focus on Oxidative Stress

Glu

versus

*Well-known oxidative stressor neurodegenerative
models*

7 Description of *in vitro* neurodegenerative models using cultured murine primary cortical neurons

Mouse Neocortical Neuronal Cell Culture Preparation

Neocortical neurons (gestational days 15 or 16) obtained from foetal cortices of Swiss albino mice were used to prepare the primary cultures employing previously described procedures with modifications (Cheung *et al.*, 2000). Microdissected cortices were subjected to trypsin digestion and mechanical trituration. Cells were collected by centrifugation and resuspended in NB medium containing 2.5% B-27 supplement, 1% penicillin, 1% streptomycin, 0.25% GlutaMAX-1 supplement and 10% dialyzed FCS. 24-well plates previously coated with poly-D-lysine (100 µg/ml) were seeded with cells to a density of 2×10^5 cells/cm² and used for subsequent experiments. The cultures were maintained in a humidified 5% CO₂ and 95 % air incubator at 37 °C. Immunocytochemical staining of the cultures at day 5 *in vitro* for microtubule-associated protein 2 and glia fibrillary acidic protein revealed > 95% of the cells were neurons with minimal contamination by glia (Cheung *et al.*, 1998). All experiments involving animals were approved by the National University of Singapore, and were in accordance with the US Public Health Service guide for the care and use of laboratory animals.

Drug preparation for application on neuronal cultures over a 24h period

All pharmacological drugs listed in the table below were freshly prepared individually in their respective solvent before each neuronal culture treatment. Desired concentrations were achieved via dilution with NB medium. EC₅₀ for each drug has been previously ascertained in our laboratory via MTT cell viability assay, and this concentration is

Chapter 7:
***In vitro* oxidative stressor models**

employed to induce neuronal injury over a 24h incubation period in day 5 or 7 cultured neurons. Total RNA was harvested at over at designated time-points over the 24h post-treatment period, and subjected to microarray analysis. All microarray data reported here are described in accordance with MIAME guidelines, and has been deposited in the NCBI's Gene Expression Omnibus (GEO; [http://www. ncbi.nlm.nih.gov/geo/](http://www.ncbi.nlm.nih.gov/geo/)) and are accessible through the following GEO Series accession number.

Drug Treatment	Solvent	Stock Concentration	Treatment concentration	GEO Accession
NOC-18 [Nitric oxide (NO) donor] [DETA-NONOate, (Z)-1-[2-(2-Aminoethyl)-N-(2-ammonioethyl)amino]diazene-1-ium-1,2-diolate]	10mM Sodium hydroxide (NaOH)	100mM	0.5mM	GSE22087
Hypochlorous acid (HOCl)*	Water	300mM	250uM	-
Rotenone	DMSO	10mM	10nM	GSE22997
Lactacystin	DMSO	100mM	1mM	GSE23155
Glu	100mM NaOH	100mM	250uM	GSE19936

*The HOCl stock solution was aliquoted into small quantities and stored at 4°C in the dark for up to 1h prior to use due to its instability and susceptibility to dissociate into free oxygen and HCl. HOCl concentration was quantified spectrophotometrically at 290nm (pH 12.0, $\epsilon = 350\text{M}^{-1}\text{cm}^{-1}$) prior to use (Morris, 1996). HOCl was diluted in cold water to a concentration of 300mM and stored on ice for no longer than 1min (Whiteman et al., 2005b). HOCl was diluted in Earle's balanced salt solution (EBSS) warmed to 37°C to desired concentration.

7.1 Introduction

Several patho-physiological mechanisms such as oxidative stress, neuroinflammation, cell cycle re-entry and excitotoxicity are not exclusive to any one neurodegenerative disease or neurological disorder, but are frequently found to occur concurrently in several neuropathies. Particularly, oxidative stress can be considered to be a universal patho-physiological phenomenon consistently observed in chronic neurodegenerative disorders such as AD (Sultana and Butterfield, 2009) and PD (Jenner, 2007) and acute neurological disorders such as stroke (Niizuma et al., 2009). Even though this phenomenon has been ubiquitously detected in post-mortem brains of these neurological disorders through its consequential effects, the significance of its implication during neuronal death progression remains unclear. As such, comparative microarray analysis of specific neuropathy-representing models becomes an invaluable avenue to decipher the pathological mechanisms upstream and/or downstream of oxidative stress. From there, novel insights into the signaling transduction pathways modulated upon its occurrence would form the foundation for screening platform in the identification of potential universal biological targets useful in the area of therapeutic management.

Adopting cultured murine primary cortical neurons as the basis of the *in vitro* model, focus on the commonality of the signaling pathways regulated upon individual time-course neuronal treatments with four well-characterized oxidative stressors: HOCl, NO, Glu and rotenone. They are most appropriately selected as they either have been implicated in the pathogenesis of several neurological dysfunctions, or are well-

represented agents of neurodegenerative models through reproduction of pathological morphological characteristics of the disease state.

Involvement of HOCl has been documented in numerous inflammatory and oxidative stress-related diseases namely atherosclerosis (Hazell et al., 1996), cystic fibrosis (Kettle et al., 2004) and neurodegenerative disorders such as PD (Choi et al., 2005) and AD (Green et al., 2004). As compared to other fields of disease study, the role of HOCl in neurodegenerative disorders is still lacking. In the mammalian brain, HOCl is produced predominantly by concerted activations of NADPH oxidase and myeloperoxidase (MPO) in activated microglia and infiltrated neutrophils and monocytes during inflammatory pathological conditions (Bianca et al., 1999; Gonzalez-Scarano and Baltuch, 1999). However, expression of NADPH oxidase and MPO in neurons has also been reported (Green et al., 2004; Noh and Koh, 2000; Tammariello et al., 2000; Vallet et al., 2005). In PD, an up-regulation of MPO with a corresponding elevation of HOCl-modified proteins has been demonstrated in the ventral midbrain of post-mortem brains and disease mouse models. Further, in AD brains, 3-chlorotyrosine, a biomarker of HOCl, existed at three-fold that of control brains (Green et al., 2004).

Similarly, excessive endogenous NO production has been identified in neurological disorders linked to oxidative stress such as ischemia (Cuzzocrea et al., 2001), ALS (Cookson and Shaw, 1999), AD (Good et al., 1996) and PD (Good et al., 1998). Apart from its conformational activation of GC, NO, due to its extreme thermodynamic instability, is able to undergo vigorous chemical reactions with gaseous molecules, anions

and ROS to form NO_2^- , NO_3^- and particularly ONOO^- . Under physiological conditions, these electrophilic reactions are important in the modulation of protein activity through selective post-translational modifications such as nitrotyrosination (Ischiropoulos and Beckman, 2003) and *S*-nitrosylation (Broillet, 1999), and alteration of mitochondrial energy metabolism (Brown and Cooper, 1994; Cleeter et al., 1994) and synthesis (Nisoli et al., 2003). However, upon physio-pathological state, excess NO reacts quickly with O_2^- to form ONOO^- to escape its sequestration by the antioxidant systems, of which the latter decomposes further into multiple toxic products (Beckman et al., 1990). During this transformation process, intermediate products such as ROS and free radicals are being produced. Abundant presence of NO-originated intermediates and byproducts induces dysregulated modifications of cellular molecules (lipids, proteins and DNA) through oxidation (Butterfield, 1997), nitration (Souza et al., 1999) or nitrosylation (Stamler et al., 1997).

Rotenone, a specific mitochondrial complex I inhibitor, is well known for its ability to mimic the pathological characteristics of PD (e.g. presence of Lewy bodies) within dopaminergic neurons. Mitochondrial complex I is involved in the superoxide formation during physiological respiration and its dysfunction is denoted as a hallmark feature of PD identified in the substantia nigra par compacta of disease patients (Lin and Beal, 2006; Mancuso et al., 2006). It has been further suggested that partial inactivation of the complex activity observed in PD would enhance ROS production as compared to that of full inhibition, aggravating the extent of cellular damages (Pitkanen and Robinson, 1996; Votyakova and Reynolds, 2001).

Chapter 7:
***In vitro* oxidative stressor models**

Pharmacological proteasomal inhibitor, lactacystin, can trigger oxidative stress indirectly via the promotion of aberrant, toxic protein buildup as a result of UPS dysfunction, and thus induce apoptosis in cultured mouse cortical neurons (Cheung et al., 2004; Yew et al., 2005). With specific regard to the CNS, proteasomal inhibition has been linked to the cellular toxicity and pathology observed in the brain during normal aging, in neurodegenerative diseases such as PD and AD as well as cerebral ischemia (Ding and Keller, 2001; Grune et al., 2004; Keller et al., 2004; Keller et al., 2000b). Incidentally, proteasomal inhibition is most severe in the brain region that exhibits the largest amount of pathology (Keller et al., 2000a; McNaught et al., 2001). Proteasomal inhibition is also reported to mediate deleterious alterations in cell cycle regulation, inflammatory processes, protein aggregation and trigger the cell death pathway (Demasi and Davies, 2003; Rideout et al., 2003; Rockwell et al., 2000; Yew et al., 2005). Recently, studies have shown that the inhibition of proteasome using a proteasomal inhibitor such as PS-341 induced apoptosis through the induction of ER stress-reactive oxygen species (Fribley et al., 2004).

Collectively these agents are appropriately selected as each has been implicated in the pathogenesis of numerous inflammatory and oxidative stress-related neurological dysfunctions. Furthermore, they are well-represented agents of neurodegenerative models through recapitulation of various pathological or morphological characteristics of the diseased state. Major biological pathways that are activated by the four stressors were monitored, to provide information on the detailed signal transduction processes and to enhance our understanding of the mechanisms invoked.

7.2 Results

Even with a focus on the elucidation of pathogenesis of cerebral ischemia, it is beneficial to identify signaling pathway commonality of this neurological deficit condition to the other neurodegenerative diseases such as PD, AD and ALS. Four *in vitro* oxidative stressor models namely, NO, HOCl, rotenone and lactacystin representative of the neuropathological characteristics of these common neurodegenerative diseases were employed for comparative global transcriptomic comparison to that of Glu.

7.2.1 Generation of NO global gene profile

On day 7 *in vitro*, the cultured neurons were treated with escalating concentrations of NOC-18 in NB medium. MTT cell viability assay revealed the IC₅₀ for NO was 0.5mM (51.2 ± 4.0% cell viability). Morphological analysis of 0.5mM NOC-18 treated neurons by Hoffman modulation contrast imaging demonstrated cell shrinkage into round apoptotic cell bodies with absence of neuritic outgrowths and when compared to the healthy control neurons (Peng et al., 2008). There was an absence of rapid swelling indicating that accidental necrosis was not involved (Nagley et al., 2010). In addition, Hoescht stain illustrated the presence of chromatin condensation in these round cell bodies as opposed to that of control cells, further confirming induction of neuronal death predominantly by apoptotic-like injury by 0.5mM of NOC-18 (Peng et al., 2008). In the present study, 0.5mM of NOC-18 was chosen for subsequent time-course experiments.

Microarray analysis was carried out on day 7 neuronal cultures treated with 0.5mM NOC-18 post-24h using 14 GeneChip Mouse Genome 430 2.0 array (Affymetrix, Santa

Clara, CA), which contain 45,000 probe sets and can analyze the expression level of over 39,000 transcripts and variants from over 34,000 well-characterized mouse genes. The assignment of the arrays (GeneChip) was as follows: vehicle-treated control (n=5); NOC-18-treatment for 8h, 15h and 24h NOC-18 treatment (n=3 for each time point). Out of a total of 45,000 probe sets representing over 34,000 well-characterized mouse genes, 3,672 probe sets were profiled after 0.5mM NOC-18 treatment. DAVID interpretation recognized 3,484 biologically- and functionally-reported genes from various biological databases for NO treatment.

7.2.2 Generation of HOCl global gene profile

Neurons at day 5 *in vitro* were treated with 0.5ml of HOCl in EBSS culture medium. The addition of HOCl did not significantly alter the pH of the reaction mixture. After 3h, EBSS was removed and followed by the addition of 0.3ml of Dulbecco's modified Eagle medium (DMEM)/F-12 culture medium to allow neuronal injury to proceed for a further 8h and 24h respectively. Appropriate vehicle controls were run in parallel.

Previous data have shown that HOCl induced a concentration-dependent apoptotic-necrotic continuum cell death in cultured murine cortical neurons (Yap et al., 2006). The focus of the present study was on the transcriptomic regulatory response of neurons upon apoptotic injury mediated by HOCl. HOCl concentrations lower than 300 μ M induced apoptosis in cultured cortical neurons (Yap et al., 2006). Cell viability of 250 μ M HOCl-treated neurons decreased to approximately 70% after 24 h of exposure (data not shown), reminiscent of our previous work (Yap et al., 2006). HOCl-induced apoptosis of cortical

neurons was evaluated by morphological changes and Hoechst/propidium iodide (PI) staining (Yap et al., 2006). Morphological photomontage demonstrated HOCl induced neuronal shrinkage and loss of neuritic networks when viewed. After 24h of treatment, cell bodies of HOCl-treated neurons shrink when viewed under light microscopy. Those injured neurons still preserve their plasma membrane integrity as demonstrated by PI staining. Nuclear changes were examined by Hoechst stain. Both revealed chromatin condensation in HOCl-treated neurons. As such, 250 μ M HOCl was the concentration of choice for microarray analysis.

HOCl global transcriptional profile was previously conducted in our laboratory and has been published (Yap et al., 2006). Ten Affymetrix murine genome array U74A (Affymetrix, Santa Clara, CA) containing probe sets presenting all known mouse genes and 6000 ESTs were used. The controls/treatments were carried out as followed: control (n=5), 8h (n=2), and 24h post-HOCl treatment (n=3). 2,203 probe sets were profiled to be significantly regulated. DAVID interpretation recognized 2,016 biologically- and functionally-reported genes from various biological databases for HOCl treatment.

7.2.3 Generation of rotenone global gene profile

Previous study in our laboratory on rotenone-mediated neuronal injury demonstrated significant loss of cell survival and major apoptotic morphological changes characterized by cell shrinkage and membrane blebbing in cortical neurons at rotenone concentrations at 5nM and 10nM, respectively (Chen et al., 2006). Morphological observations of the neurons treated with rotenone concentrations of more than 50nM showed rapid cell

swelling, indicating that cells died primarily via necrosis (Chen et al., 2006). Furthermore, morphological evaluation using Hoechst 33258 staining and fluorescence microscopy revealed DNA condensation and fragmentation in primary cortical neurons treated with 25nM rotenone for 24h, a major morphological characteristic of apoptosis (Chen et al., 2006). This indicates that rotenone induces an apoptotic-necrotic continuum cell death. IC₅₀ value for rotenone from cell viability assay was revealed to be 10nM, and was subsequently employed for microarray analysis over a 24h period.

A total of 13 arrays from the Illumina® Mouse Ref8 Ver.1.1 hybridization beadchips was used for rotenone global gene profiling purpose in my Ph.D. study: Control (n=4); exposure to 10nM lactacystin for 8h (n=3), 15h (n=3) and 24 h (n=3). 5,935 gene probes, which corresponded to 4,629 DAVID-recognizable candidates with reported up-to-date biological functions, were found to be significantly regulated.

7.2.4 Generation of lactacystin global gene profile

Previous study from our laboratory demonstrated a time-dependent decrease of neuronal cell viability after treatment with 1µM of lactacystin with a significant decrease 24h after lactacystin treatment (Choy et al., 2010). Fluorometric analysis of caspase activities demonstrated that CASP- 2, 3, 6, 8 and 10 are pro-apoptotic caspases, suggesting that up to 15h is needed to trigger the activation of the pro-apoptotic proteases after lactacystin treatment in cultured cortical neurons (Choy et al., 2010). Morphological study revealed that nucleus condensation and chromatin fragmentation were obvious in cells 24 h after the lactacystin treatment (Choy et al., 2010).

Transcriptomic profiling adopting the Illumina Mouse Ref8 V1.1 Beadchips was carried out on lactacystin-treated neuronal RNA samples harvested over a period of 24h. A total of 18 arrays was used in this experiment: Control (n=6); exposure to 10nM lactacystin for 5h (n=3), 8h (n=3), 15h (n=3) and 24 h (n=3). A genelist of 4,292 gene probes, were statistically significantly regulated. Upon online DAVID classification, 3,424 genes with known biological functions were demonstrated. Part of this lactacystin global gene profile (24h lactacystin versus control) generated in my Ph.D. project has been published in (Choy et al., 2010).

7.2.5 Comparative global transcriptomic analysis across all five distinct oxidative stressor models (Common genes perspective)

As several microarray platforms were adopted in this comparative bioinformatics study, to avoid differences in degree of sensitivity and specificity resulting in loss of potential significantly regulated genes, differentially expressed genes common to the five treatments (NO, HOCl, rotenone, lactacystin and Glu) were defined on the criteria of a minimum of ± 1.5 fold change in each of the treatment time-point and passed statistical testing by one-way ANOVA, $p < 0.05$ and Benjamini-Hochberg FDR Correction. Genes which were differentially expressed were annotated using DAVID 6.7 and PubMed search. Due to the limitation of the paper size and the vast amount of microarray data from all five transcriptomic profiles, comparative profile analysis in this chapter seeks to focus on the identification of the common genes and signaling pathways found to be potentially modulated, and in doing so, comparing their overall temporal regulatory

trends. This is crucial and informative in the elucidation of the universal signaling mechanisms at work during neurodegeneration.

59 gene probes, corresponding to 51 DAVID-identifiable IDs, were identified as commonly differentially regulated across all five oxidative stressor models. Functional cluster of these genes only provided two enriched biological processes (Table 7.1). Oxidative stress was clearly experienced by neurons subjected to oxidative insults with potential modulation of the anti-oxidant Nrf2-inducible transcription and GSH pathway. Genes that were involved in promoting cell survival demonstrated a generally down-regulatory transcriptional response.

Table 7.1 Selected enriched biological processes consisting of common differentially regulated genes common to five oxidative stressors-induced neuronal injury models. Cultured mouse primary cortical neurons (dissected from brains of gestation day 15-16 Swiss white albino embryos; Cheung et al., 1996) were treated with 250µM HOCl, 0.5mM NOC-18, 10nM rotenone, 1µM lactacystin and 250µM Glu respectively and RNA collected over a 24h timeframe. The first significant numerical fold-change value exceeding ± 1.5 up or down –regulated \pm sem, with their respective time-point (in bracket) was presented. Up (\uparrow) or Down (\downarrow) arrow after gene symbol denotes the overall regulatory trend over a 24h time-course transcriptomic study for each oxidative stressor model, i.e. a specific gene which show early up-regulation at the initial phase, with subsequent down-regulation at a later time-point is assigned with a $\uparrow\downarrow$ arrow and vice versa. If the latter up/down-regulation is in a fold-change of opposite mathematical sign (+ or -) and above 1.5 expression level, it would also be demonstrated in the table.

Genbank	Gene Title	Symbol	HOCl	NOC-18	Rotenone	Lactacystin	Glu
Oxidative stress							
- Oxidative stress induced gene expression via Nrf2							
NM_010234	FBJ osteosarcoma oncogene	c-Fos	20.94 \pm 3.01 (8h) $\uparrow\downarrow$	31.00 \pm 1.08 (8h) $\uparrow\downarrow$	3.29 \pm 0.21 (8h) \uparrow	2.70 \pm 0.86 (5h) \downarrow	3.95 \pm 0.86 (5h) \downarrow
NM_009716	Activating transcription factor 4	Atf4	1.80 \pm 0.49 (8h) \downarrow	1.59 \pm 0.31 (5h) \uparrow	2.36 \pm 0.16 (15h) \uparrow	1.50 \pm 0.56 (8h) $\uparrow\downarrow$	-1.67 \pm 0.24 (15h) \downarrow
NM_010442	Heme oxygenase (decycling) 1	Hmox1	5.14 \pm 0.50 (8h) $\uparrow\downarrow$	18.03 \pm 8.04 (5h) \uparrow	14.26 \pm 2.29 (24h) \uparrow	1.87 \pm 0.49 (5h) \uparrow	1.59 \pm 0.34 (5h) $\uparrow\downarrow$
NM_010902	Nuclear factor erythroid-related factor 2	Nrf2	1.82 \pm 0.45 (24h) \uparrow	2.66 \pm 0.31 (5h) $\uparrow\downarrow$	3.55 \pm 0.42 (15h) \uparrow	1.56 \pm 0.51 (24h) \uparrow	1.61 \pm 0.58 (5h) $\uparrow\downarrow$
- Glutathione metabolism							
NM_010357	Glutathione S-transferase, alpha 4	Gsta4	3.25 \pm 0.45 (24h) \uparrow	5.78 \pm 0.48 (15h) \uparrow	2.91 \pm 0.32 (15h) \uparrow	-1.68 \pm 0.13 (5h) 1.63 \pm 0.36 (24h) $\downarrow\uparrow$	2.58 \pm 0.63 (15h) $\uparrow\downarrow$
NM_019946	Microsomal glutathione S-transferase 1	mGst1	1.93 \pm 0.41 (24h) \uparrow	2.65 \pm 0.48 (15h) $\uparrow\downarrow$	2.56 \pm 0.35 (15h) $\uparrow\downarrow$	-1.68 \pm 0.19 (8h) \downarrow	3.21 \pm 0.87 (15h) $\uparrow\downarrow$
NM_009104	Ribonucleotide reductase M2	Rrm2	-1.56 \pm 0.50	-1.65 \pm 0.48 (15h) \downarrow	-1.85 \pm 0.07 (24h) \downarrow	-2.51 \pm 0.14 (15h) \downarrow	1.80 \pm 0.46 (5h) \downarrow
Cell survival							
NM_153547	Guanine nucleotide binding protein-like 3 (nucleolar)	Gnl3	2.10 \pm 0.50 (8h) \downarrow	1.54 \pm 0.48 (15h) \uparrow	1.78 \pm 0.11 (24h) \uparrow	2.03 \pm 0.48 (8h) \uparrow	1.72 \pm 0.40 (5h) \downarrow
NM_021099	Kit oncogene	Kit	-2.74 \pm 0.49 (8h) \downarrow	-2.09 \pm 0.48 (15h) \downarrow	-4.13 \pm 0.06 (15h) \downarrow	-1.53 \pm 0.17 (8h) \downarrow	-1.55 \pm 0.12 (5h) \downarrow
NM_009129	Secretogranin II	Scg2	1.95 \pm 0.49 (8h) $\uparrow\downarrow$	1.79 \pm 0.31 (5h) \uparrow	-1.86 \pm 0.07 (8h) \downarrow	1.76 \pm 0.43 (8h) $\uparrow\downarrow$	-4.09 \pm 0.07 (5h) \downarrow

7.2.6 Comparative global transcriptomic analysis across all five distinct oxidative stressor models (Common pathway perspective)

As demonstrated from Table 7.1, through functional classification of genes common to all five models, there is not much useful information extracted with regards to the understanding of the commonality of the signaling pathway. As such, another approach was derived. Gene functional classification and biological process clustering were performed on the global transcriptomic profile of individual model. Enriched biological processes were generated and compared for identification of common pathways. This prevents the potential of eliminating potential genes related to a particular significant pathway that were not universally significantly regulated in all models, and which could otherwise be filtered off if selection of genes common to all models was to be done. Furthermore, this approach is plausible as it allows a more affirmative conclusion of the overall regulatory trend of the signaling pathways through evaluation of all genes encoding for members of a particular signaling cascade.

Table 7.2 displayed genes (in their gene symbols due to the limitation of space) that were significantly modulated according to the microarray parameters previously mentioned with the up (↑) or down (↓) arrows to demonstrate their overall temporal regulatory trend in a 24h treatment timeframe. In this case, several promising and cell injury-associated signaling pathways were identified.

Table 7.2 Selected enriched biological processes consisting of significantly up-regulated genes common to four oxidative stressors-induced neuronal injury models. The genes demonstrated in the table were chosen based on the criteria of having at least ± 1.5 fold transcriptional expression in a minimum of one times-point and passed statistical testing, one-way ANOVA, $p < 0.05$ in each oxidative stressor transcriptomic profile. Cultured mouse primary cortical neurons (dissected from brains of gestation day 15-16 Swiss white albino embryos; Cheung et al., 1996) were treated with 250 μ M HOCl, 0.5mM NOC-18, 10nM rotenone and 250 μ M Glu respectively and RNA collected over a 24h timeframe. Individual transcriptomic profile was subjected to functional-gene ontology classification using the online bioinformatics database DAVID 2008. Selected biological processes (shown in table below) were generated through gene enrichment and statistically validated by gene-term enrichment score through modified Fisher's exact test and Benjamini correction (Huang et al., 2009; Dennis et al., 2003). Up (\uparrow) and/or Down (\downarrow) arrow after gene symbol denotes the overall regulatory trend over a 24h time-course transcriptomic study for each oxidative stressor model, i.e. a specific gene which show early up-regulation at the initial phase, with subsequent down-regulation at a later time are indicated with opposed arrows ($\uparrow\downarrow$).

Biological Processes	Oxidative Stressors				
	HOCl	NOC-18	Rotenone	Lactacystin	Glu
Response to oxidative Stress <ul style="list-style-type: none"> Oxidative stress-induced expression via Nrf2 	\uparrow Nrf2, Gst (alpha)	\uparrow Nrf2, Gst (alpha), Hmox1, Atf4, Pkc, Fos, Jun, Ugt	\uparrow Nrf2, Gst (alpha), Hmox1, Atf4, Fos, Ugt	\uparrow Nrf2, Gst (alpha), Hmox1, Atf4, Fos, Ugt	\uparrow Nrf2, Hmox1, Gst (alpha), Fos, Ugt
<ul style="list-style-type: none"> Heat shock proteins (Hsps) and molecular chaperones 	\uparrow ApoE, Nqo1, Txnl2, Prdx(1, 6)	\uparrow Nqo1, Ptgs2, Npn3, Prdx (1, 6)	\uparrow Nqo1, Gab1 / Gab3, Ptgs2, Npn3, Prdx6, Sesn3	\uparrow Npn3, Txnl1, Ptgs2 \downarrow ApoE, Prdx (2, 3, 5, 6)	\uparrow ApoE, Nqo1, Gab1, Npn3, Prdx (1, 6), Mt (1, 2, 3), Sesn3
<ul style="list-style-type: none"> Glutathione (GSH) anti-oxidant pathway 	\uparrow Gst (alpha, mu, pi), mGst1, Gsr1, Gcl	\uparrow Gst (alpha, mu, theta), mGst1, Gpx1, Gss, Gsr1, Gcl, Idh2 \uparrow	\uparrow Gst (alpha, mu, pi), mGst1, Gpx1 / Gpx7, Gss, Idh2	\uparrow Gst (alpha), Gsr1, Gcl \downarrow Gst (mu, theta, zeta), mGst, Idh2	\uparrow Gpx1, Gst (alpha, mu, theta), mGst1, Idh2

Table 7.2 (continue)

Biological Processes	Oxidative Stressors				
	HOCl	NOC-18	Rotenone	Lactacystin	Glu
Endoplasmic reticulum (ER) stress via unfolded protein response (UPR)	<p>↑Serpinh1</p> <p>↑↓Hspa1a, Hsp (ca, cb), Hsp105, Chaperonin 10, Hsp (a2, a8), Txdc4 ↑↓</p>	<p>↑Hspa8, Hspb8, Hspa9a, Hsp14, Serpinh1, Txdc4, Perk, Der11, Ero11, Herpud1</p>	<p>↑Hsp (a1, a8), Hspa9a, Txdc4, Ern2</p>	<p>↑Hspa1a, Hsp (a5, a8), Hspa9a, Hspb1, Hspd1, Hspe1, Hsp (ca, cb), Chaperonin 10, Hsp105, Serpinh1, Perk, Ero11, Herpud1</p>	<p>↑Hsp (a2, a8), Serpinh1, Perk</p>
Ubiquitin-Proteasome System (UPS)	<p>↑Ube2a,</p> <p>↑↓Ube2e, Usp (5, 19, 22), Psma (1, 7), Psm8</p>	<p>↑Usp (2, 36)</p> <p>↓Ube2c, Ube2n, Ube3c, Psma1</p>	<p>↓Ube1x, Ube2d, Ube2n, Ube3b, Psma (1, 3)</p>	<p>↑Ubc, Ube2g2, Ube3a, Ufd11, Usp (8, 16, 40), Psma (1, 7), Psmb (3, 7), Psmc1</p> <p>↑↓Usp (3, 30), Psmb1, Psmc (2, 3, 4, 5)</p> <p>↓Usp (29, 36, 43), Psmb10</p>	<p>↑Usp3</p> <p>↑↓Psma1</p> <p>↓Ube1x, Ube2n</p>
Mitochondrial respiratory chain	<p>↑Acad, Cyp7b1, Cyp4v3</p> <p>↑↓Gpd2, ETC complex-I (Ndufa3), ETC complex-III (Uqcr), ETC complex-IV (Cox4i1, Cox7b, Cox7c)</p>	<p>↑Acad, Idh2, ETC complex-IV (Cox6a2, Cox7c)</p> <p>↓ ETC complex-IV (Cox7a1), Gpd1</p>	<p>↑Acad, Idh2, ETC complex-IV (Cox7b), Cyp1b1, Cyp4v3, Cyp4a14, Cyb5r1, Cyb5r2</p> <p>↓ ETC complex-I (Nduf), ETC complex-II (Sdhb, Sdhc), ETC complex-III (Uqcr), ETC complex-IV (Cox5b, Cox6a2)</p>	<p>↑Acad, Cyp26b1, Cyp4b1, Cyp7b1, Etfb</p> <p>↓ ETC complex-I (Ndufa6), ETC complex-III (Uqcr), ETC complex-IV (Cox5b, Cox6a2, Cox6b, Cox6c, Cox7b), Idh2, Cyb561, Cyb5</p>	<p>↑Acad, Idh2, Etf (a, d), ETC complex-IV (Cox6b, Cox8b), ETC complex-IV (Cox6a)</p>

Table 7.2 (continue)

Biological Processes	Oxidative Stressors				
	HOCl	NOC-18	Rotenone	Lactacystin	Glu
Calcium ion binding and homeostasis	<p>↑Trpc4, S100A (1, 6, 10, 11), Fah, Cib2 AnxA (2, 3)</p> <p>↑↓Gpd2, Lman</p>	<p>↑Trpm7, S100A (1, 4), S100b, Atp2c, Pkca, Fk506bp (9, 10), Lamc1, AnxA (2, 3, 4, 5) ↑</p>	<p>↑S100A (1, 6, 10, 11), Fk506bp (9, 10), AnxA (2, 3, 5)</p>	<p>↑S100A (10, 13), AnxA2</p> <p>↓ Fk506bp (2, 4, 8)</p>	<p>↑S100A (6, 11), FK506bp (9, 10), Calml4, Lamb2, AnxA (2, 3, 5), Capn2</p>
Programmed cell death	<p>↑Bax, Bad</p> <p>↑↓Casp (3, 8, 9), Cytc</p>	<p>↑Tnfrsf (1a, 12a), Pawr, Dap, Btg, Siva, Puma, Noxa</p> <p>↑↓ Dapk2</p>	<p>↑Tnfrsf (1a, 10b, 12a), Traf1, Pawr, Dap, Casp8, Fas</p>	<p>↑Fas, Puma, Noxa</p>	<p>↑Casp6, Dap, Pawr, Aif</p> <p>↑↓Tnfrsf12a</p>

7.3 Discussion

7.3.1 RESPONSE TO OXIDATIVE STRESS

- Oxidative stress-induced expression via Nrf2

Various endogenous and exogenous sources contribute to the increase in oxidative load. Mitochondria being the primary cellular factory for energy production are a rich endogenous source of ROS through its respiratory electron transport chain which constantly undergoes fluctuations in redox states (Halliwell, 2006). Other cellular processes leading to ROS formation include lipid peroxidation, metal ion-associated Fenton reactions, NO-mediated protein nitrosylation and matrix enzymatic interactions (Chinopoulos and Adam-Vizi, 2006; Halliwell, 2006). Cellular oxidative stress can trigger two opposing cellular responses: pro-survival and pro-death reactions. Pro-survival response to oxidative stress can be implemented at two different molecular stages, targeting at the transcriptional and post-translational modification levels respectively.

NRF2, a pro-survival transcription factor primarily localized in the cell nucleus, is ubiquitously expressed in a wide variety of tissue and cell types (McMahon et al., 2001). Neuroprotective role of NRF2 has been demonstrated in *in vitro* and *in vivo* models of neuropathy (Johnson et al., 2008), amidst its assertive anti-cancerous and anti-inflammatory functions in tumor growth and tissue injuries (Reddy et al., 2009; Ramoz-Gomez et al., 2001). It is involved in the transcriptional activation of ARE-containing genes encoding detoxifying enzymes and cytoprotective antioxidant proteins (e.g. superoxide dehydrogenase, Nqo1, and glutathione *S*-transferase (Gst) upon oxidative and electrophilic stresses (Zhao et al., 2007). Under physiological basal conditions, induction

Chapter 7:
***In vitro* oxidative stressor models**

of NRF2 target gene expression is inhibited by NRF2 retention in the cytoplasm by its interacting inhibitory partner, KEAP1 which targets it for degradation by the UPS (Reviewed in Kaspar et al., 2009). In the event of cellular stress, rise in intracellular ROS and electrophiles induce the activation of several protein kinases, including PKC, ERK, MAPK, and PKR-like ER kinase (PERK) (Buckley et al., 2003). These protein kinases induce the phosphorylation of NRF2, releasing it from KEAP1 sequestration and facilitating its translocation into the cell nucleus where it binds to ARE sequence, leading to transcriptional activation of antioxidant enzymes (Nguyen et al., 2000; Buckley et al., 2003) (Bloom and Jaiswal, 2003; Huang et al., 2002; Zipper and Mulcahy, 2000; Cullinan et al., 2003).

Individual analytical results from the time-course global expression profiles of HOCl-, NO-, rotenone-, lactacystin- and Glu-treated neurons revealed a strong NRF2-mediated transcriptional elevation of oxidative stress-responsive neuroprotective genes. NRF2-targeted pro-survival genes (e.g. Pkc, activating transcription factor 4 (Atf4), Gst subunits, Hmox1 and Hsps (categorized under Endoplasmic reticulum stress via unfolded protein response in Table 7.2) demonstrated consistent transcriptional up-regulation with concomitant along with Nrf2 elevated gene expression in all five oxidative stressor models. It is worthy to note that proteins encoded by Nrf2-induced transcriptional target genes also have prominent roles in the unfolded protein response (UPR) triggered upon ER stress, establishing the intimate regulatory feedback relationship between processes activated upon cellular oxidative and ER tensions.

-Hsps and molecular chaperones

Oxidative damages to existing cellular proteins can also be mitigated at the post-translational stage through the mobilization and activation of HSPs and metal ion molecular chaperones. HSPs and molecular chaperones are crucial in the facilitation of the refolding of misfolded proteins to avoid their aggregation and accumulation in the cell (Meriin and Sherman, 2005). They cooperate with the ubiquitin-proteasome system (UPS) to prevent intracellular buildup of aberrant toxic proteins, and regulate the degradation of excess cytoplasmic proteins. HSPs confer cellular protection mainly through two mechanisms: firstly, as mentioned, HSPs act as molecular chaperones to ensure correct formation and maintenance of native conformation of cytosolic proteins and stabilization of actin filaments; secondly, suppression of the pro-apoptotic member of the BCL2 family, BID, by HSP70 (HSPA8) and HSP27 (HSPB8) prevents cytochrome c (CYTC) release (reviewed in Franklin et al., 2005).

The present comparative gene expression profiling study demonstrated a generally similar elevation in gene expression trend of several Hsps such as Hspb1, Hsp2, Hspa8, Hsp9a and Serpinh1 (Hsp47) (categorized under Endoplasmic reticulum stress via unfolded protein response in Table 7.2). The same phenomenon is observed for peroxiredoxins (Prx1 and Prx6), prostaglandin-endoperoxide synthase 2 (Ptgs2; also known as cyclo-oxygenase 2) and neoplastic progression 3 (Npn3; also known as sulfiredoxin) and members of the metal ion chaperones, metallothionein family (Mt1, Mt2 and Mt3) in all models with the exception of lactacystin.

- *Glutathione (GSH) anti-oxidant pathway*

Further to the cytoprotective effects offered by the HSPs and chaperones, the GSH pathway also serves to be a major effective mean to reduce oxidative stress via sequestration of NO, ONOO⁻ and ROS. Genes related to GSH biosynthesis induced in the presence of oxidative stress acts as a cellular defense mechanism. During oxidative stress, increased NADP⁺ concentration will lead to activation of glucose-6-phosphate dehydrogenase, an enzyme that catalyses the first rate-limiting step in the oxidative branch of pentose phosphate pathway (PPP), and subsequently stimulation of PPP (Ursini et al., 1997). Studies have showed that stimulation of PPP in neurons and astrocytes conferred protection against ROS-induced toxicity by producing NADPH (Ben-Yoseph et al., 1996). The induction of detoxification enzymes such as GST, NQO1, mitochondrial aldehyde dehydrogenase (ALDH), and Aldh dehydrogenase/reductase 8 (DHRS8) which use GSH and NADPH as co-factors are important in detoxifying quinines and maintaining the cellular redox balance. One common feature of these proteins is that they use GSH and NADPH as co-factor. So, for efficient detoxification and maintenance of cellular redox status, it would be beneficial to increase these proteins together with GSH and NADPH. Hsps genes were also regulated in a GSH-dependent manner (Calabrese et al., 2003). Fratelli et al., 2005 showed that HSP40 and HSP70 are strongly induced by GSH depletion.

Indeed, from the microarray analyses, initiation and persistent activation of the GSH anti-oxidative pathway were evident from the concerted transcriptional up-regulation of its pathway members (Gcl, Gst, Gsr and Gpx1) and associated detoxifying enzymes (Nqo1

and Npn3) and Hsps (Serpinh1 and Hspa8) in HOCl, NO, rotenone and Glu models (Table 7.2). Intriguingly, lactacystin-mediated neuronal injury demonstrated a mixed transcriptional response within the different Gst subunits.

Altogether, the transcriptional up-regulation of detoxification enzymes, antioxidant proteins and Hsps upon oxidative stress is a result of activation by NRF2 via the ARE motif found in their promoters followed by alteration of thiol redox state (Wasserman and Fahl, 1997). Thus, the coordinate up-regulation of these genes can have a synergistic effect in the maintenance of GSH levels as well as detoxification of reactive intermediates. It can be inferred that NRF2-induced pathway plays a crucial role in propagating a strong anti-oxidative, pro-survival response against oxidative stress.

7.3.2 ENDOPLASMIC RETICULUM (ER) STRESS VIA UNFOLDED PROTEIN RESPONSE (UPR)

ER, with a pivotal pleiotropic physiological role in cellular biogenesis, metabolism, signaling and survival, is also a vital homeostatic organellar regulator of cellular stress (Travers et al., 2000). It is the site for the proper synthesis, folding and post-translational modification of cellular proteins (Ron et al., 2007) as well as production of steroids, cholesterols and other lipids (Chang et al., 2006). It also serves as a major intracellular Ca²⁺ store (Verkhatsky, 2005).

Presence of ER stress has been reported in AD (Hoozemans et al., 2005), PD (Kitao et al., 2007) and ischemic stroke (DeGracie and Montie, 2004). ER stress, characterized by

the accumulation of unfolded proteins in the ER lumen, is frequently inflicted upon by the presence of oxidative stress. This stress induction can occur upon perturbation of any of ER cellular functions, i.e. via protein oxidation, disturbance of Ca^{2+} signaling, and alteration of the homeostatic redox balance (Gorlach et al., 2006). An intimate communicative, functional coupling relationship between ER and mitochondria has also been established on the basis of these cellular functions. One instance would be the maintenance of Ca^{2+} equilibrium, crucial for the proper functioning of both organelles (Csordás et al., 2006). Mitochondria act as an emergency Ca^{2+} store upon sudden transient surge in cytosolic Ca^{2+} level, to buffer the ER against any functional disruption. Furthermore, several members of the Bcl2 family prominent for their roles in regulation of mitochondrial-mediated apoptosis also participate in ER-induced cell death and Ca^{2+} signaling between the ER and mitochondria (Gorlach et al., 2006; Rao et al., 2004). Initiation of ER stress has been demonstrated to occur upon mitochondrial energy deficits (Flores-Diaz et al., 2004).

Upon ER stress, UPR is triggered to restore homeostatic balance (Schröder, 2008). UPR serves as a double edge sword inducing resultant pro- and anti-apoptotic effects. During the initial phase of oxidative stress when incurrence of cellular oxidative damage is still within ER tolerable threshold, UPR activates two signaling pathways mediated by two ER-resident kinases, PERK and inositol-requiring enzyme (IRE1), and transcription factors Atf4 and Atf6 which promote cell survival through the alleviation of ER burden. Mitigation of ER stress is achieved via two cellular routes: firstly, ER dynamic capacity to process unfolded and/or misfolded proteins is increased through elevated expression of

Chapter 7:
***In vitro* oxidative stressor models**

ER chaperones via IRE1-induced expression of Xbp1, a transcription factor that activates transcription of genes coding for proteins needed for the ER protein folding and processing reactions (Schroder, 2008), and inhibition of cellular protein translation to decrease the buildup of newly synthesized, unassembled proteins by PERK-mediated inhibitory phosphorylation of the eukaryotic initiation factor (eIF2 α) (Harding et al., 1999).

However, once ER stress proceeds beyond the tolerable limit and homeostasis cannot be restored, UPR evokes a detrimental effect to send the cell to its demise. Programmed cell death pathways originating from ER stress responses can occur dependent and/or independent of mitochondria (Li et al., 2006). Prolonged extensive ER damage triggers apoptosis via the production of unfolded proteins or the release of Ca²⁺ into the cytoplasm (Rao et al., 2004). ER stress can activate its resident protease, caspase-12 and Atf6-induced CHOP expression, causing mitochondrial membrane permeabilization which eventually leads to either classical apoptosis or other mitochondrial cell death pathways (van der Sanden et al., 2003). In addition, the Ca²⁺ release from ER can induce calpains which are normally kept inactive by their endogenous inhibitor calpastatin, eventually leading to programmed necrosis (Wang, 2000). Excessive calpain activation *in vitro* can lead to non-specific degradation of constituent proteins, including cytoskeletal proteins, and growth factor receptors.

Substantial ER stress is prominent from the gene expression profiles of all five oxidative stressor models with significant increase in gene expression of Atf4, Nrf2 and Perk, an

indication of UPR activation (Table 7.2). The increase expression of these UPR-related genes can occur as a consequence of Nrf2 transcriptional activation, as previously mentioned. Furthermore, ER-stress inducible chaperones (Txdc4 and Hsps) and pro-apoptotic proteins (Puma and Noxa) (discussed in details Cell Death section) also showed transcriptional up-regulation. This is a clear inference of the occurrence of ER stress upon cellular oxidative tension, resulting in trigger of UPR to counteract the accumulation of aberrant oxidized proteins and dysregulated intracellular ionic concentrations.

7.3.3 UBIQUITIN-PROTEASOME SYSTEM (UPS)

The UPS is a complex system which plays a primary role in eukaryotic protein clearance and quality control, where misfolded and/or excessively produced proteins are molecularly marked with poly-ubiquitins and dedicated for degradation by the proteasome system (Schroder and Kaufman, 2005). Compromise in UPS efficiency has been reported in the aging process (reviewed in Gaczynska et al., 2001) and neurodegenerative disorders where aberrant protein inclusions have been observed (Mandel et al., 2005). A down-regulation of genes encoding proteasome subunits in the substantia nigra pars compacta of PD brain has been reported by Mandel et al., 2005, indicating the essentiality of maintenance of functional proteasomal expression for neuronal survival under stress conditions. UPS can be segregated into two distinct processes which starts off with ubiquitinylation of the proteins mediated by three enzymes namely, ubiquitin-activating enzyme E1 (UBE1), ubiquitin-conjugating enzyme E2 (UBE2) and ubiquitin protein ligase E3 (UBE3), followed by the targeting of the ubiquitin-linked protein/polypeptide to the proteasome for clearance.

Chapter 7:
***In vitro* oxidative stressor models**

Observations based on the temporal regulatory trend of UPS-related genes in the transcriptomic profiles of all oxidative stressor models with the exception of HOCl and lactacystin suggested the occurrence of an UPS dysfunction based on a general down-regulation of genes encoding ubiquitinylation enzymes and certain proteasome subunits (Table 7.2). These genes include those encoding for the proteasome subunits (Psm1 and Psm3), Ube1 (Ube1x), Ube2 (Ube2c, Ube2a, Ube2d2 and Ube2n) and Ube3 (Ube3b and Ube3c). On the other hand, ubiquitin-specific peptidases (Usp2, Usp3, Usp22, Usp36), which function as deubiquitinating enzymes, demonstrated significant up-regulation, a further evidence of the decreased efficiency of UPS function.

An early initial up-regulation of UPS genes that eventually falters with time is especially prominent in HOCl-mediated neuronal injury (Table 7.2), suggestive of a regulatory feedback mechanism in an attempt to reverse the detrimental effects of proteasomal inhibition in the event of a proteasome dysfunction-induced cell death (Yew et al., 2005). This mirrors a partial regulatory trend of the UPS genes (Usp3, Usp30, Psm1, Psmc(2-5)) in lactacystin-mediated neuronal injury. On the other hand, the remaining genes were up-regulated in lactacystin profile. These include genes that encode for the proteasome subunits (Psm1, Psm7, Psm3 and Psm7), ubiquitins (Ubc), ubiquitin-conjugating enzyme E2(Ube2g2), ubiquitin protein ligase E3 (Ube3a) and ubiquitin fusion degradation 1 like (Ufd11). This is consistent with report by Meiners et al, 2003 that remarked that proteasomal inhibition triggered a transient and concerted up-regulation of all 26S proteasome subunit mRNAs and enhanced synthesis of all proteasomal subunits, and increase in the number of proteasomes.

7.3.4 MITOCHONDRIAL RESPIRATORY CHAIN / NON-RESPIRATORY CHAIN ENZYMES

The mitochondrial network plays a vital role in the supply of cellular energy currency in the form of ATP to ensure the proper functioning of a variety of metabolic processes within a cell. Simpler molecules resulting from the cellular cyclic processing of macromolecular nutrients transfer electrons to carrier proteins such as NAD⁺ and FAD⁺ producing NADH and FADH₂, which transfer the electrons to the ETC localized at the inner mitochondrial membrane (Saraste, 1999). Due to the constitutive cyclic fluctuation of the redox status between ETC enzymatic protein complexes with consequent high consumption of cellular oxygen in the oxidative phosphorylation process, mitochondria are assumed to be the main cellular producers of ROS (Orrenius et al., 2007). Escaping electrons from the ETC can potentially reduce oxygen to form the highly reactive free radical superoxide anion, which can undergo further Fenton reaction to generate hydroxyl radical and hydrogen peroxide which similarly can cause detrimental cellular damages (Boveris et al., 1972).

As a result of this pivotal physiological function of mitochondria which if not properly managed can have adverse effects on cell survival, mitochondrial functionality has been proposed to be a crucial regulator and indicator of cellular homeostasis. Indeed, decline in mitochondrial functionality has been closely linked to increasing age of mammals. This age-correlated respiratory chain deficiency is especially prevalent in only a subset of mammalian tissues, such as heart, skeletal muscle, colonic crypts and neurons (Dufour et al., 2008). A recent study by Dufour et al., 2008 demonstrated that the co-existence of

functional respiratory chain-deprived and normal neurons accelerated the neurodegenerative process of the adjacent normal cells through a trans-neuronal signaling mechanism.

Transcriptomic analysis revealed substantial differential regulation in gene expression of majority of the mitochondrial enzymatic proteins involved in the oxidative phosphorylation and ETC processes. Main players of the mitochondrial ETC, namely complexes I to IV, demonstrated primarily significant down-regulation scattered across five oxidative stressor models, with the rotenone treatment being especially prominent with all four complexes being transcriptionally affected (Table 7.2). Mitochondrial complex IV demonstrated significant transcriptional regulation across all five oxidative stressor models.

On the contrary, other non-mitochondrial microsomal electron transferring pathways such as the cytochrome p450 family (Cyp), and cytochrome b5 reductase (Cyb5) demonstrated up-regulation, a probable compensatory attempt to make up for the cellular energy deficit (Table 7.2). Similarly, other proteins also involved in oxidative phosphorylation (e.g. glycerol-3-phosphate dehydrogenase (Gpd), acetyl-coenzyme A dehydrogenase (Acad) and isocitrate dehydrogenase (Idh)) also showed elevated gene expression.

7.3.5 CALCIUM ION BINDING AND HOMEOSTASIS

Delicate management of calcium ion homeostasis is critical to cellular wellbeing due to the presence of a variety of Ca^{2+} -activated protein families which can evoke two antagonizing outcomes: survival and proliferation, or cell death. These opposing consequences are mediated by Ca^{2+} released from specific Ca^{2+} compartments through different calcium channel subtypes, which stimulate Ca^{2+} -dependent proteins at differential subcellular localizations. As such, cells have an intrinsic fail-safe system implemented by the mitochondria to combat sudden and temporary surge in intracellular Ca^{2+} level as a result of oxidative stress (reviewed in Chinopoulos and Adam-Vizi, 2006). Mitochondria regulate cellular Ca^{2+} signals by acting as a temporary Ca^{2+} buffer and respond to Ca^{2+} elevations by increasing the cell energy supply (Santo-Domingo and Demarex, 2010). However, upon abnormal calcium ion homeostasis arising from prolonged ER stress and increase ROS production, a series of intracellular signaling cascades is activated which can lead to apoptosis through the activation of Ca^{2+} -activated calpains (Crocker et al., 2003).

Detailed analysis of the transcriptomic profiling of all five oxidative stressor models in the present study demonstrated significant up-regulated gene expression of proteins involved in calcium ion binding and homeostasis which comprised of Ca^{2+} -activated proteins such as S100A and FK506 Ca^{2+} -binding protein families and annexins (Anxs) (Table 7.2). Further, a transcriptional up-regulation of the Ca^{2+} -activated protease calpain-2 (Capn2), prominently implicated in programmed necrosis (discussed in details in Cell Death), was observed in the Glu-mediated neuronal injury model. This is a

probable indication of the presence of atypical, high intracellular Ca^{2+} level which enhanced Ca^{2+} signaling resulting in an increased demand for elevated expression of its Ca^{2+} -dependent members.

7.3.6 CELL DEATH

PCD as previously mentioned in Chapter 1: Introduction has broaden its definition, other than apoptosis (PCD-I), to include further two cell death subtypes namely autophagy (PCD-II) and programmed necrosis (PCD-III). Due to the increased complexity and overlapping in processes across the 3 modes of PCD, it is difficult to distinctively assign which PCD type is at work for each individual cell death occurrence. This is because all three PCD modes can consecutively or simultaneously be involved in an apoptotic-necrotic continuum in a cell. Alternatively, within a homogenous population of cell type subjected to a single cytotoxic insult, there can be a co-existence of heterogenous PCD types in operation among neighbouring cells.

It is evident from the microarray analysis that the apoptotic mechanisms, both mitochondrial-dependent and –independent, were at work in the facilitation of neuronal death in the four distinct oxidative stressor models. However, the up-regulated set of PCD genes differs across models even though the genes encode for proteins involving in the same pathway. Transcriptional up-regulation of the main players in mitochondrial-dependent pathway, comprising of cytochrome c (Cyt_c), caspase 3 (Casp3), BH3 interacting domain death agonist (Bid), Bcl2-associated x protein (Bax) and apoptosis-inducing factor (Aif), and that of the extrinsic apoptotic pathway, including the tumour

necrosis factor receptors (Tnfrsf1), Fas, caspase 8 (Casp8) and death associated protein (Dap), were detected (Table 7.2).

- Intrinsic mitochondrial-dependent apoptosis

Activation of the intrinsic mitochondrial apoptotic pathway as a response to elevated ROS production and mitochondrial DNA damage facilitates outer membrane permeabilization and mitochondrial-cytoplasmic translocation of CYTC, AIF, or SMAC/DIABLO, which induce downstream caspase-dependent or -independent cytosolic signaling events (Ryter et al., 2007). In the event of the occurrence of former, CYTC interacts with APAF1 to form the apoptosome complex which further recruits and activates the zymogen of CASP9. The fully assembled apoptosome then proceeds to induce cleavage of downstream effectors CASP3 and CASP7. In the form of positive feedback mechanism, activated CASP3 promotes CASP2 and CASP6 activation that further promote CASP9 processing (Slee et al., 1999). Concurrently, the antagonistic effect of Smac/Diablo on the inhibitors of apoptotic proteins (IAPs) enhances caspase activation. On the other hand, AIF mediates caspase-independent signaling through cytoplasmic-nuclear translocation to mediate nuclear chromatin condensation and DNA fragmentation (Sussin et al., 1999). From Table 7.2, it is apparent that HOCl and Glu – mediated neuronal injuries engaged the mitochondrial-dependent apoptotic pathway as demonstrated by the transcriptional up-regulation of Cytc, Bax, Bad, Casp (3, 6 and 9) and Aif in both models.

-Extrinsic tumour necrosis factor receptors (TNFRs)-mediated apoptosis

The extrinsic apoptotic pathway is triggered by the activation of death receptors present on the exterior of plasma membrane through ligand-receptor interactions resulting in the eventual activation of the initiator caspases through protein-protein interactions. These death receptors include Fas, TNFRSF, and TNF-related apoptosis-inducing ligand (TRAIL) receptors (Ashkenazi and Dixit 1999), of which the former two demonstrated transcriptional up-regulation in all five oxidative stressor models (Table 7.2). The Fas/Fas ligand (FasL) pathway is one of the extensively studied mechanisms in extrinsically stimulated death receptors-mediated apoptosis (Reviewed in Circu and Aw, 2010). With the binding of Fas/FasL, the Fas-associated death domain (FADD) and procaspase 8 are recruited to form the death-inducing signaling complex (DISC) which is then endocytosed (Watanabe et al., 1988). The accumulation of cytoplasmic DISC after its release from the endosomes and detachment from the receptors promotes activation of the initiator CASP8 (Lee et al., 2006). The relative degree of CASP8 activation determines the types of downstream signaling courses being induced: substantial CASP8 activation can directly activates CASP3, whereas low CASP8 activation adopts intrinsic mitochondrial-dependent pathway as previously to activate CASP3 (Barnhart et al., 2003). The extrinsic pathways mediated by the plasma membrane integrated death receptors (TNFRs) play a major role in cell death promotion in all five oxidative stressor models by demonstrating transcriptional up-regulation over the 24h gene profiling period (Table 7.2).

- p53-mediated apoptosis

p53 (alternatively known as transformation-related p53 (Trp53)) is a well-known transcription factor for its physiologic role in guarding the integrity of the DNA genome by keeping the cell cycle process in check. However, recent discoveries have shifted the research attention onto its role in cell death induction through activation of ER stress-responsive apoptotic genes such as p53-unregulated modulator of apoptosis (PUMA; BCL2 binding component 3 (Bbc3)) and phorbol-12-myristate-13-acetate-induced protein 1 (NOXA; phorbol-12-myristate-13-acetate-induced protein 1 (Pmaip1)) (Yu and Zhang, 2003) as well as its non-transcriptional-dependent mediation of cell death through its non-nuclear localization (Yee and Vorsden, 2004). p53 has also been demonstrated to associate with and inactivate the anti-apoptotic/pro-survival members of the BCL2 superfamily such as BCL2 and BCL-xL (Erster and Moll, 2005). On the other hand, PUMA and NOXA are BH3-containing proteins which have the ability to displace BCL2 and BCL-xL inhibitory interactions with the pro-apoptotic proteins BAX and/or BAK (also members of the BCL2 superfamily), thus leading to the latter duo activation, resulting in mitochondrial outer membrane permeabilization and release of apoptogenic factors such as CYTC (Kim et al., 2009). Interestingly, BCL-xL has been reported to be involved in the inhibition of cytoplasmic p53 activity, and that transcriptional activation of Puma by nuclear p53 is required for the PUMA protein to release cytoplasmic p53 from BCL-xL to activate BAX (Chipuk et al., 2005). Only in NO and lactacystin - mediated neuronal death models did PUMA and NOXA demonstrated significant transcriptional up-regulation, indicative of the activation of p53 signaling pathway induced by ER stress (Table 7.2).

7.3.7 Summary of the comparative microarray analysis across the five oxidative stressors models

Elaboration of the type of data obtained by transcriptional analysis, as shown above, will shed further light on specific details of the apoptosis-necrosis continuum of neuronal death, which takes place consequential to induction of oxidative stress. As such, with the presence of regulatory feedback loops existed among different modes of PCD, it is impossible to distinctly dissect one mode from the other. Furthermore, adding on to the equation is each player having concurrent functions in different modes, complicating the whole PCD process. This can be an advantage when identifying potential biological targets within the PCD cascades, as there is the possibility of inhibiting multiple pro-death pathways through single target suppression. As such, it is important that PCD be viewed as a single complex, multi-pathways process.

In conclusion, comparative analysis of the global transcriptomic profiles of HOCl, NO, rotenone, lactacystin and Glu, all of which are prominent oxidative stressors of neurological disorders such as AD, PD and ischemic stroke models, enable us to achieve novel insights into neuronal oxidative stress. This would greatly facilitates downstream experimental works via identification of novel biological targets which singular effects through manipulative means (e.g. suppression or over-expression) would prove to be effective in the impediment of neurodegeneration in a variety of neuropathies. The enriched biological processes discussed here centralized and highlighted the significant implication of mitochondria and other organelles including ER, in a multi-process aggravation of neuronal injury. Furthermore, in the context of most oxidative stress-

Chapter 7:
***In vitro* oxidative stressor models**

related neurodegenerative diseases such as AD, PD, ALS and even in ischemic stroke, which are also recognized as protein aggregation disorders, the presence of these aggregates provide an additional aspect aggravating the cellular stresses leading to neurodegeneration and cell death. While studies at the cellular level have limitations in terms of understanding the detailed pathophysiological process leading to disease in the intact organism (humans or animal models of particular diseases), they do provide the key underpinnings of molecular and cellular pathways, on the basis of which the behaviors of cells, tissues and organs in the more complex milieu of the mammal can be deciphered.

Chapter 8: Conclusion and Future Directions

8.1 Conclusion

8.1.1 Summary of major findings from *in vitro* models

Previous pharmacological studies employing selective iGluRs antagonists demonstrated that H₂S-mediated neuronal injury involved iGluRs (namely NMDARs and KARs) - mediated excitotoxicity resulting in lysosomal rupture (Cheung et al., 2007). By employing functional GluRs-expressing cultured primary cortical neurons as the foundation of *in vitro* model, it would be worthy to determine the significance of NMDARs and KARs –activated signaling cascade in H₂S-mediated neuronal injury by employing their specific agonists. As such, microarray analysis was conducted on H₂S, NMDA and KAR-mediated neuronal injury models to elucidate this dependence of the excitotoxicity pathways during H₂S-mediated neuronal injury. Comparative global gene profiling of these three models demonstrated a significant overlap of NMDA and KA profiles against that of H₂S, indicating a high degree of reliance of the iGluRs, i.e. NMDARs and KARs in the infliction of excitotoxicity-mediated cellular damage, which constitute a significant contribution to the overall H₂S-mediated neuronal injury.

Excitotoxicity is primarily initiated by aberrant rise in cytosolic Ca²⁺ level through activation of iGluRs and ionic channels on plasma membrane. It has become an increasing hallmark in several neurodegenerative diseases such as AD, PD, HD and ALS, as well as acute neurological disorders as such as cerebral ischemia and TBI. Since excitotoxicity has been frequently documented as an upstream cellular event with great emphasis placed on its role in induction of neuronal loss, it would be of great research importance and relevance to ascertain the mechanistic impact of the iGluRs subtype in

excitotoxicity during Glu-mediated neuronal injury. This is because Glu is a major excitatory neurotransmitter in the mammalian brain, and an agonist to a huge GluRs superfamily that comprises of ionotropic and metabotropic (G-protein-coupled) subtypes which initiate very distinct signaling cascades with diverse cellular outcomes. Under neuropathological conditions, Glu in the extracellular matrix is accumulated to high cellular toxic concentrations as a result of its release from damaged neurons and the reversal action of Glu pumps on astrocyte plasma membrane. This high level of Glu then proceeds to induce activation of all its interacting GluRs, be them ionotropic or metabotropic subtypes resulting in neuronal death. As such, Glu –mediated neuronal injury involves a mixed cellular response from two different subtypes of GluRs. Even though excitotoxicity is frequently associated with hyper and constitutive activation of iGluRs, it has not been ascertained quantitatively in terms of the signaling pathways the whole subfamily transduced, and the main cellular processes potentially being the culprits for neuronal demise.

iGluRs subfamily is made up of three members, AMPAR, KAR and NMDAR, all named after their specific pharmacological agonists. Simultaneous comparison of the global transcriptomic profiles of AMPA, KA, NMDA and Glu –mediated excitotoxicity injuries revealed a higher degree of correlation in terms of number of similarly-regulated genes for KA and NMDA rather than AMPA profiles against that of Glu as background. This may signify a higher amplification of signaling transduction from KARs and NMDARs activation as a result of greater surface expression as in the case of the latter, intrinsic receptor ionic conductance and/or divergence of elicited downstream pathways. Other

than not being as highly expressed as NMDARs, AMPARs demonstrate differential Ca^{2+} permeability which is governed by the GluR2 subunit, as such the ratio of GluR2 – present to absence ratio would play a role in its regulatory response time to rise in Glu stimulus. Furthermore, in the case of Glu, the delayed in cellular process activation may be accounted for by the dilution of the effective concentration of the agonist to activate iGluRs, due to concurrent sequestration of Glu molecules by metabotropic GluRs.

Functional annotation revealed oxidative stress and cell cycle re-activation as the main cellular components triggered by excitotoxicity. This is the first time that the origin of cell cycle-reactivation has been defined and clearly linked to iGluRs activation. Simultaneous transcriptional upheaval of both processes supported the “two-hit” hypothesis originally formulated for AD pathogenesis, suggesting that oxidative stress and cell cycle dysregulation contribute hand-in-hand to neuronal loss during neurodegeneration.

8.1.2 Summary of major findings from *in vivo* models

As the mammalian brain comprises of heterogeneity of brain cell populations and blood vasculature, sole employment of the *in vitro* models allow would not suffice the understanding of excitotoxicity implication under disease pathogenesis as it does not entirely mimic the *in vivo* interactive brain environment. Stroke, commonly known as cerebral ischemia, has been well associated to excitotoxicity being one of its most prominent downstream cellular processes. Together with its pathogenesis still not fully elucidated coupled with the seriously deprivation of available therapeutic options, *in vivo*

cerebral ischemia rodent models from neonatal to adult brains, and transient to permanent occlusion, were adopted to extensively study the main injury-governing processes.

Two main patho-mechanisms namely, oxidative stress and inflammation, were consistently observed *in vivo* in all three forms of cerebral ischemia, in accordance with current up-to-date literature. Presence of oxidative stress is defined by the transcriptional upregulation of organellar (ER/lysosomal) stress-inducible genes and anti-oxidant proteins such as Hsps, molecular chaperones and GSH enzymes. The detrimental role of oxidative stress is further accentuated by the employment of Gpx1^{-/-} transgenic mouse, which demonstrated higher vulnerability to pro-oxidants, indicative of the need of functional anti-oxidative mechanisms in place to combat rise in oxidative burden. Inflammation is also evident by the increase in gene expression of inflammatory molecules such as chemokines, cytokines, interleukins and CAMs which serves to facilitate leukocyte chemotaxis and infiltration into the ischemic region.

Interestingly, cell cycle re-entry is not significantly over-represented in the *in vivo* models, even though up-regulation of pro-mitogenic and some cell cycle proteins were observed. Few Cdks and cyclins were significantly modulated. Oxidative stress and inflammation are downstream outcomes of cerebral ischemia, and occurrence of excitotoxicity, a rapid process, preceded these two events. The inability to transcriptionally detect cell cycle re-activation might be due to the much earlier occurrence of this event, resulting in even the early profiling time-point (5h) to only capture the aftermath of its regulation. In order to confirm that excitotoxicity-induced

cell cycle re-activation was present physiologically in the mammalian brain, inhibitor of a cell cycle protein kinase family, AURKs (selective for AURKA and AURKB), whose transcriptional up-regulation has been observed in all four *in vitro* models was post-administered into the rodent brain after induction of permanent focal cerebral ischemia. Promisingly and unprecedentedly, AURKs inhibitor demonstrated significant abrogation of ischemic damage with substantial reduction in infarct volume.

Up-to-date, preclinical experiments employing inhibitors (Flavopiridol, Olomoucine or Roscovitine) of another cell cycle protein kinase family, CDKs, demonstrated improved behavioral outcomes and increased neuronal survival in a series of CNS disease models such as AD (Copani et al., 2001; Jorda et al., 2003; Verdaguer et al., 2004b), PD (Kruman and Schwartz, 2006), stroke (Osuga et al., 2000; Wang et al., 2002a) and TBI (Hilton et al., 2008). However, it is worried that these beneficial effects may be ousted by the potential side-effects arise from the non-specificity of those CDK inhibitors, and furthermore, may also imply the possibility of the neuroprotection conferred by other unknown molecules inhibited by the drugs (Bain et al., 2003; Bain et al., 2007; Sridhar et al., 2006).

All in all, the combined microarray findings from *in vitro* excitotoxicity and *in vivo* cerebral ischemia models serve their purpose as a screening platform to on one hand, facilitate the understanding of the pathogenesis of stroke, and on the other hand, identify a novel biological target (AURKs) which would be promising in the development of therapeutic interventions not just for stroke, but for other neurodegenerative diseases

where cell cycle re-entry is prominent, as in the case for CDKs.

8.2 Future Directions

My current study has established the origin of cell cycle re-entry to be attributed iGluRs activation during excitotoxicity. Further, AURKs, a cell cycle protein kinase family, appeared to play a substantial role in the initiation and propagation of the cell cycle re-entry process, through firstly, the significant transcriptional up-regulation of AurKA/B interacting partners in *in vitro* models and secondly, selective AURKA/B protein inhibition demonstrating successful abrogation of cerebral ischemic infarct damage in *in vivo* rat brain. However, there still exist a missing link between these two processes which requires urgent addressing with particular focus on AURKs, mainly A and B, involvement since these two members though being have been well documented to be involved in cell cycle division especially pertaining to cancer oncology field, their roles under neuropathological conditions which in most cases excitotoxicity is causative remains to be elucidated.

First, it is important to identify the relative neuronal survival influence of AURKA/B in cell cycle re-entry in relation to excitotoxicity, and determine if their individual role in this neuropathological process is attributed to their intrinsic phosphorylation activation of their downstream targets. This is important as AURKA and AURKB functions have been assigned to different stages in the cell cycle. This can be achieved via knockdown and over-expression functional studies of AURKA/B in *in vitro* cultured primary cortical neurons which are subsequently subjected to excitotoxic insults. Consequentially, overall outcome of AURKA/B can be concluded via cell viability assays (e.g. MTT reduction assay, LDH release assay, Annexin V labelling and Hoescht stain) to determine their

Chapter 8.2: Future directions

respective influence on cell survival and the mode of cell death they each induces. Manipulation of AURKA/B protein expression can be achieved by lentiviral transduction techniques, which yields high level of targeted and controllable manipulative efficiency (that can be quantitated via immunoblotting or microscopic techniques through the use of green fluorescence tags), as compared to the employment of pharmacological inhibitors. A step further, it would be worthy to ascertain if the intrinsic phosphorylation ability of AURKA/B is crucial in mediation of excitotoxicity-induced cell cycle re-activation via the over-expression of AURKA/B kinase-dead mutants.

As AURKA and AURKB are relatively newly discovered proteins as compared to CDKs, and their relevance to neuropathy has been recently established, much research work still remains underway to fully elucidate their up/downstream interactive pathways and endogenous regulatory mechanisms in the cell cycle process under neurodegenerative conditions. As such, the second proposed future study would involve the dissection of AURKA/B up/downstream signaling pathways at the transcriptional and translational levels would prove to be of utmost relevance in the understanding of AURKA/B signaling mechanistic activation and regulation. At the transcriptional level, miRNA global expression profiling from the present project has identified several 13 miRNAs significantly modulated upon AURKs inhibitor administration after permanent focal cerebral ischemia. As miRNAs are endogenous transcriptional repressors with each controlling a handful of downstream target genes, the present miRNA global expression data provides us an advantage in the identification of the miRNA responsible for the transcriptional modulation of AURKA/B expression. This can be facilitated through the

Chapter 8.2: Future directions

application of miRNA mimetics to *in vitro* neuronal cultures prior to excitotoxicity insults, with subsequent determination of their effects on neuronal viability. At the translational level, literature has reported several AURKA (PKC, PLK and TPX2) and AURKB (BIRC5 and INCEP) interacting partners during mitotic cell division. Manipulative elevation and/or silencing of protein expression of these interacting partners would provide insights into the criticality of these interacting partners on AURKA/B functionality (in terms of activation and phosphorylation ability) and/or expression. These insights could mean the unravelling of a positive/inhibitory feedback loop and substitution of an interacting partner with another. Apart from existing reported protein partners, a yeast-two-hybrid screening can be conducted to identify new interacting partners of AURKA/B to elicit cell cycle re-entry or other cellular processes which all in all contributed to neuronal damage under neuropathological conditions. All approaches towards the uncovering of AURKA/B-mediated signaling cascade are advantageous as they concurrently also permit identification of additional biological targets, i.e. AURKA/B interacting partners whose inhibitions showed better efficacy as well as other cell cycle-related signaling roles of AURKA/B if present, which all in all contribute to exacerbation of excitotoxicity-triggered cerebral ischemic damage.

Lastly, one may ask if the significant role of AURKA/B during excitotoxicity-mediated cell cycle re-activation as seen in the *in vitro* model also applies to the *in vivo* situation which comprises of heterogeneity of brain cell populations and complex architectural interactions such as the blood-brain barrier. This can be verified indirectly through the application of AURKA and AURKB –specific inhibitors to induce functional suppression

Chapter 8.2: Future directions

in neuropathological (focal cerebral ischemia) model where excitotoxicity is causative. The efficacy of each AURK-type specific inhibitor can be accessed through animal behavioural studies to determine cognitive dysfunction as well as biochemical tests on the post-mortem rodent brains. Further work can also be set up to determine the therapeutic window of these inhibitors that can be administered post-stroke episode.

References

- Abe K. 2008. [Neuroprotective therapy for ischemic stroke with free radical scavenger and gene-stem cell therapy]. *Rinsho Shinkeigaku* 48(11):896-898.
- Abe K, Kimura H. 1996. The possible role of hydrogen sulfide as an endogenous neuromodulator. *J Neurosci* 16(3):1066-1071.
- Abe T, Sugihara H, Nawa H, Shigemoto R, Mizuno N, Nakanishi S. 1992. Molecular characterization of a novel metabotropic glutamate receptor mGluR5 coupled to inositol phosphate/Ca²⁺ signal transduction. *J Biol Chem* 267(19):13361-13368.
- Abumiya T, Lucero J, Heo JH, Tagaya M, Koziol JA, Copeland BR, del Zoppo GJ. 1999. Activated microvessels express vascular endothelial growth factor and integrin alpha(v)beta3 during focal cerebral ischemia. *J Cereb Blood Flow Metab* 19(9):1038-1050.
- Acalovschi D, Wiest T, Hartmann M, Farahmi M, Mansmann U, Auffarth GU, Grau AJ, Green FR, Grond-Ginsbach C, Schwaninger M. 2003. Multiple levels of regulation of the interleukin-6 system in stroke. *Stroke* 34(8):1864-1869.
- Adhami F, Liao G, Morozov YM, Schloemer A, Schmithorst VJ, Lorenz JN, Dunn RS, Vorhees CV, Wills-Karp M, Degen JL, Davis RJ, Mizushima N, Rakic P, Dardzinski BJ, Holland SK, Sharp FR, Kuan CY. 2006. Cerebral ischemia-hypoxia induces intravascular coagulation and autophagy. *Am J Pathol* 169(2):566-583.
- Aizenman E, Lipton SA, Loring RH. 1989. Selective modulation of NMDA responses by reduction and oxidation. *Neuron* 2(3):1257-1263.
- Akashiba H, Ikegaya Y, Nishiyama N, Matsuki N. 2008. Differential involvement of cell cycle reactivation between striatal and cortical neurons in cell death induced by 3-nitropropionic acid. *J Biol Chem* 283(10):6594-6606.
- Akazawa C, Shigemoto R, Bessho Y, Nakanishi S, Mizuno N. 1994. Differential expression of five N-methyl-D-aspartate receptor subunit mRNAs in the cerebellum of developing and adult rats. *J Comp Neurol* 347(1):150-160.
- Albers GW, Thijs VN, Wechsler L, Kemp S, Schlaug G, Skalabrin E, Bammer R, Kakuda W, Lansberg MG, Shuaib A, Coplin W, Hamilton S, Moseley M, Marks MP. 2006. Magnetic resonance imaging profiles predict clinical response to early reperfusion: the diffusion and perfusion imaging evaluation for understanding stroke evolution (DEFUSE) study. *Ann Neurol* 60(5):508-517.
- Amantea D, Nappi G, Bernardi G, Bagetta G, Corasaniti MT. 2009. Post-ischemic brain damage: pathophysiology and role of inflammatory mediators. *FEBS J* 276(1):13-26.
- Ames A, 3rd, Wright RL, Kowada M, Thurston JM, Majno G. 1968. Cerebral ischemia. II. The no-reflow phenomenon. *Am J Pathol* 52(2):437-453.
- Amici M, Lupidi G, Angeletti M, Fioretti E, Eleuteri AM. 2003. Peroxynitrite-induced oxidation and its effects on isolated proteasomal systems. *Free Radic Biol Med* 34(8):987-996.
- Andresen J, Shafi NI, Bryan RM, Jr. 2006. Endothelial influences on cerebrovascular tone. *J Appl Physiol* 100(1):318-327.
- Aoshima H, Inoue Y, Tanaka D. 1992. A minimal model to account for the response of N-Methyl-D-aspartate receptors expressed in *Xenopus* oocyte injected with rat brain mRNA. *Neurochem Int* 20(3):299-306.

- Aronowski J, Strong R, Grotta JC. 1997. Reperfusion injury: demonstration of brain damage produced by reperfusion after transient focal ischemia in rats. *J Cereb Blood Flow Metab* 17(10):1048-1056.
- Arumugam TV, Woodruff TM, Lathia JD, Selvaraj PK, Mattson MP, Taylor SM. 2009. Neuroprotection in stroke by complement inhibition and immunoglobulin therapy. *Neuroscience* 158(3):1074-1089.
- Arundine M, Tymianski M. 2004. Molecular mechanisms of glutamate-dependent neurodegeneration in ischemia and traumatic brain injury. *Cell Mol Life Sci* 61(6):657-668.
- Aschner JL, Lum H, Fletcher PW, Malik AB. 1997. Bradykinin- and thrombin-induced increases in endothelial permeability occur independently of phospholipase C but require protein kinase C activation. *J Cell Physiol* 173(3):387-396.
- Azad MB, Chen Y, Henson ES, Cizeau J, McMillan-Ward E, Israels SJ, Gibson SB. 2008. Hypoxia induces autophagic cell death in apoptosis-competent cells through a mechanism involving BNIP3. *Autophagy* 4(2):195-204.
- Bahr BA, Bendiske J. 2002. The neuropathogenic contributions of lysosomal dysfunction. *J Neurochem* 83(3):481-489.
- Bahr BA, Hoffman KB, Kessler M, Hennegriff M, Park GY, Yamamoto RS, Kawasaki BT, Vanderklish PW, Hall RA, Lynch G. 1996. Distinct distributions of alpha-amino-3-hydroxy-5-methyl-4-isoxazolepropionate (AMPA) receptor subunits and a related 53,000 M(R) antigen (GR53) in brain tissue. *Neuroscience* 74(3):707-721.
- Bain J, McLauchlan H, Elliott M, Cohen P. 2003. The specificities of protein kinase inhibitors: an update. *Biochem J* 371(Pt 1):199-204.
- Bain J, Plater L, Elliott M, Shpiro N, Hastie CJ, McLauchlan H, Klevernic I, Arthur JS, Alessi DR, Cohen P. 2007. The selectivity of protein kinase inhibitors: a further update. *Biochem J* 408(3):297-315.
- Balazs R, Hack N, Jorgensen OS. 1988. Stimulation of the N-methyl-D-aspartate receptor has a trophic effect on differentiating cerebellar granule cells. *Neurosci Lett* 87(1-2):80-86.
- Bang OY, Buck BH, Saver JL, Alger JR, Yoon SR, Starkman S, Ovbiagele B, Kim D, Ali LK, Sanossian N, Jahan R, Duckwiler GR, Vinuela F, Salamon N, Villablanca JP, Liebeskind DS. 2007. Prediction of hemorrhagic transformation after recanalization therapy using T2*-permeability magnetic resonance imaging. *Ann Neurol* 62(2):170-176.
- Bannai S, Kitamura E. 1980. Transport interaction of L-cystine and L-glutamate in human diploid fibroblasts in culture. *J Biol Chem* 255(6):2372-2376.
- Barber M, Langhorne P, Rumley A, Lowe GD, Stott DJ. 2006. D-dimer predicts early clinical progression in ischemic stroke: confirmation using routine clinical assays. *Stroke* 37(4):1113-1115.
- Barone FC, Feuerstein GZ. 1999. Inflammatory mediators and stroke: new opportunities for novel therapeutics. *J Cereb Blood Flow Metab* 19(8):819-834.
- Barr AR, Gergely F. 2007. Aurora-A: the maker and breaker of spindle poles. *J Cell Sci* 120(Pt 17):2987-2996.

References

- Baskar R, Li L, Moore PK. 2007. Hydrogen sulfide-induces DNA damage and changes in apoptotic gene expression in human lung fibroblast cells. *Faseb J* 21(1):247-255.
- Baumgartner HK, Gerasimenko JV, Thorne C, Ferdek P, Pozzan T, Tepikin AV, Petersen OH, Sutton R, Watson AJ, Gerasimenko OV. 2009. Calcium elevation in mitochondria is the main Ca²⁺ requirement for mitochondrial permeability transition pore (mPTP) opening. *J Biol Chem* 284(31):20796-20803.
- Bayliss R, Sardon T, Vernos I, Conti E. 2003. Structural basis of Aurora-A activation by TPX2 at the mitotic spindle. *Mol Cell* 12(4):851-862.
- Beart PM, Lim ML, Chen B, Diwakarla S, Mercer LD, Cheung NS, Nagley P. 2007. Hierarchical recruitment by AMPA but not staurosporine of pro-apoptotic mitochondrial signaling in cultured cortical neurons: evidence for caspase-dependent/independent cross-talk. *J Neurochem* 103(6):2408-2427.
- Beckman JS, Beckman TW, Chen J, Marshall PA, Freeman BA. 1990. Apparent hydroxyl radical production by peroxynitrite: implications for endothelial injury from nitric oxide and superoxide. *Proc Natl Acad Sci U S A* 87(4):1620-1624.
- Belayev L, Busto R, Zhao W, Ginsberg MD. 1996. Quantitative evaluation of blood-brain barrier permeability following middle cerebral artery occlusion in rats. *Brain Res* 739(1-2):88-96.
- Ben-Ari Y, Cossart R. 2000. Kainate, a double agent that generates seizures: two decades of progress. *Trends Neurosci* 23(11):580-587.
- Benchoua A, Braudeau J, Reis A, Couriaud C, Onteniente B. 2004. Activation of proinflammatory caspases by cathepsin B in focal cerebral ischemia. *J Cereb Blood Flow Metab* 24(11):1272-1279.
- Benjelloun N, Renolleau S, Represa A, Ben-Ari Y, Charriaut-Marlangue C. 1999. Inflammatory responses in the cerebral cortex after ischemia in the P7 neonatal Rat. *Stroke* 30(9):1916-1923; discussion 1923-1914.
- Berman FW, Murray TF. 1997. Domoic acid neurotoxicity in cultured cerebellar granule neurons is mediated predominantly by NMDA receptors that are activated as a consequence of excitatory amino acid release. *J Neurochem* 69(2):693-703.
- Beyer K, Lao JI, Carrato C, Rodriguez-Vila A, Latorre P, Mataro M, Llopis MA, Mate JL, Ariza A. 2004. Cystathionine beta synthase as a risk factor for Alzheimer disease. *Curr Alzheimer Res* 1(2):127-133.
- Bianca VD, Dusi S, Bianchini E, Dal Pra I, Rossi F. 1999. beta-amyloid activates the O-2 forming NADPH oxidase in microglia, monocytes, and neutrophils. A possible inflammatory mechanism of neuronal damage in Alzheimer's disease. *J Biol Chem* 274(22):15493-15499.
- Bjorkman JA, Abrahamsson TI, Nerme VK, Mattsson CJ. 2005. Inhibition of carboxypeptidase U (TAFIa) activity improves rt-PA induced thrombolysis in a dog model of coronary artery thrombosis. *Thromb Res* 116(6):519-524.
- Bliss TV, Collingridge GL. 1993. A synaptic model of memory: long-term potentiation in the hippocampus. *Nature* 361(6407):31-39.

- Blomgren K, Leist M, Groc L. 2007. Pathological apoptosis in the developing brain. *Apoptosis* 12(5):993-1010.
- Boland B, Nixon RA. 2006. Neuronal macroautophagy: from development to degeneration. *Mol Aspects Med* 27(5-6):503-519.
- Bona E, Andersson AL, Blomgren K, Gilland E, Puka-Sundvall M, Gustafson K, Hagberg H. 1999. Chemokine and inflammatory cell response to hypoxia-ischemia in immature rats. *Pediatr Res* 45(4 Pt 1):500-509.
- Bonda DJ, Bajic VP, Spremo-Potparevic B, Casadesus G, Zhu X, Smith MA, Lee HG. 2010. Review: cell cycle aberrations and neurodegeneration. *Neuropathol Appl Neurobiol* 36(2):157-163.
- Boujrad H, Gubkina O, Robert N, Krantic S, Susin SA. 2007. AIF-mediated programmed necrosis: a highly regulated way to die. *Cell Cycle* 6(21):2612-2619.
- Bouma BN, Meijers JC. 2003. Thrombin-activatable fibrinolysis inhibitor (TAFI, plasma procarboxypeptidase B, procarboxypeptidase R, procarboxypeptidase U). *J Thromb Haemost* 1(7):1566-1574.
- Boutin H, LeFeuvre RA, Horai R, Asano M, Iwakura Y, Rothwell NJ. 2001. Role of IL-1alpha and IL-1beta in ischemic brain damage. *J Neurosci* 21(15):5528-5534.
- Boveris A, Oshino N, Chance B. 1972. The cellular production of hydrogen peroxide. *Biochem J* 128(3):617-630.
- Bowie D, Mayer ML. 1995. Inward rectification of both AMPA and kainate subtype glutamate receptors generated by polyamine-mediated ion channel block. *Neuron* 15(2):453-462.
- Bozinovski S, Cristiano BE, Marmy-Conus N, Pearson RB. 2002. The synthetic peptide RPRAATF allows specific assay of Akt activity in cell lysates. *Anal Biochem* 305(1):32-39.
- Bracci R, Perrone S, Buonocore G. 2006. The timing of neonatal brain damage. *Biol Neonate* 90(3):145-155.
- Brea D, Sobrino T, Ramos-Cabrer P, Castillo J. 2009. Inflammatory and neuroimmunomodulatory changes in acute cerebral ischemia. *Cerebrovasc Dis* 27 Suppl 1:48-64.
- Breckenridge DG, Germain M, Mathai JP, Nguyen M, Shore GC. 2003. Regulation of apoptosis by endoplasmic reticulum pathways. *Oncogene* 22(53):8608-8618.
- Broillet MC. 1999. S-nitrosylation of proteins. *Cell Mol Life Sci* 55(8-9):1036-1042.
- Brouns R, De Deyn PP. 2009. The complexity of neurobiological processes in acute ischemic stroke. *Clin Neurol Neurosurg* 111(6):483-495.
- Brouns R, Heylen E, Sheorajpanday R, Willemse JL, Kunnen J, De Surgeloose D, Hendriks DF, De Deyn PP. 2009. Carboxypeptidase U (TAFIa) decreases the efficacy of thrombolytic therapy in ischemic stroke patients. *Clin Neurol Neurosurg* 111(2):165-170.
- Brouns R, Heylen E, Willemse JL, Sheorajpanday R, De Surgeloose D, Verkerk R, De Deyn PP, Hendriks DF. 2010. The decrease in procarboxypeptidase U (TAFI) concentration in acute ischemic stroke correlates with stroke severity, evolution and outcome. *J Thromb Haemost* 8(1):75-80.
- Brown CE, Wong C, Murphy TH. 2008. Rapid morphologic plasticity of peri-infarct dendritic spines after focal ischemic stroke. *Stroke* 39(4):1286-1291.

- Brown GC, Cooper CE. 1994. Nanomolar concentrations of nitric oxide reversibly inhibit synaptosomal respiration by competing with oxygen at cytochrome oxidase. *FEBS Lett* 356(2-3):295-298.
- Buckley BJ, Marshall ZM, Whorton AR. 2003. Nitric oxide stimulates Nrf2 nuclear translocation in vascular endothelium. *Biochem Biophys Res Commun* 307(4):973-979.
- Buller AL, Monaghan DT. 1997. Pharmacological heterogeneity of NMDA receptors: characterization of NR1a/NR2D heteromers expressed in *Xenopus* oocytes. *Eur J Pharmacol* 320(1):87-94.
- Burnashev N, Monyer H, Seeburg PH, Sakmann B. 1992. Divalent ion permeability of AMPA receptor channels is dominated by the edited form of a single subunit. *Neuron* 8(1):189-198.
- Busser J, Geldmacher DS, Herrup K. 1998. Ectopic cell cycle proteins predict the sites of neuronal cell death in Alzheimer's disease brain. *J Neurosci* 18(8):2801-2807.
- Butterfield DA. 1997. beta-Amyloid-associated free radical oxidative stress and neurotoxicity: implications for Alzheimer's disease. *Chem Res Toxicol* 10(5):495-506.
- Byrnes KR, Faden AI. 2007. Role of cell cycle proteins in CNS injury. *Neurochem Res* 32(10):1799-1807.
- Calautti C, Baron JC. 2003. Functional neuroimaging studies of motor recovery after stroke in adults: a review. *Stroke* 34(6):1553-1566.
- Camins A, Pallas M, Silvestre JS. 2008. Apoptotic mechanisms involved in neurodegenerative diseases: experimental and therapeutic approaches. *Methods Find Exp Clin Pharmacol* 30(1):43-65.
- Camins A, Verdaguer E, Folch J, Beas-Zarate C, Canudas AM, Pallas M. 2007. Inhibition of ataxia telangiectasia-p53-E2F-1 pathway in neurons as a target for the prevention of neuronal apoptosis. *Curr Drug Metab* 8(7):709-715.
- Camps M, Nichols A, Arkinstall S. 2000. Dual specificity phosphatases: a gene family for control of MAP kinase function. *Faseb J* 14(1):6-16.
- Canu N, Tufi R, Serafino AL, Amadoro G, Ciotti MT, Calissano P. 2005. Role of the autophagic-lysosomal system on low potassium-induced apoptosis in cultured cerebellar granule cells. *J Neurochem* 92(5):1228-1242.
- Cao G, Xing J, Xiao X, Liou AK, Gao Y, Yin XM, Clark RS, Graham SH, Chen J. 2007. Critical role of calpain I in mitochondrial release of apoptosis-inducing factor in ischemic neuronal injury. *J Neurosci* 27(35):9278-9293.
- Carloni S, Buonocore G, Balduini W. 2008. Protective role of autophagy in neonatal hypoxia-ischemia induced brain injury. *Neurobiol Dis* 32(3):329-339.
- Carmena M, Ruchaud S, Earnshaw WC. 2009. Making the Auroras glow: regulation of Aurora A and B kinase function by interacting proteins. *Curr Opin Cell Biol* 21(6):796-805.
- Carragher NO. 2006. Calpain inhibition: a therapeutic strategy targeting multiple disease states. *Curr Pharm Des* 12(5):615-638.
- Carson MJ, Sutcliffe JG. 1999. Balancing function vs. self defense: the CNS as an active regulator of immune responses. *J Neurosci Res* 55(1):1-8.

- Cassina AM, Hodara R, Souza JM, Thomson L, Castro L, Ischiropoulos H, Freeman BA, Radi R. 2000. Cytochrome c nitration by peroxynitrite. *J Biol Chem* 275(28):21409-21415.
- Castillo PE, Malenka RC, Nicoll RA. 1997. Kainate receptors mediate a slow postsynaptic current in hippocampal CA3 neurons. *Nature* 388(6638):182-186.
- Chakravarthi S, Jessop CE, Bulleid NJ. 2006. The role of glutathione in disulphide bond formation and endoplasmic-reticulum-generated oxidative stress. *EMBO Rep* 7(3):271-275.
- Chan PH. 1996. Role of oxidants in ischemic brain damage. *Stroke* 27(6):1124-1129.
- Chan PH. 2001. Reactive oxygen radicals in signaling and damage in the ischemic brain. *J Cereb Blood Flow Metab* 21(1):2-14.
- Chang TY, Chang CC, Ohgami N, Yamauchi Y. 2006. Cholesterol sensing, trafficking, and esterification. *Annu Rev Cell Dev Biol* 22:129-157.
- Charpak S, Gahwiler BH, Do KQ, Knopfel T. 1990. Potassium conductances in hippocampal neurons blocked by excitatory amino-acid transmitters. *Nature* 347(6295):765-767.
- Chatterton JE, Awobuluyi M, Premkumar LS, Takahashi H, Talantova M, Shin Y, Cui J, Tu S, Sevarino KA, Nakanishi N, Tong G, Lipton SA, Zhang D. 2002. Excitatory glycine receptors containing the NR3 family of NMDA receptor subunits. *Nature* 415(6873):793-798.
- Chen C, Hu Q, Yan J, Yang X, Shi X, Lei J, Chen L, Huang H, Han J, Zhang JH, Zhou C. 2009. Early inhibition of HIF-1alpha with small interfering RNA reduces ischemic-reperfused brain injury in rats. *Neurobiol Dis* 33(3):509-517.
- Chen C, Ostrowski RP, Zhou C, Tang J, Zhang JH. 2010a. Suppression of hypoxia-inducible factor-1alpha and its downstream genes reduces acute hyperglycemia-enhanced hemorrhagic transformation in a rat model of cerebral ischemia. *J Neurosci Res* 88(9):2046-2055.
- Chen MJ, Peng ZF, Manikandan J, Melendez AJ, Tan GS, Chung CM, Li QT, Tan TM, Deng LW, Whiteman M, Beart PM, Moore PK, Cheung NS. 2010b. Gene profiling reveals hydrogen sulphide recruits death signaling via the N-methyl-D-aspartate receptor identifying commonalities with excitotoxicity. *J Cell Physiol*.
- Chen MJ, Yap YW, Choy MS, Koh CH, Seet SJ, Duan W, Whiteman M, Cheung NS. 2006. Early induction of calpains in rotenone-mediated neuronal apoptosis. *Neurosci Lett* 397(1-2):69-73.
- Chen N, Moshaver A, Raymond LA. 1997. Differential sensitivity of recombinant N-methyl-D-aspartate receptor subtypes to zinc inhibition. *Mol Pharmacol* 51(6):1015-1023.
- Cheng W, Fu YX, Porres JM, Ross DA, Lei XG. 1999. Selenium-dependent cellular glutathione peroxidase protects mice against a pro-oxidant-induced oxidation of NADPH, NADH, lipids, and protein. *Faseb J* 13(11):1467-1475.
- Cheung NS, Choy MS, Halliwell B, Teo TS, Bay BH, Lee AY, Qi RZ, Koh VH, Whiteman M, Koay ES, Chiu LL, Zhu HJ, Wong KP, Beart PM, Cheng HC. 2004. Lactacystin-induced apoptosis of cultured mouse cortical neurons is

- associated with accumulation of PTEN in the detergent-resistant membrane fraction. *Cell Mol Life Sci* 61(15):1926-1934.
- Cheung NS, Pascoe CJ, Giardina SF, John CA, Beart PM. 1998. Micromolar L-glutamate induces extensive apoptosis in an apoptotic-necrotic continuum of insult-dependent, excitotoxic injury in cultured cortical neurones. *Neuropharmacology* 37(10-11):1419-1429.
- Cheung NS, Peng ZF, Chen MJ, Moore PK, Whiteman M. 2007. Hydrogen sulfide induced neuronal death occurs via glutamate receptor and is associated with calpain activation and lysosomal rupture in mouse primary cortical neurons. *Neuropharmacology* 53(4):505-514.
- Chinopoulos C, Adam-Vizi V. 2006. Calcium, mitochondria and oxidative stress in neuronal pathology. Novel aspects of an enduring theme. *FEBS J* 273(3):433-450.
- Cho BB, Toledo-Pereyra LH. 2008. Caspase-independent programmed cell death following ischemic stroke. *J Invest Surg* 21(3):141-147.
- Choi DK, Pennathur S, Perier C, Tieu K, Teismann P, Wu DC, Jackson-Lewis V, Vila M, Vonsattel JP, Heinecke JW, Przedborski S. 2005. Ablation of the inflammatory enzyme myeloperoxidase mitigates features of Parkinson's disease in mice. *J Neurosci* 25(28):6594-6600.
- Choi DW. 1985. Glutamate neurotoxicity in cortical cell culture is calcium dependent. *Neurosci Lett* 58(3):293-297.
- Choi DW. 1987. Ionic dependence of glutamate neurotoxicity. *J Neurosci* 7(2):369-379.
- Choi DW. 1995. Calcium: still center-stage in hypoxic-ischemic neuronal death. *Trends Neurosci* 18(2):58-60.
- Choi DW. 1996. Ischemia-induced neuronal apoptosis. *Curr Opin Neurobiol* 6(5):667-672.
- Choi DW, Koh JY, Peters S. 1988. Pharmacology of glutamate neurotoxicity in cortical cell culture: attenuation by NMDA antagonists. *J Neurosci* 8(1):185-196.
- Chong ZZ, Xu QP, Sun JN. 2001. Effects and mechanisms of triacetylshikimic acid on platelet adhesion to neutrophils induced by thrombin and reperfusion after focal cerebral ischemia in rats. *Acta Pharmacol Sin* 22(8):679-684.
- Choy MS, Chen MJ, Manikandan J, Peng ZF, Jenner AM, Melendez AJ, Cheung NS. 2010. Up-regulation of endoplasmic reticulum stress-related genes during the early phase of treatment of cultured cortical neurons by the proteasomal inhibitor lactacystin. *J Cell Physiol*.
- Chua BT, Guo K, Li P. 2000. Direct cleavage by the calcium-activated protease calpain can lead to inactivation of caspases. *J Biol Chem* 275(7):5131-5135.
- Ciabarra AM, Sevarino KA. 1997. An anti-chi-1 antibody recognizes a heavily glycosylated protein in rat brain. *Brain Res Mol Brain Res* 46(1-2):85-90.
- Ciabarra AM, Sullivan JM, Gahn LG, Pecht G, Heinemann S, Sevarino KA. 1995. Cloning and characterization of chi-1: a developmentally regulated member of a novel class of the ionotropic glutamate receptor family. *J Neurosci* 15(10):6498-6508.

References

- Ciechomska IA, Goemans GC, Skepper JN, Tolkovsky AM. 2009. Bcl-2 complexed with Beclin-1 maintains full anti-apoptotic function. *Oncogene* 28(21):2128-2141.
- Clarke NP, Bevan MD, Cozzari C, Hartman BK, Bolam JP. 1997. Glutamate-enriched cholinergic synaptic terminals in the entopeduncular nucleus and subthalamic nucleus of the rat. *Neuroscience* 81(2):371-385.
- Clarke NP, Bolam JP. 1998. Distribution of glutamate receptor subunits at neurochemically characterized synapses in the entopeduncular nucleus and subthalamic nucleus of the rat. *J Comp Neurol* 397(3):403-420.
- Clarke PG. 1990. Developmental cell death: morphological diversity and multiple mechanisms. *Anat Embryol (Berl)* 181(3):195-213.
- Clarke R, Smith AD, Jobst KA, Refsum H, Sutton L, Ueland PM. 1998. Folate, vitamin B12, and serum total homocysteine levels in confirmed Alzheimer disease. *Arch Neurol* 55(11):1449-1455.
- Cleeter MW, Cooper JM, Darley-Usmar VM, Moncada S, Schapira AH. 1994. Reversible inhibition of cytochrome c oxidase, the terminal enzyme of the mitochondrial respiratory chain, by nitric oxide. Implications for neurodegenerative diseases. *FEBS Lett* 345(1):50-54.
- Clemens JA, Stephenson DT, Dixon EP, Smalstig EB, Mincy RE, Rash KS, Little SP. 1997. Global cerebral ischemia activates nuclear factor-kappa B prior to evidence of DNA fragmentation. *Brain Res Mol Brain Res* 48(2):187-196.
- Colangelo V, Schurr J, Ball MJ, Pelaez RP, Bazan NG, Lukiw WJ. 2002. Gene expression profiling of 12633 genes in Alzheimer hippocampal CA1: transcription and neurotrophic factor down-regulation and up-regulation of apoptotic and pro-inflammatory signaling. *J Neurosci Res* 70(3):462-473.
- Comperat E, Camparo P, Haus R, Chartier-Kastler E, Radenen B, Richard F, Capron F, Paradis V. 2007. Aurora-A/STK-15 is a predictive factor for recurrent behaviour in non-invasive bladder carcinoma: a study of 128 cases of non-invasive neoplasms. *Virchows Arch* 450(4):419-424.
- Conn PJ, Pin JP. 1997. Pharmacology and functions of metabotropic glutamate receptors. *Annu Rev Pharmacol Toxicol* 37:205-237.
- Connolly ES, Jr., Winfree CJ, Stern DM, Solomon RA, Pinsky DJ. 1996. Procedural and strain-related variables significantly affect outcome in a murine model of focal cerebral ischemia. *Neurosurgery* 38(3):523-531; discussion 532.
- Contractor A, Swanson G, Heinemann SF. 2001. Kainate receptors are involved in short- and long-term plasticity at mossy fiber synapses in the hippocampus. *Neuron* 29(1):209-216.
- Copani A, Uberti D, Sortino MA, Bruno V, Nicoletti F, Memo M. 2001. Activation of cell-cycle-associated proteins in neuronal death: a mandatory or dispensable path? *Trends Neurosci* 24(1):25-31.
- Cowan F, Rutherford M, Groenendaal F, Eken P, Mercuri E, Bydder GM, Meiners LC, Dubowitz LM, de Vries LS. 2003. Origin and timing of brain lesions in term infants with neonatal encephalopathy. *Lancet* 361(9359):736-742.
- Cowell RM, Xu H, Galasso JM, Silverstein FS. 2002. Hypoxic-ischemic injury induces macrophage inflammatory protein-1alpha expression in immature rat brain. *Stroke* 33(3):795-801.

- Coyle JT, Puttfarcken P. 1993. Oxidative stress, glutamate, and neurodegenerative disorders. *Science* 262(5134):689-695.
- Crack PJ, Taylor JM, Ali U, Mansell A, Hertzog PJ. 2006. Potential contribution of NF-kappaB in neuronal cell death in the glutathione peroxidase-1 knockout mouse in response to ischemia-reperfusion injury. *Stroke* 37(6):1533-1538.
- Crack PJ, Taylor JM, Flentjar NJ, de Haan J, Hertzog P, Iannello RC, Kola I. 2001. Increased infarct size and exacerbated apoptosis in the glutathione peroxidase-1 (Gpx-1) knockout mouse brain in response to ischemia/reperfusion injury. *Journal of neurochemistry* 78(6):1389-1399.
- Craig AM, Blackstone CD, Haganir RL, Banker G. 1993. The distribution of glutamate receptors in cultured rat hippocampal neurons: postsynaptic clustering of AMPA-selective subunits. *Neuron* 10(6):1055-1068.
- Crespo-Biel N, Camins A, Pelegri C, Vilaplana J, Pallas M, Canudas AM. 2007. 3-Nitropropionic acid activates calpain/cdk5 pathway in rat striatum. *Neurosci Lett* 421(1):77-81.
- Crocker SJ, Smith PD, Jackson-Lewis V, Lamba WR, Hayley SP, Grimm E, Callaghan SM, Slack RS, Melloni E, Przedborski S, Robertson GS, Anisman H, Merali Z, Park DS. 2003. Inhibition of calpains prevents neuronal and behavioral deficits in an MPTP mouse model of Parkinson's disease. *J Neurosci* 23(10):4081-4091.
- Csordas G, Renken C, Varnai P, Walter L, Weaver D, Buttle KF, Balla T, Mannella CA, Hajnoczky G. 2006. Structural and functional features and significance of the physical linkage between ER and mitochondria. *J Cell Biol* 174(7):915-921.
- Culmsee C, Zhu C, Landshamer S, Becattini B, Wagner E, Pellecchia M, Blomgren K, Plesnila N. 2005. Apoptosis-inducing factor triggered by poly(ADP-ribose) polymerase and Bid mediates neuronal cell death after oxygen-glucose deprivation and focal cerebral ischemia. *J Neurosci* 25(44):10262-10272.
- Cuzzocrea S, Riley DP, Caputi AP, Salvemini D. 2001. Antioxidant therapy: a new pharmacological approach in shock, inflammation, and ischemia/reperfusion injury. *Pharmacol Rev* 53(1):135-159.
- D'Ambrosio AL, Pinsky DJ, Connolly ES. 2001. The role of the complement cascade in ischemia/reperfusion injury: implications for neuroprotection. *Mol Med* 7(6):367-382.
- Danysz W, Parsons CG. 1998. Glycine and N-methyl-D-aspartate receptors: physiological significance and possible therapeutic applications. *Pharmacol Rev* 50(4):597-664.
- Dawson SL, Panerai RB, Potter JF. 2003. Serial changes in static and dynamic cerebral autoregulation after acute ischaemic stroke. *Cerebrovasc Dis* 16(1):69-75.
- Dawson VL, Dawson TM, London ED, Brecht DS, Snyder SH. 1991. Nitric oxide mediates glutamate neurotoxicity in primary cortical cultures. *Proc Natl Acad Sci U S A* 88(14):6368-6371.
- de Haan JB, Bladier C, Griffiths P, Kelner M, O'Shea RD, Cheung NS, Bronson RT, Silvestro MJ, Wild S, Zheng SS, Beart PM, Hertzog PJ, Kola I. 1998. Mice with a homozygous null mutation for the most abundant glutathione peroxidase,

- Gpx1, show increased susceptibility to the oxidative stress-inducing agents paraquat and hydrogen peroxide. *J Biol Chem* 273(35):22528-22536.
- de Haan JB, Bladier C, Lotfi-Miri M, Taylor J, Hutchinson P, Crack PJ, Hertzog P, Kola I. 2004. Fibroblasts derived from Gpx1 knockout mice display senescent-like features and are susceptible to H₂O₂-mediated cell death. *Free radical biology & medicine* 36(1):53-64.
- De Long MJ, Santamaria AB, Talalay P. 1987. Role of cytochrome P1-450 in the induction of NAD(P)H:quinone reductase in a murine hepatoma cell line and its mutants. *Carcinogenesis* 8(10):1549-1553.
- DeGracia DJ, Montie HL. 2004. Cerebral ischemia and the unfolded protein response. *J Neurochem* 91(1):1-8.
- Deisz RA, Fortin G, Zieglansberger W. 1991. Voltage dependence of excitatory postsynaptic potentials of rat neocortical neurons. *J Neurophysiol* 65(2):371-382.
- del Zoppo GJ, Hallenbeck JM. 2000. Advances in the vascular pathophysiology of ischemic stroke. *Thromb Res* 98(3):73-81.
- del Zoppo GJ, Mabuchi T. 2003. Cerebral microvessel responses to focal ischemia. *J Cereb Blood Flow Metab* 23(8):879-894.
- del Zoppo GJ, Schmid-Schonbein GW, Mori E, Copeland BR, Chang CM. 1991. Polymorphonuclear leukocytes occlude capillaries following middle cerebral artery occlusion and reperfusion in baboons. *Stroke* 22(10):1276-1283.
- Demasi M, Davies KJ. 2003. Proteasome inhibitors induce intracellular protein aggregation and cell death by an oxygen-dependent mechanism. *FEBS Lett* 542(1-3):89-94.
- Deng W. 2010. Neurobiology of injury to the developing brain. *Nat Rev Neurol* 6(6):328-336.
- Dennis G, Jr., Sherman BT, Hosack DA, Yang J, Gao W, Lane HC, Lempicki RA. 2003. DAVID: Database for Annotation, Visualization, and Integrated Discovery. *Genome Biol* 4(5):P3.
- Desagher S, Osen-Sand A, Nichols A, Eskes R, Montessuit S, Lauper S, Maundrell K, Antonsson B, Martinou JC. 1999. Bid-induced conformational change of Bax is responsible for mitochondrial cytochrome c release during apoptosis. *J Cell Biol* 144(5):891-901.
- Desai MA, Conn PJ. 1991. Excitatory effects of ACPD receptor activation in the hippocampus are mediated by direct effects on pyramidal cells and blockade of synaptic inhibition. *J Neurophysiol* 66(1):40-52.
- deVeber G, Roach ES, Riela AR, Wiznitzer M. 2000. Stroke in children: recognition, treatment, and future directions. *Semin Pediatr Neurol* 7(4):309-317.
- Dietrich WD. 1994. Morphological manifestations of reperfusion injury in brain. *Ann N Y Acad Sci* 723:15-24.
- Ding Q, Keller JN. 2001. Proteasomes and proteasome inhibition in the central nervous system. *Free Radic Biol Med* 31(5):574-584.
- Dirnagl U, Iadecola C, Moskowitz MA. 1999. Pathobiology of ischaemic stroke: an integrated view. *Trends in neurosciences* 22(9):391-397.
- Diwakarla S, Mercer LD, Kardashsyan L, Chu PW, Shin YS, Lau CL, Hughes ML, Nagley P, Beart PM. 2009a. GABAergic striatal neurons exhibit caspase-independent,

- mitochondrially mediated programmed cell death. *J Neurochem* 109 Suppl 1:198-206.
- Diwakarla S, Nagley P, Hughes ML, Chen B, Beart PM. 2009b. Differential insult-dependent recruitment of the intrinsic mitochondrial pathway during neuronal programmed cell death. *Cell Mol Life Sci* 66(1):156-172.
- Doble A. 1999. The role of excitotoxicity in neurodegenerative disease: implications for therapy. *Pharmacol Ther* 81(3):163-221.
- Dombkowski RA, Russell MJ, Olson KR. 2004. Hydrogen sulfide as an endogenous regulator of vascular smooth muscle tone in trout. *Am J Physiol Regul Integr Comp Physiol* 286(4):R678-685.
- Donevan SD, McCabe RT. 2000. Conantokin G is an NR2B-selective competitive antagonist of N-methyl-D-aspartate receptors. *Mol Pharmacol* 58(3):614-623.
- Donevan SD, Rogawski MA. 1995. Intracellular polyamines mediate inward rectification of Ca(2+)-permeable alpha-amino-3-hydroxy-5-methyl-4-isoxazolepropionic acid receptors. *Proc Natl Acad Sci U S A* 92(20):9298-9302.
- Donnan GA, Fisher M, Macleod M, Davis SM. 2008. Stroke. *Lancet* 371(9624):1612-1623.
- Doraiswamy PM. 2003a. Alzheimer's disease and the glutamate NMDA receptor. *Psychopharmacol Bull* 37(2):41-49.
- Doraiswamy PM. 2003b. The role of the N-methyl-D-aspartate receptor in Alzheimer's disease: therapeutic potential. *Curr Neurol Neurosci Rep* 3(5):373-378.
- Du Y, Bales KR, Dodel RC, Hamilton-Byrd E, Horn JW, Czilli DL, Simmons LK, Ni B, Paul SM. 1997. Activation of a caspase 3-related cysteine protease is required for glutamate-mediated apoptosis of cultured cerebellar granule neurons. *Proc Natl Acad Sci U S A* 94(21):11657-11662.
- Dufour E, Terzioglu M, Sterky FH, Sorensen L, Galter D, Olson L, Wilbertz J, Larsson NG. 2008. Age-associated mosaic respiratory chain deficiency causes trans-neuronal degeneration. *Hum Mol Genet* 17(10):1418-1426.
- Dugan LL, Sensi SL, Canzoniero LM, Handran SD, Rothman SM, Lin TS, Goldberg MP, Choi DW. 1995. Mitochondrial production of reactive oxygen species in cortical neurons following exposure to N-methyl-D-aspartate. *J Neurosci* 15(10):6377-6388.
- Durand GM, Bennett MV, Zukin RS. 1993. Splice variants of the N-methyl-D-aspartate receptor NR1 identify domains involved in regulation by polyamines and protein kinase C. *Proc Natl Acad Sci U S A* 90(14):6731-6735.
- Durand GM, Zukin RS. 1993. Developmental regulation of mRNAs encoding rat brain kainate/AMPA receptors: a northern analysis study. *J Neurochem* 61(6):2239-2246.
- Duvoisin RM, Zhang C, Ramonell K. 1995. A novel metabotropic glutamate receptor expressed in the retina and olfactory bulb. *J Neurosci* 15(4):3075-3083.
- Dykens JA. 1994. Isolated cerebral and cerebellar mitochondria produce free radicals when exposed to elevated CA2+ and Na+: implications for neurodegeneration. *J Neurochem* 63(2):584-591.

References

- Eames PJ, Blake MJ, Dawson SL, Panerai RB, Potter JF. 2002. Dynamic cerebral autoregulation and beat to beat blood pressure control are impaired in acute ischaemic stroke. *J Neurol Neurosurg Psychiatry* 72(4):467-472.
- Eddleston M, de la Torre JC, Oldstone MB, Loskutoff DJ, Edgington TS, Mackman N. 1993. Astrocytes are the primary source of tissue factor in the murine central nervous system. A role for astrocytes in cerebral hemostasis. *J Clin Invest* 92(1):349-358.
- Eghbal MA, Pennefather PS, O'Brien PJ. 2004. H₂S cytotoxicity mechanism involves reactive oxygen species formation and mitochondrial depolarisation. *Toxicology* 203(1-3):69-76.
- Egler RA, Fernandes E, Rothermund K, Sereika S, de Souza-Pinto N, Jaruga P, Dizdaroglu M, Prochownik EV. 2005. Regulation of reactive oxygen species, DNA damage, and c-Myc function by peroxiredoxin 1. *Oncogene* 24(54):8038-8050.
- Ekdahl CT, Kokaia Z, Lindvall O. 2009. Brain inflammation and adult neurogenesis: the dual role of microglia. *Neuroscience* 158(3):1021-1029.
- Eliassen JC, Boespflug EL, Lamy M, Allendorfer J, Chu WJ, Szaflarski JP. 2008. Brain-mapping techniques for evaluating poststroke recovery and rehabilitation: a review. *Top Stroke Rehabil* 15(5):427-450.
- Emilsson L, Saetre P, Jazin E. 2006. Alzheimer's disease: mRNA expression profiles of multiple patients show alterations of genes involved with calcium signaling. *Neurobiol Dis* 21(3):618-625.
- Enari M, Sakahira H, Yokoyama H, Okawa K, Iwamatsu A, Nagata S. 1998. A caspase-activated DNase that degrades DNA during apoptosis, and its inhibitor ICAD. *Nature* 391(6662):43-50.
- Estrada V, Tellez MJ, Moya J, Fernandez-Durango R, Egido J, Fernandez Cruz AF. 1994. High plasma levels of endothelin-1 and atrial natriuretic peptide in patients with acute ischemic stroke. *Am J Hypertens* 7(12):1085-1089.
- Evans MD, Cooke MS. 2004. Factors contributing to the outcome of oxidative damage to nucleic acids. *Bioessays* 26(5):533-542.
- Eyers PA, Erikson E, Chen LG, Maller JL. 2003. A novel mechanism for activation of the protein kinase Aurora A. *Curr Biol* 13(8):691-697.
- Eyers PA, Maller JL. 2004. Regulation of Xenopus Aurora A activation by TPX2. *J Biol Chem* 279(10):9008-9015.
- Fan X, Heijnen CJ, van der Kooij MA, Groenendaal F, van Bel F. 2009. The role and regulation of hypoxia-inducible factor-1alpha expression in brain development and neonatal hypoxic-ischemic brain injury. *Brain Res Rev* 62(1):99-108.
- Feeley Kearney JA, Albin RL. 2003. mGluRs: a target for pharmacotherapy in Parkinson disease. *Exp Neurol* 184 Suppl 1:S30-36.
- Feldmeyer D, Cull-Candy S. 1996. Functional consequences of changes in NMDA receptor subunit expression during development. *J Neurocytol* 25(12):857-867.
- Ferrand-Drake M, Zhu C, Gido G, Hansen AJ, Karlsson JO, Bahr BA, Zamzami N, Kroemer G, Chan PH, Wieloch T, Blomgren K. 2003. Cyclosporin A prevents calpain activation despite increased intracellular calcium concentrations, as

- well as translocation of apoptosis-inducing factor, cytochrome c and caspase-3 activation in neurons exposed to transient hypoglycemia. *J Neurochem* 85(6):1431-1442.
- Ferrarese C, Mascarucci P, Zoia C, Cavarretta R, Frigo M, Begni B, Sarinella F, Frattola L, De Simoni MG. 1999. Increased cytokine release from peripheral blood cells after acute stroke. *J Cereb Blood Flow Metab* 19(9):1004-1009.
- Ferrer I, Planas AM. 2003. Signaling of cell death and cell survival following focal cerebral ischemia: life and death struggle in the penumbra. *Journal of neuropathology and experimental neurology* 62(4):329-339.
- Ferriero DM. 2004. Neonatal brain injury. *N Engl J Med* 351(19):1985-1995.
- Fisher M, Francis R. 1990. Altered coagulation in cerebral ischemia. Platelet, thrombin, and plasmin activity. *Arch Neurol* 47(10):1075-1079.
- Flavin MP, Coughlin K, Ho LT. 1997. Soluble macrophage factors trigger apoptosis in cultured hippocampal neurons. *Neuroscience* 80(2):437-448.
- Flores-Diaz M, Higuera JC, Florin I, Okada T, Pollesello P, Bergman T, Thelestam M, Mori K, Alape-Giron A. 2004. A cellular UDP-glucose deficiency causes overexpression of glucose/oxygen-regulated proteins independent of the endoplasmic reticulum stress elements. *J Biol Chem* 279(21):21724-21731.
- Forrest D, Yuzaki M, Soares HD, Ng L, Luk DC, Sheng M, Stewart CL, Morgan JJ, Connor JA, Curran T. 1994. Targeted disruption of NMDA receptor 1 gene abolishes NMDA response and results in neonatal death. *Neuron* 13(2):325-338.
- Fox K, Henley J, Isaac J. 1999. Experience-dependent development of NMDA receptor transmission. *Nat Neurosci* 2(4):297-299.
- Frangogiannis NG. 2007. Chemokines in ischemia and reperfusion. *Thromb Haemost* 97(5):738-747.
- Frank CL, Tsai LH. 2009. Alternative functions of core cell cycle regulators in neuronal migration, neuronal maturation, and synaptic plasticity. *Neuron* 62(3):312-326.
- Franklin TB, Krueger-Naug AM, Clarke DB, Arrigo AP, Currie RW. 2005. The role of heat shock proteins Hsp70 and Hsp27 in cellular protection of the central nervous system. *Int J Hyperthermia* 21(5):379-392.
- French PJ, Bijman J, Edixhoven M, Vaandrager AB, Scholte BJ, Lohmann SM, Nairn AC, de Jonge HR. 1995. Isozyme-specific activation of cystic fibrosis transmembrane conductance regulator-chloride channels by cGMP-dependent protein kinase II. *J Biol Chem* 270(44):26626-26631.
- Fribley A, Zeng Q, Wang CY. 2004. Proteasome inhibitor PS-341 induces apoptosis through induction of endoplasmic reticulum stress-reactive oxygen species in head and neck squamous cell carcinoma cells. *Mol Cell Biol* 24(22):9695-9704.
- Friedman LK, Pellegrini-Giampietro DE, Sperber EF, Bennett MV, Moshe SL, Zukin RS. 1994. Kainate-induced status epilepticus alters glutamate and GABA_A receptor gene expression in adult rat hippocampus: an in situ hybridization study. *J Neurosci* 14(5 Pt 1):2697-2707.
- Friedman LK, Sperber EF, Moshe SL, Bennett MV, Zukin RS. 1997. Developmental regulation of glutamate and GABA(A) receptor gene expression in rat

- hippocampus following kainate-induced status epilepticus. *Dev Neurosci* 19(6):529-542.
- Fu J, Bian M, Jiang Q, Zhang C. 2007. Roles of Aurora kinases in mitosis and tumorigenesis. *Mol Cancer Res* 5(1):1-10.
- Furlan AJ, Katzan IL, Caplan LR. 2003. Thrombolytic Therapy in Acute Ischemic Stroke. *Curr Treat Options Cardiovasc Med* 5(3):171-180.
- Gadalla MM, Snyder SH. 2010. Hydrogen sulfide as a gasotransmitter. *J Neurochem* 113(1):14-26.
- Gan L, Ye S, Chu A, Anton K, Yi S, Vincent VA, von Schack D, Chin D, Murray J, Lohr S, Patthy L, Gonzalez-Zulueta M, Nikolich K, Urfer R. 2004. Identification of cathepsin B as a mediator of neuronal death induced by Abeta-activated microglial cells using a functional genomics approach. *J Biol Chem* 279(7):5565-5572.
- Gasche Y, Copin JC, Sugawara T, Fujimura M, Chan PH. 2001. Matrix metalloproteinase inhibition prevents oxidative stress-associated blood-brain barrier disruption after transient focal cerebral ischemia. *J Cereb Blood Flow Metab* 21(12):1393-1400.
- Gawaz M. 2004. Role of platelets in coronary thrombosis and reperfusion of ischemic myocardium. *Cardiovasc Res* 61(3):498-511.
- Geiger JR, Melcher T, Koh DS, Sakmann B, Seeburg PH, Jonas P, Monyer H. 1995. Relative abundance of subunit mRNAs determines gating and Ca²⁺ permeability of AMPA receptors in principal neurons and interneurons in rat CNS. *Neuron* 15(1):193-204.
- Gendron TF, Mealing GA, Paris J, Lou A, Edwards A, Hou ST, MacManus JP, Hakim AM, Morley P. 2001. Attenuation of neurotoxicity in cortical cultures and hippocampal slices from E2F1 knockout mice. *J Neurochem* 78(2):316-324.
- Gerard C, Rollins BJ. 2001. Chemokines and disease. *Nat Immunol* 2(2):108-115.
- Gereau RW, Conn PJ. 1995. Multiple presynaptic metabotropic glutamate receptors modulate excitatory and inhibitory synaptic transmission in hippocampal area CA1. *J Neurosci* 15(10):6879-6889.
- Geschwind DH. 2000. Mice, microarrays, and the genetic diversity of the brain. *Proc Natl Acad Sci U S A* 97(20):10676-10678.
- Gidday JM, Gasche YG, Copin JC, Shah AR, Perez RS, Shapiro SD, Chan PH, Park TS. 2005. Leukocyte-derived matrix metalloproteinase-9 mediates blood-brain barrier breakdown and is proinflammatory after transient focal cerebral ischemia. *Am J Physiol Heart Circ Physiol* 289(2):H558-568.
- Gill MB, Perez-Polo JR. 2008. Hypoxia ischemia-mediated cell death in neonatal rat brain. *Neurochem Res* 33(12):2379-2389.
- Gill R, Tsung A, Billiar T. 2010. Linking oxidative stress to inflammation: Toll-like receptors. *Free Radic Biol Med* 48(9):1121-1132.
- Ginsberg SD, Hemby SE, Lee VM, Eberwine JH, Trojanowski JQ. 2000. Expression profile of transcripts in Alzheimer's disease tangle-bearing CA1 neurons. *Ann Neurol* 48(1):77-87.
- Golstein P, Kroemer G. 2007. Cell death by necrosis: towards a molecular definition. *Trends Biochem Sci* 32(1):37-43.

References

- Gomez-Santos C, Ferrer I, Santidrian AF, Barrachina M, Gil J, Ambrosio S. 2003. Dopamine induces autophagic cell death and alpha-synuclein increase in human neuroblastoma SH-SY5Y cells. *J Neurosci Res* 73(3):341-350.
- Gonzalez-Scarano F, Baltuch G. 1999. Microglia as mediators of inflammatory and degenerative diseases. *Annu Rev Neurosci* 22:219-240.
- Gonzalez-Zulueta M, Ensz LM, Mukhina G, Lebovitz RM, Zwacka RM, Engelhardt JF, Oberley LW, Dawson VL, Dawson TM. 1998. Manganese superoxide dismutase protects nNOS neurons from NMDA and nitric oxide-mediated neurotoxicity. *J Neurosci* 18(6):2040-2055.
- Goodwin LR, Francom D, Dieken FP, Taylor JD, Warenycia MW, Reiffenstein RJ, Dowling G. 1989. Determination of sulfide in brain tissue by gas dialysis/ion chromatography: postmortem studies and two case reports. *J Anal Toxicol* 13(2):105-109.
- Gorlach A, Klappa P, Kietzmann T. 2006. The endoplasmic reticulum: folding, calcium homeostasis, signaling, and redox control. *Antioxid Redox Signal* 8(9-10):1391-1418.
- Gorter JA, Petrozzino JJ, Aronica EM, Rosenbaum DM, Opitz T, Bennett MV, Connor JA, Zukin RS. 1997. Global ischemia induces downregulation of Glur2 mRNA and increases AMPA receptor-mediated Ca²⁺ influx in hippocampal CA1 neurons of gerbil. *J Neurosci* 17(16):6179-6188.
- Gozdz A, Habas A, Jaworski J, Zielinska M, Albrecht J, Chlystun M, Jalili A, Hetman M. 2003. Role of N-methyl-D-aspartate receptors in the neuroprotective activation of extracellular signal-regulated kinase 1/2 by cisplatin. *J Biol Chem* 278(44):43663-43671.
- Graber S, Maiti S, Halpain S. 2004. Cathepsin B-like proteolysis and MARCKS degradation in sub-lethal NMDA-induced collapse of dendritic spines. *Neuropharmacology* 47(5):706-713.
- Grana X, Reddy EP. 1995. Cell cycle control in mammalian cells: role of cyclins, cyclin dependent kinases (CDKs), growth suppressor genes and cyclin-dependent kinase inhibitors (CKIs). *Oncogene* 11(2):211-219.
- Green DR, Reed JC. 1998. Mitochondria and apoptosis. *Science* 281(5381):1309-1312.
- Green PS, Mendez AJ, Jacob JS, Crowley JR, Growdon W, Hyman BT, Heinecke JW. 2004. Neuronal expression of myeloperoxidase is increased in Alzheimer's disease. *J Neurochem* 90(3):724-733.
- Griffiths GM, Mueller C. 1991. Expression of perforin and granzymes in vivo: potential diagnostic markers for activated cytotoxic cells. *Immunol Today* 12(11):415-419.
- Grooms SY, Opitz T, Bennett MV, Zukin RS. 2000. Status epilepticus decreases glutamate receptor 2 mRNA and protein expression in hippocampal pyramidal cells before neuronal death. *Proc Natl Acad Sci U S A* 97(7):3631-3636.
- Grune T, Jung T, Merker K, Davies KJ. 2004. Decreased proteolysis caused by protein aggregates, inclusion bodies, plaques, lipofuscin, ceroid, and 'aggresomes' during oxidative stress, aging, and disease. *Int J Biochem Cell Biol* 36(12):2519-2530.

- Guerineau NC, Gahwiler BH, Gerber U. 1994. Reduction of resting K⁺ current by metabotropic glutamate and muscarinic receptors in rat CA3 cells: mediation by G-proteins. *J Physiol* 474(1):27-33.
- Gursoy-Ozdemir Y, Can A, Dalkara T. 2004. Reperfusion-induced oxidative/nitrative injury to neurovascular unit after focal cerebral ischemia. *Stroke* 35(6):1449-1453.
- Haapaniemi E, Soenne L, Syrjala M, Kaste M, Tatlisumak T. 2004. Serial changes in fibrinolysis and coagulation activation markers in acute and convalescent phase of ischemic stroke. *Acta Neurol Scand* 110(4):242-247.
- Habas A, Kharebava G, Szatmari E, Hetman M. 2006. NMDA neuroprotection against a phosphatidylinositol-3 kinase inhibitor, LY294002 by NR2B-mediated suppression of glycogen synthase kinase-3 β -induced apoptosis. *J Neurochem* 96(2):335-348.
- Haeusler KG, Schmidt WU, Fohring F, Meisel C, Helms T, Jungehulsing GJ, Nolte CH, Schmolke K, Wegner B, Meisel A, Dirnagl U, Villringer A, Volk HD. 2008. Cellular immunodepression preceding infectious complications after acute ischemic stroke in humans. *Cerebrovasc Dis* 25(1-2):50-58.
- Hakak Y, Walker JR, Li C, Wong WH, Davis KL, Buxbaum JD, Haroutunian V, Fienberg AA. 2001. Genome-wide expression analysis reveals dysregulation of myelination-related genes in chronic schizophrenia. *Proc Natl Acad Sci U S A* 98(8):4746-4751.
- Hallenbeck JM, Dutka AJ. 1990. Background review and current concepts of reperfusion injury. *Arch Neurol* 47(11):1245-1254.
- Halliwell B. 1992. Reactive oxygen species and the central nervous system. *J Neurochem* 59(5):1609-1623.
- Halliwell B. 2006. Oxidative stress and neurodegeneration: where are we now? *J Neurochem* 97(6):1634-1658.
- Hamann GF, Okada Y, Fitridge R, del Zoppo GJ. 1995. Microvascular basal lamina antigens disappear during cerebral ischemia and reperfusion. *Stroke* 26(11):2120-2126.
- Hanisch UK, Kettenmann H. 2007. Microglia: active sensor and versatile effector cells in the normal and pathologic brain. *Nat Neurosci* 10(11):1387-1394.
- Hansen TM, Nagley P. 2003. AIF: a multifunctional cog in the life and death machine. *Sci STKE* 2003(193):PE31.
- Hara A, Niwa M, Yoshimi N, Mori H. 1997. Apoptotic cell death in vulnerable subpopulation of cerebellar granule cells. *Acta Neuropathol* 94(5):517-518.
- Hara H, Huang PL, Panahian N, Fishman MC, Moskowitz MA. 1996. Reduced brain edema and infarction volume in mice lacking the neuronal isoform of nitric oxide synthase after transient MCA occlusion. *J Cereb Blood Flow Metab* 16(4):605-611.
- Hara MR, Agrawal N, Kim SF, Cascio MB, Fujimuro M, Ozeki Y, Takahashi M, Cheah JH, Tankou SK, Hester LD, Ferris CD, Hayward SD, Snyder SH, Sawa A. 2005. S-nitrosylated GAPDH initiates apoptotic cell death by nuclear translocation following Siah1 binding. *Nat Cell Biol* 7(7):665-674.
- Hara MR, Snyder SH. 2007. Cell signaling and neuronal death. *Annu Rev Pharmacol Toxicol* 47:117-141.

- Hardingham GE, Bading H. 2002. Coupling of extrasynaptic NMDA receptors to a CREB shut-off pathway is developmentally regulated. *Biochim Biophys Acta* 1600(1-2):148-153.
- Hayashi T, Saito A, Okuno S, Ferrand-Drake M, Dodd RL, Chan PH. 2005. Damage to the endoplasmic reticulum and activation of apoptotic machinery by oxidative stress in ischemic neurons. *J Cereb Blood Flow Metab* 25(1):41-53.
- Hayashi Y, Momiyama A, Takahashi T, Ohishi H, Ogawa-Meguro R, Shigemoto R, Mizuno N, Nakanishi S. 1993. Role of a metabotropic glutamate receptor in synaptic modulation in the accessory olfactory bulb. *Nature* 366(6456):687-690.
- Hazell LJ, Arnold L, Flowers D, Waeg G, Malle E, Stocker R. 1996. Presence of hypochlorite-modified proteins in human atherosclerotic lesions. *J Clin Invest* 97(6):1535-1544.
- Hengartner MO. 2000. The biochemistry of apoptosis. *Nature* 407(6805):770-776.
- Heo JH, Han SW, Lee SK. 2005. Free radicals as triggers of brain edema formation after stroke. *Free Radic Biol Med* 39(1):51-70.
- Hetman M, Cavanaugh JE, Kimelman D, Xia Z. 2000. Role of glycogen synthase kinase-3beta in neuronal apoptosis induced by trophic withdrawal. *J Neurosci* 20(7):2567-2574.
- Heurteaux C, Lauritzen I, Widmann C, Lazdunski M. 1995. Essential role of adenosine, adenosine A1 receptors, and ATP-sensitive K⁺ channels in cerebral ischemic preconditioning. *Proc Natl Acad Sci U S A* 92(10):4666-4670.
- Higgins GC, Beart PM, Nagley P. 2009. Oxidative stress triggers neuronal caspase-independent death: endonuclease G involvement in programmed cell death-type III. *Cell Mol Life Sci* 66(16):2773-2787.
- Higgins GC, Beart PM, Shin YS, Chen MJ, Cheung NS, Nagley P. 2010. Oxidative stress: emerging mitochondrial and cellular themes and variations in neuronal injury. *J Alzheimers Dis* 20 Suppl 2:S453-473.
- Hill WD, Hess DC, Martin-Studdard A, Carothers JJ, Zheng J, Hale D, Maeda M, Fagan SC, Carroll JE, Conway SJ. 2004. SDF-1 (CXCL12) is upregulated in the ischemic penumbra following stroke: association with bone marrow cell homing to injury. *J Neuropathol Exp Neurol* 63(1):84-96.
- Hilton GD, Stoica BA, Byrnes KR, Faden AI. 2008. Roscovitine reduces neuronal loss, glial activation, and neurologic deficits after brain trauma. *J Cereb Blood Flow Metab* 28(11):1845-1859.
- Hirota T, Kunitoku N, Sasayama T, Marumoto T, Zhang D, Nitta M, Hatakeyama K, Saya H. 2003. Aurora-A and an interacting activator, the LIM protein Ajuba, are required for mitotic commitment in human cells. *Cell* 114(5):585-598.
- Hjort N, Wu O, Ashkanian M, Solling C, Mouridsen K, Christensen S, Gyldensted C, Andersen G, Ostergaard L. 2008. MRI detection of early blood-brain barrier disruption: parenchymal enhancement predicts focal hemorrhagic transformation after thrombolysis. *Stroke* 39(3):1025-1028.
- Hoglinger GU, Breunig JJ, Depboylu C, Rouaux C, Michel PP, Alvarez-Fischer D, Boutillier AL, Degregori J, Oertel WH, Rakic P, Hirsch EC, Hunot S. 2007. The

- pRb/E2F cell-cycle pathway mediates cell death in Parkinson's disease. *Proc Natl Acad Sci U S A* 104(9):3585-3590.
- Hollmann M, Boulter J, Maron C, Beasley L, Sullivan J, Pecht G, Heinemann S. 1993. Zinc potentiates agonist-induced currents at certain splice variants of the NMDA receptor. *Neuron* 10(5):943-954.
- Hollmann M, Hartley M, Heinemann S. 1991. Ca²⁺ permeability of KA-AMPA-gated glutamate receptor channels depends on subunit composition. *Science* 252(5007):851-853.
- Hollmann M, Heinemann S. 1994. Cloned glutamate receptors. *Annu Rev Neurosci* 17:31-108.
- Hoozemans JJ, Veerhuis R, Van Haastert ES, Rozemuller JM, Baas F, Eikelenboom P, Scheper W. 2005. The unfolded protein response is activated in Alzheimer's disease. *Acta Neuropathol* 110(2):165-172.
- Hosomi N, Lucero J, Heo JH, Koziol JA, Copeland BR, del Zoppo GJ. 2001. Rapid differential endogenous plasminogen activator expression after acute middle cerebral artery occlusion. *Stroke* 32(6):1341-1348.
- Hossmann KA. 1988a. Resuscitation potentials after prolonged global cerebral ischemia in cats. *Crit Care Med* 16(10):964-971.
- Hossmann KA. 1988b. Thresholds of ischemic injury. In: Ginsberg MD, Bogousslavsky J, Malden UK, editors. *Cerebrovascular Disease: Pathophysiology Diagnosis and Management*: Blackwell Science. p 193-204.
- Htun P, Fateh-Moghadam S, Tomandl B, Handschu R, Klinger K, Stellos K, Garlich C, Daniel W, Gawaz M. 2006. Course of platelet activation and platelet-leukocyte interaction in cerebrovascular ischemia. *Stroke* 37(9):2283-2287.
- Hu LF, Lu M, Tiong CX, Dawe GS, Hu G, Bian JS. 2010. Neuroprotective effects of hydrogen sulfide on Parkinson's disease rat models. *Aging Cell* 9(2):135-146.
- Hu LF, Lu M, Wu ZY, Wong PT, Bian JS. 2009. Hydrogen sulfide inhibits rotenone-induced apoptosis via preservation of mitochondrial function. *Mol Pharmacol* 75(1):27-34.
- Huang da W, Sherman BT, Lempicki RA. 2009. Systematic and integrative analysis of large gene lists using DAVID bioinformatics resources. *Nat Protoc* 4(1):44-57.
- Huang DW, Sherman BT, Lempicki RA. 2009. Systematic and integrative analysis of large gene lists using DAVID Bioinformatics Resources. *Nature Protoc* 4(1):44-57.
- Huang EJ, Reichardt LF. 2001. Neurotrophins: roles in neuronal development and function. *Annu Rev Neurosci* 24:677-736.
- Huang ZG, Xue D, Preston E, Karbalai H, Buchan AM. 1999. Biphasic opening of the blood-brain barrier following transient focal ischemia: effects of hypothermia. *Can J Neurol Sci* 26(4):298-304.
- Huie RE, Padmaja S. 1993. The reaction of NO with superoxide. *Free Radic Res Commun* 18(4):195-199.
- Hynd MR, Scott HL, Dodd PR. 2004a. Differential expression of N-methyl-D-aspartate receptor NR2 isoforms in Alzheimer's disease. *J Neurochem* 90(4):913-919.
- Hynd MR, Scott HL, Dodd PR. 2004b. Selective loss of NMDA receptor NR1 subunit isoforms in Alzheimer's disease. *J Neurochem* 89(1):240-247.

- Ichijo H, Nishida E, Irie K, ten Dijke P, Saitoh M, Moriguchi T, Takagi M, Matsumoto K, Miyazono K, Gotoh Y. 1997. Induction of apoptosis by ASK1, a mammalian MAPKKK that activates SAPK/JNK and p38 signaling pathways. *Science* 275(5296):90-94.
- Ignarro LJ. 1991. Signal transduction mechanisms involving nitric oxide. *Biochem Pharmacol* 41(4):485-490.
- Ikonomidou C, Bosch F, Miksa M, Bittigau P, Vockler J, Dikranian K, Tenkova TI, Stefovaska V, Turski L, Olney JW. 1999. Blockade of NMDA receptors and apoptotic neurodegeneration in the developing brain. *Science* 283(5398):70-74.
- Imai F, Suzuki H, Oda J, Ninomiya T, Ono K, Sano H, Sawada M. 2007. Neuroprotective effect of exogenous microglia in global brain ischemia. *J Cereb Blood Flow Metab* 27(3):488-500.
- Inoue J, Misawa A, Tanaka Y, Ichinose S, Sugino Y, Hosoi H, Sugimoto T, Imoto I, Inazawa J. 2009. Lysosomal-associated protein multispansing transmembrane 5 gene (LAPTM5) is associated with spontaneous regression of neuroblastomas. *PLoS One* 4(9):e7099.
- Iqbal K, Grundke-Iqbal I. 2008. Alzheimer neurofibrillary degeneration: significance, etiopathogenesis, therapeutics and prevention. *J Cell Mol Med* 12(1):38-55.
- Ischiropoulos H, Beckman JS. 2003. Oxidative stress and nitration in neurodegeneration: cause, effect, or association? *J Clin Invest* 111(2):163-169.
- Ishigami M, Hiraki K, Umemura K, Ogasawara Y, Ishii K, Kimura H. 2009. A source of hydrogen sulfide and a mechanism of its release in the brain. *Antioxid Redox Signal* 11(2):205-214.
- Ishii T, Moriyoshi K, Sugihara H, Sakurada K, Kadotani H, Yokoi M, Akazawa C, Shigemoto R, Mizuno N, Masu M, et al. 1993. Molecular characterization of the family of the N-methyl-D-aspartate receptor subunits. *J Biol Chem* 268(4):2836-2843.
- Ivacko JA, Sun R, Silverstein FS. 1996. Hypoxic-ischemic brain injury induces an acute microglial reaction in perinatal rats. *Pediatr Res* 39(1):39-47.
- Iwasato T, Erzurumlu RS, Huerta PT, Chen DF, Sasaoka T, Ulupinar E, Tonegawa S. 1997. NMDA receptor-dependent refinement of somatotopic maps. *Neuron* 19(6):1201-1210.
- Jaeger PA, Wyss-Coray T. 2009. All-you-can-eat: autophagy in neurodegeneration and neuroprotection. *Mol Neurodegener* 4:16.
- Jenner P. 2007. Oxidative stress and Parkinson's disease. *Handb Clin Neurol* 83:507-520.
- Jensen FE. 2002a. Relationship between encephalopathy and abnormal neuronal activity in the developing brain. *Int Rev Neurobiol* 49:23-35.
- Jensen FE. 2002b. The role of glutamate receptor maturation in perinatal seizures and brain injury. *Int J Dev Neurosci* 20(3-5):339-347.
- Jimbo A, Fujita E, Kouroku Y, Ohnishi J, Inohara N, Kuida K, Sakamaki K, Yonehara S, Momoi T. 2003. ER stress induces caspase-8 activation, stimulating cytochrome c release and caspase-9 activation. *Exp Cell Res* 283(2):156-166.

- Jin K, Sun Y, Xie L, Childs J, Mao XO, Greenberg DA. 2004. Post-ischemic administration of heparin-binding epidermal growth factor-like growth factor (HB-EGF) reduces infarct size and modifies neurogenesis after focal cerebral ischemia in the rat. *J Cereb Blood Flow Metab* 24(4):399-408.
- Johnson EM, Jr., Deckwerth TL. 1993. Molecular mechanisms of developmental neuronal death. *Annu Rev Neurosci* 16:31-46.
- Johnston TH, Fox SH, McIlldowie MJ, Piggott MJ, Brotchie JM. 2010. Reduction of L-DOPA-induced dyskinesia by the selective metabotropic glutamate receptor 5 antagonist 3-[(2-methyl-1,3-thiazol-4-yl)ethynyl]pyridine in the 1-methyl-4-phenyl-1,2,3,6-tetrahydropyridine-lesioned macaque model of Parkinson's disease. *J Pharmacol Exp Ther* 333(3):865-873.
- Jones NM, Kardashyan L, Callaway JK, Lee EM, Beart PM. 2008. Long-term functional and protective actions of preconditioning with hypoxia, cobalt chloride, and desferrioxamine against hypoxic-ischemic injury in neonatal rats. *Pediatr Res* 63(6):620-624.
- Jonnala RR, Buccafusco JJ. 2001. Inhibition of nerve growth factor signaling by peroxy nitrite. *J Neurosci Res* 63(1):27-34.
- Jorda EG, Verdaguer E, Canudas AM, Jimenez A, Bruna A, Caelles C, Bravo R, Escubedo E, Pubill D, Camarasa J, Pallas M, Camins A. 2003. Neuroprotective action of flavopiridol, a cyclin-dependent kinase inhibitor, in colchicine-induced apoptosis. *Neuropharmacology* 45(5):672-683.
- Jordan-Sciutto KL, Dorsey R, Chalovich EM, Hammond RR, Achim CL. 2003. Expression patterns of retinoblastoma protein in Parkinson disease. *J Neuropathol Exp Neurol* 62(1):68-74.
- Juul SE, McPherson RJ, Bauer LA, Ledbetter KJ, Gleason CA, Mayock DE. 2008. A phase I/II trial of high-dose erythropoietin in extremely low birth weight infants: pharmacokinetics and safety. *Pediatrics* 122(2):383-391.
- Kabeya Y, Mizushima N, Ueno T, Yamamoto A, Kirisako T, Noda T, Kominami E, Ohsumi Y, Yoshimori T. 2000. LC3, a mammalian homologue of yeast Apg8p, is localized in autophagosome membranes after processing. *EMBO J* 19(21):5720-5728.
- Kamiya T, Katayama Y, Kashiwagi F, Terashi A. 1993. The role of bradykinin in mediating ischemic brain edema in rats. *Stroke* 24(4):571-575; discussion 575-576.
- Kanno H, Ozawa H, Sekiguchi A, Itoi E. 2009. Spinal cord injury induces upregulation of Beclin 1 and promotes autophagic cell death. *Neurobiol Dis* 33(2):143-148.
- Kastrup A, Engelhorn T, Beaulieu C, de Crespigny A, Moseley ME. 1999. Dynamics of cerebral injury, perfusion, and blood-brain barrier changes after temporary and permanent middle cerebral artery occlusion in the rat. *J Neurol Sci* 166(2):91-99.
- Kato Y, Tapping RI, Huang S, Watson MH, Ulevitch RJ, Lee JD. 1998. Bmk1/Erk5 is required for cell proliferation induced by epidermal growth factor. *Nature* 395(6703):713-716.
- Kaur N, Lu B, Monroe RK, Ward SM, Halvorsen SW. 2005. Inducers of oxidative stress block ciliary neurotrophic factor activation of Jak/STAT signaling in neurons. *J Neurochem* 92(6):1521-1530.

- Kawahara N, Mishima K, Higashiyama S, Taniguchi N, Tamura A, Kirino T. 1999. The gene for heparin-binding epidermal growth factor-like growth factor is stress-inducible: its role in cerebral ischemia. *J Cereb Blood Flow Metab* 19(3):307-320.
- Keller JN, Dimayuga E, Chen Q, Thorpe J, Gee J, Ding Q. 2004. Autophagy, proteasomes, lipofuscin, and oxidative stress in the aging brain. *Int J Biochem Cell Biol* 36(12):2376-2391.
- Keller JN, Hanni KB, Markesbery WR. 2000a. Impaired proteasome function in Alzheimer's disease. *J Neurochem* 75(1):436-439.
- Keller JN, Huang FF, Zhu H, Yu J, Ho YS, Kindy TS. 2000b. Oxidative stress-associated impairment of proteasome activity during ischemia-reperfusion injury. *J Cereb Blood Flow Metab* 20(10):1467-1473.
- Kernie SG, Parent JM. 2010. Forebrain neurogenesis after focal Ischemic and traumatic brain injury. *Neurobiol Dis* 37(2):267-274.
- Kettle AJ, Chan T, Osberg I, Senthilmohan R, Chapman AL, Mocatta TJ, Wagener JS. 2004. Myeloperoxidase and protein oxidation in the airways of young children with cystic fibrosis. *Am J Respir Crit Care Med* 170(12):1317-1323.
- Kidwell CS, Latour L, Saver JL, Alger JR, Starkman S, Duckwiler G, Jahan R, Vinuela F, Kang DW, Warach S. 2008. Thrombolytic toxicity: blood brain barrier disruption in human ischemic stroke. *Cerebrovasc Dis* 25(4):338-343.
- Kim AH, Puram SV, Bilimoria PM, Ikeuchi Y, Keough S, Wong M, Rowitch D, Bonni A. 2009. A centrosomal Cdc20-APC pathway controls dendrite morphogenesis in postmitotic neurons. *Cell* 136(2):322-336.
- Kim DY, Kim SH, Choi HB, Min C, Gwag BJ. 2001. High abundance of GluR1 mRNA and reduced Q/R editing of GluR2 mRNA in individual NADPH-diaphorase neurons. *Mol Cell Neurosci* 17(6):1025-1033.
- Kim JS, Gautam SC, Chopp M, Zaloga C, Jones ML, Ward PA, Welch KM. 1995. Expression of monocyte chemoattractant protein-1 and macrophage inflammatory protein-1 after focal cerebral ischemia in the rat. *J Neuroimmunol* 56(2):127-134.
- Kim SH, Fraser PE, Westaway D, St George-Hyslop PH, Ehrlich ME, Gandy S. 2010. Group II metabotropic glutamate receptor stimulation triggers production and release of Alzheimer's amyloid(beta)42 from isolated intact nerve terminals. *J Neurosci* 30(11):3870-3875.
- Kimura H. 2010. Hydrogen sulfide: from brain to gut. *Antioxid Redox Signal* 12(9):1111-1123.
- Kimura SH, Nojima H. 2002. Cyclin G1 associates with MDM2 and regulates accumulation and degradation of p53 protein. *Genes Cells* 7(8):869-880.
- Kimura Y, Dargusch R, Schubert D, Kimura H. 2006. Hydrogen sulfide protects HT22 neuronal cells from oxidative stress. *Antioxid Redox Signal* 8(3-4):661-670.
- Kimura Y, Goto Y, Kimura H. 2010. Hydrogen sulfide increases glutathione production and suppresses oxidative stress in mitochondria. *Antioxid Redox Signal* 12(1):1-13.
- Kimura Y, Kimura H. 2004. Hydrogen sulfide protects neurons from oxidative stress. *Faseb J* 18(10):1165-1167.

- Kitao Y, Imai Y, Ozawa K, Kataoka A, Ikeda T, Soda M, Nakimawa K, Kiyama H, Stern DM, Hori O, Wakamatsu K, Ito S, Itohara S, Takahashi R, Ogawa S. 2007. Pael receptor induces death of dopaminergic neurons in the substantia nigra via endoplasmic reticulum stress and dopamine toxicity, which is enhanced under condition of parkin inactivation. *Hum Mol Genet* 16(1):50-60.
- Klehmet J, Harms H, Richter M, Prass K, Volk HD, Dirnagl U, Meisel A, Meisel C. 2009. Stroke-induced immunodepression and post-stroke infections: lessons from the preventive antibacterial therapy in stroke trial. *Neuroscience* 158(3):1184-1193.
- Klionsky DJ. 2006. Neurodegeneration: good riddance to bad rubbish. *Nature* 441(7095):819-820.
- Koh JY. 2001. Zinc and disease of the brain. *Mol Neurobiol* 24(1-3):99-106.
- Koike M, Shibata M, Tadakoshi M, Gotoh K, Komatsu M, Waguri S, Kawahara N, Kuida K, Nagata S, Kominami E, Tanaka K, Uchiyama Y. 2008. Inhibition of autophagy prevents hippocampal pyramidal neuron death after hypoxic-ischemic injury. *Am J Pathol* 172(2):454-469.
- Koizumi J, Yoshida Y, Nakazawa T, Ooneda G. 1986. Experimental studies of ischemic brain edema. I: a new experimental model of cerebral embolism in rats in which recirculation can be introduced in the ischemic area. *Jpn J Stroke* 8:1-8.
- Konig HG, Rehm M, Gudorf D, Krajewski S, Gross A, Ward MW, Prehn JH. 2007. Full length Bid is sufficient to induce apoptosis of cultured rat hippocampal neurons. *BMC Cell Biol* 8:7.
- Kontos HA. 1985. George E. Brown memorial lecture. Oxygen radicals in cerebral vascular injury. *Circ Res* 57(4):508-516.
- Kontos HA. 2001. Oxygen radicals in cerebral ischemia: the 2001 Willis lecture. *Stroke* 32(11):2712-2716.
- Krantic S, Mechawar N, Reix S, Quirion R. 2005. Molecular basis of programmed cell death involved in neurodegeneration. *Trends Neurosci* 28(12):670-676.
- Kreutzberg GW. 1996. Microglia: a sensor for pathological events in the CNS. *Trends Neurosci* 19(8):312-318.
- Kriz J, Lalancette-Hebert M. 2009. Inflammation, plasticity and real-time imaging after cerebral ischemia. *Acta Neuropathol* 117(5):497-509.
- Kroemer G, Galluzzi L, Brenner C. 2007. Mitochondrial membrane permeabilization in cell death. *Physiol Rev* 87(1):99-163.
- Kroemer G, Galluzzi L, Vandenabeele P, Abrams J, Alnemri ES, Baehrecke EH, Blagosklonny MV, El-Deiry WS, Golstein P, Green DR, Hengartner M, Knight RA, Kumar S, Lipton SA, Malorni W, Nunez G, Peter ME, Tschopp J, Yuan J, Piacentini M, Zhivotovsky B, Melino G. 2009. Classification of cell death: recommendations of the Nomenclature Committee on Cell Death 2009. *Cell Death Differ* 16(1):3-11.
- Kroemer G, Levine B. 2008. Autophagic cell death: the story of a misnomer. *Nat Rev Mol Cell Biol* 9(12):1004-1010.
- Kruman, II, Wersto RP, Cardozo-Pelaez F, Smilenov L, Chan SL, Chrest FJ, Emokpae R, Jr., Gorospe M, Mattson MP. 2004. Cell cycle activation linked to neuronal cell death initiated by DNA damage. *Neuron* 41(4):549-561.

- Kruman I, Schwartz E. 2006. Methods of neuroprotection by cyclin-dependent kinase inhibition. US 20080182853.
- Kufer TA, Sillje HH, Korner R, Gruss OJ, Meraldi P, Nigg EA. 2002. Human TPX2 is required for targeting Aurora-A kinase to the spindle. *J Cell Biol* 158(4):617-623.
- Kuroiwa T, Ting P, Martinez H, Klatzo I. 1985. The biphasic opening of the blood-brain barrier to proteins following temporary middle cerebral artery occlusion. *Acta Neuropathol* 68(2):122-129.
- Kutsuwada T, Kashiwabuchi N, Mori H, Sakimura K, Kushiya E, Araki K, Meguro H, Masaki H, Kumanishi T, Arakawa M, et al. 1992. Molecular diversity of the NMDA receptor channel. *Nature* 358(6381):36-41.
- Kyriakis JM, Avruch J. 2001. Mammalian mitogen-activated protein kinase signal transduction pathways activated by stress and inflammation. *Physiol Rev* 81(2):807-869.
- Lafon-Cazal M, Pietri S, Culcasi M, Bockaert J. 1993. NMDA-dependent superoxide production and neurotoxicity. *Nature* 364(6437):535-537.
- Lakhan SE, Kirchgessner A, Hofer M. 2009. Inflammatory mechanisms in ischemic stroke: therapeutic approaches. *J Transl Med* 7:97.
- Lalancette-Hebert M, Gowing G, Simard A, Weng YC, Kriz J. 2007. Selective ablation of proliferating microglial cells exacerbates ischemic injury in the brain. *J Neurosci* 27(10):2596-2605.
- Landshamer S, Hoehn M, Barth N, Duvezin-Caubet S, Schwake G, Tobaben S, Kazhdan I, Becattini B, Zahler S, Vollmar A, Pellecchia M, Reichert A, Plesnila N, Wagner E, Culmsee C. 2008. Bid-induced release of AIF from mitochondria causes immediate neuronal cell death. *Cell Death Differ* 15(10):1553-1563.
- Larm JA, Cheung NS, Beart PM. 1997. Apoptosis induced via AMPA-selective glutamate receptors in cultured murine cortical neurons. *J Neurochem* 69(2):617-622.
- Lassmann S, Shen Y, Jutting U, Wiehle P, Walch A, Gitsch G, Hasenburg A, Werner M. 2007. Predictive value of Aurora-A/STK15 expression for late stage epithelial ovarian cancer patients treated by adjuvant chemotherapy. *Clin Cancer Res* 13(14):4083-4091.
- Lau KL, Kong SK, Ko WH, Kwan HY, Huang Y, Yao X. 2003. cGMP stimulates endoplasmic reticulum Ca(2+)-ATPase in vascular endothelial cells. *Life Sci* 73(16):2019-2028.
- Lee HG, Casadesus G, Zhu X, Castellani RJ, McShea A, Perry G, Petersen RB, Bajic V, Smith MA. 2009. Cell cycle re-entry mediated neurodegeneration and its treatment role in the pathogenesis of Alzheimer's disease. *Neurochem Int* 54(2):84-88.
- Lee HM, Greeley GH, Jr., Englander EW. 2000. Effects of aging on expression of genes involved in regulation of proliferation and apoptosis in the colonic epithelium. *Mech Ageing Dev* 115(3):139-155.
- Lee JM, Zipfel GJ, Choi DW. 1999. The changing landscape of ischaemic brain injury mechanisms. *Nature* 399(6738 Suppl):A7-14.
- Leist M, Nicotera P. 1998a. Apoptosis, excitotoxicity, and neuropathology. *Exp Cell Res* 239(2):183-201.

References

- Leist M, Nicotera P. 1998b. Calcium and neuronal death. *Rev Physiol Biochem Pharmacol* 132:79-125.
- Leist M, Volbracht C, Kuhnle S, Fava E, Ferrando-May E, Nicotera P. 1997. Caspase-mediated apoptosis in neuronal excitotoxicity triggered by nitric oxide. *Mol Med* 3(11):750-764.
- Leker RR, Lasri V, Chernoguz D. 2009. Growth factors improve neurogenesis and outcome after focal cerebral ischemia. *J Neural Transm* 116(11):1397-1402.
- Lennon SV, Martin SJ, Cotter TG. 1991. Dose-dependent induction of apoptosis in human tumour cell lines by widely diverging stimuli. *Cell Prolif* 24(2):203-214.
- Leonardi-Bee J, Bath PM, Phillips SJ, Sandercock PA. 2002. Blood pressure and clinical outcomes in the International Stroke Trial. *Stroke* 33(5):1315-1320.
- Leonardo CC, Pennypacker KR. 2009. Neuroinflammation and MMPs: potential therapeutic targets in neonatal hypoxic-ischemic injury. *J Neuroinflammation* 6:13.
- Lerma J. 2003. Roles and rules of kainate receptors in synaptic transmission. *Nat Rev Neurosci* 4(6):481-495.
- Lester RA, Clements JD, Westbrook GL, Jahr CE. 1990. Channel kinetics determine the time course of NMDA receptor-mediated synaptic currents. *Nature* 346(6284):565-567.
- Leurs J, Hendriks D. 2005. Carboxypeptidase U (TAF1a): a metallo-carboxypeptidase with a distinct role in haemostasis and a possible risk factor for thrombotic disease. *Thromb Haemost* 94(3):471-487.
- Lev S, Moreno H, Martinez R, Canoll P, Peles E, Musacchio JM, Plowman GD, Rudy B, Schlessinger J. 1995. Protein tyrosine kinase PYK2 involved in Ca²⁺-induced regulation of ion channel and MAP kinase functions. *Nature* 376(6543):737-745.
- Levine S. 1960. Anoxic-ischemic encephalopathy in rats. *Am J Pathol* 36:1-17.
- Levine S, Klein M. 1960. Ischemic infarction and swelling in the rat brain. *Arch Pathol* 69:544-553.
- Li D, Zhu J, Firozi PF, Abbruzzese JL, Evans DB, Cleary K, Friess H, Sen S. 2003. Overexpression of oncogenic STK15/BTAK/Aurora A kinase in human pancreatic cancer. *Clin Cancer Res* 9(3):991-997.
- Li J, Baud O, Vartanian T, Volpe JJ, Rosenberg PA. 2005. Peroxynitrite generated by inducible nitric oxide synthase and NADPH oxidase mediates microglial toxicity to oligodendrocytes. *Proc Natl Acad Sci U S A* 102(28):9936-9941.
- Li J, Pelletier MR, Perez Velazquez JL, Carlen PL. 2002. Reduced cortical synaptic plasticity and GluR1 expression associated with fragile X mental retardation protein deficiency. *Mol Cell Neurosci* 19(2):138-151.
- Lin MT, Beal MF. 2006. Mitochondrial dysfunction and oxidative stress in neurodegenerative diseases. *Nature* 443(7113):787-795.
- Lip GY, Blann AD, Farooqi IS, Zarifis J, Sagar G, Beevers DG. 2002. Sequential alterations in haemorheology, endothelial dysfunction, platelet activation and thrombogenesis in relation to prognosis following acute stroke: The West Birmingham Stroke Project. *Blood Coagul Fibrinolysis* 13(4):339-347.

- Liu DZ, Cheng XY, Ander BP, Xu H, Davis RR, Gregg JP, Sharp FR. 2008. Src kinase inhibition decreases thrombin-induced injury and cell cycle re-entry in striatal neurons. *Neurobiol Dis* 30(2):201-211.
- Liu PK, Hsu CY, Dizdaroglu M, Floyd RA, Kow YW, Karakaya A, Rabow LE, Cui JK. 1996. Damage, repair, and mutagenesis in nuclear genes after mouse forebrain ischemia-reperfusion. *J Neurosci* 16(21):6795-6806.
- Lledo PM, Zhang X, Sudhof TC, Malenka RC, Nicoll RA. 1998. Postsynaptic membrane fusion and long-term potentiation. *Science* 279(5349):399-403.
- Lo EH, Dalkara T, Moskowitz MA. 2003. Mechanisms, challenges and opportunities in stroke. *Nat Rev Neurosci* 4(5):399-415.
- Lockhart DJ, Barlow C. 2001. Expressing what's on your mind: DNA arrays and the brain. *Nat Rev Neurosci* 2(1):63-68.
- Longa EZ, Weinstein PR, Carlson S, Cummins R. 1989. Reversible middle cerebral artery occlusion without craniectomy in rats. *Stroke* 20(1):84-91.
- Lopes CS, Casares F. 2010. hth maintains the pool of eye progenitors and its downregulation by Dpp and Hh couples retinal fate acquisition with cell cycle exit. *Dev Biol* 339(1):78-88.
- Lopes JP, Blurton-Jones M, Yamasaki TR, Agostinho P, LaFerla FM. 2009a. Activation of cell cycle proteins in transgenic mice in response to neuronal loss but not amyloid-beta and tau pathology. *J Alzheimers Dis* 16(3):541-549.
- Lopes JP, Oliveira CR, Agostinho P. 2009b. Cell cycle re-entry in Alzheimer's disease: a major neuropathological characteristic? *Curr Alzheimer Res* 6(3):205-212.
- Lorberboym M, Lampl Y, Sadeh M. 2003. Correlation of 99mTc-DTPA SPECT of the blood-brain barrier with neurologic outcome after acute stroke. *J Nucl Med* 44(12):1898-1904.
- Love S. 1999. Oxidative stress in brain ischemia. *Brain Pathol* 9(1):119-131.
- Lucas SM, Rothwell NJ, Gibson RM. 2006. The role of inflammation in CNS injury and disease. *Br J Pharmacol* 147 Suppl 1:S232-240.
- Luthi A, Gahwiler BH, Gerber U. 1996. A slowly inactivating potassium current in CA3 pyramidal cells of rat hippocampus in vitro. *J Neurosci* 16(2):586-594.
- Macas J, Nern C, Plate KH, Momma S. 2006. Increased generation of neuronal progenitors after ischemic injury in the aged adult human forebrain. *J Neurosci* 26(50):13114-13119.
- MacDermott AB, Mayer ML, Westbrook GL, Smith SJ, Barker JL. 1986. NMDA-receptor activation increases cytoplasmic calcium concentration in cultured spinal cord neurones. *Nature* 321(6069):519-522.
- Madinier A, Bertrand N, Mossiat C, Prigent-Tessier A, Beley A, Marie C, Garnier P. 2009. Microglial involvement in neuroplastic changes following focal brain ischemia in rats. *PLoS One* 4(12):e8101.
- Madison DV, Schuman EM. 1991. LTP, post or pre? A look at the evidence for the locus of long-term potentiation. *New Biol* 3(6):549-557.
- Maiuri MC, Criollo A, Tasdemir E, Vicencio JM, Tajeddine N, Hickman JA, Geneste O, Kroemer G. 2007a. BH3-only proteins and BH3 mimetics induce autophagy by competitively disrupting the interaction between Beclin 1 and Bcl-2/Bcl-X(L). *Autophagy* 3(4):374-376.

- Maiuri MC, Le Toumelin G, Criollo A, Rain JC, Gautier F, Juin P, Tasdemir E, Pierron G, Troulinaki K, Tavernarakis N, Hickman JA, Geneste O, Kroemer G. 2007b. Functional and physical interaction between Bcl-X(L) and a BH3-like domain in Beclin-1. *EMBO J* 26(10):2527-2539.
- Majd S, Zarifkar A, Rastegar K, Takhshid MA. 2008. Different fibrillar Abeta 1-42 concentrations induce adult hippocampal neurons to reenter various phases of the cell cycle. *Brain Res* 1218:224-229.
- Malinak C, Silverstein FS. 1996. Hypoxic-ischemic injury acutely disrupts microtubule-associated protein 2 immunostaining in neonatal rat brain. *Biol Neonate* 69(4):257-267.
- Malinow R, Malenka RC. 2002. AMPA receptor trafficking and synaptic plasticity. *Annu Rev Neurosci* 25:103-126.
- Mancuso M, Coppede F, Migliore L, Siciliano G, Murri L. 2006. Mitochondrial dysfunction, oxidative stress and neurodegeneration. *J Alzheimers Dis* 10(1):59-73.
- Maragakis NJ, Rothstein JD. 2006. Mechanisms of Disease: astrocytes in neurodegenerative disease. *Nat Clin Pract Neurol* 2(12):679-689.
- Marini AM, Rabin SJ, Lipsky RH, Mocchetti I. 1998. Activity-dependent release of brain-derived neurotrophic factor underlies the neuroprotective effect of N-methyl-D-aspartate. *J Biol Chem* 273(45):29394-29399.
- Marsh BJ, Williams-Karnesky RL, Stenzel-Poore MP. 2009. Toll-like receptor signaling in endogenous neuroprotection and stroke. *Neuroscience* 158(3):1007-1020.
- Martin LJ, Al-Abdulla NA, Brambrink AM, Kirsch JR, Sieber FE, Portera-Cailliau C. 1998. Neurodegeneration in excitotoxicity, global cerebral ischemia, and target deprivation: A perspective on the contributions of apoptosis and necrosis. *Brain Res Bull* 46(4):281-309.
- Martin LJ, Blackstone CD, Levey AI, Haganir RL, Price DL. 1993. AMPA glutamate receptor subunits are differentially distributed in rat brain. *Neuroscience* 53(2):327-358.
- Masu M, Tanabe Y, Tsuchida K, Shigemoto R, Nakanishi S. 1991. Sequence and expression of a metabotropic glutamate receptor. *Nature* 349(6312):760-765.
- Matsui T, Sekiguchi M, Hashimoto A, Tomita U, Nishikawa T, Wada K. 1995. Functional comparison of D-serine and glycine in rodents: the effect on cloned NMDA receptors and the extracellular concentration. *J Neurochem* 65(1):454-458.
- Matyja E, Taraszewska A, Naganska E, Rafalowska J. 2005. Autophagic degeneration of motor neurons in a model of slow glutamate excitotoxicity in vitro. *Ultrastruct Pathol* 29(5):331-339.
- Mayer ML, Vyklicky L, Jr., Clements J. 1989. Regulation of NMDA receptor desensitization in mouse hippocampal neurons by glycine. *Nature* 338(6214):425-427.
- Mayer ML, Westbrook GL. 1984. Mixed-agonist action of excitatory amino acids on mouse spinal cord neurones under voltage clamp. *J Physiol* 354:29-53.

References

- Mayer ML, Westbrook GL, Guthrie PB. 1984. Voltage-dependent block by Mg²⁺ of NMDA responses in spinal cord neurones. *Nature* 309(5965):261-263.
- McCullough KD, Martindale JL, Klotz LO, Aw TY, Holbrook NJ. 2001. Gadd153 sensitizes cells to endoplasmic reticulum stress by down-regulating Bcl2 and perturbing the cellular redox state. *Mol Cell Biol* 21(4):1249-1259.
- McDonald JW, Johnston MV. 1990. Physiological and pathophysiological roles of excitatory amino acids during central nervous system development. *Brain Res Brain Res Rev* 15(1):41-70.
- McDonald JW, Johnston MV, Young AB. 1990. Differential ontogenic development of three receptors comprising the NMDA receptor/channel complex in the rat hippocampus. *Exp Neurol* 110(3):237-247.
- McGinnis KM, Gnegy ME, Park YH, Mukerjee N, Wang KK. 1999. Procaspase-3 and poly(ADP)ribose polymerase (PARP) are calpain substrates. *Biochem Biophys Res Commun* 263(1):94-99.
- McNaught KS, Olanow CW, Halliwell B, Isacson O, Jenner P. 2001. Failure of the ubiquitin-proteasome system in Parkinson's disease. *Nat Rev Neurosci* 2(8):589-594.
- McRae A, Gilland E, Bona E, Hagberg H. 1995. Microglia activation after neonatal hypoxic-ischemia. *Brain Res Dev Brain Res* 84(2):245-252.
- McShea A, Harris PL, Webster KR, Wahl AF, Smith MA. 1997. Abnormal expression of the cell cycle regulators P16 and CDK4 in Alzheimer's disease. *Am J Pathol* 150(6):1933-1939.
- McShea A, Lee HG, Petersen RB, Casadesus G, Vincent I, Linford NJ, Funk JO, Shapiro RA, Smith MA. 2007. Neuronal cell cycle re-entry mediates Alzheimer disease-type changes. *Biochim Biophys Acta* 1772(4):467-472.
- McShea A, Wahl AF, Smith MA. 1999. Re-entry into the cell cycle: a mechanism for neurodegeneration in Alzheimer disease. *Med Hypotheses* 52(6):525-527.
- Meguro H, Mori H, Araki K, Kushiya E, Kutsuwada T, Yamazaki M, Kumanishi T, Arakawa M, Sakimura K, Mishina M. 1992. Functional characterization of a heteromeric NMDA receptor channel expressed from cloned cDNAs. *Nature* 357(6373):70-74.
- Meikrantz W, Schlegel R. 1995. Apoptosis and the cell cycle. *J Cell Biochem* 58(2):160-174.
- Meriin AB, Sherman MY. 2005. Role of molecular chaperones in neurodegenerative disorders. *Int J Hyperthermia* 21(5):403-419.
- Middleton FA, Mirnics K, Pierri JN, Lewis DA, Levitt P. 2002. Gene expression profiling reveals alterations of specific metabolic pathways in schizophrenia. *J Neurosci* 22(7):2718-2729.
- Miller JT, Bartley JH, Wimborne HJ, Walker AL, Hess DC, Hill WD, Carroll JE. 2005. The neuroblast and angioblast chemotactic factor SDF-1 (CXCL12) expression is briefly up regulated by reactive astrocytes in brain following neonatal hypoxic-ischemic injury. *BMC Neurosci* 6:63.
- Minger SL, Ekonomou A, Carta EM, Chinoy A, Perry RH, Ballard CG. 2007. Endogenous neurogenesis in the human brain following cerebral infarction. *Regen Med* 2(1):69-74.

References

- Mirnics K, Middleton FA, Marquez A, Lewis DA, Levitt P. 2000. Molecular characterization of schizophrenia viewed by microarray analysis of gene expression in prefrontal cortex. *Neuron* 28(1):53-67.
- Mizushima N, Levine B, Cuervo AM, Klionsky DJ. 2008. Autophagy fights disease through cellular self-digestion. *Nature* 451(7182):1069-1075.
- Mizushima N, Yamamoto A, Hatano M, Kobayashi Y, Kabeya Y, Suzuki K, Tokuhiya T, Ohsumi Y, Yoshimori T. 2001. Dissection of autophagosome formation using Apg5-deficient mouse embryonic stem cells. *J Cell Biol* 152(4):657-668.
- Mojsilovic-Petrovic J, Callaghan D, Cui H, Dean C, Stanimirovic DB, Zhang W. 2007. Hypoxia-inducible factor-1 (HIF-1) is involved in the regulation of hypoxia-stimulated expression of monocyte chemoattractant protein-1 (MCP-1/CCL2) and MCP-5 (Ccl12) in astrocytes. *J Neuroinflammation* 4:12.
- Moldes O, Sobrino T, Millan M, Castellanos M, Perez de la Ossa N, Leira R, Serena J, Vivancos J, Davalos A, Castillo J. 2008. High serum levels of endothelin-1 predict severe cerebral edema in patients with acute ischemic stroke treated with t-PA. *Stroke* 39(7):2006-2010.
- Moldrich RX, Beart PM, Pascoe CJ, Cheung NS. 2000. Low-affinity kainate receptor agonists induce insult-dependent apoptosis and necrosis in cultured murine cortical neurons. *J Neurosci Res* 59(6):788-796.
- Moldrich RX, Cheung NS, Pascoe CJ, Beart PM. 1999. Excitotoxic injury profiles of low-affinity kainate receptor agonists in cortical neuronal cultures. *Eur J Pharmacol* 378(2):R1-3.
- Momeni HR, Kanje M. 2006. Calpain inhibitors delay injury-induced apoptosis in adult mouse spinal cord motor neurons. *Neuroreport* 17(8):761-765.
- Momiyama A, Feldmeyer D, Cull-Candy SG. 1996. Identification of a native low-conductance NMDA channel with reduced sensitivity to Mg²⁺ in rat central neurones. *J Physiol* 494 (Pt 2):479-492.
- Monn JA, Valli MJ, Massey SM, Wright RA, Salhoff CR, Johnson BG, Howe T, Alt CA, Rhodes GA, Robey RL, Griffey KR, Tizzano JP, Kallman MJ, Helton DR, Schoepp DD. 1997. Design, synthesis, and pharmacological characterization of (+)-2-aminobicyclo[3.1.0]hexane-2,6-dicarboxylic acid (LY354740): a potent, selective, and orally active group 2 metabotropic glutamate receptor agonist possessing anticonvulsant and anxiolytic properties. *J Med Chem* 40(4):528-537.
- Montaner J, Molina CA, Monasterio J, Abilleira S, Arenillas JF, Ribo M, Quintana M, Alvarez-Sabin J. 2003. Matrix metalloproteinase-9 pretreatment level predicts intracranial hemorrhagic complications after thrombolysis in human stroke. *Circulation* 107(4):598-603.
- Monyer H, Burnashev N, Laurie DJ, Sakmann B, Seeburg PH. 1994. Developmental and regional expression in the rat brain and functional properties of four NMDA receptors. *Neuron* 12(3):529-540.
- Monyer H, Sprengel R, Schoepfer R, Herb A, Higuchi M, Lomeli H, Burnashev N, Sakmann B, Seeburg PH. 1992. Heteromeric NMDA receptors: molecular and functional distinction of subtypes. *Science* 256(5060):1217-1221.

- Mori E, del Zoppo GJ, Chambers JD, Copeland BR, Arfors KE. 1992. Inhibition of polymorphonuclear leukocyte adherence suppresses no-reflow after focal cerebral ischemia in baboons. *Stroke* 23(5):712-718.
- Moriyoshi K, Masu M, Ishii T, Shigemoto R, Mizuno N, Nakanishi S. 1991. Molecular cloning and characterization of the rat NMDA receptor. *Nature* 354(6348):31-37.
- Moroni F. 2008. Poly(ADP-ribose)polymerase 1 (PARP-1) and postischemic brain damage. *Curr Opin Pharmacol* 8(1):96-103.
- Mueller-Steiner S, Zhou Y, Arai H, Roberson ED, Sun B, Chen J, Wang X, Yu G, Esposito L, Mucke L, Gan L. 2006. Anti-amyloidogenic and neuroprotective functions of cathepsin B: implications for Alzheimer's disease. *Neuron* 51(6):703-714.
- Murakami K, Kondo T, Chan PH. 1997. Reperfusion following focal cerebral ischemia alters distribution of neuronal cells with DNA fragmentation in mice. *Brain Res* 751(1):160-164.
- Murphy TH, Miyamoto M, Sastre A, Schnaar RL, Coyle JT. 1989. Glutamate toxicity in a neuronal cell line involves inhibition of cystine transport leading to oxidative stress. *Neuron* 2(6):1547-1558.
- Nagley P, Higgins GC, Atkin JD, Beart PM. 2010. Multifaceted deaths orchestrated by mitochondria in neurones. *Biochim Biophys Acta* 1802(1):167-185.
- Nagy Z, Esiri MM. 1998. Neuronal cyclin expression in the hippocampus in temporal lobe epilepsy. *Exp Neurol* 150(2):240-247.
- Nakagawa T, Yuan J. 2000. Cross-talk between two cysteine protease families. Activation of caspase-12 by calpain in apoptosis. *J Cell Biol* 150(4):887-894.
- Nakajima K, Yamamoto S, Kohsaka S, Kurihara T. 2008. Neuronal stimulation leading to upregulation of glutamate transporter-1 (GLT-1) in rat microglia in vitro. *Neurosci Lett* 436(3):331-334.
- Nakajima Y, Iwakabe H, Akazawa C, Nawa H, Shigemoto R, Mizuno N, Nakanishi S. 1993. Molecular characterization of a novel retinal metabotropic glutamate receptor mGluR6 with a high agonist selectivity for L-2-amino-4-phosphonobutyrate. *J Biol Chem* 268(16):11868-11873.
- Namura S, Zhu J, Fink K, Endres M, Srinivasan A, Tomaselli KJ, Yuan J, Moskowitz MA. 1998. Activation and cleavage of caspase-3 in apoptosis induced by experimental cerebral ischemia. *J Neurosci* 18(10):3659-3668.
- Neumann J, Sauerzweig S, Ronicke R, Gunzer F, Dinkel K, Ullrich O, Gunzer M, Reymann KG. 2008. Microglia cells protect neurons by direct engulfment of invading neutrophil granulocytes: a new mechanism of CNS immune privilege. *J Neurosci* 28(23):5965-5975.
- Newman DK, Hoffman S, Kotamraju S, Zhao T, Wakim B, Kalyanaraman B, Newman PJ. 2002. Nitration of PECAM-1 ITIM tyrosines abrogates phosphorylation and SHP-2 binding. *Biochem Biophys Res Commun* 296(5):1171-1179.
- Nguyen MD, Boudreau M, Kriz J, Couillard-Despres S, Kaplan DR, Julien JP. 2003. Cell cycle regulators in the neuronal death pathway of amyotrophic lateral sclerosis caused by mutant superoxide dismutase 1. *J Neurosci* 23(6):2131-2140.

- Nicholls DG. 2008. Oxidative stress and energy crises in neuronal dysfunction. *Ann N Y Acad Sci* 1147:53-60.
- Nicholls DG, Budd SL, Ward MW, Castilho RF. 1999. Excitotoxicity and mitochondria. *Biochem Soc Symp* 66:55-67.
- Nicotera P, Melino G. 2004. Regulation of the apoptosis-necrosis switch. *Oncogene* 23(16):2757-2765.
- Niizuma K, Endo H, Chan PH. 2009. Oxidative stress and mitochondrial dysfunction as determinants of ischemic neuronal death and survival. *J Neurochem* 109 Suppl 1:133-138.
- Niizuma K, Endo H, Nito C, Myer DJ, Kim GS, Chan PH. 2008. The PIDDosome mediates delayed death of hippocampal CA1 neurons after transient global cerebral ischemia in rats. *Proc Natl Acad Sci U S A* 105(42):16368-16373.
- Nishi M, Hinds H, Lu HP, Kawata M, Hayashi Y. 2001. Motoneuron-specific expression of NR3B, a novel NMDA-type glutamate receptor subunit that works in a dominant-negative manner. *J Neurosci* 21(23):RC185.
- Nishida N, Nagasaka T, Kashiwagi K, Boland CR, Goel A. 2007. High copy amplification of the Aurora-A gene is associated with chromosomal instability phenotype in human colorectal cancers. *Cancer Biol Ther* 6(4):525-533.
- Nisoli E, Clementi E, Paolucci C, Cozzi V, Tonello C, Sciorati C, Bracale R, Valerio A, Francolini M, Moncada S, Carruba MO. 2003. Mitochondrial biogenesis in mammals: the role of endogenous nitric oxide. *Science* 299(5608):896-899.
- Nixon RA, Cataldo AM, Mathews PM. 2000. The endosomal-lysosomal system of neurons in Alzheimer's disease pathogenesis: a review. *Neurochem Res* 25(9-10):1161-1172.
- Noh KM, Koh JY. 2000. Induction and activation by zinc of NADPH oxidase in cultured cortical neurons and astrocytes. *J Neurosci* 20(23):RC111.
- Northington FJ, Ferriero DM, Flock DL, Martin LJ. 2001. Delayed neurodegeneration in neonatal rat thalamus after hypoxia-ischemia is apoptosis. *J Neurosci* 21(6):1931-1938.
- Noshita N, Lewen A, Sugawara T, Chan PH. 2001. Evidence of phosphorylation of Akt and neuronal survival after transient focal cerebral ischemia in mice. *J Cereb Blood Flow Metab* 21(12):1442-1450.
- Nowak L, Bregestovski P, Ascher P, Herbert A, Prochiantz A. 1984. Magnesium gates glutamate-activated channels in mouse central neurones. *Nature* 307(5950):462-465.
- Nunomura A, Moreira PI, Lee HG, Zhu X, Castellani RJ, Smith MA, Perry G. 2007. Neuronal death and survival under oxidative stress in Alzheimer and Parkinson diseases. *CNS Neurol Disord Drug Targets* 6(6):411-423.
- Oberstein A, Jeffrey PD, Shi Y. 2007. Crystal structure of the Bcl-XL-Bcl-1 peptide complex: Bcl-1 is a novel BH3-only protein. *J Biol Chem* 282(17):13123-13132.
- Okada Y, Copeland BR, Fritridge R, Koziol JA, del Zoppo GJ. 1994a. Fibrin contributes to microvascular obstructions and parenchymal changes during early focal cerebral ischemia and reperfusion. *Stroke* 25(9):1847-1853; discussion 1853-1844.

References

- Okada Y, Copeland BR, Mori E, Tung MM, Thomas WS, del Zoppo GJ. 1994b. P-selectin and intercellular adhesion molecule-1 expression after focal brain ischemia and reperfusion. *Stroke* 25(1):202-211.
- Okamoto K, Li H, Jensen MR, Zhang T, Taya Y, Thorgeirsson SS, Prives C. 2002. Cyclin G recruits PP2A to dephosphorylate Mdm2. *Mol Cell* 9(4):761-771.
- Okamoto N, Hori S, Akazawa C, Hayashi Y, Shigemoto R, Mizuno N, Nakanishi S. 1994. Molecular characterization of a new metabotropic glutamate receptor mGluR7 coupled to inhibitory cyclic AMP signal transduction. *J Biol Chem* 269(2):1231-1236.
- Oliveira-Filho J, Silva SC, Trabuco CC, Pedreira BB, Sousa EU, Bacellar A. 2003. Detrimental effect of blood pressure reduction in the first 24 hours of acute stroke onset. *Neurology* 61(8):1047-1051.
- Olney JW. 1969. Brain lesions, obesity, and other disturbances in mice treated with monosodium glutamate. *Science* 164(880):719-721.
- Ono K, Trautwein W. 1991. Potentiation by cyclic GMP of beta-adrenergic effect on Ca²⁺ current in guinea-pig ventricular cells. *J Physiol* 443:387-404.
- Ono S, Ishizaki Y, Tokuda E, Tabata K, Asami S, Suzuki T. 2007. Different patterns in the induction of metallothionein mRNA synthesis among isoforms after acute ethanol administration. *Biol Trace Elem Res* 115(2):147-156.
- Opdenakker G, Van den Steen PE, Dubois B, Nelissen I, Van Coillie E, Masure S, Proost P, Van Damme J. 2001. Gelatinase B functions as regulator and effector in leukocyte biology. *J Leukoc Biol* 69(6):851-859.
- Orrenius S, Gogvadze V, Zhivotovsky B. 2007. Mitochondrial oxidative stress: implications for cell death. *Annu Rev Pharmacol Toxicol* 47:143-183.
- Ossowska K, Konieczny J, Wardas J, Pietraszek M, Kuter K, Wolfarth S, Pilc A. 2007. An influence of ligands of metabotropic glutamate receptor subtypes on parkinsonian-like symptoms and the striatopallidal pathway in rats. *Amino Acids* 32(2):179-188.
- Osuga H, Osuga S, Wang F, Fetni R, Hogan MJ, Slack RS, Hakim AM, Ikeda JE, Park DS. 2000. Cyclin-dependent kinases as a therapeutic target for stroke. *Proc Natl Acad Sci U S A* 97(18):10254-10259.
- Ozkan OV, Yuzbasioglu MF, Ciralik H, Kurutas EB, Yonden Z, Aydin M, Bulbuloglu E, Semerci E, Goksu M, Atli Y, Bakan V, Duran N. 2009. Resveratrol, a natural antioxidant, attenuates intestinal ischemia/reperfusion injury in rats. *Tohoku J Exp Med* 218(3):251-258.
- Pan J, Konstas AA, Bateman B, Ortolano GA, Pile-Spellman J. 2007. Reperfusion injury following cerebral ischemia: pathophysiology, MR imaging, and potential therapies. *Neuroradiology* 49(2):93-102.
- Pang Z, Bondada V, Sengoku T, Siman R, Geddes JW. 2003. Calpain facilitates the neuron death induced by 3-nitropropionic acid and contributes to the necrotic morphology. *J Neuropathol Exp Neurol* 62(6):633-643.
- Panikashvili D, Mechoulam R, Beni SM, Alexandrovich A, Shohami E. 2005. CB1 cannabinoid receptors are involved in neuroprotection via NF-kappa B inhibition. *J Cereb Blood Flow Metab* 25(4):477-484.
- Park DS, Morris EJ, Bremner R, Keramaris E, Padmanabhan J, Rosenbaum M, Shelanski ML, Geller HM, Greene LA. 2000. Involvement of retinoblastoma

- family members and E2F/DP complexes in the death of neurons evoked by DNA damage. *J Neurosci* 20(9):3104-3114.
- Patneau DK, Mayer ML. 1990. Structure-activity relationships for amino acid transmitter candidates acting at N-methyl-D-aspartate and quisqualate receptors. *J Neurosci* 10(7):2385-2399.
- Pattingre S, Tassa A, Qu X, Garuti R, Liang XH, Mizushima N, Packer M, Schneider MD, Levine B. 2005. Bcl-2 antiapoptotic proteins inhibit Beclin 1-dependent autophagy. *Cell* 122(6):927-939.
- Paulson OB, Strandgaard S, Edvinsson L. 1990. Cerebral autoregulation. *Cerebrovasc Brain Metab Rev* 2(2):161-192.
- Pekny M, Nilsson M. 2005. Astrocyte activation and reactive gliosis. *Glia* 50(4):427-434.
- Pelegri C, Duran-Vilaregut J, del Valle J, Crespo-Biel N, Ferrer I, Pallas M, Camins A, Vilaplana J. 2008. Cell cycle activation in striatal neurons from Huntington's disease patients and rats treated with 3-nitropropionic acid. *Int J Dev Neurosci* 26(7):665-671.
- Pellegrini-Giampietro DE, Bennett MV, Zukin RS. 1994. AMPA/kainate receptor gene expression in normal and Alzheimer's disease hippocampus. *Neuroscience* 61(1):41-49.
- Pellegrini-Giampietro DE, Zukin RS, Bennett MV, Cho S, Pulsinelli WA. 1992. Switch in glutamate receptor subunit gene expression in CA1 subfield of hippocampus following global ischemia in rats. *Proc Natl Acad Sci U S A* 89(21):10499-10503.
- Peng ZF, Chen MJ, Yap YW, Manikandan J, Melendez AJ, Choy MS, Moore PK, Cheung NS. 2008. Proteasome inhibition: an early or late event in nitric oxide-induced neuronal death? *Nitric Oxide* 18(2):136-145.
- Perl TM, Bedard L, Kosatsky T, Hockin JC, Todd EC, Remis RS. 1990. An outbreak of toxic encephalopathy caused by eating mussels contaminated with domoic acid. *N Engl J Med* 322(25):1775-1780.
- Perrone S, Szabo M, Bellieni CV, Longini M, Bango M, Kelen D, Treszl A, Negro S, Tataranno ML, Buonocore G. 2010. Whole body hypothermia and oxidative stress in babies with hypoxic-ischemic brain injury. *Pediatr Neurol* 43(4):236-240.
- Peterfalvi A, Molnar T, Banati M, Pusch G, Miko E, Bogar L, Pal J, Szereday L, Illes Z. 2009. Impaired function of innate T lymphocytes and NK cells in the acute phase of ischemic stroke. *Cerebrovasc Dis* 28(5):490-498.
- Petralia RS, Wenthold RJ. 1992. Light and electron immunocytochemical localization of AMPA-selective glutamate receptors in the rat brain. *J Comp Neurol* 318(3):329-354.
- Ping Z, Liu W, Kang Z, Cai J, Wang Q, Cheng N, Wang S, Zhang JH, Sun X. 2010. Sulforaphane protects brains against hypoxic-ischemic injury through induction of Nrf2-dependent phase 2 enzyme. *Brain Res* 1343:178-185.
- Pitkanen S, Robinson BH. 1996. Mitochondrial complex I deficiency leads to increased production of superoxide radicals and induction of superoxide dismutase. *J Clin Invest* 98(2):345-351.

- Plesnila N, Zinkel S, Le DA, Amin-Hanjani S, Wu Y, Qiu J, Chiarugi A, Thomas SS, Kohane DS, Korsmeyer SJ, Moskowitz MA. 2001. BID mediates neuronal cell death after oxygen/ glucose deprivation and focal cerebral ischemia. *Proc Natl Acad Sci U S A* 98(26):15318-15323.
- Podack ER, Hengartner H, Lichtenheld MG. 1991. A central role of perforin in cytolysis? *Annu Rev Immunol* 9:129-157.
- Pollard H, Heron A, Moreau J, Ben-Ari Y, Khrestchatisky M. 1993. Alterations of the GluR-B AMPA receptor subunit flip/flop expression in kainate-induced epilepsy and ischemia. *Neuroscience* 57(3):545-554.
- Polster BM, Basanez G, Etxebarria A, Hardwick JM, Nicholls DG. 2005. Calpain I induces cleavage and release of apoptosis-inducing factor from isolated mitochondria. *J Biol Chem* 280(8):6447-6454.
- Poon HF, Calabrese V, Scapagnini G, Butterfield DA. 2004. Free radicals: key to brain aging and heme oxygenase as a cellular response to oxidative stress. *J Gerontol A Biol Sci Med Sci* 59(5):478-493.
- Porn-Ares MI, Samali A, Orrenius S. 1998. Cleavage of the calpain inhibitor, calpastatin, during apoptosis. *Cell Death Differ* 5(12):1028-1033.
- Posner A, Raser KJ, Hajimohammadreza I, Yuen PW, Wang KK. 1995. Aurintricarboxylic acid is an inhibitor of mu- and m-calpain. *Biochem Mol Biol Int* 36(2):291-299.
- Power JH, Blumbergs PC. 2009. Cellular glutathione peroxidase in human brain: cellular distribution, and its potential role in the degradation of Lewy bodies in Parkinson's disease and dementia with Lewy bodies. *Acta Neuropathol* 117(1):63-73.
- Prince HC, Tzingounis AV, Levey AI, Conn PJ. 2000. Functional downregulation of GluR2 in piriform cortex of kindled animals. *Synapse* 38(4):489-498.
- Qu K, Chen CP, Halliwell B, Moore PK, Wong PT. 2006. Hydrogen sulfide is a mediator of cerebral ischemic damage. *Stroke* 37(3):889-893.
- Quintana A, Giralt M, Rojas S, Penkowa M, Campbell IL, Hidalgo J, Molinero A. 2005. Differential role of tumor necrosis factor receptors in mouse brain inflammatory responses in cryolesion brain injury. *J Neurosci Res* 82(5):701-716.
- Raivich G, Bohatschek M, Kloss CU, Werner A, Jones LL, Kreutzberg GW. 1999. Neuroglial activation repertoire in the injured brain: graded response, molecular mechanisms and cues to physiological function. *Brain Res Brain Res Rev* 30(1):77-105.
- Rallidis LS, Zolindaki MG, Vikelis M, Kaliva K, Papadopoulos C, Kremastinos DT. 2009. Elevated soluble intercellular adhesion molecule-1 levels are associated with poor short-term prognosis in middle-aged patients with acute ischaemic stroke. *Int J Cardiol* 132(2):216-220.
- Ranganathan S, Bowser R. 2003. Alterations in G(1) to S phase cell-cycle regulators during amyotrophic lateral sclerosis. *Am J Pathol* 162(3):823-835.
- Rao HV, Thirumangalakudi L, Desmond P, Grammas P. 2007. Cyclin D1, cdk4, and Bim are involved in thrombin-induced apoptosis in cultured cortical neurons. *J Neurochem* 101(2):498-505.

- Rao RV, Ellerby HM, Bredesen DE. 2004. Coupling endoplasmic reticulum stress to the cell death program. *Cell Death Differ* 11(4):372-380.
- Rashmi R, Pillai SG, Vijayalingam S, Ryerse J, Chinnadurai G. 2008. BH3-only protein BIK induces caspase-independent cell death with autophagic features in Bcl-2 null cells. *Oncogene* 27(10):1366-1375.
- Reinhard M, Roth M, Guschlbauer B, Harloff A, Timmer J, Czosnyka M, Hetzel A. 2005. Dynamic cerebral autoregulation in acute ischemic stroke assessed from spontaneous blood pressure fluctuations. *Stroke* 36(8):1684-1689.
- Represa A, Tremblay E, Ben-Ari Y. 1987. Kainate binding sites in the hippocampal mossy fibers: localization and plasticity. *Neuroscience* 20(3):739-748.
- Reynolds IJ, Hastings TG. 1995. Glutamate induces the production of reactive oxygen species in cultured forebrain neurons following NMDA receptor activation. *J Neurosci* 15(5 Pt 1):3318-3327.
- Ribeiro FM, Paquet M, Ferreira LT, Cregan T, Swan P, Cregan SP, Ferguson SS. 2010. Metabotropic glutamate receptor-mediated cell signaling pathways are altered in a mouse model of Huntington's disease. *J Neurosci* 30(1):316-324.
- Rice JE, 3rd, Vannucci RC, Brierley JB. 1981. The influence of immaturity on hypoxic-ischemic brain damage in the rat. *Ann Neurol* 9(2):131-141.
- Richardson CJ, Magee EA, Cummings JH. 2000. A new method for the determination of sulphide in gastrointestinal contents and whole blood by microdistillation and ion chromatography. *Clin Chim Acta* 293(1-2):115-125.
- Rideout HJ, Wang Q, Park DS, Stefanis L. 2003. Cyclin-dependent kinase activity is required for apoptotic death but not inclusion formation in cortical neurons after proteasomal inhibition. *J Neurosci* 23(4):1237-1245.
- Rink C, Roy S, Khan M, Ananth P, Kuppusamy P, Sen CK, Khanna S. 2010. Oxygen-sensitive outcomes and gene expression in acute ischemic stroke. *J Cereb Blood Flow Metab* 30(7):1275-1287.
- Robinson DM, Keating GM. 2006. Memantine: a review of its use in Alzheimer's disease. *Drugs* 66(11):1515-1534.
- Rockwell P, Yuan H, Magnusson R, Figueiredo-Pereira ME. 2000. Proteasome inhibition in neuronal cells induces a proinflammatory response manifested by upregulation of cyclooxygenase-2, its accumulation as ubiquitin conjugates, and production of the prostaglandin PGE(2). *Arch Biochem Biophys* 374(2):325-333.
- Ron D, Walter P. 2007. Signal integration in the endoplasmic reticulum unfolded protein response. *Nat Rev Mol Cell Biol* 8(7):519-529.
- Rosell A, Cuadrado E, Ortega-Aznar A, Hernandez-Guillamon M, Lo EH, Montaner J. 2008. MMP-9-positive neutrophil infiltration is associated to blood-brain barrier breakdown and basal lamina type IV collagen degradation during hemorrhagic transformation after human ischemic stroke. *Stroke* 39(4):1121-1126.
- Rosenberg GA, Cunningham LA, Wallace J, Alexander S, Estrada EY, Grossetete M, Razhagi A, Miller K, Gearing A. 2001. Immunohistochemistry of matrix metalloproteinases in reperfusion injury to rat brain: activation of MMP-9 linked to stromelysin-1 and microglia in cell cultures. *Brain Res* 893(1-2):104-112.

References

- Rosenberg GA, Estrada EY, Dencoff JE. 1998. Matrix metalloproteinases and TIMPs are associated with blood-brain barrier opening after reperfusion in rat brain. *Stroke* 29(10):2189-2195.
- Rosenmund C, Stern-Bach Y, Stevens CF. 1998. The tetrameric structure of a glutamate receptor channel. *Science* 280(5369):1596-1599.
- Rothlein R, Dustin ML, Marlin SD, Springer TA. 1986. A human intercellular adhesion molecule (ICAM-1) distinct from LFA-1. *J Immunol* 137(4):1270-1274.
- Ruchaud S, Carmena M, Earnshaw WC. 2007. Chromosomal passengers: conducting cell division. *Nat Rev Mol Cell Biol* 8(10):798-812.
- Rumbaugh G, Prybylowski K, Wang JF, Vicini S. 2000. Exon 5 and spermine regulate deactivation of NMDA receptor subtypes. *J Neurophysiol* 83(3):1300-1306.
- Salt TE, Eaton SA. 1995. Distinct presynaptic metabotropic receptors for L-AP4 and CCG1 on GABAergic terminals: pharmacological evidence using novel alpha-methyl derivative mGluR antagonists, MAP4 and MCCG, in the rat thalamus in vivo. *Neuroscience* 65(1):5-13.
- Salt TE, Eaton SA, Turner JP. 1996. Characterization of the metabotropic glutamate receptors (mGluRs) which modulate GABA-mediated inhibition in the ventrobasal thalamus. *Neurochem Int* 29(3):317-322.
- Samantaray S, Ray SK, Ali SF, Banik NL. 2006. Calpain activation in apoptosis of motoneurons in cell culture models of experimental parkinsonism. *Ann N Y Acad Sci* 1074:349-356.
- Sanchez RM, Koh S, Rio C, Wang C, Lamperti ED, Sharma D, Corfas G, Jensen FE. 2001. Decreased glutamate receptor 2 expression and enhanced epileptogenesis in immature rat hippocampus after perinatal hypoxia-induced seizures. *J Neurosci* 21(20):8154-8163.
- Sandberg R, Yasuda R, Pankratz DG, Carter TA, Del Rio JA, Wodicka L, Mayford M, Lockhart DJ, Barlow C. 2000. Regional and strain-specific gene expression mapping in the adult mouse brain. *Proc Natl Acad Sci U S A* 97(20):11038-11043.
- Saraste M. 1999. Oxidative phosphorylation at the fin de siecle. *Science* 283(5407):1488-1493.
- Sattler R, Charlton MP, Hafner M, Tymianski M. 1998. Distinct influx pathways, not calcium load, determine neuronal vulnerability to calcium neurotoxicity. *J Neurochem* 71(6):2349-2364.
- Saugstad JA, Kinzie JM, Mulvihill ER, Segerson TP, Westbrook GL. 1994. Cloning and expression of a new member of the L-2-amino-4-phosphonobutyric acid-sensitive class of metabotropic glutamate receptors. *Mol Pharmacol* 45(3):367-372.
- Savage JC, Gould DH. 1990. Determination of sulfide in brain tissue and rumen fluid by ion-interaction reversed-phase high-performance liquid chromatography. *J Chromatogr* 526(2):540-545.
- Scarpulla RC. 2002. Nuclear activators and coactivators in mammalian mitochondrial biogenesis. *Biochim Biophys Acta* 1576(1-2):1-14.
- Scheuer K, Maras A, Gattaz WF, Cairns N, Forstl H, Muller WE. 1996. Cortical NMDA receptor properties and membrane fluidity are altered in Alzheimer's disease. *Dementia* 7(4):210-214.

References

- Schmidt C, Hollmann M. 2008. Apparent homomeric NR1 currents observed in *Xenopus* oocytes are caused by an endogenous NR2 subunit. *J Mol Biol* 376(3):658-670.
- Schoepp DD, Goldsworthy J, Johnson BG, Salhoff CR, Baker SR. 1994. 3,5-dihydroxyphenylglycine is a highly selective agonist for phosphoinositide-linked metabotropic glutamate receptors in the rat hippocampus. *J Neurochem* 63(2):769-772.
- Schroder M, Kaufman RJ. 2005. ER stress and the unfolded protein response. *Mutat Res* 569(1-2):29-63.
- Seifert G, Rehn L, Weber M, Steinhauser C. 1997. AMPA receptor subunits expressed by single astrocytes in the juvenile mouse hippocampus. *Brain Res Mol Brain Res* 47(1-2):286-294.
- Seifert G, Weber M, Schramm J, Steinhauser C. 2003. Changes in splice variant expression and subunit assembly of AMPA receptors during maturation of hippocampal astrocytes. *Mol Cell Neurosci* 22(2):248-258.
- Sen N, Hara MR, Kornberg MD, Cascio MB, Bae BI, Shahani N, Thomas B, Dawson TM, Dawson VL, Snyder SH, Sawa A. 2008. Nitric oxide-induced nuclear GAPDH activates p300/CBP and mediates apoptosis. *Nat Cell Biol* 10(7):866-873.
- Shacka JJ, Lu J, Xie ZL, Uchiyama Y, Roth KA, Zhang J. 2007. Kainic acid induces early and transient autophagic stress in mouse hippocampus. *Neurosci Lett* 414(1):57-60.
- Shalak L, Perlman JM. 2004. Hypoxic-ischemic brain injury in the term infant-current concepts. *Early Hum Dev* 80(2):125-141.
- Shankaran S, Laptook AR, Ehrenkranz RA, Tyson JE, McDonald SA, Donovan EF, Fanaroff AA, Poole WK, Wright LL, Higgins RD, Finer NN, Carlo WA, Duara S, Oh W, Cotten CM, Stevenson DK, Stoll BJ, Lemons JA, Guillet R, Jobe AH. 2005. Whole-body hypothermia for neonates with hypoxic-ischemic encephalopathy. *N Engl J Med* 353(15):1574-1584.
- Shao S, Wang Y, Jin S, Song Y, Wang X, Fan W, Zhao Z, Fu M, Tong T, Dong L, Fan F, Xu N, Zhan Q. 2006. Gadd45a interacts with aurora-A and inhibits its kinase activity. *J Biol Chem* 281(39):28943-28950.
- Sherman MY, Goldberg AL. 2001. Cellular defenses against unfolded proteins: a cell biologist thinks about neurodegenerative diseases. *Neuron* 29(1):15-32.
- Sherr CJ. 1994. G1 phase progression: cycling on cue. *Cell* 79(4):551-555.
- Sherr CJ. 1995. D-type cyclins. *Trends Biochem Sci* 20(5):187-190.
- Shichita T, Sugiyama Y, Ooboshi H, Sugimori H, Nakagawa R, Takada I, Iwaki T, Okada Y, Iida M, Cua DJ, Iwakura Y, Yoshimura A. 2009. Pivotal role of cerebral interleukin-17-producing gammadeltaT cells in the delayed phase of ischemic brain injury. *Nat Med* 15(8):946-950.
- Shigemoto R, Kinoshita A, Wada E, Nomura S, Ohishi H, Takada M, Flor PJ, Neki A, Abe T, Nakanishi S, Mizuno N. 1997. Differential presynaptic localization of metabotropic glutamate receptor subtypes in the rat hippocampus. *J Neurosci* 17(19):7503-7522.
- Shigemoto R, Mizuno N. 2000. Metabotropic glutamate receptors-Immunocytochemical and in situ hybridization analyses. In: Otterson OP S-

- MJ, editor. Handbook of Chemical Neuroanatomy. Amsterdam: Elsevier Science. p 63-98.
- Siesjo BK, Agardh CD, Bengtsson F. 1989. Free radicals and brain damage. *Cerebrovasc Brain Metab Rev* 1(3):165-211.
- Silva D, Dikkes P, Barnes M, Lopez MF. 2009. Decreased motoneuron survival in Igf2 null mice after sciatic nerve transection. *Neuroreport* 20(16):1414-1418.
- Siman R, Noszek JC, Kegerise C. 1989. Calpain I activation is specifically related to excitatory amino acid induction of hippocampal damage. *J Neurosci* 9(5):1579-1590.
- Simeone TA, Sanchez RM, Rho JM. 2004. Molecular biology and ontogeny of glutamate receptors in the mammalian central nervous system. *J Child Neurol* 19(5):343-360; discussion 361.
- Simpkins KL, Guttman RP, Dong Y, Chen Z, Sokol S, Neumar RW, Lynch DR. 2003. Selective activation induced cleavage of the NR2B subunit by calpain. *J Neurosci* 23(36):11322-11331.
- Single FN, Rozov A, Burnashev N, Zimmermann F, Hanley DF, Forrest D, Curran T, Jensen V, Hvalby O, Sprengel R, Seeburg PH. 2000. Dysfunctions in mice by NMDA receptor point mutations NR1(N598Q) and NR1(N598R). *J Neurosci* 20(7):2558-2566.
- Smith DJ, Ng H, Kluck RM, Nagley P. 2008. The mitochondrial gateway to cell death. *IUBMB Life* 60(6):383-389.
- Smith RA, Walker T, Xie X, Hou ST. 2003. Involvement of the transcription factor E2F1/Rb in kainic acid-induced death of murine cerebellar granule cells. *Brain Res Mol Brain Res* 116(1-2):70-79.
- Soane L, Kahraman S, Kristian T, Fiskum G. 2007. Mechanisms of impaired mitochondrial energy metabolism in acute and chronic neurodegenerative disorders. *J Neurosci Res* 85(15):3407-3415.
- Somogyi P, Tamas G, Lujan R, Buhl EH. 1998. Salient features of synaptic organisation in the cerebral cortex. *Brain Res Brain Res Rev* 26(2-3):113-135.
- Song I, Huganir RL. 2002. Regulation of AMPA receptors during synaptic plasticity. *Trends Neurosci* 25(11):578-588.
- Southern E, Mir K, Shchepinov M. 1999. Molecular interactions on microarrays. *Nat Genet* 21(1 Suppl):5-9.
- Souza JM, Daikhin E, Yudkoff M, Raman CS, Ischiropoulos H. 1999. Factors determining the selectivity of protein tyrosine nitration. *Arch Biochem Biophys* 371(2):169-178.
- Sprengel R, Single FN. 1999. Mice with genetically modified NMDA and AMPA receptors. *Ann N Y Acad Sci* 868:494-501.
- Spruston N, Jonas P, Sakmann B. 1995. Dendritic glutamate receptor channels in rat hippocampal CA3 and CA1 pyramidal neurons. *J Physiol* 482 (Pt 2):325-352.
- Sribnick EA, Matzelle DD, Banik NL, Ray SK. 2007. Direct evidence for calpain involvement in apoptotic death of neurons in spinal cord injury in rats and neuroprotection with calpain inhibitor. *Neurochem Res* 32(12):2210-2216.
- Sridhar J, Akula N, Pattabiraman N. 2006. Selectivity and potency of cyclin-dependent kinase inhibitors. *AAPS J* 8(1):E204-221.

- Stamler JS, Toone EJ, Lipton SA, Sucher NJ. 1997. (S)NO signals: translocation, regulation, and a consensus motif. *Neuron* 18(5):691-696.
- Steinbrenner H, Sies H. 2009. Protection against reactive oxygen species by selenoproteins. *Biochim Biophys Acta* 1790(11):1478-1485.
- Stern P, Behe P, Schoepfer R, Colquhoun D. 1992. Single-channel conductances of NMDA receptors expressed from cloned cDNAs: comparison with native receptors. *Proc Biol Sci* 250(1329):271-277.
- Stoll G, Jander S. 1999. The role of microglia and macrophages in the pathophysiology of the CNS. *Prog Neurobiol* 58(3):233-247.
- Sucher NJ, Akbarian S, Chi CL, Leclerc CL, Awobuluyi M, Deitcher DL, Wu MK, Yuan JP, Jones EG, Lipton SA. 1995. Developmental and regional expression pattern of a novel NMDA receptor-like subunit (NMDAR-L) in the rodent brain. *J Neurosci* 15(10):6509-6520.
- Sugihara H, Moriyoshi K, Ishii T, Masu M, Nakanishi S. 1992. Structures and properties of seven isoforms of the NMDA receptor generated by alternative splicing. *Biochem Biophys Res Commun* 185(3):826-832.
- Sugiura S, Kitagawa K, Tanaka S, Todo K, Omura-Matsuoka E, Sasaki T, Mabuchi T, Matsushita K, Yagita Y, Hori M. 2005. Adenovirus-mediated gene transfer of heparin-binding epidermal growth factor-like growth factor enhances neurogenesis and angiogenesis after focal cerebral ischemia in rats. *Stroke* 36(4):859-864.
- Sullivan JM, Traynelis SF, Chen HS, Escobar W, Heinemann SF, Lipton SA. 1994. Identification of two cysteine residues that are required for redox modulation of the NMDA subtype of glutamate receptor. *Neuron* 13(4):929-936.
- Sultana R, Butterfield DA. 2009. Oxidatively modified, mitochondria-relevant brain proteins in subjects with Alzheimer disease and mild cognitive impairment. *J Bioenerg Biomembr* 41(5):441-446.
- Susin SA, Lorenzo HK, Zamzami N, Marzo I, Snow BE, Brothers GM, Mangion J, Jacotot E, Costantini P, Loeffler M, Larochette N, Goodlett DR, Aebersold R, Siderovski DP, Penninger JM, Kroemer G. 1999. Molecular characterization of mitochondrial apoptosis-inducing factor. *Nature* 397(6718):441-446.
- Swanson RA, Ying W, Kauppinen TM. 2004. Astrocyte influences on ischemic neuronal death. *Curr Mol Med* 4(2):193-205.
- Szegezdi E, Logue SE, Gorman AM, Samali A. 2006. Mediators of endoplasmic reticulum stress-induced apoptosis. *EMBO Rep* 7(9):880-885.
- Takadera T, Matsuda I, Ohyashiki T. 1999. Apoptotic cell death and caspase-3 activation induced by N-methyl-D-aspartate receptor antagonists and their prevention by insulin-like growth factor I. *J Neurochem* 73(2):548-556.
- Takadera T, Ohyashiki T. 2004. Glycogen synthase kinase-3 inhibitors prevent caspase-dependent apoptosis induced by ethanol in cultured rat cortical neurons. *Eur J Pharmacol* 499(3):239-245.
- Takahashi T, Forsythe ID, Tsujimoto T, Barnes-Davies M, Onodera K. 1996. Presynaptic calcium current modulation by a metabotropic glutamate receptor. *Science* 274(5287):594-597.

- Takahashi T, Katada S, Onodera O. 2010. Polyglutamine diseases: where does toxicity come from? what is toxicity? where are we going? *J Mol Cell Biol* 2(4):180-191.
- Takano J, Tomioka M, Tsubuki S, Higuchi M, Iwata N, Itohara S, Maki M, Saido TC. 2005. Calpain mediates excitotoxic DNA fragmentation via mitochondrial pathways in adult brains: evidence from calpastatin mutant mice. *J Biol Chem* 280(16):16175-16184.
- Tammariello SP, Quinn MT, Estus S. 2000. NADPH oxidase contributes directly to oxidative stress and apoptosis in nerve growth factor-deprived sympathetic neurons. *J Neurosci* 20(1):RC53.
- Tanabe Y, Masu M, Ishii T, Shigemoto R, Nakanishi S. 1992. A family of metabotropic glutamate receptors. *Neuron* 8(1):169-179.
- Tanabe Y, Nomura A, Masu M, Shigemoto R, Mizuno N, Nakanishi S. 1993. Signal transduction, pharmacological properties, and expression patterns of two rat metabotropic glutamate receptors, mGluR3 and mGluR4. *J Neurosci* 13(4):1372-1378.
- Tanaka T, Kimura M, Matsunaga K, Fukada D, Mori H, Okano Y. 1999. Centrosomal kinase AIK1 is overexpressed in invasive ductal carcinoma of the breast. *Cancer Res* 59(9):2041-2044.
- Tang G, Wu L, Wang R. 2010. Interaction of hydrogen sulfide with ion channels. *Clin Exp Pharmacol Physiol* 37(7):753-763.
- Tanne D, Macko RF, Lin Y, Tilley BC, Levine SR. 2006. Hemostatic activation and outcome after recombinant tissue plasminogen activator therapy for acute ischemic stroke. *Stroke* 37(7):1798-1804.
- Tarca AL, Romero R, Draghici S. 2006. Analysis of microarray experiments of gene expression profiling. *Am J Obstet Gynecol* 195(2):373-388.
- Tenneti L, D'Emilia DM, Troy CM, Lipton SA. 1998. Role of caspases in N-methyl-D-aspartate-induced apoptosis in cerebrocortical neurons. *J Neurochem* 71(3):946-959.
- Terai K, Matsuo A, McGeer EG, McGeer PL. 1996. Enhancement of immunoreactivity for NF-kappa B in human cerebral infarctions. *Brain Res* 739(1-2):343-349.
- Terman A, Gustafsson B, Brunk UT. 2006. Mitochondrial damage and intralysosomal degradation in cellular aging. *Mol Aspects Med* 27(5-6):471-482.
- Thayer SA, Wang GJ. 1995. Glutamate-induced calcium loads: effects on energy metabolism and neuronal viability. *Clin Exp Pharmacol Physiol* 22(4):303-304.
- Thomas KL, Davis S, Hunt SP, Laroche S. 1996. Alterations in the expression of specific glutamate receptor subunits following hippocampal LTP in vivo. *Learn Mem* 3(2-3):197-208.
- Thomas KL, Davis S, Laroche S, Hunt SP. 1994. Regulation of the expression of NR1 NMDA glutamate receptor subunits during hippocampal LTP. *Neuroreport* 6(1):119-123.
- Thornberry NA, Lazebnik Y. 1998. Caspases: enemies within. *Science* 281(5381):1312-1316.
- Timsit S, Menn B. 2007. Cerebral ischemia, cell cycle elements and Cdk5. *Biotechnol J* 2(8):958-966.

- Todde V, Veenhuis M, van der Klei IJ. 2009. Autophagy: principles and significance in health and disease. *Biochim Biophys Acta* 1792(1):3-13.
- Tong T, Zhong Y, Kong J, Dong L, Song Y, Fu M, Liu Z, Wang M, Guo L, Lu S, Wu M, Zhan Q. 2004. Overexpression of Aurora-A contributes to malignant development of human esophageal squamous cell carcinoma. *Clin Cancer Res* 10(21):7304-7310.
- Tong Y, Ben-Shlomo A, Zhou C, Wawrowsky K, Melmed S. 2008. Pituitary tumor transforming gene 1 regulates Aurora kinase A activity. *Oncogene* 27(49):6385-6395.
- Travers KJ, Patil CK, Wodicka L, Lockhart DJ, Weissman JS, Walter P. 2000. Functional and genomic analyses reveal an essential coordination between the unfolded protein response and ER-associated degradation. *Cell* 101(3):249-258.
- Tseveleki V, Rubio R, Vamvakas SS, White J, Taoufik E, Petit E, Quackenbush J, Probert L. 2010. Comparative gene expression analysis in mouse models for multiple sclerosis, Alzheimer's disease and stroke for identifying commonly regulated and disease-specific gene changes. *Genomics* 96(2):82-91.
- Tsubokawa H, Oguro K, Masuzawa T, Kawai N. 1994. Ca(2+)-dependent non-NMDA receptor-mediated synaptic currents in ischemic CA1 hippocampal neurons. *J Neurophysiol* 71(3):1190-1196.
- Tsuji M, Higuchi Y, Shiraishi K, Kume T, Akaike A, Hattori H. 2000. Protective effect of aminoguanidine on hypoxic-ischemic brain damage and temporal profile of brain nitric oxide in neonatal rat. *Pediatr Res* 47(1):79-83.
- Tsujimoto Y, Shimizu S. 2007. Role of the mitochondrial membrane permeability transition in cell death. *Apoptosis* 12(5):835-840.
- Tsuru-Aoyagi K, Potts MB, Trivedi A, Pfankuch T, Raber J, Wendland M, Claus CP, Koh SE, Ferriero D, Noble-Haeusslein LJ. 2009. Glutathione peroxidase activity modulates recovery in the injured immature brain. *Ann Neurol* 65(5):540-549.
- Tu XK, Yang WZ, Shi SS, Wang CH, Zhang GL, Ni TR, Chen CM, Wang R, Jia JW, Song QM. 2010. Spatio-temporal distribution of inflammatory reaction and expression of TLR2/4 signaling pathway in rat brain following permanent focal cerebral ischemia. *Neurochem Res* 35(8):1147-1155.
- Tymianski M, Charlton MP, Carlen PL, Tator CH. 1993. Source specificity of early calcium neurotoxicity in cultured embryonic spinal neurons. *J Neurosci* 13(5):2085-2104.
- Uberti D, Carsana T, Francisconi S, Ferrari Toninelli G, Canonico PL, Memo M. 2004. A novel mechanism for pergolide-induced neuroprotection: inhibition of NF-kappaB nuclear translocation. *Biochem Pharmacol* 67(9):1743-1750.
- Urra X, Cervera A, Villamor N, Planas AM, Chamorro A. 2009. Harms and benefits of lymphocyte subpopulations in patients with acute stroke. *Neuroscience* 158(3):1174-1183.
- Vader G, Lens SM. 2008. The Aurora kinase family in cell division and cancer. *Biochim Biophys Acta* 1786(1):60-72.

- Vairapandi M, Balliet AG, Hoffman B, Liebermann DA. 2002. GADD45b and GADD45g are cdc2/cyclinB1 kinase inhibitors with a role in S and G2/M cell cycle checkpoints induced by genotoxic stress. *J Cell Physiol* 192(3):327-338.
- Vallano ML. 1998. Developmental aspects of NMDA receptor function. *Crit Rev Neurobiol* 12(3):177-204.
- Vallet P, Charnay Y, Steger K, Ogier-Denis E, Kovari E, Herrmann F, Michel JP, Szanto I. 2005. Neuronal expression of the NADPH oxidase NOX4, and its regulation in mouse experimental brain ischemia. *Neuroscience* 132(2):233-238.
- van Handel M, Swaab H, de Vries LS, Jongmans MJ. 2007. Long-term cognitive and behavioral consequences of neonatal encephalopathy following perinatal asphyxia: a review. *Eur J Pediatr* 166(7):645-654.
- Vannucci RC. 1990. Experimental biology of cerebral hypoxia-ischemia: relation to perinatal brain damage. *Pediatr Res* 27(4 Pt 1):317-326.
- Venugopal R, Jaiswal AK. 1996. Nrf1 and Nrf2 positively and c-Fos and Fra1 negatively regulate the human antioxidant response element-mediated expression of NAD(P)H:quinone oxidoreductase1 gene. *Proc Natl Acad Sci U S A* 93(25):14960-14965.
- Verdaguer E, Jimenez A, Canudas AM, Jorda EG, Sureda FX, Pallas M, Camins A. 2004a. Inhibition of cell cycle pathway by flavopiridol promotes survival of cerebellar granule cells after an excitotoxic treatment. *J Pharmacol Exp Ther* 308(2):609-616.
- Verdaguer E, Jorda EG, Canudas AM, Jimenez A, Pubill D, Escubedo E, Camarasa J, Pallas M, Camins A. 2004b. Antiapoptotic effects of roscovitine in cerebellar granule cells deprived of serum and potassium: a cell cycle-related mechanism. *Neurochem Int* 44(4):251-261.
- Verdaguer E, Jorda EG, Canudas AM, Jimenez A, Sureda FX, Rimbau V, Pubill D, Escubedo E, Camarasa J, Pallas M, Camins A. 2003. 3-Amino thioacridone, a selective cyclin-dependent kinase 4 inhibitor, attenuates kainic acid-induced apoptosis in neurons. *Neuroscience* 120(3):599-603.
- Verdoorn TA, Burnashev N, Monyer H, Seeburg PH, Sakmann B. 1991. Structural determinants of ion flow through recombinant glutamate receptor channels. *Science* 252(5013):1715-1718.
- Verkhatsky A. 2005. Physiology and pathophysiology of the calcium store in the endoplasmic reticulum of neurons. *Physiol Rev* 85(1):201-279.
- Vicini S, Wang JF, Li JH, Zhu WJ, Wang YH, Luo JH, Wolfe BB, Grayson DR. 1998. Functional and pharmacological differences between recombinant N-methyl-D-aspartate receptors. *J Neurophysiol* 79(2):555-566.
- Vignes M, Clarke VR, Parry MJ, Bleakman D, Lodge D, Ornstein PL, Collingridge GL. 1998. The GluR5 subtype of kainate receptor regulates excitatory synaptic transmission in areas CA1 and CA3 of the rat hippocampus. *Neuropharmacology* 37(10-11):1269-1277.
- Vignes M, Collingridge GL. 1997. The synaptic activation of kainate receptors. *Nature* 388(6638):179-182.
- Vincent I, Jicha G, Rosado M, Dickson DW. 1997. Aberrant expression of mitotic cdc2/cyclin B1 kinase in degenerating neurons of Alzheimer's disease brain. *J Neurosci* 17(10):3588-3598.

- Vogelgesang A, Grunwald U, Langner S, Jack R, Broker BM, Kessler C, Dressel A. 2008. Analysis of lymphocyte subsets in patients with stroke and their influence on infection after stroke. *Stroke* 39(1):237-241.
- Votyakova TV, Reynolds IJ. 2001. DeltaPsi(m)-Dependent and -independent production of reactive oxygen species by rat brain mitochondria. *J Neurochem* 79(2):266-277.
- Wada E, Shigemoto R, Kinoshita A, Ohishi H, Mizuno N. 1998. Metabotropic glutamate receptor subtypes in axon terminals of projection fibers from the main and accessory olfactory bulbs: a light and electron microscopic immunohistochemical study in the rat. *J Comp Neurol* 393(4):493-504.
- Wang F, Corbett D, Osuga H, Osuga S, Ikeda JE, Slack RS, Hogan MJ, Hakim AM, Park DS. 2002a. Inhibition of cyclin-dependent kinases improves CA1 neuronal survival and behavioral performance after global ischemia in the rat. *J Cereb Blood Flow Metab* 22(2):171-182.
- Wang GJ, Thayer SA. 1996. Sequestration of glutamate-induced Ca²⁺ loads by mitochondria in cultured rat hippocampal neurons. *J Neurophysiol* 76(3):1611-1621.
- Wang KK, Posmantur R, Nadimpalli R, Nath R, Mohan P, Nixon RA, Talanian RV, Keegan M, Herzog L, Allen H. 1998. Caspase-mediated fragmentation of calpain inhibitor protein calpastatin during apoptosis. *Arch Biochem Biophys* 356(2):187-196.
- Wang L, Li Y, Chen X, Chen J, Gautam SC, Xu Y, Chopp M. 2002b. MCP-1, MIP-1, IL-8 and ischemic cerebral tissue enhance human bone marrow stromal cell migration in interface culture. *Hematology* 7(2):113-117.
- Wang W, Bu B, Xie M, Zhang M, Yu Z, Tao D. 2009. Neural cell cycle dysregulation and central nervous system diseases. *Prog Neurobiol* 89(1):1-17.
- Wang X, Phelan SA, Forsman-Semb K, Taylor EF, Petros C, Brown A, Lerner CP, Paigen B. 2003. Mice with targeted mutation of peroxiredoxin 6 develop normally but are susceptible to oxidative stress. *J Biol Chem* 278(27):25179-25190.
- Wang Y, Han R, Liang ZQ, Wu JC, Zhang XD, Gu ZL, Qin ZH. 2008. An autophagic mechanism is involved in apoptotic death of rat striatal neurons induced by the non-N-methyl-D-aspartate receptor agonist kainic acid. *Autophagy* 4(2):214-226.
- Wang Y, Qin ZH. 2010. Molecular and cellular mechanisms of excitotoxic neuronal death. *Apoptosis*.
- Ward MW, Rehm M, Duesmann H, Kacmar S, Concannon CG, Prehn JH. 2006. Real time single cell analysis of Bid cleavage and Bid translocation during caspase-dependent and neuronal caspase-independent apoptosis. *J Biol Chem* 281(9):5837-5844.
- Warenycia MW, Goodwin LR, Benishin CG, Reiffenstein RJ, Francom DM, Taylor JD, Dieken FP. 1989. Acute hydrogen sulfide poisoning. Demonstration of selective uptake of sulfide by the brainstem by measurement of brain sulfide levels. *Biochem Pharmacol* 38(6):973-981.

- Watanabe M, Inoue Y, Sakimura K, Mishina M. 1992. Developmental changes in distribution of NMDA receptor channel subunit mRNAs. *Neuroreport* 3(12):1138-1140.
- Watanabe M, Inoue Y, Sakimura K, Mishina M. 1993a. Distinct distributions of five N-methyl-D-aspartate receptor channel subunit mRNAs in the forebrain. *J Comp Neurol* 338(3):377-390.
- Watanabe M, Inoue Y, Sakimura K, Mishina M. 1993b. Distinct spatio-temporal distributions of the NMDA receptor channel subunit mRNAs in the brain. *Ann N Y Acad Sci* 707:463-466.
- Watanabe M, Mishina M, Inoue Y. 1994a. Distinct distributions of five NMDA receptor channel subunit mRNAs in the brainstem. *J Comp Neurol* 343(4):520-531.
- Watanabe M, Mishina M, Inoue Y. 1994b. Distinct spatiotemporal expressions of five NMDA receptor channel subunit mRNAs in the cerebellum. *J Comp Neurol* 343(4):513-519.
- Wei EP, Kontos HA, Christman CW, DeWitt DS, Povlishock JT. 1985. Superoxide generation and reversal of acetylcholine-induced cerebral arteriolar dilation after acute hypertension. *Circ Res* 57(5):781-787.
- Weisbrot-Lefkowitz M, Reuhl K, Perry B, Chan PH, Inouye M, Mirochnitchenko O. 1998. Overexpression of human glutathione peroxidase protects transgenic mice against focal cerebral ischemia/reperfusion damage. *Brain Res Mol Brain Res* 53(1-2):333-338.
- Wen YD, Sheng R, Zhang LS, Han R, Zhang X, Zhang XD, Han F, Fukunaga K, Qin ZH. 2008. Neuronal injury in rat model of permanent focal cerebral ischemia is associated with activation of autophagic and lysosomal pathways. *Autophagy* 4(6):762-769.
- Wenthold RJ, Petralia RS, Blahos J, II, Niedzielski AS. 1996. Evidence for multiple AMPA receptor complexes in hippocampal CA1/CA2 neurons. *J Neurosci* 16(6):1982-1989.
- Whalin ME, Scammell JG, Strada SJ, Thompson WJ. 1991. Phosphodiesterase II, the cGMP-activatable cyclic nucleotide phosphodiesterase, regulates cyclic AMP metabolism in PC12 cells. *Mol Pharmacol* 39(6):711-717.
- White HS, McCabe RT, Armstrong H, Donevan SD, Cruz LJ, Abogadie FC, Torres J, Rivier JE, Paarmann I, Hollmann M, Olivera BM. 2000. In vitro and in vivo characterization of conantokin-R, a selective NMDA receptor antagonist isolated from the venom of the fish-hunting snail *Conus radiatus*. *J Pharmacol Exp Ther* 292(1):425-432.
- Whiteman M, Armstrong JS, Chu SH, Jia-Ling S, Wong BS, Cheung NS, Halliwell B, Moore PK. 2004. The novel neuromodulator hydrogen sulfide: an endogenous peroxynitrite 'scavenger'? *J Neurochem* 90(3):765-768.
- Whiteman M, Cheung NS, Zhu YZ, Chu SH, Siau JL, Wong BS, Armstrong JS, Moore PK. 2005a. Hydrogen sulphide: a novel inhibitor of hypochlorous acid-mediated oxidative damage in the brain? *Biochem Biophys Res Commun* 326(4):794-798.
- Whiteman M, Ketsawatsakul U, Halliwell B. 2002. A reassessment of the peroxynitrite scavenging activity of uric acid. *Ann N Y Acad Sci* 962:242-259.

- Whiteman M, Li L, Kostetski I, Chu SH, Siau JL, Bhatia M, Moore PK. 2006. Evidence for the formation of a novel nitrosothiol from the gaseous mediators nitric oxide and hydrogen sulphide. *Biochem Biophys Res Commun* 343(1):303-310.
- Whiteman M, Rose P, Siau JL, Cheung NS, Tan GS, Halliwell B, Armstrong JS. 2005b. Hypochlorous acid-mediated mitochondrial dysfunction and apoptosis in human hepatoma HepG2 and human fetal liver cells: role of mitochondrial permeability transition. *Free Radic Biol Med* 38(12):1571-1584.
- Willemse JL, Brouns R, Heylen E, De Deyn PP, Hendriks DF. 2008. Carboxypeptidase U (TAFIa) activity is induced in vivo in ischemic stroke patients receiving thrombolytic therapy. *J Thromb Haemost* 6(1):200-202.
- Willemse JL, Hendriks DF. 2007. A role for procarboxypeptidase U (TAFI) in thrombosis. *Front Biosci* 12:1973-1987.
- Williams K. 1993. Ifenprodil discriminates subtypes of the N-methyl-D-aspartate receptor: selectivity and mechanisms at recombinant heteromeric receptors. *Mol Pharmacol* 44(4):851-859.
- Wong CH, Bozinovski S, Hertzog PJ, Hickey MJ, Crack PJ. 2008. Absence of glutathione peroxidase-1 exacerbates cerebral ischemia-reperfusion injury by reducing post-ischemic microvascular perfusion. *J Neurochem* 107(1):241-252.
- Wong CH, Crack PJ. 2008. Modulation of neuro-inflammation and vascular response by oxidative stress following cerebral ischemia-reperfusion injury. *Current medicinal chemistry* 15(1):1-14.
- Woods J, Snape M, Smith MA. 2007. The cell cycle hypothesis of Alzheimer's disease: suggestions for drug development. *Biochim Biophys Acta* 1772(4):503-508.
- Woodward RM, Huettner JE, Guastella J, Keana JF, Weber E. 1995a. In vitro pharmacology of ACEA-1021 and ACEA-1031: systemically active quinoxalinediones with high affinity and selectivity for N-methyl-D-aspartate receptor glycine sites. *Mol Pharmacol* 47(3):568-581.
- Woodward RM, Huettner JE, Tran M, Guastella J, Keana JF, Weber E. 1995b. Pharmacology of 5-chloro-7-trifluoromethyl-1,4-dihydro-2,3-quinoxalinedione: a novel systemically active ionotropic glutamate receptor antagonist. *J Pharmacol Exp Ther* 275(3):1209-1218.
- Wu J, Kaufman RJ. 2006. From acute ER stress to physiological roles of the Unfolded Protein Response. *Cell Death Differ* 13(3):374-384.
- Xia Z, Dickens M, Raingeaud J, Davis RJ, Greenberg ME. 1995. Opposing effects of ERK and JNK-p38 MAP kinases on apoptosis. *Science* 270(5240):1326-1331.
- Xu W, Liu L, Charles IG, Moncada S. 2004. Nitric oxide induces coupling of mitochondrial signaling with the endoplasmic reticulum stress response. *Nat Cell Biol* 6(11):1129-1134.
- Xue L, Fletcher GC, Tolkovsky AM. 1999. Autophagy is activated by apoptotic signaling in sympathetic neurons: an alternative mechanism of death execution. *Mol Cell Neurosci* 14(3):180-198.
- Yamagata K, Ichinose S, Miyashita A, Tagami M. 2008. Protective effects of ebselen, a seleno-organic antioxidant on neurodegeneration induced by hypoxia and

- reperfusion in stroke-prone spontaneously hypertensive rat. *Neuroscience* 153(2):428-435.
- Yamashima T, Kohda Y, Tsuchiya K, Ueno T, Yamashita J, Yoshioka T, Kominami E. 1998. Inhibition of ischaemic hippocampal neuronal death in primates with cathepsin B inhibitor CA-074: a novel strategy for neuroprotection based on 'calpain-cathepsin hypothesis'. *Eur J Neurosci* 10(5):1723-1733.
- Yamashima T, Tonchev AB, Tsukada T, Saido TC, Imajoh-Ohmi S, Momoi T, Kominami E. 2003. Sustained calpain activation associated with lysosomal rupture executes necrosis of the postischemic CA1 neurons in primates. *Hippocampus* 13(7):791-800.
- Yamashita T, Ninomiya M, Hernandez Acosta P, Garcia-Verdugo JM, Sunabori T, Sakaguchi M, Adachi K, Kojima T, Hirota Y, Kawase T, Araki N, Abe K, Okano H, Sawamoto K. 2006. Subventricular zone-derived neuroblasts migrate and differentiate into mature neurons in the post-stroke adult striatum. *J Neurosci* 26(24):6627-6636.
- Yan C, Lu D, Hai T, Boyd DD. 2005. Activating transcription factor 3, a stress sensor, activates p53 by blocking its ubiquitination. *EMBO J* 24(13):2425-2435.
- Yang Y, Geldmacher DS, Herrup K. 2001. DNA replication precedes neuronal cell death in Alzheimer's disease. *J Neurosci* 21(8):2661-2668.
- Yap YW, Whiteman M, Bay BH, Li Y, Sheu FS, Qi RZ, Tan CH, Cheung NS. 2006. Hypochlorous acid induces apoptosis of cultured cortical neurons through activation of calpains and rupture of lysosomes. *J Neurochem* 98(5):1597-1609.
- Yenari MA, Xu L, Tang XN, Qiao Y, Giffard RG. 2006. Microglia potentiate damage to blood-brain barrier constituents: improvement by minocycline in vivo and in vitro. *Stroke* 37(4):1087-1093.
- Yeste-Velasco M, Folch J, Trullas R, Abad MA, Enguita M, Pallas M, Camins A. 2007. Glycogen synthase kinase-3 is involved in the regulation of the cell cycle in cerebellar granule cells. *Neuropharmacology* 53(2):295-307.
- Yew EH, Cheung NS, Choy MS, Qi RZ, Lee AY, Peng ZF, Melendez AJ, Manikandan J, Koay ES, Chiu LL, Ng WL, Whiteman M, Kandiah J, Halliwell B. 2005. Proteasome inhibition by lactacystin in primary neuronal cells induces both potentially neuroprotective and pro-apoptotic transcriptional responses: a microarray analysis. *J Neurochem* 94(4):943-956.
- Yilmaz G, Granger DN. 2008. Cell adhesion molecules and ischemic stroke. *Neurol Res* 30(8):783-793.
- Yin WL, He JQ, Hu B, Jiang ZS, Tang XQ. 2009. Hydrogen sulfide inhibits MPP(+)-induced apoptosis in PC12 cells. *Life Sci* 85(7-8):269-275.
- Yin XM, Luo Y, Cao G, Bai L, Pei W, Kuharsky DK, Chen J. 2002. Bid-mediated mitochondrial pathway is critical to ischemic neuronal apoptosis and focal cerebral ischemia. *J Biol Chem* 277(44):42074-42081.
- Yoneda-Kato N, Tomoda K, Umehara M, Arata Y, Kato JY. 2005. Myeloid leukemia factor 1 regulates p53 by suppressing COP1 via COP9 signalosome subunit 3. *EMBO J* 24(9):1739-1749.
- Youle RJ, Strasser A. 2008. The BCL-2 protein family: opposing activities that mediate cell death. *Nat Rev Mol Cell Biol* 9(1):47-59.

- Young HA, Bream JH. 2007. IFN-gamma: recent advances in understanding regulation of expression, biological functions, and clinical applications. *Curr Top Microbiol Immunol* 316:97-117.
- Yousefi S, Perozzo R, Schmid I, Ziemiecki A, Schaffner T, Scapozza L, Brunner T, Simon HU. 2006. Calpain-mediated cleavage of Atg5 switches autophagy to apoptosis. *Nat Cell Biol* 8(10):1124-1132.
- Yu SP, Yeh CH, Sensi SL, Gwag BJ, Canzoniero LM, Farhangrazi ZS, Ying HS, Tian M, Dugan LL, Choi DW. 1997. Mediation of neuronal apoptosis by enhancement of outward potassium current. *Science* 278(5335):114-117.
- Yu SW, Wang H, Poitras MF, Coombs C, Bowers WJ, Federoff HJ, Poirier GG, Dawson TM, Dawson VL. 2002. Mediation of poly(ADP-ribose) polymerase-1-dependent cell death by apoptosis-inducing factor. *Science* 297(5579):259-263.
- Zamai L, Ahmad M, Bennett IM, Azzoni L, Alnemri ES, Perussia B. 1998. Natural Killer (NK) Cell-mediated Cytotoxicity: Differential Use of TRAIL and Fas Ligand by Immature and Mature Primary Human NK Cells. 188(122375-122380).
- Zamanillo D, Sprengel R, Hvalby O, Jensen V, Burnashev N, Rozov A, Kaiser KM, Koster HJ, Borchardt T, Worley P, Lubke J, Frotscher M, Kelly PH, Sommer B, Andersen P, Seeburg PH, Sakmann B. 1999. Importance of AMPA receptors for hippocampal synaptic plasticity but not for spatial learning. *Science* 284(5421):1805-1811.
- Zatz M, Starling A. 2005. Calpains and disease. *N Engl J Med* 352(23):2413-2423.
- Zazulia AR, Videen TO, Powers WJ. 2007. Symptomatic autoregulatory failure in acute ischemic stroke. *Neurology* 68(5):389-390.
- Zeller JA, Lenz A, Eschenfelder CC, Zunker P, Deuschl G. 2005. Platelet-leukocyte interaction and platelet activation in acute stroke with and without preceding infection. *Arterioscler Thromb Vasc Biol* 25(7):1519-1523.
- Zeller JA, Tschoepe D, Kessler C. 1999. Circulating platelets show increased activation in patients with acute cerebral ischemia. *Thromb Haemost* 81(3):373-377.
- Zhang X, Peng B. 2005. Immunolocalization of receptor activator of NF kappa B ligand in rat periapical lesions. *J Endod* 31(8):574-577.
- Zhao W, Wang R. 2002. H₂S-induced vasorelaxation and underlying cellular and molecular mechanisms. *Am J Physiol Heart Circ Physiol* 283(2):H474-480.
- Zhu C, Kang W, Xu F, Cheng X, Zhang Z, Jia L, Ji L, Guo X, Xiong H, Simbruner G, Blomgren K, Wang X. 2009. Erythropoietin improved neurologic outcomes in newborns with hypoxic-ischemic encephalopathy. *Pediatrics* 124(2):e218-226.
- Zhu C, Wang X, Xu F, Bahr BA, Shibata M, Uchiyama Y, Hagberg H, Blomgren K. 2005. The influence of age on apoptotic and other mechanisms of cell death after cerebral hypoxia-ischemia. *Cell Death Differ* 12(2):162-176.
- Zhu X, Castellani RJ, Takeda A, Nunomura A, Atwood CS, Perry G, Smith MA. 2001. Differential activation of neuronal ERK, JNK/SAPK and p38 in Alzheimer disease: the 'two hit' hypothesis. *Mech Ageing Dev* 123(1):39-46.

References

- Zhu X, Lee HG, Perry G, Smith MA. 2007. Alzheimer disease, the two-hit hypothesis: an update. *Biochim Biophys Acta* 1772(4):494-502.
- Zhu X, Raina AK, Smith MA. 1999. Cell cycle events in neurons. Proliferation or death? *Am J Pathol* 155(2):327-329.
- Zhu Y, Yang GY, Ahlemeyer B, Pang L, Che XM, Culmsee C, Klumpp S, Kriegstein J. 2002. Transforming growth factor-beta 1 increases bad phosphorylation and protects neurons against damage. *J Neurosci* 22(10):3898-3909.
- Zindy F, Nilsson LM, Nguyen L, Meunier C, Smeyne RJ, Rehg JE, Eberhart C, Sherr CJ, Roussel MF. 2003. Hemangiosarcomas, medulloblastomas, and other tumors in *Ink4c/p53*-null mice. *Cancer Res* 63(17):5420-5427.
- Zinszner H, Kuroda M, Wang X, Batchvarova N, Lightfoot RT, Remotti H, Stevens JL, Ron D. 1998. CHOP is implicated in programmed cell death in response to impaired function of the endoplasmic reticulum. *Genes Dev* 12(7):982-995.
- Zundorf G, Kahlert S, Bunik VI, Reiser G. 2009. alpha-Ketoglutarate dehydrogenase contributes to production of reactive oxygen species in glutamate-stimulated hippocampal neurons in situ. *Neuroscience* 158(2):610-616.